



# AIRPLANE STRUCTURES

BY

ALFRED S. NILES, A.B., S.B.

PROFESSOR OF AERONAUTIC ENGINEERING,  
STANFORD UNIVERSITY

AND

JOSEPH S. NEWELL, S.B.

PROFESSOR OF AERONAUTICAL STRUCTURAL ENGINEERING,  
MASSACHUSETTS INSTITUTE OF TECHNOLOGY

VOLUME II

*THIRD EDITION*

NEW YORK

JOHN WILEY & SONS, INC.

LONDON: CHAPMAN & HALL, LIMITED

1943



THIS BOOK HAS BEEN MANUFACTURED IN  
ACCORDANCE WITH THE RECOMMENDATIONS  
OF THE WAR PRODUCTION BOARD IN THE  
INTEREST OF THE CONSERVATION OF PAPER  
AND OTHER IMPORTANT WAR MATERIALS.

COPYRIGHT, 1929, 1938, 1943  
BY ALFRED S. NILES  
AND JOSEPH S. NEWELL

*All Rights Reserved*

*This book or any part thereof must not  
be reproduced in any form without  
the written permission of the publisher.*

PRINTED IN THE UNITED STATES OF AMERICA

## PREFACE TO THE THIRD EDITION

In the third edition, the principal changes in Volume I have been the clarification of some articles with which students have had trouble, the rewriting of others to make them consistent with new material in the second volume, and the correction of typographical errors. In the second volume there are six completely new chapters which are devoted primarily to problems connected with the types of metal and plywood construction which are now being used.

Three of the new chapters cover the analysis of beams having incomplete tension-field webs, the computation of shear flow in thin shells such as monocoque wings and fuselages, and the determination of stresses in curved beams and rings. Because of the importance of stability criteria in the determination of the load-carrying capacity of compression members, one chapter is devoted to basic methods for dealing with the stability of beams and trusses, while a second presents an application of the calculus of variations to the torsion-bending stability problem in open-section columns. Allowable stress data and characteristics of some of the newer materials such as magnesium alloy, plastics, plastic-bonded plywood, and glass have been added, and a critical bibliography has been included to acquaint the student with some of the literature pertaining to structural theory, its scope and limitations.

The addition of these new chapters has necessitated presenting the enlarged work as a third edition. Though a rearrangement of the material in the two volumes, with a condensation of some articles and an expansion of others, might be desirable from a pedagogical standpoint, the authors have found that much of the material required for the complete revision of such articles is on a restricted status and may not be published during the war. Rather than revise and rewrite the entire text under these conditions it was decided to utilize the plates for the second edition wherever possible. As a result many of the references to the state of the art in 1937, particularly where progress has been slight or restricted as to publication, have not been modified. It is hoped that when the present emergency is over it will be possible to present a new edition in which the wartime advances in structural analysis methods can be freely discussed.

The two volumes present data on the more commonly used materials and methods of stress analysis, and it is the authors' experience that

students well qualified in mathematics and mechanics can master both in a course providing 180 to 200 hours of lectures and about 400 hours devoted to study of the text and the solution of problems. For use in accelerated or intensive programs it has been found possible to select topics not usually mastered by civil or mechanical engineers and to reorient graduates in these fields so that they are reasonably competent stress analysts after courses consisting of 75 to 90 lecture hours, with two hours of outside study assigned for each lecture. Such programs presuppose a mature student, usually a graduate, with some competence in the fields of mechanics and structures.

Where younger students are involved, as in some of the accelerated college programs now being given, it appears necessary to reduce the speed at which the various topics are presented. This, of course, requires the omission of certain material, and, though the choice of such material must be left to the individual instructor, the authors feel that he should make every effort to develop proficiency in his students in the construction of curves of shear and bending moments for beams, in the analysis of trusses, the computation of deflections, and the solution of redundant structures by the Maxwell-Mohr method. Such proficiency can best be developed by having the student solve representative problems, either independently or under the direct supervision of the instructor. The science, or theory, of structures may be learned from books, but the art of analyzing and designing structures by the most expeditious method comes only by practice in the solution of problems. Those presented at the end of each chapter will be found to provoke thought on the part of the student, to develop his ability to trace the paths of forces through rather complex systems of members, and to insure that he master the basic principles involved in the articles to which they are related. Whether the proposed course be normal, accelerated, or intensive, it should contain as many of these, or similar, problems as may be compatible with the time allotted to the study of structures.

ALFRED S. NILES  
JOSEPH S. NEWELL

*May, 1943*

# CONTENTS

## CHAPTER XIII

### STATICALLY INDETERMINATE STRUCTURES

ART.	PAGE
1. Degree of Redundancy . . . . .	1
2. Methods of Solving Indeterminate Structures . . . . .	2
3. The Principle of Superposition . . . . .	4
4. Structures with a Single Redundant . . . . .	5
5. Multipli-redundant Structures . . . . .	8
6. The Statically Determinate Included Structure . . . . .	10
7. General Statement of the Maxwell-Mohr Method . . . . .	11
8. Redundant Structures with Axial Loads Only . . . . .	12
9. Initial Stresses in Trusses . . . . .	15
10. Members Dropping out of Action . . . . .	17
11. The Method of Least Work. General Statement . . . . .	20
12. Alternative Method of Computing Partial Derivatives . . . . .	23
13. Expressions for Internal Work . . . . .	24
14. Numerical Example . . . . .	26
15. Value of the Maxwell-Mohr and Least-work Methods . . . . .	29
16. Principle of Relative Rigidities . . . . .	30
17. Arrangement of Computations . . . . .	31
18. Solution by Influence Lines . . . . .	34
19. The Rigid Frame Sign Convention . . . . .	36
20. Moment Distribution, Stationary Joints . . . . .	39
21. Moment Distribution, Known Joint Translation . . . . .	39
22. Moment Distribution with Unknown Deflections . . . . .	41
23. Slope Deflection . . . . .	49
24. Effect of Elastic Joints . . . . .	52

## CHAPTER XIV

### BEAM-COLUMNS

1. General Effect of an Axial Load . . . . .	63
2. Derivation of the Formulas . . . . .	65
3. Equation of Three Moments . . . . .	79
4. Numerical Example . . . . .	81
5. Formulas for Other Loadings . . . . .	90
6. Critical Loads . . . . .	109
7. Approximate Computations . . . . .	115
8. Effect of Change in Axial Load between Supports . . . . .	116
9. Secondary Shear . . . . .	117
10. Notes on the Use of the Beam-column Formulas . . . . .	119
11. Moment Distribution, Beam-columns of Constant Section . . . . .	120

ART.	PAGE
12. Numerical Example . . . . .	130
13. Beam-columns of Non-uniform Section . . . . .	132
14. Beam-columns Subjected to High Axial Stress . . . . .	140
15. Graphical Analysis of Beam-columns . . . . .	141

## CHAPTER XV

## INCOMPLETE TENSION FIELDS

1. Stresses in Complete Tension Field Beams . . . . .	157
2. Notation and Nomenclature . . . . .	159
3. Assumptions Underlying Analysis of Incomplete Tension Field Beams . . . . .	160
4. Computation of Web Stresses . . . . .	161
5. Numerical Example . . . . .	164
6. Loads on Web-chord Connecting Rivets . . . . .	166
7. Design of Web Stiffeners . . . . .	166
8. Chord Stresses . . . . .	170
9. Effects of Non-parallel Chords and Oblique Stiffeners . . . . .	171
10. Deflection of Tension Field Beams . . . . .	173
11. General Remarks . . . . .	178

## CHAPTER XVI

## SHELL ANALYSIS

1. Mid-line Method of Computing Section Properties . . . . .	180
2. Shear Flow . . . . .	182
3. Shear Flow in Tube Subjected to Torsion . . . . .	184
4. Torsion on Subdivided Shell . . . . .	187
5. Analysis of Shell-type Wing Section under Torsion . . . . .	188
6. Shear Due to Transverse Load. Introduction to the Problem . . . . .	191
7. Geometric Properties of the Effective Section . . . . .	192
8. Distribution of Normal Stress . . . . .	200
9. Computation of Trial Shear Flows . . . . .	203
10. Computation of Resultant of Trial Shear Flows . . . . .	208
11. Computation of Correction Shear Flows . . . . .	210
12. Computation of Net Shear Flows . . . . .	214
13. Effect of Lack of Symmetry . . . . .	214
14. Buckling Lag . . . . .	216
15. Shear Lag . . . . .	218
16. Distribution of Effective Material . . . . .	220
17. Remarks on Practical Procedure . . . . .	222
18. Shear-flow Determination without Locating the Shear Center . . . . .	224
19. Rib and Ring Pressure . . . . .	225
20. Normal Stresses Induced by Torsion . . . . .	227
21. Tapered Shells of Symmetrical Section . . . . .	232
22. Practical Analysis of Tapered Shells . . . . .	238
23. Effect of Sudden Change in Section . . . . .	239
24. Shear Transfer around Openings . . . . .	242
25. Illustrative Example . . . . .	247

CHAPTER XVII

CURVED BEAMS AND RINGS

ART.	PAGE
1. Bending Stresses in Curved Bars . . . . .	257
2. Graphical Method for Computing $J$ . . . . .	261
3. Illustrative Example . . . . .	262
4. Deflection of a Curved Beam . . . . .	263
5. Equation of Elastic Curves for Beams Having Circular Central Axes . . . . .	265
6. Symmetric and Anti-symmetric Loadings . . . . .	267
7. Redundant Forces on Section of Circular Ring . . . . .	269
8. Illustrative Example . . . . .	276
9. Rings Used to Maintain Form . . . . .	278

CHAPTER XVIII

CRITICAL LOADS

1. Use of Maupertuis' Theorem . . . . .	283
2. Representation of Deformation Pattern . . . . .	285
3. Principle of Virtual Work . . . . .	286
4. Development of Trigonometric Beam-deflection Formula . . . . .	289
5. Critical Load of a Column in an Elastic Medium . . . . .	291
6. Types of Instability Failure . . . . .	294
7. Stability of a Column Carrying a Variable Transverse Load . . . . .	296
8. Stability of an Elastically Supported Column . . . . .	297
9. Effect of Non-Linear Resistance to Deflection . . . . .	300
10. Effect of a Transverse Load . . . . .	300
11. Conclusions Regarding the Spring-constant Criterion . . . . .	302
12. Stability of Rigid-jointed Trusses . . . . .	303
13. Illustrative Example . . . . .	306
14. Empirical Determination of the Critical Load . . . . .	309
15. Present Status of Theory of Instability Failure . . . . .	311

CHAPTER XIX

TORSIONAL COLUMN FAILURE

1. The Purpose of the Calculus of Variations . . . . .	317
2. Calculus of Variations. Notation and Nomenclature . . . . .	318
3. Application to a Pin-ended Column . . . . .	320
4. Warping of Thin Metal Members . . . . .	323
5. Formulas for Unit Warping . . . . .	326
6. Relations among Stress, Strain, and Warping . . . . .	330
7. Energy of a Bent and Twisted Column . . . . .	332
8. General Differential Equations for a Column; Rotation Axis Unknown . . . . .	334
9. Action of Column with Doubly Symmetrical Section . . . . .	336
10. Action of Columns with Singly Symmetrical Section . . . . .	338
11. Action of Unsymmetrical Section Column . . . . .	340
12. General Equation for a Column with Known Axis of Rotation . . . . .	343
13. Practical Evaluation of Warping Moments and Constants . . . . .	345
14. Experimental Verification for Formulas . . . . .	351
15. General Remarks on Torsional Failure . . . . .	353

## CHAPTER XX

## ALLOWABLE STRESS DATA

ART.	PAGE
1. Materials Used in Compact Sections.....	359
2. Materials Used in Thin Elements.....	360
3. References.....	360
4. Glass.....	367
5. Plastics.....	369
6. Use of Plastics in Airplane Construction.....	372
7. Plastics Used as Sealants.....	373
8. Types of Plastic-bonded Plywood.....	374
9. Tensile Properties of Plastic-bonded Plywoods.....	376
10. Plastic-bonded Plywoods Subjected to Compression.....	379
11. Resistance to Shear and Buckling.....	383
12. Moisture Absorption of Plastic-bonded Plywoods.....	385
13. Connections between Plastic-bonded Plywood Parts.....	385
14. Magnesium Alloys.....	388

## BIBLIOGRAPHY

Section I. Books.....	393
Section II. Reports and Papers.....	401

# AIRPLANE STRUCTURES

## CHAPTER XIII

### STATICALLY INDETERMINATE STRUCTURES

As stated in Chapter III there are certain types of structure in which the outer forces, the reactions, or the inner forces, the loads in the various parts of the structure, cannot be determined from the conditions of equilibrium alone. Such structures are known as statically indeterminate or redundant structures since there are more unknown magnitudes, directions, and points of application of the reactions, or more internal forces on the elements of the structure, than there are independent equations that can be written by the application of the conditions of statics. In this chapter some of the more important methods of analyzing structures of this type will be described and illustrated.

**13 : 1. Degree of Redundancy** — For any structure, the relationships between the forces in the structure imposed by the conditions of static equilibrium can be represented by algebraic equations. Each condition of equilibrium when applied to the whole or any part of a structure can be represented by one and only one independent equation. If the structure is statically determinate the number of independent equations that can be obtained in this way will be equal to the number of unknown quantities appearing in them. All the reactions on or stresses in the structure can then be found by solving the equations. If the equations deducible from the conditions of equilibrium are written for a redundant structure and its parts, it will be found that there will be  $n$  less independent equations than there are unknown quantities appearing in them. The structure is then said to be statically indeterminate or redundant in the  $n$ th degree.

It will sometimes happen that  $p + r$  equations can be written for a structure on the basis of the conditions of equilibrium, and that a group of these equations  $p$  in number will contain only  $p$  unknowns. The remaining  $r$  equations will contain  $r + n$  unknowns in addition to those appearing in the  $p$  equations. This indicates that the parts of the structure represented by the  $p$  equations are statically determinate



and can be solved directly, while the remainder represented by the  $r$  equations are redundant in the  $n$ th degree. In such cases it is necessary for the complete analysis of the structure to obtain  $n$  new independent equations which will be based, not on the requirements for equilibrium, but on some other principle.

It is not always easy to determine the degree of redundancy of a structure, and very often the designer will write down equations that are mutually dependent in the belief that they are independent. When this is done certain of the equations will reduce to an identity or, due to lack of precision, to equations which are almost identical. In such cases, one of the mutually dependent equations must be thrown out. The only sure way of determining the degree of redundancy is to write down the equations based on the conditions of equilibrium and solve them as far as possible, eliminating such equations as prove to be dependent. The number of unknowns that cannot be eliminated by the methods of algebra will then indicate the degree of redundancy.

**13 : 2. Methods of Solving Indeterminate Structures**—The simplest method of determining the values of the redundant unknowns is to make sufficient arbitrary assumptions. A good example of this is the common procedure of assuming a truss to be composed of members connected by frictionless pins, thus fixing the directions and points of application of the loads acting at the ends of the various members. Another is the assumption that a continuous beam acts as a series of disconnected simple beams, each resting on only two supports. This is a highly approximate method, which should be used only when great accuracy is not desired, or when it is known that the assumptions made for the structure being analyzed will give sufficiently precise results. Some assumptions of this character, however, are practically always needed, and most structures that are analyzed as statically determinate are really redundant structures in which the redundant unknowns have been eliminated by simplifying assumptions.

For many structures the designer can visualize fairly clearly the deformations and deflections that would be caused by the external loads to which they are subjected. Thus referring to the beam shown in Fig. 13 : 1*a*, it should be obvious that, under the load indicated, the elastic curve would be of the type shown in Fig. 13 : 1*b*. From the load and deflection curves it can be similarly deduced that the bending-moment curve will be of the type shown in Fig. 13 : 1*c*. Finally, it can be deduced from the moment curve that the reactions will be in the directions shown in Fig. 13 : 1*a*.

As the loading consists exclusively of concentrated loads (including the reactions) the moment curve must consist of straight lines. From

Fig. 13 : 1b it is evident that there must be two points of inflection. To be consistent with the essential characteristics of the moment curve these points must be approximately at the locations shown by the small circles. Between  $C$  and  $D$  the moment curve must be a single straight line as there is no change in shear in that bay. Also this line must intersect the axis at  $D$  since a pinned support at that point is indicated

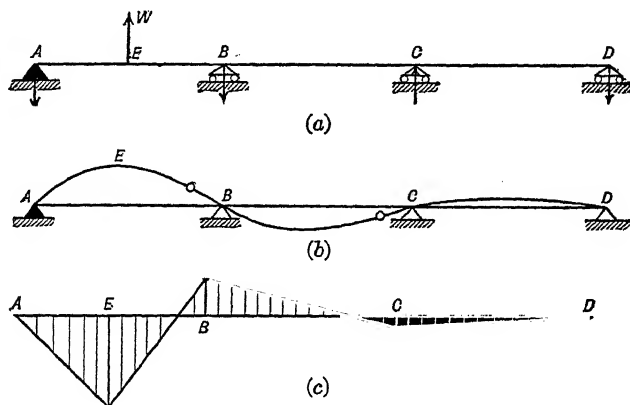


FIG. 13 : 1

in Fig. 13 : 1a. Therefore it cannot intersect the axis at any other point to indicate a point of inflection between  $C$  and  $D$ . Similarly there can be no point of inflection between  $A$  and  $E$ , nor more than one such point between  $E$  and  $B$ , or  $B$  and  $C$ . Thus far the locations of the points of inflection are determined purely by the requirements that the elastic curve pass through the (assumed stationary) supporting points, and that the bending moment be the second integral of the loading. That one point of inflection should be closer to  $B$  than to  $E$  and the other closer to  $C$  than to  $B$  should be clear from a very rough mental analysis of the beam by the Cross method.

Once the locations of all points of inflection are known or assumed, a structure can be analyzed either as statically determinate or as one of a much reduced degree of redundancy. Even though qualitative deflection and moment curves like those illustrated by Fig. 13 : 1b and 13 : 1c cannot serve to determine the exact locations of the points of inflection they are of great help to the designer. With practice, he can draw such curves for much more complex structures, and they will greatly assist him in visualizing the action of structures under load, a prerequisite for intelligent design. They also facilitate locating points of inflection with such accuracy that a trial design based on an analysis in which they are utilized to make suitable simplifying assumptions is

quite likely to be found satisfactory or need only minor modifications. When drawing such qualitative deflection and moment curves it is desirable to plot moments on that side of a member which they tend to subject to compression. Then for a horizontal member positive bending moments will be plotted above the member.

The rational method of computing the redundant unknowns is to apply the principle of consistent deformations. This principle is: In any redundant structure, the distribution of stresses will be such that not only are the conditions of equilibrium satisfied, but also that the deformations of all parts of the structure will be consistent with respect to each other. The application of this principle may take any one of several forms, but no matter which method is used, if it is used correctly, the same stress distributions will be found in the various members. Its chief disadvantage is that, since the deformation of any member is a function of the area and stress in the member, the size of the members of the structure must be determined before the stresses in them can be computed. In certain special cases the principle of consistent deformations can be used for members of unknown size if it is known that they are to be of constant section or that the values of  $EI$  and  $AE$  of the different members will be in previously determined ratios.

One application of the principle of consistent deformations was made in Chapter V in the development of the three-moment equations from the proposition that the slope of the elastic curve just to the left of a support is necessarily the same as its slope just to the right of the support.

**13 : 3. The Principle of Superposition** — Most of the practical methods of analyzing redundant structures assume the validity of the principle of superposition as well as that of consistent deformations. The general principle of superposition is that the resultant effect of a group of causes acting simultaneously is the algebraic sum of the effects of the individual causes acting separately. This principle applies whenever the resultant effect may be expressed algebraically as a linear function of the various causes. Thus the resultant deflection in any given direction of any point  $a$  of a structure to which the principle applies may be expressed by the formula

$$\delta_a = \delta_{ao} + X_a\delta_{aa} + X_b\delta_{ab} + X_c\delta_{ac} + \dots \quad 13 : 1$$

where

$\delta_a$  = resultant deflection of point  $a$  in the given direction.

$\delta_{ao}$  = deflection of  $a$  in that direction due to external forces and couples of known magnitude.

$X_a$  = magnitude of any unknown external force at  $a$  in the direction of  $\delta_a$ .

- $\delta_{aa}$  = deflection of point  $a$  due to a unit external load at  $a$  in the direction of  $X_a$ .
- $X_b, X_c, \dots$  = magnitudes of unknown external forces (or couples) acting at points  $b, c, \dots$  respectively.
- $\delta_{ab}, \delta_{ac}, \dots$  = deflections of point  $a$  due to unit values of  $X_b, X_c, \dots$  respectively.

Similar equations can be written for other quantities to which the principle of superposition may apply, such as slope, bending moment, shear, or axial load.

The principle of superposition does not apply when the material in a structure is stressed beyond the limit of proportionality, nor when the stresses in some of its members are dependent on the deformations. The methods of analysis described in this chapter all presuppose the validity of the principle. The most important type of member used in airplane design to which the principle does not apply is the beam subjected to combined bending and axial loads. An appropriate method for the analysis of such members is taken up in Chapter XIV.

**13 : 4. Structures with a Single Redundant**—The most general method of applying the principles of consistent deformation and superposition to the solution of redundant structures is that first suggested by Professor Maxwell and later developed by Professor Mohr. It will be convenient to apply the method to a few simple problems first and then generalize the procedure employed.

As a first example consider the beam of Fig. 13 : 2, fixed at  $A$ , simply supported at  $B$ , and subjected to a uniformly distributed load of  $w$  pounds per inch. It will be assumed that the support at  $B$  is sufficiently rigid that it will not move vertically under the assumed loading. In other words, the net deflection of  $B$  from the tangent to the elastic curve at  $A$  will remain zero. It should be obvious that the reactions, bending moments, etc., of the redundant beam of the figure will be the same as those of a cantilever beam of the same material and cross-section, supported at  $A$  and subjected to the uniformly distributed load,  $w$ , and to a concentrated load,  $V_b$ , at  $B$  of sufficient magnitude to make the net deflection of point  $B$  from the tangent at  $A$  equal to zero. The deflection of the cantilever due to the uniformly distributed load would be equal to  $wL^4/8 EI$ ,<sup>1</sup> and that due to  $V_b$ , were it to act upward as shown, would be  $V_b L^3/3 EI$ . Therefore we may write as

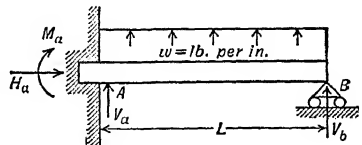


FIG. 13 : 2

<sup>1</sup> For the deflection formulas used in this discussion see Table 4 : 1.

an "equation of deformation"

$$\frac{wL^4}{8EI} + \frac{V_b L^3}{3EI} = 0$$

whence

$$V_b = -\frac{3wL}{8}$$

When  $V_b$  has been thus evaluated the equations of equilibrium may be applied and the other external forces found as follows:

$$\Sigma V = 0 = V_a + wL - \frac{3wL}{8} \quad V_a = -\frac{5wL}{8}$$

$$\Sigma H = 0 = H_a \quad H_a = 0$$

$$\Sigma M = 0 = \frac{wL^2}{2} - \frac{3wL^2}{8} - M_a \quad M_a = \frac{wL^2}{8}$$

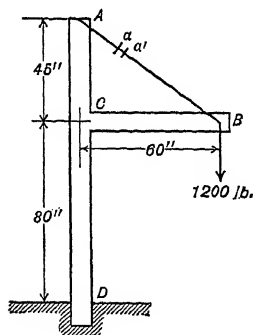
If it had been assumed that the external loading had caused support  $B$  to deflect some amount,  $\delta_b$ , normal to the tangent at  $A$ , the procedure would have been the same except that the right-hand side of equation  $a$  would have been  $\delta_b$  instead of zero.

The same problem can also be solved by considering the beam to be simply supported at  $A$  and  $B$  and subjected to a redundant moment  $M_a$ , at  $A$ , of the magnitude required to make the net slope at  $A$  equal to zero. In this case the slope at  $A$  due to the distributed load will be  $wL^3/24EI$ , and that due to the moment will be  $-M_a L/3EI$ . The deformation equation is then

$$\frac{wL^3}{24EI} - \frac{M_a L}{3EI} = 0$$

whence

$$M_a = \frac{wL^2}{8}$$



For  $A$  and  $I$  of members, see  
Table 13:1

FIG. 13:3

If the equations of equilibrium are now applied the same values will be obtained for  $V_a$ ,  $V_b$ , and  $H_a$  as before.

The same basic method is applicable when the structure is redundant to the first degree with respect to the internal forces. Consider, for example, the structure shown in Fig. 13:3. If the wire  $AB$  were cut this structure would be statically determinate and the relative move-

ment apart of the two faces of the cut,  $a$  and  $a'$ , could be obtained by the method of virtual work from the formula

$$\delta_{ao} = \sum \frac{p_a P_0 L}{AE} + \int \frac{m_a M_0 dx}{EI} \quad b^1$$

in which  $\delta_{ao}$  = deflection of  $a$  with respect to  $a'$  due to the external loads.

$p_a$  = axial load in a member due to equal and opposite unit loads applied at  $a$  and  $a'$ .

$m_a$  = bending moment due to equal and opposite unit loads at  $a$  and  $a'$ .

$P_0$  = axial load due to the external loads on the structure.

$M_0$  = bending moment due to external loads on the structure.

$L$ ,  $A$ ,  $E$ , and  $I$  have their usual significance.

The computations of  $\delta_{ao}$  for this structure from Eq.  $b$  are recorded in Table 13 : 1, from which  $E\delta_{ao} = -10,368,000$ . The minus sign in connection with the assumed directions for the unit loads indicates that the distance  $AB$  would be increased by the application of the 1,200-lb. load at  $B$ .

Consider now the effect on the relative movement of  $a$  and  $a'$  of applying 1 lb. of tension at each of those points. The resultant relative movement of the two points will then be

$$\delta_{aa} = \sum \frac{p_a^2 L}{AE} + \int \frac{m_a^2 dx}{EI} \quad c$$

The numerical value of  $\delta_{aa}$  is also computed in Table 13 : 1 and is found to be  $11,390/E$ . Here the plus sign indicates that the distance  $AB$  would be decreased.

If the statically determinate structure obtained by cutting  $AB$  is to have the same distribution of forces as the actual redundant structure, the tensions imposed at  $a$  and  $a'$  must be just sufficient to bring those points again into contact, i.e., to make their net relative deflection equal to zero. Thus we have as a deformation equation, by applying the principle of superposition,

$$-\frac{10,368,000}{E} + \frac{11,390 P_{ab}}{E} = 0$$

whence

$$P_{ab} = 910 \text{ lb.} \quad d$$

The remaining unknowns can now be found by applying the equations of equilibrium from which  $P_{ac} = -546 \text{ lb.}$ ,  $P_{bc} = -728 \text{ lb.}$ ,

<sup>1</sup> See Art. 12 : 12.

$S_{ac} = 728$  lb.,  $S_{bc} = 1,200 - 546 = 654$  lb.,  $M_{ca} = 728 \times 45 = 32,760$  in.-lb., and  $M_{cb} = 654 \times 60 = 39,240$  in.-lb. These values of  $M_{ca}$  and  $M_{cb}$  when added amount to 72,000 in.-lb., which is the moment in  $CD$  as found from applying the conditions of equilibrium to the whole structure.

The same results can be obtained by assuming that, instead of cutting the member  $AB$ , the member  $CB$  is attached to  $AD$  at  $C$  by a frictionless pin, and computing the moments to be applied at  $C$  to  $CA$  and  $CB$  to make the net change in the angle between those members equal to zero.

TABLE 13 : 1  
SOLUTION OF SINGLY REDUNDANT STRUCTURE

Member	$AB$	$AC$	$BC$	$CD$	Total
Length, $L$ in.	75	45	60	80	
Area, $A$ sq. in.	0.02	2.5	2.0	2.5	
$I$ , in. <sup>4</sup>	0	8.0	5.0	8.0	
$P_0$	0	0	0	-1,200	
$M_0$	0	0	-1,200 $x$	-72,000	
Origin at	.....	$A$	$B$	$C$	
$p_a$	+1.00	-0.60	-0.80	0	
$m_a$	0	-0.80 $x$	+0.60 $x$	0	
$p_a P_0 L / A$	0	0	0	0	0
$m_a M_0 / I$	0	0	-144 $x^2$	0	
$\int \frac{m_a M_0 dx}{1,000 I}$	0	0	-10,368	0	-10,368
$p_a^2 L^3 / A$	3,750	6.48	19.2	0	3,776
$m_a^2 / I$	0	0.080 $x^2$	0.072 $x^2$	0	
$\int m_a^2 dx / I$	0	2,430	5,184	0	7,614

**13 : 5. Multipli-Redundant Structures** — The same method can be extended to structures with more than one redundant. Take for example the beam of Fig. 13 : 4, subjected to a uniformly distributed load of

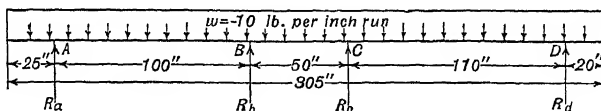


FIG. 13 : 4

— 10 lb. per in. and supported at four points. For simplicity the supports will be assumed stationary under load, and  $EI$  will be considered constant.

Assume that this beam is supported at  $A$  and  $D$  only. Then taking

# MULTIPLY-REDUNDANT STRUCTURES

moments about  $D$

$$R_a \times 260 - 10 \times 305 \times 132.5 = 0$$

whence  $R_a = 1,555$  lb. and  $R_d = 3,050 - 1,555 = 1,495$  lb.

$$S_{-a} = -10 \times 25 = -250 \text{ lb.}$$

$$S_{+a} = -250 + 1,555 = +1,305 \text{ lb.}$$

$$M_a = -250 \times 12.5 = -3,125 \text{ in.-lb.}$$

From Case 11, Table 4 : 1

$$EI\delta = x(x-L) \left[ \frac{M_a}{2} + \frac{S_{+a}}{6}(x+L) + \frac{w}{24}(x^2 + xL + L^2) \right]$$

$$EI\delta_{bo} = 100 \times (-160) \left[ -\frac{3,125}{2} + \frac{1,305}{6} \times 360 - \frac{10}{24}(100^2 + 100 \times 260 + 260^2) \right]$$

$$\delta_{bo} = \frac{537,128,000}{EI}$$

$$EI\delta_{co} = 150 \times (-110) \left[ -\frac{3,125}{2} + \frac{1,305}{6} \times 410 - \frac{10}{24}(150^2 + 150 \times 260 + 260^2) \right]$$

$$\delta_{co} = -\frac{558,032,000}{EI}$$

In these computations,  $\delta_{bo}$  and  $\delta_{co}$  are the deflections of  $B$  and  $C$  that would result from the application of the known distributed load if the supports at those points were absent. In the same way  $\delta_{bb}$  and  $\delta_{cb}$  will be the deflections of  $B$  and  $C$  due to a unit load at  $B$ , while  $\delta_{bc}$  and  $\delta_{cc}$  will be the deflections due to a unit load at  $C$ .

Assume the beam supported at  $A$  and  $D$  to be subjected to a unit load acting upward at  $B$ . The deflections  $\delta_{bb}$  and  $\delta_{cb}$  can then be obtained from the formula of Case 7, Table 4 : 1.

$$EI\delta = Wa(L-x) \frac{2Lx - a^2 - x^2}{6L}$$

$$EI\delta_{bb} = 100 \times 160 \frac{2 \times 260 \times 100 - 2 \times 100^2}{6 \times 260}$$

$$\delta_{bb} = \frac{328,000}{EI}$$

$$EI\delta_{cb} = 100 \times 110 \frac{2 \times 260 \times 150 - 100^2 - 150^2}{6 \times 260}$$

$$\delta_{cb} = \frac{321,000}{EI}$$



The deflections  $\delta_{bc}$  and  $\delta_{cb}$  can be computed from the effect of a unit load acting upward at  $C$ .

By the principle of reciprocal deflections,

$$\delta_{bc} = \delta_{cb} = \frac{321,000}{EI}$$

$$EI\delta_{cc} = 150 \times 110^2 \times 260 \times 150 - 2 \times 150^2$$

$$\delta_{cc} = \frac{349,000}{EI}$$

There being no net deflection of points  $B$  and  $C$ , we may write the following equations of the type of 13 : 1

$$\begin{aligned}\delta_{bo} + R_b\delta_{bb} + R_c\delta_{bc} &= 0 \\ \delta_{co} + R_b\delta_{cb} + R_c\delta_{cc} &= 0\end{aligned}$$

Substituting the numerical values and multiplying all terms by  $EI/1,000$

$$\begin{aligned}-537,128 + 328 R_b + 321 R_c &= 0 \\ -558,032 + 321 R_b + 349 R_c &= 0\end{aligned}$$

Whence  $R_b = +727.5 \text{ lb}$  and  $R_c = +929.9 \text{ lb}$ .

Considering the beam supported at  $A$  and  $D$  under the originally specified known external loading and the reactions just computed acting together, and taking moments about  $D$

$$R_a \times 260 + 727.5 \times 160 + 929.9 \times 110 - 10 \times 305 \times 132.5 = 0$$

Whence  $R_a = +713.2 \text{ lb}$ .

and  $R_d = 3,050 - (713.2 + 727.5 + 929.9) = 679.4 \text{ lb}$ .

The reactions having been obtained in this manner, the shears and bending moments can be computed as usual for the entire beam.

**13 : 6. The Statically Determinate Included Structure** — In each of the above examples the first step was to define a statically determinate structure by the removal of sufficient parts to make the number of independent unknowns equal to the number of independent equations derivable from the conditions of equilibrium. This procedure is practicable for any redundant structure. For structures statically indeterminate with respect to the outer forces, it would involve one or both of the following operations: complete removal of certain supports, or modification of the structure at certain supports so that the directions or points of application of the reactions would be fixed instead of

unknown. The second of these operations includes any modification fixing a definite relationship between the components of the reactions affected or a modification that prevents moments being developed as part of the reactions. In general these operations either reduce the number of unknowns directly or provide additional "equations of condition" and thus reduce the degree of redundancy. Structures statically indeterminate with respect to the inner forces can similarly be made determinate by the omission or cutting of members, or the fixation, by means of pinned connections, of the relations between the bending moments at the ends of certain members and the axial loads in them. Usually the pins are assumed to be placed on the axes of the members, so the end moments will be zero. The structure remaining after the changes that are necessary to make the number of unknowns equal to the independent equations of equilibrium have been made may be called the "included statically determinate structure" or more briefly the "included determinate structure."

Usually there are a number of alternative included statically determinate systems in any redundant structure, but the final results will be the same whichever system is used in the stress and deflection computations. The computer tries to select the one for which the numerical work will be the least tedious and, if possible, that on which the effect of the unknown external loads will be a minimum. Care must be taken, however, that the included structure selected for the computations is truly statically determinate, as it is easy to try to use one, part of which is unstable and part indeterminate.

**13 : 7. General Statement of the Maxwell-Mohr Method**—As each part was removed from the redundant structure to obtain the included determinate one, it was assumed to be replaced by an unknown external load acting on the remaining structure, identical in magnitude and distribution with that previously exerted by the part removed. The load distribution in, and hence the deformations of, the included determinate structure so loaded would be identical with those of the original redundant structure. The computer thus obtains a statically determinate structure, but one subjected to loads of unknown as well as loads of known magnitude. This process of defining the included determinate structure may also be described as the selection of the unknown (or unknowns) to be considered redundant.

From the definitions of the problems, the resultant movement of the point of application of each of the unknowns selected as redundant was known. In the above examples it was known to be zero, but that was not essential. Therefore it was possible to apply the principle of superposition and write a deformation equation of the type of Eq.

13 : 1, for the point of application of each redundant force. By this means sufficient additional independent equations were obtained to make the solution possible. In the above examples the deformation equations were first solved by themselves and the results substituted in the equations of equilibrium which were then solved simultaneously. Sometimes it may be more convenient to combine the deformation and equilibrium equations and solve them as a single simultaneous group.

The Maxwell-Mohr method of solving redundant structures therefore consists essentially of substituting for the actual redundant structure a hypothetical included determinate structure, and applying the principle of superposition to write the deformation equations that must be satisfied if the two structures are to have the same deformations and stress distributions. The method can be applied only when the net deflections (or rotations) of a number of points on the redundant structure equal to the degree of redundancy are known, but this is true in nearly all practical problems.

The deformation equations used in applying the method are of the type illustrated by Eq. 13 : 1. Using this equation as a model, the computer can easily write a similar equation for either the rotation or deflection at any point on the structure and include terms for the effects of any number of unknown redundants.

In practice it will sometimes be found that it is more convenient to work with redundant couples and the rotations of their planes of application than with redundant forces and their points of application. In other cases it will be convenient to have the redundants include both forces and couples.

The distinctive feature of the general Maxwell-Mohr method as described here is that the terms of the deformation equations developed are the actual deflections or rotations of the points of application of the redundants. In some of its special applications and in some alternative methods of analysis these deflections and rotations do not appear directly in the computations.

**13 : 8. Redundant Structure with Axial Loads Only** — When a structure is composed of a number of members, each of which is subjected to axial loads only, it is often convenient to modify the typical deformation equation, 13 : 1, in such a way as to avoid computation of the actual values of  $\delta$  or  $E\delta$ . If we substitute Eq. 12 : 3 in Eq. 13 : 1 we get

$$= \sum \frac{p_a^2 L}{AE} \quad AE \quad \sum :$$

If we now write  $Q = L/AE$  for each member, this becomes

$$- X_c \Sigma p_a p_c Q + \dots \quad 13 : 3$$

Similar equations can be written for  $\delta_b$ ,  $\delta_c$ , etc., using 13 : 3 as a model.

These equations are most useful for the analysis of redundant space frames in which the members are assumed to be connected by frictionless pins. In many cases it is more convenient to consider that  $Q = L/A$  instead of  $L/AE$ ; then the left side of each deformation equation would be  $E\delta$  instead of  $\delta$ .

When the structure is assumed to be without initial stresses, and the redundant members are cut to obtain an included determinate structure, the net relative deflections of the two faces of each cut (i.e.,  $\delta_a$  of Eq. 13 : 3) will be zero. This method of analysis will be illustrated by applying it to the structure shown in Fig. 13 : 5.

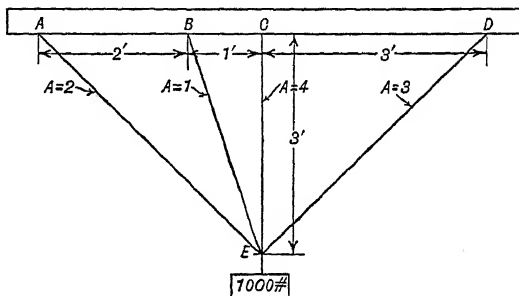


FIG. 13 : 5

This figure shows a weight of 1,000 lb. suspended from four wires,  $AE$ ,  $BE$ ,  $CE$ , and  $DE$ , the cross-sectional areas of which are in the ratios, 2, 1, 4, 3, respectively. It is desired to find the load in each wire.

As all four wires meet at  $E$ , lie in the same plane, and carry only axial load, there are four unknowns but only two available equations of equilibrium. There are thus two redundancies, or the structure is statically indeterminate in the second degree. It can also be seen that any two of the wires might be considered as the included determinate structure, since any other pair might be removed and the structure would still retain its stability. (This is not strictly true if wires are used, but would be if members capable of carrying compression were substituted.)

The first step is to determine which of the members shall be considered redundant. Any two may be chosen, and as they illustrate the problem best we will assume  $CE$  and  $DE$  to be redundant while  $AE$  and  $BE$  form the included determinate structure. Next determine the loads in the included determinate structure caused by the load of 1,000 lb. and by unit tensions in the redundant members.

Under the load of 1,000 lb.

$$\begin{aligned}\Sigma V &= 0 & 0.707 P_a + 0.949 P_b &= 1,000 \\ \Sigma H &= 0 & 0.707 P_a + 0.316 P_b &= 0 \\ & & P_a + 1.342 P_b &= 1,414.2 \\ & & -P_a - 0.447 P_b &= 0 \\ & & 0.895 P_b &= 1,414.2 \\ & & P_b &= +1581 \text{ lb. } P_a = -707 \text{ lb.}\end{aligned}$$

Under a load of 1 lb. tension in  $CE$

$$P_a = +0.707 \text{ lb. } P_b = -1.581 \text{ lb.}$$

Under a load of 1 lb. tension in  $DE$

$$\begin{aligned}\Sigma V &= 0 & 0.707 P_a + 0.949 P_b &= -0.707 \\ \Sigma H &= 0 & 0.707 P_a + 0.316 P_b &= +0.707 \\ & & +0.633 P_b &= -1.414 \\ & & P_b &= -2.236 \text{ lb. } P_a = +2.000 \text{ lb.}\end{aligned}$$

The values of  $Q$  are then obtained for all four members. In this case, the areas being given in terms of  $A_b$ , the area of member  $BE$ , and  $E$  being assumed a constant, it will save labor if  $Q$  is expressed in terms  $/A_b E$ . Then

$$Q_a \quad 4.2426 = 2.1213 \quad Q_b = 3.1623$$

$$Q_c = \quad = 0.7500$$

These quantities and the computations of the terms to be substituted in the equations of the type of 13 : 3 are given in Table 13 : 2.

TABLE 13 : 2

Member	$Q$	$P_0$	$p_c$	$p_d$	$P_0 p_c Q$	$P_0 p_d Q$	$p_c p_d Q$	$p_c^2 Q$	$p_d^2 Q$
$AE$	2.1213	-707	+0.707	+2.000	-1060	-3000	+3.000	+1.060	+8.485
$BE$	3.1623	+1581	-1.581	-2.236	-7904	-11179	+11.179	+7.904	+15.811
$CE$	0.7500	0	+1.000	0	0	0	0	+0.750	0
$DE$	1.4142	0	0	+1.000	0	0	0	0	+1.414
Sum					-8964	-14179	+14.179	+9.714	+25.710

Substituting in equations of the type of 13 : 3

$$-8,964 + 9.714 X_c + 14.179 X_d = 0$$

$$-14,179 + 14.179 X_c + 25.710 X_d = 0$$

$$X_c + 1.460 X_d = +922.8$$

$$-X_c - 1.813 X_d = -1000.0$$

$$- 0.354 X_d = -77.2$$

$$\text{Load in } DE = X_d = +218.2 \text{ lb.}$$

$$\text{Load in } CE = X_c = +604.3 \text{ lb.}$$

$$\text{Load in } AE = -707 + 0.707 \times 604.3 + 2.000 \times 218.2 = +156.7 \text{ lb.}$$

$$\text{Load in } BE = +1581 - 1.581 \times 604.3 - 2.236 \times 218.2 = +137.6 \text{ lb.}$$

This method is much more tedious for the structure used for illustrative purposes than the method of least work described below, but is much easier to apply for the solution of more complex structures. Its chief defect is that it is not suitable for structures including members subjected to bending or torsion unless the formulas are modified, and frequently the modifications involved are too complex to be practical.

**13 : 9. Initial Stresses in Trusses** — If a statically determinate pin-jointed truss were subjected to no external loads there would be no internal stresses in its members other than those caused by the dead weight. This can be proved by trying to compute the stresses in any such truss. When external forces are absent, the equations of equilibrium will show that the internal forces are all zero.

A statically indeterminate pin-jointed truss, however, may have loads in its various members even though it is subjected to no external loads. The nature of these loads can best be explained if we consider the indeterminate truss as built up by the addition of redundant members to an original determinate truss. If the lengths of the redundant members are just equal to the distances between the pins on the original truss to which they are connected, they can be inserted without subjecting the original truss or the redundant members to any loads. If any of the redundant members are not of just the right length, both they and the original truss must be deformed to permit their insertion. This will cause the redundant truss to be subjected to "initial stresses."

Suppose, for example, that the length of a redundant member  $AB$  is less than the distance between joints  $A$  and  $B$  of the original truss by an amount  $\delta$ , which may be called the "initial deformation" for member  $AB$ . If one end of the redundant member is connected to joint  $B$  of the truss, the other end will fall short of joint  $A$  by the distance  $\delta$ . Equal and opposite forces must therefore be applied to the free end of the redundant member and to joint  $A$ , of sufficient magnitude to give

them a relative deflection equal to  $\delta$ , before the connection at  $A$  can be made. After the connection is made the internal stresses produced in this operation will remain in the structure as initial stresses.

In applying Eq. 13 : 3 to the solution of the example of Art. 13 : 8 it was assumed that there were no initial stresses, and so it was proper to write the deformation equations with the net deflections equal to zero. This procedure is correct only when no initial deformations were necessary to insert the redundant members. If such initial deformations existed, it would be necessary to equate the sum of the relative deflections due to the known external loads and those due to the loads on the cut faces (the loads in the redundant members) to the various initial deformations. The deformation equations for a truss with initial deformations and stresses are therefore of the type of 13 : 3 with the initial deformations for the redundant members in which the loads are  $X_a$ ,  $X_b$ ,  $X_c$ , etc., used as the values of  $\delta_a$ ,  $\delta_b$ ,  $\delta_c$ , etc., respectively.

The loads in the redundant members could be divided into two parts, the initial loads producing the deformations  $\delta$ , and the subsequent loads induced by the known external loads. The initial loads for any given set of values of  $\delta$  could be obtained from deformation equations of the type of 13 : 3 with the  $\Sigma p P_0 Q$  terms omitted. The subsequent loads would then be obtainable from the complete equations of the type of 13 : 3 with the values of  $\delta$  all assumed equal to zero. As the principle of superposition applies, however, the net loads in the redundant members can be obtained in a single operation using all terms of the equations of the type of 13 : 3 as well as values of  $\delta$  equal to the initial deformations. If the initial deformations are due to the redundant members being too short, they will cause tensions in those members and the values of  $\delta$  should be considered positive, and vice versa.

It might be thought that if the initial deformations were known or assumed the initial stresses in the redundant members could be computed very simply by calculating the loads required to change the length of each redundant member an amount equal to the corresponding initial deformation. This would not give the correct result because  $\delta$  is the relative deflection of the cut faces, or of the end of the member and the joint to which it is to be attached. Only a part of this deflection is due to change in length of the redundant member, the remainder being due to changes in length of members of the original truss and to changes in length of any other redundant members.

When the effects of initial deformations are being determined, the computer cannot use values of  $Q$  in terms of  $EA$  or  $E$  as was done in the example of Art. 13 : 8 unless he substitutes values of  $EA\delta$  or  $E\delta$  for  $\delta$  in the formulas of the type of 13 : 3. In many cases he will find





[illegible]

Whence

$$X_a = -1,339.1 \text{ lb.} \quad X_b = -1,006.4 \text{ lb.} \quad X_c = -1,016.6 \text{ lb.}$$

All these are purely hypothetical loads as the members are wires and cannot carry compression. What these figures really indicate is that all three wires would be out of action, as would be expected since they were assumed to be subjected to no initial stress.

If each wire is assumed to have been originally stressed due to initial deformations of 0.1 in., the formulas would be

$$\begin{aligned} 4,756,800 + 3,436.8 X_a + 153.6 X_b &= 3,000,000 \\ 3,820,800 + 153.6 X_a + 3,436.8 X_b + 153.6 X_c &= 3,000,000 \\ 4,812,800 &+ 153.6 X_b + 4,582.4 X_c = 3,000,000 \end{aligned}$$

Whence

$$X_a = -502 \text{ lb.} \quad X_b = -199 \text{ lb.} \quad X_c = -389 \text{ lb.}$$

Comparison of the results shows that the redundant members would not have dropped out so soon in the second as in the first case. It may be necessary, however, to determine at what percentages of the total external loads the various redundant wires would go out of action. If  $k$  is the percentage of the external load in action at any moment, the above equations can be written

$$\begin{aligned} 4,756,800 k + 3,436.8 X_a + 153.6 X_b &= 3,000,000 \\ 3,820,800 k + 153.6 X_a + 3,436.8 X_b + 153.6 X_c &= 3,000,000 \\ 4,812,800 k &+ 153.6 X_b + 4,582.4 X_c = 3,000,000 \end{aligned}$$

Whence

$$\begin{aligned} X_a &= 836.8 - 1,339.1 k \\ X_b &= 807.4 - 1,006.4 k \\ X_c &= 627.6 - 1,016.6 k \end{aligned}$$

in which the constant is the initial tension in the wire and the  $k$  term the effect of the external loads.

From the above values of  $X_a$ , it appears that  $AG$  would go out of action when  $k = 836.8/1,339.1 = 0.625$ . Similarly  $X_b$  would become zero, indicating that member  $BH$  was on the point of becoming inactive when  $k = 807.4/1,006.4 = 0.802$ . The critical point for member  $CK$  would be that when  $k = 627.6/1,016.6 = 0.617$ . The lowest of these values is that for  $CK$ , showing that it would be the first of the three wires to go out of action.

When  $CK$  has gone out of action, the structure becomes indeterminate in only the second degree, and to determine stresses when  $k$  is a little

larger than 0.617, the equations must be modified by dropping out all terms referring to  $CK$ . The equations then become

$$\begin{aligned} 4,756,800 k + 3,436.8 X_a + 153.6 X_b &= 3,000,000 \\ 3,820,800 k + 153.6 X_a + 3,436.8 X_b &= 3,000,000 \end{aligned}$$

Whence

$$X_a = 835.6 - 1,337.1 k \quad \text{and} \quad X_b = 835.2 - 1,051.2 k$$

These expressions for  $X_a$  and  $X_b$  differ from those computed first, but give the same values when  $k = 0.617$ . They indicate that member  $AG$  would go out of action when  $k = 835.6/1,337.1 = 0.625$  and that  $BH$  would drop out when  $k = 835.2/1,051.2 = 0.795$ .

When  $AG$  has gone out of action,  $BH$  is the only redundant wire remaining in action, and the load in it can be determined from

$$3,820,800 k + 3,436.8 X_b = 3,000,000$$

whence

$$X_b = 872.9 - 1,111.7 k$$

This member would go out of action when  $k = 872.9/1,111.7 = 0.802$ .

It happens that, in this case, the complete computations show that the redundant wires all go out of action at the percentages of full load indicated in the first computation. This is due to the fact that these values of  $k$  were computed to only three significant figures, and that there was not much spread between the values of  $k$  at which the wires went out of action. It could not be counted on to happen generally, though the error in assuming that the various wires would go out of action at the percentages of the total load indicated from the computations based on all redundant wires being in action is not likely to be large in any practical case. It is much less likely to be serious than errors in the assumed values of the initial deformations.

**13 : 11. The Method of Least Work. General Statement** — In Art. 12 : 17 the validity of Castigliano's first theorem was established, namely, that the deflection of any point due to the imposition of a closed system of forces on a structure is equal to the derivative of the internal work done by the application of those forces with respect to an external force acting at the point in the direction of that deflection. In the great majority of redundant structures analyzed in practice the net deflections of the points of application of the redundants are, or are assumed to be, equal to zero. For such structures, therefore, the equations of the type of 13 : 1 may be replaced by

$$\frac{\partial U}{\partial X_a} = 0; \quad \frac{\partial U}{\partial X_b} = 0; \quad \text{etc.} \qquad 13 : 4$$

where  $U$  is the total internal work and  $X_a, X_b, \dots$  the various redundants.

As  $U$  is a function of the independent variables,  $X_a, X_b, \dots$  and its partial derivatives with respect to all these variables are equal to zero, Eq. 13 : 4 indicate that the redundant forces will be of such magnitudes, consistent with the conditions of equilibrium, that the energy transfer resulting from applying the external loads to the structure will be a minimum. From this fact, known as Castigliano's second theorem, the use of equations of the type of 13 : 4 as the deformation equations in solving redundant structures is known as the method of least work.

For many structures the computations carried out in applying the method of least work are identical with those used in applying the Maxwell-Mohr method. There are some types of structure, however, for which the computations are considerably simplified by using Eq. 13 : 4 instead of 13 : 1. The equations of the type of 13 : 3 can be derived equally well from either 13 : 1 or 13 : 4.

The first step in the practical application of the method of least work is to write down all the independent equations representing relations between the forces in the structure that can be obtained by applying the conditions of equilibrium,  $\Sigma M = 0$ , etc. The structure being indeterminate to the  $n$ th degree, there will be  $n$  more unknowns appearing in the equations thus obtained than there are equations.

There will also be several groups of  $n$  unknowns which might be simultaneously equal to zero without affecting the stability of the structure. One of these groups should be chosen and the values of all stresses in the structure determined in terms of the  $n$  unknowns. This is done by solving in the usual manner the simultaneous equations already obtained. The work done in all the members of the structure is now expressed in terms of the  $n$  unknowns and differentiated with respect to each unknown in turn, all unknowns except the one with respect to which the differentiation is being performed being treated as constants. Setting each of the  $n$  partial derivatives equal to zero produces  $n$  new independent equations which can be solved in the usual manner. All the unknowns can then be evaluated.

This method of solution will be illustrated by the example of Art. 13 : 8. Writing down the two available equations of equilibrium, we have

$$\begin{array}{ll} \Sigma V = 0 & V_a + V_b + V_c + V_d - 1,000 = 0 \quad a \\ \Sigma H = 0 & H_a + H_b - H_c - H_d = 0 \quad b \end{array}$$

where  $V_a$  and  $H_a$  are the vertical and horizontal components of the load in  $AE$ , and so on for the other members.

Expressing these equations in terms of the direct loads  $P_a$ ,  $P_b$ , etc.,

$$0.707 P_a + 0.949 P_b + 1.000 P_c + 0.707 P_d = 1,000 \quad c$$

$$0.707 P_a + 0.316 P_b - 0.707 P_d = 0 \quad d$$

From  $d$ ,  $P_a = P_d - 0.447 P_b$

Substituting this value of  $P_a$  in  $c$  and solving for  $P_c$ ,

$$P_c = 1,000 - 1.414 P_d - 0.633 P_b$$

The four forces being known in terms of two of them, the expression for the internal work done can be written. For the structure in question, this expression will be

$$\begin{aligned} & \frac{P_a^2 L_a}{2 A_a E} + \frac{P_b^2 L_b}{2 A_b E} + \frac{P_c^2 L_c}{2 \times 4 A_b E} + \frac{P_d^2 L_d}{2 \times 3 A_b E} \\ &= \frac{4.2426 P_a^2}{2 \times 2 A_b E} + \frac{3.1623 P_b^2}{2 A_b E} + \frac{3.0000 P_c^2}{2 \times 4 A_b E} + \frac{4.2426 P_d^2}{2 \times 3 A_b E} \\ & (1.0607 P_a^2 + 1.5812 P_b^2 + 0.3750 P_c^2 + 0.7071 P_d^2) \quad e \end{aligned}$$

Substituting the values of  $P_a$  and  $P_c$  in terms of  $P_b$  and  $P_d$ ,

$$\begin{aligned} U &= \frac{1}{2 A_b E} (P_d - 0.447 P_b)^2 + 1.5812 P_b^2 + 0.3750 \\ & (1,000 - 1.414 P_d - 0.633 P_b)^2 + 0.7071 P_d^2 \quad f \end{aligned}$$

Differentiating  $U$  with respect to  $P_b$  and  $P_d$  in turn and setting the partial derivatives equal to zero we obtain

$$\begin{aligned} \frac{\partial U}{\partial P_b} = 0 &= \frac{1}{A_b E} [1.0607 \times 2 (-0.447) (P_d - 0.447 P_b) + 2 \times 1.5812 P_b \\ & + 0.3750 \times 2 (-0.633) (1,000 - 1.414 P_d - 0.633 P_b)] \quad g \end{aligned}$$

$$\begin{aligned} \frac{\partial U}{\partial P_d} = 0 &= \frac{1}{A_b E} [1.0607 \times 2 (P_d - 0.447 P_b) + 0.3750 \times 2 (-1.414) \\ & (1,000 - 1.414 P_d - 0.633 P_b) + 2 \times 0.7071 P_d] \quad h \end{aligned}$$

Simplifying Eq.  $g$  and  $h$

$$\begin{aligned} -0.4744 P_d + 0.2122 P_b + 1.5812 P_b - 237.2 + 0.3355 P_d \\ + 0.1500 P_b = 0 \quad a' \end{aligned}$$

$$1.0607 P_d - 0.4744 P_b - 530.3 + 0.7500 P_d + 0.3355 P_b + 0.7071 P_d = 0 \quad h'$$

$$\begin{aligned} 1.9434 P_b - 0.1189 P_d &= 237.2 \\ -0.1389 P_b + 2.5178 P_d &= 530.3 \\ P_b - 0.0715 P_d &= 122.1 \\ -P_b + 18.1267 P_d &= 3,818.2 \\ 18.0552 P_d &= 3,940.3 \\ P_d &= 218.2 \text{ lb.} \\ P_b &= 137.7 \text{ lb.} \end{aligned}$$

Substituting these values of  $P_b$  and  $P_d$  in the expressions for  $P_a$  and  $P_c$ ,

$$\begin{aligned} P_a &= 218.2 - 61.6 = 156.6 \text{ lb.} \\ P_c &= 1,000 - 87.1 - 308.6 = 604.3 \text{ lb.} \end{aligned}$$

These values should be checked by substituting them in the original Eq.  $c$  and  $d$ , which become

$$\begin{aligned} 110.7 + 130.6 + 604.3 + 154.3 - 1,000 &= -0.1 \text{ instead of zero} \\ 110.7 + 43.5 - 154.3 &= -0.1 \text{ instead of zero} \end{aligned}$$

The check is not exact but is close enough for any practical purposes. Such a check is always advisable as it shows that the system of forces found satisfies the conditions of statics. It is not, however, a positive check because any pair of values for  $P_b$  and  $P_d$ , if substituted in the expressions for  $P_a$  and  $P_c$ , would give a set of values that would satisfy it. Great care should therefore be taken that the expression for the internal work is correct and that no errors are made in the differentiation or in solving the equations obtained by that operation.

It should be noted that the results of the above computation check those of Art. 13 : 8, in which the same structure was analyzed, with a maximum deviation of only 0.1 lb.

**13 : 12. Alternative Method of Computing Partial Derivatives —** The method of solution illustrated above becomes excessively tedious and liable to error if there are many members in the structure. A simplification that is extremely useful for a moderate number of members subjected to axial loads and even more useful when bending is present is the application of the relation

$$\frac{du}{dx} = \frac{du}{dy} \cdot \frac{dy}{dx}$$

If this relationship is borne in mind it is not necessary to write the work expression exclusively in terms of the unknowns with respect to which it is to be differentiated, as in Eq.  $f$ , but the differentiations can

be made at the stage of Eq. *e*. Using this shortcut, the computations down to and including Eq. *e* would be the same as before.

$$U = \frac{1}{A_b E} (1.0607 P_a^2 + 1.5812 P_b^2 + 0.3750 P_c^2 + 0.7071 P_d^2)$$

Differentiating with respect to  $P_b$  and  $P_d$

$$\frac{\partial U}{\partial P_b} = \frac{1}{A_b E} \left[ 2 \times 1.0607 P_a \frac{\partial P_a}{\partial P_b} + 2 \times 1.5812 P_b + 2 \times 0.3750 P_c \frac{\partial P_c}{\partial P_b} \right] = 0 \quad g''$$

$$\frac{\partial U}{\partial P_d} = \frac{1}{A_b E} \left[ 2 \times 1.0607 P_a \frac{\partial P_a}{\partial P_d} + 2 \times 0.3750 P_c \frac{\partial P_c}{\partial P_d} + 2 \times 0.7071 P_d \right] = 0 \quad h''$$

Eliminating the term  $2/(A_b E)$  which is common to both equations, and substituting the values of  $P_a$  and  $P_c$  and their derivatives with respect to  $P_b$  and  $P_d$ , we obtain from  $g''$  and  $h''$

$$1.0607 (-0.447) (P_d - 0.447 P_b) + 1.5812 P_b + 0.3750 (-0.633) (1,000 - 1.414 P_d - 0.633 P_b) = 0 \quad g'''$$

$$1.0607 (P_d - 0.447 P_b) + 0.3750 (-1.414) (1,000 - 1.414 P_d - 0.633 P_b) + 0.7071 P_d = 0 \quad h'''$$

These equations are evidently identical with  $g$  and  $h$ , and the remaining computations would be the same as before. In this illustration, this method of obtaining the partial derivatives of the internal work is no easier than the one first employed, but experience has shown that it makes the work much less tedious and much easier to check when the structure is more complex.

**13 : 13. Expressions for Internal Work**—The structure of the illustrative example above was one in which the only type of deformation to be considered was elongation. The internal work done could therefore be expressed by the equation

$$U = \sum \frac{P^2 L}{2 A E} \quad 13 : 5$$

In the general case of a structure subjected to bending, shear, and torsion, as well as axial load, the expression for the internal work becomes

$$U = \sum \frac{P^2 L}{2 A E} + \int \frac{M^2 dx}{2 E I} + \int \frac{k V^2 dx}{2 A G} + \int \frac{T}{2} d\phi \quad 13 : 6$$

in which the nomenclature is the same as in Eq. 12 : 9, Art. 12 : 12.

When the member is a round shaft or tube of metal the last term on the right-hand side of Eq. 13 : 6 becomes  $1.25 \int T^2 dx / 2 EI$ .

In applying Eq. 13 : 6 the integrations should extend over the entire structure. If  $M^2/EI$ ,  $kV^2/AG$ , or  $T d\phi$  cannot be represented as a single continuous function of  $x$ , the structure must be divided into a group of elements for each of which these quantities can be represented as a single continuous function of  $x$ . In such cases the integrations are made between the ends of each of these elements in the same general manner as when the method of virtual work is used to compute deflections.

It has previously been stated that the methods described in this chapter do not apply strictly to members subjected to combined axial and bending loads. This is not due to any lack of applicability of Eq. 13 : 6 to such members, but to the fact that the bending moments in such members are not directly proportional to the external loads on the structure, and the principle of superposition therefore does not apply. If, however, the axial load is tension or a compression that is small in comparison with the Euler load ( $\pi^2 EI/L^2$ ), the error involved in assuming the bending moments proportional to the external loads is small. With such members it is common practice to employ the method of least work as though it were strictly applicable.

When the bending moment in any member is a constant, the work due to bending in that member will be  $M^2 L / 2 EI$ . Similar changes can be made in the expressions for the work due to shear and torsion when  $V$  and  $T$  are constants.

A special case of varying bending moment that is often encountered is that in which the variation is uniform, there being no transverse load on the portion of the member being considered. For this,

$$\int_0^L \frac{M^2 dx}{EI} = \frac{L}{2 EI} \left( M_1^2 \pm LM_1 V + \frac{L^2 V^2}{3} \right) \quad 13 : 7$$

where  $M_1$  is the bending moment at one end and  $V$  is the shear on the member. (There being no transverse load, this is a constant.) The plus sign in the parenthesis is used when the shear tends to increase the bending moment as  $x$  increases; the minus sign, when it tends to decrease the moment.

Formula 13 : 7 can be applied to a member with concentrated side loads by dividing the member into sections between adjacent loads and applying it to each section. It cannot be applied to sections subjected to a distributed side load. In such cases the value of  $M$  expressed in terms of  $x$  must be substituted in Eq. 13 : 6.



For a simply supported beam without overhangs and subjected to a uniform load the internal work done is  $w^2 L^5 / 120 EI$ .

Though the internal work done by the axial load may be added to that due to bending to obtain the total work in a structure, the bending load cannot be divided into portions (such as a constant bending, a uniformly varying bending, and a bending due to a uniformly distributed load), the work done by each of these portions computed, and the results added to obtain the total work in bending, because  $(A + B)^2 = A^2 + 2AB + B^2$  not  $A^2 + B^2$ .

In many problems labor can be saved by differentiating the expression for total work (Eq. 13 : 6) with respect to each of the unknown redundant forces before integrating with respect to distance along the axes of the members.

In order to simplify the computations the internal work done as the result of relatively small deformations is usually neglected. This is particularly true of shear deformation, which is seldom taken into account. To a lesser extent it is true of elongation in structures in which the bending or torsional deformations are paramount.

**13 : 14. Numerical Example** — The application of the method of least work to a case involving members subjected to combined bending and compression can be illustrated by a numerical example. Figure

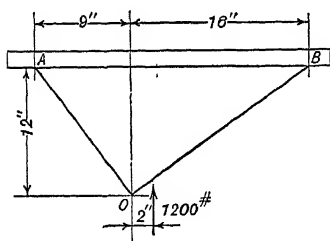


FIG. 13 : 7

13 : 7 shows a structure composed of two tubes  $OA$  and  $OB$  connected to a horizontal member  $AB$  and subjected to an upward load of 1,200 lb. acting 2 in. to the right of  $O$ . The problem is to determine the loads in  $OA$  and  $OB$ , neglecting the work done in  $AB$ , but assuming that the joints at  $A$  and  $B$  are capable of transmitting bending moment. This is a simplified case of the general chassis

analysis problem. The tubes are both of 1-in. outer diameter and 0.035-in. wall thickness, and the material is steel.

Seven external forces are acting on the structure: the vertical load of 1,200 lb., the axial loads  $P_a$  at  $A$  and  $P_b$  at  $B$ , the shear loads  $S_a$  at  $A$  and  $S_b$  at  $B$ , and the moments  $M_a$  at  $A$  and  $M_b$  at  $B$ .  $S$  is used here to designate the shear forces since they are not vertical, and it is desired to avoid having them confused with vertical forces. Figure 13 : 8 shows the forces at  $A$  and  $B$  in the directions in which they are assumed positive.

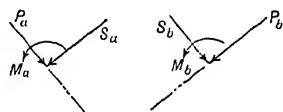


FIG. 13 : 8

Applying the conditions of equilibrium to the structure we obtain three equations:

$$\begin{aligned}\Sigma V &= 0; & 0.8 P_a + 0.6 S_a + 0.6 P_b + 0.8 S_b &= 1,200 \\ \Sigma H &= 0; & 0.6 P_a - 0.8 S_a - 0.8 P_b + 0.6 S_b &= 0 \\ \Sigma M &= 0; & 15.0 S_a - 20.0 S_b + M_a + M_b &= -2,400\end{aligned}$$

Whence

$$\begin{aligned}P_b &= -S_a + 720 \\ S_b &= -P_a + 960 \\ M_b &= -M_a - 15 S_a - 20 P_a + 16,800\end{aligned}$$

The expression for total work is

$$U = \Sigma \left[ \frac{P^2 L}{2 A E} + \frac{L}{2 E I} \left( M^2 + L M S + \frac{L^2 S^2}{3} \right) \right] \quad a$$

Substituting the numerical values for the specific problem

$$\begin{aligned}EU &= \frac{15 P_a^2}{2 \times 0.10611} + \frac{15}{2 \times 0.01237} \left[ M_a^2 + 15 M_a S_a + \frac{225 S_a^2}{3} \right] \\ &+ \frac{20 P_b^2}{2 \times 0.10611} + \frac{20}{2 \times 0.01237} \left[ M_b^2 - 20 M_b S_b + \frac{400 S_b^2}{3} \right] \\ EU &= 70.68 P_a^2 + 606.30 (M_a^2 + 15 M_a S_a + 75 S_a^2) + 94.24 P_b^2 \\ &+ 808.40 (M_b^2 - 20 M_b S_b + 133.33 S_b^2)\end{aligned}$$

As the values of the unknowns with the subscript  $b$  have already been determined in terms of those with the subscript  $a$ , we will differentiate the above work expression with respect to each of the latter and set the partial derivatives equal to zero, thus obtaining the three additional equations needed for the solution of the problem. It may be noted that in this case the expression being differentiated is that for  $EU$  rather than that for  $U$ , but as  $E$  is a constant, and as the partial derivatives are all to be assumed equal to zero, the resulting equations are the same as if  $E$  had been kept on the right side and canceled out after the differentiations had been made.

$$\begin{aligned}\frac{\partial EU}{\partial P_a} &= 2 \times 70.68 P_a + 808.40 (-20 \times 2 M_b + 20 \times 20 S_b \\ &+ 20 M_b - 2 \times 133.33 S_b) = 0\end{aligned}$$

$$\begin{aligned}\frac{\partial EU}{\partial S_a} &= 606.30 (15 M_a + 2 \times 75 S_a) - 2 \times 94.24 P_b \\ &+ 808.40 (-2 \times 15 M_b + 20 \times 15 S_b) = 0\end{aligned}$$

$$\frac{\partial EU}{\partial M_a} = 606.30 (2 M_a + 15 S_a) + 808.40 (-2 M_b + 20 S_b) = 0$$

$$\begin{array}{rcl}
 \text{Whence} & 70.68 P_a + 53,893 S_b - 8,084.0 M_b = 0 \\
 90,945.0 S_a + 9,094.5 M_a - 188.48 P_b + 242,520 S_b - 24,252.0 M_b = 0 \\
 9,094.5 S_a + 1,212.6 M_a & + & 16,168 S_b - 1.616.8 M
 \end{array}$$

Owing to the method of differentiation used, the unknowns with the subscript  $b$  have reappeared in these "deformation equations." One method of attack would be to combine these deformation equations with the three original equations of equilibrium and solve the resulting group of six simultaneous equations. A somewhat simpler procedure would be to substitute the values of  $P_b$ ,  $S_b$ , and  $M_b$  in terms of  $P_a$ ,  $S_a$ , and  $M_a$  already computed into the deformation equations, thus obtaining a group of only three simultaneous equations with three unknowns. In this particular example, it will be seen that as  $P_a$  and  $P_b$  appear in the deformation equations only once, and  $M_a$  only twice, the work would be simplified if the values of those three unknowns in terms of the other three were substituted. This is particularly advantageous on account of the simple relations that can be used. Making these substitutions, the deformation equations become:

$$\begin{array}{rcl}
 & 53,822.3 S_b - 8,084.0 M_b = & -67,852.8 \\
 -45,284.0 S_a + 424,410.0 S_b - 33,346.5 M_b = & +21,962,505.6 \\
 -9,094.5 S_a + 40,420.0 S_b - 2,829.4 M_b = & +2,910,240.0
 \end{array}$$

$$\begin{array}{rcl}
 \text{Whence} & S_a = & -131.8 \text{ lb.} \\
 & S_b = & 80.4 \text{ lb.} \\
 & M_b = & 543.8 \text{ in.-lb.}
 \end{array}$$

Substituting these values in the original equations of equilibrium,

$$\begin{array}{rcl}
 P_a = & 879.6 \text{ lb.} \\
 P_b = & 851.8 \text{ lb.} \\
 M_a = & 641.1 \text{ in.-lb.}
 \end{array}$$

The minus sign of  $S_a$  indicates that it acts in the direction opposite to that shown in Fig. 13 : 8. The plus sign of the other quantities indicate that they act in the directions shown in that figure.

With the components of the reactions at  $A$  and  $B$  known, the bending moment and shear at any point in  $OA$  and  $OB$  can be computed by the methods already discussed.

The computations required are usually very tedious, this example being a relatively simple one, and the method is often avoided for that reason. Nevertheless it is the most precise method available for many designs. The labor of computation varies with the number of redundant unknowns and is greatly decreased if certain of those unknowns can be given assumed values. In the above problem, for example, the work

of computation would have been greatly decreased if the moments at *A* and *B* had been assumed equal to zero, i.e., that the joints at these locations were pinned.

The above example also illustrates two weaknesses of the method of least work. Often, as in this case, the work done in the structure supporting that being investigated must be neglected either to reduce the labor of computation to a reasonable amount or because the design of that structure has not yet been made. This causes an error of unknown amount. The other weakness is that although the cross-sections of members at joints usually differ from those between joints it is customary to assume the members as of constant section and to extend from center-line intersection to center-line intersection.

It may also be noticed that the work done by the axial load was so small in comparison with that due to bending that the former could have been omitted from the total work expression without seriously affecting the results. In approximate and preliminary computations, much labor can often be saved if this practice is followed with members other than wires. Similarly in applying the Maxwell-Mohr method those portions of the deflections that are due to elongations of members also subjected to bending can often be neglected without serious loss of accuracy. This can be seen from a study of the computations of Art. 13 : 4.

**13 : 15. Value of the Maxwell-Mohr and Least-work Methods —** Although the computations involved in analyzing indeterminate structures by the methods discussed in this chapter are often very tedious, and it is hard to catch arithmetical errors except by independent checking, the computations are not at all difficult, unless the number of redundant quantities becomes excessive. In most airplane structures there are a large number of redundancies that would have to be considered if an exact analysis were attempted. Most of them have a negligible effect on the stress systems, however, and should be neglected. This is the more justified since an attempt to allow for all redundancies would not suffice for a precise analysis owing to inherent errors in the method. Among these inherent errors are: the basic formulas presuppose that the principle of superposition is applicable, though this is not true with respect to members subjected to combined axial and bending loads; the exact amounts of all the initial deformations in the structure can never be known and will usually differ between different articles of the same design; the cross-sections and moduli of elasticity of the members are never just what they are assumed to be in the computations; in practice it would be impossible to take account of all variations in cross-section affecting only a small portion of the length of the member

IISc Lib B'lore

629.1341 N43.2

II ■■■■■■■■■■■■■■■■■■

affected; it is impossible to determine the work done in complex connecting fittings with their complex and unknown stress distributions; and the supports are never fully rigid and the degree of rigidity attained by them can seldom be known. Finally, even though all the above defects could be overcome, the external loads are never known with complete accuracy, and it is useless to attempt to compute the internal loads to a greater degree of accuracy than that to which the external loads are known.

The existence of these defects in the methods for analyzing redundant structures does not mean that they are useless or that they should be superseded by arbitrary assumptions. It means only that they should be used with judgment, and their limitations recognized.

As a designer becomes more practiced in the use of these methods of analysis he will learn what redundancies can safely be left out of account in familiar types of structure. He will also learn how to avoid much work of detailed computation by neglecting such of the terms in the work expression as will have little influence on the final results. In addition he will be able to make much more reasonable arbitrary assumptions as to the magnitudes of the redundant unknowns than if he lacked this experience.

**13 : 16. Principle of Relative Rigidities** — Any redundant structure can be considered as a combination of included determinate structures, each of which carries a part of the total external load. If no part of the total structure is included in more than one such included structure, these included structures may be considered as independent of each other. In most cases, however, many parts of the total structure will be included in two or more of the included ones which thus become interdependent.

In order to satisfy the principle of consistent deformations the deflections of all points common to more than one of the included structures must be identical. Therefore the external loading will be divided between the included structures in such proportions that this will be the case. If we define the external load required to cause unit deflection of an included structure as the rigidity of that structure, the actual external load will be divided among the included structures in proportion to their rigidities. Thus if there are but two included structures and it requires twice as much load to deflect one a given amount as it does to deflect the other the same amount, the first structure will carry two-thirds, and the second one-third, of the total load.

This principle of relative rigidities can be used in practical quantitative computations only when there is but one external load and the included structures are independent of each other. Under other

conditions it is too difficult to develop quantitative measures of the rigidities of the included structures, though fairly satisfactory approximations can often be made. In any redundant structure, however, the principle applies to the extent that if any member is increased in stiffness or rigidity the distribution of stresses will be changed in such a manner that that member will be called upon to carry a larger load. Thus, if a member is found, as the result of a precise analysis, to be called on to carry a load say 10 per cent in excess of its strength, it will not be sufficient to increase the strength of that member by just 10 per cent. A larger increase is needed as the increased rigidity of the included structures of which that member is a portion will cause the load on the member to be increased. Sometimes the design can be made more satisfactory by decreasing the sizes of some overstrength members in the included structures that contain the weak member. By thus reducing the rigidity of these structures the load on the member may be brought down to its strength. If this is done, however, the loads in the other included structures will be increased. Although this principle of relative rigidities can seldom be applied to the quantitative solution of redundant structures, it is of great assistance when deciding on the changes to be made in a trial design that is not wholly satisfactory.

**13 : 17. Arrangement of Computations** — The labor involved in analyzing complex redundant structures can usually be greatly reduced if the computations are carried out in a systematic form. The suggested practice outlined below for organizing the computations by the method outlined in Art. 13 : 8 has been found by experience to be very helpful. It is taken from Air Corps Information Circular 495, "Application of the Method of Least Work to Redundant Structures," by C. J. Rowe, in which its use is illustrated by a numerical example.

(1) Show completely dimensioned line drawings of the framework to be analyzed.

(2) Tabulate the physical properties and directional components of the members in the framework and any others which will affect the stresses in these members.

(3) Make line drawings of the framework, showing the point of application and the magnitude and direction of all applied loads affecting the framework. Give the nomenclature to be used.

(4) Very carefully select the redundant members, trying to choose those which may go out of action.

(5) Write deformation equations of the type of 13 : 3 which will be equal in number to the number of redundant members.

(6) Make a line drawing to show the statically determinate structure obtained by temporarily removing the redundant members, and solve this structure for the stresses due to applied loads. These values should be tabulated under the heading  $P_0$ . Show, in the right or left margin of the page, which member is being solved for by the equation on that line.

(7) Show, by line drawings, that part of the framework affected by a unit load in each of the redundant members, and solve for the stresses due to this load. Tabulate these values under the heading  $p$  with subscripts designating the various redundant members.

(8) Tabulate the foregoing values and solve for the numerical values required in the deformation equations.

(9) Before solving the deformation equations, arrange the various terms so that those representing members which may be found to be out of action will appear either at the beginning or the end of the equations.

(10) Arrange the various equations in a series so that those composed entirely of functions of the loads in the doubtful members will appear at the beginning or end of the series.

(11) Tabulate and solve the equations according to some method such as is described below.

(12) Multiply the stresses in the various members, due to unit loads in the redundant members by the actual loads obtained in these members, and take the algebraic sum of these stresses together with those under the heading  $P_0$  and obtain the final stress in each member of the framework.

In the same report from which the above recommendations are quoted, Mr. Rowe gives the following suggestions regarding the solution of a number of simultaneous linear equations.

(a) Write the equations to be solved in tabular form, one line for each equation, and one column for each variable. It will save labor if the symbol for the variable ( $x$ ,  $y$ , etc.) is placed only at the head of the column, the coefficients alone appearing in the lines below. If one of the variables does not appear in one of the equations, the space at the intersection of the corresponding line and column should be left blank or a zero inserted at the option of the computer.

(b) In a column at one side of the table of equations each should be numbered or lettered for reference.

(c) Divide each equation by plus or minus the coefficient of the variable in the first column and write down the resulting equations directly below the first set. The same columns should be used for each variable. The plus or minus sign should be used with these divisors in such a manner that the coefficients of the variables in the first column will be alternately plus one and minus one. The equations of this second set should be referenced by the same numbers or letters as those of the first set.

(d) Add adjacent equations of the second set to obtain the equations of the third set, and write the latter directly below, using the same column for each variable. As the coefficients of the first variable are plus and minus unity, this variable will disappear. By this process both the number of variables and the number of independent equations will be reduced by one.

(e) Reference this third set of equations by a new set of numbers or letters, and show in the column where the referencing symbols appear, how the new equation was formed. Thus, if equations 1 and 2 were added to obtain equation 6, the note in the column of referencing symbols should read " $1 + 2 = 6$ ."

(f) Repeat the above operations until a numerical value is obtained for one of the unknown variables.

(g) Substitute this value in both of the equations of the set with two unknowns, in which the coefficients of the other variable appearing are plus and minus one,

and solve for that variable. Consider the mean of the values obtained as the correct value. If these two values differ appreciably an error has been made that should be sought out and corrected.

(h) Repeat the above operation until all of the unknown variables have been evaluated.

After one of the variables has been evaluated, it is quicker to use only one of each set of equations in computing the values of the other variables, but the likelihood of error is greater. In this case, the values of all the variables should be checked by substituting them in all the equations of the first set to determine whether identities result. Exact identities may not be obtained owing to the use of a limited number of significant figures, but if the deviation from an identity is large, an error has been made and the computations must be corrected.

If the number of equations to be solved simultaneously is large the errors resulting from the dropping of excess significant figures is likely to become so great that the method of solution outlined above becomes impracticable. If, as often happens in this case, one of the coefficients in each equation and in each column when the equations are written down as suggested above is much larger than the other coefficients in the same line and column, the group of equations can usually be solved most expeditiously by successive trials.

Take for example the first set of equations in Art. 13 : 10. Here the largest coefficients are those of  $X_a$  in the first line and column,  $X_b$  in the second line and column, and  $X_c$  in the third line and column. For the first trial either the smaller coefficients in each equation may be neglected (which implies that the unknowns they modify are temporarily assumed equal to zero), or they may be added to the largest coefficient (which implies the assumption that all the unknowns are equal). If we make the latter assumption, the results of the first trial are

$$X_a = -\frac{4,756,800}{3,590.4} = -1,325$$

$$X_b = -\frac{3,820,800}{3,744.0} = -1,020$$

$$X_c = -\frac{4,812,800}{4,736.0} = -1,019.$$

In the second trial  $X_b = -1,020$  would be substituted in the first equation which would then be solved for a revised value of  $X_a$ . The revised value of  $X_a$  and the above value of  $X_c$  would be substituted in the second equation which would be solved for a revised value of  $X_b$ . This process would be continued until the changes in the resulting values of the unknowns became negligible. One advantage of this method is



that the work may be stopped when the unknowns have been evaluated to any desired degree of precision.

**13 : 18. Solution by Influence Lines** — The solution of redundant structures can often be facilitated by the use of influence lines obtained with the aid of Maxwell's reciprocal theorem discussed in Art. 12 : 16. This is particularly true when the loading is complex and there is but one redundant, as with the beam shown in Fig. 13 : 9.

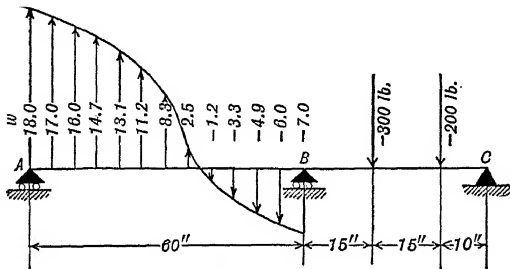


FIG. 13 : 9

If we assume support  $B$  to be redundant, Eq. 13 : 1 becomes  $R_b = -\delta_{bo}/\delta_{bb}$ . In this expression  $\delta_{bo}$  is the deflection that would be produced by the given external loads if the support at  $B$  were removed,

and is the sum of the deflections that would be produced by each of the loads acting by itself. From Maxwell's theorem the deflection of  $B$  due to a unit load at any point  $x$  is equal to the deflection of  $x$  due to a unit load at  $B$ . Therefore the deflection curve for a unit load at  $B$  is also an influence line for deflection at  $B$ , i.e., each ordinate indicates the deflection that would be produced at  $B$  by a unit load placed at the point for which the ordinate is drawn. If each ordinate of this influence line is multiplied by the corresponding ordinate of the loading diagram to locate a new curve, the area under this new curve will be equal to the deflection of  $B$  due to the given loading. This area can be divided by the value of  $\delta_{bb}$ , the ordinate of the deflection curve-influence line at  $B$ , to find the magnitude of the reaction at  $B$ . Usually it is found more convenient to locate an influence line for reaction at  $B$  by dividing all ordinates of the deflection curve for a unit load at  $B$  by the ordinate at  $B$ .

The computations involved in applying this method to the beam of Fig. 13 : 9, assuming it to be of constant  $EI$ , are outlined in Table 13 : 4. Column 1 shows the distance of each ordinate from the left end. Column 2 gives  $EI$  times the deflection due to 1 lb. at  $B$  (Station 60) computed from the formulas of Case 7 of Table 4 : 1. In column 3 are values of the ratio of the deflection at each point to that at  $B$ . These are the ordinates of the influence line for reaction at  $B$ . The ordinates of the assumed loading curve for span  $AB$  are in column 4. Column 5 is obtained by multiplying corresponding figures in columns 3 and 4. The part of the reaction at  $B$  which is due to load on span  $AB$  will be equal

to the area under the curve defined by the ordinates in this column. This area may be computed under the assumption it is composed of a number of trapezoids, using the method of Art. 3 : 11. Greater precision can be obtained with little additional labor by using Simpson's rule.

This rule applies only when the curve is defined by an odd number of equally spaced ordinates. Starting at either end, the successive ordinates are multiplied by 1, 4, 2, 4, 2, . . . 2, 4, 2, 4, 1, and the products added. The result is multiplied by the common distance between ordinates and divided by 3 to obtain the area. These operations are carried out in Table 13 : 4 where Simpson's multipliers are listed in

TABLE 13 : 4

1 Station	2 $EI\delta_{xb}$	3 $\delta_{xb}/\delta_{bb}$	4 $w$	5	6	7
0, <i>A</i>	0	0	18.0	0	1	0
5	2,792	0.145	17.0	2.465	4	9.860
10	5,533	0.288	16.0	4.608	2	9.216
15	8,175	0.426	14.7	6.262	4	25.048
20	10,667	0.556	13.1	7.284	2	14.568
25	12,958	0.675	11.2	7.560	4	30.240
30	15,000	0.781	8.3	6.482	2	12.964
35	16,742	0.872	2.5	2.180	4	8.720
40	18,133	0.944	-1.2	-1.133	2	-2.266
45	19,125	0.996	-3.3	-3.287	4	-13.148
50	19,667	1.024	-4.9	-5.018	2	-10.036
55	19,708	1.026	-6.0	-6.156	4	-24.624
60, <i>B</i>	19,200	1.000	-7.0	-7.000	1	-7.000
65	18,112	0.943				
70	16,500	0.859				53.542
75	14,437	0.752				5
80	12,000	0.625				
85	9,263	0.482				3)267.710
90	6,300	0.328				
95	3,187	0.166				89.237
100, <i>C</i>	0	0				

At Sta. 75,  $0.752 (-300) = -225.6$ . At Sta. 90,  $0.328 (-200) = -65.6$   
 $-225.6 - 65.6 = -291.2$

$$R_B = 291.2 - 89.2 = +202.0 \text{ lb.}$$

column 6 and the products of those multipliers and the ordinates of column 5 are shown in column 7. If the method of Art. 3 : 11 had been used, the area under the curve would have been 88.735 instead of 89.237. The difference represents area between a smooth curve with the ordinates of column 5 and the straight lines assumed to represent that curve in the method of Art. 3 : 11.

The contributions of the concentrated loads to the reaction at *B* are obtained by multiplying each load and the corresponding ordinate

of the influence line from column 3, and are computed on the lower portion of the table.

In many cases it is most convenient to obtain an influence line for a reaction directly by testing a model. For the beam of Fig. 13 : 9 the model would be a spline of constant section, held at points representing *A* and *C* and caused to deflect by a concentrated load applied at the point corresponding to *B*. The influence line for reaction at *B* would then be obtained directly by drawing the deflection curve of the spline and adjusting the scale so that the ordinate at *B* would be unity. This method of obtaining influence lines by testing models can be extended to multipli-redundant structures, and has been highly developed by Professor Beggs, Dr. Gottschalk, and others.

Although illustrated by a case where  $EI$  was assumed constant, the influence-line method is most useful when applied to structures of varying section, both when the influence lines are computed and when they are obtained by model tests. The method is also of great value in analyzing continuous trusses, provided it is allowable to assume that there is no play in the joints. When there is play in the joints neither this method nor the method of least work is applicable. The Maxwell-Mohr method can be adapted to the problem, but the necessary computations are very tedious.

**13 : 19. The Rigid Frame Sign Convention** — When a redundant structure is composed of members in which the only deformations of importance are those due to bending, the most convenient method of analysis is normally the Cross method of moment distribution. The application of this method to continuous beams has already been described. When it is applied to more complex structures it is desirable to adopt a convention for the signs of the bending moments at the ends of the members which differs from that employed in Chapter V.

With a continuous beam it is convenient to consider bending moments causing compression in the upper fibers as positive, and those causing tension in the upper fibers as negative. This convention, which will be termed the "beam convention," becomes ambiguous unless an additional convention is adopted to determine which is the "upper" side of a non-horizontal member. Professor Cross recommends that the left side of a vertical member be considered "upper," but it is difficult to devise any extension of the beam convention that will apply to all sloping members without ambiguity. The best solution of the problem is to adopt a special convention making the signs of moments on the ends of the separate spans depend on whether they are counter-clockwise or clockwise. In this book a counter-clockwise moment on the end of a member is considered positive and a clockwise moment nega-

tive.<sup>1</sup> This will be termed the "rigid frame convention," and the moments to which it applies will be termed "end moments" to distinguish them from bending moments for which the signs are determined by the beam convention.

It is highly important to distinguish between the "bending moment" at the end of a span and the "end moment" at that point, although both have the same numerical value. The term "bending moment" applies to both the external couple representing the action of the joint, or an adjacent span, on the boundary section of the span under consideration, and to the equal and opposite internal couple representing the action of the span on that boundary section. Therefore the sign of a bending moment cannot be determined from a convention of counter-clockwise or clockwise since the term refers to two couples, one in each of these senses. The term "end moment," however, refers only to the external couple acting on the boundary section of the span under consideration, and its sign can be determined by its sense. This is as true for a vertical or sloping member as for one that is horizontal.

The relations between the end moments and the bending moments on a beam can be summarized as follows:

1. The end moment and the bending moment at the left end of a span have opposite signs.
2. The end moment and the bending moment at the right end of a span have the same sign.
3. If the end moments are of the same sign, an odd number of points of inflection will be found in the span.
4. If the end moments are of opposite sign there will be either no points of inflection or an even number of such points in the span.

What were called the "support moments" in Chapter V are essentially the end moments for the spans of continuous beams. The moment at any given support is numerically equal to, and of the same sign as, the end moment for the span to the left of that support. It is also numerically equal, but of opposite sign, to the end moment for the span to the right of that support.

In the analysis of continuous beams by the method of moment distribution many engineers prefer to work with end moments and the rigid frame sign convention until the support moments have been computed, instead of using bending moments and the beam convention for

<sup>1</sup> The opposite convention is used by some authors and has much to be said in its favor. The chief reason for selecting the counter-clockwise end moment as positive is that by so doing the slope produced by a positive end moment will be positive according to the convention used throughout this volume.

signs as illustrated in Chapter V. Had this been done in the development of Eq. 5 : 4 to 5 : 14, it would have resulted in the following changes.

1. In Eq. 5 : 4 the sign of the carry-over factor would have been plus instead of minus.

2. The signs of the expressions for the stiffness factors in Eq. 5 : 5 to 5 : 8 would have been changed so as to give positive instead of negative results.

3. In Eq. 5 : 9 to 5 : 11 the sign of the fixed-end moment at the left end of a span,  $M_{Fa}$ , would have been reversed, but that of  $M_{Fb}$  would have been unchanged.

4. In Eq. 5 : 12 for the moment due to relative deflection of the ends of a span the sign of  $M_a$  would have been reversed, but that of  $M_b$  would have been unchanged. As a result, Eq. 5 : 13 would have become

$$M_a = M_b = -6 EKR \quad 13 : 8$$

5. Eq. 5 : 14 for checking the results of moment distribution calculations would have been

$$\begin{aligned} \Delta M_{ab} - 0.5 \Delta M_{ba} & K_{ab} \\ \Delta M_{ad} - 0.5 \Delta M_{da} & K_{ad} \end{aligned} \quad 13 : 9$$

It is to be noted that these changes affect only the signs, and never the numerical values, of the quantities being determined.

An important result of using the rigid frame sign convention is that a joint is balanced by making the algebraic sum of the end moments at that joint equal to zero. This is fundamentally the same as making the bending moments on each side of a support algebraically equal, but is a more convenient method of defining the operation, particularly when it is carried out at a joint where three or more members meet.

If the rigid frame sign convention had been employed in the numerical examples of Chapter V the only changes in the computations would have been in the signs of the moments at the left ends of the spans, all of which would have been reversed. The signs of moments at the right ends and all the numerical values would have been unchanged.

Although it may take a little practice for the engineer who is used to applying the beam convention for signs to become accustomed to the rigid frame convention, he will find that the time and effort required were well spent, particularly if he wishes to analyze more complex structures than continuous beams by the method of moment distribution. The chief defect of the rigid frame convention is that it cannot be used in computing bending moments between the ends of a span.

This can be obviated by reverting to the beam convention as soon as the end moments have been computed. Usually it will be found desirable to draw a line diagram of the structure and plot the end moments on the compression sides of the members on which they act as soon as they are computed. Then any necessary bending moments at intermediate points can be computed and a moment diagram completed for the structure with each ordinate plotted on the side of the member which the corresponding bending moment tends to subject to compression. This method of indicating the character of the bending moment at each point in a rigid frame is much clearer and simpler than any system of using plus and minus signs.

**13 : 20. Moment Distribution, Stationary Joints** — When there is no translation of the joints the moment distribution analysis of a rigid jointed frame differs very little from that of a continuous beam, particularly if the rigid frame sign convention is used in the latter. In a rigid jointed frame there may be three or more, instead of just two, members meeting at a joint, and therefore the method of computing distribution factors must be slightly revised. Since all the members meeting at a joint must be assumed to rotate the same amount when the joint is released, the unbalanced moment must be distributed among all the members in proportion to their stiffnesses. Therefore, in general, the distribution factor for any one member is equal to the stiffness factor for that member divided by the sum of the stiffness factors for all the members acting at the joint. Thus, if the members are all of constant  $EI$ , the distribution factor for any member  $A$  will be equal to  $K_a/\Sigma K$ , where  $K_a = I/L$  for member  $A$ , and  $\Sigma K$  is the sum of the values of  $I/L$  for the members at the joint. If a member has its far end pinned,  $0.75 K$  would be used instead of  $K$  for that member in computing the distribution factors. This modification is so simple that it is considered unnecessary to describe in more detail the extension of the method of moment distribution to structures where there is no translation of the joints.

**13 : 21. Moment Distribution, Known Joint Translation** — In many cases to which it is desired to apply the method of moment distribution there will be translational movement of one or more of the joints when the structure is subjected to the external load. The procedure to be adopted for these depends on whether the movements of the joints can be computed independently. If they can be, the problem is handled in essentially the same manner as that of a continuous beam with deflecting supports as illustrated in Art. 5 : 15. The joints are first assumed fixed in their original positions. Then it is assumed that they are moved without rotation to their deflected positions, developing end

moments that may be computed from Eq. 13 : 8. These deflection moments are added to any fixed-end moments that would result from applying loads in the various spans, and the normal procedure of moment distribution is then carried out.

A common application of this process is in determining the bending moments in the members of a truss constructed with rigid (riveted or welded) joints. The first step is to neglect the effects of joint rigidity and compute the axial loads in the various members, assuming them connected with frictionless pins, by the conventional methods of truss analysis. The second step is to compute the rotations of the members. This may be done by the application of Eq. 12 : 11 if desired, but the most practical methods are those of elastic loads and the Williot diagram. In Chapter XII these methods were described as methods of computing deflections rather than rotations, but they can be easily adapted to the latter purpose. In the method of elastic loads, the shear on any portion of the conjugate beam is numerically equal to the rotation of the corresponding link of the bar-chain. Once the rotations of the members of the bar-chain are known, those of the other members can be easily computed by adding and subtracting the various angle changes.<sup>1</sup> If it is desired to obtain the rotation of a member from the Williot diagram, one can measure off the distance,  $D$ , the relative deflection of the ends of a member normal to its axis, directly. This distance is represented by the length of the normal drawn from the end of the line representing the change in length of the member. Thus in Fig. 12 : 21, the distance,  $D$ , for member  $AC$ , is represented by  $c'c$ , and that for member  $BC$  by  $c''c$ . The rotation,  $R$ , is the distance  $D$  divided by the length of the member  $L$ .

The rotations of the members having been computed, the third step is to compute the resulting deflection moments and distribute them by the Cross method. Usually the engineer stops at this point although the effect of the moments due to joint rigidity is to modify the axial loads and rotations of the truss members. Experience has shown, however, that the resulting changes in these quantities are normally

<sup>1</sup> It is not necessary to determine the actual rotations of the members, but that of any member of the structure may be assumed at any desired amount, and the corresponding rotations of the remaining members computed from the angle changes. If all the members of a truss are rotated through an angle  $\alpha$ , the unbalanced moment at each joint would be  $-\Sigma \delta EK\alpha$ . This moment, however, would be distributed back to the members in the same proportions, so the sum of the deflection moment and the distributed moment for each member would be zero. There would be carry-over moments from this first cycle, but they also would be neutralized in the same manner during the next cycle. Thus if an arbitrary constant,  $\alpha$ , is added to all the true values of  $R$ , that action will not alter the final results.

so small that it is reasonable to neglect them. If, for some reason, more precise results are desired, the computer may assume that this first set of moments is correct and recompute the axial loads on and rotations of the truss members, and then recompute the moments due to joint rigidity. This process may be carried through any desired number of cycles.

**13 : 22. Moment Distribution with Unknown Deflections** — The method of Art. 13 : 21 is directly applicable only when the joint deflections due to bending deformations are negligible in comparison with those due to elongations. This is normal with trusses that would remain stable even though the members were connected by frictionless pins. With Vierendeel trusses, the conventional building frame, and many other structures where resistance of the joints to bending moments is essential for stability, the joint deflections are due almost entirely to bending deformations and the effects of elongation may be neglected. No general extension of the method of moment distribution has been developed to cover all cases of this kind, but one which is often useful, though of limited applicability, is outlined below in connection with the analysis of the light-weight railroad car side-frame shown diagrammatically in Fig. 13 : 10.

A basic requirement for any structural analysis is that the criteria of equilibrium must be satisfied. The most obvious of these is that there must be no unbalanced moment at any joint. With many structures there is but one set of end moments that will satisfy this criterion as

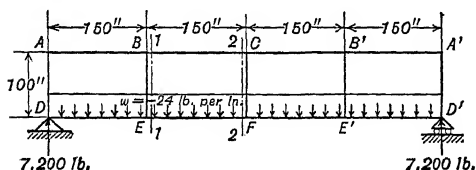


FIG. 13 : 10

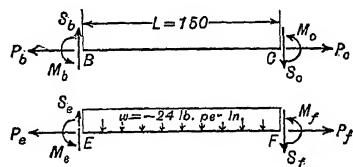


FIG. 13 : 11

well as those imposed by known movements of the joints, and the methods of the two preceding articles are applicable. In the structure of Fig. 13 : 10, however, the relative vertical deflections of the joints are unknown, and a separate solution satisfying the principle of consistent deformations and equilibrium of end moments at each joint will exist for each conceivable set of deflection values, but only that conforming to the deflections that would actually be produced would be correct. In a case of this kind it is often possible to develop other criteria from studies of the equilibrium of suitably selected free bodies assumed isolated from the remainder of the structure. Suppose, for



example, we isolate a free body by passing the section 1-1 through the truss just to the right of member  $BE$  and section 2-2 just to the left of member  $CF$ . The resulting free body and the forces acting on it will be as shown in Fig. 13 : 11. The end moments and shears shown have the directions implied by positive values.

Taking moments about either  $B$  or  $E$  we have

$$\Sigma M = 0 = M_b + M_c + M_e + M_f - S_c L - S_f L + \frac{wL^2}{2}$$

Noting that  $S_c + S_f = \Sigma S_2$ , the sum of the shears on sections cut by line 2-2, and writing  $\Sigma M_e$  for the sum of the end moments on the sections cut by lines 1-1 and 2-2, this relation may be written

$$\Sigma M_e = \Sigma S_2 L - \frac{wL^2}{2} \quad 13 : 10$$

Equation 13 : 10 is the form taken for this special case by what is commonly termed the "bent equation." The bent equation is usually derived for a number of columns in one story of a building frame subjected to horizontal loads assumed to be concentrated at the various floors. Then the  $w$  term drops out and the equation as usually written is

$$= Sh \quad 13 : 11$$

where  $\Sigma M_{tc}$  and  $\Sigma M_{bc}$  are the sums of the end moments on the tops and bottoms of the columns;  $S$ , the total shear on the story; and  $h$ , the story height. The form of the bent equation will be the same regardless of how many parallel members are cut by the parallel planes defining the free body for which it is written. If the external load normal to the members is not uniformly distributed the necessary modifications of Eq. 13 : 10 can be easily developed.

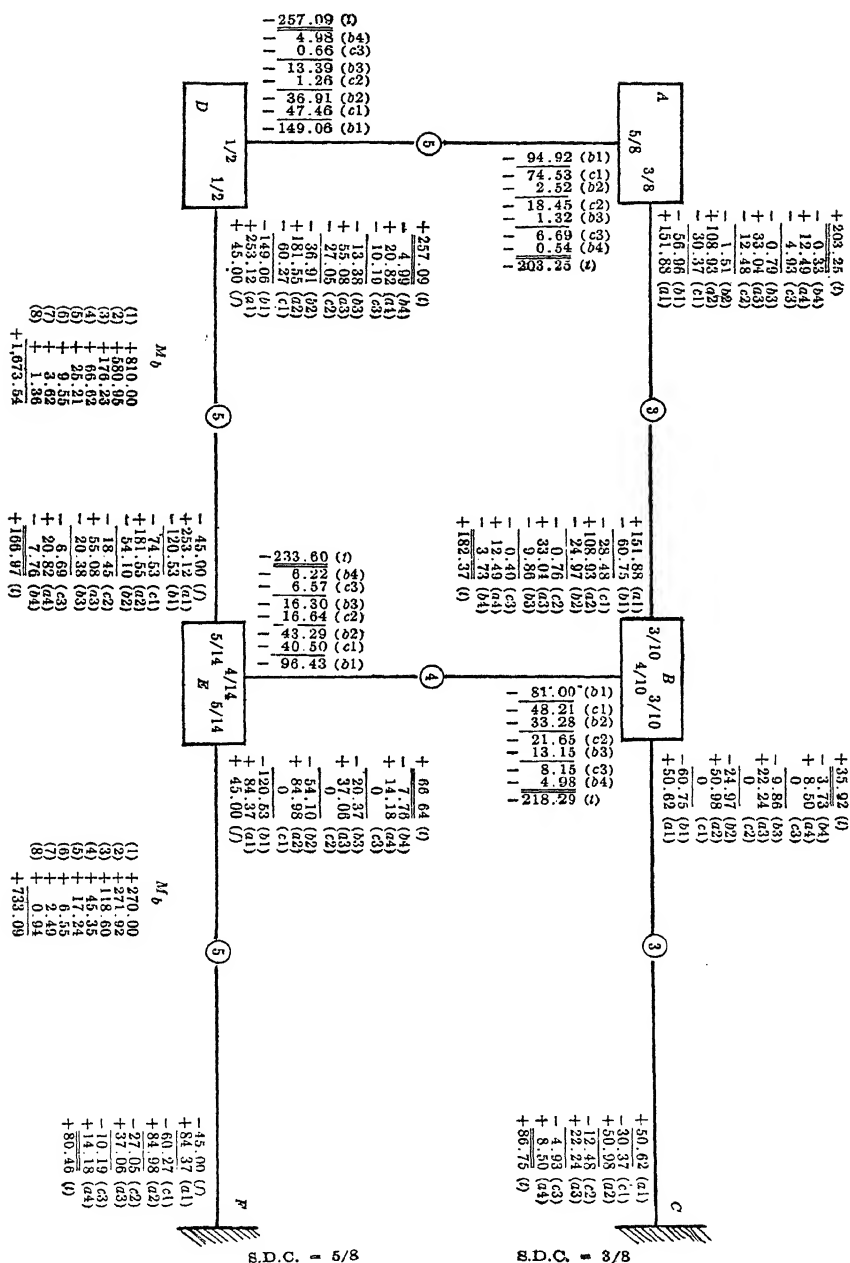
In the structure under consideration the total shear on either side of member  $CF$  is zero and that on either side of member  $BE$  is +3,600 lb. The length of each bay is 150 in., and the uniformly distributed load is -24 lb. per in. Therefore, for the left end bay the bent equation becomes

$$\Sigma M_e = 3,600 \times 150 + 24 \times 150 \times 75 = 810,000 \text{ in.-lb.} \quad a$$

Similarly for the left center bay

$$\Sigma M_e = 0 + 24 \times 150 \times 75 = 270,000 \text{ in.-lb.} \quad b$$

These relations must be satisfied in addition to having no unbalanced moments at the joints, and their existence makes it possible to analyze the frame of Fig. 13 : 10 by the method of moment distribution.



Since this frame is symmetrical as to both dimensions and load, the final slopes of the chord members at the center line will be zero and member  $CF$  will be subjected to no bending moments. Therefore it is allowable to analyze but one-half of the actual structure, assuming it to be a cantilever with the chord members fixed at  $C$  and  $F$ , and subjected to a concentrated load of 7,200 lb. at the free end and a uniformly distributed load of  $-24$  lb. per in. along the lower chord. It will also be convenient, in order to conserve space, to make the unit of moments the "inch-kip" equal to 1,000 in.-lb.

The first step in such an analysis would be to prepare a work sheet and enter the  $K$  values and distribution factors on it according to the system described in Chapter V. In Fig. 13 : 12 the  $K$  values used are relative values arbitrarily assigned for the purposes of illustration. The moment distribution computations may be carried out in the following stages.

1. Assume all joints fixed, compute fixed-end moments due to loads applied between joints, and enter results on the "(f) lines." In this example the only fixed-end moments are  $\pm 0.024 \times 150^2/12 = \pm 45.00$  in.-kips at the ends of the lower chord members.

2. Assume joints  $A$ ,  $B$ ,  $D$ , and  $E$  to move vertically without rotation until the end moments on the chords satisfy the bent equations,  $a$  and  $b$ . The magnitudes of these movements need not be computed, but the total moment required to satisfy the bent equation for each bay should be determined and entered in a convenient location as line (1) of a column of values of " $M_b$ ." The subscript indicates that these moments are those used to satisfy the bent equation.

3. Distribute the values of  $M_b$  computed in stage 2 among the ends of the chord members. The procedure for doing this may be developed as follows. If the ends of a member are moved without rotation to produce a deflection,  $D$ , of either end with respect to the tangent to the elastic curve at the other, the end moments developed will be given by Eq. 5 : 12, modified to conform to the rigid frame sign convention, as

$$M_a = \frac{D}{A_a (x_a - x_b)} \quad M_b = \frac{D}{A_b (x_a - x_b)} \quad 13 : 12$$

The corresponding shear in the member will be

$$S = \frac{M_a + M_b}{L} = \frac{(A_a + A_b) D}{A_a A_b (x_a - x_b) L} \quad 13 : 13$$

In a structure like that of Fig. 13 : 10 it is allowable to neglect the shortening of members due to axial load and assume the deflections of the two ends of each vertical member to be the same. Therefore, if

the deflections of stage 2 take place without rotations of the joints, the shear on any bay and the end moments required to satisfy the bent equation for that bay will be distributed between the chords in proportion to their "shear distribution factors."<sup>1</sup>

$$\begin{array}{ccc} S.D.F. & A_b) & \\ & (x_a - & 13 : 14 \end{array}$$

This will be true wherever a number of parallel members have their ends subjected to equal transverse deflections without rotation, as when the tops of all the columns in one story of a building are subjected to a common horizontal deflection due to movement of the floor above. If all the members of such a group are of constant  $EI$  the shear distribution factors of Eq. 13 : 14 become proportional to  $I/L^2$ . Therefore if they are also of equal length, as in the structure under consideration, the quantity  $K = I/L$  may be used as the shear distribution factor as well as for the relative stiffness factor for each member. The distribution of the end moments between the two ends of any member will be such that  $M_a/M_b = A_b/A_a$ . When  $EI$  is constant this implies that  $M_a = M_b$ .

In the structure of Fig. 13 : 10 the relative  $K$  values for the two chords are 3 and 5. Therefore the shear distribution factors are  $\frac{3}{8}$  for the upper and  $\frac{5}{8}$  for the lower chord. These quantities are entered on Fig. 13 : 12 near the right-hand margin. In the left end panel the value of  $M_b$  to be distributed is +810.00 in.-kips. Of this total,  $\frac{3}{8}$  is equally divided between  $M_{ab}$  and  $M_{ba}$ , and the remainder equally divided between  $M_{de}$  and  $M_{ed}$ . These quantities and the corresponding values for the second bay are entered on the (a1) lines of Fig. 13 : 12. Since no horizontal joint movement is assumed there will be no moments distributed to the vertical members in this stage.

4. Assume joints  $A$ ,  $B$ ,  $D$ , and  $E$  released, and distribute the unbalanced moments. The distributed moments are to be entered on the (b1) lines and short lines drawn to indicate that the joints are now in balance. Joints  $C$  and  $F$  are not released in this stage (or in any of those following) since they are considered fixed.

5. Carry over moments in the usual manner, and enter the figures in the (c1) lines.

6. Since the joints are now unbalanced by the carried-over moments, it would be possible to distribute these and continue the computations through several cycles until the quantities handled had become negligible before paying further attention to the bent equations. Such action, however, would greatly lengthen the analysis without any com-

<sup>1</sup> Usually called the "column distribution factor" in structural practice.

pensating advantages. The bent equation for each bay will now be found to be unbalanced by the total amount of the entries in the (b1) and (c1) lines for the ends of the chords of that bay. These totals should be computed and entered with reversed signs in the second line of the  $M_b$  columns. In computing these totals one may either add all the pertinent entries in both (b1) and (c1) lines, or add those in the (c1) lines and multiply by 3.

7. Assume joints  $A$ ,  $B$ ,  $D$ , and  $E$  again moved vertically without further rotation until the moments at the ends of the chord members again satisfy the bent equations. In this case the bent equation for the left end bay was thrown out of balance by  $-580.95$  in.-kips by the moments computed in stages 4 and 5. It is rebalanced by adding  $+580.95$  in.-kips distributed between the joints in the same proportions as the original figure of  $+810.00$ , the individual amounts applied at the separate joints being recorded on the (a2) lines. The other bay is similarly rebalanced by distributing  $+271.92$  in.-kips among its joints.

8. The joints are again released and the moments balanced, the balancing moments being entered on the (b2) lines and the resulting carry-over moments on the (c2) lines.

TABLE 13 : 5  
CHECK OF MOMENT DISTRIBUTION COMPUTATIONS

1	2	3	4	5	6	7	8	9	10	11
Joint	Mem- ber	$M$	$M_f$	$M_b$	$\Delta M_n$	$-0.5$ $\Delta M_f$	$\Delta M_n -$ $0.5 \Delta M_f$	$K$	$\Delta M_n -$ $0.5 \Delta M_f$ $K$	$M_{s.d.}$
$A$	$AB$	+203.25	0	+313.79	-110.54	+65.72	-44.82	3	-14.04	+203.298
	$AD$	-203.25	0	0	-203.25	+128.55	-74.70	5	-14.94	-203.340
$B$	$BA$	+182.37	0	+313.80	-131.43	+55.27	-76.16	3	-25.39	+182.424
	$BC$	+35.92	0	+137.45	-101.53	+25.36	-76.17	3	-25.39	+35.988
	$BE$	-218.29	0	0	-218.29	+116.80	-101.49	4	-25.37	-218.440
$C$	$CB$	+86.73	0	+137.45	-50.72	+50.77	+0.05	3	+0.02	+86.772
	$DA$	-257.09	0	0	-257.09	+101.62	-155.47	5	-31.09	-257.130
$D$	$DE$	+257.09	+45.00	+522.98	-311.01	+155.51	-155.50	5	-31.10	+257.120
	$ED$	+166.97	-45.00	+522.99	-311.02	+155.51	-155.51	5	-31.10	+166.990
	$EB$	-233.60	0	0	-233.60	+109.15	-124.45	4	-31.11	-233.744
$E$	$EF$	+66.64	+45.00	+229.08	-207.44	+51.82	-155.62	5	-31.12	+66.720
	$FE$	+80.46	-45.00	+229.10	-103.64	+103.72	+0.08	5	+0.02	+80.490

This procedure of balancing the bent equations, balancing the individual joints, carrying over, and repeating is continued until the quantities handled become negligible. The various columns are then added to determine the total end moments for each member. In Fig. 13 : 12 the complete computations are recorded for only four cycles, but

the values of  $M_b$  are given for eight cycles and the totals are those obtained after eight cycles.

After the end moments have been computed the check of Eq. 13 : 9 may be applied as shown in Table 13 : 5. There the values of  $M_b$  in the fifth column may be found either by a separate addition of the quantities in the (a) lines for each end moment, or by distributing the sum of the values of  $M_b$  for each bay in the proportions used to determine the quantities for the (a) lines in each cycle. In preparing Table 13 : 5 the first of these methods was used. Checking by the second method, the first quantity in the column would be  $+1,673.54 \times \frac{3}{16} = +313.79$ . The quantity  $\Delta M_n$  in the sixth column is the moment increment at the "near end" of the member. Thus  $-110.54$  in the first line is the moment increment on end A of member AB. It is computed by subtracting the algebraic sum of the values of  $M_f$  and  $M_b$  in columns 4 and 5 from that of  $M$  in column 3. Similarly  $0.5 \Delta M_f$  is half the moment increment at the "far end" of the member. Thus  $+65.72$  is minus one-half the moment increment on end B of member AB. From Eq. 13 : 9 all members acting at any joint should have quantities in column 8 that are proportional to their  $K$  values. This can be most easily checked by dividing each quantity in that column by the proper value of  $K$  to obtain the figures of column 10. Since the latter are essentially measures of the rotations of the joints, the figures for joints C and F, at the plane of symmetry, should be zero. A glance at column 10 shows that the end moments of column 3 satisfy the principle of consistent deformations as well as that of equilibrium and therefore whatever errors may have been made in the moment distributions were of negligible importance. The values of  $M$  listed in column 11 were computed by the method outlined in the next article. They are included in Table 13 : 5 to show that the two methods give essentially the same results.

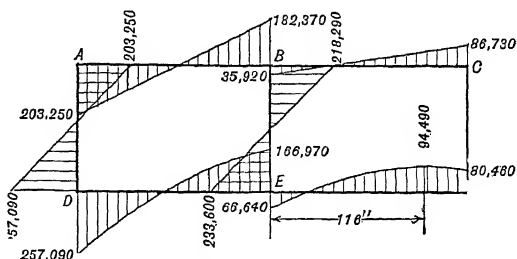


FIG. 13 : 13

After the end moments have been checked it is advisable to make a moment diagram for the structure, plotting *bending moments* on that side of each member that they tend to subject to compression. Such a diagram is shown in Fig. 13 : 13. With the exception of the lower chord, none of the members are subjected to transverse loads, and the bending-moment diagrams are straight lines joining points located by

the values of the end moments. For the lower chord members it is necessary to plot some intermediate values to locate the bending-moment curve. For member  $DE$  the shear at  $D$  will be  $+1,800 + (257,090 + 166,970)/150 = +1,800 + 2,827 = +4,627$  lb. The bending moment 50 in. to the right of  $D$  will then be  $-257,090 + 4,627 \times 50 - 24 \times 50 \times 25 = -55,740$  in.-lb. Similarly the moment 100 in. to the right of  $D$  is found to be  $+85,610$  in.-lb. On member  $EF$  the shear at  $E$  is similarly found to be  $+2,781$  lb., whence there is a point of zero shear, and maximum moment,  $2,781/24 = 116$  in. to the right of  $E$ . The bending moment at this point is  $-66,640 + 2,781 \times 116 - 24 \times 116 \times 58 = +94,490$  in.-lb. The student will find that checking these values will contribute to his understanding of the method by which they were obtained.

If the deflections of the joints should be desired they can be determined from a simple extension of the computations of Fig. 13 : 12 and Table 13 : 5. Each time the bent equation was balanced it was implied that there was a definite relative vertical movement of the joints at the ends of each bay, proportional to the magnitude of  $M_b$ , distributed to the ( $a$ ) lines. The sum of such movements is therefore measured by the values of  $M_b$  in Table 13 : 5, and can be obtained by means of Eq. 13 : 8. This formula connects the rotation of a member and the corresponding value of  $M_b$  at one end. However, the relative deflection of the ends of any member is  $D = RL$ , and the equation may be written

$$D = - \frac{M_b L}{6 EI} = - \frac{M_b L^2}{6 EI} \quad 13 : 15$$

Applying this expression to the left end bay we get

$$D_1 = - \frac{313,800 \times 150 \times 150}{6 EI_u} = - \frac{1,176,750,000}{EI_u}$$

from the upper chord moments, and

$$D_1 = - \frac{522,980 \times 150 \times 25}{EI_l} = - \frac{1,961,175,000}{EI_l}$$

from the lower. Similarly for the left center bay,

$$D_2 = - \frac{137,450 \times 150 \times 25}{EI_u} = - \frac{515,437,500}{EI_u}$$

or

$$D_2 = - \frac{229,090 \times 150 \times 25}{EI_l} = - \frac{859,087,500}{EI_l}$$

For each bay the deflections computed in this manner should be proportional to the  $K$  values of the chords, and it will be found that the above values satisfy this criterion to a high degree of precision. The total deflections of joints  $C$  and  $F$  with respect to a line through the supports at the ends of the frame will be equal to  $D_1 + D_2$ .

Although the computations of this example were carried through eight cycles, sufficient precision for most practical purposes would have been obtained if the distributions had been stopped at an earlier stage. This is shown by the values that would have been obtained for  $M_{de}$  if the additions had been made after each balancing of the joints. These figures are +149.06, +233.43, +248.08, +253.72, +255.85, +256.66, +256.97, and +257.09. It should be noted that these values constitute a constantly increasing series converging on a figure slightly in excess of the last one computed. This is true of all the end moments considered in this example and indicates that all the values in column 3 of Table 13 : 5 are a little too small. It should also be noted that sufficient precision for most purposes could have been obtained if a smaller number of significant figures had been used.

The above discussion of the Cross method of moment distribution is very sketchy, and many shortcuts and alternative methods of procedure have been omitted. For the more thorough discussion of the method, the reader is referred to Professor Cross's book.

**13 : 23. Slope Deflection** — An alternative to the method of moment distribution for the analysis of rigid jointed frames is the Slope Deflection method. A closely similar method was proposed for the analysis of bending moments due to joint rigidity by Manderla in 1878. Manderla's method was further developed by Professor Mohr in 1892 and extended to a wider range of problems by Professor G. A. Maney in 1915. For some types of problem this method is more convenient than that of moment distribution, and it is desirable to outline its fundamental characteristics.

From Eq.  $a$  of Art. 5 : 16 the rotation at end  $a$  of a member  $ab$  of constant  $EI$  is given by

$$3EK\theta_a = \Delta M_{ab} - 0.5 \Delta M_{ba}^1 \quad 13 : 16a$$

where  $\theta_a$  = the rotation of end  $a$  of the member.

$E$  = Young's modulus.

$K = I/L$  for the member.

$\Delta M_{ab}$  = the "moment increment" at end  $a$  as defined in Art. 5 : 16.

$\Delta M_{ba}$  = the "moment increment" at end  $b$ .

<sup>1</sup> The sign of  $\Delta M_{ab}$  is reversed to make it conform to the rigid frame sign convention.



Similarly the rotation at end  $b$  is given by

$$3 EK\theta_b = -0.5 \Delta M_{ab} + \Delta M_{ba} \quad 13 : 16b$$

Solving these equations to obtain  $\Delta M_{ab}$  and  $\Delta M_{ba}$  in terms of  $\theta_a$  and  $\theta_b$ , we find

$$\Delta M_{ab} = 2 EK (2\theta_a + \theta_b) \quad 13 : 17a$$

$$\Delta M_{ba} = 2 EK (\theta_a + 2\theta_b) \quad 13 : 17b$$

These "moment increments" do not include either the fixed-end moments or the moments due to rotation of the member.<sup>1</sup> Since the latter are equal to  $-6 EKR$  (see Eq. 13 : 8), the total moments at the ends of the member are given by

$$M_{ab} = 2 EK (2\theta_a + \theta_b - 3R) + M_{Fab} \quad 13 : 18a$$

$$M_{ba} = 2 EK (\theta_a + 2\theta_b - 3R) + M_{Fba} \quad 13 : 18b$$

Similar equations can be written until the end moments on all the members of a structure have been expressed in terms of the rotations of the joints ( $\theta$  values) and the rotations of the members ( $R$  values). By substituting these expressions for the end moments in the available equations of equilibrium, the latter are changed from equations in which the unknowns are the values of the end moments to equations in which the unknowns are the values of  $\theta$  and  $R$ . In many cases this process reduces the number of unknowns in the equations of equilibrium to the number of such equations. When this is true, the equations of equilibrium can be solved simultaneously to find the values of  $\theta$  and  $R$  and the results inserted in the equations of the type of 13 : 18 to evaluate the end moments. The equilibrium equations suitable for use in this method are normally of two types, "joint equations" and "bent equations." The joint equations are those expressing the fact that the algebraic sum of all the end moments at any joint must be zero. The bent equations are the same as the bent equations described in Art. 13 : 22 for use with the method of moment distribution.

The first step in applying this method to the frame of Fig. 13 : 10 is to write equations expressing the equilibrium of moments at each joint, using expressions of the type of Eq. 13 : 18 for the various moments. Thus

$$\Sigma M_a = M_{ab} + M_{ad} = 0 = 2E \times 3 (2\theta_a + \theta_b - 3R_1) + 2E \times 5 (2\theta_a + \theta_d) \quad a$$

$$\Sigma M_d = M_{da} + M_{de} = 0 = 2E \times 5 (2\theta_d + \theta_a) + 2E \times 5 (2\theta_d + \theta_e - 3R_1) + 45,000 \quad b$$

and similarly for joints  $B$  and  $E$ . In these equations  $R_1$  is the rotation of the chord members of the left end bay, and that of the left center bay

<sup>1</sup> I.e., Rotation of the straight line joining the ends of the member.

would be designated by  $R_2$ ;  $\theta_c$  and  $\theta_f$  would be zero on account of the symmetry of the structure and loading; and  $R$  would be zero for each of the verticals, any rotation due to changes in length being neglected.

Four equations containing the six unknowns,  $\theta_a$ ,  $\theta_b$ ,  $\theta_d$ ,  $\theta_e$ ,  $R_1$ , and  $R_2$ , would be obtained in this manner. For the other two equations needed, the bent equations, 13 : 10, would be written for each bay in the same manner. That for the left end bay would be

$$2 E \times 3 (2 \theta_a + \theta_b - 3 R_1) + 2 E \times 3 (2 \theta_b + \theta_a - 3 R_1) - 2 E \times 5 (2 \theta_d + \theta_e - 3 R_1) + 45,000 + 2 E \times 5 (2 \theta_e + \theta_d - 3 R_1) - 45,000 = 3,600 \times 150 + 3,600 \times 75 = 810,000 \quad c$$

Through simplification and combination of terms, the six equations thus obtained would become

$$\begin{array}{rclcl} 16 \theta_a + 3 & + & 5 \theta_d & - & 9 R_1 & = & 0 \\ 3 \theta_a + 20 & & & + & 4 \theta_e - 9 R_1 - 9 R_2 & = & 0 \\ 5 \theta_a & & + 20 \theta_d + 5 \theta_e - 15 R_1 & & & = & -22,500/E \\ & 4 \theta_b + 5 \theta_d + 28 \theta_e - 15 R_1 - 15 R_2 & = & 0 \\ 9 \theta_a + 9 \theta_b + 15 \theta_d + 15 \theta_e - 48 R_1 & & & & & = & 405,000/E \\ & 9 \theta_b & + & 15 \theta_e & 48 R_2 & = & 135,000/E \end{array}$$

Whence, by the usual methods of solution,

$$\begin{array}{lll} E\theta_a = -4,985 & E\theta_b = -8,464 & E\theta_d = -10,364 \\ E\theta_e = -10,377 & ER_1 = -17,439 & ER_2 = -7,642 \end{array}$$

Using these values in the equations of the type of 13 : 18 the end moments can be determined.

$$\begin{array}{ll} M_{ab} = 2 \times 3 (-9,970 - 8,464 + 52,317) = +203,298 \\ M_{ad} = 2 \times 5 (-9,970 - 10,364) = -203,340 \end{array}$$

The other values found in this manner are listed in the last column of Table 13 : 5, where it is readily seen that they check the results of the moment distribution computations very closely. In this example all the end moments obtained by the slope deflection method are slightly larger than those obtained by moment distribution, and indicate the values toward which the latter converge. This is to be expected since the two methods are based on the same principles and assumptions and are basically alternative methods of solving the same group of equations.

It should be noted that in these computations, as long as the values used for  $K$  are in the proper ratios, the resulting end moments will be the same. For this reason relative  $K$  values are often used in place of the actual values of  $I/L$ . When this is done the computed values of  $R$  and  $\theta$  are not the true values but are quantities proportional to them.

When it is desired to apply the slope deflection method to the com-

putation of bending moments due to rigid truss joints, bent equations similar to those used in the above example are not available. In such problems the practice is to compute the values of  $R$  on the assumption of pin joints, in the same manner as when the method of moment distribution is to be used. Then the only unknowns in the equilibrium equations will be the values of  $\theta$ , of which there will be one for each joint. As there will also be an equilibrium equation for each joint a solution is possible. In problems of this type care must be taken to use the actual  $K$  values instead of relative ones.

In some problems the moment at one end (which will be called end  $b$ ) of a member can be determined directly by applying the principle of equilibrium. The most common examples are when one end of a member is pinned and the only member, if any, rigidly connected to that end is a cantilever. Then the moment at end  $a$  can be expressed in terms of  $\theta_a$  and  $R$  by the equation

$$M_{ab} = 2 EK (1.5 \theta_a - 1.5 R) + M_{Fab} - 0.5 M_{Fba} + 0.5 M_{ba} \quad 13 : 19$$

This is developed by solving Eq. 13 : 18b for  $\theta_b$  and substituting the result in 13 : 18a. It is of value only when  $M_{ba}$  is known. Its use is analogous to the use of 0.75 true relative  $K$  in the method of moment distribution in similar situations.

The chief defect of the slope deflection method is that with complex structures the solution of an excessive number of simultaneous equations is required. Recently several modifications have been proposed with the aim of eliminating this defect. Among these should be mentioned Goldberg's<sup>1</sup> method of solving the equations by successive approximations; Wilbur's method of solving the equations in groups,<sup>2</sup> and Schwalbe's method of solving the equations by iteration.<sup>3</sup>

**13 : 24. Effect of Elastic Joints**—In the methods of analysis of frames outlined above, it has been assumed that the joints were rigid, so that the rotations of the ends of all the members at any joint would be identical. In practical structures this is an ideal that is only approximated, though approached very closely when the connections have ample gussets or are made by welding. If the elastic characteristics of the joints used are known it is possible to extend either the method of moment distribution or the method of slope deflection to allow for the properties of the actual joints. Methods of accomplishing this have

<sup>1</sup> "Wind Stresses by Slope Deflection and Converging Approximations," by John E. Goldberg, *Transactions, Am. Soc. C. E.*, Vol. 99, p. 962, 1934.

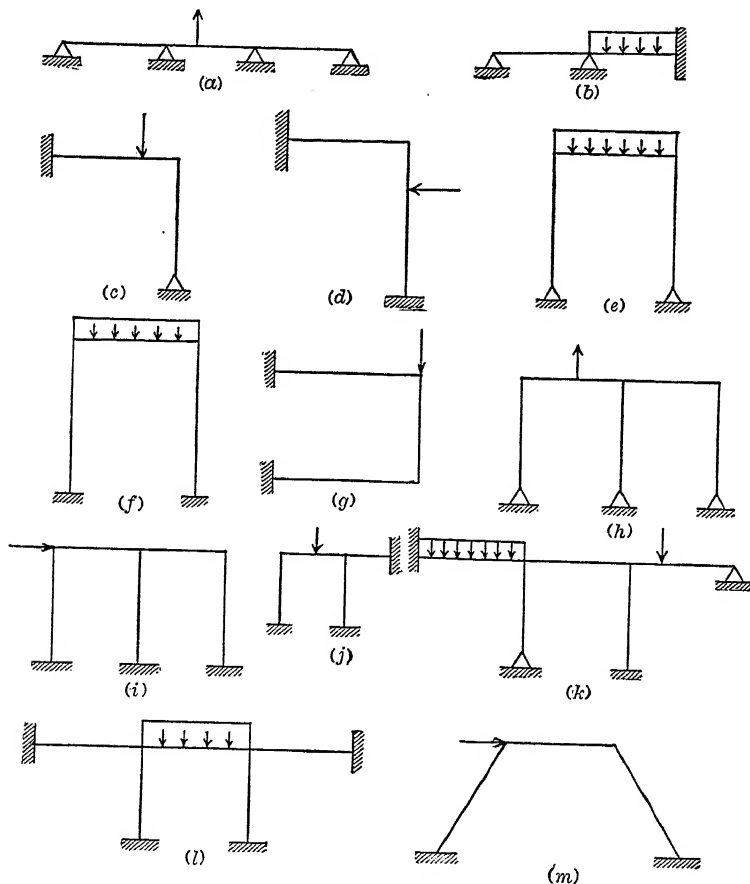
<sup>2</sup> "Successive Elimination of Unknowns in the Slope Deflection Method," by John B. Wilbur, *Transactions, Am. Soc. C. E.*, Vol. 102, p. 346, 1937.

<sup>3</sup> "Simultaneous Equations in Mechanics Solved by Iteration," by W. L. Schwalbe, *Transactions, Am. Soc. C. E.*, Vol. 102, p. 939, 1937.

been described by J. C. Rathbun.<sup>1</sup> These methods are very new and have not yet been generally adopted. At present the usual procedure is to neglect the effect of joint elasticity or to make alternative analyses, one assuming rigid joints and the other assuming pin joints or similar arbitrary assumptions. The design is then made to satisfy the more severe condition for each section of the structure.

PROBLEMS

**13 : 1.** Draw qualitative bending moment and deflection curves similar to those of Fig. 13 : 1 for each of the structures shown. Assume all members rigidly connected to each other, and plot bending moments on the side of a member which they tend to subject to compression.

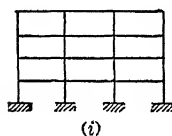
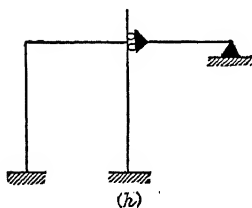
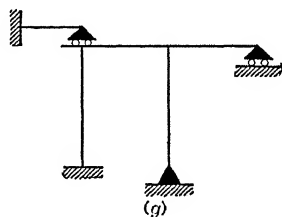
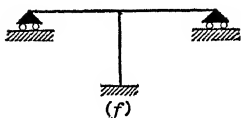
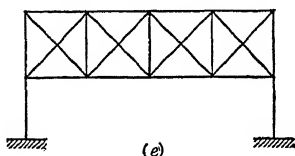
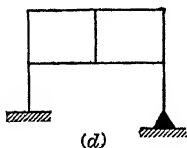
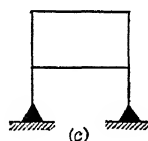
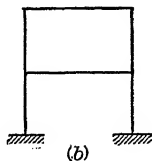
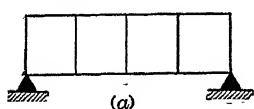


PROB. 13 : 1

<sup>1</sup> "Elastic Properties of Riveted Connections," by J. Charles Rathbun, *Transactions, Am. Soc. C. E.*, Vol. 101, p. 524, 1936.

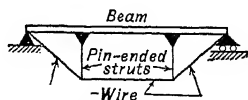
**13 : 2.** Determine the degree of redundancy of each of the structures of Prob. 13 : 1.

**13 : 3.** Determine the degree of redundancy of each of the rigid jointed frames shown in the figures.

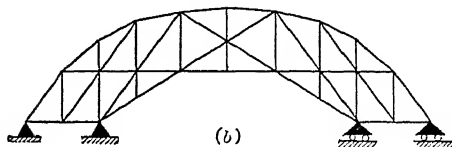
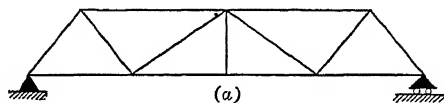


PROB. 13 : 3

**13 : 4.** What is the degree of redundancy of the "queen post truss" shown in the figure?

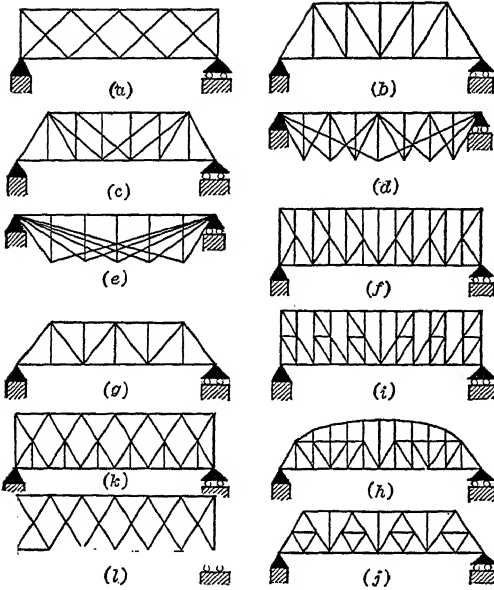


PROB. 13 : 4



PROB. 13 : 5

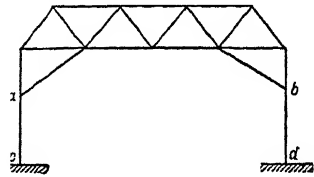
**13 : 5.** Determine the degree of redundancy of each of the trusses shown, assuming first that all joints are pinned, and second that all joints are rigid.



PROB. 13 : 6

**13 : 6.** Determine which of the pin-jointed trusses shown in the figures are statically determinate, and state the degree to which each of the others are redundant.

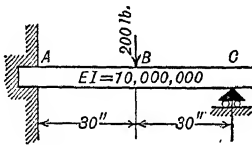
**13 : 7.** Determine the degree of redundancy of the structure shown: (a) assuming all joints rigid; (b) assuming all joints pinned except  $a$  and  $b$  and the supports  $c$  and  $d$ ; at  $a$  and  $b$  the diagonals are to be assumed pinned to the continuous vertical posts.



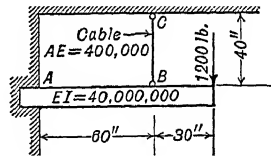
PROB. 13 : 7

**13 : 8.** Assuming no deflection of support  $c$ , determine the magnitude of the reaction at that point.

**13 : 9.** Determine the load in cable  $BC$  by the Maxwell-Mohr method.

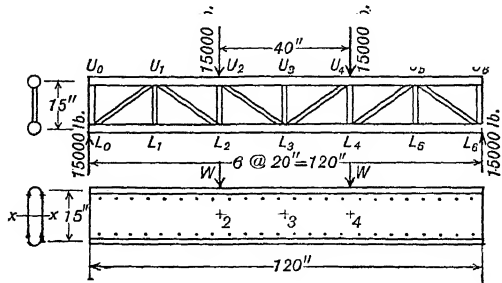


PROB. 13 : 8



PROB. 13 : 9

**13 : 10.** The stub wing of an airplane has a steel tubular truss front spar which, in landing, is loaded as shown above. The top chords are  $2\frac{1}{2}$  by 0.095 tubes, the lower chords  $2\frac{1}{2}$  by 0.065. The vertical web members are  $1\frac{5}{8}$  by 0.049, the diagonals  $1\frac{5}{8}$  by 0.065. The deflection of the spar is considered to be excessive, and it is proposed to stiffen the structure by building a stainless-steel beam which can be slid over the original truss and spot-welded to it. The fit is to be close enough so that both truss and beam will deflect to the same elastic curve.  $E = 28,000,000$  for both truss and beam.



PROB. 13 : 10

Determine the deflection of  $L_2, L_3, L_4$  of the truss on the basis of its carrying the entire load. Determine the deflection of points 2, 3, and 4 of the beam,  $I_{xx} = 36.0$ , on the assumption that it carries the entire load.

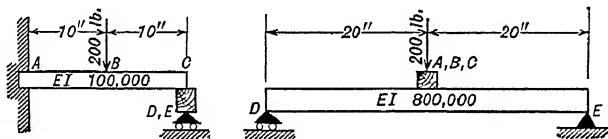
On the basis of the relative deflections of  $L_3$  and point 3, how much of the load will be carried by the truss, how much by the beam when they are constrained to act together?

What is the deflection of the combination spar at midspan, measured from an axis connecting the ends of the spar?

**13 : 11.** Using the truss and loading for Prob. 13 : 10 determine the stress in each tube and the deflection of  $L_3$  below an axis through  $L_0-L_6$ . What is the  $EI$  of an equivalent beam which, for the same span and loading, will give the same deflection at midspan? On the basis of the  $EI$  of this equivalent beam as compared with the  $EI$  of the stainless-steel beam of Prob. 13 : 10 what proportion of the total load is carried by the truss, by the stainless beam, when the two work together?

**13 : 12.** Using the truss and loading for Prob. 13 : 10 with the addition of an axial compressive load of 20,000 lb., applied so that each chord carries 10,000 lb., determine the stress in each tube and the deflection of  $L_3$  below an axis through  $L_0-L_6$ . What is the  $EI$  of an equivalent beam, which for the same span and loading will give the same midspan deflection when the axial load is neglected? Using a beam of this  $EI$ , taking the axial load into account and using the precise method, draw a curve of bending moments for the beam, computing ordinates at 20-in. intervals. By means of the method of moments and this curve of bending moments determine the load in each member of the top and bottom chords of the truss and compare these loads with those obtained when the secondary moments and deflections were neglected. Which member of the truss is most affected?

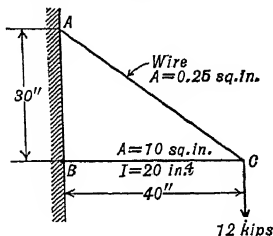
**13 : 13.** Determine the bending moment at point  $A^*$  for the structure shown.



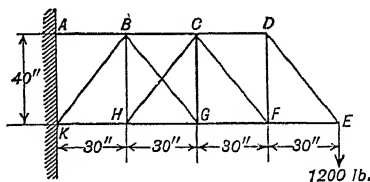
PROB. 13 : 13

**13 : 14.**  $BC$  is a cantilever beam supporting a weight of 12 kips at its outer end, and reinforced by the wire  $AC$  attached to that end. Assuming the wire incapable of carrying bending, and taking account of deformations due to both axial loads and bending moments, compute the axial loads and bending moments in the two members.

**13 : 15.** Assume the truss shown to be pin jointed and  $EA$  of each member proportional to its length in inches. Compute the axial load in each member.



PROB. 13 : 14



PROB. 13 : 15

**13 : 16.** The rear portion of a fuselage side truss is reinforced by the additional wires  $AH$ ,  $BJ$ , and  $CK$  as shown. Compute the axial loads in the various members assuming  $E = 30,000,000$  and the sizes to be as follows:

$ABC - 1\frac{1}{4}$  by 0.049

$CDE - 1$  by 0.035

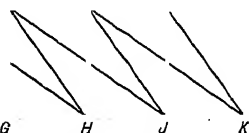
$FGH - 1\frac{1}{2}$  by 0.049

$HJK - 1\frac{1}{4}$  by 0.049

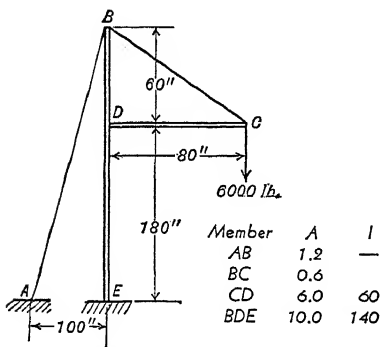
All verticals —  $1\frac{1}{4}$  by 0.035

All diagonals — Single  $\frac{1}{4}$ -28 round swaged tie rods. ( $A = 0.0254 \text{ in.}^2$ )

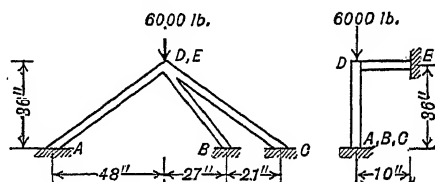
400 lb. 400 lb. 400 lb. 400 lb.



PROB. 13 : 16



PROB. 13 : 17

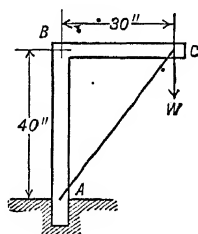


PROB. 13 : 18

**13 : 18.** A 6,000-lb. load is supported on four steel tubes as shown.  $AD$  is  $1\frac{1}{2}$  by 0.049,  $BD$  is  $1\frac{1}{4}$  by 0.049, and both  $CD$  and  $ED$  are 1 by 0.049. Assuming pin joints, compute the axial load in each tube.

**13 : 19.** Compute the initial tension in wire  $AC$  assuming it originally 0.1 in. too short. The properties of the members are,

Member	A	I
$AB$	0.650	0.825
$BC$	0.650	0.825
$AC$	0.0125	

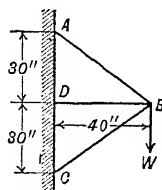


PROB. 13 : 19

**13 : 20.** Members  $AB$  and  $CB$  are  $\frac{1}{4}$ -28 S.L. wires, sectional area 0.0234 sq. in.  $BD$  is a  $2\frac{1}{2}$  by 0.083 steel tube, sectional area 0.6302 sq. in., hinged at  $D$ .

a. Assume  $BC$  to be 0.08 in. too short to fit, and compute the initial stresses in the three members. Assume  $E = 30,000,000 \text{ p.s.i.}$

b. If the load  $W$  is applied gradually, what will be its magnitude when  $BC$  drops out of action, assuming  $BC$  incapable of carrying compression?



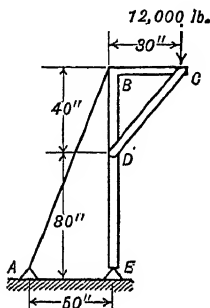
PROB. 13 : 20

**13 : 21.** Work Prob. 13 : 20 assuming member  $BD$  fixed at  $D$ .

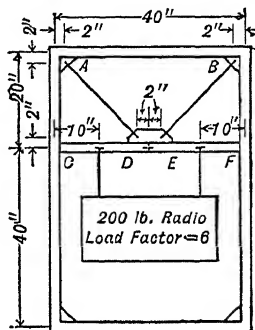


**13 : 22.** In the structure shown,  $CBE$  is a continuous member with  $A = 5$  sq. in. and  $I = 36$  in.<sup>4</sup> The brace  $CD$  is pinned at both ends. Its sectional properties are  $A = 3$  sq. in.,  $I = 12$  in.<sup>4</sup> The sectional area of the guy wire,  $AB$ , is 0.25 sq. in. Compute the axial loads and bending moments in the members of the structure.

**13 : 23.** A radio set weighing 200 lb. is supported from tube  $CF$  which is pin-connected to the vertical members of a fuselage at  $C$  and  $F$  by fittings not shown in the figure. Cables  $AD$  and  $BE$  have an  $EA$  of 200,000; tube  $CF$  an  $EA$  of 5,000,000 and an  $EI$  of 1,000,000. Determine the load in the cables and the bending moment at the center of tube  $CF$  by the method of least work.

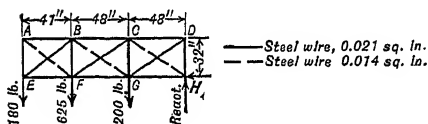


PROB. 13 : 22



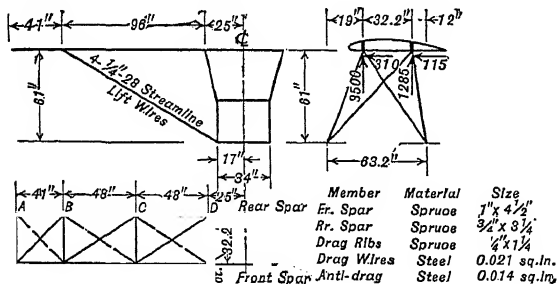
PROB. 13 : 23

**13 : 24.** Rear spar  $AD$  is spruce,  $\frac{3}{4}$  in. by 3 in. Front spar  $EH$  is 1 in. by 4 in. Compression ribs are all  $1\frac{1}{4}$  in. by  $1\frac{1}{4}$  in. square spruce members. All wires are steel ( $E = 29,000,000$ ) and were rigged to an initial tension of 500 lb. each before the panel loads shown were applied. Determine the final loads in all members.



PROB. 13 : 24

**13 : 25.** Assuming the wires of Prob. 13 : 24 to be replaced by 1 by 0.049 steel tubes throughout, all wood members remaining unchanged, determine the loads in all members of the truss by the method of least work.



PROB. 13 : 28

**13 : 26.** Determine the reaction at  $c$  of Prob. 13 : 8 by the method of least work.

**13 : 27.** Determine the axial load in wire  $BC$  of Prob. 13 : 19 by the method of least work.

**13 : 28.** The sketch shows the dimensions of and loads on the upper wing and lift wires of a biplane. The loads of

3,500 and 1,285 lb. represent the lift components of upper and lower wing which are transmitted to the lift wires at the points shown. The 115- and 310-lb. loads

are drag components from the interplane struts. These combine with a 200-lb. drag load to give the 625-lb. at  $F$ . The 180- and 200-lb. loads are due to the drag on the upper wing (anti-drag in this case).

Determine the axial loads in all lift and drag truss wires, in the spars and compression ribs. Assume that the work due to bending of the spars is negligible.

**13 : 29.** Determine the stresses due to axial loads, bending, and torsion in the tubular members of this chassis when in the deflected position, shown dotted. The vertical component of the applied load is 7,660 lb.; the drag component is 4,680 lb. acting toward the tail post. There is no side component on the wheel.

All tubes are chrome-molybdenum steel except the axle which is heat-treated nickel tubing.

Strut  $OB$  is  $1\frac{3}{4}$  by 0.049

Strut  $OC$  is  $2\frac{1}{2}$  by 0.049

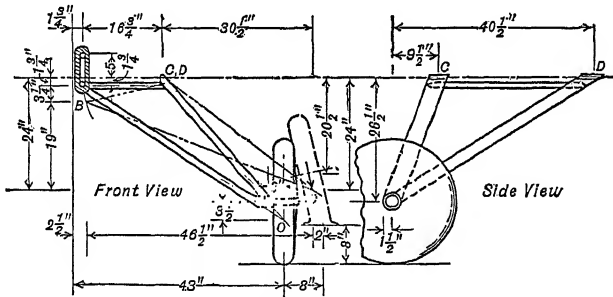
Strut  $OD$  is  $1\frac{3}{4}$  by 0.049

Strut  $BC$  is  $1\frac{3}{4}$  by 0.049

Strut  $BD$  is  $\frac{5}{8}$  by 0.035

All tubes are drawn streamline sections conforming to profile of Fig. 10 : 21 of Volume I.

The structure shown here is a trial design. Joint  $B$  takes only vertical load through the shock chord.  $CD$  represents the hinge line. All joints are welded.

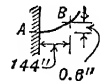


PROB. 13 : 29

**13 : 30.** By the use of Maxwell's theorem construct an influence line for a reaction at  $a$  on the structure of Prob. 12 : 28, assuming one to be introduced there, and determine its magnitude if the 12,000-lb. loads are applied to the truss at all lower chord joints, including  $a$ .

**13 : 31.** Remove the 200-lb. load from point  $b$  of the structure of Prob. 13 : 8 and draw a curve of deflections, ordinates every 10 in., for the beam under a 100-lb. upward force at  $c$ . Construct an influence line for reaction at  $c$ , and check the result obtained in Prob. 13 : 8.

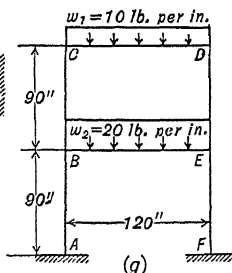
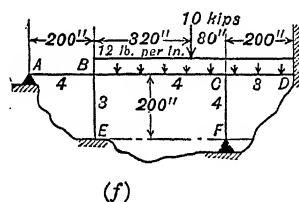
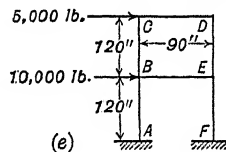
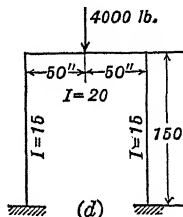
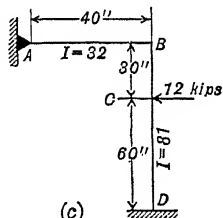
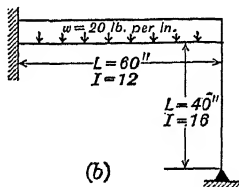
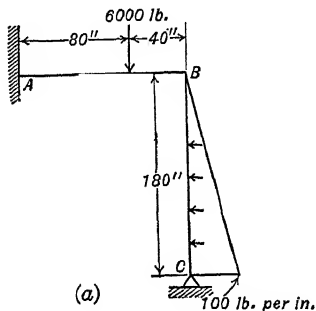
**13 : 32.** A fuselage for a very large airplane is built with a rectangular steel frame which is covered with birch plywood  $\frac{3}{8}$  in. thick. The designing engineer arbitrarily assumes 75 per cent of the load to be carried by the frame and the other 25 per cent to be taken by the plywood. On this basis a computation of the deflections of the frame shows that the first panel point, 12 ft. behind the point of attachment to the wings at point  $A$ , deflects 0.6 in. above the tangent at  $A$ . The curve of deflections is



PROB. 13 : 32

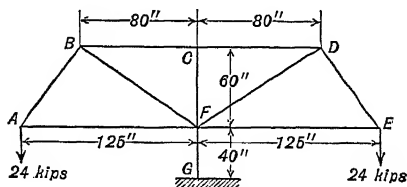
essentially a circular arc and can be assumed to be circular. What is the stress in the birch plywood covering at point  $A$  if  $E = 2,200,000$  p.s.i.,  $I = 515,000$  in.<sup>4</sup>, and  $y = 115$  in.?

**13 : 33.** Compute the end moments of the members, and draw bending-moment diagrams for the structures shown. Use method of Maxwell-Mohr, moment distribution, or slope deflection, as specified.



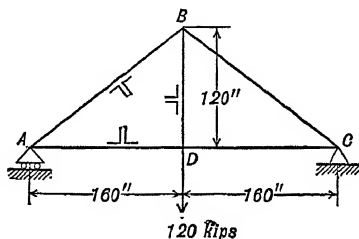
PROB. 13 : 33

**13 : 34.** Compute the secondary stresses at the joints and the maximum combined unit stress in each member of the rigid frame shown. Assume that all members are channels 4.00 in. deep, with  $A = 2.5$  sq. in. and  $I = 6.00$  in.<sup>4</sup>. Construct a bending-moment diagram for the structure with all ordinates on the compression sides of the members.



PROB. 13 : 34

**13 : 35.** Compute the angular rotations of the members of the truss shown, using the cotangent formula and checking by a Williot diagram. Compute the secondary bending moments due to rigidity of the joints, and construct a bending-moment diagram for the structure.  $AB$  and  $BC$  are pairs of 7 by 4 by  $\frac{3}{8}$  in. angles.  $AD$  and  $CD$  are pairs of 4 by 3 by  $\frac{1}{2}$  in. angles, and  $BD$  is a pair of 5 by  $3\frac{1}{2}$  by  $\frac{3}{8}$  in. angles. In all cases the short legs are normal to the plane of the truss, and in the chord members they are along the perimeter of the truss.



PROB. 13 : 35

**13 : 36.** Check the total end moments computed in the example of Art. 13 : 22 by carrying out the distributions omitted from Fig. 13 : 12.

**13 : 37.** Check the results obtained in the example of Art. 13 : 23, carrying out in full the steps omitted from the text.

## CHAPTER XIV

### BEAM-COLUMNS

One of the most interesting types of airplane member that the structural engineer is called upon to design is the "beam-column," or member subjected simultaneously to axial and bending loads, particularly that in which the axial load is one of compression. Such members are very common in all types of structural work, but in most fields it is allowable to make conservative assumptions which permit the members to be designed with little more difficulty than is involved in the investigation of an ordinary column or simple beam. As such assumptions must be conservative, they involve making the members heavier than necessary, and since the importance of economy of weight is greater in airplane design than in most structural work the aeronautical engineer is not satisfied with their use. Furthermore, the airplane designer is in the habit of using long and slender columns for which the usual assumptions that are satisfactory in bridge and building design are not conservative, but exceedingly unsafe.

Basic formulas for beam-columns were published by Müller-Breslau in 1902 or earlier, but they were so difficult to use and of so little practical advantage in structural work that they were neglected. During the War, Müller-Breslau worked out his formulas in more detail and supplied tables of complex functions that made possible their use in practical design. At the same time the English, working independently, developed similar equations and tables of functions. The English equations and tables were put into their most useful form by Arthur Berry and are usually known by his name.

The Berry formulas were adopted by the United States Navy during the War, but the Army continued to employ certain approximate formulas. In 1922 a thorough study of the problem was begun by the Engineering Division of the Army Air Corps in which it was found that the Berry and Müller-Breslau formulas were fundamentally identical, the only differences being in nomenclature and in the location of the origin. Neither set of formulas was adopted, however, as it was believed that a set resting on the same theoretical basis but much easier to apply could be developed. Such formulas were worked out by the present authors for the case covered by Berry and the more

important ones covered by Müller-Breslau, and also for certain cases often arising in airplane design but covered by neither. At the same time sufficient experimental work was done to demonstrate that the use of the formulas was justified.

**14 : 1. General Effect of an Axial Load** — Owing to the side load alone, the strut, Fig. 14 : 1, would deflect a distance,  $y'$ , at a distance  $x$  from the left support, and the bending moment at that point would be

$$M = \frac{wx}{2} - \frac{wLx}{2}$$

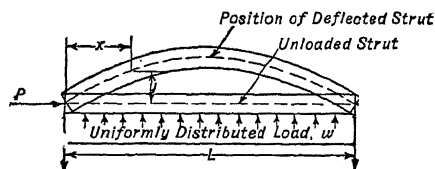


FIG. 14 : 1

If a compressive load,  $P$ , were to be applied as shown, the moment at  $x$  would be increased by  $-Py'$ , since the load,  $P$ , would act at a distance,  $y'$ , from the axis of the deflected member. This increase in moment would cause a greater deflection at  $x$  which, in turn, would result in a further increase in the moment. If the load,  $P$ , were not too great, these increments of the moment and deflection would become smaller and smaller until, eventually, the strut would reach a state of equilibrium. If, however, the load,  $P$ , were sufficiently large, the increments of deflection would be successively greater and greater until failure occurred. It is apparent, then, that it should be possible to represent increments of deflection or bending moment by a mathematical series of some kind which, if the axial compression were not too great, would converge, so that the limit of the series could be taken to represent conditions when the member reached a state of equilibrium.

The bending moment that would be caused by the lateral load acting alone is called the "primary bending moment," and the deflection under that load acting alone is the "primary deflection." The sums of the infinite series of increments of bending moment and deflection due to the interaction of the axial and lateral loads are called the "secondary" bending moments and deflections.

If  $P$  were tension instead of compression, the deflection,  $y'$ , due to the side load alone would be reduced instead of increased; and, as  $P$  was increased, the beam would tend to straighten and the moment at any point would be reduced. The failure, when it occurred, would be a tension failure, and there would be no tendency toward elastic instability or buckling as would be the case with a compressive axial load.

Thus it is evident that an axial compressive load, which increases the bending moment at every point, is of far greater importance in the

design of members under combined loads than an axial tension, which tends to decrease the bending moment. For this reason the formulas developed in this chapter apply mainly to cases including a compressive load, although some attention has been given to axial tension.

If the member is continuous over two or more supports, the bending moments will be increased throughout by the application of an axial compressive load. The ordinary three-moment equation, which would be used on a continuous beam in conjunction with any of the standard approximate methods for evaluating the effect of the axial load, makes no provision for this change in moment over the supports and so vitiates the effect of any power series or other device used in such formulas. The methods developed in this chapter, however, provide for the axial load both in the three-moment equation and in the formulas for the moments in the spans by the use of mathematical series. It so happens that the series used with axial compression are identical with those of the trigonometric functions, sines, cosines, and tangents.

In working with the formulas of this chapter the term "sin  $x$ " should always be thought of as representing the infinite series

$$\sin x = x - \frac{x^3}{!3} + \frac{x^5}{!5} - \frac{x^7}{!7} + \dots$$

and "cos  $x$ " the series

$$\cos x = 1 - \frac{x^2}{!2} + \frac{x^4}{!4} - \frac{x^6}{!6} + \dots$$

instead of ratios between the sides of a right triangle. The other functions such as  $\tan x$  and  $\sec x$  should be thought of as quotients, reciprocals, etc., of the basic  $\sin x$  and  $\cos x$  series, the relationships being those with which the reader is familiar from his study of trigonometry. It is quite correct mathematically to consider the relationships between the sides of a right triangle usually employed to define the sine and cosine of  $x$  to be coincidences that are true when one angle of a right triangle is  $x$  radians in magnitude. If the reader will get the habit of thinking of the sine and other "trigonometrical" functions as abbreviations for the corresponding infinite series, he will find it much easier to see the justification for the use of the formulas and will not spend his time looking in vain for angles that do not exist, nor will he doubt the validity of the formulas because the angles cannot be found. If  $\sin x$  is thought of as a trigonometrical relationship only, its appearance in the formulas will seem absurd, but if thought of as an infinite series its appearance becomes most appropriate.

**14 : 2. Derivation of the Formulas** — The derivation of the formulas for the most common type of loading, a uniformly distributed lateral load in conjunction with an axial compression, is carried out in detail in this and the next article while the expressions for other types of loading are given in Art. 14 : 5, so they may be used when needed in design work. For brevity, computations involving only simple algebra or arithmetic are omitted.

Figure 14 : 2 shows a member supported at two points and subjected to a uniformly distributed transverse load, an axial compression, and restraining moments applied at the points of support.

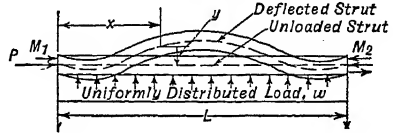


FIG. 14 : 2

The expression for the moment at any point is

$$M = M_1 + \frac{-M_1}{L}x - \frac{wLx}{2} + \frac{wx^2}{2} - Py \quad 14 : 1$$

Differentiating twice with respect to  $x$ , and making the usual assumption of the beam theory, that  $d^2y/dx^2 = M/EI$ , we obtain

$$\frac{d^2M}{dx^2} + \frac{P}{EI}M = w$$

If we write  $j^2$  for  $EI/P$ , this becomes

$$\frac{d^2M}{dx^2} + \frac{M}{j^2} = w \quad a$$

One form of the complete solution of this differential equation is

$$M = C_1 \sin \frac{x}{j} + C_2 \cos \frac{x}{j} + wj^2 \quad 14 : 2$$

$C_1$  and  $C_2$  being the constants of integration.

When  $x = 0$ ,  $M = M_1$ , and when  $x = L$ ,  $M = M_2$ ; hence

$$C_1 = \frac{M_2 - wj^2}{\sin \frac{L}{j}} - \frac{M_1 - wj^2}{\tan \frac{L}{j}} = \frac{M_2 - wj^2 - (M_1 - wj^2) \cos \frac{L}{j}}{\sin \frac{L}{j}}$$

and

$$C_2 = M_1 - wj^2$$



For brevity:

$$D_1 = M_1 - wj^2$$

and

$$D_2 = M_2 - wj^2$$

The moment at any point on the span is

$$M = \frac{D_2 - D_1 \cos \frac{L}{j}}{\sin \frac{L}{j}} \sin \frac{x}{j} + D_1 \cos \frac{x}{j} + wj^2 \quad 14 : 3$$

To find the location of the section of maximum moment, differentiate Eq. 14 : 2, equate the first derivative to zero, and solve; whence

$$\frac{dM}{dx} = 0 = \frac{C_1}{j} \cos \frac{x}{j} - \frac{C_2}{j} \sin \frac{x}{j}$$

and

$$\tan \frac{x}{j} = \frac{C_1}{C_2} = \frac{D_2 - D_1 \cos \frac{L}{j}}{D_1 \sin \frac{L}{j}} \quad 14 : 4$$

From the value of  $x/j$ , determined from Eq. 14 : 4 and the use of Table 14 : 1, the distance,  $x$ , to the section of maximum moment, is readily obtained. The value of  $x$ , obtained in this way, must lie between zero and  $L$ . Otherwise, either  $M_1$  or  $M_2$  is the maximum on the member.

The maximum moment may be found by substituting the value from Eq. 14 : 4 in Eq. 14 : 3 and simplifying:

$$M_{\max} = \frac{D_1}{\cos \frac{x}{j}} + wj^2 \quad 14 : 5$$

The bending moment determined from Eq. 14 : 5 is the moment at the section where the slope of the moment curve changes sign. It may be either a maximum or a minimum numerically, and may also be smaller than the bending moments at the ends of the span. Even though it is not the largest bending moment on the beam the margin of safety at its section should always be investigated as it is likely to be critical, the allowable unit stress being smaller between supports than at a support.

The deflection at any point is found by substituting the value of  $M$  from Eq. 14 : 2 in Eq. 14 : 1 and solving for  $y$ ,

$$y = \frac{1}{P} \left( M_1 + \frac{M_2 - M_1}{L} x - \frac{wLx}{2} + \frac{wx^2}{2} - \frac{D_2 - D_1 \cos \frac{L}{j}}{\sin \frac{L}{j}} \sin \frac{x}{j} - D_1 \cos \frac{x}{j} - wj^2 \right) \quad 14 : 6$$

The first derivative of Eq. 14 : 6 gives the slope of the tangent to the elastic curve at any point:

$$\theta^1 = \frac{1}{P} \left( \frac{M_2 - M_1}{L} - \frac{wL}{2} + wx - \frac{C_1}{j} \cos \frac{x}{j} + \frac{C_2}{j} \sin \frac{x}{j} \right) \quad 14 : 7$$

Since  $L/j$  and  $x/j$  are first computed as numbers, the formulas of this chapter are very awkward to apply when the engineer has available only the common type of trigonometric tables with the argument in degrees and fractions. The constant shift from radian measure to degree measure and back again is not only tedious and annoying but reduces the precision of the computations and increases the chances of error. This is particularly true when  $L/j$  or  $x/j$  exceeds  $\pi/2$ . To facilitate the use of these formulas the authors present the following table of sines, cosines, and tangents of natural numbers from 0 to 3.50 at intervals of 0.01. These tables will be found more useful than the common type in all computations involving small angles most conveniently expressed in radian measure, such as angles of beam slope.

One convenient feature of Table 14 : 1 is that the table of cosines may be used as a table of differences between adjoining values in the table of sines, and vice versa. From Taylor's theorem

$$f(x + a) = f(x) + \frac{df(x)}{dx} a + \frac{d^2f(x)}{dx^2} \frac{a^2}{!2} + \frac{d^3f(x)}{dx^3} \frac{a^3}{!3} + \dots$$

When  $f(x) = \sin x$  and  $a = 0.01$  this becomes

$$\sin(x + 0.01) = \sin x + 0.01 \cos x - 0.00005 \sin x - 0.00000017 \cos x + \dots$$

Thus the difference between any two adjoining values in the table of

<sup>1</sup> Since  $\alpha$  is used in this chapter to represent one of the functions employed with the equation of three moments, slope angles will be indicated by  $\theta$ .

TABLE 14 : 1

NATURAL SINES, COSINES, AND TANGENTS OF ANGLES IN RADIANS

$L/j$ in radians	Sine $\frac{L}{j}$	Cosine $\frac{L}{j}$	Tangent $\frac{L}{j}$	$L/j$ in radians	Sine $\frac{L}{j}$	Cosine $\frac{L}{j}$	Tangent $\frac{L}{j}$
0.00	0.00000	1.00000	0.00000	0.50	0.47943	0.87758	0.54630
0.01	0.01000	0.99995	0.01000	0.51	0.48818	0.87274	0.55936
0.02	0.02000	0.99980	0.02000	0.52	0.49688	0.86782	0.57256
0.03	0.03000	0.99955	0.03001	0.53	0.50553	0.86281	0.58592
0.04	0.03999	0.99920	0.04002	0.54	0.51414	0.85771	0.59943
0.05	0.04998	0.99875	0.05004	0.55	0.52269	0.85252	0.61311
0.06	0.05996	0.99820	0.06007	0.56	0.53119	0.84726	0.62695
0.07	0.06994	0.99755	0.07011	0.57	0.53963	0.84190	0.64097
0.08	0.07991	0.99680	0.08017	0.58	0.54802	0.83646	0.65517
0.09	0.08988	0.99595	0.09024	0.59	0.55636	0.83094	0.66956
0.10	0.09983	0.99500	0.10033	0.60	0.56464	0.82534	0.68414
0.11	0.10978	0.99396	0.11045	0.61	0.57287	0.81965	0.69892
0.12	0.11971	0.99281	0.12058	0.62	0.58104	0.81388	0.71391
0.13	0.12963	0.99156	0.13074	0.63	0.58914	0.80803	0.72911
0.14	0.13954	0.99022	0.14092	0.64	0.59720	0.80210	0.74454
0.15	0.14944	0.98877	0.15114	0.65	0.60519	0.79608	0.76020
0.16	0.15932	0.98723	0.16138	0.66	0.61312	0.78999	0.77610
0.17	0.16918	0.98558	0.17166	0.67	0.62099	0.78382	0.79225
0.18	0.17903	0.98384	0.18197	0.68	0.62879	0.77757	0.80866
0.19	0.18886	0.98200	0.19232	0.69	0.63654	0.77125	0.82534
0.20	0.19867	0.98007	0.20271	0.70	0.64422	0.76484	0.84229
0.21	0.20846	0.97803	0.21314	0.71	0.65183	0.75836	0.85953
0.22	0.21823	0.97590	0.22362	0.72	0.65938	0.75181	0.87707
0.23	0.22798	0.97367	0.23414	0.73	0.66687	0.74517	0.89492
0.24	0.23770	0.97134	0.24472	0.74	0.67429	0.73847	0.91309
0.25	0.24740	0.96891	0.25534	0.75	0.68164	0.73169	0.93160
0.26	0.25708	0.96639	0.26602	0.76	0.68892	0.72484	0.95045
0.27	0.26673	0.96377	0.27676	0.77	0.69614	0.71791	0.96967
0.28	0.27636	0.96106	0.28755	0.78	0.70328	0.71091	0.98926
0.29	0.28595	0.95824	0.29841	0.79	0.71035	0.70385	1.00924
0.30	0.29552	0.95534	0.30934	0.80	0.71736	0.69671	1.02964
0.31	0.30506	0.95233	0.32033	0.81	0.72429	0.68950	1.05046
0.32	0.31457	0.94924	0.33139	0.82	0.73115	0.68222	1.07171
0.33	0.32404	0.94604	0.34252	0.83	0.73793	0.67488	1.09343
0.34	0.33349	0.94275	0.35374	0.84	0.74464	0.66746	1.11563
0.35	0.34290	0.93937	0.36503	0.85	0.75128	0.65998	1.13834
0.36	0.35227	0.93590	0.37640	0.86	0.75784	0.65244	1.16155
0.37	0.36162	0.93233	0.38786	0.87	0.76433	0.64483	1.18533
0.38	0.37092	0.92866	0.39941	0.88	0.77074	0.63715	1.20967
0.39	0.38019	0.92491	0.41105	0.89	0.77707	0.62941	1.23460
0.40	0.38942	0.92106	0.42279	0.90	0.78333	0.62161	1.26016
0.41	0.39861	0.91712	0.43463	0.91	0.78950	0.61375	1.28637
0.42	0.40776	0.91309	0.44657	0.92	0.79560	0.60582	1.31326
0.43	0.41687	0.90897	0.45862	0.93	0.80162	0.59783	1.34088
0.44	0.42594	0.90475	0.47078	0.94	0.80756	0.58979	1.36923
0.45	0.43497	0.90045	0.48306	0.95	0.81342	0.58168	1.39838
0.46	0.44395	0.89605	0.49545	0.96	0.81919	0.57352	1.42836
0.47	0.45289	0.89157	0.50797	0.97	0.82489	0.56530	1.45920
0.48	0.46178	0.88699	0.52061	0.98	0.83050	0.55702	1.49096
0.49	0.47063	0.88233	0.53339	0.99	0.83603	0.54869	1.52368
0.50	0.47943	0.87758	0.54630	1.00	0.84147	0.54030	1.55741

## DERIVATION OF THE FORMULAS

69

TABLE 14: 1 — (Continued)

NATURAL SINES, COSINES, AND TANGENTS OF ANGLES IN RADIANs

$L/j$ in radians	Sine $\frac{L}{j}$	Cosine $\frac{L}{j}$	Tangent $\frac{L}{j}$	$L/j$ in radians	Sine $\frac{L}{j}$	Cosine $\frac{L}{j}$	Tangent $\frac{L}{j}$
1.00	0.84147	0.54030	1.55741	1.50	0.99749	0.07074	14.10142
1.01	0.84683	0.53186	1.59221	1.51	0.99815	0.06076	16.42209
1.02	0.85211	0.52337	1.62813	1.52	0.99871	0.05077	19.66953
1.03	0.85730	0.51482	1.66525	1.53	0.99917	0.04079	24.49841
1.04	0.86240	0.50622	1.70361	1.54	0.99953	0.03079	32.46114
1.05	0.86742	0.49757	1.74332	1.55	0.99978	0.02079	48.07848
1.06	0.87236	0.48887	1.78442	1.56	0.99994	0.01080	92.62047
1.07	0.87720	0.48012	1.82703	1.57	1.00000	0.00080	1,255.76559
1.08	0.88196	0.47133	1.87122	1.58	0.99996	-0.00920	-108.64920
1.09	0.88663	0.46249	1.91710	1.59	0.99982	-0.01920	-52.06698
1.10	0.89121	0.45360	1.96476	1.60	0.99957	-0.02920	-34.23254
1.11	0.89570	0.44466	2.01434	1.61	0.99923	-0.03919	-25.49475
1.12	0.90010	0.43568	2.06595	1.62	0.99879	-0.04918	-20.30728
1.13	0.90441	0.42666	2.11975	1.63	0.99825	-0.05917	-16.87111
1.14	0.90863	0.41759	2.17588	1.64	0.99760	-0.06915	-14.42702
1.15	0.91276	0.40849	2.23449	1.65	0.99687	-0.07912	-12.59926
1.16	0.91680	0.39934	2.29580	1.66	0.99602	-0.08909	-11.18055
1.17	0.92075	0.39015	2.35998	1.67	0.99508	-0.09904	-10.04718
1.18	0.92461	0.38092	2.42726	1.68	0.99404	-0.10899	-9.12077
1.19	0.92837	0.37166	2.49790	1.69	0.99290	-0.11892	-8.34923
1.20	0.93204	0.36236	2.57215	1.70	0.99166	-0.12884	-7.69660
1.21	0.93562	0.35302	2.65033	1.71	0.99033	-0.13875	-7.13726
1.22	0.93910	0.34365	2.73276	1.72	0.98889	-0.14865	-6.65245
1.23	0.94249	0.33424	2.81982	1.73	0.98735	-0.15853	-6.22809
1.24	0.94578	0.32480	2.91194	1.74	0.98572	-0.16840	-5.85353
1.25	0.94898	0.31532	3.00957	1.75	0.98399	-0.17825	-5.52037
1.26	0.95209	0.30582	3.11328	1.76	0.98215	-0.18808	-5.22209
1.27	0.95510	0.29628	3.22363	1.77	0.98022	-0.19789	-4.95340
1.28	0.95802	0.28672	3.34135	1.78	0.97820	-0.20768	-4.71010
1.29	0.96084	0.27712	3.46721	1.79	0.97607	-0.21745	-4.48866
1.30	0.96356	0.26750	3.60210	1.80	0.97385	-0.22720	-4.28627
1.31	0.96618	0.25785	3.74708	1.81	0.97153	-0.23693	-4.10050
1.32	0.96872	0.24818	3.90335	1.82	0.96911	-0.24663	-3.92937
1.33	0.97115	0.23848	4.07231	1.83	0.96659	-0.25631	-3.77118
1.34	0.97348	0.22875	4.25562	1.84	0.96398	-0.26596	-3.62450
1.35	0.97572	0.21901	4.45523	1.85	0.96128	-0.27559	-3.48806
1.36	0.97786	0.20924	4.67344	1.86	0.95847	-0.28519	-3.36083
1.37	0.97991	0.19945	4.91306	1.87	0.95557	-0.29476	-3.24188
1.38	0.98185	0.18964	5.17744	1.88	0.95258	-0.30430	-3.13039
1.39	0.98370	0.17981	5.47069	1.89	0.94949	-0.31381	-3.02566
1.40	0.98545	0.16997	5.79788	1.90	0.94630	-0.32329	-2.92710
1.41	0.98710	0.16010	6.16537	1.91	0.94302	-0.33274	-2.83414
1.42	0.98865	0.15023	6.58112	1.92	0.93965	-0.34215	-2.74630
1.43	0.99010	0.14033	7.05546	1.93	0.93618	-0.35153	-2.66316
1.44	0.99146	0.13042	7.60182	1.94	0.93261	-0.36087	-2.58433
1.45	0.99271	0.12050	8.23810	1.95	0.92896	-0.37018	-2.50947
1.46	0.99387	0.11057	8.98862	1.96	0.92521	-0.37945	-2.43828
1.47	0.99492	0.10063	9.88738	1.97	0.92137	-0.38868	-2.37049
1.48	0.99588	0.09067	10.98338	1.98	0.91744	-0.39788	-2.30582
1.49	0.99674	0.08071	12.34986	1.99	0.91341	-0.40703	-2.24408
1.50	0.99749	0.07074	14.10142	2.00	0.90930	-0.41615	-2.18504

TABLE 14:1 — (Continued)

NATURAL SINES, COSINES, AND TANGENTS OF ANGLES IN RADIANS

$L/j$ in radians	Sine $\frac{L}{j}$	Cosine $\frac{L}{j}$	Tangent $\frac{L}{j}$	$L/j$ in radians	Sine $\frac{L}{j}$	Cosine $\frac{L}{j}$	Tangent $\frac{L}{j}$
2.00	0.90930	-0.41615	-2.18504	2.50	0.59847	-0.80114	-0.74702
2.01	0.90509	-0.42522	-2.12853	2.51	0.59043	-0.80709	-0.73156
2.02	0.90079	-0.43425	-2.07437	2.52	0.58233	-0.81295	-0.71632
2.03	0.89641	-0.44323	-2.02242	2.53	0.57417	-0.81873	-0.70129
2.04	0.89193	-0.45218	-1.97252	2.54	0.56596	-0.82444	-0.68648
2.05	0.88736	-0.46107	-1.92456	2.55	0.55768	-0.83005	-0.67186
2.06	0.88271	-0.46992	-1.87841	2.56	0.54936	-0.83559	-0.65745
2.07	0.87796	-0.47873	-1.83396	2.57	0.54097	-0.84104	-0.64322
2.08	0.87313	-0.48748	-1.79112	2.58	0.53253	-0.84641	-0.62917
2.09	0.86821	-0.49619	-1.74977	2.59	0.52405	-0.85169	-0.61530
2.10	0.86321	-0.50485	-1.70984	2.60	0.51550	-0.85689	-0.60160
2.11	0.85812	-0.51345	-1.67127	2.61	0.50691	-0.86200	-0.58806
2.12	0.85294	-0.52201	-1.63395	2.62	0.49826	-0.86703	-0.57468
2.13	0.84768	-0.53051	-1.59785	2.63	0.48957	-0.87197	-0.56145
2.14	0.84233	-0.53896	-1.56287	2.64	0.48082	-0.87682	-0.54837
2.15	0.83690	-0.54738	-1.52898	2.65	0.47203	-0.88158	-0.53544
2.16	0.83138	-0.55570	-1.49610	2.66	0.46319	-0.88626	-0.52264
2.17	0.82579	-0.56399	-1.46419	2.67	0.45431	-0.89085	-0.50997
2.18	0.82010	-0.57221	-1.43321	2.68	0.44537	-0.89534	-0.49743
2.19	0.81434	-0.58039	-1.40310	2.69	0.43640	-0.89975	-0.48502
2.20	0.80850	-0.58850	-1.37382	2.70	0.42738	-0.90407	-0.47273
2.21	0.80257	-0.59656	-1.34534	2.71	0.41832	-0.90830	-0.46055
2.22	0.79657	-0.60455	-1.31761	2.72	0.40921	-0.91244	-0.44848
2.23	0.79048	-0.61249	-1.29060	2.73	0.40007	-0.91648	-0.43653
2.24	0.78432	-0.62036	-1.26429	2.74	0.39088	-0.92044	-0.42467
2.25	0.77807	-0.62817	-1.23863	2.75	0.38166	-0.92430	-0.41292
2.26	0.77175	-0.63592	-1.21360	2.76	0.37240	-0.92807	-0.40126
2.27	0.76535	-0.64361	-1.18916	2.77	0.36310	-0.93175	-0.38970
2.28	0.75888	-0.65123	-1.16531	2.78	0.35376	-0.93533	-0.37822
2.29	0.75233	-0.65879	-1.14199	2.79	0.34439	-0.93883	-0.36683
2.30	0.74571	-0.66628	-1.11921	2.80	0.33499	-0.94222	-0.35553
2.31	0.73901	-0.67370	-1.09694	2.81	0.32555	-0.94553	-0.34431
2.32	0.73223	-0.68106	-1.07514	2.82	0.31608	-0.94873	-0.33316
2.33	0.72538	-0.68834	-1.05381	2.83	0.30658	-0.95185	-0.32208
2.34	0.71846	-0.69556	-1.03292	2.84	0.29704	-0.95486	-0.31108
2.35	0.71147	-0.70271	-1.01247	2.85	0.28748	-0.95779	-0.30015
2.36	0.70441	-0.70979	-0.99242	2.86	0.27789	-0.96061	-0.28928
2.37	0.69728	-0.71680	-0.97276	2.87	0.26827	-0.96334	-0.27847
2.38	0.69007	-0.72374	-0.95349	2.88	0.25862	-0.96598	-0.26773
2.39	0.68280	-0.73060	-0.93457	2.89	0.24895	-0.96852	-0.25704
2.40	0.67546	-0.73739	-0.91602	2.90	0.23925	-0.97096	-0.24641
2.41	0.66806	-0.74411	-0.89779	2.91	0.22953	-0.97330	-0.23582
2.42	0.66058	-0.75075	-0.87989	2.92	0.21978	-0.97555	-0.22529
2.43	0.65304	-0.75732	-0.86230	2.93	0.21002	-0.97770	-0.21481
2.44	0.64544	-0.76382	-0.84502	2.94	0.20023	-0.97975	-0.20437
2.45	0.63776	-0.77023	-0.82801	2.95	0.19042	-0.98170	-0.19397
2.46	0.63003	-0.77657	-0.81130	2.96	0.18060	-0.98356	-0.18362
2.47	0.62223	-0.78283	-0.79485	2.97	0.17075	-0.98531	-0.17330
2.48	0.61437	-0.78901	-0.77866	2.98	0.16089	-0.98697	-0.16301
2.49	0.60645	-0.79512	-0.76272	2.99	0.15101	-0.98853	-0.15277
2.50	0.59847	-0.80114	-0.74703	3.00	0.14112	-0.98999	-0.14255

TABLE 14 : 1 — (Concluded)  
NATURAL SINES, COSINES, AND TANGENTS OF ANGLES IN RADIANS

$L/j$ in radians	Sine $\frac{L}{j}$	Cosine $\frac{L}{j}$	Tangent $\frac{L}{j}$	$L/j$ in radians	Sine $\frac{L}{j}$	Cosine $\frac{L}{j}$	Tangent $\frac{L}{j}$
3.00	0.14112	-0.98999	-0.14255	3.25	-0.10820	-0.99413	0.10883
3.01	0.13121	-0.99135	-0.13235	3.26	-0.11813	-0.99300	0.11896
3.02	0.12129	-0.99262	-0.12219	3.27	-0.12805	-0.99177	0.12912
3.03	0.11136	-0.99378	-0.11206	3.28	-0.13797	-0.99044	0.13930
3.04	0.10142	-0.99484	-0.10195	3.29	-0.14786	-0.98901	0.14951
3.05	0.09146	-0.99581	-0.09185				
3.06	0.08150	-0.99667	-0.08177	3.30	-0.15775	-0.98748	0.15975
3.07	0.07153	-0.99744	-0.07171	3.31	-0.16761	-0.98585	0.17002
3.08	0.06155	-0.99810	-0.06167	3.32	-0.17746	-0.98413	0.18033
3.09	0.05157	-0.99867	-0.05164	3.33	-0.18729	-0.98230	0.19067
				3.34	-0.19711	-0.98038	0.20105
3.10	0.04158	-0.99914	-0.04162	3.35	-0.20690	-0.97836	0.21148
3.11	0.03159	-0.99950	-0.03161	3.36	-0.21668	-0.97624	0.22195
3.12	0.02159	-0.99977	-0.02160	3.37	-0.22643	-0.97403	0.23246
3.13	0.01159	-0.99993	-0.01160	3.38	-0.23616	-0.97172	0.24303
3.14	0.00159	-1.00000	-0.00159	3.39	-0.24586	-0.96931	0.25365
3.15	-0.00841	-0.99996	0.00841				
3.16	-0.01841	-0.99983	0.01841	3.40	-0.25554	-0.96680	0.26432
3.17	-0.02840	-0.99960	0.02841	3.41	-0.26520	-0.96419	0.27504
3.18	-0.03840	-0.99926	0.03843	3.42	-0.27482	-0.96149	0.28583
3.19	-0.04839	-0.99883	0.04845	3.43	-0.28443	-0.95870	0.29668
				3.44	-0.29400	-0.95581	0.30759
3.20	-0.05837	-0.99829	0.05847	3.45	-0.30354	-0.95282	0.31857
3.21	-0.06835	-0.99766	0.06852	3.46	-0.31305	-0.94974	0.32962
3.22	-0.07833	-0.99693	0.07857	3.47	-0.32254	-0.94656	0.34074
3.23	-0.08829	-0.99609	0.08864	3.48	-0.33199	-0.94328	0.35195
3.24	-0.09825	-0.99516	0.09873	3.49	-0.34140	-0.93992	0.36322
3.25	-0.10820	-0.99413	0.10883	3.50	-0.35078	-0.93646	0.37459

sines can be seen to be very nearly equal to 0.01 times the value of corresponding cosines.

In preparing Table 14 : 1 many of the values of sines and cosines were checked by the use of the formulas on page 64 for values of the argument differing by 0.1 and interpolating the intermediate values by means of the above formula derived from Taylor's theorem. The same system is useful in the occasional situation when it is desired to obtain trigonometric functions to a greater number of significant figures than are available in published tables.

No such simple method of interpolating in the table of tangents is available since  $\frac{d}{dx} \tan x = \sec^2 x$ . Therefore when a straight line interpolation to obtain a tangent is considered insufficiently precise, the best method is to compute  $\sin x$  and  $\cos x$  by the method suggested above, the tangent then being found by division.

No cotangents, secants, or cosecants are listed in Table 14 : 1, but they can easily be computed when desired since they are reciprocals of the functions that are tabulated.

TABLE 14 : 2  
FUNCTIONS FOR THREE-MOMENT EQUATIONS —  $\alpha$ ,  $\beta$ , AND  $\gamma$  FUNCTIONS FOR AXIAL  
COMPRESSION

$$6 (L/j \operatorname{cosec} L/j - 1)$$

$$3 (1 - L/j \cot L/j)$$

$$3 (\tan L/2j - L/2j)$$

A general relation existing between  $\alpha$ ,  $\beta$ , and  $\gamma$  is  $\alpha + 2\beta - 3 = \gamma (L/2j)^2$

$\Delta\beta$				$L/j$			
0	1.0000	0.0008	1.0000	1.0000	0.0010	0	0
0.10	1.0008	0.0039	1.0007	0.0020	1.0010	0.0030	0.10
0.20	1.0047	0.0059	1.0027	0.0034	1.0040	0.0051	0.20
0.30	1.0106	0.0083	1.0061	0.0047	1.0091	0.0072	0.30
0.40	1.0189	0.0110	1.0108	0.0063	1.0163	0.0094	0.40
0.50	1.0299	0.0138	1.0171	0.0078	1.0257	0.0117	0.50
0.60	1.0437	0.0166	1.0249	0.0094	1.0374	0.0142	0.60
0.70	1.0603	0.0198	1.0343	0.0111	1.0516	0.0168	0.70
0.80	1.0801	0.0232	1.0454	0.0131	1.0684	0.0198	0.80
0.90	1.1033	0.0271	1.0585	0.0152	1.0882	0.0231	0.90
1.00	1.1304	0.0315	1.0737	0.0185	1.1113	0.0268	1.00
1.05	1.1455	0.0362	1.0822	0.0200	1.1241	0.0283	1.05
1.10	1.1617	0.0415	1.0912	0.0215	1.1379	0.0298	1.10
1.15	1.1792	0.0475	1.1009	0.0230	1.1527	0.0313	1.15
1.20	1.1979	0.0540	1.1114	0.0245	1.1686	0.0328	1.20
1.25	1.2180	0.0610	1.1225	0.0260	1.1856	0.0343	1.25
1.30	1.2396	0.0685	1.1345	0.0275	1.2039	0.0358	1.30
1.35	1.2628	0.0765	1.1473	0.0290	1.2235	0.0373	1.35
1.40	1.2878	0.0850	1.1610	0.0305	1.2445	0.0388	1.40
1.45	1.3146	0.0940	1.1757	0.0320	1.2671	0.0403	1.45
1.50	1.3434	0.1035	1.1915	0.0335	1.2914	0.0418	1.50
1.55	1.3744	0.1135	1.2084	0.0350	1.3174	0.0433	1.55
1.60	1.4078	0.1240	1.2266	0.0365	1.3455	0.0448	1.60
1.65	1.4439	0.1350	1.2462	0.0380	1.3758	0.0463	1.65
1.70	1.4830	0.1465	1.2673	0.0395	1.4085	0.0478	1.70
1.75	1.5252	0.1585	1.2901	0.0410	1.4438	0.0493	1.75
1.80	1.5710	0.1710	1.3147	0.0425	1.4821	0.0508	1.80
1.85	1.6208	0.1840	1.3414	0.0440	1.5237	0.0523	1.85
1.90	1.6750	0.1975	1.3704	0.0455	1.5689	0.0538	1.90
1.95	1.7343	0.2115	1.4020	0.0470	1.6182	0.0553	1.95
2.00	1.7993	0.2260	1.4365	0.0485	1.6722	0.0568	2.00

TABLE 14 : 2

FUNCTIONS FOR THREE-MOMENT EQUATIONS —  $\alpha$ ,  $\beta$ , AND  $\gamma$  FUNCTIONS FOR AXIAL COMPRESSION — (Continued)

$L/j$	$\alpha$	$\Delta\alpha$	$\beta$	$\Delta\beta$	$\gamma$	$\Delta\gamma$	$L/j$
2.00	1.7993		1.4365		1.6722		2.00
		0.0137		0.0073		0.0114	
2.01	1.8130		1.4438		1.6836		2.01
		0.0140		0.0074		0.0117	
2.02	1.8270		1.4512		1.6953		2.02
		0.0143		0.0075		0.0118	
2.03	1.8413		1.4587		1.7071		2.03
		0.0145		0.0077		0.0121	
2.04	1.8558		1.4664		1.7192		2.04
		0.0148		0.0078		0.0122	
2.05	1.8706		1.4742		1.7314		2.05
		0.0152		0.0080		0.0126	
2.06	1.8858		1.4822		1.7440		2.06
		0.0154		0.0082		0.0128	
2.07	1.9012		1.4904		1.7568		2.07
		0.0156		0.0083		0.0130	
2.08	1.9168		1.4987		1.7698		2.08
		0.0161		0.0084		0.0134	
2.09	1.9329		1.5071		1.7832		2.09
		0.0164		0.0087		0.0135	
2.10	1.9493		1.5158		1.7967		2.10
		0.0168		0.0088		0.0139	
2.11	1.9661		1.5246		1.8106		2.11
		0.0170		0.0090		0.0141	
2.12	1.9831		1.5336		1.8247		2.12
		0.0174		0.0091		0.0145	
2.13	2.0005		1.5427		1.8392		2.13
		0.0179		0.0094		0.0147	
2.14	2.0184		1.5521		1.8539		2.14
		0.0182		0.0095		0.0150	
2.15	2.0366		1.5616		1.8689		2.15
		0.0186		0.0097		0.0154	
2.16	2.0552		1.5713		1.8843		2.16
		0.0189		0.0100		0.0157	
2.17	2.0741		1.5813		1.9000		2.17
		0.0194		0.0101		0.0160	
2.18	2.0935		1.5914		1.9160		2.18
		0.0198		0.0104		0.0163	
2.19	2.1133		1.6018		1.9323		2.19
		0.0203		0.0106		0.0168	
2.20	2.1336		1.6124		1.9491		2.20
		0.0207		0.0109		0.0172	
2.21	2.1543		1.6233		1.9663		2.21
		0.0211		0.0110		0.0174	
2.22	2.1754		1.6343		1.9837		2.22
		0.0218		0.0114		0.0179	
2.23	2.1972		1.6457		2.0016		2.23
		0.0222		0.0115		0.0183	
2.24	2.2194		1.6572		2.0199		2.24
		0.0228		0.0118		0.0187	
2.25	2.2422		1.6690		2.0386		2.25
		0.0232		0.0122		0.0192	
2.26	2.2654		1.6812		2.0578		2.26



TABLE 14:2

FUNCTIONS FOR THREE-MOMENT EQUATIONS —  $\alpha$ ,  $\beta$ , AND  $\gamma$  FUNCTIONS FOR AXIAL COMPRESSION — (Continued)

$L/j$	$\alpha$	$\Delta\alpha$	$\beta$	$\Delta\beta$	$\gamma$	$\Delta\gamma$	$L/j$
2.26	2.2654		1.6812		2.0578		2.26
		0.0237		0.0124		0.0197	
2.27	2.2891		1.6936		2.0775		2.27
		0.0244		0.0126		0.0201	
2.28	2.3135		1.7062		2.0976		2.28
		0.0249		0.0130		0.0205	
2.29	2.3384		1.7192		2.1181		2.29
		0.0256		0.0133		0.0211	
2.30	2.3640		1.7325		2.1392		2.30
		0.0262		0.0136		0.0216	
2.31	2.3902		1.7461		2.1608		2.31
		0.0269		0.0140		0.0222	
2.32	2.4171		1.7601		2.1830		2.32
		0.0277		0.0143		0.0227	
2.33	2.4448		1.7744		2.2057		2.33
		0.0283		0.0147		0.0233	
2.34	2.4731		1.7891		2.2290		2.34
		0.0291		0.0150		0.0239	
2.35	2.5022		1.8041		2.2529		2.35
		0.0298		0.0154		0.0245	
2.36	2.5320		1.8195		2.2774		2.36
		0.0305		0.0159		0.0251	
2.37	2.5625		1.8354		2.3025		2.37
		0.0314		0.0162		0.0259	
2.38	2.5939		1.8516		2.3284		2.38
		0.0323		0.0167		0.0266	
2.39	2.6262		1.8683		2.3550		2.39
		0.0334		0.0171		0.0272	
2.40	2.6596		1.8854		2.3822		2.40
		0.0339		0.0177		0.0281	
2.41	2.6935		1.9031		2.4103		2.41
		0.0352		0.0181		0.0288	
2.42	2.7287		1.9212		2.4391		2.42
		0.0362		0.0186		0.0296	
2.43	2.7649		1.9398		2.4687		2.43
		0.0372		0.0191		0.0306	
2.44	2.8021		1.9589		2.4993		2.44
		0.0382		0.0197		0.0313	
2.45	2.8403		1.9786		2.5306		2.45
		0.0395		0.0203		0.0324	
2.46	2.8798		1.9989		2.5630		2.46
		0.0406		0.0209		0.0334	
2.47	2.9204		2.0198		2.5964		2.47
		0.0420		0.0215		0.0343	
2.48	2.9624		2.0413		2.6307		2.48
		0.0432		0.0222		0.0355	
2.49	3.0056		2.0635		2.6662		2.49
		0.0446		0.0229		0.0365	
2.50	3.0502		2.0864		2.7027		2.50
		0.0461		0.0236		0.0378	
2.51	3.0963		2.1100		2.7405		2.51
		0.0475		0.0243		0.0389	
2.52	3.1438		2.1343		2.7794		2.52

TABLE 14:2

FUNCTIONS FOR THREE-MOMENT EQUATIONS —  $\alpha$ ,  $\beta$ , AND  $\gamma$  FUNCTIONS FOR AXIAL COMPRESSION — (Continued)

$L/j$	$\alpha$	$\Delta\alpha$	$\beta$	$\Delta\beta$	$\gamma$	$\Delta\gamma$	$L/j$
2.52	3.1438	0.0493	2.1343	0.0252	2.7794	0.0403	2.52
2.53	3.1931	0.0506	2.1595	0.0260	2.8197	0.0415	2.53
2.54	3.2437	0.0526	2.1855	0.0269	2.8612	0.0431	2.54
2.55	3.2963	0.0545	2.2124	0.0278	2.9043	0.0445	2.55
2.56	3.3508	0.0564	2.2402	0.0288	2.9488	0.0461	2.56
2.57	3.4072	0.0585	2.2690	0.0298	2.9949	0.0478	2.57
2.58	3.4657	0.0605	2.2988	0.0309	3.0427	0.0495	2.58
2.59	3.5262	0.0628	2.3297	0.0321	3.0922	0.0513	2.59
2.60	3.5890	0.0652	2.3618	0.0332	3.1435	0.0533	2.60
2.61	3.6542	0.0678	2.3950	0.0345	3.1968	0.0554	2.61
2.62	3.7220	0.0705	2.4295	0.0359	3.2522	0.0575	2.62
2.63	3.7925	0.0734	2.4654	0.0373	3.3097	0.0599	2.63
2.64	3.8659	0.0762	2.5027	0.0388	3.3696	0.0623	2.64
2.65	3.9421	0.0797	2.5415	0.0404	3.4319	0.0650	2.65
2.66	4.0218	0.0829	2.5819	0.0422	3.4969	0.0677	2.66
2.67	4.1047	0.0867	2.6241	0.0439	3.5646	0.0707	2.67
2.68	4.1914	0.0906	2.6680	0.0460	3.6353	0.0739	2.68
2.69	4.2820	0.0946	2.7140	0.0479	3.7092	0.0771	2.69
2.70	4.3766	0.0991	2.7619	0.0502	3.7863	0.0808	2.70
2.71	4.4757	0.1038	2.8121	0.0527	3.8671	0.0846	2.71
2.72	4.5795	0.1090	2.8648	0.0551	3.9517	0.0888	2.72
2.73	4.6885	0.1144	2.9199	0.0579	4.0405	0.0932	2.73
2.74	4.8029	0.1204	2.9778	0.0608	4.1337	0.0980	2.74
2.75	4.9233	0.1266	3.0386	0.0641	4.2317	0.1032	2.75
2.76	5.0499	0.1336	3.1027	0.0675	4.3349	0.1087	2.76
2.77	5.1835	0.1410	3.1702	0.0712	4.4436	0.1148	2.77
2.78	5.3245		3.2414		4.5584		2.78

TABLE 14:2

FUNCTIONS FOR THREE-MOMENT EQUATIONS —  $\alpha$ ,  $\beta$ , AND  $\gamma$  FUNCTIONS FOR AXIAL COMPRESSION — (Continued)

$L/j$	$\alpha$	$\Delta\alpha$	$\beta$	$\Delta\beta$	$\gamma$	$\Delta\gamma$	$L/j$
2.78	5.3245		3.2414		4.5584		2.78
		0.1491		0.0752		0.1213	
2.79	5.4736		3.3166		4.6797		2.79
		0.1579		0.0797		0.1285	
2.80	5.6315		3.3963		4.8082		2.80
		0.1675		0.0844		0.1362	
2.81	5.7990		3.4807		4.9444		2.81
		0.1780		0.0897		0.1448	
2.82	5.9770		3.5704		5.0892		2.82
		0.1894		0.0955		0.1540	
2.83	6.1664		3.6659		5.2432		2.83
		0.2021		0.1017		0.1643	
2.84	6.3685		3.7676		5.4075		2.84
		0.2160		0.1088		0.1757	
2.85	6.5845		3.8764		5.5832		2.85
		0.2315		0.1164		0.1881	
2.86	6.8160		3.9928		5.7713		2.86
		0.2486		0.1251		0.2020	
2.87	7.0646		4.1179		5.9733		2.87
		0.2676		0.1346		0.2174	
2.88	7.3322		4.2525		6.1907		2.88
		0.2890		0.1452		0.2348	
2.89	7.6212		4.3977		6.4255		2.89
		0.3131		0.1573		0.2543	
2.90	7.9343		4.5550		6.6798		2.90
		0.3402		0.1709		0.2763	
2.91	8.2745		4.7259		6.9561		2.91
		0.3710		0.1862		0.3012	
2.92	8.6455		4.9121		7.2573		2.92
		0.4061		0.2039		0.3298	
2.93	9.0516		5.1160		7.5871		2.93
		0.4466		0.2241		0.3625	
2.94	9.4982		5.3401		7.9496		2.94
		0.4933		0.2474		0.4004	
2.95	9.9915		5.5875		8.3500		2.95
		0.5478		0.2747		0.4446	
2.96	10.5393		5.8622		8.7946		2.96
		0.6117		0.3066		0.4964	
2.97	11.1510		6.1688		9.2910		2.97
		0.6876		0.3446		0.5579	
2.98	11.8386		6.5134		9.8489		2.98
		0.7785		0.3901		0.6315	
2.99	12.6171		6.9035		10.4804		2.99
		0.8886		0.4451		0.7209	
3.00	13.5057		7.3486		11.2013		3.00
		1.0238		0.5127		0.8304	
3.01	14.5295		7.8613		12.0317		3.01
		1.1924		0.5970		0.9671	
3.02	15.7219		8.4583		12.9988		3.02
		1.4063		0.7040		1.1405	
3.03	17.1282		9.1623		14.1393		3.03
		1.6834		0.8426		1.3651	
3.04	18.8116		10.0049		15.5044		3.04

TABLE 14:2

FUNCTIONS FOR THREE-MOMENT EQUATIONS— $\alpha$ ,  $\beta$ , AND  $\gamma$  FUNCTIONS FOR AXIAL COMPRESSION— (Continued)

$L/j$	$\alpha$	$\Delta\alpha$	$\beta$	$\Delta\beta$	$\gamma$	$\Delta\gamma$	$L/j$
3.04	18.8116		10.0049		15.5044		3.04
3.05	20.8629	2.0513	11.0314	1.0265	17.1677	1.6633	3.05
3.06	23.4176	2.5547	12.3096	1.2782	19.2388	2.0711	3.06
3.07	26.6860	3.2684	13.9446	1.6350	21.8886	2.6498	3.07
3.08	31.0160	4.3300	16.1105	2.1659	25.3989	3.5103	3.08
3.09	37.0244	6.0084	19.1156	3.0051	30.2701	4.8712	3.09
3.10	45.9234	8.8990	23.5659	4.4503	37.4839	7.2138	3.10
3.11	60.4566	14.5332	30.8334	7.2675	49.2647	11.7808	3.11
3.12	88.4522	27.9956	44.8321	13.9987	71.9577	22.6930	3.12
3.13	164.7487	76.2965	82.9812	38.1491	133.8017	61.8440	3.13
3.14	1199.1629	1034.4142	600.1900	517.2088	972.2562	838.4545	3.14
3.15	-227.1668	$\infty$	-112.9747	$\infty$	-183.8716	$\infty$	3.15
3.16	-103.7576	123.4092	-51.2692	61.7055	-83.8391	100.0325	3.16
3.17	-67.2348	36.5228	-33.0068	18.2624	-54.2342	29.6049	3.17
3.18	-49.7313	17.5035	-24.2541	8.7527	-40.0458	14.1884	3.18
3.19	-39.4600	10.2713	-19.1176	5.1365	-31.7195	8.3263	3.19
3.20	-32.7063	6.7537	-15.7398	3.3778	-26.2445	5.4750	3.20
3.21	-27.9276	4.7787	-13.3495	2.3903	-22.3703	3.8742	3.21
3.22	-24.3683	3.5593	-11.5688	1.7807	-19.4845	2.8858	3.22
3.23	-21.6142	2.7541	-10.1909	1.3779	-17.2515	2.2330	3.23
3.24	-19.4202	2.1940	-9.0929	1.0980	-15.4725	1.7790	3.24
3.25	-17.6312	1.7890	-8.1975	0.8954	-14.0218	1.4507	3.25
3.26	-16.1447	1.4865	-7.4532	0.7443	-12.8161	1.2057	3.26
3.27	-14.8899	1.2548	-6.8248	0.6284	-11.7983	1.0178	3.27
3.28	-13.8166	1.0733	-6.2872	0.5376	-10.9276	0.8707	3.28
3.29	-12.8881	0.9285	-5.8220	0.4652	-10.1743	0.7533	3.29
3.30	-12.0770	0.8111	-5.4154	0.4066	-9.5162	0.6581	3.30

TABLE 14:2

FUNCTIONS FOR THREE-MOMENT EQUATIONS —  $\alpha$ ,  $\beta$ , AND  $\gamma$  FUNCTIONS FOR AXIAL COMPRESSION — (Concluded)

$L/j$	$\alpha$	$\Delta\alpha$	$\beta$	$\Delta\beta$	$\gamma$	$\Delta\gamma$	$L/j$
3.30	-12.0770		-5.4154		-9.5162		3.30
		4.6522		2.3367		3.7784	
3.40	-7.4248		-3.0787		-5.7378		3.40
		2.0479		1.0354		1.6681	
3.50	-5.3769		-2.0433		-4.0697		3.50
		1.1477		0.5861		0.9389	
3.60	-4.2292		-1.4572		-3.1308		3.60
		0.7302		0.3785		0.6016	
3.70	-3.4990		-1.0787		-2.5292		3.70
		0.5029		0.2659		0.4179	
3.80	-2.9961		-0.8128		-2.1113		3.80
		0.3647		0.1981		0.3070	
3.90	-2.6314		-0.6147		-1.8043		3.90
		0.2744		0.1544		0.2349	
4.00	-2.3570		-0.4603		-1.5694		4.00
		0.2116		0.1248		0.1854	
4.10	-2.1454		-0.3355		-1.3840		4.10
		0.1662		0.1038		0.1498	
4.20	-1.9792		-0.2317		-1.2342		4.20
		0.1317		0.0887		0.1237	
4.30	-1.8475		-0.1430		-1.1105		4.30
		0.1046		0.0778		0.1036	
4.40	-1.7429		-0.0652		-1.0069		4.40
		0.0826		0.0696		0.0881	
4.50	-1.6603		0.0044		-0.9188		4.50
		0.0641		0.0638		0.0757	
4.60	-1.5962		0.0682		-0.8431		4.60
		0.0810		0.1169		0.1235	
4.80	-1.5152		0.1851		-0.7196		4.80
		0.0238		0.1124		0.0962	
5.00	-1.4914		0.2975		-0.6234		5.00
		0.0568		0.1520		0.0938	
5.25	-1.5482		0.4495		-0.5296		5.25
		0.1964		0.1975		0.0733	
5.5	-1.7446		0.6470		-0.4563		5.5
		0.4898		0.3277		0.0589	
5.75	-2.2344		0.9747		-0.3974		5.75
		1.5111		0.8268		0.0482	
6.0	-3.7455		1.8015		-0.3492		6.0
		25.3412		12.7331		0.0404	
6.25	-29.0867		14.5346		-0.3088		6.25
		$\infty$		$\infty$		0.0048	
$2\pi$	$\pm\infty$		$\pm\infty$		-0.3040		$2\pi$
		$\infty$		$\infty$		0.0295	
6.5	4.1490		-2.0242		-0.2745		6.5

**14 : 3. Equation of Three Moments**—In two contiguous spans, shown in Fig. 14 : 3, the slope of the tangent to the elastic curve at the center support will be the same for both spans, the member being continuous over this support.

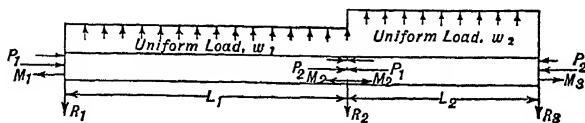


FIG. 14 : 3

At  $R_2$ ,  $x_1 = L_1$  for the left-hand, and  $x_2 = 0$  for the right-hand span. Using subscripts or primes to differentiate between the symbols for the respective spans and substituting these values in the expressions for slope at  $R_2$ ,

$$\theta_1 = \frac{M_2 - M_1}{L_1 P_1} - \frac{w_1 L_1}{2 P_1} + \frac{w_1 L_1}{P_1} - \frac{C_1 \cos \frac{L_1}{j_1}}{j_1 P_1} + \frac{C_2 \sin \frac{L_1}{j_1}}{j_1 P_1} \quad 14 : 8$$

in which

$$C_1 = \frac{M_2 - w_1 j_1^2 - (M_1 - w_1 j_1^2) \cos \frac{L_1}{j_1}}{\sin \frac{L_1}{j_1}}$$

and

$$C_2 = M_1 - w_1 j_1^2$$

$$\theta_2 = \frac{M_3 - M_2}{L_2 P_2} - \frac{w_2 L_2}{2 P_2} - \frac{C'_1}{j_2 P_2} \quad 14 : 9$$

in which

$$C'_1 = \frac{M_3 - w_2 j_2^2 - (M_2 - w_2 j_2^2) \cos \frac{L_2}{j_2}}{\sin \frac{L_2}{j_2}}$$

However,  $\theta_1 = \theta_2$  at the center support. Substituting the values for  $C_1$ ,  $C'_1$  and  $C_2$  in Eq. 14 : 8 and 14 : 9, combining the terms, and simplifying, the following result is obtained:

$$\begin{aligned}
& \frac{M_1 L_1}{I_1} \left( \frac{\frac{L_1}{j_1} \operatorname{cosec} \frac{L_1}{j_1} - 1}{\left(\frac{L_1}{j_1}\right)^2} \right) + \frac{M_3 L_2}{I_2} \left( \frac{\frac{L_2}{j_2} \operatorname{cosec} \frac{L_2}{j_2} - 1}{\left(\frac{L_2}{j_2}\right)^2} \right) \\
& + M_2 \left\{ \frac{L_1}{I_1} \left( \frac{\left(1 - \frac{L_1}{j_1} \cot \frac{L_1}{j_1}\right)}{\left(\frac{L_1}{j_1}\right)^2} \right) + \frac{L_2}{I_2} \left( \frac{\left(1 - \frac{L_2}{j_2} \cot \frac{L_2}{j_2}\right)}{\left(\frac{L_2}{j_2}\right)^2} \right) \right\} \\
& = \frac{w_1 L_1^3}{I_1} \left( \frac{\tan \frac{L_1}{2 j_1} - \frac{L_1}{2 j_1}}{\left(\frac{L_1}{j_1}\right)^3} \right) + \frac{w_2 L_2^3}{I_2} \left( \frac{\tan \frac{L_2}{2 j_2} - \frac{L_2}{2 j_2}}{\left(\frac{L_2}{j_2}\right)^3} \right) \quad 14 : 10
\end{aligned}$$

Multiplying Eq. 14 : 10 by 6, it becomes

$$\begin{aligned}
& \frac{M_1 L_1 \alpha_1}{I_1} + 2 M_2 \left( \frac{L_1}{I_1} \beta_1 + \frac{L_2}{I_2} \beta_2 \right) + \frac{M_3 L_2 \alpha_2}{I_2} \\
& = \frac{w_1 L_1^3}{4 I_1} \gamma_1 + \frac{w_2 L_2^3}{4 I_2} \gamma_2 \quad 14 : 11
\end{aligned}$$

in which, with subscripts for  $L$  and  $j$  corresponding to the spans:

$$\begin{aligned}
\alpha &= 6 \frac{\left( \frac{L}{j} \operatorname{cosec} \frac{L}{j} - 1 \right)}{\left(\frac{L}{j}\right)^2} \\
\beta &= 3 \frac{\left( 1 - \frac{L}{j} \cot \frac{L}{j} \right)}{\left(\frac{L}{j}\right)^2} \\
\gamma &= 3 \frac{\left( \tan \frac{L}{2 j} - \frac{L}{2 j} \right)}{\left(\frac{L}{2 j}\right)^3}
\end{aligned}$$

The sines, cosines, and tangents of  $L/j$ , and also the values of  $\alpha$ ,  $\beta$ , and  $\gamma$ , corresponding to the different values of  $L/j$ , will be found in Tables 14 : 1 and 14 : 2. .

In Chapter V, it was shown how the three-moment equation for beams subjected to no axial load could be written for the cases in which an external moment is applied at the intermediate support. Equation 14 : 11 can be similarly modified to apply to the corresponding cases when axial compression is present, giving

$$\begin{aligned} \frac{M_1 L_1 \alpha_1}{I_1} + 2 M_{-2} \frac{L_1}{I_1} \beta_1 + 2 M_{+2} \frac{L_2}{I_2} \beta_2 + \frac{M_3 L_2 \alpha_2}{I_2} \\ = \frac{w_1 L_1^3 \gamma_1}{4 I_1} + \frac{w_2 L_2^3 \gamma_2}{4 I_2} \end{aligned} \quad 14 : 12$$

In Eq. 14 : 12,  $M_{-2}$  and  $M_{+2}$  are the moments an infinitesimal distance to the left and right, respectively, of the point of support. Equation 14 : 12 contains an additional unknown which necessitates another equation for a solution. This is obtained from the relation between  $M_{-2}$  and  $M_{+2}$ ,  $M_{+2}$  being equal to  $M_{-2}$  plus or minus the eccentric moment,  $M_e$ . Care must be taken with the sign of  $M_e$ . It should be considered positive if it increases the bending moment from  $M_{-2}$  to  $M_{+2}$  as one goes from left to right over the point of support.

In Eq. 5 : 3 (Chapter V of vol. I) two terms are shown on the right-hand side of the equation to allow for the effect of deflection of the supports. The same two terms may be properly added to the right-hand side of Eq. 14 : 11 for the same purpose. No modification of these deflection terms is needed when an axial load is present.

**14 : 4. Numerical Example** — To illustrate the use of the formulas just developed, an investigation will be made of the rear upper spar required for the airplane framework shown in Fig. 8 : 11. The spar will be assumed to be a spruce I-section, continuous between wing tips, and with a center height not over 4.00 in. From Table 8 : 5 we find the average axial load in the rear upper spar between the interplane and cabane struts to be  $(\frac{1}{2})(3,044 + 3,235) = 3,140$  lb., while the axial load in the center section, between cabane struts, is 3,388 lb. The use of the average axial load instead of the maximum between points of support is justified by several years of experience wherein this practice has been followed.

The bending moment at the outer support,  $M_1$ , is 1,200 in.-lb. for a load of 1.0 lb. per in., as computed in Art. 8 : 8, so it would become  $M_1 = 10,800$  in.-lb. for the design load of 9.0 lb. per in.

Following airplane practice, the spar section at the panel points of the lift and drag trusses will be rectangular except for the bevel of the upper and lower surfaces required to conform to the wing contour. Between those points it will be assumed routed to an I-section. For



a first trial the width of the spar will be taken between  $\frac{1}{4}$  and  $\frac{1}{3}$  of the depth, i.e., between 1.00 and 1.33 in., say 1.25 in. The routing for this trial will be assumed to cut away about 40 per cent of the rectangle, leaving the section shown in Fig. 14:4. Although this section is beveled and has fillets between the web and flanges, the geometrical properties used in the computations will be based upon the equivalent section, shown by the dotted lines, which has the same center height and flange thickness as the actual section, but in which the bevels and fillets are neglected. The properties of this section are then:

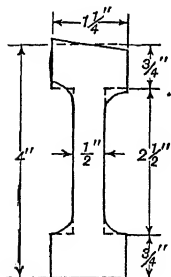


FIG. 14:4

$$A = 1.25 \times 4.00 - 0.75 \times 2.50 = 3.125 \text{ in.}^2$$

$$I = \frac{1.25 \times 4.00^3}{12} - \frac{0.75 \times 2.50^3}{12} = 5.69 \text{ in.}^4$$

Because the lengths of the unrouted rectangular sections are small in comparison with the distances between supports, hence have little effect on the deflection of the beam and the secondary bending moments, the solution of the three-moment equation will be based on the properties of the routed section only. The effect of this procedure which is rather conservative is to compensate, in part at least, for the somewhat unsafe use of the average axial load instead of the maximum. Computing the bending moments by the aid of the precise formulas involves the use of the values tabulated below.

## Span 1-2 (Outer Bay)

$$\begin{aligned} w_1 &= 9.00 \\ M_1 &= 10,800 \\ I_1 &= 5.69 \\ E_1 &= 1,300,000 \\ E_1 I_1 &= 7,397,000 \\ P_1 &= 3,140 \\ j_1^2 &= \frac{E_1 I_1}{P_1} = 2355.7 \\ j_1 &= 48.54 \\ w_1 j_1^2 &= 21,202 \\ L_1 &= 96 \\ \frac{L_1}{j_1} &= 1.978 \\ \alpha_1 &= 1.7707 \\ \beta_1 &= 1.4213 \\ \gamma_1 &= 1.6484 \end{aligned}$$

## Span 2-3 (Center Section)

$$\begin{aligned} w_2 &= 9.00 \\ M_2 &= M_3 \text{ by symmetry} \\ I_2 &= 5.69 \\ E_2 &= 1,300,000 \\ E_2 I_2 &= 7,397,000 \\ P_2 &= 3,388 \\ j_2^2 &= \frac{E_2 I_2}{P_2} = 2183.3 \\ j_2 &= 46.73 \\ w_2 j_2^2 &= 19,650 \\ L_2 &= 48 \\ \frac{L_2}{j_2} &= 1.027 \\ \alpha_2 &= 1.1385 \\ \beta_2 &= 1.0783 \\ \gamma_2 &= 1.1182 \end{aligned}$$

Since  $I_1 = I_2$  the three-moment equation for this case is

$$M_1 L_1 \alpha_1 + 2 M_2 (L_1 \beta_1 + L_2 \beta_2) + M_2 L_2 \alpha_2 = \frac{w_1 L_1^3 \gamma_1}{4} + \frac{w_2 L_2^3 \gamma_2}{4}$$

$$10,800 \times 96 \times 1.7707 + 2 M_2 (96 \times 1.4213 + 48 \times 1.0783) +$$

$$M_2 \times 48 \times 1.1385 = \frac{9.0 \times 96^3 \times 1.6484}{4} + \frac{9.0 \times 48^3 \times 1.1182}{4}$$

$$1,835,860 + 376.41 M_2 + 54.65 M_2 = 3,281,400 + 278,140$$

$$431.06 M_2 = 1,723,680$$

$$M_2 = M_3 = 3,999 \text{ in.-lb.}$$

The next step is to determine the magnitudes of the maximum bending moments in the outer bay and center section. In the latter the point of zero slope of the moment curve — the mathematical maximum or minimum — will be at the center of the span, since the loading is symmetrical. The loading on the outer bay, however, is not symmetrical, so the location of the point of maximum bending moment must be computed from Eq. 14 : 4:

$$\tan \frac{x_1}{j_1} = \frac{D_2 - D_1 \cos \frac{L_1}{j_1}}{D_1 \sin \frac{L_1}{j_1}}$$

where

$$D_1 = M_1 - w_1 j_1^2 = 10,800 - 21,202 = -10,402$$

$$D_2 = M_2 - w_1 j_1^2 = 3,999 - 21,202 = -17,203$$

and from Table 14 : 1

$$\cos \frac{L_1}{j_1} = \cos 1.978 = -0.39604$$

$$\sin \frac{L_1}{j_1} = \sin 1.978 = 0.91823$$

Then

$$\tan \frac{x_1}{j_1} = \frac{-17,203 - (-10,402)(-0.39604)}{(-10,402)(0.91823)} = 2.2325$$

$$\frac{x_1}{j_1} = \tan^{-1} 2.2325 = 1.1497$$

The point of maximum moment is then  $x_1 = 48.54 \times 1.1497 = 55.80$  in. from  $R_1$  at the outer strut.

$$M_{1-2 \max} = \frac{D_1}{\cos \frac{x_1}{j_1}} + w_1 j_1^2 = \frac{-10,402}{0.40876} + 21,202 = -4,246 \text{ in.-lb.}$$

In the center section,  $\frac{x_2}{j_2} = \frac{L_2}{2 j_2} = 0.514$

$$M_{2-3 \max} = \frac{3,999 - 19,650}{0.87077} + 19,650 = +1,676 \text{ in.-lb.}$$

It is now possible to compute the stresses due to bending at the most-stressed sections, compare these stresses with the allowables, and revise the dimensions of the cross-section according to whether it is too strong or too weak. The cross-sections of this spar most stressed in bending will be the rectangular section at  $R_1$ , where  $M_1 = 10,800$  in.-lb., and  $P_1 = 3,044$  lb.; the section near  $R_1$  where the rectangular section stops and the I-section starts, and the section of  $M_{1-2 \max} = -4,246$  in.-lb., where  $P_1 = 3,140$  lb. if the average be taken, but 3,235 lb. if the more conservative method of taking the actual axial stress (see Table 8 : 5) is to be followed. Unless there be a large difference between average and actual stress at the section, the average is generally used. The moments at  $R_2$  and in span 2-3 are, for this spar, not critical even though the axial load in that span is greater than in span 1-2.

The allowable stresses in combined bending and compression for wood beam-columns are computed by the method developed at the Forest Products Laboratory by Newlin and Trayer.<sup>1</sup> No attempt will be made here to recapitulate the theory underlying this method, but its application will be illustrated by detailed computations of the margin of safety of the trial section at the point of maximum moment in the outer bay, where  $M = -4,246$  in.-lb.,  $P = -3,140$  lb.,  $j = 48.54$  in.,  $w_j^2 = 21,202$  in.-lb.,  $I = 5.69$  in.<sup>4</sup>, and  $A = 3.125$  in.<sup>2</sup> The total depth of the equivalent section,  $h$ , is 4.00 in.; the distance,  $y$ , from the neutral axis to the most-stressed fiber is 2.00 in.; the thickness of the compression flange,  $t_c$ , is 0.75 in.; the total width of the section,  $b$ , is 1.25 in.; and the web thickness,  $b'$ , is 0.50 in. From the above data we compute: the radius of gyration,  $\rho = \sqrt{I/A} = 1.35$  in.; the bending stress on the extreme fiber,  $f_b = My/I = 4,246 \times 2/5.69 = 1,493$  p.s.i.; the com-

<sup>1</sup> N.A.C.A. Technical Reports 181 and 188, "The Influence of the Form of a Wooden Beam on its Stiffness and Strength," by J. A. Newlin and G. W. Trayer.

pressive stress due to axial load,  $f_c = P/A = 3,140/3.125 = 1,005$  p.s.i.; the total stress,  $f_b + f_c = 1,493 + 1,005 = 2,498$  p.s.i.; the ratio  $f_b/f_t = 1,493/2,498 = 0.597$ ;  $t_c/h = 0.75/4.00 = 0.1875$ ; and  $b'/b = 0.50/1.25 = 0.40$ .

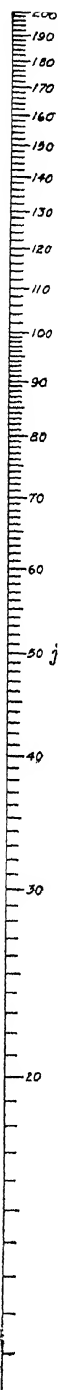
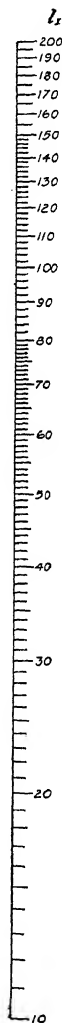
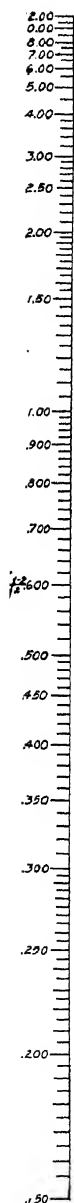
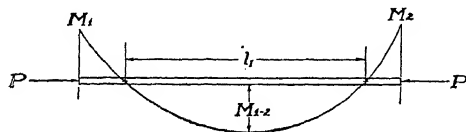
The distance  $L_I$  between the points of inflection of the outer bay is also needed for the determination of the effective slenderness ratio.  $L_I$  is obtained from Fig. 14 : 5, which is a nomogram for solving the equation for maximum moment on a pin-ended beam-column subjected to uniformly distributed side load and axial compression, the first formula listed in Table 14 : 4. Drawing a line from  $M_{1-2}/wj^2 = 4,246/21,202 = 0.200$  on the left scale to  $j = 48.54$  on the right, we find it intersects the center scale at  $L_I = 57.0$  in. Hence there are points of zero bending moment  $57.0/2 = 28.5$  in. to each side of the point of maximum moment in span 1-2, and  $L_I/\rho = 57.0/1.35 = 42.2$ .

We now have all the quantities needed to determine the allowable stress,  $F_t$ , from Fig. 14 : 6. With the values of  $b'/b$  and  $t_c/h$ , we enter the right half of the figure and locate points  $A$  and  $B$  at the intersections of the vertical drawn through  $t_c/h = 0.1875$  with  $b'/b = 0.4$ . Point  $A$ , the intersection with the curve of the lower set, represents the fiber stress at elastic limit in bending for this section. Point  $B$  gives the modulus of rupture for simple bending. Points  $A$  and  $B$  are projected horizontally to the central line in the chart, giving  $C$  and  $D$ . In the left half of the chart are two families of curves, one labeled with the values of  $L/\rho$  to which they apply, and the other without designation. The latter are known as the "elastic limit stress" curves since they indicate the variation of elastic limit with the ratio  $f_b/f_t$ . Through  $C$  we interpolate an elastic limit stress curve and follow it to its intersection with the curve for  $L/\rho = 42.2$ . It is to be noted that no such intersection can be obtained in this case since the lowest value of  $L/\rho$  for which a curve is shown on the chart is 50. Therefore, we locate  $E$  at the point on the  $f_b/f_t = 0$  line which represents the allowable stress for a short column of  $L/\rho = 42.2$ .

We now have point  $D$  which represents the modulus of rupture in simple bending, and point  $E$  which indicates the allowable stress intensity in compression on the segment of the spar considered as a pin-ended column between the points of inflection. Since the actual load is a combination of bending and compression, the spar would be expected to fail under a load intermediate between  $D$  and  $E$ . Assuming a rectilinear variation — an assumption which has been substantiated by numerous tests — we draw a straight line from  $D$  to  $E$  and find its intersection with the abscissa representing  $f_b/f_t = 0.597$ , point  $F$ . The ordinate value for point  $F$  is 5,950 p.s.i. The allowable stress  $F_t$  is then 5,950

DISTANCE BETWEEN POINTS OF INFLECTION ON  
SPAR WITH AXIAL COMPRESSIVE AND UNIFORM LATERAL LOADS

$$\frac{M_{1-2}}{Wj^2} = EK \sec \frac{l_1}{2j} \sim j^2 \frac{EI}{P}$$



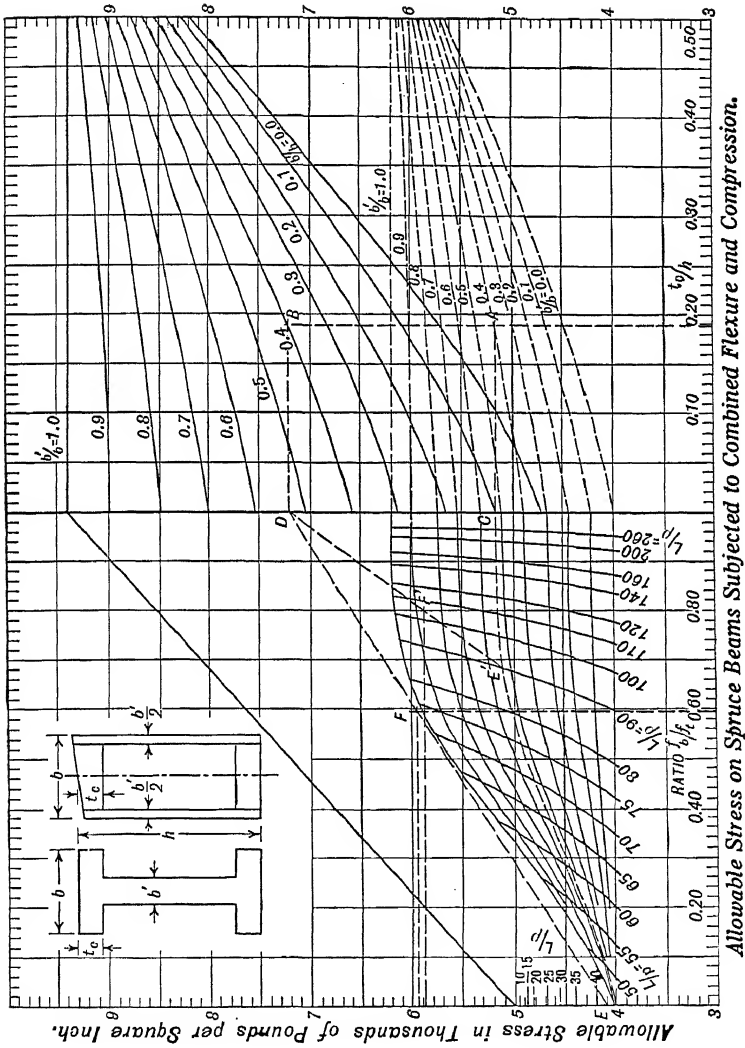


FIG. 14 : 6

Allowable Stress on Spruce Beams Subjected to Combined Flexure and Compression.

p.s.i. and the margin of safety of the beam is  $(5,950/2,498) - 1 = 1.38$  or 138 per cent. The trial section is stronger than necessary, but it will not be investigated further here. In all probability the margin of safety for this beam cannot be reduced to zero without making the spar so narrow that it will buckle laterally, or its web so thin that it will not carry the longitudinal shear near the supports. A very rough rule, but one which works well over a range of 10 to 15 per cent change in spar area, is that the margin of safety will vary as the area of the cross-section, for a given cross-section carrying a given bending moment and axial load. The trial section, being more than twice as strong as necessary, will require considerable reduction in area to render it satisfactory and economical of weight.

Had  $L/\rho$  been 90 and  $f_b/f_t$  been 0.80, point  $E$  would have been at  $E'$ , point  $F$  at  $F'$ , the intersection of  $DE'$  and  $f_b/f_t = 0.80$ ; and the allowable unit stress,  $F_t$ , would have been reduced to 5,890 p.s.i. Were  $f_b/f_t = 0.60$  and  $L/\rho = 90$ , points  $A, B, C, D, E'$  and  $F'$  would be unnecessary.  $F_t$  would be indicated directly by the intersection of the curve for  $L/\rho = 90$  with  $f_b/f_t = 0.60$ , that is, at 4,000 p.s.i.

In using the right half of Fig. 14 : 6 to determine the modulus of rupture of a box beam with plywood webs, the total thickness of the webs should be used for  $b'$  in computing the ratio  $b'/b$ , although but half the web thickness may be assumed effective when computing  $A$  and  $I$  for the section.

The modulus of rupture values of Fig. 14 : 6 apply to the compression flange since that is normally critical. For spruce beams of any shape the allowable tensile stress may safely be taken as 10,000 p.s.i. whether it is the result of simple bending or of combined bending and axial load. With beam-columns subjected to axial tension, the allowable net compressive stress should be taken as the modulus of rupture in simple bending.

The slenderness ratio to be used with Fig. 14 : 6 should be that between points of inflection. When the ends of the member are restrained, this need not be computed with excessive precision, and the following practice is well established. In any span of a continuous or restrained beam,  $L$  may be taken as the distance between points of inflection under side load alone or may be obtained for the combined loading as was done above, by using Fig. 14 : 5. The latter procedure is preferred. At points of support  $L$  is taken as the distance between adjacent points of inflection except at the end supports where it is assumed to be twice the distance from the given support to the outer point of inflection. In computing  $\rho$ , filler blocks may be neglected and for tapered spars the average value may be used. Filler blocks, if

rigidly attached to the spar, may be included in the section when computing its properties and determining  $f_b$ ,  $f_c$ , and  $f_t$ .

In some instances in which axial compression is combined with bending there are no points of inflection between which the slenderness ratio can be logically measured. One such is that of a spar in an internally braced cantilever monoplane. It is subjected to large bending moments from the beam loads on the wing and to axial compression owing to its being a member of the internal drag truss. A reasonable method of handling this case, and others in which the unit stress due to axial load is small in comparison to the unit stress due to bending, is to assume the allowable total stress,  $F_t$ , equal to the modulus of rupture as obtained from the right-hand side of Fig. 14 : 6 multiplied by the ratio of  $f_b/f_t$ .

In a few cases spans will be found where the stress due to axial load is a large part of the total stress but in which there are no points of inflection on account of the large size of the end moments as compared to the length of the span and the magnitude of the lateral load. This condition brings up two questions: "Where should the point of the inflection be assumed when investigating the strength of the end sections?" and "What distance between points of inflection should be assumed when investigating sections near the center of the span?" A reasonable answer to the first is to assume a point of inflection where the curve of bending moment in the span changes slope, i.e., at the point of zero shear in the span. A reasonable answer to the second is to assume the distance in question to be the length of the span.

Figure 14 : 6 is complicated, but it has been demonstrated by experience to give beam-columns of adequate strength. An alignment chart, much simpler to use, has recently been presented by Mr. R. M. Carlson;<sup>1</sup> it will be found applicable to most airplane wing spars. It represents conditions on the straight-line portion of the allowable stress curve,  $DE'$  of Fig. 14 : 6, but leads to erroneous results when  $f_b/f_t$  is low enough to cause the allowable stress to lie on the part of the curve represented by the appropriate  $L/\rho$  line. Another method for obtaining allowable stresses in continuous beam-columns has been described by J. A. Newlin and G. W. Trayer in N.A.C.A. Report 347, but has not been used by airplane designers because it is less conservative, by about 15 per cent, than the procedure described above. To increase allowable stresses by 15 per cent is the same as reducing design requirements by approximately that amount, and designers have felt that such a reduction would not be justified. The older method based on equivalent

<sup>1</sup> "An Alignment Chart for Allowable Stresses for Spruce Beams in Bending and Compression," R. M. Carlson, Vol. 4, No. 12, p. 502, *Journal of the Aeronautical Sciences*, October, 1937.



pin-ended beam-columns has therefore persisted for the design of spruce spars.

While data for wood beam-columns are reasonably complete and satisfactory, few exist for checking the adequacy of metal members. Methods for computing margins of safety for metal beams subjected to simple bending have been outlined in Chapter VI; those for columns subjected to axial compression are covered in Chapter X. In general the present practice is to use these methods to obtain the stress ratios,  $R_b$  and  $R_c$ , and to apply Eq. 7 : 14, with  $m$  and  $n$  each equal to unity, to determine whether the member is adequate. For a few commonly used shapes, the A.N.C. Committee on Aircraft Requirements has published data to facilitate the application of this general method, and it is to be expected that the ground covered by their specific recommendations will be extended as rapidly as continued research permits.

**14 : 5. Formulas for Other Loadings.** *Single Span with Axial Compression* — The aeronautical engineer often has to deal with beam-columns subjected to transverse loads that are not uniformly distributed over the entire span, or beam-columns in which the axial load is tension instead of compression. Formulas for the bending moments, etc., and extended three-moment equations for such beam-columns with any specified type of transverse load can be derived by the method outlined above for axial compression and a uniformly distributed side load. If this be done, it will be found that, for axial compression and the transverse loads listed in Table 14 : 3, the formula for the bending moment in a single span always takes the form

$$M = C_1 \sin \frac{x}{j} + C_2 \cos \frac{x}{j} + f(w) \quad 14 : 13$$

in which  $f(w)$  is a term containing  $w$  and possibly  $j$ ,  $x$ , and  $L$ , but neither the axial load  $P$  nor the end moments,  $M_1$  and  $M_2$ . The particular expressions for  $C_1$ ,  $C_2$ , and  $f(w)$  depend on the character of the transverse load.

If Eq. 14 : 13 be differentiated with respect to  $x$ , we obtain

$$S = \frac{dM}{dx} = \frac{C_1}{j} \cos \frac{x}{j} - \frac{C_2}{j} \sin \frac{x}{j} + f'(w) \quad 14 : 14$$

in which  $f'(w)$  is the derivative of  $f(w)$  with respect to  $x$ . The physical significance of the quantity  $S$ , which will be termed the "total shear," is discussed in Art. 14 : 9.

If the "primary" bending moment and shear<sup>1</sup> be designated by

<sup>1</sup> The bending moment and shear that would be produced by the transverse loads and end moments acting without the axial load.

$M_0$  and  $S_0$ , respectively, the deflection and slope can be obtained from the relations

$$\delta = \frac{M_0 - M}{P} \quad 14 : 15$$

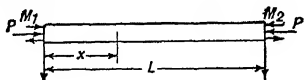
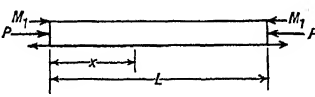
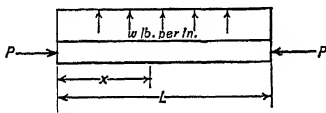
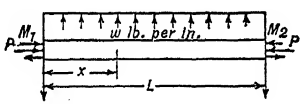
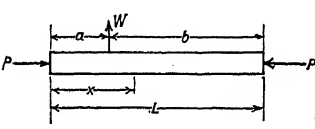
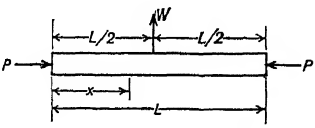
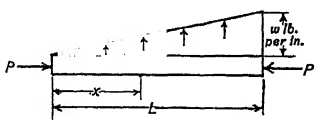
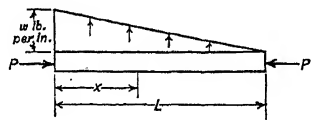
$$\theta = \frac{S_0 - S}{P} \quad 14 : 16$$

Formulas for  $C_1$ ,  $C_2$ , and  $f(w)$  for axial compression and the more commonly encountered types of transverse loads are listed in Tables 14 : 3 and 14 : 6. In some computations the engineer will find the alternative formulas of Table 14 : 6 more convenient than their more concise equivalents of Table 14 : 3.

It has already been shown that the principle of superposition does not apply to a beam-column, since the bending moments due to a transverse load and an axial load acting simultaneously are not the same as the sum of the bending moments caused by those loads acting separately. On the other hand it will be found that the bending moments due to a transverse loading  $A$  acting simultaneously with an axial load,  $P$ , added to the bending moments due to another transverse loading  $B$  acting simultaneously with the same axial load  $P$  will be identical with the bending moments due to the transverse loadings  $A$  and  $B$  and the axial load  $P$  acting simultaneously. Thus one might say that the method of superposition can be applied provided each of the superimposed bending moments is the effect of the combined action of one or more of the transverse loads and the entire axial load. In this connection an end moment is to be considered as a transverse load. In order, therefore, to write the proper formula for the bending moment on a beam-column subjected to two or more transverse loads, all that is necessary is to add the values from Table 14 : 3 for each of the transverse loads to obtain the values of  $C_1$ ,  $C_2$ , and  $f(w)$  to be used in Eq. 14 : 13. The method of superposition can be applied in the same manner to determine the total shear, slope, or deflection due to an axial compression acting in combination with two or more transverse loads.

For example, let us obtain a formula for bending moment for a loading which combines Case 1, end moments, Case 2, uniformly distributed load, Case 4, concentrated load at a distance  $a$  from the left end of the span, and Case 5, uniformly varying load increasing to the right. The combination of Cases 1 and 2 is given in the table as Case 3, so our problem may be treated as a combination of Cases 3, 4, and 5. In order to distinguish the uniformly distributed load from the uniformly varying let us designate the former by  $w_u$  and the latter by  $w_v$ . For values of  $x$  less than  $a$ , the constants  $C_1$  and  $C_2$  may be built up from the data of

TABLE 14:3  
TERMS FOR BEAM-COLUMN FORMULAS  
AXIAL COMPRESSION

Case	Loading	$C_1$
1 	End moments	$\frac{M_2 - M_1 \cos \frac{L}{j}}{\sin \frac{L}{j}}$
1a 	Equal end moments	$M_1 \tan \frac{L}{2j}$
2 	Uniform	$\frac{wj^2 \left( \cos \frac{L}{j} - 1 \right)}{\sin \frac{L}{j}}$
3 	Uniform plus end moments	$\frac{D_2 - D_1 \cos \frac{L}{j}}{\sin \frac{L}{j}}$
4 	Concentrated load	$\begin{aligned} z < a & - \frac{Wj \sin \frac{b}{j}}{\sin \frac{L}{j}} \\ z > a & \frac{Wj \sin \frac{a}{j}}{\tan \frac{L}{j}} \end{aligned}$
4a 	Concentrated load at $z = L/2$	$\begin{aligned} z < \frac{L}{2} & - \frac{Wj}{2} \sec \frac{L}{2j} \\ z > \frac{L}{2} & \frac{Wj}{2} \cos \frac{L}{2j} \sec \frac{L}{2j} \end{aligned}$
5 	Uniformly varying increasing to right	$-\frac{wj^2}{\sin \frac{L}{j}}$
6 	Uniformly varying decreasing to right	$\frac{wj^2}{\tan \frac{L}{j}}$

\*  $D_1 = M_1 - wj^2$ ,  $D_2 = M_2 - wj^2$

TABLE 14:3  
TERMS FOR BEAM-COLUMN FORMULAS  
AXIAL COMPRESSION

$C_2$	$f(w)$	Terms for Three-moment Equation	
		Left Bay	Right Bay
$M_1$	0	0	0
$M_2$	0	0	0
$-wj^2$	$wj^2$	$\frac{w_1 L_1^3 \gamma_1}{4 I_1}$	$\frac{w_2 L_2^3 \gamma_2}{4 I_2}$
$D_1^*$	$wj^2$	Same as Case 2	Same as Case 2
0 $-Wj \sin \frac{a}{j}$	0 0	$\frac{6 W j_1^2}{I_1} \left[ \frac{\sin \frac{a_1}{j_1}}{\sin \frac{L_1}{j_1}} - \frac{a_1}{L_1} \right]$	$\frac{6 W j_2^2}{I_2} \left[ \frac{\sin \frac{b_2}{j_2}}{\sin \frac{L_2}{j_2}} - \frac{b_2}{L_2} \right]$
0 $-Wj \sin \frac{L}{2j}$	0 0	$\frac{3 W j_1^2}{I_1} \left( \sec \frac{L_1}{2j_1} - 1 \right)$	$\frac{3 W j_2^2}{I_2} \left( \sec \frac{L_2}{2j_2} - 1 \right)$
0	$\frac{w j^2 x}{L}$	$\frac{2 w_1 L_1 j_1^2 (\beta_1 - 1)}{I_1}$	$\frac{w_2 L_2 j_2^2 (\alpha_2 - 1)}{I_2}$
$-wj^3$	$wj^3 \left( 1 - \frac{x}{L} \right)$	$\frac{w_1 L_1 j_1^2 (\alpha_1 - 1)}{I_1}$	$\frac{2 w_2 L_2 j_2^2 (\beta_2 - 1)}{I_2}$

TABLE 14:3 (Continued)  
TERMS FOR BEAM-COLUMN FORMULAS  
AXIAL COMPRESSION

Case	Loading	$C_1$
<p>7</p>	Symmetrical triangle	$x < \frac{L}{2} \quad - \frac{2wj^2}{L \cos \frac{L}{2j}}$ $x > \frac{L}{2} \quad \frac{2wj^2 \cos \frac{L}{j}}{L \cos \frac{L}{2j}}$
<p>8</p>	Partial uniformly distributed	$x < a \quad - \frac{2wj^2 \sin \frac{d}{2j} \sin \frac{x}{j}}{\sin \frac{L}{j}}$ $a < x < b \quad \frac{2wj^2 \sin \frac{d}{2j} \sin \frac{e}{j}}{\tan \frac{L}{j}} - wj^2 \sin \frac{b}{j}$ $b < x < L \quad \frac{2wj^2 \sin \frac{d}{2j} \sin \frac{e}{j}}{\tan \frac{L}{j}}$
<p>8a</p>	Symmetrical partial uniformly distributed	$x < a \quad - wj^2 \sin \frac{d}{2j} \sec \frac{L}{2j}$ $a < x < L - a \quad - wj^2 \tan \frac{L}{2j} \cos \frac{a}{j}$ $L - a < x < L \quad wj^2 \sin \frac{d}{2j} \sec \frac{L}{2j} \cos \frac{L}{j}$
<p>9</p>	Two symmetrical concentrated loads	$x < a \quad - Wj \frac{\cos \frac{b}{2j}}{\cos \frac{L}{2j}}$ $a < x < L - a \quad - Wj \sin \frac{a}{j} \tan \frac{L}{2j}$ $L - a < x < L \quad Wj \frac{\cos \frac{L}{j} \cos \frac{b}{2j}}{\cos \frac{L}{2j}}$
<p>10</p>	Clockwise Couple	$x < a \quad - \frac{m \cos \frac{b}{j}}{\sin \frac{L}{j}}$ $x > a \quad - \frac{m \cos \frac{a}{j}}{\tan \frac{L}{j}}$

TABLE 14 : 3  
TERMS FOR BEAM-COLUMN FORMULAS  
AXIAL COMPRESSION

$C_s$	$f(w)$	Terms for Three-moment Equation	
		Left Bay	Right Bay
$0$  $-\frac{4wj^2}{L} \sin \frac{L}{2j}$	$\frac{2wj^2x}{L}$  $2wj^2 \left(1 - \frac{x}{L}\right)$	$\frac{12wj_1^2}{I_1} \left[ \frac{j_1^2}{L_1} \left( \sec \frac{L_1}{2j_1} - 1 \right) - \frac{L_1}{8} \right]$	$\frac{12wj_2^2}{I_2} \left[ \frac{j_2^2}{L_2} \left( \sec \frac{L_2}{2j_2} - 1 \right) - \frac{L_2}{8} \right]$
$0$  $-wj^2 \cos \frac{a}{j}$  $-2wj \sin \frac{d}{2j} \sin \frac{e}{j}$	$0$  $wj^2$  $0$	$\frac{12wj_1^2}{I_1} \left[ \frac{j_1 \sin \frac{e_1}{j_1} \sin \frac{d_1}{2j_1}}{\sin \frac{L_1}{j_1}} - \frac{d_1 e_1}{2L_1} \right]$	$\frac{12wj_2^2}{I_2} \left[ \frac{j_2 \sin \frac{f_2}{j_2} \sin \frac{d_2}{2j_2}}{\sin \frac{L_2}{j_2}} - \frac{d_2 f_2}{2L_2} \right]$
$0$  $-wj^2 \cos \frac{a}{j}$  $-2wj^2 \sin \frac{d}{2j} \sin \frac{L}{2j}$	$0$  $wj^2$  $0$	$\frac{3wj_1^2}{I_1} \left[ \frac{2j_1 \sin \frac{d_1}{2j_1}}{\cos \frac{L_1}{2j_1}} - d_1 \right]$	$\frac{3wj_2^2}{I_2} \left[ \frac{2j_2 \sin \frac{d_2}{2j_2}}{\cos \frac{L_2}{2j_2}} - d_2 \right]$
$0$  $-Wj \sin \frac{a}{j}$  $-Wj \frac{\sin \frac{L}{j} \cos \frac{b}{2j}}{\cos \frac{L}{2j}}$	$0$  $0$  $0$	$\frac{6Wj_1^2}{I_1} \left[ \frac{\cos \frac{b_1}{2j_1}}{\cos \frac{L_1}{2j_1}} - 1 \right]$	$\frac{6Wj_2^2}{I_2} \left[ \frac{\cos \frac{b_2}{2j_2}}{\cos \frac{L_2}{2j_2}} - 1 \right]$
$0$  $m \cos \frac{a}{j}$	$0$  $0$	$\frac{6mj_1^2}{I_1} \left[ \frac{j_1}{L_1} - \frac{\cos \frac{a_1}{j_1}}{\sin \frac{L_1}{j_1}} \right]$	$\frac{6mj_2^2}{I_2} \left[ \frac{j_2}{L_2} - \frac{\cos \frac{a_2}{j_2}}{\sin \frac{L_2}{j_2}} \right]$

Table 14 : 3 to give

$$C_1 = \frac{D_2 - D_1 \cos \frac{L}{j} - Wj \sin \frac{b}{j} - w_v j^2}{\sin \frac{L}{j}}$$

$$C_2 = D_1 \quad \text{and} \quad f(w) = w_u j^2 + \frac{w_v j^2 x}{L}$$

The resulting formula for bending moment at any section between the left end of the span and the concentrated load  $W$  is, then,

$$M = \frac{D_2 - D_1 \cos \frac{L}{j} - Wj \sin \frac{b}{j} - w_v j^2}{\sin \frac{L}{j}} \sin \frac{x}{j} + D_1 \cos \frac{x}{j} + w_u j^2 + \frac{w_v j^2 x}{L}$$

Were the formula to be written for a section to the right of the concentrated load the parts of  $C_1$  and  $C_2$  dependent upon  $W$  would be altered to those for  $x > a$ . Experience proves that care must be exercised to have this seemingly obvious detail correct.

The location of the maximum bending moment on a beam-column is found by the same basic procedure as that used for locating the maximum bending moment on a simple beam. Since Eq. 14 : 14 represents the slope of the bending-moment curve, any value of  $x$  at which the total shear is zero represents a possible location of the section of maximum bending moment. For those loadings for which  $f'(w) = 0$ , the total shear will be zero when

$$\tan \frac{x}{j} = \frac{C_1}{C_2} \quad 14 : 17$$

Then, from well-known trigonometrical relations,

$$\sin \frac{x}{j} = \frac{C_1}{\sqrt{C_1^2 + C_2^2}} \quad \text{and} \quad \cos \frac{x}{j} = \frac{C_2}{\sqrt{C_1^2 + C_2^2}}$$

Substituting these values in Eq. 14 : 13 and simplifying, we obtain for the magnitude of the maximum moment

$$+ C_2^2 + f(w) \quad 14 : 18$$

This formula is ambiguous to the extent that there are a positive and a negative root to the expression under the radical. It can be shown

that, for values of  $x$  between 0 and  $L$ , the root to be taken should be the one with the same sign as  $C_1$ .<sup>1</sup>

The value of  $x$  to satisfy Eq. 14 : 17 should be determined for each of the segments of the beam-column for which a separate equation of the type of 14 : 13 is needed. Those values of  $x$  which fall outside the limits of applicability of the corresponding values of  $C_1$  and  $C_2$  should be disregarded, but Eq. 14 : 18 or its equivalent should be used to determine the moments at the sections represented by any remaining values of  $x$ . When  $f'(w) \neq 0$  the formulas corresponding to 14 : 17 and 14 : 18 are much too cumbersome for practical use and the simplest method of attack is to compute the moments at three or four points from Eq. 14 : 13, plot the results, and obtain a maximum value from a smooth curve through the points plotted. In addition to the sections of zero total shear located by means of Eq. 14 : 17 or by plotting, the bending moment may have its maximum value at one end of the span or at a concentrated transverse load. In the latter case it will be found that the total shears on the two sides of the load are of opposite sign. In practice all sections at which the bending moment is likely to be a maximum should be investigated.

When the transverse loading is symmetrical the maximum moment will obviously be at midspan. In such cases the maximum moment can usually be found most conveniently from the formulas of Table 14 : 4 in which the nomenclature is the same as in Table 14 : 3. The method of superposition can be applied to these formulas under the same limitations as for the formulas of Table 14 : 3.

Many of the beam-columns encountered in practice are of the class represented by case 1 of Table 14 : 3. In this case, when  $M_2 = 0$ , Eq. 14 : 17 becomes  $\tan x/j = -\cot L/j$ . Then if  $L/j$  is less than  $\pi/2$ , there will be no point of zero shear on the span of the member, and the maximum bending moment will be  $M_1$ . If  $L/j$  exceeds  $\pi/2$ , however, there will be a point of zero shear on the span at which the bending moment will be a maximum,<sup>2</sup> and equal to  $M_1 \operatorname{cosec} L/j$ . If  $M_2$  is not zero but there is a point of inflection in the span, and  $L/j$  is less than  $\pi/2$ , it should be evident that the maximum bending moment will be at one end.

<sup>1</sup> The radical of Eq. 14 : 18 is a simplification of  $(C_1^2 + C_2^2) \cos \frac{x}{j} / C_2$ . Study of this expression for values of  $x/j$  less than  $\pi$  will show that it will always have the same sign as  $C_1$ . It will be shown later that this range of values of  $x/j$  covers all practical cases.

<sup>2</sup> For this case  $C_1^2 + C_2^2 = M_1^2 (\cot^2 L/j + 1) = M_1^2 \operatorname{cosec}^2 L/j$ .



TABLE 14 : 4  
 FORMULAS FOR MAXIMUM MOMENT  
 BEAM-COLUMNS WITH AXIAL COMPRESSION

## CASE 2

$$M_{\max} = wj^2 \left( 1 - \sec \frac{L}{2j} \right)$$

Approximate formulas for this case are  
 Johnson's formula

$$M_{\max} = \frac{M_0}{1 - \frac{PL^2}{10EI}} \quad \text{or (more precisely)} \quad \frac{M_0}{1 - \frac{5PL^2}{48EI}}$$

and Perry's formula

$$M_{\max} = \frac{M_0 Q}{Q - P}$$

in which  $M_0 = -wL^2/8$  and  $Q = \pi^2 EI/L^2$

## CASE 3

$$M_{\max} = \frac{D_1}{\cos \frac{x}{j}} + wj^2$$

where  $D_1 = M_1 - wj^2$ . This formula may also be used for Cases 1 and 2.

## CASES 4a AND 1a COMBINED

$$M_{\max} = \frac{M_1}{\cos \frac{L}{2j}} - \frac{Wj}{2} \tan \frac{L}{2j}$$

## CASES 7 AND 1a COMBINED

$$M_{\max} = \frac{M_1}{\cos \frac{L}{2j}} - \frac{2wj^2}{L} \tan \frac{L}{2j} + wj^2$$

## CASES 8a AND 1a COMBINED

$$M_{\max} = \frac{M_1}{\cos \frac{L}{2j}} + wj^2 \left[ 1 - \frac{\cos \frac{a}{j}}{\cos \frac{L}{2j}} \right]$$

## CASES 9 AND 1a COMBINED

$$M_{\max} = \frac{M_1}{\cos \frac{L}{2j}} - Wj \frac{\sin \frac{a}{j}}{\cos \frac{L}{2j}}$$

*Single Span with Axial Tension* — In developing formulas for a beam-column subjected to axial tension and a given type of transverse load the starting point is an equation of the type of Eq. 14 : 1. This equation is identical with that for the same type of transverse load and axial compression except that the last term on the right-hand side is  $+Py$  instead of  $-Py$ . The consequences of this change of sign are that, wherever a trigonometric function appears in a formula for axial compression, the corresponding hyperbolic function appears in the corresponding formula for axial tension, and in many cases the signs are changed. As the changes in sign do not follow any simple rule, the formulas paralleling Eq. 14 : 13 to 14 : 18 are given below, and the values of  $C_1$ ,  $C_2$ , and  $f(w)$  to be used in these formulas are listed in Tables 14 : 5 and 14 : 6.

$$\text{Total shear} \quad S = \frac{C_1}{j} \cosh \frac{x}{j} + \frac{C_2}{j} \sinh \frac{x}{j} + f'(w) \quad 14 : 19$$

$$\text{Total moment} \quad M = C_1 \sinh \frac{x}{j} + C_2 \cosh \frac{x}{j} + f(w) \quad 14 : 20$$

$$\text{Slope} \quad \theta = \frac{S - S_0}{P} \quad 14 : 21$$

$$\text{Deflection} \quad \delta = \frac{M - M_0}{P} \quad 14 : 22$$

Location of point of zero shear when  $f'(w) = 0$

$$\tanh \frac{x}{j} = -\frac{C_1}{C_2} \quad 14 : 23$$

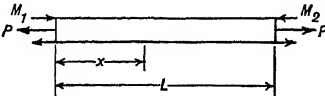
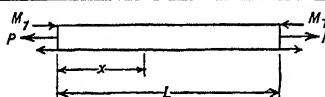
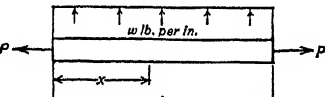
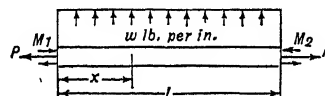
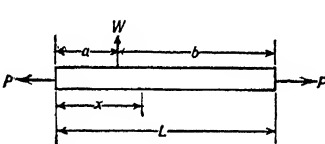
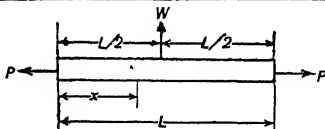
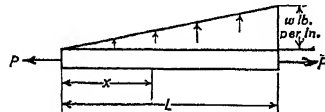
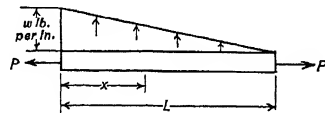
When  $C_1$  and  $C_2$  are of the same sign,  $x$  from Eq. 14 : 23 will be negative, indicating that the point of zero total shear is to the left of the span, and the corresponding value of  $M$  is of no practical interest. If  $C_1$  and  $C_2$  are of opposite sign, the bending moment at the section where the slope of the moment curve is zero can be obtained from the formula

$$M_{\min} = \sqrt{C_2^2 - C_1^2} + f(w) \quad 14 : 24$$

In applying this formula the quantity under the radical sign should be given the same sign as the numerically larger of the two constants. Usually the bending moment obtained from Eq. 14 : 24 is an arithmetical minimum rather than a maximum.

The method of superposition can be applied to beam-columns with axial tension in the same manner as when the axial load is compression.

TABLE 14:5  
TERMS FOR BEAM-COLUMN FORMULAS  
AXIAL TENSION

Case	Loading	$C_1$
1 	Unequal end moments	$\frac{M_2 - M_1 \cosh \frac{L}{j}}{\sinh \frac{L}{j}}$
1a 	Equal end moments	$-M_1 \tanh \frac{L}{2j}$
2 	Uniformly distributed	$\frac{wj^2 (1 - \cosh \frac{L}{j})}{\sinh \frac{L}{j}}$
3 	Uniform plus end moments	$\frac{D_2 - D_1 \cosh \frac{L}{j}}{\sinh \frac{L}{j}}$
4 	Concentrated load	$x < a \quad - \frac{Wj \sinh \frac{b}{j}}{\sinh \frac{L}{j}}$ $x > a \quad \frac{Wj \sinh \frac{a}{j}}{\tanh \frac{L}{j}}$
4a 	Concentrated load at center	$x < \frac{L}{2} \quad - \frac{Wj}{2} \operatorname{sech} \frac{L}{2j}$ $x > \frac{L}{2} \quad \frac{Wj}{2} \cosh \frac{L}{j} \operatorname{sech} \frac{L}{2j}$
5 	Uniformly varying increase to right	$\frac{wj^2}{\sinh \frac{L}{j}}$
6 	Uniformly varying decrease to right	$- \frac{wj^2}{\tanh \frac{L}{j}}$

$$* D_1 = M_1 + wj^2, \quad D_2 = M_2 + wj^2$$

TABLE 14 : 5  
TERMS FOR BEAM-COLUMN FORMULAS  
AXIAL TENSION

$C_2$	$f(w)$	Terms for Three-moment Equation	
		Left Bay	Right Bay
$M_1$	0	0	0
$M_1$	0	0	0
$wj^2$	$-wj^2$	$\frac{w_1 L_1^2 \gamma h_1}{4I_1}$	$\frac{w_2 L_2^2 \gamma h_2}{4I_2}$
$D_1^*$	$-wj^2$	Same as Case 2	Same as Case 2
0 $-Wj \sinh \frac{\alpha}{j}$	0 0	$\frac{6W_1 j_1^2}{I_1} \left[ \frac{a_1}{L_1} - \frac{\sinh \frac{a_1}{j_1}}{\sinh \frac{L_1}{j_1}} \right]$	$\frac{6W_2 j_2^2}{I_2} \left[ \frac{b_2}{L_2} - \frac{\sinh \frac{b_2}{j_2}}{\sinh \frac{L_2}{j_2}} \right]$
0 $-Wj \sinh \frac{L}{2j}$	0 0	$\frac{3W_1 j_1^2}{I_1} \left( 1 - \operatorname{sech} \frac{L_1}{2j_1} \right)$	$\frac{3W_2 j_2^2}{I_2} \left( 1 - \operatorname{sech} \frac{L_2}{2j_2} \right)$
0	$-\frac{wj^2 x}{L}$	$\frac{2w_1 L_1 j_1^2 (1 - \beta_{h1})}{I_1}$	$\frac{w_2 L_2 j_2^2 (1 - \alpha_{h2})}{I_2}$
$wj^2$	$-wj^2 \left( 1 - \frac{x}{L} \right)$	$\frac{w_1 L_1 j_1^2 (1 - \alpha_{h1})}{I_1}$	$\frac{2w_2 L_2 j_2^2 (1 - \beta_{h2})}{I_2}$

TABLE 14:5 (Continued)  
TERMS FOR BEAM-COLUMN FORMULAS  
AXIAL TENSION

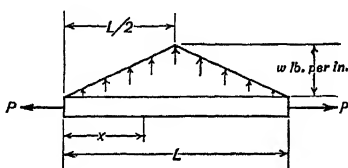
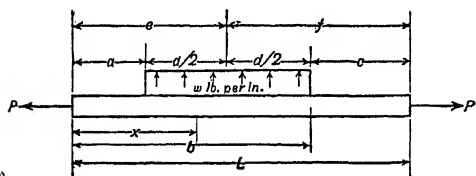
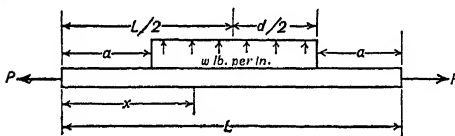
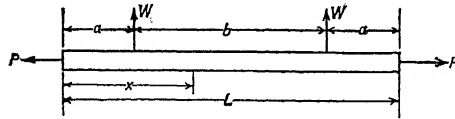
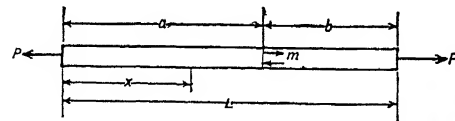
Case	Loading	$C_1$
<p>7</p> 	Symmetrical triangle	$z < \frac{L}{2} \quad \frac{2wj^2}{L \cosh \frac{L}{2j}}$ $z > \frac{L}{2} \quad - \frac{2wj^2 \cosh \frac{L}{2j}}{L \cosh \frac{L}{2j}}$
<p>8</p> 	Partial uniformly distributed	$z < a \quad - \frac{2wj^2 \sinh \frac{d}{2j} \sinh \frac{f}{j}}{\sinh \frac{L}{j}}$ $a < z < b \quad \frac{2wj^2 \sinh \frac{d}{2j} \sinh \frac{e}{j}}{\tanh \frac{L}{j}} - wj^2 \sinh \frac{b}{j}$ $b < z < L \quad \frac{2wj^2 \sinh \frac{d}{2j} \sinh \frac{e}{j}}{\tanh \frac{L}{j}}$
<p>8a</p> 	Symmetrical partial uniformly distributed	$z < a \quad - \frac{wj^2 \sinh \frac{d}{2j}}{\cosh \frac{L}{2j}}$ $a < z < L - a \quad - wj^2 \cosh \frac{a}{j} \tanh \frac{L}{2j}$ $L - a < z < L \quad \frac{wj^2 \sinh \frac{d}{2j} \cosh \frac{L}{j}}{\cosh \frac{L}{2j}}$
<p>9</p> 	Two symmetrical concentrated loads	$z < a \quad - \frac{Wj \cosh \frac{b}{2j}}{\cosh \frac{L}{2j}}$ $a < z < L - a \quad Wj \sinh \frac{a}{j} \tanh \frac{L}{2j}$ $L - a < z < L \quad \frac{Wj \cosh \frac{L}{j} \cosh \frac{b}{2j}}{\cosh \frac{L}{2j}}$
<p>10</p> 	Clockwise Couple	$z < a \quad \frac{m \cosh \frac{b}{j}}{\sinh \frac{L}{j}}$ $z > a \quad - \frac{m \cosh \frac{a}{j}}{\tanh \frac{L}{j}}$

TABLE 14 : 5  
TERMS FOR BEAM-COLUMN FORMULAS  
AXIAL TENSION

$C_2$	$f(w)$	Terms for Three-moment Equation	
		Left Bay	Right Bay
$0$  $\frac{4wj^3}{L} \sinh \frac{L}{2j}$	$-\frac{2wj^2x}{L}$  $-2wj^2 \left(1 - \frac{x}{L}\right)$	$\frac{12wj_1^2}{I_1} \left[ \frac{j_1^2}{L_1} \left( \operatorname{sech} \frac{L_1}{2j_1} - 1 \right) + \frac{L_1}{8} \right]$	$\frac{12wj_2}{I_2} \left[ \frac{j_2^2}{L_2} \left( \operatorname{sech} \frac{L_2}{2j_2} - 1 \right) + \frac{L_2}{8} \right]$
$0$  $wj^2 \cosh \frac{a}{j}$  $-2wj^2 \sinh \frac{d}{2j} \sinh \frac{e}{j}$	$0$  $-wj^2$  $0$	$\frac{12wj_1^2}{I_1} \left[ \frac{d_1 e_1}{2L_1} - \frac{j_1 \sinh \frac{d_1}{2j_1} \sinh \frac{e_1}{j_1}}{\sinh \frac{L_1}{j_1}} \right]$	$\frac{12wj_2}{I_2} \left[ \frac{d_2 j_2}{2L_2} - \frac{j_2 \sinh \frac{d_2}{2j_2} \sinh \frac{j_2}{j_2}}{\sinh \frac{L_2}{j_2}} \right]$
$0$  $wj^2 \cosh \frac{a}{j}$  $-2wj^2 \sinh \frac{d}{2j} \sinh \frac{L}{2j}$	$0$  $-wj^2$  $0$	$\frac{3wj_1^2}{I_1} \left[ d_1 - \frac{2j_1 \sinh \frac{d_1}{2j_1}}{\cosh \frac{L_1}{2j_1}} \right]$	$\frac{3wj_2^2}{I_2} \left[ d_2 - \frac{2j_2 \sinh \frac{d_2}{2j_2}}{\cosh \frac{L_2}{2j_2}} \right]$
$0$  $-Wj \sinh \frac{a}{j}$  $\frac{Wj \sinh \frac{L}{j} \cosh \frac{b}{2j}}{\cosh \frac{L}{2j}}$	$0$  $0$  $0$	$\frac{6Wj_1^2}{I_1} \left[ 1 - \frac{\cosh \frac{b_1}{2j_1}}{\cosh \frac{L_1}{2j_1}} \right]$	$\frac{6Wj_2^2}{I_2} \left[ 1 - \frac{\cosh \frac{b_2}{2j_2}}{\cosh \frac{L_2}{2j_2}} \right]$
$0$  $m \cosh \frac{a}{j}$	$0$  $0$	$\frac{6mj_1}{I_1} \left[ \frac{\cosh \frac{a_1}{j_1}}{\sinh \frac{L_1}{j_1}} - \frac{j_1}{L_1} \right]$	$\frac{6mj_2}{I_2} \left[ \frac{j_2}{L_2} - \frac{\cosh \frac{b_2}{j_2}}{\sinh \frac{L_2}{j_2}} \right]$

TABLE 14:6  
TERMS FOR BEAM-COLUMN FORMULAS  
VARIANT FORMS  
Axial Compression

CASE 4  $x < a$

$$C_1 = \frac{Wj \sin \frac{a}{j}}{\tan \frac{L}{j}} - Wj \cos \frac{a}{j}$$

CASE 8  $x < a$

$$C_1 = wj^2 \left[ \frac{\cos \frac{a}{j} - \cos \frac{b}{j}}{\tan \frac{L}{j}} + \sin \frac{a}{j} - \sin \frac{b}{j} \right] \quad C_2 = 0$$

$a < x < b$

$$C_1 = wj^2 \left[ \frac{\cos \frac{a}{j} - \cos \frac{b}{j}}{\tan \frac{L}{j}} - \sin \frac{b}{j} \right] \quad C_2 = -wj^2 \cos \frac{a}{j}$$

$b < x < L$

$$C_1 = wj^2 \left[ \frac{\cos \frac{a}{j} - \cos \frac{b}{j}}{\tan \frac{L}{j}} \right] \quad C_2 = wj^2 \left( \cos \frac{b}{j} - \cos \frac{a}{j} \right)$$

CASE 9  $L - a < x < L$

$$C_2 = -2 Wj \sin \frac{L}{2j} \cos \frac{b}{2j}$$

CASE 10  $x < a$

$$C_1 = -\frac{m \cos \frac{a}{j}}{\tan \frac{L}{j}} - m \sin \frac{a}{j}$$

Axial Tension

CASE 4  $x < a$

$$C_1 = \frac{Wj \sinh \frac{a}{j}}{\tanh \frac{L}{j}} - Wj \cosh \frac{a}{j}$$

TABLE 14 : 6 — (Continued)

CASE 8  $x < a$

$$C_1 = wj^2 \left[ \frac{\cosh \frac{b}{j} - \cosh \frac{a}{j}}{\tanh \frac{L}{j}} + \sinh \frac{a}{j} - \sinh \frac{b}{j} \right] \quad C_2 = 0$$

$a < x < b$

$$C_1 = wj^2 \left[ \frac{\cosh \frac{b}{j} - \cosh \frac{a}{j}}{\tanh \frac{L}{j}} - \sinh \frac{b}{j} \right] \quad C_2 = wj^2 \cosh \frac{a}{j}$$

$b < x < L$

$$C_1 = wj^2 \left[ \frac{\cosh \frac{b}{j} - \cosh \frac{a}{j}}{\tanh \frac{L}{j}} \right] \quad C_2 = wj^2 \left( \cosh \frac{a}{j} - \cosh \frac{b}{j} \right)$$

CASE 9  $L - a < x < L$

$$C_2 = -2 Wj \sinh \frac{L}{2j} \cosh \frac{b}{2j}$$

CASE 10  $x < a$

$$C_1 = - \frac{m \cosh \frac{a}{j}}{\tanh \frac{L}{j}} + m \sinh \frac{a}{j}$$

The usual effect of axial tension is to make the total bending moment at any point less than the primary bending moment. Since most designers therefore follow the conservative practice of using the primary instead of the total moment in computing the margin of safety, the formulas of Table 14 : 5 are seldom used unless specially precise figures are desired. For this reason, it does not appear necessary to tabulate formulas similar to those of Table 14 : 4 for cases with axial tension.

*Three-moment Equations* — The form of the left side of the three-moment equation when an axial load is present is similar to that with no axial load except that each term is modified by a coefficient to provide for the effect of the axial load. When the axial load causes compression in the span the left side of the equation is

$$\frac{M_1 L_1 \alpha_1}{I_1} + 2 M_{-2} \frac{L_1}{I_1} \beta_1 + 2 M_{+2} \frac{L_2}{I_2} \beta_2 + \frac{M_3 L_2 \alpha_2}{I_2}$$

When the axial load causes tension in the span the left side of the



equation is

$$\frac{M_1 L_1 \alpha_{h1}}{I_1} + 2 M_{-2} \frac{L_1}{I_1} \beta_{h1} + 2 M_{+2} \frac{L_2}{I_2} \beta_{h2} + \frac{M_3 L_2 \alpha_{h2}}{I_2}$$

Values of  $\alpha$ ,  $\beta$ ,  $\alpha_h$ , and  $\beta_h$  are given in Tables 14 : 2 and 14 : 7.

Attention is called to the fact that the  $\alpha$  and  $\beta$  values for the case of axial compression are dependent on the common circular functions, whereas those for axial tension are based upon the hyperbolic functions. The subscript,  $h$ , is therefore used to differentiate between the two sets of functions, and care should be exercised to take the proper values in each case.

The terms on the right side of the equation depend on the type of loading on the spans. They are similar to those used when there is no axial load, except for the coefficients which provide for such load. The terms to be used with axial compression are listed in Table 14 : 3, and those for use with axial tension in Table 14 : 5. In both tables two terms are given for each type of loading, one to be used when the load is on the left-hand bay and the other when it is on the right. If the load on any bay is composed of a series of loads, the right side of the three-moment equation may be built up by applying the method of superposition in the same manner as when no axial load is present. Care must be taken that the correct values of the coefficients are used, depending on whether the axial load is tensile or compressive.

The terms providing for deflection of the supports are identical with those for the cases of no axial load as given in Art. 5 : 2. These terms are added to the right side of the equation in the same way as they appear in Eq. 5 : 3 in that article. They are not modified by coefficients to provide for the effect of the axial load. On the other hand, when there is deflection of the supports, care must be exercised in computing the reactions to take proper account of the effect of the axial load. If the transverse loads and the reactions are vertical, and the supports remain on a horizontal line, the reactions will not be directly affected by the axial loads in the various spans, since those loads will have no vertical components. If, however, one end of a span is higher than the other its axial load will have a vertical component equal to  $P (y_2 - y_1)/L$ , in which  $y_1$  and  $y_2$  are the vertical distances of the ends of the span from a horizontal base line. If the right end is higher than the left, and the axial load is compressive, the left reaction should contain an upward and the right reaction a downward force of that magnitude in addition to the forces computed from the transverse loads and end moments. The adjustments to be made if the left end is the higher or the axial load is tension should be evident.

TABLE 14:7

FUNCTIONS FOR THREE-MOMENT EQUATIONS —  $\alpha_h, f$  AND  $\gamma_h$  FUNCTIONS FOR AXIAL TENSION

$L/j$	$\alpha_h$	$\Delta\alpha_h$	$\beta_h$	$\Delta\beta_h$	$\gamma_h$	$\Delta\gamma_h$	$L/j$
0.00	1.0000		1.0000		1.0000		0.00
0.50	0.9716	0.0284	0.9837	0.0163	0.9756	0.0244	0.50
1.00	0.8945	0.0771	0.9391	0.0446	0.9092	0.0664	1.00
1.05	0.8848	0.0097	0.9334	0.0057	0.9009	0.0083	1.05
1.10	0.8748	0.0100	0.9276	0.0058	0.8922	0.0087	1.10
1.15	0.8647	0.0101	0.9216	0.0060	0.8833	0.0089	1.15
1.20	0.8542	0.0105	0.9155	0.0061	0.8743	0.0090	1.20
1.25	0.8436	0.0106	0.9093	0.0062	0.8651	0.0092	1.25
1.30	0.8328	0.0108	0.9028	0.0065	0.8557	0.0094	1.30
1.35	0.8218	0.0110	0.8963	0.0065	0.8461	0.0096	1.35
1.40	0.8107	0.0111	0.8897	0.0066	0.8364	0.0097	1.40
1.45	0.7994	0.0113	0.8830	0.0067	0.8266	0.0098	1.45
1.50	0.7881	0.0113	0.8762	0.0068	0.8167	0.0099	1.50
1.55	0.7767	0.0114	0.8694	0.0068	0.8067	0.0100	1.55
1.60	0.7652	0.0115	0.8625	0.0069	0.7967	0.0100	1.60
1.65	0.7537	0.0115	0.8555	0.0070	0.7867	0.0100	1.65
1.70	0.7421	0.0116	0.8485	0.0070	0.7766	0.0101	1.70
1.75	0.7305	0.0116	0.8415	0.0071	0.7664	0.0102	1.75
1.80	0.7189	0.0116	0.8344	0.0071	0.7560	0.0103	1.80
1.85	0.7073	0.0116	0.8273	0.0071	0.7457	0.0103	1.85
1.90	0.6958	0.0115	0.8202	0.0071	0.7355	0.0102	1.90
1.95	0.6843	0.0115	0.8131	0.0071	0.7253	0.0102	1.95
2.00	0.6728	0.0115	0.8060	0.0071	0.7152	0.0101	2.00
2.05	0.6614	0.0114	0.7989	0.0071	0.7051	0.0101	2.05
2.10	0.6501	0.0113	0.7918	0.0071	0.6950	0.0101	2.10
2.15	0.6389	0.0112	0.7847	0.0071	0.6850	0.0100	2.15
2.20	0.6278	0.0111	0.7777	0.0070	0.6750	0.0100	2.20

TABLE 14:7  
FUNCTIONS FOR THREE-MOMENT EQUATIONS— $\alpha_h$ ,  $\beta_h$ , AND  $\gamma_h$  FUNCTIONS FOR AXIAL  
TENSION — (Concluded)

$L/j$	$\alpha_h$	$\Delta\alpha_h$	$\beta_h$	$\Delta\beta_h$	$\gamma_h$	$\Delta\gamma_h$	$L/j$
2.20	0.6278		0.7777		0.6750		2.20
		0.0111		0.0070		0.0098	
2.25	0.6167	0.0109	0.7707	0.0070	0.6652	0.0097	2.25
2.30	0.6058	0.0108	0.7637	0.0069	0.6555	0.0098	2.30
2.35	0.5950	0.0107	0.7568	0.0069	0.6457	0.0097	2.35
2.40	0.5843	0.0106	0.7499	0.0069	0.6360	0.0095	2.40
2.45	0.5737	0.0104	0.7430	0.0068	0.6265	0.0095	2.45
2.50	0.5633	0.0103	0.7362	0.0067	0.6170	0.0093	2.50
2.55	0.5530	0.0101	0.7295	0.0067	0.6077	0.0092	2.55
2.60	0.5429	0.0100	0.7228	0.0066	0.5985	0.0092	2.60
2.65	0.5329	0.0099	0.7162	0.0065	0.5893	0.0090	2.65
2.70	0.5230	0.0097	0.7097	0.0065	0.5803	0.0088	2.70
2.75	0.5133	0.0096	0.7032	0.0065	0.5715	0.0088	2.75
2.80	0.5037	0.0094	0.6967	0.0064	0.5627	0.0085	2.80
2.85	0.4943	0.0092	0.6903	0.0063	0.5542	0.0085	2.85
2.90	0.4851	0.0091	0.6840	0.0062	0.5457	0.0085	2.90
2.95	0.4760	0.0090	0.6778	0.0062	0.5372	0.0084	2.95
3.00	0.4670	0.0087	0.6716	0.0061	0.5288	0.0083	3.00
3.05	0.4583	0.0087	0.6655	0.0060	0.5205	0.0080	3.05
3.10	0.4496	0.0085	0.6595	0.0059	0.5125	0.0080	3.10
3.15	0.4411	0.0083	0.6536	0.0060	0.5045	0.0077	3.15
3.20	0.4328		0.6476		0.4968		3.20

The expressions for the bending moment, etc., on an axially loaded beam differ considerably in form from those for beams with the same types of lateral load but no axial load. In many cases, if the axial load and therefore  $L/j$  is zero, the formulas reduce to the indeterminate forms  $0/0$  and  $\infty/\infty$ . Such forms can be evaluated by the standard method described in works on differential calculus, and when this is done will give expressions that are identical with the usual formulas for beams without axial load. Thus the coefficients of the three-moment

equation for a beam with a uniformly distributed lateral load all become equal to unity when  $L/j = 0$ , making this equation the same as that derived in Chapter V.

All the formulas of this article are based upon the assumption that the moment of inertia of the strut or continuous beam is a constant throughout each span, though it may differ as between spans. If the moment of inertia varies, they will give incorrect results, though if the variation is small or extends over but a small part of the span, they will give results of sufficient precision. For more precise work, the method described in Art. 14 : 13 must be used.

**14 : 6. Critical Loads** — As the axial load  $P$  in a member increases, the value of  $L/j$  also increases. When  $P = L/j = 0$ , there is no axial load to multiply by the deflection and therefore there is no secondary bending, hence the primary bending moment is identical with the total bending moment. For small values of  $P$  and  $L/j$  the secondary bending is small in comparison with the primary bending but the ratio of the former to the latter increases with an increase in  $P$  and  $L/j$ . If the axial load is compressive and increases further, a point is reached when the sum of the series of increments of bending moment constituting the secondary bending becomes infinite. The loading at which this takes place is known as the "critical load," or "critical value of  $L/j$ ." The critical load and the ultimate load — the load that would cause failure — are not the same except for the ideal Euler strut.

The maximum fiber stress on any cross-section of a member subjected to combined bending and compression is represented by the formula

If  $M_0$  is the primary bending moment, and  $\delta$  the deflection, this formula can be written:

$$f = \frac{P}{A} + \frac{P\delta y}{I} + \frac{M_0 y}{I}$$

As the deflection  $\delta$  increases, the unit stress  $f$  will increase, the ultimate compressive strength of the material will be reached, and the member will fail at a load below the critical. The critical load is therefore not the maximum load that an actual physical member can carry, but rather the load under which the member would be elastically unstable and would fail even if the material had infinite compressive strength.

The expressions for bending moment and deflection are of such character that, even though they are used with values of  $P$  and  $L/j$

greater than the critical, the moments and deflections obtained will be finite. Obviously, however, they do not apply when  $P$  and  $L/j$  are so large, and it is therefore of importance to the designer to be able to determine the critical load of the member he is designing, or at least be certain that the load to be carried is less than the critical one.

Study of any of the formulas for combined bending and compression will show that, for any type of lateral load, as the axial load  $P$  and hence  $L/j$  increase, the bending moment and deflection also increase, although the lateral load may remain constant. This increase will continue until the critical value of  $L/j$  is reached, when the formulas indicate that the bending moment and deflection are infinite. To determine the critical load, however, care must be taken to make sure that the formulas really give the value of infinity for the bending moment or deflection, as there are several special cases where they give the indeterminate forms  $0/0$  and  $\infty/\infty$ .

The formula for the bending moment at any point in a single span subjected to axial compression and a uniformly distributed lateral load is

$$M = \frac{D_2 - D_1 \cos \frac{L}{j}}{\sin \frac{L}{j}} \sin \frac{x}{j} + D_1 \cos \frac{x}{j} + wj^2$$

This expression for  $M$  is determinate for all values of  $L/j$  less than  $\pi$ ; but when  $L/j = \pi$  then  $\sin L/j = 0$  and the first term appears to become infinite. In most cases it will become infinite, indicating that

the critical load is such that  $L \div \sqrt{\frac{EI}{P}} = \pi$ , or  $P = \frac{\pi^2 EI}{L^2}$ . This value of  $P$  is the Euler load for the member if considered as a pin-ended column, and its appearance as the critical load for this case is a reflection of the fact that the critical load is independent of the magnitude or distribution of the transverse load.

There is one case, however, in which  $\pi$  is not the critical value for  $L/j$  in the above formula. If  $D_2 = D_1 \cos \pi$ , the expression for  $M$  takes the indeterminate form  $0/0 + D_1 \cos \pi + wj^2$ . As  $\cos \pi = -1$ , we would get this result if  $M_2 - wj^2 + M_1 - wj^2 = 0$  or  $M_2 = 2wj^2 - M_1$ . It will be found, however, that this is precisely the relation between  $M_1$ ,  $M_2$ , and  $w$  in a span of a *continuous* beam for which  $L/j = \pi$ . Similar relations will be found for other types of transverse load when  $L/j = \pi$  and the beam-column forms one span of a continuous beam.

If the span being investigated is the only one,  $\pi$  is the critical value of

$L/j$ . If, however, it is one of a rigidly connected series,  $\pi$  is not the critical value of  $L/j$ , but the critical value is that due to some larger axial load that would cause an infinite bending moment over one of the supports.<sup>1</sup> Such a result may seem unreasonable at first glance, but a little study will show that it is quite in line with what should be expected.

If the axial compression in the span shown in Fig. 14 : 7 is such that  $L/j = \pi$ , the center portion of the span will tend to deflect infinitely — and will deflect, in fact, until the material fails. The loads on the cantilevers may give the beam a little reversed curvature at the supports, but they will not be able to prevent rotation of the beam about those supports due to the action of the combined lateral and axial loads

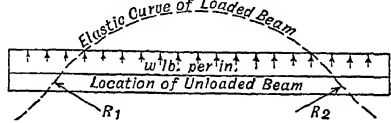


FIG. 14 : 7

in the span. In the case of a continuous beam, the conditions are different. Suppose  $L/j = \pi$  in the left-hand span of the beam in Fig. 14 : 8 and is less than  $\pi$  in the right-hand span. While the load on the left-hand cantilever cannot prevent rotation of the beam about support 1, rotation about support 2 is limited by the action of the right-hand span and the reaction at support 3. The bending moment at support 2 depends in part upon this action; and when  $M_2$  is such that  $D_1 = D_2 \cos \pi$ , a condition of equilibrium is reached. The result is

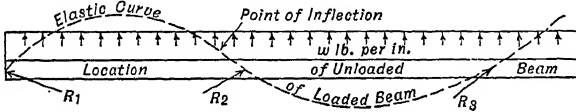


FIG. 14 : 8

that there is a point of inflection fixed a short distance to the left of support 2 and the span may be considered as made up of two parts: a cantilever from support 2 to the point of inflection, and a beam with one end restrained and the other pinned between support 1 and the point of inflection. The latter beam may have a value of  $L/j$  less than  $\pi$  although  $L/j$  for the entire left-hand span is greater than  $\pi$ , and may thus be stable.

The critical load for a continuous beam-column is that which (if the formulas of this chapter still applied in spite of the elastic limit being passed) would produce infinite bending moment over one or more of the

<sup>1</sup> An exception to this general rule is that, when  $L/j = \pi$  in all spans simultaneously and the beam-column is free to rotate at the end supports, the critical load has been reached.

supports. In any specific case the combinations of axial loads in the various spans that would be found critical can be determined from a study of the three-moment equations that would be used to compute the redundant support moments. These equations should be written down in the manner suggested in Art. 13 : 17, with the terms for the known transverse loads, the deflections of the supports, and any statically determinate moments at the supports on the right-hand side of the equality signs. These terms will then form a column which will be termed the "column of known quantities." On the left-hand side of the equality signs there will then be a column for each of the redundant support moments, and its coefficients. If the symbols for the redundant moments are omitted, the coefficients of these moments will be in the form of a determinant which will be called the "denominator determinant." Then each of the redundant moments may be found by dividing the denominator determinant into the determinant formed by replacing the coefficients of that moment in the denominator determinant by the column of known quantities. From this procedure for evaluating the redundant support moments, it can be seen that the critical load will be one which will cause the value of the denominator determinant to become zero. It also shows that the critical load is independent of the magnitude and distribution of the transverse load, but depends solely on the dimensions and material of the beam-column, the axial loads in the spans, and the locations and types of support.

Suppose it is desired to determine the critical load for a beam-column of constant cross-section with fixed-end supports, two spans of equal length, and the same axial load in both spans. As  $I$  is constant and the values of  $L$ ,  $\alpha$ , and  $\beta$  will be the same for both spans, the three-moment equations for this case may be written

$$\begin{aligned} 2\beta LM_1 + \alpha LM_2 &= k_1 \\ \alpha LM_1 + 4\beta LM_2 + \alpha LM_3 &= k_2 \\ \alpha LM_2 + 2\beta LM_3 &= k_3 \end{aligned}$$

where  $k_1$ ,  $k_2$ , and  $k_3$  are the terms representing the effects of transverse loads and deflections of the supports. The denominator determinant for this case is then

$$\begin{vmatrix} 2\beta L & \alpha L & 0 \\ \alpha L & 4\beta L & \alpha L \\ 0 & \alpha L & 2\beta L \end{vmatrix} = 16\beta^3 L^3 - 4\alpha^2 \beta L^3$$

The value of the denominator determinant will be zero when  $\beta = 0$  or  $\alpha = \pm 2\beta$ . From Table 14 : 2 we find that  $\alpha = 2\beta$  when  $L/j = \pi$  or  $2\pi$ , and that  $\beta = 0$  when  $L/j = 4.49+$ . When  $L/j = \pi$ , it will be found that the numerator determinants formed by substituting the

column of known quantities for one of the columns of the denominator determinant will also become zero and the resulting value of  $0/0$  will be finite. This will not be the case, however, when  $L/j = 4.49+$ , so the axial load which produces that value of  $L/j$  will be the critical one.

If the transverse loading had been assumed symmetrical, the denominator determinant for the case under consideration would have been

$$2 \alpha L \quad 4 \beta L \quad \alpha L \\ = 8 \beta^2 L^2 - 2 \alpha^2 L^2$$

The resulting critical load would then be that making  $\alpha = \pm 2 \beta$ , or  $L/j = 2 \pi$ . In this case, however, for values of  $L/j$  between  $4.49+$  and  $2 \pi$  the beam-column would be in unstable equilibrium, and the slightest departure from perfect symmetry of construction or loading would result in its collapse. Similarly, if the criterion is applied to any symmetrical continuous beam-column a fictitiously high critical load may result. It should therefore always be applied to the three-moment equations that would be used if the transverse loading were unsymmetrical.

This method of attack can be used in any case in which the ratios of the axial loads in the various spans remain constant, but is likely to involve tedious computations to determine the critical values of  $L/j$ .

An alternative method of determining the critical loads has been developed and applied to a few simple cases by Professor John E. Younger of the University of California. The most important of these cases is that of a beam-column resting on three supports, with or without overhanging cantilever ends. For simplicity it will be assumed that each span is subjected to a uniformly distributed load, though the criterion applies regardless of the type of transverse load assumed. It will also be assumed that the values of  $L/j$  for the left-hand span are consistently greater than those in the right-hand span, that the ratio  $P_1/P_2$  is a constant, and that the lateral load on each span is uniformly distributed. As the bending moments  $M_1$  and  $M_3$  over the outer supports are determined by the loads on the cantilever overhangs, if any, they may be treated as known constants, and the moment  $M_2$  over the center support remains to be determined by the three-moment equation. The three-moment equation for this case is Eq. 14 : 11 given in Art. 14 : 3. For the present discussion it is advisable to rearrange its terms and write

$$M_2 = \frac{I_1}{2 \left( \frac{1}{\beta_1} + \frac{1}{\beta_2} \right)}$$



As the axial loads in the two spans increase, the coefficients  $\alpha$ ,  $\beta$ , and  $\gamma$  increase but the formula gives a finite value for  $M_2$ . When  $L_1/j_1 = \pi$ ;  $\alpha_1$ ,  $\beta_1$ , and  $\gamma_1$  all become infinite and we have the value of  $M_2$  given by the indeterminate expression  $\infty/\infty$ . This expression can be evaluated by the standard method for handling indeterminate forms and then becomes  $M_2 = 2 w j^2 - M_1$ , a finite quantity.

If the axial load is further increased, we will have  $L_1/j_1$  greater than  $\pi$  and  $L_2/j_2$  still less than  $\pi$  but both increasing. Study of the tables of  $\alpha$ ,  $\beta$ , and  $\gamma$  will show that these quantities for the left-hand bay are negative and decreasing in absolute magnitude, while for the right-hand bay they are positive and increasing in magnitude. At first, then, the complex quantity  $\frac{L_1}{I_1} \beta_1 + \frac{L_2}{I_2} \beta_2$  will be negative, the first term being negative and of greater absolute magnitude than the second. As the values of  $L/j$  increase further the absolute magnitude of the first term will decrease while that of the second will increase until a point is reached where the whole expression  $\frac{L_1}{I_1} \beta_1 + \frac{L_2}{I_2} \beta_2$  will be equal to zero.

When this happens, it is hardly likely that the numerator of the expression for  $M_2$  will also be zero, so we can safely assume that at this loading  $M_2$  becomes infinite, indicating that the loading causing this condition is the critical load.

If the axial loading is still further increased, the absolute magnitude of  $\frac{L_1}{I_1} \beta_1$  will continue to decrease while that of  $\frac{L_2}{I_2} \beta_2$  will increase, and their sum will therefore be positive until  $L_2/j_2$  becomes equal to  $\pi$ . When both values of  $L/j$  are greater than  $\pi$ , both  $\beta_1$  and  $\beta_2$  will be negative.

The criteria for the critical loads for the case being considered can therefore be summarized as follows: If  $L/j$  is less than  $\pi$  for both spans the axial loading is less than the critical, but if it is greater than  $\pi$  for both spans the axial loading is greater than the critical. If  $L/j$  is less than  $\pi$  for one span and greater than  $\pi$  for the other, and the quantity  $\frac{L_1}{I_1} \beta_1 + \frac{L_2}{I_2} \beta_2$  is negative, the axial loading is less than the critical; but if the quantity  $\frac{L_1}{I_1} \beta_1 + \frac{L_2}{I_2} \beta_2$  is positive the axial loading is greater than the critical.

The criteria for continuous beam-columns may be summarized as follows. When  $L/j$  is less than  $\pi$  for all spans the critical load has not been reached. When  $L/j$  exceeds  $2\pi$  for any span the critical load has

been exceeded. The only debatable cases are those in which  $L/j$  for some spans is less than  $\pi$  while for others it is between  $\pi$  and  $2\pi$ . The critical loads for such cases can be determined by either of the methods discussed above. In most practical designs, however, when  $L/j$  in any span exceeds  $\pi$  the deflections and secondary moments are so great that the member would fail as the result of excessive compression on its most-stressed fibers. It is therefore a good rule to avoid designs involving values of  $L/j$  greater than  $\pi$  whenever possible.

The above discussion has been confined to single spans and continuous beams. The airplane designer is often interested also in the critical loads for members of rigid jointed trusses such as those used in welded tube fuselages. In such cases also, if  $L/j < \pi$  for all compression members the structure is stable, and if  $L/j > 2\pi$  for any compression member the structure is unstable. Several investigators have developed methods for determining the critical loads in the intermediate range. That which appears most practical is discussed in Art. 18 : 12.

**14 : 7. Approximate Computations** — In preliminary design work and similar approximate computations much labor can often be saved by the use of approximate formulas. If the first few terms of the infinite series are substituted for the secant term in the precise formula for the maximum moment on a pin-ended strut with uniformly distributed transverse load (Case 2, Table 14 : 4) it becomes

$$M = 1 - \frac{5 PL^2}{48 EI}$$

where  $M_0 = -wL^2/8$  the primary bending moment due to side load alone. If for  $5/48$  we substitute  $1/10$  we obtain Johnson's approximate formula for this case, while the substitution of  $1/\pi^2$  will give Perry's formula,

$$M = M_0 \frac{Q}{Q - P}$$

where  $Q$  is the Euler load of the strut in question.

The formulas above show that for the loading under consideration there are definite relationships between the ratios  $M/M_0$ ,  $P/Q$ , and  $L/j$ . In Fig. 14 : 9 are plotted curves showing the corresponding values of these ratios. If the locations of two points of inflection are definitely known, and the load between them is uniformly distributed, these curves can be used to compute the actual maximum total bending moment between those points of inflection from the maximum primary moment. Usually, however, the positions of the points of inflection

are not known definitely, as one effect of the axial load is to shift them to locations that differ from those when the primary moment is zero. The experienced designer, however, can estimate the amount of this shift and make a reasonable approximation of the maximum total moment from the primary moments and the curves of Fig. 14 : 9.

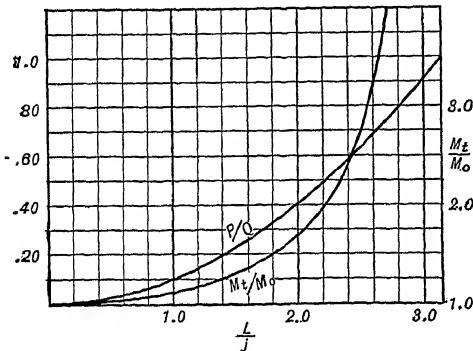


FIG. 14 : 9

The curves can also be used in this manner when the transverse load is not uniformly distributed, but with some decrease in the accuracy of the approximation.

**14 : 8. Effect of Change in Axial Load Between Supports** — The drag truss bays in an airplane are generally shorter than those of the lift truss, there usually being two or three drag bays to one lift

bay. The stresses in the drag, or anti-drag, wires produce axial loads in the spars so that the value of  $P$  cannot be taken as constant throughout a lift truss bay. In addition to this variation in the axial load the spar sections themselves are often varied in the different drag bays so that the moment of inertia is not constant. The precise formulas developed in the foregoing articles are therefore not accurate for these conditions since they assume a constant axial load and a constant moment of inertia between supports. The following method may be used for approximating the moments on the spars under such circumstances.

Figure 14 : 10 shows one bay of a lift truss of length  $L_1$ , which is subdivided by the drag truss into three bays of length  $L'$ ,  $L''$ , and  $L'''$ . The axial loads are  $P'$ ,  $P''$ , and  $P'''$ , and it will be assumed that the section is changed in each bay so that the moments of inertia are  $I'$ ,  $I''$ , and  $I'''$  respectively.

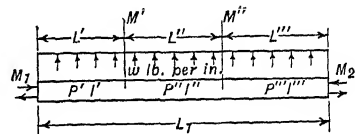


FIG. 14 : 10

$$\text{Let } P_1 \quad \begin{array}{l} P'L' + P''L'' + P'''L''' \\ L' + L'' + L''' \\ I'L' \quad \quad \quad + I'''L''' \\ L' + L'' + L''' \end{array}$$

and compute  $j$  in the usual way. This value of  $j$  should be used in the three-moment equation.

This method of using weighted values for  $P$  and  $I$  is somewhat more accurate than that of using the arithmetical mean but the difference is so slight as to be negligible in most cases. Where the changes in load or section between bays is great this method of weighting the values of  $P$  and  $I$  may be used, but it is, in most cases, an unnecessary refinement.

**14 : 9. Secondary Shear** — In most beam computations the shear at any point along the beam axis is assumed to be the shear on a section through that point and perpendicular to the location of the beam axis before the loads were applied. For purposes of web design it would be more correct to compute the shear on sections perpendicular to tangents to the elastic curve of the beam at the points in question. Since the angle between such a tangent and the original location of the beam axis (the slope  $\theta$ ) is always assumed to be very small, the usual practice is justified; first, because the error is both negligible and on the safe side; and second, because the computations are greatly simplified.

In the cases of beams subjected to axial loads that are large in comparison to the transverse loads (and most airplane spars fall into this class), the error involved in the usual method of computing the shear is no longer negligible, and for proper design the shear on sections perpendicular to the elastic curve must be computed. In a study of airplane spar tests made to determine the constants to be used in the design of webs for box beams, Roy A. Miller<sup>1</sup> found cases in which the shear on sections perpendicular to the elastic curve was as much as 20 per cent greater than that on sections perpendicular to the original location of the beam axis. His results also showed that this additional shear should be taken into account in design.

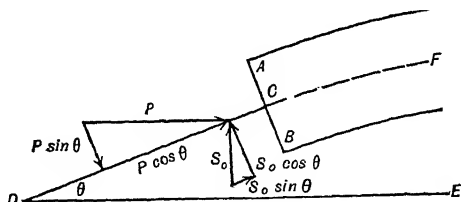


FIG. 14 : 11

The magnitude of the total shear on a section perpendicular to the elastic curve of a beam can easily be computed. In Fig. 14 : 11,  $CF$  is the elastic curve of the beam;  $CD$ , a tangent to  $CF$  at  $C$ ;  $DE$ , the original location of the beam axis before loading; and  $AB$ , a section through the beam at  $C$  and perpendicular to  $DC$ . In the same diagram the forces acting on the section  $AB$  from the portion to the left are represented by  $P$  and  $S_0$ , parallel and perpendicular, respectively, to the original axis  $DE$ .  $P$  is what is usually thought of as the axial load, and  $S_0$ , the shear as usually computed.

<sup>1</sup> Air Corps Information Circular 516, "Design of Plywood Webs for Box Beams."

The normal force on section  $AB$  is then obviously equal to  $P \cos \theta + S_0 \sin \theta$ , and the shear force is  $S_0 \cos \theta - P \sin \theta$ . If the slope,  $\theta$ , is assumed to be small,  $\cos \theta = 1.00$  and  $\sin \theta = \theta$ , practically. Then the normal force on section  $AB$  will be  $P' = P + S_0\theta$ , and the shear will be  $S = S_0 - P\theta$ .

Formula 14 : 15 of Art. 14 : 5 may be written

$$M = M_0 - P\delta \quad 14 : 25$$

From Eq. 3 : 2 the shear on a section perpendicular to the original axis of a beam (i.e., the primary shear) is  $S_0 = dM_0/dx$ . Differentiating Eq. 14 : 25 with respect to  $x$  and substituting this value and the value of  $dM/dx$  given in Eq. 14 : 14, we get

$$S = S_0 - P \frac{d\delta}{dx} \quad 14 : 26$$

But  $d\delta/dx$  is the slope  $\theta$ . Therefore the "total shear" of Art. 14 : 5 is the shear on a section perpendicular to the tangent to the elastic curve. It can easily be proved that this statement applies equally whether the axial load is compression or tension.

If the expression for the total shear,  $S$ , is differentiated with respect to  $x$ , we have  $\frac{dS}{dx} = \frac{dS_0}{dx} - P \frac{d\theta}{dx}$ , the axial load  $P$  being assumed constant.

The first term on the right side of this expression is the rate of change of load normal to the original axis, and the second term the rate of change of the component of  $P$  perpendicular to the elastic curve.

Thus we can also say that  $S = \int w \, dx$  for the axially loaded beam as well as for that without axial load. When using this general differential equation for an axially loaded beam, however, it must be remembered that the loads and shears represented are those perpendicular to the elastic curve, and that parts of them are components of the axial load  $P$  parallel to the original axis of the beam. The objection may be made to the above illustrations of the applicability of the general differential equation for beams to the relations between load, shear, and bending moment, that the bending moment at the section has not been considered. Such an objection is not valid, however, as the only effect of the bending moment is to change the point of application of the load  $P$ . It would not affect the equations of equilibrium on which the illustrations are based.

In the derivation of the equations given in this chapter, the only deflections considered were those due to bending. In addition to such deflection, the deflection due to shear should sometimes be considered.

In Air Corps Information Circular 493, "The Investigation of Structural Members under Combined Axial and Transverse Loads — Section II," the authors have investigated this phase of the problem and found that the result of this shear deflection is to reduce the critical load below that indicated by the formulas. A similar problem arises for beams without axial load, as the total deflection is the sum of that due to bending and that due to shear. The usual procedure for wood beams of both classes is to use a standard value for the modulus of elasticity somewhat smaller than the true value. Using this standard value of  $E$  in the computations results in larger computed deflections than would be obtained from the use of the true value, the difference being an allowance for shear deflection. Though this is a rule-of-thumb method and is obviously inaccurate, it gives satisfactory results and is almost universally used. It is necessary to make precise computations of the shear deflections only in the design of metal beams with very thin webs.

When it is desired to obtain formulas for single spans with axial compression in which the effect of shear deflection is taken into account, this can be done by making the following changes in the formulas of Art. 14 : 5.

- a. Substitute  $J$  for  $j$  in all trigonometric expressions such as  $\sin (x/j)$ .
- b. Retain  $wj^2$  unchanged.
- c. Substitute  $WJ/Q^2$  for  $Wj$ .

For these substitutions  $Q^2 = 1 + PK$ ,  $J = jQ$ , and  $K = -k/AG$  as used in Eq. 13 : 6.

**14 : 10. Notes on the Use of the Beam-column Formulas** — It is recommended that at least four significant figures be used in all computations involving the formulas in this chapter. In preliminary investigations or for the purpose of obtaining a rough check on a spar, three figures will be sufficient but, since the final result of several of these formulas depends on small differences between large quantities, three significant figures will often give misleading results. This fact should be borne in mind and the number of significant figures necessary to give the required precision in the results should be used. This matter is especially important when the value of  $L/j$  is near  $\pi$ , as the functions  $\alpha$ ,  $\beta$ , and  $\gamma$  are all changing rapidly in that range.

Special care must be taken to use the proper signs throughout the computations or serious errors will result. This is particularly true of the signs of the terms for loads and deflections. The conventions for signs are given in Art. 14 : 5.

In applying the precise formulas to design, it is necessary to decide upon a size of member before the final values of the bending moments

can be obtained. This makes the process of design a matter of successive trials; but by first computing the bending moments and axial loads without allowing for secondary stresses and using those moments and loads suitably modified by the judgment of the designer on the first trial, the number of trials needed to obtain a satisfactory design should not be excessive.

In discussions of the precise methods of computing stresses due to combined loadings in this volume and by other authors (as Cowley and Levy in "Aeronautics in Theory and Experiment," etc.), failure is usually assumed to mean failure due to elastic instability or "buckling." Usually, before such failure would occur in practice, the member would have failed by rupture of the material due to excessive unit stresses, and statements regarding the criteria for failure must be read with these facts in mind. The criteria for failure in buckling implicitly assume that the material has a constant finite modulus of elasticity and an infinite proportional limit and ultimate allowable stress. Of course, no engineering material has such properties, but the precise formulas and resulting criteria for buckling failure are nevertheless very useful in determining the loads under which failure by rupture of the material is likely to occur.

#### **14 : 11. Moment Distribution Beam-columns of Constant Section —**

The method of moment distribution described in Chapters V and XIII can be applied to continuous beam-columns, and rigid frames including beam-columns, if the effect of the axial load on fixed-end moments, stiffness factors, and carry-over factors is taken into account. These quantities can be found for beam-columns in basically the same manner as for beams without axial load. The only difference in procedure is that the formulas of this chapter must be used to compute slopes, deflections, and moments instead of those used in the earlier chapters. The resulting values for beam-columns of constant section of the carry-over factors, stiffness factors, and fixed-end moments for various types of transverse load are shown graphically in Fig. 14 : 12 to 14 : 22 as functions of  $L/j$ . These curves are taken from the thesis of Mr. B. W. James,<sup>1</sup> which also gives the derivation of the formulas from which they were plotted and numerical examples of their use.

Carry-over factors are shown in Fig. 14 : 12, one curve giving the values when the axial load is compression, and another giving those for axial tension. Stiffness factor coefficients are shown in Fig. 14 : 13. In this case there are two sets of curves, one for beam-columns with the far end fixed against rotation, and one for those with the far end pinned.

<sup>1</sup> "Principal Effects of Axial Load on Moment-Distribution Analysis of Rigid Structures," N.A.C.A. Technical Note 534.

Each set is composed of one curve for axial compression and another for axial tension. The value of  $C$  to be read from Fig. 14 : 13 is not the absolute stiffness factor (i.e., the ratio of the moment applied at one end of a beam-column to the rotation at that end) but rather a stiffness coefficient to be multiplied by  $K = I/L$  to obtain a convenient relative stiffness factor. Thus the relative stiffnesses of two or more beam-columns will be represented by the respective values of  $C(I/L)$ ,

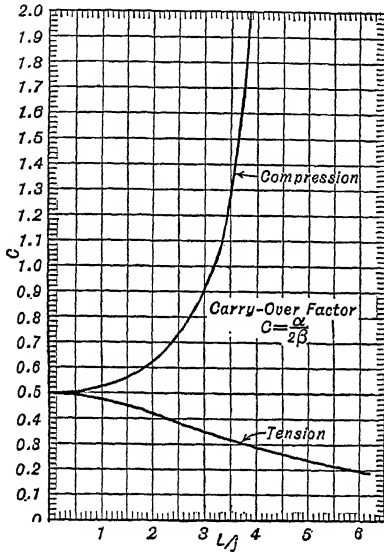


FIG. 14 : 12

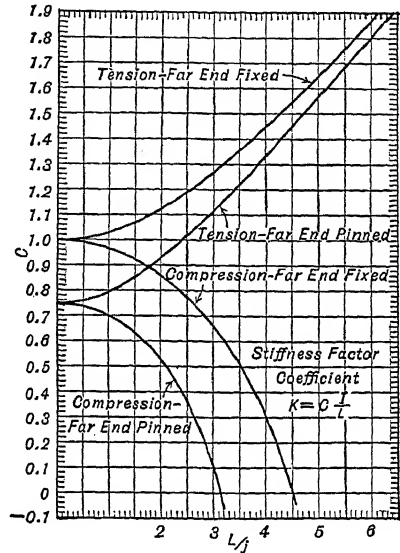


FIG. 14 : 13

but the absolute stiffness factor of a beam-column will be  $+4 CEI/L$ . The equations represented by the curves for the stiffness coefficients are as follows:

For far end fixed

$$C = 3\beta \quad 14 : 27$$

For far end pinned

$$14 : 28$$

In using these equations for beam-columns with the axial load compression,  $\alpha$  and  $\beta$  are the functions of  $L/j$  listed in Table 14 : 2. If the axial load is tension,  $\alpha$  and  $\beta$  are the functions listed in Table 14 : 7. Numerical values for both carry-over and relative stiffness factors for various values of  $L/j$  are listed in Tables 14 : 8 and 14 : 9.



TABLE 14:8  
MOMENT-DISTRIBUTION COEFFICIENTS FOR AXIAL COMPRESSION

$(L/j)_{\text{eff.}}$	Carry-over Factor	Stiffness Coefficients		Fixed End Moment Coefficients	
		Far End Pinned	Far End Fixed	Uniformly Dis- tributed Load	Concentrated Load at Midspan
	$\frac{\alpha}{2\beta}$	$\frac{3}{4\beta}$	$\frac{3\beta}{4\beta^2 - \alpha^2}$	$\frac{4(2\beta + \alpha)}{\gamma}$	$\frac{\left(\frac{L}{j}\right)^2 (2\beta + \alpha)}{3\left(\sec \frac{L}{2j} - 1\right)}$
0	0.5000	0.7500	1.0000	12.000	8.000
0.1	0.5002	0.7495	0.9997	11.998	7.998
0.2	0.5010	0.7480	0.9987	11.992	7.993
0.3	0.5023	0.7455	0.9970	11.982	7.985
0.4	0.5040	0.7420	0.9947	11.968	7.973
0.5	0.5063	0.7374	0.9916	11.950	7.958
0.6	0.5092	0.7318	0.9879	11.928	7.940
0.7	0.5126	0.7251	0.9836	11.902	7.918
0.8	0.5166	0.7174	0.9785	11.871	7.893
0.9	0.5211	0.7085	0.9727	11.837	7.865
1.0	0.5264	0.6985	0.9662	11.799	7.833
1.1	0.5323	0.6873	0.9590	11.756	7.797
1.2	0.5389	0.6748	0.9511	11.709	7.758
1.3	0.5463	0.6611	0.9424	11.658	7.716
1.4	0.5546	0.6460	0.9329	11.602	7.670
1.5	0.5637	0.6295	0.9227	11.543	7.621
1.6	0.5739	0.6114	0.9116	11.478	568
1.7	0.5851	0.5918	0.8998	11.410	512
1.8	0.5974	0.5704	0.8871	11.337	452
1.9	0.6111	0.5473	0.8735	11.259	389
2.0	0.6263	0.5221	0.8590	11.176	322
2.1	0.6430	0.4948	0.8436	11.089	251
2.2	0.6616	0.4651	0.8273	10.997	177
2.3	0.6823	0.4329	0.8099	10.900	99
2.4	0.7053	0.3978	0.7915	10.797	7.017
2.5	0.7310	0.3595	0.7720	10.690	6.931
2.6	0.7598	0.3176	0.7513	10.577	6.840
2.7	0.7923	0.2715	0.7295	10.459	6.746
2.8	0.8291	0.2208	0.7064	10.336	6.648
2.9	0.8709	0.1647	0.6819	10.206	6.546
3.0	0.9189	0.1021	0.6560	10.071	6.440
3.1	0.9744	0.03183	0.6287	9.930	6.330
$\pi$	1.000	0	0.6169	9.870	6.283
3.2	1.039	-0.04765	0.5997	9.783	6.216
3.3	1.115	-0.1385	0.5691	9.629	6.097
3.4	1.206	-0.2436	0.5366	9.468	5.974
3.5	1.316	-0.3670	0.5021	9.301	5.846
3.6	1.451	-0.5147	0.4655	9.127	5.714

TABLE 14:8 — (Continued)

## MOMENT-DISTRIBUTION COEFFICIENTS FOR AXIAL COMPRESSION

$(L/j)_{\text{eff.}}$	Carry-over Factor	Stiffness Coefficients		Fixed End Moment Coefficients	
		Far End Pinned	Far End Fixed	Uniformly Dis- tributed Load	Concentrated Load at Midspan
	$\alpha$ $2\beta$	$\frac{3}{4\beta}$	$\frac{3\beta}{4\beta^2 - \alpha^2}$	$\frac{4(2\beta + \alpha)}{\gamma}$	$\left(\frac{L}{j}\right)^2 (2\beta + \alpha)$ $3\left(\sec \frac{L}{2j} - 1\right)$
3.7	1.622	-0.6953	0.4265	8.945	5.577
3.8	1.843	-0.9227	0.3850	8.756	5.435
3.9	2.140	-1.220	0.3407	8.559	5.288
4.0	2.560	-1.629	0.2933	8.354	5.137
4.1	3.197	-2.235	0.2424	8.140	4.980
4.2	4.271	-3.237	0.1878	7.917	4.818
4.3	6.461	-5.246	0.1287	7.684	4.651
4.31	6.812	-5.566	0.1226	7.661	4.635
4.32	7.204	-5.922	0.1164	7.637	4.618
4.33	7.643	-6.322	0.1101	7.613	4.600
4.34	8.140	-6.773	0.1038	7.589	4.583
4.35	8.706	-7.287	0.09742	7.565	4.566
4.36	9.357	-7.877	0.09100	7.540	4.549
4.37	10.11	-8.562	0.08453	7.516	4.531
4.38	11.00	-9.368	0.07801	7.492	4.514
4.39	12.07	-10.33	0.07143	7.467	4.496
4.40	13.36	-11.50	0.06480	7.442	4.479
4.41	14.96	-12.94	0.05811	7.418	4.461
4.42	16.99	-14.78	0.05136	7.392	4.444
4.43	19.67	-17.19	0.04455	7.368	4.426
4.44	23.35	-20.52	0.03769	7.342	4.408
4.45	28.73	-25.36	0.03077	7.317	4.391
4.46	37.33	-33.11	0.02378	7.292	4.373
4.47	53.27	-47.48	0.01674	7.267	4.355
4.48	93.00	-83.27	0.009629	7.241	4.337
4.49	365.8	-329.0	0.002459	7.216	4.319
4.50	-188.7	170.5	-0.004788	7.190	4.301
4.51	-75.17	68.20	-0.01207	7.164	4.283
4.52	-46.90	42.74	-0.01944	7.138	4.265
4.53	-34.08	31.19	-0.02687	7.112	4.247
4.54	-26.77	24.60	-0.03437	7.086	4.228
4.55	-22.04	20.33	-0.04194	7.059	4.210
4.56	-18.73	17.35	-0.04958	7.033	4.191
4.57	-16.29	15.14	-0.05729	7.007	4.173
4.58	-14.41	13.44	-0.06507	6.980	4.155
4.59	-12.92	12.10	-0.07293	6.953	4.136
4.60	-11.71	11.00	-0.08086	6.926	4.117
4.61	-10.70	10.09	-0.08887	6.899	4.099

TABLE 14:8 — (Concluded)

MOMENT-DISTRIBUTION COEFFICIENTS FOR AXIAL COMPRESSION

$(L/j)_{\text{eff.}}$	Carry-over Factor	Stiffness Coefficients		Fixed End Moment Coefficients	
		Far End Pinned	Far End Fixed	Uniformly Dis- tributed Load	Concentrated Load at Midspan
	$\frac{\alpha}{2\beta}$	$\frac{3}{4\beta}$	$\frac{3\beta}{4\beta^2 - \alpha^2}$	$\frac{4(2\beta + \alpha)}{\gamma}$	$\frac{\left(\frac{L}{j}\right)^2 (2\beta + \alpha)}{3\left(\sec \frac{L}{2j} - 1\right)}$
4.62	-9.861	9.330	-0.09695	6.872	4.080
4.63	-9.140	8.676	-0.1051	6.845	4.061
4.64	-8.518	8.112	-0.1134	6.818	4.042
4.65	-7.976	7.619	-0.1217	6.790	4.023
4.66	-7.499	7.184	-0.1301	6.763	4.004
4.67	-7.076	6.799	-0.1386	6.735	3.985
4.68	-6.698	6.454	-0.1471	6.707	3.966
4.69	-6.359	6.144	-0.1558	6.679	3.947
4.70	-6.053	5.864	-0.1645	6.652	3.928
4.8	-4.093	4.052	-0.2572	6.365	3.732
4.9	-3.102	3.110	-0.3607	6.065	3.531
5.0	-2.507	2.521	-0.4772	5.752	3.323
5.1	-2.112	2.110	-0.6099	5.424	3.108
5.2	-1.833	1.799	-0.7629	5.081	2.887
5.3	-1.626	1.550	-0.9422	4.721	2.660
5.4	-1.470	1.341	-1.156	4.345	2.425
5.5	-1.348	1.159	-1.418	3.949	2.183
5.6	-1.253	0.9949	-1.748	3.533	1.933
5.7	-1.177	0.8426	-2.180	3.095	1.675
5.8	-1.119	0.6977	-2.778	2.634	1.409
5.9	-1.073	0.5566	-3.668	2.148	1.134
6.0	-1.040	0.4163	-5.159	1.6330	0.8507
6.1	-1.017	0.2742	-8.234	1.0878	0.5588
6.2	-1.003	0.1275	-18.59	0.5092	0.2581
$2\pi$	-1.000	0	$\infty$	0	0

TABLE 14:9

MOMENT-DISTRIBUTION COEFFICIENTS FOR AXIAL TENSION

$(L/j)_{\text{eff.}}$	Carry-over Factor	Stiffness Coefficients		Fixed End Moment Coefficients	
		Far End Pinned	Far End Fixed	Uniformly Dis- tributed Load	Concentrated Load at Midspan
	$\frac{\alpha_h}{2\beta_h}$	$\frac{3}{4\beta_h}$	$\frac{3\beta_h}{4\beta_h^2 - \alpha_h^2}$	$\frac{4(2\beta_h + \alpha_h)}{\gamma_h}$	$\left(\frac{L}{j}\right)^2 (2\beta_h + \alpha_h)$ $3 \left(1 - \text{sech} \frac{L}{2j}\right)$
0	0.5000	0.7500	1.000	12.000	8.000
0.1	0.4998	0.7505	1.000	12.000	8.002
0.2	0.4990	0.7520	1.001	12.008	8.007
0.3	0.4978	0.7545	1.003	12.018	8.015
0.4	0.4961	0.7580	1.005	12.032	8.027
0.5	0.4938	0.7624	1.008	12.050	8.042
0.6	0.4912	0.7678	1.012	12.072	8.060
0.7	0.4881	0.7742	1.016	12.098	8.081
0.8	0.4845	0.7814	1.021	12.127	8.106
0.9	0.4806	0.7896	1.027	12.161	8.135
1.0	0.4762	0.7986	1.033	12.199	8.166
1.1	0.4716	0.8085	1.040	12.240	8.201
1.2	0.4665	0.8192	1.047	12.285	8.239
1.3	0.4612	0.8307	1.055	12.334	8.280
1.4	0.4556	0.8429	1.064	12.387	8.324
1.5	0.4497	0.8559	1.073	12.443	8.372
1.6	0.4436	0.8696	1.083	12.503	8.422
1.7	0.4373	0.8839	1.093	12.566	8.476
1.8	0.4308	0.8989	1.104	12.634	8.533
1.9	0.4242	0.9144	1.115	12.704	8.593
2.0	0.4174	0.9306	1.127	12.778	8.656
2.1	0.4105	0.9472	1.139	12.856	8.722
2.2	0.4036	0.9644	1.152	12.936	8.791
2.3	0.3966	0.9820	1.165	13.020	8.863
2.4	0.3896	1.000	1.179	13.107	8.938
2.5	0.3825	1.019	1.193	13.198	9.015
2.6	0.3755	1.038	1.208	13.291	9.096
2.7	0.3685	1.057	1.223	13.388	9.180
2.8	0.3615	1.076	1.238	13.487	9.266
2.9	0.3546	1.096	1.254	13.590	9.355
3.0	0.3477	1.117	1.270	13.695	9.447
3.1	0.3409	1.137	1.287	13.803	9.541
3.2	0.3341	1.158	1.304	13.913	9.638
3.3	0.3275	1.179	1.321	14.027	9.738
3.4	0.3210	1.200	1.338	14.143	9.840
3.5	0.3146	1.222	1.356	14.261	9.945
3.6	0.3083	1.244	1.374	14.382	10.052
3.7	0.3021	1.265	1.393	14.505	10.161

TABLE 14 : 9 — (Concluded)

$(L/j)$ eff.	Carry-over Factor	Stiffness Coefficients		Fixed End Moment Coefficients	
		Far End Pinned	Far End Fixed	Uniformly Distributed Load	Concentrated Load at Midspan
	$\frac{\alpha_h}{2\beta_h}$	$\frac{3}{4\beta_h}$	$\frac{3\beta_h}{4\beta_h^2 - \alpha_h^2}$	$\frac{4(2\beta_h + \alpha_h)}{\gamma_h}$	$\left(\frac{L}{j}\right)^2 (2\beta_h + \alpha_h)$ $3 \left(1 - \operatorname{sech} \frac{L}{2j}\right)$
3.8	0.2960	1.288	1.411	14.631	10.273
3.9	0.2900	1.310	1.430	14.759	10.388
4.0	0.2842	1.332	1.449	14.889	10.504
5.0	0.2231	1.562	1.652	16.298	11.788
6.0	0.1940	1.800	1.870	17.867	13.257
7.0	0.1645	2.042	2.098	19.550	14.872
8.0	0.1421	2.286	2.333	21.314	16.597
9.0	0.1247	2.531	2.571	23.136	18.404
10.0	0.1110	2.778	2.812	24.997	20.272
11.0	0.09996	3.025	3.056	26.888	22.181
12.0	0.09090	3.273	3.300	28.799	24.119
13.0	0.08333	3.521	3.545	30.727	26.078
14.0	0.07692	3.769	3.792	32.667	28.051
15.0	0.07143	4.018	4.038	34.615	30.033
16.0	0.06667	4.267	4.286	36.571	32.021
17.0	0.06250	4.516	4.533	38.534	34.014
18.0	0.05882	4.765	4.781	40.500	36.009
19.0	0.05556	5.014	5.029	42.470	38.006
20.0	0.05263	5.263	5.278	44.444	40.004
25.0	0.04167	6.510	6.522	54.388	50.000
30.0	0.03448	7.759	7.768	64.288	60.000
35.0	0.02941	9.007	9.015	74.243	70.000
40.0	0.02564	10.26	10.26	84.211	80.000
45.0	0.02273	11.51	11.51	94.178	90.000
50.0	0.02041	12.76	12.76	104.167	100.000

When a span of a continuous beam-column is bisected by an axis of symmetry, that span may be treated as though the far end were pinned and its relative stiffness factor obtained by a special procedure. Either the stiffness factor for the far-end-pinned condition may be divided by unity plus the carry-over factor for the far-end-fixed condition or it may be computed from the formula

$$\text{Relative stiffness factor for symmetrical span} = \left[ \frac{L}{4j} \cot \frac{L}{2j} \right] \div 14 : 29$$

The two methods give identical results. When this special stiffness factor is used no moment need be carried over across the symmetrical span.

Fixed-end moments can be found from the curves of Fig. 14 : 14 to 14 : 21. Most of these curves give coefficients to be inserted in the for-

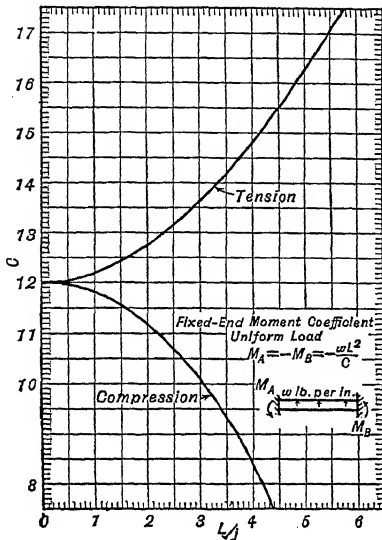


FIG. 14 : 14

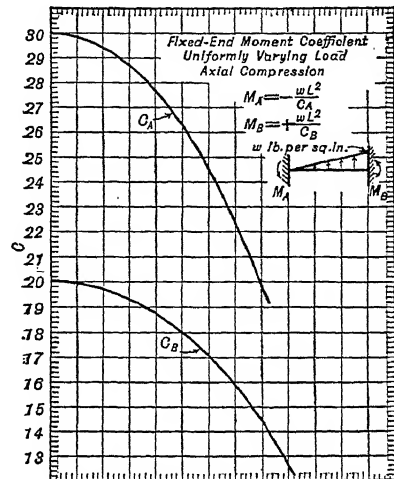


FIG. 14 : 15

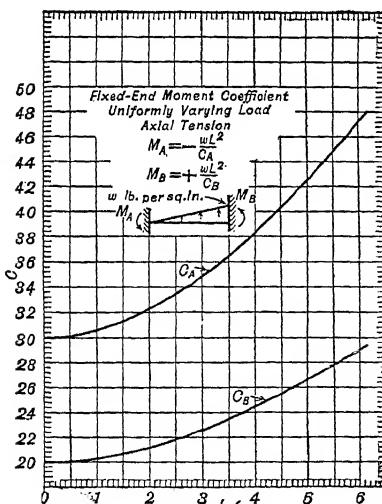


FIG. 14 : 16

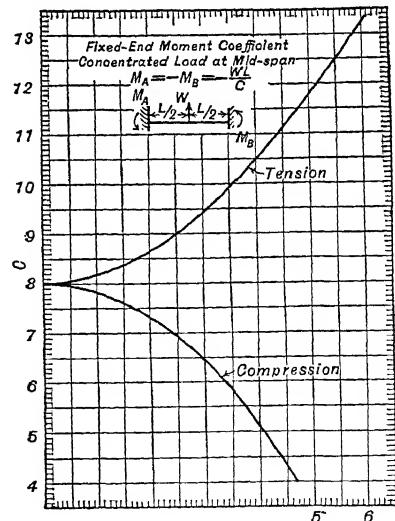


FIG. 14 : 17

mulas for fixed-end moments shown on the same figures. For a concentrated load at any point on the span and a load distributed uniformly over only a part of the span, the formulas for fixed-end moments as

shown on the figures for the corresponding fixed-end moment coefficients are inconvenient to solve. The computer will find his work greatly lightened in these cases by the curves of Fig. 14 : 19. The equations of the curves of fixed-end-moment coefficient are:

For uniformly distributed load (Fig. 14 : 14),

$$C = \frac{4 (2 \beta + \alpha)}{\gamma} \quad 14 : 30$$

For uniformly varying load at end where  $w = 0$  (Figs. 14 : 15 and 14 : 16),

$$14 : 31$$

For same loading at end where  $w = w$ ,

$$C = \left( \frac{4 \beta^2 - \alpha^2}{\gamma} \right) \quad 14 : 32$$

For concentrated load at midspan (Fig. 14 : 17)

$$C = \left( \frac{4}{3 (\sec (L/2j) - 1)} \right) \quad 14 : 33$$

The formulas for the curves of Figs. 14 : 18, 14 : 20, and 14 : 21 may be found in N.A.C.A. Technical Note 534. In using these formulas, values of  $\alpha$ ,  $\beta$ , and  $\gamma$  should be taken from Table 14 : 2 if the axial load is compression and from Table 14 : 7 if the axial load is tension. Values of the coefficients,  $1/C$ , for the uniformly distributed load and the concentrated load at midspan are listed in Tables 14 : 8 and 14 : 9.

The shear distribution factor,  $2\beta - \alpha$ , plotted in Fig. 14 : 22, has two functions. In Art. 13 : 22 it was shown that, in the analysis of a Vierendeel truss, the moments added to the chords in each cycle to balance the bent equation should be distributed among the chords in proportion to their values of  $I/L^2$ . That practice is strictly accurate only when there is no axial load in the chords. If axial loads are present, the distribution should be proportional to the values of  $\frac{I}{L^2 (2\beta - \alpha)}$ .

The other use of the coefficient,  $2\beta - \alpha$ , is in computations of beam-columns when it is assumed that there is deflection of the supports. In Art. 5 : 15 it was shown that the effect of such deflection could be taken into account by adding or subtracting  $6EKR$  to the fixed-end moments due to transverse loads, when the axial load was zero. When axial load is present, the corresponding correction to the fixed-end moment would be  $6EKR / (2\beta - \alpha)$ .

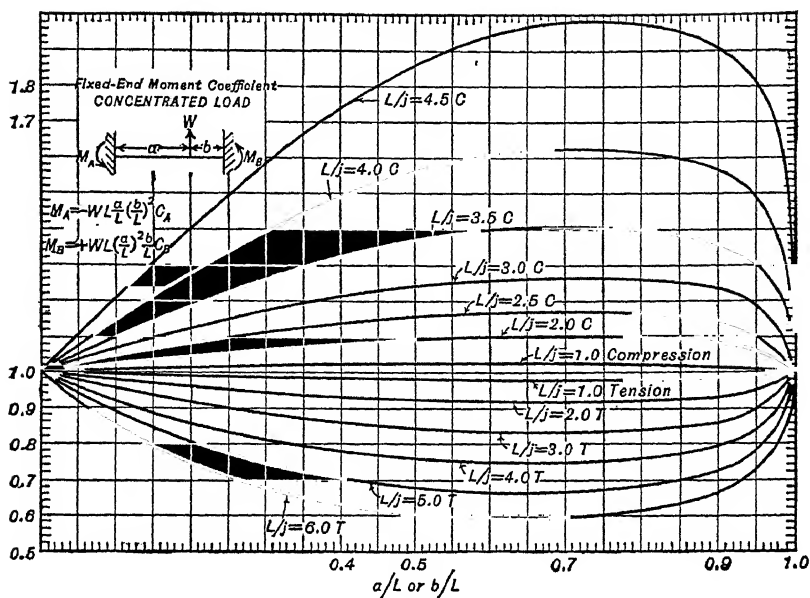


FIG. 14 : 18

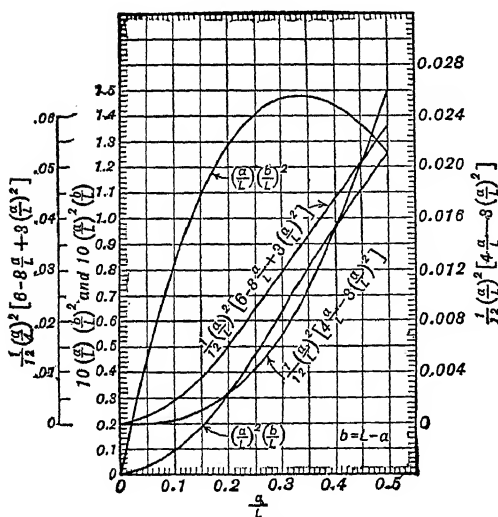


FIG. 14 : 19

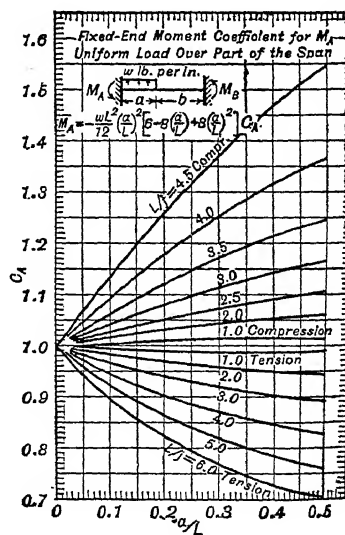


FIG. 14 : 20



When the transverse loading on a span is made up of a combination of the loadings for which the fixed-end moments are given in Fig. 14 : 14 to 14 : 21, the fixed-end moments for the combination may be obtained by the method of superposition.

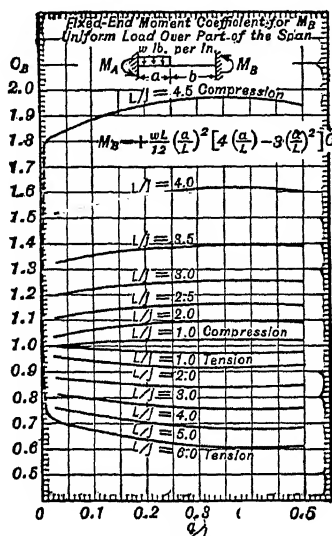


FIG. 14 : 21

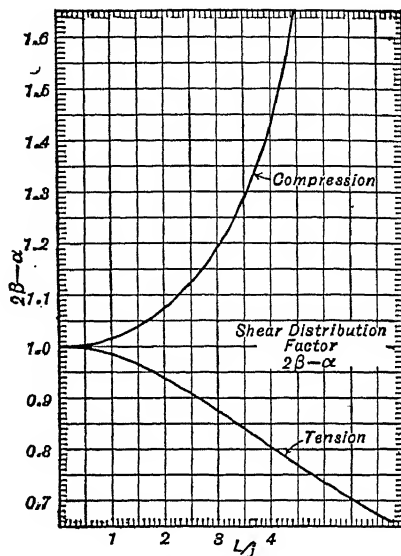


FIG. 14 : 22

**14 : 12. Numerical Example** — Compute the moments over the supports of the elevator spar shown in Fig. 14 : 23, under the loading shown. Assume the spar to be a  $1\frac{1}{4}$  by 0.035 aluminum alloy tube with  $I = 0.02467 \text{ in.}^4$  and  $E = 10,400,000 \text{ p.s.i.}$  Assume that, after loading,

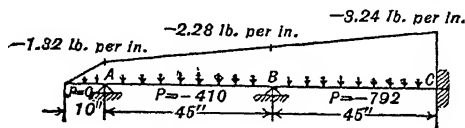


FIG. 14 : 23

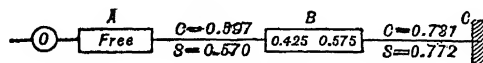


FIG. 14 : 24

joint A deflects  $\frac{1}{4}$  in., and joint B  $\frac{1}{8}$  in. below joint C. It may be noticed that this is the same as the illustrative example of Art. 5 : 15 except for the addition of the axial loads.

Before proceeding to the distribution of the moments it is necessary to make the computations recorded in Table 14 : 10.

TABLE 14 : 10

Item	Span AB	Span BC	Reference
Axial load, $P$ in pounds	-410	-792	Fig. 14 : 23
$EI$ in pound-inch units	256,000	256,000	
$j^2 = EI/P$	625	324	
$j$	25	18	
$L/j$	1.80	2.50	Fig. 14 : 12
Carry-over factor	0.597	0.731	
Stiffness factor coefficient	0.570 <sup>a</sup>	0.772 <sup>b</sup>	Fig. 14 : 13
Shear distribution factor	1.058	1.123	Fig. 14 : 22

<sup>a</sup> For far end pinned.<sup>b</sup> For far end fixed.

The fixed-end moments due to the transverse loads will be

$$M_{Fa0} = -1.32 \times 5 \times 10/3 = -22 \text{ in.-lb.}^1$$

$$M_{Fab} = +0.96 \times 45^2/28.10 + 1.32 \times 2,025/11.34 = +69.18 + 235.80 = +304.98 \text{ in.-lb.}$$

$$M_{Fba} = -1,944/19.01 - 1.32 \times 2,025/11.34 = -102.26 - 235.80 = -338.06 \text{ in.-lb.}$$

$$M_{Fbc} = +1,944/26.29 + 2.28 \times 2,025/10.69 = +73.94 + 431.90 = +505.84 \text{ in.-lb.}$$

$$M_{Fcb} = -1,944/18.01 - 2.28 \times 2,025/10.69 = -107.94 - 431.90 = -539.84 \text{ in.-lb.}$$

The fixed-end moments due to the assumed deflections of the supports will be

$$M_{Fab} = +M_{Fba} = -\frac{6 \times 256,000}{8 \times 2,025 \times 1.058} = -89.82 \text{ in.-lb.}$$

$$M_{Fbc} = +M_{Fcb} = -\frac{6 \times 256,000}{8 \times 2,025 \times 1.123} = -84.62 \text{ in.-lb.}$$

The above computations having been made, the line diagram of Fig. 14 : 24 is prepared. The stiffness and carry-over factors are first entered on the line diagram near the centers of the respective spans, and the fixed-end moments due to transverse loads and support deflection are entered on lines (f) and (d) adjacent to the joints. From the stiffness factors of the members entering each joint the distribution factors

<sup>1</sup> In this example the "rigid frame convention" for end moments is used throughout.

are computed and entered in the figures inserted in the line diagram for the purpose. The computer is then ready to distribute moments, which he does in the following manner:

Joint *A* is balanced by adding  $-193$  to  $M_{ab}$  and a line is drawn to indicate that the joint is in balance.

A moment of  $-193 \times 0.597$  is carried over from *A* to *B*, making the unbalanced moment at that joint equal to  $-543 + 421 = -122$  in.-lb. This is distributed,  $+122 \times 0.425 = +52$  in.-lb. to  $M_{ba}$  and  $+122 \times 0.575 = +70$  in.-lb. to  $M_{bc}$ . The line to indicate that the joint *B* is in balance is now drawn.

As the distribution factors for joint *B* were computed assuming joint *A* pinned there will be no moment carried over from *B* to *A*, but  $+70 \times 0.731$  will be carried over from *B* to *C*. As joint *C* is assumed fixed the distribution of moments is now complete, the lines indicating joint balance can be doubled to signify this fact, and the quantities in each column added to determine the total moments.

This example covers a very simple case, but the application of the method of moment distribution is changed so little by the consideration of the effects of axial load that it should be sufficient for illustrative purposes.

**14 : 13. Beam-columns of Non-uniform Section** — When a beam-column is of non-uniform section,  $M/EI$  becomes such a complex function of  $x$  that it is impossible to develop practical formulas similar to those of Art. 14 : 5. In many cases it is sufficiently accurate to use the formulas of that article with average values of  $EI$ . When this is not desirable, the simplest method of procedure is to use the method of moment distribution, computing the carry-over factors and similar quantities needed by a method originated by Mr. D. Williams of the Royal Aircraft Establishment and published in R. and M. 1670. As described by Mr. Williams this is a graphical method; the following discussion pertains to its "semi-graphical" equivalent.

As the method can be explained most readily in connection with a numerical example, some of the carry-over factors, stiffness factors, etc., will be found for the beam shown in Fig. 14 : 25. The modulus of elasticity,  $E$ , is assumed to be 1,500,000 p.s.i., and the moment of inertia varies linearly from 5 in.<sup>4</sup> at *A* to 10 in.<sup>4</sup> at *B*. It may be noted that this beam is the same as that of Art. 5 : 17 with the addition of an axial load.

*Carry-over and Stiffness Factors* — The carry-over factor from *B* to *A* may be defined as the moment required at *A* to make the deflection of *B* from the tangent to the elastic curve at *A* equal to zero when the beam is simply supported and subjected to a unit couple at *B*. Similarly the

stiffness factor for end  $B$  assuming end  $A$  fixed is equal to the reciprocal of the slope at  $B$  when the beam is simply supported and subjected to a unit moment at  $B$  and a moment equal to the carry-over factor from  $B$  to  $A$  at  $A$ . These quantities should be determined first for the case when the axial load is zero by the method of Art. 5:17 and then corrected for the effect of the axial load. A method for making these corrections is described below.

If the axial load is zero, the carry-over factor from  $B$  to  $A$  is 0.4172, and the deflections from the line  $AB$ , which is also the tangent to the elastic curve at  $A$ , due to 1,000 in.-lb. at  $B^1$  and 417.2 in.-lb. at  $A$  may be found from

$$E\delta_0 = -0.4172 E\delta_{0a} + E\delta_{0b}$$

where  $\delta_0$  is the "primary deflection" due to the end moments.

$\delta_{0a}$  is the deflection due to 1,000 in.-lb. at  $A$  as given in Table 5:1.

$\delta_{0b}$  is the deflection due to 1,000 in.-lb. at  $B$  as given in Table 5:2.

TABLE 14:11

COMPUTATION OF FIRST SECONDARY MOMENTS

$$M_a = 417.2 \text{ in.-lb.} \quad M_b = 1,000 \text{ in.-lb.}$$

Station	$E\delta_{0a}$	$-0.4172 E\delta_{0a}$	$E\delta_{0b}$	$E\delta_0$	$M_{s1}$	$I$	$M_{s1}/I$
0	0	0	0	0	0	5	0
10	8,330	-3,480	830	-2,650	+17.7	6	2.9
20	30,470	-12,710	4,760	-7,950	+53.0	7	7.6
30	61,480	-25,650	14,250	-11,400	+76.0	8	9.5
40	97,680	-40,750	31,130	-9,620	+64.1	9	7.1
50	136,250	-56,840	56,840	0	0	10	0

<sup>1</sup> The couple at  $B$  is assumed to be 1,000 in.-lb. instead of 1 in.-lb. to avoid having to deal with excessively small quantities. The final figures for carry-over and stiffness factors, however, will be those that would have resulted from the use of 1 in.-lb.

The values of  $E\delta_0$  are computed from this expression in Table 14 : 11 and must be divided by  $E = 1,500,000$  to obtain  $\delta$  in inches.

If an axial load of 10,000 lb. compression is now imposed on the beam, it will produce a secondary moment equal to  $-10,000 \delta_0 = -E\delta_0/150$  at each section. These will be called the "first secondary moments" and will be designated by  $M_{s1}$ . They will cause additional deflections in the same manner as bending moments due to transverse loads. If these were the only additional moments imposed on the beam they would cause the changes in slope and deflection from the tangent at  $A$  computed in Table 14 : 12 by the method used in Art. 5 : 17 to obtain the slopes and deflections due to end moments and transverse loads.

TABLE 14 : 12  
COMPUTATION OF FIRST SECONDARY DEFLECTIONS,  $\delta_{t1}$

Station	$M_{s1}/I$	Sum	$E \Delta \theta_{t1}$	$E\theta_{t1}$	Sum	$E \Delta \delta_{t1}$	$E\delta_{t1}$
0	0			0			0
10	2.9	2.9	14.5	14.5	14.5	72.5	72.5
20	7.6	10.5	52.5	67.0	81.5	407.5	480.0
30	9.5	17.1	85.5	152.5	219.5	1,097.5	1,577.5
40	7.1	16.6	83.0	235.5	388.0	1,940.0	3,517.5
50	0	7.1	35.5	271.0	506.5	2,532.5	6,050.0

The resulting deflections from the tangent at  $A$  are designated  $\delta_{t1}$  to indicate that they are what may be termed the "first secondary deflections" from the tangent. If, therefore, the deflection of  $B$  from the tangent at  $A$  is to remain zero, an additional or "first secondary fixing moment" must be applied at  $A$ . From Table 5 : 1 the deflection of  $B$  from the tangent at  $A$  due to 1.00 in.-lb. applied at  $A$  would be  $136.25/E$  in. Therefore the first secondary fixing moment at  $A$  will be  $6,050/136.25 = 44.4$  in.-lb. Then the "first secondary deflections" from the line  $AB$ , designated  $\delta_{s1}$ , will be equal to  $\delta_{t1} - 0.0444 \delta_{0a}$ . These values are computed in Table 14 : 13. Qualitative curves of  $\delta_0$ ,  $\delta_{t1}$  and  $\delta_{s1}$  are shown in Fig. 14 : 26.

The products of the axial load and the first deflections  $\delta_{s1}$  will be the "second secondary moments,"  $M_{s2}$ . These will cause "second secondary deflections" which may be computed in the same manner as the first secondary deflections. In fact, there will be infinite series of such secondary moments and deflections, but, unless the axial load approaches the critical load for the member, the convergence of each series is rapid and only one or two of the terms need be computed. The

second secondary deflections from the tangent at  $A$ ,  $\delta_{t2}$ , are shown for this case in Table 14 : 13 though some of the steps in calculating them are omitted. From these values we find the "second secondary fixing moment" at  $A$  to be  $635/136.25 = 4.66$  in.-lb. If we assume these secondary fixing moments at  $A$  to constitute a geometric series, the geometric constant will be  $r = 4.66/44.4 = 0.105$ . The sum of the series will then be  $44.4/(1.00 - 0.105) = 49.6$  in.-lb.

TABLE 14 : 13  
COMPUTATION OF SECOND SECONDARY DEFLECTIONS,  $\delta_{t2}$

Station	$E\delta_{t1}$	$-0.0444 E\delta_{0a}$	$E\delta_{s1}$	$M_{s2}$	$E\delta_{t2}$
0	0	0	0	0	0
10	72.5	-370	-297	+2.0	8
20	480	-1,350	-870	+5.8	54
30	1,580	-2,730	-1,150	+7.7	173
40	3,520	-4,340	-820	+5.5	377
50	6,050	-6,050	0	0	635

Thus when the beam is subjected to an axial load of 10,000 lb. compression and a couple of 1,000 in.-lb. at  $B$ , if the deflection of  $B$  from the tangent at  $A$  is to be zero, a couple of  $417.2 + 49.6 = 466.8$  in.-lb. must be applied at  $A$ . Dividing by 1,000 to determine the effect of a unit couple at  $B$ , we find the fixing moment at  $A$ , and thus the carry-over factor from  $B$  to  $A$  to be 0.4668.

When the beam is subjected to an axial load of 10,000 lb. compression, a unit couple at  $B$  and 0.4668 in.-lb. at  $A$ ,  $E$  times the resultant slope at  $B$  will be the algebraic sum of 3.043 due to the couple at  $B$ ,  $-0.4668 \times 3.912 = -1.826$  due to the couple at  $A$ , and  $0.271/0.895 = 0.303$  due to the infinite series of secondary bending moments. The stiffness factor for end  $B$ , assuming end  $A$  fixed, will therefore be  $E/(3.043 - 1.826 + 0.303) = E/1.520 = 0.658 E$ .

The carry-over factor from  $A$  to  $B$  and the stiffness factor for end  $A$  assuming end  $B$  fixed can be obtained in the same manner. To obtain these quantities, however, it is necessary to integrate the  $M/I$  curves from right to left. If this is done, and the second and following secondary moments and deflections are ignored (which is allowable in most practical cases) the results are: carry-over factor from  $A$  to  $B$  equals  $0.6227 + 0.0684 = 0.691$ , and stiffness factor for end  $A$  assuming end  $B$  fixed equals  $E/2.156 = 0.4638 E$ .

The stiffness factor assuming the far end pinned is obtainable in very

much the same manner. If the stiffness factor for end  $A$  is desired, the beam is assumed freely supported at both ends and subjected to a moment of 1,000 in.-lb. at  $A$ . The deflections from the tangent to the elastic curve at  $A$  are then the values of  $\delta_{0a}$  as given in Table 5 : 1. In this case the tangent at  $A$  does not pass through  $B$  but the deflections from the line  $AB$  can be computed by subtracting  $x/L$  times the deflection,  $\delta_{0a}$ , of point  $B$  from the corresponding values of  $\delta_{0a}$ . Such computations are shown in Table 14 : 14, the resultant deflections from the

TABLE 14 : 14  
COMPUTATION OF SECONDARY DEFLECTIONS,  $M_a = 1,000$  in.-lb.

Station	$E\delta_{a0}$	$E\delta b x/L$	$E\delta_0$	$M_{s1}$	$\delta_{t1}$	$\delta_{s1}$	$M_{s2}$	$\delta_{t2}$
0	0	0	0	0	0	0	0	0
10	8,330	-27,250	-18,920	+126.1	530	-3,370	+22.5	94
20	30,470	-54,500	-24,030	+160.2	2,670	-5,130	+34.2	507
30	61,480	-81,750	-20,270	+135.1	6,910	-4,780	+31.9	1,349
40	97,680	-109,000	-11,320	+75.5	12,780	-2,810	+18.7	2,564
50	136,250	-136,250	0	0	19,490	0	0	3,983

line  $AB$  being designated  $\delta_0$ . If the axial load of 10,000 lb. is now added to the system the first secondary moments,  $M_{s1}$ , are produced, each equal to  $-10,000 \delta_0 = -E\delta_0/150$ . Integrating the curve of  $M_{s1}/I$  twice from left to right gives the values of  $\delta_{t1}$ , the first secondary deflections from the tangent at  $A$ . These figures are shown in Table 14 : 14. In this case the deflection of  $B$  is  $19,490/E$ . The first secondary deflections from the line  $AB$ ,  $\delta_{s1}$ , are then found by subtracting  $19,490 x/L$  from  $E\delta_{t1}$ . The process can be repeated, if desired, and the second secondary deflections from the tangent at  $A$ ,  $\delta_{t2}$ , computed. For point  $B$ ,  $\delta_{t2} = 3,983/E$ . Assuming the secondary deflections to form a geometric series, the geometric constant will be  $3,983/19,490 = 0.204$ . The sum of the secondary deflections of  $B$  from the tangent at  $A$  will therefore be  $19,490/0.796 E = 24,500/E$ . From the above figures it can be seen that the deflection of  $B$  from the tangent at  $A$  due to the axial load and a couple of 1 in.-lb. at  $A$  would be  $136.25/E + 24.50/E = 160.75/E$  in. The rotation of the tangent at  $A$  will thus be  $160.75/50 E = 3.205/E$ . The stiffness factor for end  $A$  assuming end  $B$  pinned will therefore be  $E/3.205 = 0.3120 E$ . The stiffness factor for end  $B$  assuming end  $A$  pinned can be obtained in similar fashion from the curve of  $\delta_{0b}$  of Table 5 : 2, the integrations necessary being made from right to left.

*Fixed-end Moments* — To compute the fixed-end moments the first step is to calculate the ordinates of the deflection curve when the ends of the beam are fixed and it is subjected to the side load, but no axial load. For a transverse load of 1,000 lb. at Sta. 20 these ordinates will be equal to the deflections,  $E\delta_{0a}$ , of Table 5 : 1 multiplied by the fixed-end moment,  $M_{Fa}$ , of 6.042; plus the deflections,  $E\delta_{0b}$ , of Table 5 : 2 multiplied by the fixed-end moment,  $M_{Fb}$ , of 5.898; plus the deflections,  $E\delta_{0w}$ , of Table 5 : 3. These quantities and the resulting values of the primary deflection,  $E\delta_0$ , are shown in Table 14 : 15. As the actual transverse load is assumed to be 2,000 lb. and the axial load is 10,000 lb. the first secondary moments  $M_{s1}$  can be obtained by multiplying the values of  $E\delta_0$  by  $-2/150$ . By double integration the area under the curve of  $M_{s1}/I$  is found to be  $-3,273$ , and its moment about  $B$  to be  $-89,150$ . Then the distance from  $B$  to the centroid of this area is  $89,150/3,273 = 27.24$ , and the distance from  $A$  to the centroid is  $50 - 27.24 = 22.76$  in.

TABLE 14 : 15  
COMPUTATION OF SECONDARY MOMENTS,  $M_{s1}$   
FIXED ENDS AND CONCENTRATED SIDE LOAD

Station	$E\delta_{0a}$	$E\delta_{0b}$	$E\delta_w$	6.042 $E\delta_{0a}$	5.898 $E\delta_{0b}$	$E\delta_0$	$M_{s1}$
0	0	0	0	0	0	0	0
10	8,330	830	-25,000	50,300	4,900	30,200	-404
20	30,470	4,760	-142,800	184,100	28,100	69,400	-925
30	61,480	14,250	-396,400	371,500	84,000	59,100	-788
40	97,680	31,130	-753,900	590,200	183,600	19,900	-265
50	136,250	56,840	-1,158,600	823,200	335,200	200	0

As the ends are assumed to remain fixed in both orientation and position these secondary moments,  $M_{s1}$ , must be accompanied by secondary fixing moments at  $A$  and  $B$  which can be computed from Eq. 5 : 9 modified as suggested in Art. 13 : 19.

$$M_{Fa1} = + \frac{A_w (x_w - x_b)}{A_a (x_a - x_b)} = - \frac{3,273 (22.76 - 31.32)}{3,912 (15.17 - 31.32)} = -0.444 \quad \text{or} \quad -444 \text{ in.-lb.}$$

$$M_{Fb1} = - \frac{A_w (x_w - x_a)}{A_b (x_b - x_a)} = + \frac{3,273 (22.76 - 15.17)}{3,043 (31.32 - 15.17)} = +0.505 \quad \text{or} \quad +505 \text{ in.-lb.}$$



The ordinates of the first secondary deflection curve can now be found as the resultant effect of these first secondary fixed-end moments and the first secondary moments,  $M_{s1}$ . From these the second secondary deflections and moments can be computed by repeating the process described above. In this case the second secondary fixed-end moments are found to be  $M_{Fa2} = -0.0182$  and  $M_{Fb2} = +0.0234$ . Assuming the secondary fixed-end moments to constitute a geometric series, the geometric constants are 0.041 for  $M_{Fa}$  and 0.046 for  $M_{Fb}$ . The total fixed-end moments are therefore

$$M_{Fa} = -2,000 \times 6.042 - \frac{444}{0.959} = -12,084 - 464 = -12,548 \text{ in.-lb.}$$

$$M_{Fb} = +2,000 \times 5.898 + \frac{505}{0.954} = +11,796 + 530 = +12,326 \text{ in.-lb.}$$

*Deflection End Moments* — It remains to determine the end moments resulting from moving the end  $B$  a distance  $D$  normal to the original position of the axis, the ends being assumed prevented from rotation. In Art. 5 : 17 it was found that if there were no axial load the resulting bending moment at  $A$  would be  $DE/63.18$  in.-lb. and that at  $B$  would be  $-DE/49.14$  in.-lb. Multiplying these values by  $E = 1,500,000$  we get as the primary deflection moments,  $M_{0a} = 23,740 D$  in.-lb. and  $M_{0b} = -30,520 D$  in.-lb. The deflections from the tangent at  $A$  due to these moments will be  $D/63.18$  times the values of  $E\delta$  from Table 5 : 1 minus  $D/49.14$  times the values of  $E\delta$  from Table 5 : 2. These deflections are computed in terms of  $D$  in Table 14 : 16, where they are

TABLE 14 : 16  
COMPUTATION OF SECONDARY MOMENTS,  $M_{s1}/D$

Station	$\frac{D\delta_{0a}}{63.18 D}$	$\frac{D\delta_{0b}}{49.14 D}$	$\frac{\delta_{t0}}{D}$	$\frac{x}{L}$	$\frac{\delta_{c0}}{D}$	$\frac{M_{s1}}{D}$
0	0	0	0	0	0	0
10	0.132	-0.017	0.115	0.200	-0.085	+850
20	0.482	-0.097	0.385	0.400	-0.015	+150
30	0.973	-0.290	0.683	0.600	+0.068	-680
40	1.546	-0.633	0.913	0.800	+0.113	-1,130
50	2.157	-1.157	1.000	1.000	0	0

designated  $\delta_{t0}$ . If a compressive load of 10,000 lb. is now applied along the line joining the deflected positions of  $A$  and  $B$ , its eccentricity at any point will be  $\delta_{c0} = \delta_{t0} - xD/L$ . The values of  $\delta_{c0}/D$  are also

computed in Table 14 : 16. These quantities multiplied by the axial load give the ordinates of the first secondary moment curve,  $M_{s1}/D$ , which are also shown in the table.

Table 14 : 17 shows the double integration of the ordinate of the curve of  $M_{s1}/DI$  to obtain values of  $E\theta_1$  and  $E\delta_1$  representing the changes in slope and deflection that would be produced by the secondary

TABLE 14 : 17  
COMPUTATION OF SECONDARY DEFLECTIONS,  $\delta_1$

Station	$M_{s1}/ID$	Sum	$E \Delta\theta_1$	$E\theta_1$	Sum	$E \Delta\delta_1$	$E\delta_1$
0	0			0			0
10	+142	+142	+710	+710	+710	+3,550	+3,550
20	+21	+163	+815	+1,525	+2,235	+11,175	+14,725
30	-85	-64	-320	+1,205	+2,730	+13,650	+28,375
40	-125	-210	-1,050	+155	+1,360	+6,800	+35,175
50	0	-125	-625	-470	-315	-1,575	+33,600

moments,  $M_{s1}$ , acting alone. The area under the curve of  $M_{s1}/I$  is found to be -470 and its moment about  $B$  to be +33,600. Its centroid is therefore  $33,600/470 = 71.49$  in. to the right of  $B$ , whence  $A_w = -470$  and  $x_w = 121.49$  in. By hypothesis, however, the moments,  $M_{s1}$ , are not permitted to act alone, but as the ends  $A$  and  $B$  are rigidly held in both orientation and position, additional secondary end moments,  $M_{a1}$  and  $M_{b1}$ , are developed. Since the latter moments must be such that they change neither the slope nor the deflection at  $B$ , they can be computed by the modified Eq. 5 : 9 for fixed-end moments, as follows:

$$M_{a1} = + \frac{A_w (x_w - x_b)}{A_a (x_a - x_b)} = - \frac{470 (121.49 - 31.32)}{3.912 (15.17 - 31.32)} = +671 \text{ in.-lb.}$$

$$M_{b1} = - \frac{A_w (x_w - x_a)}{A_b (x_b - x_a)} = + \frac{470 (121.49 - 15.17)}{3.043 (31.32 - 15.17)} = +1,017 \text{ in.-lb.}$$

The net end moments corresponding to the deflection, including the first secondaries, are therefore  $M_a = -23,740 + 670 = -23,070$  in.-lb., and  $M_b = -30,520 + 1,020 = -29,500$  in.-lb.

It will be noticed that both  $M_{a1}$  and  $M_{b1}$  are positive. That is, the deflection moments at  $A$  and  $B$  are reduced in absolute magnitude by the presence of axial compression. That this is to be expected can be seen from Fig. 14 : 22 which gives corresponding figures for beam-columns of constant section.

The calculations of the deflection moments could be carried through another cycle to obtain the effects of the second and following secondary moments, but the reader should have no difficulty in doing this if he desires.

*Shear Distribution Factor* — If member  $AB$  is one of a series of parallel members that resist a transverse load with a common deflection,  $D$ , the resulting shears and end moments carried by it will be in proportion to  $23.07 + 29.50 = 52.57$ , which number may be termed the shear distribution factor for the member. These moments will be divided between ends  $A$  and  $B$  in the ratio of 23.07 to 29.50.

**14 : 14. Beam-columns Subjected to High Axial Stress** — When the average axial stress,  $P/A$ , of a beam-column exceeds the elastic limit of the material, proper allowances should be made in the analysis. The simplest method of doing this is to use  $\bar{E}$  as defined in Art. 10 : 11 in place of  $E$  in computing  $j$  and  $L/j$ . This practice should be followed both when using the formulas of Art. 14 : 5 and the moment-distribution method of Art. 14 : 11. Usually it is sufficient to determine  $\bar{E}$  from the formulas of Art. 10 : 11. If desired, this value of  $\bar{E}$  may be corrected slightly to allow for the differences between the shape of cross-section under investigation and that used in the tests on which the column formula of Art. 10 : 11 was based. Such corrections normally entail the use of the tangent modulus of elasticity in conjunction with the initial or Young's modulus. Timoshenko discusses the "double-modulus" problem in his "Theory of Elastic Stability," and W. R. Osgood treats it in "The Double-modulus Theory of Column Action" in *Civil Engineering* for March, 1935, and in N.A.C.A. Technical Reports 615 and 656.

In Art. 10 : 11 it is recommended that, when the axial load is tension, the assumed value of  $\bar{E}$  should be the same as for the same average intensity of compressive stress, or, if the average tensile stress exceeds the maximum allowable for a column of the same material,  $\bar{E}$  should be assumed equal to zero. These assumptions were proposed as being conservative, but some engineers believe that they are actually on the unsafe side. The writers are now among those who believe it better to assume  $\bar{E} = E$  for all intensities of tensile stress. This problem should be subjected to further study with the objective of developing a more satisfactory and rational procedure for determining the value of  $\bar{E}$  to be used with highly stressed tension members.

**14 : 15. Graphical Analysis of Beam-columns** — Whenever the transverse loading of a beam-column subjected to axial compression is composed of any combination of external couples, concentrated loads, and uniformly distributed loads, the member may be divided into segments for each of which the relation between bending moment and deflection may be written in the form

$$M + Py = M_0 \quad 14 : 34$$

where  $M_0$  is the “ primary bending moment ” and  $M$  the total moment for the given loading. Differentiating twice with respect to  $x$  gives the relation

$$\frac{d^2M}{dx^2} + \frac{M}{j^2} = w^1 \quad 14 : 35$$

In Art. 14 : 2 the solution of this differential equation is given as

$$M = C_1 \sin \frac{x}{j} + C_2 \cos \frac{x}{j} + wj^2$$

An equivalent alternative form for writing the solution is

$$m = M - wj^2 = C \cos \left( \frac{x}{j} - \eta \right) \quad 14 : 36$$

which, being differentiated, gives

$$S = \frac{dM}{dx} = -\frac{C}{j} \sin \left( \frac{x}{j} - \eta \right) \quad 14 : 37$$

The form of solution represented by Eq. 14 : 36 and 14 : 37 is of interest as the basis of a convenient graphical method of analyzing beam-columns.

Assuming  $m$  and  $x/j$  to be the variables and plotting on polar coordinates, the curve for Eq. 14 : 36 is a circle passing through the pole,  $O$ , with a diameter,  $OX$ , equal to  $C$ , and an angle  $\eta$  between  $OX$  and the origin line  $OA$ . The point  $X$  at the other end of the diameter through the origin is called the “ apex ” of the curve of  $m$ . In practice the problem is to find the apices of the  $m$  curves for the different segments of a span. Methods of doing this for several common types of loading follow.

*Case I. End Moments with No Side Load.* To construct the “ polar diagram ” for the loading shown in Fig. 14 : 27a, draw the radius

<sup>1</sup> With uniformly varying and other complex distributed loadings  $d^2M_0/dx^2$  becomes a function of  $x$  and Eq. 14 : 34 and 14 : 35 are not applicable.

vectors  $OA$  and  $OB$  with the angle between them equal to  $L/j$  radians.<sup>1</sup> Locate points  $A$  and  $B$  by laying off  $OA = M_A$  and  $OB = M_B$  to some convenient scale. Then construct a circle to pass through points  $O$ ,  $A$ , and  $B$ . For this purpose erect a perpendicular to  $OA$  at  $A$  and a perpendicular to  $OB$  at  $B$ . The intersection,  $X$ , of these perpendiculars is the "apex" of the desired circle; i.e.,  $OX$  is a diameter of that circle, and its length represents the magnitude of the constant of integration,  $C$ , of Eq. 14 : 36 and 14 : 37.

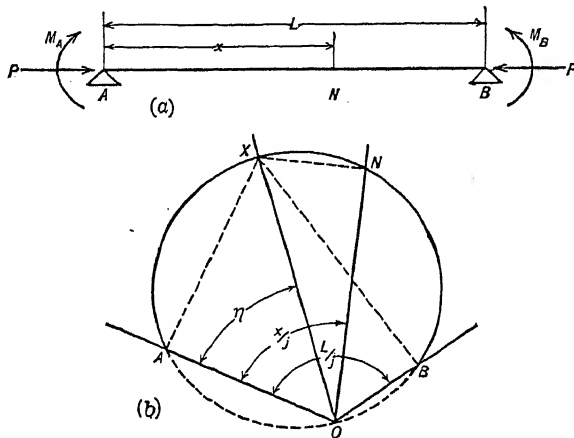


FIG. 14 : 27

To determine the magnitude of the bending moment and shear at any distance,  $x$ , from  $A$ , the left end of the beam, draw the radius vector  $ON$  with the angle  $AON = x/j$ , and also the line  $NX$ .  $ON$  then represents the bending moment and  $NX$  represents  $j$  times the shear desired. Thus the arc  $AXNB$  of Fig. 14 : 27b may be used as both a moment and a shear diagram for the beam of Fig. 14 : 27a. In this diagram the angle  $AOX = \eta$ , the second constant of integration of Eq. 14 : 36 and 14 : 37.

In this example, both  $M_A$  and  $M_B$  are positive and therefore  $OA$  and  $OB$  are laid off above the origin  $O$ . If either had been negative, it would have been laid off below  $O$ . Since the whole of the arc  $AXNB$  is above  $O$ , the bending moment is positive along the entire span.

The shear is positive when the apex,  $X$ , is to the right when looking in the positive direction (i.e., upwards) along the radius vector representing the moment, and negative when it is to the left of that vector.

<sup>1</sup> All angles used in the constructions described in this article are to be measured in radians.

Thus at  $N$  in the example, the shear is negative, but nearer the left end of the span, where  $x/j < \eta$ , the shear is positive.

The validity of this construction for representing Eq. 14 : 36 and 14 : 37 can be easily checked.

*Case II. End Moments with Uniformly Distributed Side Load.* For this case the polar diagram of Fig. 14 : 28 is constructed as follows. First draw the radius vectors  $OF$  and  $OF'$  with the included angle equal to  $L/j$ . Next construct the circular arc  $FF'$  with a radius equal

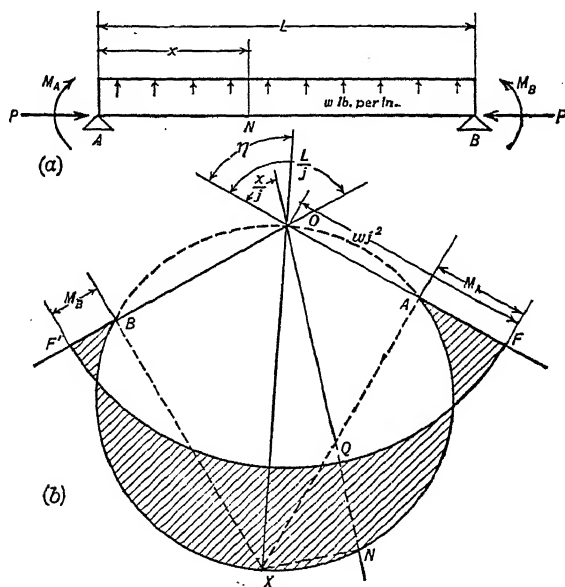


FIG. 14 : 28

to  $wj^2$ . If  $w$  is positive, as in the example, the arc  $FF'$  should be drawn below the origin,  $O$ . Now lay off  $FA = M_A$  and  $F'B = M_B$ . When the end moments are positive, as in the example, points  $A$  and  $B$  should be located above the arc  $FF'$ . A perpendicular to  $OA$  drawn through  $A$  and a perpendicular to  $OB$  through  $B$  will intersect at  $X$ , the desired apex. The diagram is completed by drawing a circle on  $OX$  as a diameter.

To find the moment at  $N$  at a distance  $x$  from end  $A$ , construct the radius vector  $ON$  making an angle of  $x/j$  with  $OA$ . The intercept  $QN$  between the arc  $FF'$  and the arc  $ANXB$  represents the desired bending moment. In this case, since  $N$  is below  $Q$ , the moment is negative. Near each end of the span the arc  $ANXB$  is above  $FF'$  and the moments

are positive. The cross-hatched area of Fig. 14 : 28b is thus a moment diagram for the loading of Fig. 14 : 28a. The shear at point  $N$  is represented by the length of line  $NX$ . In the case shown it is negative since  $X$  is to the left of  $NO$  when looking along that line in the positive direction.

As in the construction for Case I, the distance  $OX$  and the angle  $AOX$  are equal to the constants of integration  $C$  and  $\eta$  of Eq. 14 : 36 and 14 : 37. The validity of the construction is therefore easily checked.

*Case III. End Moments and Single Concentrated Side Load.* For each of the two segments into which the span is divided by the con-

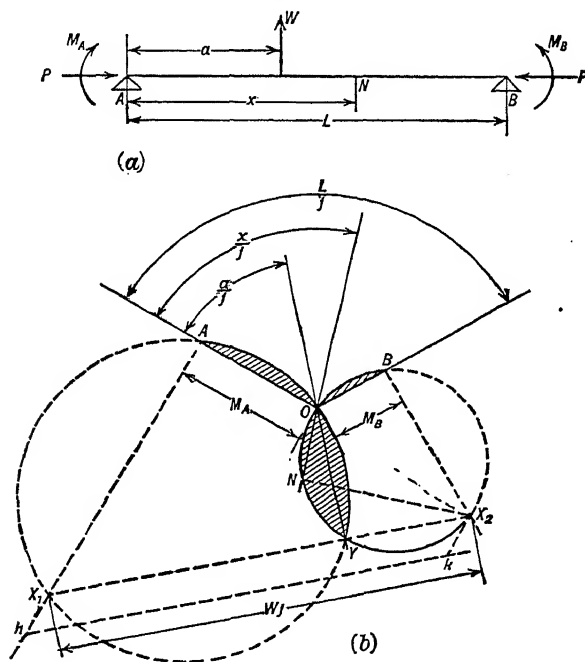


FIG. 14 : 29

centrated load the diagram is like that for the first case. At the concentrated load, however, there is a sudden change in the constants of integration,  $C$  and  $\eta$ , due to a change in the shear equal to  $W$ , but no sudden change in the bending moment. The problem is to locate the apices of the two interload segments so the resulting diagram will conform to these boundary conditions.

Lay off  $OA = M_A$  and  $OB = M_B$ , as before, on radius vectors at an angle of  $L/j$  to each other, and erect perpendiculars to those vectors at  $A$  and  $B$ . The perpendicular through  $A$  will be the locus of the apex for the left segment and that through  $B$  the locus of the apex for

the right segment. Also lay off  $OY$  at an angle of  $\alpha/j$  to  $OA$  to represent the location of the concentrated load  $W$ .

Through any point  $h$  on the perpendicular through  $A$  draw a line  $hk$  perpendicular to  $OY$  and of length  $Wj$ . In this case, since  $W$  is positive, this distance should be laid off to the right of point  $h$ . From  $k$  draw a line parallel to  $Ah$ . The intersection  $X_2$ , of this line with the perpendicular through  $B$  is the apex for the right segment of the span. The location of the apex for the left segment can now be found by drawing  $X_2X_1$  parallel to  $hk$  and intersecting  $Ah$  at  $X_1$ . The construction is completed by drawing the circles  $AOYX_1$  and  $BOYX_2$ . The cross-hatched area of Fig. 14:29b then constitutes the desired moment diagram.

To find the moment and shear at any point,  $N$ , draw the radius vector  $ON$  at an angle  $\alpha/j$  to  $OA$ , and from  $N$  draw  $NX_2$  to the apex of the circle on which  $N$  is located. The desired moment is then represented by the length of  $ON$  and the shear by the length of  $NX_2$  divided by  $j$ . In the case shown,  $M$  is negative, since  $N$  is below the origin  $O$ , and  $S$  is positive, since  $X_2$  is to the right of  $NO$ .

At the point of application of the concentrated load  $jS$  changes from  $-X_1Y$  to  $+YX_2$ , a total change of  $Wj$ , since  $X_1X_2 = hk = Wj$  but there is no sudden change in the bending moment. The construction is thus seen to satisfy the conditions of the problem.

*Case IV. End Moments and Sudden Change in Uniformly Distributed Side Load.* In this case the apex is displaced parallel to the radius vector at the point of discontinuity instead of perpendicular to it, as in the case of a concentrated load. The construction is as follows.

Draw the radius vectors  $OA$ ,  $OB$ , and  $OY$  for the ends of the span and the point of discontinuity, and also the " $wj^2$  arcs"  $FG'$  and  $F'G$ . Lay off  $FA = M_A$  and  $GB = M_B$ , and erect perpendiculars at  $A$  and  $B$ . These perpendiculars are the loci of the desired apices.

From any point  $h$  on the  $A$  perpendicular, lay off  $hk = (w_1 - w_2)j^2$  parallel to  $OY$ . The distance  $hk$  will be equal to  $G'F'$ , and  $k$  should be in the same position relative to  $h$  as  $F'$  is with respect to  $G'$ . The intersection,  $X_2$ , of the  $B$  perpendicular and a line through  $k$  parallel to  $Ah$  is the apex for the right segment of the span. The apex,  $X_1$ , for the left segment is at the intersection of  $Ah$  and a line through  $X_2$  drawn parallel to  $OY$  and  $hk$ .

The construction is completed by drawing the circular arcs  $AKX_1$  and  $BX_2H$ . The resulting moment diagram is shown cross-hatched in Fig. 14:30. Since  $X_1$  and  $X_2$  are the apices of the arcs  $AKX_1$  and  $BX_2H$ , straight lines  $KX_1$  and  $HX_2$  would be normal to  $OY$ , and  $X_1X_2$  is parallel to  $OY$  by construction. Hence  $HKX_1X_2$  is a rec-



tangle. Therefore  $HK = X_1X_2 = hk = F'G'$ , and  $F'H = G'K$ . Also  $HX_2 = KX_1$ . Thus there is no sudden change in either moment or shear at the section of discontinuity of loading, and the diagram conforms to the conditions of the problem.

The perpendicular to  $OA$  through  $A$  is the locus of  $X_1$  for the given value of  $M_A$ , and the line through  $k$  and parallel to it is the locus of  $X_2$ . If there were additional changes in loading, parallel loci for the additional apices could be drawn, and the apex for the right-hand segment

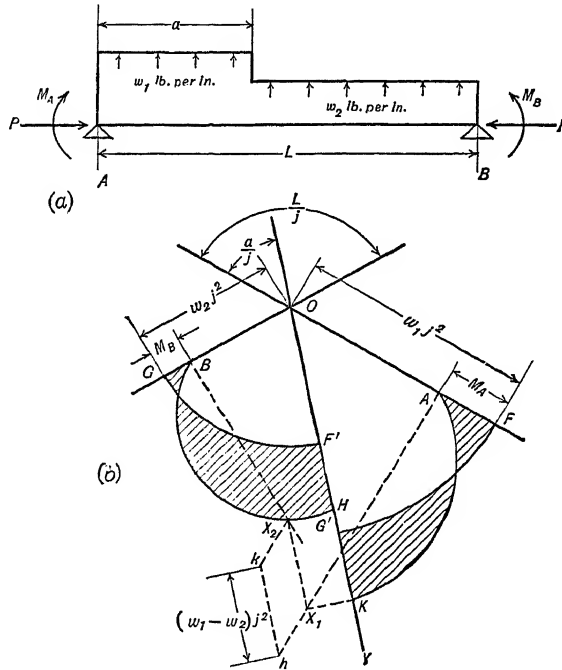


FIG. 14 : 30

found at the intersection of the corresponding perpendicular to the  $A$  perpendicular and the perpendicular to  $OB$  through  $B$ . The method can therefore be extended to any number of discontinuities of loading. The method of handling more than one discontinuity will be shown in Case VI.

*Case V. End Moments and Uniformly Distributed Side Load with Sudden Change in Moment of Inertia.* Each of the cases so far considered can be handled readily by analytical methods if desired. When, however, there is a sudden change of moment of inertia within a span, the analytical methods become impracticable but the graphical method is readily extended to cover the situation.

To construct the polar diagram for the span of Fig. 14 : 31a, first draw the radius vectors  $OA$ ,  $OB$ , and  $OY$  for the ends of the span and the section where the change in moment of inertia results in a change of  $j$  from  $j_1$  to  $j_2$ . Then construct the arcs  $FG'$  and  $F'G$  with their centers at  $O$  and radii equal to  $wj_1^2$  and  $wj_2^2$ , respectively. From  $F$ , lay off  $FA = M_A$ , and from  $G$  lay off  $GB = M_B$ . In the example, since  $M_A$  is negative, it is laid off below the arc  $FG'$ , while  $M_B$ , being positive, is laid off above  $F'G$ .

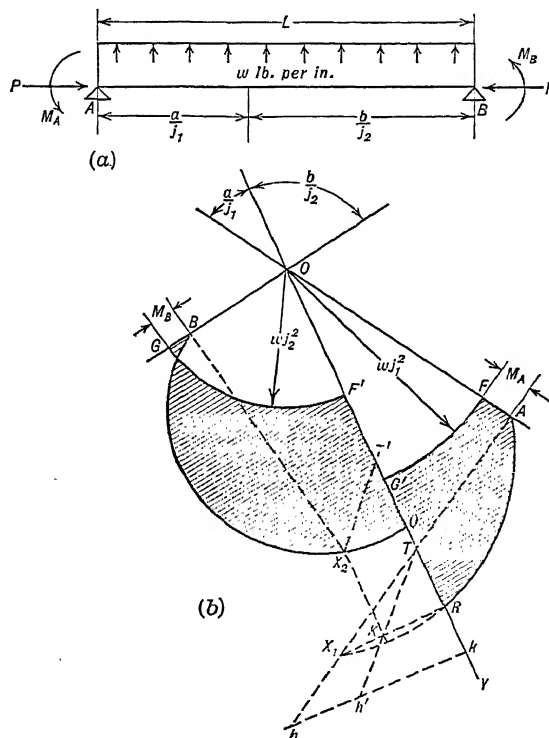


FIG. 14 : 31

is laid off above  $F'G$ . Through  $A$  and  $B$  draw perpendiculars to  $OA$  and  $OB$ , thus obtaining the loci of the desired apices.

From any point,  $h$ , on the  $A$  perpendicular draw  $hk$  perpendicular to  $OY$ , and locate point  $h'$  so that  $hk/h'k = j_1/j_2$ . From  $T$ , the intersection of  $Ah$  and  $OY$ , draw  $Th'$ . Also locate  $T'$  on  $OY$  so that  $TT' = G'F' = w(j_1^2 - j_2^2)$ . The position of  $T'$  with respect to  $T$  should be the same as that of  $F'$  with respect to  $G'$ . Then the intersection of the  $B$  perpendicular and a line through  $T'$  parallel to  $Th'$  is  $X_2$ , the apex for the right segment of the span.

To locate the apex for the left segment, draw  $X_2K$  parallel to  $OY$  and intersecting  $Th'$  at  $K$ . The intersection of a perpendicular to  $OY$  passing through  $K$  and  $Ah$  is  $X_1$ , the point desired. Constructing circular arcs  $AR$  and  $BQ$  on  $OX_1$  and  $OX_2$  as diameters completes the moment diagram indicated by the cross-hatching in Fig. 14 : 31b.

In this diagram, since  $X_1K$  is perpendicular to  $OY$  it would pass through  $R$ , if extended, and  $X_1R$  represents  $j_1$  times the shear at the point of discontinuity. The distance  $X_2Q$  represents  $j_2$  times the same shear. Since  $X_1R$  and  $X_2Q$  are both normal to, and  $X_2K$  is parallel to,  $OY$ , the figure  $QRKX_2$  is a rectangle,  $X_2Q = KR$ , and  $QR = X_2K = TT' = w(j_1^2 - j_2^2)$ . By similar triangles,  $KR/X_1R = h'k/hk = j_2/j_1$ . Therefore  $X_2Q/X_1R = j_2/j_1$  as is necessary for both lines to represent the same shear multiplied by the appropriate value of  $j$ . Also since  $QR$  and  $F'T'$  are both equal to  $w(j_1^2 - j_2^2)$ ,  $QF' = RT'$  and the diagram gives the same value for the moment at the point of discontinuity of moment of inertia, regardless of which segment is used.

It should be noted that, in this case, not only is the apex displaced a distance equal to the change in  $wj^2$  parallel to  $OY$ , but the perpendicular to  $OA$  through  $A$  is rotated about its intersection with  $OY$  through an angle dependent on the ratio of  $j_2$  to  $j_1$ . The line  $Th'$  is called the "adjusted locus" of  $X_1$ .

*Case VI. General Case.* To illustrate how to apply the method when a span is subjected to a combination of loads and sudden changes of moment of inertia, the diagram of Fig. 14 : 32b is drawn for the loading of Fig. 14 : 32a. In this example it is assumed that the proportions of the distributed loads are as shown in the figure and that  $I_2 > I_1 > I_3$ . To simplify the drawing it is also assumed that the end moments,  $M_A$  and  $M_B$ , are both equal to zero. The construction is carried out in the following stages.

(a) Calculate all required values of  $j$ ,  $a/j$ ,  $wj^2$ , and  $Wj$ .

(b) Draw end radii, dividing radii, and arcs representing  $wj^2$  for each segment. These are  $OA$ ,  $OB$ ,  $Op$ ,  $Oq$ ,  $AF'$ ,  $G'G$ , and  $FB$ .

(c) Locate  $A$  and  $B$  from the ends of the arcs to represent  $M_A$  and  $M_B$ . In this case, since  $M_A = M_B = 0$ ,  $A$  and  $B$  are at the ends of the arcs  $AF'$  and  $FB$ .

(d) Draw perpendiculars to  $OA$  and  $OB$  through  $A$  and  $B$ , respectively. These lines are the loci of  $X_1$  and  $X_3$ , the apices for the end segments.

(e) From any point,  $h$ , on the  $A$  perpendicular, draw  $hk$  perpendicular to  $Op$  and locate  $h'$  so that  $h'k/hk = j_2/j_1$ . If the value of  $j$  is increased in passing from segment  $Ap$  to segment  $pq$ ,  $h'k$  will be greater than  $hk$ , and vice versa. The line  $h'T$  through  $h'$  and the intersection of  $Ah$  and  $Op$  is the "adjusted locus" of  $X_1$ , the rotation of  $hT$  with

respect to the  $A$  perpendicular representing the adjustment of the scale of shear necessitated by the change in value of  $j$  from  $j_1$  to  $j_2$ .

(f) The adjusted locus of  $X_1$  must now be displaced by distances corresponding to the concentrated load,  $W_1$ , and the change in  $wj^2$ . From  $h'$  lines  $h'f'$  and  $j'f$  are drawn parallel and perpendicular to  $Op$ , with  $h'f' = F'G' = w_2j_2^2 - w_1j_1^2$  and  $ff' = W_1j_2$ . Since  $W_1$  acts down,  $f'f$  is drawn to the left from  $f'$ . Note also that  $W_1$  is multiplied by  $j_2$ ,

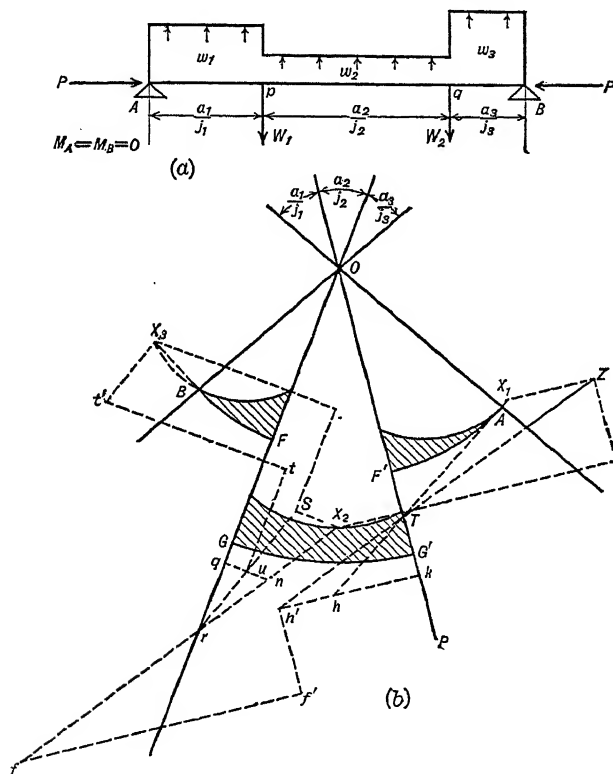


FIG. 14 : 32

the value of  $j$  for segment  $pq$ , since the adjustment for shear scale has already been made. The line  $fr$ , parallel to  $h'T$  and intersecting  $Oq$  at  $r$ , thus obtained by the successive "adjustment" and displacement of the locus of  $X_1$ , is the locus of  $X_2$ , the apex for the segment  $pq$ . The choice of point  $h$  is arbitrary, and the construction for locating  $fr$  can be started from any convenient point on the  $A$  perpendicular.

(g) The adjustment and displacement of the apex are repeated at every dividing radius until the intersection of the locus thus obtained

for the apex of the last segment and the  $B$  perpendicular completely locates the apex for that segment. The adjustment at radius vector  $Oq$  is made as follows. From any point,  $n$ , on  $fr$ , a line  $nq$ , perpendicular to  $Oq$  is drawn and point  $u$  so located that  $uq/nq = j_3/j_2$ . In this case  $u$  lies between  $n$  and  $q$ , since  $j_3$  is less than  $j_2$ . The line  $ur$  is the adjusted locus of  $X_2$ . The displacement of the apex is determined by drawing the line  $ut$  parallel to  $Oq$  and equal to  $GF = w_3j_3^2 - w_2j_2^2$ , and  $tt'$  perpendicular to  $Oq$  and equal to  $W_2j_3$ . Since  $W_2$  also acts down,  $tt'$  is measured to the left from  $t$ . The line through  $t'$  parallel to  $ur$  is a locus of  $X_3$ , and that apex is therefore located at the intersection of this line and the perpendicular to  $OB$  through  $B$ .

(h) The apex for the right-hand segment having been located, the other apices can now be located by reversing the construction. Lines drawn from  $X_3$  equal and parallel to  $t't$  and  $tu$  come to the point  $S$  on  $ur$ . The normal to  $Oq$  through  $S$  intersects  $fr$  at  $X_2$ , the apex for segment  $pq$ . Lines from  $X_2$  equal and parallel to  $ff'$  and  $f'h'$  come to point  $Z$  on  $h'T$ . The normal to  $Op$  through  $Z$  intersects  $Ah$  at  $X_1$  the apex for segment  $Ap$ .

(i) The diagram is completed by drawing circles on the diameters  $OX_1$ ,  $OX_2$ , and  $OX_3$ . The cross-hatched area of Fig. 14 : 32b is the moment diagram for the problem under consideration.

*General Remarks on the Method* — If desired the same general method can be used to construct shear force diagrams. Such diagrams are seldom used since the shear at any point can be readily determined from the moment diagram. When this is done care must be taken to choose the appropriate apex and value of  $j$ .

In some of the above figures the entire circle representing the specific case of Eq. 14 : 36 has been drawn. In practice it normally results in a less confusing figure if only that portion of the circle which forms part of the final moment diagram is drawn. In the figures these portions are indicated by solid lines, any additional portions being indicated by dotted lines. It may be noticed that in Fig. 14 : 30 to 14 : 32 some of the circles are extended to their apices, and this will sometimes be found convenient for relating an apex to the proper circle.

Since the angles used in this method are computed in radian measure, if any extended use of the method is planned, it will be found advisable to construct a protractor graduated in radian measure rather than to translate from radian to degree measure each time an angle is to be laid off.

The graphical method outlined above was first proposed about 1919 by J. Ratzersdorfer in a paper which received little notice in either this country or England. About 1928 it was rediscovered by H. B.

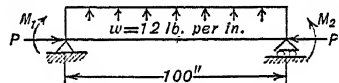
Howard, extended to other load conditions and to continuous beams. The application to continuous beams is not described here since the authors consider it inferior to the analytical method described in this chapter. In this country the method has been further developed by Prof. W. R. Jones, who introduced the term "beam-column," and by his pupils. Theoretically the method can be applied to beam-columns subjected to a uniformly varying side load, but for that case the curve to be drawn is an Archimedean spiral instead of a circle, a fact which makes it too cumbersome for practical use.

Prior to Mr. Howard's work, Miss B. Gough developed a graphical method of handling a limited number of cases of continuous beam-columns of varying cross-section which was described in the first edition of this work. As this method is more limited in scope and more difficult to apply than the Williams adaptation of the method of moment distribution to such problems it has been omitted from the present edition.

PROBLEMS

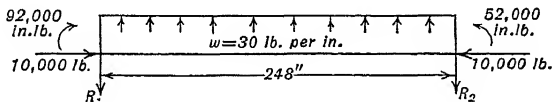
- 14 : 1. Find the maximum moment on the beam shown in the figure. Assume

$$\begin{aligned} P &= -12,600 \text{ lb.} \\ M_1 &= 10,000 \text{ in.-lb.} \\ M_2 &= 15,000 \text{ in.-lb.} \\ I &= 10 \text{ in.}^4 \\ E &= 1,300,000 \text{ p.s.i.} \end{aligned}$$



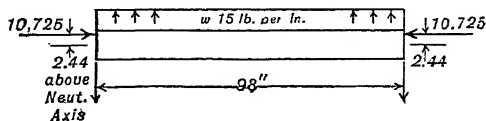
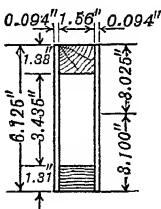
PROB. 14 : 1

- 14 : 2. Determine as closely as possible on the slide rule the location and magnitude of the maximum bending moment on the beam shown. Assume  $EI = 64,000,000$ .



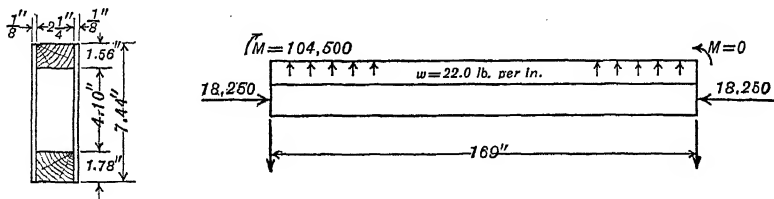
PROB. 14 : 2

- 14 : 3. Determine the magnitude and location of the section of maximum bending moment, the sections of zero bending moment, and draw a bending-moment curve for the beam and loading shown. The beam is of standard airplane spruce,  $E = 1,300,000$  p.s.i.



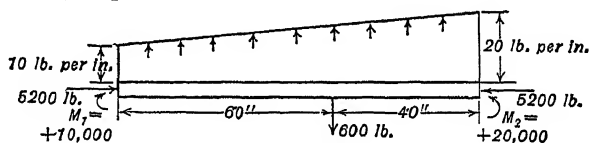
PROB. 14 : 3

14 : 4. Draw a curve of bending moments for the spar and loading shown, using  $M_1$ ,  $M_2$ ,  $M_{1-2}$  and the points of inflection to determine the curve. Neglect the plywood webs entirely in computing  $A$  and  $I$ .



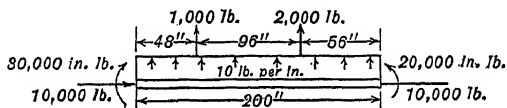
PROB. 14 : 4

14 : 5. Determine the bending moment at the center of the beam-column shown. Assume  $E = 1,300,000$  p.s.i.  $I = 10$  in.<sup>4</sup>



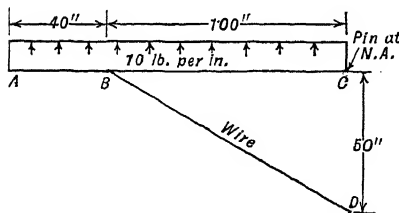
PROB. 14 : 5

14 : 6. Determine the bending moments at the load points and at the center of the beam-column shown. Assume  $EI = 64,000,000$ .



PROB. 14 : 6

14 : 7. Assume the beam of the figure to be of rectangular cross-section, 3.50 in. high, and 1.00 in. wide, with  $E = 1,400,000$  p.s.i.

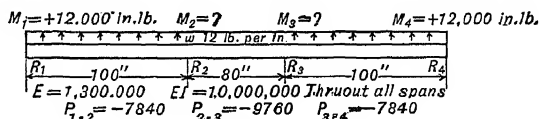


PROB. 14 : 7

a. Compute the axial load in  $BC$  neglecting secondary effects.

b. Compute the location and magnitude of maximum moment in span  $BC$  including the secondary moment due to axial load, and construct the bending-moment curve for the beam  $ABC$ .

14 : 8. Determine the support moments and the maximum bending moment between each pair of supports for the beam-column and loading shown.

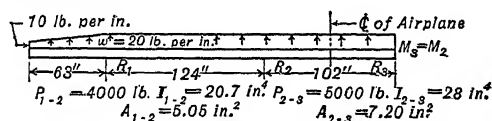


PROB. 14 : 8

14 : 9. Using the beam, spans, and so on of Prob. 14 : 8 and assuming that axial loads,  $P_{1-2}$ ,  $P_{3-4}$ , and moments  $M_1$  and  $M_4$  increase directly as  $w$  increases, compute the values of  $L_2/j_2$ ,  $M_{1-2}$ ,  $M_2$ , and  $M_{2-3}$  for the value of  $L_1/j_1$  assigned to you. Compare your results with those in the following table, the values of which are not guaranteed, and explain the peculiar variations between consecutive values of  $M_{1-2}$ ,  $M_2$ , and  $M_{2-3}$ . At what values of  $L_1/j_1$  and  $L_2/j_2$  does this beam become unstable?

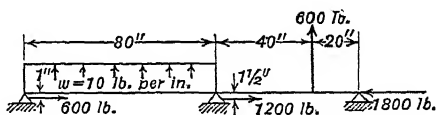
$L_1/j_1$	$w$	$P_1$	$M_1$	$M_{1-2}$	$M_2$	$L_2/j_2$	$P_2$	$M_{2-3}$
2.80	12.00	-7,840	12,000	-11,700	+9,430	2.50	-9,760	+3,300
2.90	12.89	-8,420	12,890	-14,290	+10,450	2.593	-10,470	+5,515
3.00	13.78	-9,000	13,775	-19,789	+11,824	2.678	-11,204	+10,241
3.10	14.80	-9,650	14,800	-22,300	+14,100	2.768	-12,000	+14,250
3.12	14.90	-9,734	14,900	-23,360	+14,620	2.784	-12,119	+25,365
3.14	15.09	-9,860	15,090	-41,572	+15,428	2.803	-12,280	+30,890
3.16	15.33	-9,986	15,328	-44,300	+16,539	2.819	-12,432	+38,819
3.18	15.48	-10,112	15,480	-76,600	+17,900	2.84	-12,590	+38,400
3.20	15.67	-10,240	15,670	-79,311	+20,230	2.86	-12,747	+69,900
3.30	16.67	-10,890	16,670	+126,740	-3,624	2.946	-13,550	-150,300
3.35	17.20	-11,230	17,200	+52,560	+5,540	2.99	-14,000	-72,950
3.40	17.71	-11,575	17,710	+30,500	+9,180	3.04	-14,410	-49,000

14 : 10. Draw a curve of bending moments for the spar and loading shown, the member being of standard spruce.



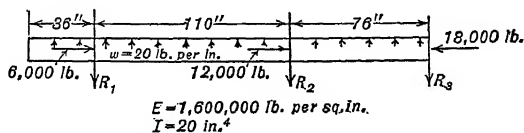
PROB. 14 : 10

14 : 11. Draw the bending-moment curve for the beam-column shown, assuming that under load the center and right-hand supports rise to a level 2.00 in. above that of the left-hand support. Assume  $E = 1,200,000 \text{ p.s.i.}$  and  $I = 10 \text{ in.}^4$



PROB. 14 : 11

14 : 12. For the beam-column shown in the figure, compute the following quantities, neglecting the effects of the axial loads: vertical components of the reactions, support moments, and the locations and magnitudes of the maximum bending moments between the supports.

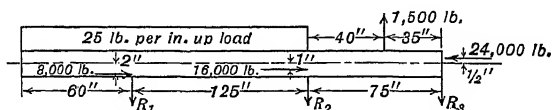


PROB. 14 : 12



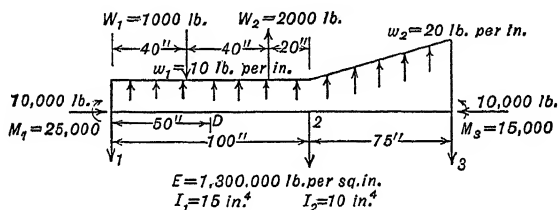
14 : 13. Compute the same quantities as in Prob. 14 : 12 taking proper account of the effects of the axial loads.

14 : 14. Construct the bending-moment curve for the beam-column shown. Assume  $E = 1,600,000$  p.s.i. and  $I = 12$  in.<sup>4</sup>



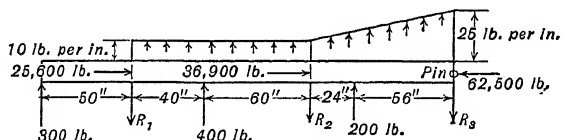
PROB. 14 : 14

14 : 15. Determine the bending moments at the center support and at point D of the beam-column shown.



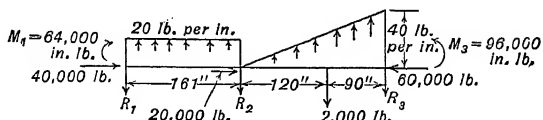
PROB. 14 : 15

14 : 16. Determine the bending moments at the supports, at the points of application of concentrated load, and midway between each pair of supports for the beam-column shown. Assume  $E = 1,600,000$  p.s.i. and  $I = 40$  in.<sup>4</sup>



PROB. 14 : 16

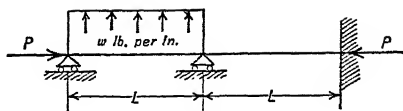
14 : 17. Determine the bending moment at the center support, at the center of each span, and at the point of application of the concentrated load for the beam-column shown. Assume  $E = 10,000,000$  p.s.i. and  $I = 36$  in.<sup>4</sup>



PROB. 14 : 17

14 : 18. Compute the total shear at each end on the beam-columns of Prob. 14 : 1 to 14 : 6.

14 : 19. Find the critical value of  $L/j$  for the beam-column shown. Assume constant  $EI$ .



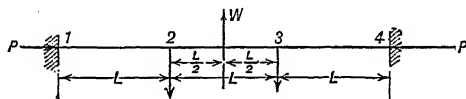
PROB. 14 : 19

14 : 20. If  $EI = 64,000,000$  for the two-span beam-column shown, would that structure be elastically stable? What is the magnitude of the axial load at which it would become unstable?



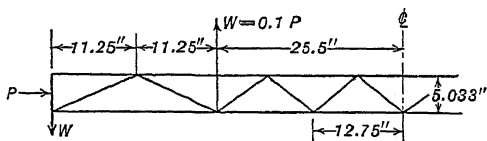
PROB. 14 : 20

14 : 21. Find the critical value of  $L/j$  for the beam-column of three equal bays with fixed ends and concentrated side load as shown. Assume constant  $EI$ .



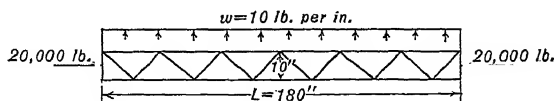
PROB. 14 : 21

14 : 22. The figure shows a line diagram of half a test spar made of chrome-molybdenum steel tubing. The chord members are of elliptical section and have the following cross-sectional areas: compression chord, 0.395 sq. in., tension chord, 0.262 sq. in. The web members are round tubes, those near the end being  $\frac{7}{8}$  by 0.035 and those in the central portion  $\frac{1}{2}$  by 0.035. The axial load  $P$  is applied at the centroid of the chord cross-sections, and the side loads  $W$  are each kept equal to  $0.1 P$ . Back figuring from simple bending tests, the value of  $EI$  for this spar was 97,100,000 in inch-pound units. When the axial load  $P = 25,000$  lb., what will be the bending moment at the center of the span, and what the shear at each end?



PROB. 14 : 22

14 : 23. A truss spar 200 in. long is subjected to a side load of 10 lb. per in. and an axial load of 20,000 lb. The chords are  $1\frac{3}{4}$  by 0.058 round steel tubes. ( $A = 0.3083$ ,  $I = 0.11046$ ,  $I/y = 0.12624$ ,  $E = 30,000,000$ .) The centroids of the chords are 10.0 in. apart. There are no end moments, the 20,000-lb. load being applied midway between the chords. Under the side load acting alone, the midpoint of the truss deflected 0.5 in. If both side load and axial load were acting, what would be the total bending moment at the center of the span, and what the total load in the compression chord at that point?



PROB. 14 : 23

## CHAPTER XV

### INCOMPLETE TENSION FIELDS

In Chapter VI two methods were outlined for analyzing metal beams. The first, based on the assumption that the shear on a section would be resisted by diagonal tensions and compressions of equal intensity, was predicated on there being no buckling of the web. The second assumed that the web would buckle, the diagonal compressions would vanish entirely, and all the shear would be carried by diagonal tensions in the web, which would therefore form a "diagonal tension field." Experience indicates, however, that after the web buckles the diagonal compressions do not disappear but actually increase in intensity, though the rate of increase is much smaller than that of the diagonal tensions. Thus the web does not form a "complete tension field" in which no compressive stresses exist but an "incomplete tension field" in which tensile stresses are associated with somewhat smaller compressive stresses. Analysis by the method of Art. 6 : 3, which presupposes the development of a complete tension field, though useful for first approximations, leads to overconservative results.

Several procedures have been devised for the analysis of beams developing incomplete tension fields in the webs, each designer having his preferred method. Most of these procedures are closely related to that described in this chapter, differing mainly in details, some of which are of a confidential nature. The procedure outlined below is normally conservative, but it can readily be modified to incorporate such refinements as experience or further research indicates to be desirable.

Nearly all methods used for the analysis of tension field beams are developments of the original work of H. Wagner.<sup>1</sup> The detailed procedure presented in this chapter is based on that proposed by Messrs. R. A. Miller and G. G. Green, of the Consolidated Aircraft Corp., as modified by Dr. E. E. Sechler, of GALCIT. The authors, however, have made numerous changes, both on their own initiative and as the result of suggestions from engineers who read a preliminary draft. The comments of Mr. J. M. Jacobson, of the Glenn L. Martin Co., and of Mr. H. M. Poyer, of Bell Aircraft Corp., were particularly helpful.

<sup>1</sup> Translated as N.A.C.A. Technical Memos. 604, 605, and 606 and summarized by P. Kuhn in N.A.C.A. Technical Note 469.

**15 : 1. Stresses in Complete Tension Field Beams** — Before considering the effect of web compression in detail, it seems advisable to complete the discussion, initiated in Art. 6 : 3, of the stresses developed if the web carries no compression. The formulas developed in that article are strictly applicable only to beams with parallel horizontal chords and vertical stiffeners subjected to constant shear. They are based on the following assumptions:

- a. The web carries the entire shear load, none being carried by the chords.
- b. The web buckles immediately when load is applied, and supports the applied shear entirely by a complete diagonal tension field.
- c. The chords are pinned to the verticals and are pin-connected at the fixed end of the beam (if the beam be a cantilever). This leads to the assumption that
- d. There is no gusset or Vierendeel truss action at the connections of the verticals to the chords.

Research indicates that, while these formulas are valid for the assumed limitations and conditions, their use in the practical analysis of deep beams should be supplemented by certain refinements if beams of optimum strength-weight ratio are to be obtained. Some of these refinements would be advisable even though the above assumptions were valid. Most of them are needed, however, because the tension field developed in the web of an airplane spar is always incomplete, and the assumption of a complete tension field leads to the design of webs, stiffeners, and other details which are heavier than need be.

In developing Eq. 6 : 11 for the tensile stress in the web, it was assumed that the chords were of infinite stiffness. Actually they bend somewhat in the plane of the web, and there is a tendency to relieve some of the web elements and to load others more heavily. Eq. 6 : 11 still gives the average value of the web tension, but to find the maximum unit stress it is necessary to multiply the figure resulting from that formula by a correction factor,  $1/R$ , given by<sup>1</sup>

$$\frac{1}{R} = \frac{f_{wt \max.}}{f_{wt \text{ ave.}}} = \frac{\phi}{2} \left[ \frac{\sinh \phi + \sin \phi}{\cosh \phi - \cos \phi} \right] \quad 15 : 1$$

where

$$\phi = 1.25 d \sin \alpha \sqrt[4]{\frac{t}{(I_c + I_t)h}} \quad 15 : 2$$

<sup>1</sup> "Flat Sheet Metal Girders with Very Thin Metal Web — Part III," H. Wagner, N.A.C.A. Technical Memo. 606, 1931.

and

$f_{wt\text{ ave.}}$  = average tensile stress in web as given by  
Eq. 6 : 11.

$f_{wt\text{ max.}}$  = maximum tensile stress developed in the web.

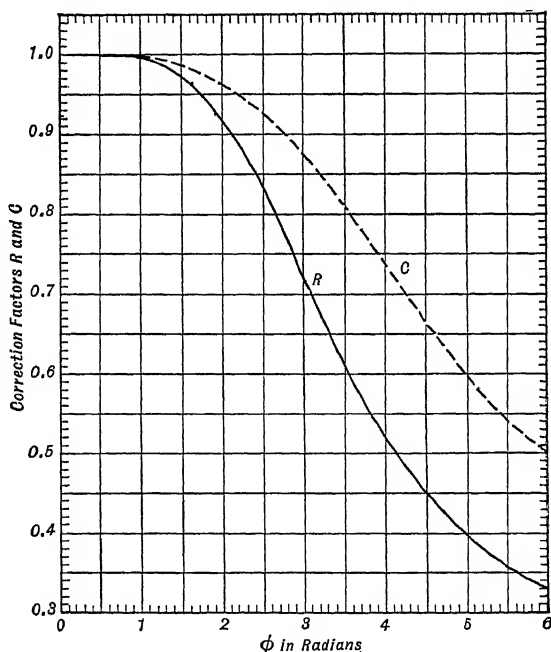
$I_c$  = moment of inertia of compression flange about  
its own neutral axis.

$I_t$  = moment of inertia of tension flange about its  
own neutral axis.

$d$  = spacing of vertical stiffeners.

$\alpha$  = slope angle of web buckles.

The correction factor  $1/R$  can be found from Fig. 15 : 1 or in Eq. 15 : 1,  $\phi$  having been computed from Eq. 15 : 2. This correction is applied



Correction Factors for R and C

FIG. 15:1

only to the tensile stress in the web. The end loads on the verticals and that portion of the load on a chord arising from the sheet tension, being practically independent of the tensile stress distribution in the web, are not appreciably affected. For many designs it will be found that  $\phi$  is less than 1.00 and the correction factor so close to unity that it can be neglected.

Though formulas have been developed to allow for the exact effect of variation in shear, which in actual beams usually varies along the span, they are little used. Normal design practice is to assume the shear to be constant and equal to the maximum between any two adjacent stiffeners. The modifications of the formulas required to allow for non-parallelism of the chords are essentially the same as those for beams with incomplete tension field webs and will not be considered separately. Occasionally the stiffeners are not perpendicular to the chords, a rather uncommon practice when the chords are parallel. Formulas to cover that design feature are not included here but may be found in Air Corps Technical Report 4313, Revised.

The basis of the formulas of Art. 6 : 3 is such that one would expect them to give reasonably accurate predicted stresses for deep beams with very thin webs. In actual practice the formula found to be most in error is that for the axial compression on the web stiffeners. It gives results which may be from two to five times the true values. The other formulas give reasonable first approximations for web thicknesses up to 0.030 in. In general the results of all the other formulas will be conservative, the degree of conservatism increasing rapidly with increasing web thickness or increasing flange stiffness.

**15 : 2. Notation and Nomenclature** — Before describing in more detail a procedure for analyzing beams incorporating incomplete tension fields, it is advisable to list the more important quantities which will appear and the notation used. In terms of pound and inch units, they are:

$V_g$  = total, or gross, shear on a cross-section of the beam or girder.

$V_s$  = shear carried by the web acting as a shear resistant member, i.e., before it buckles.

$V_t$  = shear carried by the diagonal tension field developed in the web after it buckles.

$V_{ty}$  = value of  $V_t$  when  $f_{wt \max.}$  equals the tension yield-point.

$V_{tu}$  = value of  $V_t$  when  $f_{wt \max.}$  equals the ultimate tensile strength.

$V_y$  = value of  $V_g$  associated with  $V_t = V_{ty}$ .

$V_u$  = value of  $V_g$  associated with  $V_t = V_{tu}$ .

$P_v$  = axial load on a web stiffener.

$f_s$  = shear stress in web.

$f_{s \text{ cr.}}$  = shear stress in web at start of buckling.

$f_{wc}$  = compressive stress in web.

$f_{wt}$  = tensile stress in web.

$f_{wts} = f_{wt}$  developed before buckling.

$f_{wtt} = f_{wt}$  developed after buckling.

$d$  = center-to-center spacing of web stiffeners.

$h$  = effective depth of beam, equal to distance between centroids of chords.

$q$  = shear flow, or shear force per unit distance.

$t$  = thickness of web.

$I$  = moment of inertia of cross-section about its neutral axis.

$Q$  = static moment of the cross-section of the chord about the neutral axis of the complete section.

$\alpha$  = angle between the longitudinal axis of the beam and the tension field buckles.

**15 : 3. Assumptions Underlying Analysis of Incomplete Tension Field Beams** — For analysis, the load on a beam in which the web develops an incomplete tension field may be divided into two portions. One is resisted by the development of stresses distributed like those in a shear-resistant web beam as described in Art. 6 : 2. The other is resisted by the development of stresses distributed like those in a complete tension field beam as described in Arts. 6 : 3 and 15 : 1. The total stress in any element may be found by the method of superposition if the total load is divided in the proper proportions. In this chapter it is assumed that there is no increase in diagonal compression after the web begins to wrinkle, and the first portion is therefore equal to the load that would cause wrinkling or buckling to start. This assumption is conservative since the diagonal compressions actually continue to increase after the web has started to buckle. In some designs this increase may be considerable, but methods for computing its magnitude are mostly confidential. If, however, the student really masters the procedure outlined below, he should have no undue difficulty in applying refinements by which the actual increase in diagonal compression is taken into account in the division of the total load into the two portions.

In an actual beam, part of the shear is carried by the chords, owing to their finite, though relatively small, stiffness, but by far the larger part is carried by the web. Also the intensity of shear stress in the web varies with distance from the neutral axis. Experience indicates, however, that the computations are greatly simplified, with negligible loss of accuracy, if the entire shear on a cross-section is assumed uniformly distributed over the part of the web that lies between the chord centroids. This is equivalent to assuming that the chord cross-section is concentrated at its centroid and that the junction between the web and the chord is located at the same point.

**15 : 4. Computation of Web Stresses** — The shear carried per inch of web depth, the “shear flow,” is a more convenient quantity to work with than the intensity of shearing stress in pounds per square inch. Under the assumption of the preceding article, the shear flow in the web is obtainable from

$$q = \frac{Vq}{h} \quad 15 : 3$$

where the nomenclature is that of Art. 15 : 2. This expression is consistent with Eq. 6 : 4 since it can be easily shown that, if all the effective chord area is assumed concentrated at the chord centroids,  $I = Qh$ . Actually the effective area is not so concentrated, but in practical designs the deviation of the ratio  $Qh/I$  from unity is negligible.

Equation 15 : 3 gives the shear flow on sections through the web parallel and perpendicular to the longitudinal axis. So long as the total shear is less than that required to initiate buckling, those sections are subjected to shearing stresses of intensity  $f_s = q/t$ , and sections at angles of approximately 45 degrees to that axis are subjected to tensile and compressive stresses unaccompanied by shear. At the neutral axis of the section the slopes of these diagonal stresses are just 45 degrees, and in intensity

$$f_{wc} = f_{wts} = f_s \quad 15 : 4$$

At other points on the web these relations become approximate, but they are sufficiently accurate for practical design.

These conditions may be assumed to exist until the intensity of shearing stress reaches the “critical” value at which the web begins to buckle. Then the total shear on the beam is

$$V_s = f_{s\text{ cr.}} ht \quad 15 : 5$$

and

$$f_{wc} = f_{wts} = f_{s\text{ cr.}} \quad 15 : 6$$

The value of  $f_{s\text{ cr.}}$  for metal webs may be obtained from the relation

$$f_{s\text{ cr.}} = K \frac{\pi^2 Et^2}{10.92 b^2} \quad 15 : 7$$

where  $K$  has the values listed in Table 15 : 1,  $a$  and  $b$  being the longer and shorter sides, respectively, of the rectangle defined by the centroidal axes of the chords and adjacent stiffeners. The values of  $K_s$  apply when all four sides are simply supported, and those of  $K_f$  when all four sides are fixed. It is common practice to use the values of  $K_s$  in design, though those of  $K_f$  may be useful in the interpretation of test data.



The use of the  $K_s$  based on the distance between chord centroids is quite conservative, particularly when it is assumed there will be no increase in diagonal compression after buckling begins. Some of this conservatism can be eliminated by using the distance between the lines

TABLE 15 : 1

COEFFICIENTS FOR COMPUTATION OF  $f_{s\ cr.}$  VALUES OF K FOR Eq. 15 : 7

$a/b$	1.0	1.2	1.4	1.5	1.6	1.8	2.0	2.5	3.0	Infinity
$K_s$	9.4	8.0	7.3	7.1	7.0	6.8	6.6	6.3	6.1	5.35
$K_f$	15.5	13.3	12.4	12.1	11.9	11.5	11.2	10.7	10.3	8.98

of rivets connecting the web to the chords, or even the clear distance between chords, instead of the distance between chord centroids when determining  $K_s$  from Table 15 : 1. The effect of such refinements on the computed margins of safety, however, will normally be negligible.

If Eq. 15 : 7 gives a value of  $f_{s\ cr.}$  in excess of half the tensile yield point, it indicates that plastic flow of the web material would be produced by a lower load than that required to produce buckling. Then, in computing the maximum shear that could be carried without producing permanent set, the beam should be analyzed by the method of Art. 6 : 2 for beams with shear-resistant webs. To determine the ultimate strength of such beams,  $f_{s\ cr.}$  could be computed from Eq. 15 : 7 by using a modified value of  $E$  corresponding to a direct stress equal to  $2f_{s\ cr.}$ . This modified value might be either the "effective modulus,"  $\bar{E}$ , or the "tangent modulus,"  $E_t$ , discussed in Art. 10 : 11, the latter being preferable if it is known. When a modified modulus is thus employed,  $f_{s\ cr.}$  is obtainable only by successive trials, but with beams of normal proportions this situation seldom arises.

As previously stated, when the load on the beam exceeds that which produces the critical buckling stress, it is assumed that the compressive stress in the web,  $f_{wc}$ , remains constant and equal to  $f_{s\ cr.}$ . The additional shear is assumed to be resisted by increases in the diagonal tension,  $f_{wt}$ , alone. By designating the additional web tension by  $f_{wtt}$ , the shear carried by the web acting as a tension field is therefore

$$V_t = f_{wtt}ht \sin \alpha \cos \alpha \quad 15 : 8$$

as may be seen by comparison with Eq. 6 : 7. The total average tensile stress in the web is therefore

$$f_{wt\ ave.} = f_{wtt} + f_{wts} = f_{wtt} + f_{s\ cr.} \quad 15 : 9$$

Owing to the deformation of the chords under the action of the tension field, the correction term  $R$ , of Eq. 15 : 1, must be applied to  $f_{wtt}$ .

Also, since some material is removed by the rivets connecting the web to the chords or the stiffeners, a rivet correction factor should also be applied to  $f_{wt \text{ ave.}}$  to obtain the maximum value. This correction factor may be taken as

$$C_r = \frac{\text{rivet spacing} - \text{rivet diameter}}{\text{rivet spacing}} \quad 15 : 10$$

Experience shows that while Eq. 15 : 10 is quite accurate when the tensile stresses act normal to the line of rivets, it gives quite conservative results for beam webs where the tensile stresses are at an oblique angle to the rivet line. As yet, however, there are few available test data from which a more reliable correction formula can be developed. The maximum intensity of the web tension will therefore be

$$f_{wt \text{ max.}} = \left( \frac{\frac{f_{wtt}}{R} + f_{s \text{ cr.}}}{C_r} \right) \quad 15 : 1$$

whence

$$f_{wtt} = \left( f_{wt \text{ max.}} - \frac{f_{s \text{ cr.}}}{C_r} \right) C_r R \quad 15 : 12$$

while

$$V_t = \left( f_{wt \text{ max.}} - \frac{f_{s \text{ cr.}}}{C_r} \right) C_r R h t \sin \alpha \cos \alpha \quad 15 : 13$$

For any specific value of the maximum tensile stress in the web, such as the tensile yield point or the ultimate tensile strength of the material, Eq. 15 : 13 may be used to determine the shear carried by the tension field. The value obtained when the yield point is used for  $f_{wt \text{ max.}}$  may be designated by  $V_{ty}$ , and that based on the ultimate tensile strength by  $V_{tu}$ .

Since  $V_o$ , the total shear, equals  $V_s + V_t$ , the shear that can be carried by the beam without exceeding the yield point would seem to be

$$V_y = V_s + V_{ty} \quad 15 : 14$$

Wrinkling of the web, however, produces local bending stresses, and permanent set would be produced before this value of  $V_y$  would be reached. More test data are needed to develop a formula for the minimum load at which permanent set would be produced. It has been noticed at loads causing an average web tension of as low as half the tension yield point.

The parallel formula for the ultimate shear load

$$V_u = V_s + V_{tu} \quad 15 : 15$$

is more reliable since the yielding of the material tends to neutralize the effect of local stress concentration.

The only quantity in Eq. 15 : 13 which is difficult to evaluate is  $\alpha$ , the slope angle of the diagonal tension field. At present the relations between this and the other physical properties of a beam are unknown. For design purposes it may be assumed

$$\alpha = 30 + \frac{2h}{d} \text{ in degrees} \quad 15 : 16a$$

or

$$\alpha = 0.52 + \frac{0.03h}{d} \text{ in radians} \quad 15 : 16b$$

These are empirical formulas based on tests made by the Consolidated Aircraft Corp. Since there was considerable scatter of the test data, the formulas are not as reliable as might be desired. The values of  $V_v$  and  $V_u$ , however, are not very sensitive to variations in  $\alpha$ , and it is sufficiently precise to take  $\alpha$  to the nearest degree or 0.01 radian. In fact, some designers continue to assume  $\alpha = 45$  degrees, considering the use of a more precise value a refinement that is not justified by an appreciably greater precision in the computed margins of safety.

**15 : 5. Numerical Example** — The use of these formulas may be illustrated by finding the maximum shear that the 17 ST aluminum alloy beam shown in Fig. 15 : 2 could be expected to carry. By standard methods of computation,  $I = 23.782 \text{ in.}^4$ ,  $Q = 3.784 \text{ in.}^3$ ,  $h = 6.226 \text{ in.}$ , and  $d = 3.00 \text{ in.}$

The ratio  $a/b$  for use in Table 15 : 1 is then  $6.226/3.00 = 2.075$ , whence the coefficient  $K$  for use in Eq. 15 : 7 equals 6.6. Substituting the proper values in that equation gives

$$6.6 \times \pi^2 \times 10,300,000 \times 0.032^2 =$$

Then, from Eq. 15 : 5,  $V_s = 7,000 \times 6.226 \times 0.032 = 1,395 \text{ lb.}$

Before using Eq. 15 : 13 to determine  $V_t$  it is necessary to evaluate  $\alpha$  and the correction coefficients  $C_r$  and  $R$ . The slope angle,  $\alpha$ , may be taken as equal to  $30 + 2(h/d) = 30 + 2 \times 2.075 = 34$  degrees, whence  $\sin \alpha = 0.560$ ,  $\cos \alpha = 0.829$ , and  $\tan \alpha = 0.675$ . If Table 14 : 1 is to be used,  $\alpha$  should be determined in radians. To determine the correction coefficient,  $R$ , it is first necessary to obtain the moment of inertia of a chord about an axis through its centroid. From the dimensions given, this is found to be  $I_t = I_c = 0.1049 \text{ in.}^4$ . Substitution in Eq. 15 : 2 gives  $\phi = 0.855$  and from Fig. 15 : 1  $R = 0.997$ . Since the rivet

diameter is  $\frac{3}{16}$  in. and the rivet pitch is  $\frac{3}{4}$  in., the rivet correction factor,  $C_r$ , of Eq. 15 : 10 is 0.75.

Taking the yield point of the material as 32,000 p.s.i. and the ultimate tensile strength as 55,000 p.s.i., and substituting in Eq. 15 : 13,

$$V_{ty} = (32,000 \times 0.75 - 7,000) \times 0.997 \times 6.226 \times 0.032 \times 0.560 \times 0.829 = 1,570 \text{ lb.}$$

$$V_{tu} = (55,000 \times 0.75 - 7,000) \times 0.997 \times 6.226 \times 0.032 \times 0.560 \times 0.829 = 3,160 \text{ lb.}$$

The capacity of the section to carry shear is therefore  $V_y = 1,395 + 1,570 = 2,965$  lb. if limited by the yield point and  $V_u = 1,395 + 3,160 = 4,555$  lb. if determined by the ultimate tensile strength.

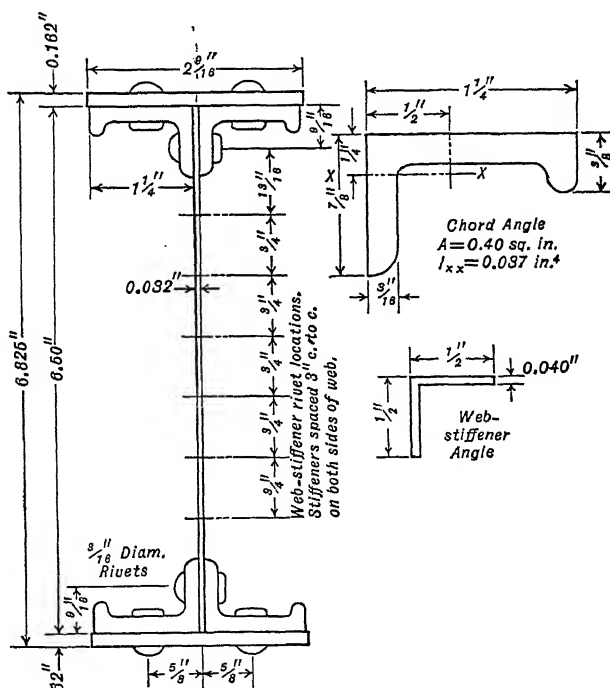


FIG. 15:2

From the geometrical properties listed at the beginning of the article, for the beam under consideration  $I/(Qh) = 23.782/(3.784 \times 6.226) = 1.01$ . This means that the chord material would carry additional shear equal to 1 per cent of the shear carried by the web. It can be shown that  $1 - I/(Qh)$  will be equal to the ratio  $\Sigma I_o/(\Sigma A d^2)$  where  $A$  is the

area of a chord,  $d$  the distance from its centroid to the neutral axis, and  $I_o$  its moments of inertia about an axis passing through its centroid. Except for very shallow beams this ratio is so small as to be negligible.

**15 : 6. Loads on Web-chord Connecting Rivets** — Until the web begins to buckle, the load per inch of span to be carried by the rivets connecting the web to the chord may be determined by the methods of Art. 11 : 9. This load acts in the direction of the beam chords and may be taken as equal to  $V_s/h$  or  $t f_{s_{cr}}$ . Under greater loadings the diagonal tension field imposes additional loads on the joint. From Art. 6 : 3 it can be seen that these would consist of a component equal to  $V_t/h$  parallel to, and a component equal to  $(V_t \tan \alpha)/h$  perpendicular to, the chords. Since  $V_s + V_t = V_w$ , the total components will be  $V_w/h$  and  $(V_t \tan \alpha)/h$ . Their resultant, which is the basis for the design of the rivets, would then be

$$q_r = \frac{1}{h} \sqrt{V_w^2 + V_t^2 \tan^2 \alpha} \quad 15 : 17$$

It should be recognized that Eq. 15 : 17 is approximate in character, but tests indicate that it is quite satisfactory for indicating whether chord rivet failures are to be expected in a given design and the shear load at which rivets may be expected to fail.

Applying this formula to the beam of Fig. 15 : 2,

$$6.226 \sqrt{(1,395 + 3,160)^2 + (3,160 \times 0.675)^2} = 807 \text{ lb. per in.}$$

It might be thought that in this computation care should be taken to use the actual distance between rivet lines instead of the distance between chord centroids as the effective depth. In that event, however, only that part of the shear which is actually carried by the portion of the web between rivet lines should be considered. If the distance between rivet lines be designated by  $h_w$ , the values of  $V_s$  and  $V_t$ , computed above, would need to be multiplied by the ratio  $h_w/h$  to obtain the stresses in the web. Also, the quantity under the radical would be divided by  $h_w$  instead of by  $h$ , so that the final result would be the same. Thus it may be seen that the suggested refinement is not worth bothering with.

**15 : 7. Design of Web Stiffeners** — In the design of thin-webbed beams it is assumed that when the web buckles the stiffeners will break up the deformation pattern into groups of wrinkles, none of which will pass from one side of a stiffener to the other. If, however, the stiffeners are too light, they will buckle simultaneously with the web plate under

a smaller load than that required to cause the type of buckling assumed in design. Timoshenko, in Chapter VII of his "Theory of Elastic Stability," has investigated the problem and developed a criterion for the minimum moment of inertia required in the stiffeners to insure that the assumed type of deformation will take place. According to his theory, the minimum allowable moment of inertia for the stiffeners of metal beams may be obtained from the relation

$$I_v = \frac{K_v d t^3}{3.64} \quad 15 : 18$$

where  $K_v$  is taken from Table 15 : 2. This table gives theoretical values for plates subjected to pure shear and divided into three panels by two equally spaced stiffeners. The experience of the Glenn L. Martin Co. is that the results are satisfactory for practical design.

TABLE 15 : 2

VALUES OF  $K_v$  FOR USE IN Eq. 15 : 18

$d/h$	1.00	0.83	0.67	0.50	0.40
$K_v$	0.64	1.37	3.53	10.7	22.6

For the illustrative example,  $d/h = 3.00/6.226 = 0.48$ , whence  $K_v = 13.1$ . Then, from Eq. 15 : 18, the required value of  $I_v$  is  $13.1 \times 3.00 \times 0.032^3/3.64 = 0.00035 \text{ in.}^4$ . A conservative figure for the moment of inertia of a pair of stiffeners can be obtained by considering only the outstanding legs and assuming them to form a rectangle 1.00 in. high and 0.040 in. thick. Their moment of inertia would then be  $1 \times 0.040/12 = 0.00267 \text{ in.}^4$ . The stiffeners provided are thus seen to be much stiffer than is called for by this criterion.

In addition to forcing the web to deform in the manner assumed in the analysis, the stiffeners must carry, as columns, the difference between the vertical components of the diagonal tensions and the vertical components of the diagonal compressions in the web. If the stiffeners were not attached to the web, it would be found, from reasoning paralleling that in Art. 6 : 3, that each stiffener would be subjected to the axial compression given by the relationship

$$P_v = \frac{V_t d \tan \alpha}{h} \quad 15 : 19$$

$V_t$ , the shear carried by the tension field, is used here instead of the total shear,  $V_g$ , since  $V_t$  is the measure of difference between the vertical components of the web tensions and compressions. The stiffeners could

then be designed as columns, of length equal to the effective depth of the beam, subjected to the load obtained from Eq. 15 : 19.

Riveting these members to the web, however, makes such a simple analysis inapplicable for two reasons. First, a certain part of the sheet must be considered to work with the stiffener proper in resisting the tendency for the chords to come together. The effective width of sheet acting in this manner is unknown and probably varies along the length of the stiffener. Secondly, in addition to the axial load produced in the stiffener by the tension field, there is a load arising from the fact that the stiffener, when riveted to the web, tends to break up the web buckles, which otherwise would be continuous between chords. These web buckles tend to deform the stiffeners torsionally and in bending and thus to precipitate failure due to localized stresses.

Because of the complexity of the problem, no satisfactory theoretical method for determining the design or the allowable stresses in the web stiffeners of tension field beams has yet been developed. Dr. E. E. Sechler has studied tests made by Consolidated on more than fifty parallel chord beams with formed sheet stiffeners on one side of the web, in which the stiffeners failed under load. From these tests he has developed the empirical formula

$$V_{tu} = 0.023 E \sqrt[3]{J_e \frac{th^2}{d}} \quad 15 : 20$$

in which  $J_e$  = effective torsion constant of the stiffener section, which for formed sheets may be taken as

$$J_e = \frac{b_v t_v^3}{3} = \frac{A_v t_v^2}{2} \quad 15 : 21$$

where  $b_v$ ,  $t_v$ , and  $A_v$  are the developed width, thickness, and sectional area, respectively, of the stiffener section.

The torsion constant rather than the moment of inertia has been taken as the important factor, since the study of the tests showed that in nearly every case the stiffener did not fail by bending but by twisting, owing to the high local stresses developed by the web buckling. As shown in Art. 7 : 7, the effective torsion constant of a formed sheet stiffener may be taken equal to that for the equivalent flat-sheet rectangle. Insufficient data are at present available to determine this value for bulb angles and other extruded sections or for closed sections, and it is suggested that in lieu of other information it be obtained from torsion tests. The validity of Eq. 15 : 20 for other than formed sections is unknown, however, and it must therefore be used with caution.

Though lacking a completely rational basis, Eq. 15 : 20 is of value since it provides a means of estimating the load at which failure of the web stiffeners may be expected. In nearly all the tests on which it was based, it gave predicted strengths within  $\pm 10$  per cent of those actually developed.

The tests underlying Eq. 15 : 20 were on beams having stiffeners on only one side of the web. A few tests on beams with the stiffeners in pairs, one on each side of the web, indicated that, if  $J_e$  were taken as twice the value of  $J_e$  for a single stiffener, Eq. 15 : 20 would give conservative results, sometimes excessively so.

The stiffeners for the beam of Fig. 15 : 2 are in pairs, and  $J_e$  for each is equal to  $0.040 \times 0.0016/3 = 0.0000213 \text{ in.}^4$  By using this value in Eq. 15 : 20, the allowable shear is

$$V_{tu} = 0.023 \times 10,300,000 \sqrt[3]{0.0000426 \times 0.032 \times 6.226 \times 6.226/3} = 6,160 \text{ lb.}$$

Since the value of  $V_{tu}$ , determined by the tensile strength of the web as found in Art. 15 : 5, is only 3,160 lb., the stiffeners shown are much stronger than is necessary.

It is very likely that for some designs stiffener failure is more dependent on the bending than on the torsional properties of the stiffener section, and more experimental work should be devoted to the problem. Such work might well result in the formulation of a third criterion calling for the design of the stiffener as a column in a manner similar to that outlined in Art. 10 : 9. For the tests on which Eq. 15 : 20 was based, however, correlation with the moments of inertia of the vertical stiffeners gave less satisfactory agreement and more experimental scatter than was obtained with that equation. On the whole, while the development of Eq. 15 : 20 represents an important forward step in solving the problem of stiffener design, it is far from the last word and much more experimental and theoretical study of the problem is needed.

Closely associated with the design of the stiffeners themselves is the determination of the forces to be transmitted by the rivets connecting the stiffeners to the chords. It is suggested that until more reliable methods have been developed the rivets connecting a stiffener to each chord be designed to transmit a force equal to  $P_v$  as obtained from Eq. 15 : 19. This figure is undoubtedly conservative for normal designs if the increase in diagonal compression after the web begins to buckle is neglected. As more accurate methods of estimating the actual increase in this compression are developed, the value of  $V_t$  used can be suitably modified.



Applying the suggested method to the beam of the illustrative example, it is found that each stiffener-to-chord joint should be designed to transmit not less than  $3,160 \times 3 \times 0.675/6.226 = 1,030$  lb. Experience indicates that this load should be divided between at least two rivets. The design shown in Fig. 15 : 2 is faulty in that provision is made for only one rivet in the stiffener-to-chord connection. In this example, however, it is difficult to see how another rivet could be added to the joint without increasing the size of stiffeners that are already larger than necessary. Situations like this constantly arise in practical design, forcing the adoption of compromises in which undesired details are used to avoid others that are even less desirable.

Little information is available regarding the forces acting on the rivets connecting the stiffeners to the web. Dr. W. T. Thompson, of the Boeing Co., suggests that they be designed to carry a load of  $22,000 A_v/d$  lb. per in. when the stiffeners are on only one side of the web, or  $30,000 A_v/d$  lb. per in. when they are on both sides. With either arrangement,  $A_v$  is the cross-sectional area of one stiffener angle. These rules are based on tests of beams about 18 in. deep, and their applicability to much deeper or much shallower beams is as yet uncertain.

**15 : 8. Chord Stresses** — The stresses in the chords may be considered to be composed of three major parts. These are:

- a. The primary beam bending stresses.
- b. Compression and tension due to the components of the diagonal tension field acting parallel to the chords.
- c. Secondary bending stresses in the chords due to the components of the diagonal tension field acting perpendicular to the chords.

Up to the point at which the web starts to buckle, the normal stresses on the chords are distributed according to the familiar formula,  $f = My/I$ . After buckling, the manner of stress distribution is more complex and has not yet been definitely determined. In practice it is therefore common to neglect the bending carried by the web, usually quite a small part of the total in any beam developing tension fields, and to find the total primary axial loads in the chords from the relation

$$P_{t,c} = \pm \frac{M}{h} \qquad 15 : 22$$

where  $P_t$  and  $P_c$  are the axial loads in the tension and compression chord respectively,  $M$  is the bending moment on the section, and  $h$  is the effective depth of the beam taken as the distance between the centroids of the chord sections. In making this approximation, neglect of the web and variation of the unit stress with distance from the neutral axis tend to neutralize each other.

In Art. 6 : 3 the load in the chords needed to resist the parallel component of the diagonal tension field was found to be  $0.5 V \cot \alpha$ . Actually only that part of the shear carried by the tension field tends to produce these loads, which will therefore be equal to  $0.5 V_t \cot \alpha$ . Thus the total axial load in the chords is given by the relation

$$P_{t,c} = \pm \frac{M}{h} - 0.5 V_t \cot \alpha \quad 15 : 23$$

Similarly the bending stresses in the chords due to the component of the tension field perpendicular to the chords can be found by using  $V_t$  instead of the total shear,  $V_g$ , in the appropriate expression from Art. 6 : 3, except that a further correction should usually be made to allow for the flexibility of the chords in bending. This allowance can be made by the introduction of the correction factor,  $C$ , from Fig. 15 : 1, whence the maximum secondary bending moment in a chord is

$$M_c = 0.10 C \frac{V_t}{d} d^2 \tan \alpha \quad 15 : 24$$

If the section of the beam of Fig. 15 : 2 is subjected to a bending moment of 120,000 in.-lb. and to a shear of 3,000 lb., the stresses in the chords may be estimated as follows. Since the effective depth  $h = 6.226$  in.,  $M/h = 120,000/6.226 = 19,260$  lb. Of the 3,000-lb. total shear,  $V_s = 1,395$  lb. would be carried by the web as shear, leaving 1,605 lb. to be carried by the tension field. From Art. 15 : 5,  $\alpha = 34$  degrees and  $\tan \alpha = 0.675$ . Thus  $0.5 V_t \cot \alpha = 803/0.675 = 1,190$  lb. The total loads are therefore  $P_t = 19,300 - 1,200 = 18,100$  lb. in the tension, and  $P_c = 19,300 + 1,200 = 20,500$  lb. in the compression chord. Since the sectional area of each chord is 1.215 sq. in., the corresponding unit stresses are +14,900 and -16,900 p.s.i.

Using the value of  $\phi$  computed in Art. 15 : 5 and Fig. 15 : 1, the correction factor,  $C$ , to allow for flange flexibility is 0.999. Then, from Eq. 15 : 24, the secondary bending moment to be assumed acting in each chord would be  $M_c = 0.10 \times 0.999 \times 1,605 \times 9 \times 0.675/6.226 = 156$  in.-lb. From the dimensions of Fig. 15 : 2 the moment of inertia of each chord is 0.1049 in.<sup>4</sup> and the distance to the outer fiber is 0.738 in. The maximum secondary stress is therefore  $156 \times 0.738/0.1049 = 1,098$  p.s.i.

**15 : 9. Effects of Non-parallel Chords and Oblique Stiffeners** — If the chords are not parallel, the forces obtained from Eq. 15 : 22 and 15 : 23 are the horizontal components of the chord loads. The resultant chord loads must act along the centroidal axes of the chords, and so their horizontal components must be accompanied by vertical components which will either reduce or add to the shear to be carried by the web. If

the slope angles of the chords are  $\gamma_t$  and  $\gamma_c$ , the sum of the vertical components of the chord loads will be  $P_t \tan \gamma_t + P_c \tan \gamma_c$ . Therefore, the total force to be carried by shear on a vertical section of web will be

$$V'_a = V_a + P_t \tan \gamma_t + P_c \tan \gamma_c \quad 15 : 25$$

For a beam tapered as shown in Fig. 15 : 3,  $P_t$  and  $\gamma_c$  are both positive, while  $P_c$  and  $\gamma_t$  are both negative. Therefore, the vertical components in both chords tend to relieve the web, since each of the last two terms is the product of a positive and a negative quantity. With the type of taper shown, the same would be true if the direction of the total shear were reversed. If, as is sometimes the case with wing spars, both

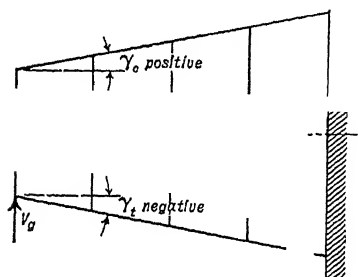


FIG. 15 : 3

chords slope upward from the fuselage toward the wing tip, the vertical component of one chord load tends to reduce, while that of the other tends to increase the shear to be carried by the web. Occasionally a beam is so proportioned that the effective depth decreases as the bending moment increases. Then the effect of the vertical components of the chord loads is to increase the load on the web. In any practical problem

the nature of the change in web shear, caused by the existence of vertical components of the chord loads, can be determined by careful attention to signs. The experienced engineer, however, can determine the nature of the effect more easily by inspection.

For a precise determination of  $V'_a$  from Eq. 15 : 25 it is necessary to resort to successive approximations, since  $P_t$  and  $P_c$  are functions of  $V'_a$ . If, however, as is often true,  $\gamma_c = -\gamma_t$ , the shear terms cancel, and numerically

$$V'_a = V_a - \frac{2 M \tan \gamma}{h} \quad 15 : 26$$

when the taper is of the type shown in Fig. 15 : 3. Even if  $\gamma_c \neq -\gamma_t$ , both are usually small angles, and it is a sufficiently close approximation to write

$$V'_a = V_a - \frac{M (\tan \gamma_c - \tan \gamma_t)}{h} \quad 15 : 27$$

It can also be shown that  $V'_a/h$ , the shear in pounds per inch of depth acting on the web, at any section will be equal to the slope of the curve

of  $M/h$  at that section. This relation is often the most convenient for practical use, especially if the chords are curved and  $\gamma_c$  and  $\gamma_t$  are variables. Proof of the validity of this relation will be left to the student.

The theoretical basis of these methods for computing the shear carried by the web is not as sound as might be desired, and they have not been validated by tests. They should therefore be used with even more than the usual degree of skepticism, particularly with beams that are highly tapered or have the end vertical very rigidly attached to the chords. Pending the procurement of data from tests designed to determine the exact effect of taper, the best a designer can do is to estimate the shear carried by the axial loads in the chords by judicious use of these formulas and to carry out the remainder of the analysis by the methods of this chapter.

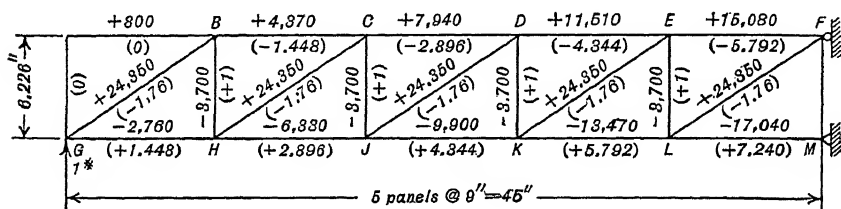
When the chords are not parallel, the stiffeners cannot be perpendicular to both, and occasionally the stiffeners of parallel chord beams are oblique. Special formulas for parallel chord beams with oblique stiffeners can be found in Air Corps Technical Report 4313, Revised. With tapered beams the stiffeners will usually be either approximately parallel to the external loads or perpendicular to the centroidal axis of the beam. Though direct evidence on the point is lacking, the errors resulting from the use of the formulas of this chapter in the analysis of such beams are generally considered negligible.

**15 : 10. Deflection of Tension Field Beams**—The methods of Chapter IV, in which the effects of shearing deformation are neglected, are usually sufficiently accurate for computing the deflections of beams whose webs do not buckle. When, however, a tension field is developed, the web panels are subjected to shearing deformations too large to be neglected. A practical method of taking them into account may be illustrated by an example.

Suppose the beam shown in Fig. 15 : 2 to be a cantilever, 45 in. long, and subjected to a concentrated downward load of 3,000 lb. at the free end. It is desired to compute the deflection of that end from a line tangent to the elastic curve at the supported end. Instead of computing the deflection directly, the computations will be those pertaining to an imaginary pin-jointed truss which constitutes one of the statically determinate structures included in the redundant beam actually of interest. A line diagram of this included truss is shown in Fig. 15 : 4. Its chords are located along the centroidal axes of the chords of the actual beam, its vertical web members coincide with every third vertical stiffener, and its diagonal web members join the intersections of these verticals with the chords. The method of locating the verticals is as follows. From Art. 15 : 5 the slope angle of the tension field is 34 degrees. Thus a

fiber parallel to the tension field and running vertically between chord centroids would have a vertical component 6.226 in. in length and a horizontal component of  $6.226/\tan \alpha = 6.226/0.675 = 9.24$  in. The horizontal distance is not an integer times the stiffener spacing of 3.00 in., but it does not differ greatly from three times that figure. Therefore the imaginary truss is provided with verticals coinciding with every third stiffener. The slope angle of the truss diagonals is thus  $\tan^{-1} (6.226/9) = 34^\circ 40'$ .

The imaginary truss thus constituted has members coinciding with fibers of the actual beam, and if the truss members are subjected to the same changes in length as the corresponding beam fibers, the deflections



Unit Stresses and Unit-load System Forces in Imaginary Truss

FIG. 15:4

of the truss joints must be the same as those of the corresponding points on the beam. The changes in length of the beam fibers corresponding to the chords and verticals of the truss can be as accurately determined as the lengths of, and unit stresses acting on, those fibers. If the truss diagonals were exactly parallel to the diagonal tension field developed in the beam web, the extensions of the corresponding beam fibers could be determined from the unit stresses developed in the tension field. As it is, some error is introduced by the fact that in order to have the horizontal component of each diagonal of the imaginary truss equal to an integral number of stiffener spacings, these diagonals are not exactly parallel to the tension field. Since, however, it is not yet possible to predict with accuracy the slope angle  $\alpha$  of the tension field, it is believed that the errors due to assuming them parallel are of minor importance, and probably smaller than those inherent in any of the alternative methods of computing the deflections of tension field beams.

If the selection of three times the stiffener spacing had not resulted in dividing the truss into a number of equal-length panels, it would have been necessary to have made at least one panel either a little shorter or a little longer than the others. That would have introduced some additional error, but if the pattern of the imaginary truss is intelligently selected, that error should not be excessive.

The change in length of each chord member of the truss will equal the average axial load in the corresponding portion of the beam multiplied by its length and divided by Young's modulus. In the beam under consideration, the bending moment varies uniformly from the free to the supported end, and the average stress in each panel of the chord will be equal to the stress at the middle of the panel. Therefore, if  $A_c$  is the sectional area of a chord,  $f_c$ , the unit stress in the chord, can be obtained from Eq. 15 : 23 as equal to  $\pm M/(hA_c) - 0.5 V_t \cot \alpha/A_c$ . Table 15 : 3 shows computations of the average stresses in the chords obtained by applying this formula. In these computations  $h = 6.226$ ,  $A_c = 1.215$  and  $0.5 V_t \cot \alpha = 1,190$ . The resulting unit stresses are indicated on the line diagram of Fig. 15 : 4.

TABLE 15 : 3  
COMPUTATION OF STRESSES IN CHORDS

Station	$M$	$\frac{M}{hA_c}$	$\frac{V_t \cot \alpha}{2A_c}$	$f_{tc}$	$f_{cc}$
4.5	13,500	1,780	980	800	-2,760
13.5	40,500	5,350	980	4,370	-6,330
22.5	67,500	8,920	980	7,940	-9,900
31.5	94,500	12,490	980	11,510	-13,470
40.5	121,500	16,060	980	15,080	-17,040

From the data of Art. 15 : 5,  $f_{s_{cr.}} = f_{wts} = 7,000$  p.s.i. and from Art. 15 : 8 when the total shear is 3,000 lb.,  $V_t = 1,605$  lb. Substituting this result in Eq. 15 : 8 gives  $f_{wtt} = 1,605/(6.226 \times 0.032 \times 0.560 \times 0.829) = 17,350$  p.s.i. The total web tension is therefore equal to  $7,000 + 17,350 = 24,350$  p.s.i. As stated above, this value divided by  $E$  is not exactly equal to the unit strain of a fiber in the position of the truss diagonals, but the difference in unit strain between fibers with slope angles of  $34^\circ$  and  $34^\circ 40'$  would not be great. In Fig. 15 : 4, therefore, the stress in each of the five diagonals is listed as  $+24,350$  p.s.i.

From Eq. 15 : 19 the axial load per stiffener is  $1,605 \times 3 \times 0.675/6.226 = 522$  lb. This is carried by a pair of angles having a sectional area of 0.080 sq. in. acting with a strip of the web plate of undetermined width. Since the computed deflection is not very sensitive to errors in estimating the width of web plate that acts as a part of the stiffener, it is allowable to use a rough approximation for that quantity, such as assuming it to equal 60 times the plate thickness. On that basis the total sectional area subjected to the 522-lb. load is  $0.080 + 60 \times 0.032^2 = 0.141$  sq. in., and the unit stress  $522/0.141 = 3,700$  p.s.i. That

figure is therefore used in Table 15 : 4 as the unit stress in each vertical.

The simplest method of computing the deflections of a truss like that of Fig. 15 : 4 is the method of virtual work. Therefore, that truss has been analyzed for a load of 1 lb. acting upward at the free end, and the resulting axial loads in the members are listed in parentheses on the line diagram in Fig. 15 : 4.

The remaining computations of  $E$  times the deflection of point  $A$  are presented in Table 15 : 4. In these computations, each chord member

TABLE 15 : 4  
COMPUTATION OF DEFLECTION

Member	$p$	$f$	$L$	$p/L$
$BC$	-1.448	+4,370	9	-56,950
$CD$	-2.896	+7,940	9	-206,950
$DE$	-4.344	+11,510	9	-449,990
$EF$	-5.792	+15,080	9	-786,090
$GH$	+1.448	-2,760	9	-35,970
$HJ$	+2.896	-6,330	9	-164,990
$JK$	+4.344	-9,900	9	-387,050
$KL$	+5.792	-13,470	9	-702,160
$LM$	+7.240	-17,040	9	-1,110,330
4 verticals	+1.000	-3,700	$4 \times 6.226$	-92,140
5 diagonals	-1.760	+24,350	$5 \times 10.92$	-2,339,940
				$E\delta_A = -6,332,560$

is treated separately, but the web members are handled in two groups, in each of which all members have the same length and are subjected to the same load in both the actual and unit load systems. The final result is  $E\delta_A = 6,332,600$ , whence, if  $E = 10,300,000$ ,  $\delta_A = 0.615$  in.

In Table 15 : 4 the values of  $p/L$  for the chords represent the effect of bending deformation, i.e., relative motion of the verticals, while the  $p/L$  values for the web members represent the effect of shearing deformation, i.e., relative parallel motion of the verticals. Considerable labor could have been saved had the effect of bending deformation been computed from the appropriate beam-deflection formula,  $\delta = (WL^3)/(3EI)$  (see Case 1, Table 4 : 1). The moment of inertia of the chord sections about the neutral axis is  $23.782 \text{ in.}^4$ ; so  $E\delta = -3,000 \times 45^3/(3 \times 23.782) = 3,832,000$ . Since the sum of the chord-member terms in Table 15 : 3 is 3,900,480, the difference is seen to be within the precision of ordinary engineering calculations and the resulting error probably less than that due to computing the actual elongations of the web members. In general, with parallel chord beams, the effect of the chord

members can thus be determined from the beam-deflection formulas, leaving only the web to be handled by the method of virtual work on an imaginary truss. The chief defects of this method are that the assumed diagonals may not be parallel to the actual wrinkles and that the diagonal compression in the web may be underestimated. When the latter occurs, the computed deflections will be excessive as a result of overestimated diagonal tensions and stiffener unit stresses.

An alternative procedure is to compute the portion of the deflection due to deformation of the web members by formulas for deflection due to shear deformation such as Eq. 12 : 7. To do so requires that an " effective shear modulus " be used to provide for the development of a tension field. Wagner showed that, where the tension field was *com-*

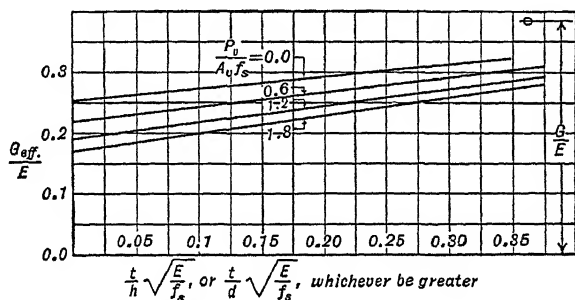


FIG. 15 : 5

plete, an effective value of five eighths the actual shear modulus for the material could be used. When the tension field is *incomplete*, however, the effective  $G$  should vary between  $0.625 G$  and  $G$  as some function of the stress in the stiffener,  $P_v/A_v$ , the web shear stress,  $f_s$ , and the dimensionless factors  $t \sqrt{\frac{E}{f_s}}$ , or  $\frac{t}{d} \sqrt{\frac{E}{f_s}}$ . Figure 15 : 5, based on Lahde and

Wagner's curves in N.A.C.A. Technical Memo. 809, shows such a relation in terms of  $G_e/E$  instead of  $G_e/G$ . Since the ratio of  $G_e/E = 0.385$  for a shear resistant material having  $\mu = 0.3$ , values of  $G_e/G$ , or  $G_e/E$  may readily be obtained from that figure.

While the curves of Fig. 15 : 5 are empirical in nature, Lahde and Wagner present test points to show that they are in good accord with results obtained from actual beams. They do not, however, indicate how the curves should be modified to apply to tapered beams. It is probable that satisfactory results can be obtained on such beams by dealing with them as a series of segments, with  $G_e$  based on the di-



mensions and stresses pertaining to the segment with which it is used.

The equivalent-truss method of computing deflections is an example of the general proposition that the deflection of any redundant structure can be computed from the deformations of any one of the included statically determinate structures. This is an important but often overlooked corollary of the principle of consistent deformations, upon which the analysis of redundant structures is based. In fact, if the deflection of a redundant structure is being computed by the method of virtual work, it follows from the principle of consistent deformation that the internal forces of the unit-load system need satisfy only the principle of equilibrium. Whether or not they also satisfy that of consistent deformation is irrelevant and immaterial. In such computations, however, although the internal forces of the unit-load system may not satisfy the principle of consistent deformation, the actual deformations used, i.e.,  $PL/AE$ ,  $Mdx/EI$ , etc., must be those which do satisfy the principle of consistent deformation. Detailed proof of the statements of this paragraph is beyond the scope of this work, but the student would find it of interest to check their validity by computing the deflection of some simple redundant structure using different distributions of the internal forces of the unit-load system.

**15 : 11. General Remarks** — The method of analysis presented in this chapter may be termed "semi-empirical." If the assumptions of Art. 15 : 3 are accepted, most of the rest of the procedure follows logically but cannot be described as wholly rational since the assumptions are only approximately valid. That they are satisfactory for practical use has been determined from tests, and parts of the procedure are on a purely empirical basis. It is desirable to know the range over which the method can be relied upon to give safe results, particularly the limiting values for  $h/t$  and  $h/d$ , but there is very little information on this point at present.

The chief known defect in the procedure is its neglect of the increase in diagonal compression after buckling begins, but this does not make much difference in the design of the web and chords. Considerable work is being done on its effect in the analysis of web stiffeners and their connections, and some progress has been made in the determination of the division of  $V_g$  between  $V_s$  and  $V_t$ . No completely rational procedure is yet available and, of the empirical methods, most are on a confidential status. The procedure outlined in this chapter can readily be modified to take account of such results when they are published, however, as they involve refinement of, rather than major changes in, the method. Students who master the basic procedure will have little trouble in mastering its refinements.

## PROBLEMS

**15 : 1.** Assume the angle of web buckles,  $\alpha$ , of the beam of Fig. 15 : 2 to be 45 degrees and determine:

- $V_y$  and  $V_z$ , the allowable values for total shear, as determined by the strength of the web plate.
- Load on web-chord connecting rivets.
- Axial stresses in chords when  $V = 3,000$  lb. and  $M = 120,000$  in.-lb.
- Secondary bending stresses in chords at the same loading.
- Deflection of the outer end of the beam under the conditions of Art. 15 : 10.

15 : 2. Assume the web of the beam of Fig. 15 : 2 reduced in thickness to 0.028 in. and determine the same quantities as in Prob. 15 : 1.

**15 : 3.** Assume the depth between cover plates of the beam of Fig. 15 : 2 to be increased from 6.50 to 8.00 in. and determine the same quantities as in Prob. 15 : 1.

15 : 4. What would be the maximum allowable shear on the beam of Prob. 15 : 3 as limited by the vertical stiffeners?

15:5. Assume the beam of Fig. 15:2 reinforced by one  $2.50 \times 0.095$  cover plate on each chord and determine the same quantities as in Prob. 15:1.

**15:6.** Assume the web-stiffener angles of the beam of Fig. 15:2 replaced by  $\frac{5}{8} \times \frac{5}{8} \times 0.040$  angles on one side of the web only and determine the allowable shear on the beam as limited by those stiffeners.

15:7. Assume the changes of problems 15:3, 15:5, and 15:6 to be made simultaneously in the beam of Fig. 15:2 and determine the same quantities as in Prob. 15:1.

**15 : 8.** Work Prob. 15 : 3, assuming  $\alpha = 45$  degrees.

**15 : 9.** Work Prob. 15 : 5, assuming  $\alpha = 45$  degrees.

**15 : 10.** Work Prob. 15 : 6, assuming  $\alpha = 45$  degrees.

**15 : 11.** Work Prob. 15 : 7, assuming  $\alpha = 45$  degrees.

**15 : 12.** Web sheet is 24-ST aluminum alloy. Angles are 24-ST extrusions.

$$I_{xx} \text{ of entire section} = 8.074 \text{ in.}^4$$

$$I_{yy} \text{ of entire section} = 0.034 \text{ in.}^4$$

$$I_{xx} \text{ without web} = 7.354 \text{ in.}^4$$

$$I_{AA} \text{ of 2 angles} = 0.0268 \text{ in.}^4$$

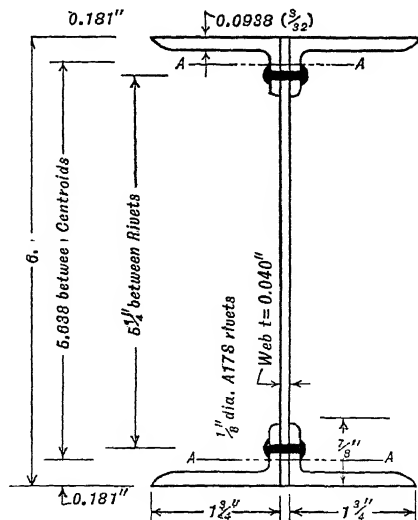
Area of entire section = 1.16 in.<sup>2</sup>

Area of 2 angles = 0.46 in.<sup>2</sup>

Assume web stiffeners of adequate strength spaced 4 in.  $\mathcal{C}$  to  $\mathcal{C}$  along web. Assume chord angle to web connection rivets at  $\frac{5}{8}$ -in. pitch.

- a. What is the maximum shear force the above beam will carry when the web plate is stressed to the ultimate tensile strength of the material?

- b. What would be the margin of safety for the chord angle to web connection rivets at that load?



PROB. 15: 12

## CHAPTER XVI

### SHELL ANALYSIS

Many structural elements of modern airplanes, notably wings and fuselages, are hollow shells of thin metal sheet reinforced by longitudinal stiffeners and transverse rings or ribs. In designing them to carry bending or torsion, several factors must be considered that are not discussed, or are but briefly treated, in the preceding chapters. Foremost of these topics is the determination of the shear-flow pattern on a closed cross-section, parts of which are not fully effective on account of local buckling or of shear deformation. Although the shells used in airplane structures are usually tapered, the normal design procedure is to analyze them as if they were cylinders of constant section and then to apply whatever corrections appear necessary to allow for the effect of taper. In this chapter attention is directed first to the determination of the shear flow developed to resist pure torsion. The distribution of shear and normal forces induced in simple bending is next considered and some associated problems are then discussed.

**16 : 1. Mid-line Method of Computing Section Properties** — The cross-sectional dimensions of the thin-walled shells used in airplane construction are usually such that precise computation of the geometric properties, such as area and moment of inertia, becomes an excessively tedious job. In practice this work is enormously reduced, with no real sacrifice in accuracy, by assuming the areas of the skin and stiffeners concentrated along their mid-lines. For computation purposes, the mid-line may be divided into infinitesimal elements of length,  $ds$ , or finite elements,  $\Delta s$  long, and the properties of the section obtained from the relations

$$A = \oint t \, ds = \Sigma t \, \Delta s \qquad 16 : 1$$

$$Q_{xx} = \oint ty \, ds = \Sigma ty \, \Delta s \qquad 16 : 2$$

$$I_{xx} = \oint ty^2 \, ds = \Sigma ty^2 \, \Delta s \qquad 16 : 3$$

$$I_p = \oint tr^2 \, ds = \Sigma tr^2 \, \Delta s \qquad 16 : 4$$

and similar formulas in which  $t ds$  or  $t \Delta s$  appears in place of  $dA$  or  $dx dy$ . In using these relations, a single integration or summation with respect to distance  $s$  measured along the mid-line replaces the double operation of surface integration, or integration first with respect to  $x$  and then with respect to  $y$ . This change is indicated by the use of the symbol  $\oint$  or  $\Sigma$  instead of  $\int_A$  or  $\iint$ .

In order to apply this method to the hollow circle of Fig. 16 : 1, it is convenient to use polar co-ordinates with the origin at  $O$ , the center of the circle, and the polar axis coincident with  $OX$ . Then  $ds = r d\theta$ , where  $r = (r_o + r_i)/2$ , the radius of the mid-line. Applying Eq. 16 : 1 and using infinitesimals, the area is found to be

$$A = \int_0^{2\pi} tr d\theta = tr \int_0^{2\pi} d\theta =$$

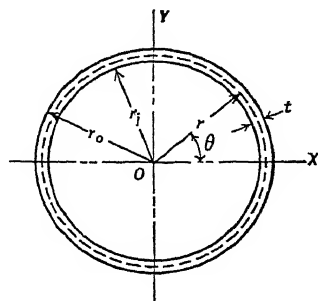


FIG. 16 : 1

From Eq. 16 : 2, since  $y = r \sin \theta$ ,

$$I_{xx} = \int_0^{2\pi} ty^2 ds = t \int_0^{2\pi} r^2 \sin^2 \theta \cdot r d\theta = \pi r^3 t$$

The expression  $Q = r^2 t$ , presented in Art. 6 : 1 for the static moment,  $Q$ , about the polar axis, of the quadrant from  $\theta = 0$  to  $\theta = \pi/2$  is obtainable by the same procedure.

With more complex sections it is necessary to divide the mid-line into segments for convenience in performing the integrations, which may be made analytically on simple sections, by tabular integration on complex.

It may be noticed that the area obtained for the hollow circle is the correct value, but that the expressions for moment of inertia and static moment are somewhat in error. This is inherent in the method since, in effect, squares and higher powers of the thickness,  $t$ , that would appear in the exact formulas are neglected. When, however,  $t$  is small compared to the other dimensions, the resulting errors are negligible, being much smaller, so far as practical members are concerned, than those resulting from probable deviations between nominal and actual dimensions. Furthermore, the computation of small differences between relatively large numbers is avoided, and the properties can easily be computed to three significant figures by slide rule, where precise formulas to obtain the same degree of precision would entail the use of four, five, or even six significant figures and much more labor. This method of com-

puting section properties is sometimes called the "mid-line" or the "center-line" method and sometimes described as "computing the properties of the mid-line and multiplying by the thickness." For practically all the thin metal sections used in aircraft it provides the best means for computing geometric properties, and it is so used by most airplane designers.

**16 : 2. Shear Flow** — With many structural elements, particularly those having thin walls, it is allowable to assume the shear stress to be uniformly distributed across the thickness of material. At some points in a cross-section the shear may have a component normal to the mid-line and the sides parallel to it, but at points along those sides such components are impossible on account of the relation proved in Art. 7 : 9. On thick portions of cross-sections these normal components may be of appreciable magnitude at points relatively remote from the sides, but in thin ones they will be so small in comparison with those tangent to the mid-line that they may be neglected. Therefore, the shear on each element may be assumed to act tangent to, and be concentrated along, the mid-line of the element. When this is done, it is usually desirable to express the intensity of shear in terms of *shear flow* in pounds per inch rather than *shear stress* in pounds per square inch. Examples of this practice are provided in the analyses of beam webs in Chapter VI and in Eq. 7 : 5 for thin-walled tubes subjected to torsion.

In general the intensity and direction of the shear flow will vary along the mid-line of a section. If the latter is divided into elements of infinitesimal length,  $ds$ , the total shear force on each will be  $q ds$ , where  $q$  is the intensity of shear flow. The resultant of the shear forces acting on a mid-line of finite length,  $L$ , is therefore

$$V = \int_0^L q ds \quad 16 : 5$$

in which  $q$  is, in general, a variable function of  $s$ . In the practical use of Eq. 16 : 5, the integration may be performed analytically, graphically, or semi-graphically, as may be most convenient.

If it is desired to determine the  $X$  and  $Y$  components of the resultant force represented by a variable shear flow along a curved line of length  $L$ , that can be done from the relations

$$V_{xx} = \int_0^L q \cos \theta ds \quad \text{and} \quad V_{yy} = \int_0^L q \sin \theta ds$$

where  $V_{xx}$  and  $V_{yy}$  are the  $X$  and  $Y$  components of the resultant force and  $\theta$  is the variable angle between the elements of length,  $ds$ , and the  $X$ - $X$  axis. If the line should be straight,  $\theta$  would be a constant and the evaluation of the integrals correspondingly simplified.

If the shear flow,  $q$ , is constant, the resultant shear force acting on any curved line will be equal to  $q$  times the straight-line distance between the ends of the curve. This resultant may be resolved into components equal to  $q$  times the components of that distance parallel to any desired axes. If the curve forms a closed circuit and the shear flow is constant, its resultant will be a couple, the magnitude of which can be determined from Eq. 16 : 8, derived in the following article.

The basic relation between shear-flow and normal-stress distribution can be developed by consideration of the equilibrium of a segment of a thin metal beam of constant section. In Fig. 16 : 2,  $AB$  and  $CD$  represent portions of the mid-lines

of two cross-sections separated by the finite distance,  $\Delta z$ , measured parallel to the beam axis.  $AD$  and  $BC$  represent portions of the mid-lines of longitudinal sections separated by the finite distance,  $\Delta s$ , measured along the mid-lines of the cross-sections. The segment  $ABCD$  may be thought of as a part of the "middle surface" of either the *web* or a *chord* of the beam. The sides  $AD$  and  $BC$ , being located

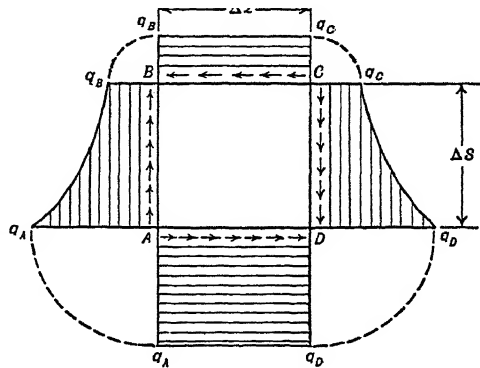


FIG. 16: 2

along longitudinal sections of a constant section beam, will be co-planar and parallel. The sides  $AB$  and  $CD$ , however, may be curved, those lines in the figure being their projections on the plane of  $AD$  and  $BC$ . In that event they would have a common projection on any plane perpendicular to the beam axis.

Assume the shear flow on  $AB$  to be represented graphically by horizontal distances from  $AB$  to the line  $q_A q_B$ , the latter line having any desired shape. From the principle of the equality of shear flows acting on mutually perpendicular lines at their intersection, the shear flows on  $AD$  and  $BC$  at  $A$  and  $B$  must be equal to the shear flow on  $AB$  at those points. If the shear flows on  $AD$  and  $BC$  are constant, as they would be if there were no change in the total shear on the beam between the cross-sections of which  $AB$  and  $CD$  are portions, the shear flows on those lines and on  $CD$  would be as shown in the figure, the line  $q_C q_D$  being symmetrical with  $q_A q_B$ . The total shear force acting on each side would be proportional to the area of the shear flow diagram drawn adjacent to it. The shear forces on  $AB$  and  $CD$  would thus be necessarily equal and opposite; but, if  $q_A$  and  $q_B$  were not equal, the shear

forces on  $AD$  and  $BC$  would be of unequal magnitude. Therefore, if equilibrium is to be maintained, normal forces must act on either  $AB$  or  $CD$  or both, and the difference between the normal forces acting on these sides of the segment must be equal to the unbalanced shear forces on  $AD$  and  $BC$ . These normal forces on  $AB$  and  $CD$  are the axial loads on the longitudinal fibers located between  $AD$  and  $BC$ . Thus it can be seen that, if the shear flow changes between any two points on the mid-line of a cross-section, the axial loads in the fibers between those points will also change as one proceeds along the direction of the beam axis. If the shear flow varied from  $B$  to  $C$  as well as from  $A$  to  $B$ , a similar study would show that there must be axial loads in the fibers between and parallel to  $AB$  and  $CD$  and that these loads would necessarily vary in intensity from  $AD$  to  $BC$ . In the situation represented in Fig. 16 : 2, the unbalanced shear force is  $(q_A - q_B)\Delta z$ , and, if the thickness of the segment is  $t$ , the average change in intensity of normal stress in the distance  $\Delta z$  would be

$$\Delta \sigma = \frac{(q_A - q_B) \Delta z}{t \Delta s} \quad 16 : 6$$

The method used to obtain Eq. 16 : 6 is the converse of that used in Art. 6 : 1 to develop the relation

$$\Delta q = \frac{VQ}{I} \quad 16 : 7$$

for the variation in shear flow associated with the type of normal stress distribution expressed by Eq. 6 : 2. The student should be certain that he understands both procedures, since the relations developed by them are fundamental to an appreciation of stress distribution in thin metal structures.

**16 : 3. Shear Flow in Tube Subjected to Torsion** — When the mid-line of a cross-section subjected to torsion is a circle, the formulas of Art. 7 : 3 are applicable. However, when the mid-line is not circular, it is best to determine the shear flow by the Bredt formula, which is applicable to any closed shape of thin-walled cross-section.

Let  $ABEFCD$  in Fig. 16 : 3 represent the mid-line of the cross-section of a constant section tube subjected to equal and opposite torsional moments,  $T$ , applied at its ends. Assume that those ends are subjected to no external forces parallel to the longitudinal fibers. To maintain equilibrium, every cross-section must be subjected to a system of internal forces, the resultant of which is a couple of magnitude  $T$ , and the stress pattern of which is the same for all cross-sections. This stress pattern consists of a shear flow at all points along the perimeter of the

mid-line. From the preceding article it can be seen that, if this shear flow were to vary from point to point along the perimeter, the longitudinal fibers would have to be subjected to linearly varying axial stresses, and external forces normal to the end cross-sections would be needed for equilibrium. By hypothesis, however, there are no such external forces. Therefore, the only forces acting on a cross-section are those represented by a *constant* shear flow,  $q$ , which, for thin tubes, may be assumed to act along the mid-line.

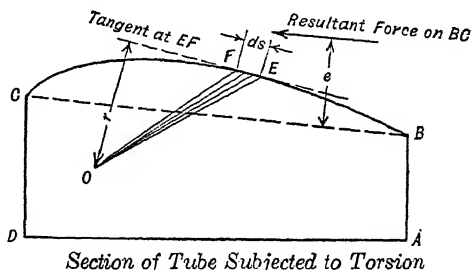


FIG. 16:3

The shear in pounds acting on a single element of the mid-line, such as  $EF$ , of length  $ds$  is equal to  $q ds$ . The moment of this force about any point,  $O$ , is  $rq ds$ , where  $r$  is the perpendicular distance from  $O$  to the tangent to the mid-line at  $EF$ . This moment is obviously equal to  $q$  times twice the area of the figure bounded by  $EF$  and radii drawn from  $O$  to  $E$  and  $F$ . This figure may be described as the area swept over by a radius vector from  $O$  as its outer end moves along the mid-line from  $E$  to  $F$ . If each element of the mid-line is treated in the same manner, the moments about  $O$  of all the shear forces acting on the mid-line are accounted for, and the total area swept over by the radius vector is the area enclosed by the mid-line of the cross-section. The total moment about  $O$  is therefore equal to  $q$  times twice that enclosed area. Thus, if the latter be represented by  $A$ ,

$$q = \frac{T}{2A} \quad 16:8$$

The unit shear stress is the quotient of this value of  $q$  divided by the thickness of section,  $t$ .

Three of the sides of the tube section of Fig. 16:3 are straight. The resultant shear force acting on each of those sides is therefore equal to  $q$  times its length, and that resultant acts along the side in question. The fourth side,  $BC$ , is curved, and, while the resultant of the shear forces acting on that side would be parallel to and equal to  $q$  times the length of the straight line  $BC$ , it would not act along that line. From reasoning similar to that used to develop Eq. 16:8, it can be shown that the moment of the shears acting on the elements of the curve between  $B$  and  $C$  about any point on the straight line joining those points will be  $2q$  times the area between the curve and the straight line. Therefore,



if that area be designated  $A'$ , the distance  $e$  from the straight line to the line of action of the resultant would be

$$e = 2 \frac{A'}{L} \quad 16 : 9$$

where  $L$  is the length of the straight line joining the ends of the curve. If  $q$  is not constant, Eq. 16 : 9 is not applicable, but the position of the resultant force can be obtained by the method used in Art. 6 : 5 to find the location of the shear center of a channel.

In addition to the shear flow developed to resist torsion on a closed tube, it is often necessary to determine the angle of twist in a given length measured along the longitudinal axis. If, as is usually true, any changes in the shape of the cross-section due to the torsion may be neglected, this can readily be done. By combining the reasoning of Arts. 12 : 13 and 12 : 17 it can be shown that the derivative of the strain energy of an elastic structure, with respect to an applied external couple, will be equal to the rotation in radians of the line of application of that couple. Consider a tube of arbitrary cross-section to be divided by transverse and longitudinal planes into elements of length,  $dz$ , measured parallel to its axis, width,  $ds$ , measured along the mid-lines of the cross-sections, and thickness,  $t$ , measured normal to those mid-lines. If the only external forces are equal and opposite torsional couples at the ends of the tube, the strain energy of each element is

$$dU = \frac{t f_s^2}{2 G} ds dz \quad 16 : 10$$

where  $f_s$  is the unit stress in shear due to torsion and  $G$  is the shearing modulus of elasticity. This formula for the strain energy of an element subjected to shear stress may be found in any good text on mechanics of materials.<sup>1</sup>

Since  $f_s = q/t$ , and  $q = T/2 A$ , the total strain energy of the tube is

$$U = \int_{z=0}^{z=L} \oint \frac{T^2 t}{8 A^2 t^2 G} ds dz$$

and

$$\theta = \frac{dU}{dT} = \int_{z=0}^{z=L} \frac{T}{4 A^2 G} \oint \frac{ds}{t} dz \quad 16 : 11$$

For a tube of constant section the line integral,  $\oint \frac{ds}{t}$ , around the perime-

<sup>1</sup> "Applied Mechanics," Fuller and Johnston, Vol. II, Art. 112, p. 243. "Strength of Materials," Timoshenko, p. 302.

ter of the area,  $A$ , is the same for all cross-sections. Therefore, since  $dU/dT$  is the rotation of one end of the tube with respect to the other, the angle of twist per inch length under constant,  $T$ , is

$$4 A^2 G J \quad t \quad - \quad 2 A G J \quad t \quad 16 : 12$$

If  $t$  is constant, the line integral is equal to  $C/t$ , where  $C$  is the length of the perimeter of the area,  $A$ , enclosed by the mid-line of the section. When this substitution is made, Eq. 16 : 12 reduces to Eq. 7 : 6. If the tube is a circular one,  $C = 2 \pi R$ ,  $A = \pi R^2$ , and  $2 \pi R^3 t = I_p$ . Equation 16 : 12 then becomes  $\theta = (TL)/(GI_p)$ , which agrees with the formula in Fig. 7 : 4.

**16 : 4. Torsion on Subdivided Shell** — Many shells used in airplane construction are not simple tubes but are subdivided, by internal diaphragms, into two or more “cells” with some common boundaries. A cross-section of a shell with three cells,  $A$ ,  $B$ , and  $C$ , is shown in Fig. 16 : 4. When such compound sections are subjected to torsion, the perimeter of each cell is subjected to a shear flow of constant intensity, which maintains equilibrium with a torsional couple equal to twice the area enclosed by the mid-line of the cell wall multiplied by the value of  $q$  for the cell. Thus when the entire tube is subjected to the clockwise

torsional couple  $T$ , the perimeter of cell  $A$  develops the resisting shear flow  $q_A$ , the resultant of which is the counter-clockwise couple  $2 q_A A_A$ . Similarly, cells  $B$  and  $C$  develop shear flows,  $q_B$  and  $q_C$ , and resisting couples,  $2 q_B A_B$  and  $2 q_C A_C$ . Those parts of the section

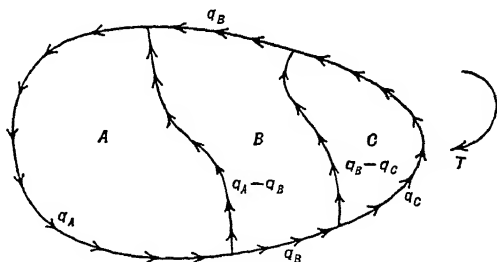


FIG. 16 : 4

mid-line that form the common boundaries of adjacent cells actually develop only the differences between the shear flows associated with those cells, while the remainder develop the shear flows associated with the single cells of which they form parts. This is indicated in Fig. 16 : 4.

To satisfy the conditions of equilibrium, the sum of the torsional couples developed by the shear flows of the individual cells must be equal to the total external torsional couple. This is represented by the general relation

$$= 2 q_A A_A + 2 q_B A_B + 2 q_C A_C + \quad 16 : 13$$

If the shape of the cross-section is assumed unchanged by the torsion, the shear flows around the cells must be in such proportions that all cells have the same angle of twist per unit length. Generalizing Eq. 16 : 12 to allow for superposition of shear flows in webs between cells, it becomes,

$$\frac{\theta}{L} = \frac{1}{2 A_n G} \left( q_n \oint \frac{ds}{t_n} - q_{n-1} \frac{s_{-n}}{t_{-n}} - q_{n+1} \frac{s_{+n}}{t_{+n}} \right) \quad 16 : 14$$

where  $A_n$  is the area of the  $n$ th cell;  $q_{n-1}$ ,  $q_n$ , and  $q_{n+1}$  are the shear flows around the  $n$ th and adjacent cells; and  $s_{-n}/t_{-n}$  and  $s_{+n}/t_{+n}$  are the ratios of mid-line length to thickness for the webs between the  $n$ th and adjacent cells. If there are  $m$  cells, the  $m - 1$  deformation equations required to supplement Eq. 16 : 13 can be formed by equating the expressions for  $\theta/L$  given by Eq. 16 : 14.

The derivation of Eqs. 16 : 12 and 16 : 14 assumes the entire cross-section fully effective in resisting shear. With many shells subjected to torsion, the skin buckles to form diagonal tension fields similar to those discussed in Chapter XV. When curved panels act in this manner, the buckles tend to flatten out the curvature, and their effective stiffness against shear is less than that of flat panels. The effective shearing modulus may therefore be less than the five-eighths  $G$  mentioned in Art. 15 : 10 as appropriate to complete tension fields, or less than the values given by Fig. 15 : 5 for flat plates. In practice it is usually simpler to assume effective thicknesses for either flat or curved plates instead of effective shearing moduli. In either procedure the ratio used must be left to the designer's judgment, no rational method having yet been developed for its accurate determination.

**16 : 5. Analysis of Shell-type Wing Section under Torsion** — The method of using Eq. 16 : 13 and 16 : 14 may be illustrated by computations to determine the shear flows developed in the shell section shown in Fig. 16 : 5 by a torsional couple of 100,000 in.-lb. This shell is the forward portion of an N.A.C.A. 23012 airfoil of 100-in. chord used as a stressed skin wing. As can be seen from the figure, it is divided into two cells by the shear web, 20 in. from the leading edge. Both vertical webs are of 0.064 material. The skin is 0.040 from the leading edge to the stiffeners, 28 in. to the rear, and 0.032 material for the remainder of the distance to the rear web. The material in the webs and in the skin from stiffener  $B$  around the lower side of the section to the rear web at  $K$  is assumed fully effective. On the upper surface between  $B$  and  $J$ , a width of skin extending 15 times its thickness from each rivet line connecting it to the stiffeners is assumed fully effective. Between these strips the skin is assumed to form diagonal tension fields and to have an effective thickness for resisting torsion, assumed, in lack of a better

figure, as five-eighths the actual thickness. The object of making these assumptions regarding the extent of effective skin is to make the torsion computation suitable for conditions like those which would exist if the section were simultaneously subjected to bending which caused portions of the skin to buckle.

The areas enclosed by the mid-lines of the cell walls can be obtained by planimetry a large-scale drawing of the cross-section or by applying Simpson's rule to the section ordinates. Use of the latter method gives  $A_F = 168.6$  sq. in. for the front and  $A_R = 445.9$  sq. in. for the rear cell.

The next quantities to be found are the line integrals of  $ds/t$  for the two cells. Since the perimeter of each cell can be divided into finite segments for each of which  $t$  is a constant, each line integral can be computed as the sum of a group of values of  $\Delta s/t$ ,  $\Delta s$  being taken as the

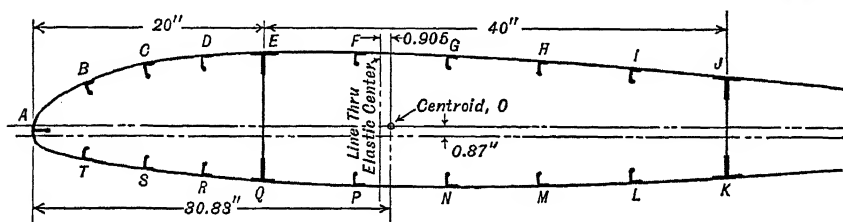


FIG. 16:5

## TABLES FOR FIG. 16:5

## SPECIFIED DATA

Airfoil Section — N.A.C.A. 23012

Nominal chord — 100 in.

Sheet thickness

Front web,  $EQ$  0.064 in.Rear web,  $JK$  0.064 in.Skin forward of  $F$  and  $P$  0.040 in.Skin to rear of  $F$  and  $P$  0.032 in.

## LONGITUDINAL STIFFENERS

Location	Number	Shape	Size	Area (sq. in.)
$E, J$	2	Angle	$2 \times 1\frac{1}{8} \times \frac{1}{8}$	0.4220
$K, Q$	2	Angle	$1\frac{3}{4} \times 1 \times 0.080$	0.2140
$A$	1	Bulb tee	$1\frac{1}{2} \times 1\frac{1}{2} \times \frac{1}{8}$	0.3773
Others	1	Bulb angle	$1\frac{1}{8} \times \frac{3}{4} \times 0.075$	0.1513

## COMPUTED PROPERTIES OF ASSUMED EFFECTIVE SECTION

Location of centroid, 30.83 in. to rear of leading edge

0.87 in. above nominal chord line

Moments of inertia about centroidal axes.

$$I_{xx} = 183.527 \text{ in.}^5 \quad I_{yy} = 3,878.42 \text{ in.}^4 \quad I_{xy} = -23.509 \text{ in.}^4$$

Distance parallel to  $X-X$  axis from centroid to elastic center,  $-0.905$  in.

distance between adjacent longitudinal stiffeners measured along the mid-line of the skin. Precise computations of these distances would be unjustifiably tedious. It is sufficiently accurate for practical purposes to use the lengths of the chords corresponding to the arcs they are assumed to represent. Values of  $\Delta s$  obtained in this manner are listed

TABLE 16 : 1  
COMPUTATIONS OF  $\Sigma \frac{\Delta s}{t}$

1 Segment	2 $\Delta s$	3 $t$	4 $\frac{\Delta s}{t_e}$
<i>ED*</i>	5.01	0.040	182.40
<i>DC*</i>	5.06	0.040	184.40
<i>CB*</i>	5.22	0.040	190.80
<i>BA</i>	6.65	0.040	166.25
<i>AT</i>	5.70	0.040	142.50
<i>TS</i>	5.04	0.040	126.00
<i>SR</i>	5.03	0.040	125.75
<i>RQ</i>	5.02	0.040	125.50
<i>QE</i>	11.43	0.064	178.59
$\Sigma_F$			1,422.19
<i>QP</i>	8.01	0.040	200.25
<i>PN</i>	8.00	0.032	250.00
<i>NM</i>	8.00	0.032	250.00
<i>ML</i>	8.00	0.032	250.31
<i>LK</i>	8.01	0.032	250.31
<i>KJ</i>	9.10	0.064	142.19
<i>JI*</i>	8.04	0.032	384.00
<i>IH*</i>	8.03	0.032	383.50
<i>HG*</i>	8.01	0.032	382.50
<i>GF*</i>	8.00	0.032	382.00
<i>FE*</i>	8.00	0.040	302.00
$\Sigma_R$			3,355.65

\* Effective  $t_e$  = five-eighths actual  $t$ .

in column 2 of Table 16 : 1. Column 3 of the table gives the actual thickness of material for each segment. In column 4 are listed values of  $\Delta s/t_e$ . For most of the segments the figures of this column may be obtained by dividing the number in column 2 by that in column 3. For the segments indicated by asterisks, this procedure is insufficient since part of the width of the segment is assumed to have an effective thickness of only five-eighths the actual thickness.

These segments can be handled as follows: Each may be divided into

two parts, one of width  $30 t$  and effective thickness  $t$ , the other of width  $\Delta s - 30 t$  and effective thickness  $0.625 t$ . Then for the whole segment

$$\frac{s}{t_e} = \frac{30 t}{t} + \frac{\Delta s - 30 t}{0.625 t} = 30 + \frac{8 \Delta s}{5 t} - 48 = \frac{\Delta s}{0.625 t} - 18$$

In adding the quantities of column 4 of Table 16 : 1 to obtain for the two cells, the value for segment  $QE$ , the front shear web, is included in both summations. It may be noticed that this is facilitated by the arrangement of lines in the table, the segments following each other in the order in which they would be encountered when proceeding counter-clockwise around each cell. The resulting values for the line integrals are 1,422.19 for the front and 3,355.65 for the rear cell.

Since the shell under analysis is composed of only two cells and  $G$  is the same for both, the deformation equation obtained from Eq. 16 : 14 would be

$$\frac{1}{2 A_F} \left( q_F \oint \frac{ds}{t_F} - q_R \frac{s_{QE}}{t_{QE}} \right) = \frac{1}{2 A_R} \left( q_R \oint \frac{ds}{t_R} - q_F \frac{s_{QE}}{t_{QE}} \right)$$

or

$$\frac{1}{2 \times 168.6} (1,422 q_F - 178.6 q_R) = \frac{1}{2 \times 445.9} (3,356 q_R - 178.6 q_F) \quad a$$

whence

$$q_R = 1.029 q_F \quad b$$

From Eq. 16 : 8, if  $q_F = q_R = 1.00$  lb. per in.,  $T_F$  would be  $2 \times 168.6 = 337.2$  in.-lb., and  $T_R$  would be  $2 \times 445.9 = 891.8$  in.-lb. If, however,  $q_R = 1.029$  lb. per in.,  $T_R$  would be  $891.8 \times 1.029 = 917.7$  in.-lb. Therefore, if the total torque is 100,000 in.-lb.,  $q_F$  would be  $100,000 / (337.2 + 917.7) = 79.7$  lb. per in. and  $q_R = 79.7 \times 1.029 = 82.0$  lb. per in. The corresponding torques would be  $T_F = 79.7 \times 337.2 = 26,870$  in.-lb. and  $T_R = 73,130$  in.-lb.

**16 : 6. Shear Due to Transverse Load. Introduction to the Problem** — When a shell like that of Fig. 16 : 5 is subjected to a transverse load which causes bending, the designer must determine the distribution of both normal and shear forces over the cross-section. In this process he must take into account several factors in addition to those considered in the analysis of more conventional types of beam. Among these are lack of symmetry, local buckling of thin elements, and shear deformation.

Much work has been done on each of these, and several methods have been proposed for taking them into account in practical design. Instead of discussing each in turn, and illustrating how they can be handled by separate illustrative problems, it is clearer to show the computations for a single illustrative problem in which all these factors are considered,

commenting on each step as it is taken. The analysis procedure employed below is one that has been developed since 1935 by a number of engineers among whom it would be difficult to apportion credit. Among them are D. Williams and W. J. Goodey, in England; R. S. Hatcher, of the Bureau of Aeronautics; P. Kuhn, of the N.A.C.A.; and F. R. Shanley and F. P. Cozzone, of Lockheed. The writers have added some ideas of their own to the work of these men and others, and believe the resulting procedure to be the most practical system of analysis yet presented for constant section shells of semi-monocoque construction.

The specific problem worked out is the determination of the distribution, over a section of the shell of Fig. 16 : 5, of the shear and normal stresses produced by external forces composed of a resultant shear of 20,000 lb. parallel to  $OY$ , acting 40 in. to the rear of the leading edge of the section, and a resultant bending moment of 1,000,000 in.-lb. about the  $OX$  axis. The shear forces are assumed to act up and the bending moment to cause compression in the upper fibers. A secondary function of this numerical example is to show how extensive computations can be clarified and facilitated by suitable tabulation and the use of "operational" and "reference notes."

**16 : 7. Geometric Properties of the Effective Section** — The most practical method of computing the distribution of normal stresses is to assume planar distribution over the "effective cross-section," allowance for the effects of buckling and shear deformation being handled primarily by assuming only a portion of the actual cross-section to take part in the resistance to external load. The first stage in the analysis must therefore consist in deciding upon the extent of the effective cross-section and the computation of its geometric properties. For the most accurate results in the delimitation of the effective section the engineer should be guided by the distribution and intensities of stress caused by the imposed loads as is done for the circular shell of Art. 6 : 9. A complete analysis is therefore a trial-and-error process in which several cycles of computations are needed. Since space limitations preclude the inclusion here of more than a single cycle (and that abbreviated), the effective area is determined on the basis of assumptions suitable for the earlier computation cycles in a practical analysis.

Since the only bending moment assumed acting is that about the  $X-X$  axis, and the deviation from symmetry about that axis is not excessive, it is assumed that the  $X-X$  axis through the centroid of the material is approximately coincident with the neutral axis. Compressive stresses close to the neutral axis are of low intensity, so that all the skin on the tension side of the  $X-X$  axis and that on the compression side

from the leading edge to the longitudinal stiffener at *B* is assumed effective. Between *B* and *J*, however, the effective skin material is assumed limited to strips of width equal to 15 times its thickness on each side of the rivet lines connecting skin to stiffeners, plus that between the pairs of rivet lines connecting the skin to the pairs of stiffening angles at *E* and *J*. Behind *J* and *K* the skin is assumed effective for a distance equal to 15 times the thickness from the rear rivet line. The rivet lines at *E*, *J*, and *K* are assumed to be located  $\frac{3}{8}$  in. inside the free edges of both angle members. The skin material between the strips assumed effective is assumed to buckle and carry no axial stress, though able to carry shear by developing diagonal tension fields. The shear webs *EQ* and *JK*, being of 0.064-in. material, are assumed fully effective.

The extent of effective material having been decided on, the next step is to compute the effective area and the location of its centroid. The computations of areas and moments for the stiffener sections are shown in Table 16 : 2. The reference axes chosen for moments are the nominal chord line for the *X-X* axis and a perpendicular at the leading edge for the *Y-Y* axis.

It should be noted that each column of the table has a number in the first line. In the next line are column headings of the usual type. The third line is reserved for the operational and reference notes. That in column 2 indicates the gross areas listed there are obtainable from Fig. 16 : 5 which includes a table of stiffener areas. The note for column 3 refers to the footnote at the bottom of the table, that note being too long for insertion in one space of the table. Both of these notes are "reference notes." That for column 4 is an "operational note" and indicates that each figure in the column is the product of the quantities listed on the same line in columns 2 and 3. The fact that it is the quantities in the columns 2 and 3 and not the natural numbers 2 and 3 that are to be multiplied is indicated by printing the numbers in bold-face type. In manuscript computations, where it is impracticable to use bold-face type, such information is often given by enclosing the column numbers in circles. The notes for columns 5 and 6 are of the reference type and indicate that the distances tabulated in those columns were obtained from Fig. 16 : 5. That figure as printed is very much reduced, and the listed dimensions were actually taken from the original drawing which was drawn half size. In practical work where dimensions are taken from drawings, the reference notes could give the serial numbers of the drawings used. The operation notes in columns 7 and 8 indicate how the tabulated moments of those columns were obtained and are of the same type as that for column 4.

On the last line of the table are shown the "totals" for the various



columns. In columns 3, 7, and 8 the figures shown are true totals. Those in columns 5 and 6, however, are not true totals but were obtained by dividing the total moments of columns 7 and 8 by the total effective area of column 4 to determine the co-ordinates of the centroid of the effective stiffener areas considered as a unit.

TABLE 16 : 2

EFFECTIVE AREAS AND MOMENTS OF STIFFENER SECTIONS ABOUT LEADING  
EDGE AND CHORD LINE

1	2	3	4	5	6	7	8
Stiffener	Gross Area	Shear Lag Factor	Effective Area	$\bar{x}$	$\bar{y}$	$M_{yy}$	$M_{zz}$
	F 16 : 5	Note A	2 × 3	F 16 : 5	F 16 : 5	4 × 5	4 × 6
A'	0.3773	1.00	0.3773	0.54	+0.50	+0.204	+0.189
B'	0.1513	1.00	0.1513	5.00	+4.38	+0.756	+0.663
C'	0.1513	1.00	0.1513	9.92	+5.90	+1.501	+0.893
D'	0.1513	1.00	0.1513	14.84	+6.66	+2.245	+1.008
E'	0.8440	1.00	0.8440	20.00	+6.84	+16.888	+5.773
F'	0.1513	0.98	0.1483	27.82	+7.09	+4.126	+1.051
G'	0.1513	0.94	0.1422	35.84	+6.87	+5.096	+0.977
H'	0.1513	0.90	0.1362	43.80	+6.41	+5.966	+0.873
I'	0.1513	0.96	0.1453	51.76	+5.75	+7.521	+0.835
J'	0.8440	1.00	0.8440	60.00	+4.80	+50.640	+4.051
K'	0.4280	1.00	0.4280	60.00	-3.05	+25.680	-1.305
L'	0.1513	1.00	0.1513	51.79	-3.60	+7.836	-0.545
M'	0.1513	1.00	0.1513	43.80	-3.89	+6.627	-0.589
N'	0.1513	1.00	0.1513	35.81	-4.02	+5.418	-0.608
P'	0.1513	1.00	0.1513	27.81	-3.90	+4.208	-0.590
Q'	0.4280	1.00	0.4280	20.00	-3.34	+8.560	-1.430
R'	0.1513	1.00	0.1513	14.83	-3.00	+2.244	-0.454
S'	0.1513	1.00	0.1513	9.90	-2.42	+1.498	-0.366
T'	0.1513	1.00	0.1513	4.90	-1.75	+0.741	-0.265
Totals			5.0063	+31.511	+2.030	+157.755	+10.161

Note A. Arbitrary figure, see Art. 16 : 15.

For computation purposes the skin is divided into segments, the areas of which are computed in Table 16 : 3. The methods employed in these calculations are indicated by the reference and operational notes of the third line. It should be noted that the co-ordinates of columns 2 and 3 in this table differ somewhat from those on the corresponding lines of Table 16 : 2. This reflects the fact that the co-ordinates of Table 16 : 2 apply to the centroids of the stiffeners, while those of Table 16 : 3 apply to the mid-line of the skin where it intersects a line

TABLE 16:3  
EFFECTIVE AREAS OF SKIN AND WEBS

1 Station	2 $x$ F 16 : 5	3 $y$ F 16 : 5	4 $\Delta x$ $\Delta 2$	5 $\Delta y$ $\Delta 3$	6 $\frac{\Delta s}{\sqrt{4^2 + 5^2}}$	7 $t$ F 16 : 5	8 $\Delta s_{\text{eff}}$ Note A	9 $A$ $7 \times 8$
A	0	+0.50						
B	5.00	+4.89	5.00	+4.39	6.65	0.040	6.65 <sup>a</sup>	0.2660
C	10.00	+6.41	5.00	+1.52	5.22	0.040	1.20 <sup>b</sup>	0.0480
D	15.00	+7.17	5.00	+0.76	5.06	0.040	1.20 <sup>b</sup>	0.0480
E	20.00	+7.48	5.00	+0.31	5.01	0.040	2.36 <sup>c</sup>	0.0944
F	28.00	+7.54	8.00	+0.06	8.00	0.040	2.36 <sup>c</sup>	0.0944
G	36.00	+7.32	8.00	-0.22	8.00	0.032	0.96 <sup>bd</sup>	0.0307
H	44.00	+6.86	8.00	-0.46	8.01	0.032	0.96 <sup>b</sup>	0.0307
I	52.00	+6.20	8.00	-0.66	8.03	0.032	0.96 <sup>b</sup>	0.0307
J	60.00	+5.45	8.00	-0.75	8.04	0.032	3.75 <sup>c</sup>	0.1200
K	60.00	-3.65	0	-9.10	9.10	0.064	9.10 <sup>a</sup>	0.5824
L	52.00	-4.05	-8.00	-0.40	8.01	0.032	9.15 <sup>f</sup>	0.2928
M	44.00	-4.34	-8.00	-0.29	8.01	0.032	8.01 <sup>a</sup>	0.2563
N	36.00	-4.47	-8.00	-0.13	8.00	0.032	8.00 <sup>a</sup>	0.2560
P	28.00	-4.35	-8.00	+0.12	8.00	0.032	8.00 <sup>ad</sup>	0.2560
Q	20.00	-3.95	-8.00	+0.40	8.01	0.040	8.01 <sup>a</sup>	0.3204
R	15.00	-3.48	-5.00	+0.47	5.02	0.040	5.02 <sup>a</sup>	0.2008
S	10.00	-2.90	-5.00	+0.58	5.03	0.040	5.03 <sup>a</sup>	0.2012
T	5.00	-2.24	-5.00	+0.66	5.04	0.040	5.04 <sup>a</sup>	0.2016
A	0.00	+0.50	-5.00	+2.74	5.70	0.040	5.70 <sup>a</sup>	0.2280
Sum			0	0				
E	20.00	+7.48	0	11.43	11.43	0.064	11.43 <sup>a</sup>	0.7315
Q	20.00	-3.95						
Sum								4.2899

Note A. The letters used as superscripts in the column indicate the following methods of computation:

- $s = 6$ .
- $s = 30 \times 7$ .
- $s = 30 \times 7 + 1.125 + 0.032$  to include distance from rivet line to centerline of web.
- No allowance made for overlap of skin material.
- $s = 45 \times 7 + 2.25 + 0.064$  to include all material between rivet lines at J and a strip 15 t in width behind the rear rivet line.
- $s = 6 + 0.625 + 0.032 + 15 \times 7$  to include all material between rivet lines at K and a strip 15 t in width behind the rear rivet line.

of rivets connecting it to a stiffener. At  $A$ ,  $E$ ,  $J$ ,  $K$ , and  $Q$ , where there are two rivet lines, the "station" is located midway between those lines. Thus there are two points of interest in connection with each stiffener; the centroid of the stiffener, and the location of its connection to the skin. In this example the former are designated by letters with primes,  $A'$ ,  $B'$ , etc., while the latter are designated by the simple letters,  $A$ ,  $B$ , etc.

The quantities in columns 2 and 3 are entered on the same lines as the designating letters for the stations since they pertain to the station locations. The quantities in the remaining columns are on intermediate lines since they pertain to the region between adjacent stations. The practice of thus classifying and separating quantities *at* from quantities *between* stations and recording the two classes on different sets of lines is highly desirable, and failure to follow it is a common cause of obscurity and error.

The symbol  $\Delta$  in the operation notes for columns 4 and 5 indicates that the quantities in the column are differences between the numbers, in the columns referred to, that are listed on the lines just above and just below the quantities in question. The operation note for column 6 indicates that the numbers in the column are obtained as the square root of the sum of the squares of the values in the same lines of columns 4 and 5. For an accurate computation of the area of skin between two stiffeners, one should compute the length of the curved mid-line between them, instead of the straight-line distances that result from the methods used to obtain the values of column 6. In the example, except for the more sharply curved segments near the leading edge, the difference is obviously negligible, and even for those segments it is so small that it appeared most reasonable to neglect it. If one desired, it would be possible to reduce the error by subdividing the more highly curved segments into narrower ones, until the resulting error was reduced to the desired limits.

The various methods used to compute the "effective" values of  $\Delta s$  in column 8 are listed in the Note  $A$  referred to in the operation note. In this note the numbers in bold-face type pertain to the quantities in the columns referred to. The other figures are natural numbers. The methods indicated in the note follow naturally from the assumptions at the beginning of this article. In addition to the computation of effective area of the skin on the external surface of the shell, Table 16 : 3 includes the computation of the area of the internal shear web. It would be awkward to include the line for  $EQ$  in the main body of the table, but it works in nicely as a kind of appendix.

The effective areas of Table 16 : 3 are used in Table 16 : 4 to obtain

the moments of the skin about the axes used in Table 16 : 2 for the stiffeners. The reference note for column 3 is composed of two numbers in bold-face type, separated by a hyphen. The first of these numbers indicates the table and the second the column of that table from which the quantities were copied. The complete reference note would be

TABLE 16 : 4

MOMENTS OF EFFECTIVE SKIN AND WEB AREAS ABOUT LEADING EDGE AND CHORD LINE; CENTROID LOCATION OF ENTIRE EFFECTIVE SECTION

1 Station	2 <i>A</i> Note A	3 <i>x</i> 3-2	4 <i>y</i> 3-3	5 <i>M<sub>yy</sub></i> 2 × 3	6 <i>M<sub>zz</sub></i> 2 × 4
A	0.2470	0	+0.50	+0	+0.123
B	0.1570	5	+4.89	+0.785	+0.768
C	0.0480	10	+6.41	+0.480	+0.308
D	0.0480	15	+7.17	+0.720	+0.344
E	0.1408	20	+7.48	+2.816	+1.053
F	0.0393	28	+7.54	+1.100	+0.296
G	0.0307	36	+7.32	+1.105	+0.225
H	0.0307	44	+6.86	+1.351	+0.211
I	0.0307	52	+6.20	+1.596	+0.190
J	0.1047	60	+5.45	+6.282	+0.571
K	0.1646	60	-3.65	+9.876	-0.601
L	0.2563	52	-4.05	+13.328	-1.038
M	0.2562	44	-4.34	+11.273	-1.112
N	0.2560	36	-4.47	+9.216	-1.144
P	0.2882	28	-4.35	+8.070	-1.254
Q	0.2606	20	-3.95	+5.212	-1.029
R	0.2010	15	-3.48	+3.015	-0.699
S	0.2014	10	-2.90	+2.014	-0.584
T	0.2148	5	-2.24	+1.074	-0.481
Web EQ	0.7315	20	+1.765	+14.630	+1.291
Web JK	0.5824	60	+0.90	+34.944	+0.524
Subtotal	4.2899	+30.005	-0.026	+128.887	-2.038
Stiffs	5.0063	+31.511	+2.030	+157.755	+10.161
Total	9.2962	+30.834	+0.874	+286.642	+8.123

Note A. Each area is half the sum of the areas of the adjacent segments, as listed in 3-9, except that near E, J, and K adjustments are made so that each element of effective skin is assumed to be concentrated at the nearest station.

16 : 3-2, but as all the tables referred to in this example are from Chapter 16, the number 16 is omitted without loss of clarity. The principle is the same as that justifying the omission of the table number when referring to a column of the same table. Sometimes when a computation is divided between several tables it is convenient to number all columns

in a single series. Inclusion of the table numbers in reference notes would then be entirely unnecessary, and if a column were repeated the computer would have the choice of designating the second appearance by a new number and giving the original one as a reference note or of merely using again the original column number.

Near the bottom of Table 16 : 4 are two lines on which are entered the quantities for the shear webs  $EQ$  and  $JK$ . The ordinates of the centroids of these elements are not to be found directly from columns 2 and 3 of Table 16 : 3 but can be easily figured from the ordinates of the ends of these elements. On the third line from the bottom of the table are sub-totals giving the area, moments, and centroid location for the group of effective skin and web areas. On the next line are the corresponding figures for the stiffeners from Table 16 : 2. The last line gives these quantities for the entire effective section. From the computations thus outlined it is found that the effective area is 9.2962 sq. in. and its centroid 30.834 in. to the rear of the leading edge and 0.874 in. above the nominal chord line. Although the effect of manufacturing tolerances is to make the last two or three figures of the computed area unreliable, they are retained to facilitate checking results. One figure, however, is dropped from the distances to the centroid, which is assumed to lie as  $x = +30.83$ ,  $y = +0.87$ , though it is exceedingly doubtful whether those figures would be correct to the nearest hundredth of an inch.

In computing the moments of inertia, and the product of inertia about  $X-X$  and  $Y-Y$  axes through the centroid, the moment of inertia of each element about an axis through its own centroid is neglected, and the desired quantities obtained from the relations  $I_{xx} = \Sigma Ay^2$ ,  $I_{yy} = \Sigma Ax^2$ , and  $I_{xy} = \Sigma Axy$ . An exception is made for the two shear webs,  $EQ$  and  $JK$ , for which the moments of inertia about  $X-X$  axes through their centroids,  $th^3/12$ , amount to 7.964 and 4.019 in.<sup>4</sup>, respectively. The necessary computations of  $Ax^2$ ,  $Ay^2$ , and  $Axy$  are abbreviated in Tables 16 : 5 and 16 : 6. Most of the lines of the original tables are omitted in this illustrative example, but by following the reference and operation notes the reader can fill in the missing figures and check the totals at the bottom of each column.

In both of these tables the operation notes for columns 3 and 4 are made up of one number in bold-face type, indicating a reference to a column in a previous table, and a natural number in normal type. Thus the quantities of column 3 are those of column 5 in Table 2 minus 30.83, the distance from the original  $Y-Y$  axis to the computed centroid. The quantities of columns 7 and 8 might have been obtained by squaring those in columns 3 and 4, respectively, and multiplying by the numbers in column 2. Columns 5 and 6, therefore, might have been omitted.

Also, column 9 might have been based on a single set of computations instead of representing the average of two sets. The operation notes indicate the procedure actually followed. The value of columns 5 and 6 is that if the axes used pass through the centroid, their sums should be zero, and the magnitude of their sums thus gives a good indication of

TABLE 16:5  
COMPUTATION OF MOMENTS OF INERTIA, STIFFENERS

1 Station	2 $A$ 2-4	3 $x$ 2-5 - 30.83	4 $y$ 2-6 - 0.87	5 $Ax$ 2 $\times$ 3	6 $Ay$ 2 $\times$ 4	7 $Ax^2$ 3 $\times$ 5	8 $Ay^2$ 4 $\times$ 6	9 $Axy$ Note A
$A'$	0.3773	-30.29	-0.37	-11.428	-0.140	346.25	0.052	+4.228
$B'$	0.1513	-25.83	+3.51	-3.908	+0.531	100.94	1.864	-13.717
$C'$	0.1513	-20.91	+5.03	-3.164	+0.761	66.16	3.828	-15.914
$D'$	0.1513	-15.99	+5.79	-2.419	+0.876	38.68	5.072	-14.006
..	.....	.....	.....	.....	.....	.....	.....	.....
..	.....	.....	.....	.....	.....	.....	.....	.....
$\Sigma$	5.0663			+3.401	+5.805	2,178.73	105.051	+4.

Note A. Average of 4  $\times$  5 and 3  $\times$  6.

TABLE 16:6  
COMPUTATION OF MOMENTS OF INERTIA, EFFECTIVE SKIN AND WEBS

1 Station	2 $A$ 4-2	3 $x$ 4-3 - 30.83	4 $y$ 4-4 - 0.87	5 $Ax$ 2 $\times$ 3	6 $Ay$ 2 $\times$ 4	7 $Ax^2$ 3 $\times$ 5	8 $Ay^2$ 4 $\times$ 6	9 $Axy$ Note A
$A$	0.2470	-30.83	-0.37	-7.615	-0.091	234.77	0.034	+2.812
$B$	0.1570	-25.83	+4.02	-4.055	+0.631	104.74	2.537	-16.300
...	.....	.....	.....	.....	.....	.....	.....	.....
...	.....	.....	.....	.....	.....	.....	.....	.....
$S$	0.2014	-20.83	-3.77	-4.195	-0.759	87.38	2.861	+15.812
$T$	0.2148	-25.83	-3.21	-5.548	-0.690	143.30	2.215	+17.815
$EQ$	0.7315	-10.83	+0.895	-7.922	+0.655	85.80	0.586	-7.092
$JK$	0.5824	+29.17	+0.03	+16.989	+0.017	495.57	0.001	+0.503
$\Sigma$ sheet	4.2899			-3.370	-5.791	1,699.69	66.493	-28.034
$\Sigma$ stiff	5.0063			+3.401	+5.805	2,178.73	105.051	+4.525
Total	9.2963			+0.031	+0.014	3,878.42	171.544	-23.509

Note A. Average of 4  $\times$  5 and 3  $\times$  6.

the accuracy of the computations of centroid location. While these sums amounted to +0.031 and +0.014 in the illustration, some such error is to be expected since the centroid location was computed only to the nearest 0.01 in. When the sizes of some of the quantities included in these sums are considered it is seen that these errors are negligible.

While it takes some time to make this check, the confidence engendered by it is of sufficient value to justify the expenditure. The time taken is far smaller than that required to correct subsequent computations if there is an error in the centroid location.

After each number in column 5 was multiplied by  $x$  from column 3 to get a figure for column 7, the same number was multiplied by  $y$  from column 4 to obtain an entry for column 9. Since the work was figured on a computing machine, this was quickly done. A check entry was obtained for column 9 in similar fashion after computing that for column 8. Agreement of the two values for column 9 constitutes a good, though not an absolute, check for the entries in columns 7 and 8 as well as for those in column 9 itself. This justifies the expenditure of extra labor involved.

Table 16 : 7 is a summary of the geometric properties of the effective section. Most of the quantities are taken from the preceding tables, but a few are obtained by additions made in the table. No reference

TABLE 16 : 7  
SUMMARY OF GEOMETRIC PROPERTIES OF EFFECTIVE SECTION

	Area	Location of Center of Gravity		$I_{xx}$		$I_{yy}$	$I_{zy}$
	$A$	$x$	$y$	$\Sigma Ay^2$	$\Sigma I_0$	$\Sigma Ax^2$	$\Sigma Axy$
Stiffs	5.0063	+31.511	+2.030	105.051		2,178.73	+4.525
Skin	4.2899	30.419	-0.475	66.493	11.983	1,699.69	-28.034
Total	9.2962	30.834	+0.874	171.544	11.983	3,878.42	-23.509
				$I_{xx} = 183.527$			

and operation notes are included since the quantities listed are the final results of the immediately preceding tables, and the checker would be unlikely to have difficulty in locating them. Caution should be exercised in making the decision to omit any pertinent reference or operation notes, and in case of doubt it is better to include the notes than to omit them. In Table 16 : 7, however, it would be difficult to include the notes in a clear manner, and their omission does not impair clarity.

**16 : 8. Distribution of Normal Stress** — Since planar distribution of normal stress over the effective cross-section has been assumed, Eq. 6 : 18 is applicable. As shown in Table 16 : 8, when  $M_{xx} = 1,000,000$  and  $M_{yy} = 0$ , this becomes  $f = -33.053 x - 5,453.0 y$  when the geometrical properties of Table 16 : 7 are inserted. Table 16 : 8 is not a true table, but is designated as one for convenience in later referencing.

Table 16 : 9 illustrates the tabulation of the computations of the normal stresses. As with Tables 16 : 5 and 16 : 6, only a portion of the actual computations are shown, but sufficient notes are given to permit the original table to be reconstructed. In practice it would often be considered convenient to repeat in this table columns of  $x$  and  $y$  instead of merely referring to the previous tables where they could be found.

Since the internal forces must be in equilibrium with the external ones, the sums of columns 6 and 7 should be zero, while that of column 8 should be +1,000,000. The error in column 6 is -157, indicating that the compression on the cross-section exceeds the tension by that many pounds. Since each of these groups of forces amounts to nearly 100,000

TABLE 16 : 8

## DEVELOPMENT OF FORMULA FOR UNIT NORMAL STRESS

Since  $M_y = 0$ , Eq. 6 : 18 becomes

$$f = \frac{M_{xx}I_{xy}x - M_{xx}I_{yy}y}{I_{xx}I_{yy} - I_{xy}^2}$$

$$I_{xx}I_{yy} - I_{xy}^2 = 183.527 \times 3,878.42 - 23.509^2 = 711,795 - 553 = 711,242$$

$$f = \frac{-23,509,000 x - 3,878,420,000 y}{711,242}$$

$$= -33.053 x - 5,453.024 y$$

lb., this error is inconsiderable and may safely be attributed to the use of a limited number of significant figures. Had the work been done on the slide rule instead of a computing machine, the error would have undoubtedly been larger. The same is true of the error of -535 in  $\Sigma Px$  of column 7. The discrepancy of 64,793 in.-lb. between the value of  $\Sigma Py$  of column 8 and the proper value of 1,000,000 is more serious. It is due, at least in part, to the fact that in the computations of Table 16 : 9, the normal forces are implicitly assumed to be concentrated at the centroids of the segments of effective material on which they act. Except for the two shear webs, the resultant errors in moment about the reference axes used are largely compensatory, and could well be neglected. The errors with respect to the two webs should be corrected, as can be done by the following computation.

Since the webs are vertical, there is no error in the values of  $Px$  for  $EQ$  and  $JK$ . In  $EQ$  the unit stress varies from -35,686 at  $E$  to +26,641 at  $Q$ , the average stress being therefore -4,522 p.s.i. Thus the total loading consists of a uniform compression of -4,522 p.s.i., which produces the moment of -2,961 in.-lb. about the  $X-X$  axis and a couple



TABLE 16:9  
COMPUTATION OF NORMAL FORCES FROM  $f = -33.053\ x - 5.453.0\ y$

1 Location	2 $-33.053\ x$	3 $-5.453.0\ y$	4 $f$ 2 + 3	5 $A$ Note A	6 $P$ 4 × 5	7 $P_x$ Note A	8 $P_y$ Note A	9 $\Delta q$ 0.02 × 6
A	+1,019	+2,018	+3,037	0.2470	+750	-23,123	-278	+15.00
A'	+1,001	+2,018	+3,019	0.3773	+1,139	-34,500	-421	+22.78
B	+854	+21,921	-21,067	0.1570	-3,308	+85,446	-13,298	-66.16
B'	+854	-19,140	-18,296	0.1513	-2,768	+71,497	-9,716	-55.36
C	+688	-30,210	-29,522	0.0480	-1,417	+29,516	-7,850	-28.34
C'	+691	-27,429	-26,738	0.1513	-4,045	+84,581	-20,346	-80.90
E	+358	-36,044	-35,686	0.1408	-5,025	+54,421	-33,215	-100.50
E'	+358	-32,554	-32,196	0.8440	-27,173	+294,284	-162,223	-543.46
EQ	+358	-4,880	-4,522	0.7315	-3,308	+35,826	-2,961	-66.16
...	...	...	...	...	...	...	...	...
J	-964	-24,975	-25,939	0.1047	-2,716	-79,226	-12,439	-54.32
J'	-964	-21,430	-22,394	0.8440	-18,901	-551,342	-74,281	-378.02
JK	-964	-164	-1,128	0.5824	-657	-19,164	-20	-13.14
K	-964	+24,648	+23,684	0.1646	+3,898	+113,705	-17,619	+77.96
K'	-964	+21,376	+20,412	0.4280	+8,736	+254,829	-34,245	+174.72
...	...	...	...	...	...	...	...	...
Q	+358	+26,283	+26,641	0.2606	+6,943	-75,193	-33,465	+138.86
Q'	+358	+22,957	+23,315	0.4280	+9,979	-108,073	-42,012	+202.72 <sup>B</sup>
...	...	...	...	...	...	...	...	...
...	...	...	...	...	...	...	...	...
Σ	+2,463	-111,159	-108,696	...	-157	-535	-935,207	0

Note A.  $x$  from 5-3 or 6-3,  $y$  from 5-4 or 6-4,  $A$  from 5-2 or 6-2.

Note B. Based on  $P = 9,979 + 157 = 10,136$ , correction made so that  $\Sigma \Delta q = 0$ .

composed of a load varying uniformly from  $-31,164$  p.s.i. at  $E$  to  $+31,164$  p.s.i. at  $Q$ . Since the distance  $EQ$  is  $11.43$  in. and the web thickness is  $0.064$  in., this couple is  $-0.064 \times 31,164 \times 11.43^2/6 = -43,428$  in.-lb. By similar computations the additional couple acting on the rear web,  $JK$ ,  $9.10$  in. long, is found to be  $-21,917$  in.-lb. Adding these figures to the value of  $\Sigma P_y$  from Table 16 : 9 makes the total of  $-1,000,552$  in.-lb., and thus reduces the error to only  $552$  in.-lb.

Considering the size of the quantities being worked with, all three errors are very small. Those in  $\Sigma P_x$  and  $\Sigma P_y$  may be neglected, but that in  $\Sigma P$  must be attended to or it will cause difficulty in the later computations. In the example this is done by changing the load acting at  $Q'$ , this point being chosen because the largest single tension acts there. A more refined method would have been to select three segments between which the  $+157$  lb. would have been distributed, making the distribution in such proportions that  $\Sigma P_x$  and  $\Sigma P_y$  would also be corrected. This would involve the solution of three simultaneous equations and might involve reductions in the loads on some of the segments selected. On the whole, it seems better either to revise the original computations until the errors are negligible or arbitrarily to increase the load on a single segment to correct  $\Sigma P$  and disregard the errors in the other two sums.

There is no fixed criterion for adjusting computations such as this, though such adjustments are often necessary in practice. When a trial design is involved, somewhat greater liberty may be taken than with final design computations, but it is well to note where and how any adjustment is made, so that a greater number of significant figures may be used in the final design or such other modifications in procedure be made as may insure the accuracy of the final figures. In large stress groups the engineer on the trial section may not be the man who makes the final analysis, and unexplained adjustments made by either may cause the other a great deal of trouble when the figures are compared to check the results before releasing the analysis to the design group.

**16 : 9. Computation of Trial Shear Flows** — The normal forces of Table 16 : 9 would be developed to resist a bending moment,  $M_{xx} = 1,000,000$  in.-lb., regardless of the location of the plane of loading or of whether that bending moment is accompanied by a torsional moment. With thin-walled shells like that of Fig. 16 : 5, buckling is usually the result of a combination of shear and normal stresses, and neither can be neglected in design. Having determined the normal stresses developed by the imposed bending moment, the next step is to compute the distribution of shear along the mid-line of the cross-section.

The first objective must be the location of a point at which the shear

flow is zero. This is vital, since formulas like Eq. 16 : 7 do not give the intensity of shear flow at a point directly but only the difference between the shear flows at two separate points. With the open or symmetrical sections discussed in Chapter VI one of the points chosen was located where the shear flow could easily be seen to be zero, so that the difference in shear flows would be equal to the actual shear flow at the other point. With the closed unsymmetrical section of Fig. 16 : 5, that procedure is impossible, and several intermediate steps must be taken before the actual shear flow at any specific point can be determined.

The general relation of the change in shear flow between two points on the mid-line of a cross-section to the rate of change in axial stress on the longitudinal fibers intersecting the cross-section between those points is discussed in Art. 16 : 2. Equation 16 : 6 of that article may be rearranged and written

$$q_A - q_B = \frac{t \Delta s \Delta f}{\Delta z} \quad 16 : 15$$

In general,  $f$  and  $\Delta f/\Delta z$  will vary between  $A$  and  $B$ , and Eq. 16 : 15 should be replaced by

$$q_A - q_B = \oint_A^B t \frac{\partial f}{\partial z} ds \quad 16 : 16$$

It should be recognized that the right side of this equation represents the rate of change, with respect to distance parallel to the longitudinal  $Z$ - $Z$  axis, of the total normal force acting on fibers intersecting the cross-section between  $A$  and  $B$ .

In the section of Fig. 16 : 5, therefore, the change in shear flow between any two points on the mid-line equals the difference between the normal force acting on the effective area between those points on the cross-section under study and that acting on the corresponding area of the cross-section 1 in. away. Since  $M_{xx} = 1,000,000$  in.-lb. and  $V_{yy} = 20,000$  lb., the change in normal force on each fiber in a distance of 1 in. from the cross-section under investigation is one-fiftieth of the normal force at that cross-section. These increments of normal force are listed in column 9 of Table 16 : 9. In computing them, the normal force on stiffener  $Q'$  is increased 157 lb. in order to make their net sum zero. Since these normal force increments are to be used as increments of shear flow, they are designated by the symbol  $\Delta q$ .

If a cross-section can be developed from a flat sheet, like a channel, there is but one possible path for the shear flow from the tension to the compression fibers, and its intensity at any point is statically determinate. In a single-cell closed section, like a tube, there are two possible

paths, and the intensity of shear flow is indeterminate to the first degree, unless, owing to symmetry, the shear flow at some point is known to be zero. In a multiple-cell unsymmetrical closed section of  $n$  cells, the shear flow is statically indeterminate to the  $n$ th degree. Thus, in the two-cell section of Fig. 16 : 5, there are three possible paths for the shear flow from any tension fiber to the compression fiber with which it may be paired and no symmetry to simplify the problem. Therefore the section is statically indeterminate to the second degree.

If each of the cells of the beam of Fig. 16 : 5 be slit longitudinally along one element of the middle surface, the shear flow becomes statically determinate. In the numerical example such slits are assumed to intersect the cross-section at a point between stations  $C$  and  $D$  and at a point between stations  $G$  and  $H$ . The distribution of shear flow, as determined by the distribution of normal force variation and the selected slit locations, is computed in Table 16 : 10. The criterion that must be satisfied by the locations of such imaginary slits is that they leave one and only one path for shear flow between any two points on the cross-section. In practice it is desirable that they should be located as near as possible to points of actual zero shear flow. The locations assumed for the example were selected as probably being close to such points.

Actually, the shear flow changes at each element of effective cross-section, but in practice it is common to assume the changes concentrated at a few points, making later corrections to take account of the actual variation where that is desirable. In the preparation of Table 16 : 10 the changes were assumed concentrated at the stations along the mid-line of the skin that were assumed as the centroids of the segments of effective skin in the computations of the geometric properties of the section. Such agreement between the computations of geometric properties and shear flow distribution is essential for consistent results. In the preparation of the table, since the imaginary slits are located on the compression side of the section, instead of following the shear flow from generating locations in the tension fibers to absorption in compression material, the opposite course is followed.

Between stations  $C$  and  $D$  the shear flow is zero since one of the slits is located between those points. From column 9 of Table 16 : 9 it is seen that stiffener  $C'$  and skin segment  $C$  absorb a total of  $80.90 + 28.34 = 109.24$  lb. per in. The shear flow between  $C$  and  $B$  is therefore 109.24 lb. per in. It is assumed that a shear flow is positive when the flow is counter-clockwise around the perimeter of a cell and negative when the flow is clockwise. Along a partition between two cells, any shear force flows counter-clockwise about one of the cells and clockwise about the other. For such situations one may assign rank

to the cells and either use the sign appropriate to the cell of higher rank or a pair of signs, the upper for the cell of higher rank. In the example the forward cell is assumed of higher rank than the rearward, and the symbol  $\pm$  used for a shear flow tending to cause counter-clockwise rotation of the forward and clockwise rotation of the rearward cell. A shear flow in the opposite direction in  $EQ$  would be indicated by the symbol  $\mp$ . This may be called the "shear flow" sign convention to distinguish it

TABLE 16 : 10  
COMPUTATION OF PRELIMINARY TRIAL SHEAR FLOWS,  $q_0$

1 Station	2 $\Delta q$ 9-9	3 $q_0$ $\Sigma_c 2$	4 Station	5 $\Delta q$ 9-9	6 $q_0$ $\Sigma_c 5$	7 Station	8 $\Delta q$ 9-9	9 $q_0$ $\Sigma_c 8$
<i>C</i>	-109.24		<i>H</i>	-105.58		<i>D</i>	-126.42	
		-109.24			+105.58			+126.42
<i>B</i>	-121.52		<i>I</i>	-97.62		<i>E</i>	-643.96	
		-230.76			+203.20			+770.38
<i>A</i>	+37.78		<i>J</i>	-432.34		..	.....	.....
		-192.98			+635.54			.....
<i>T</i>	+124.68		<i>JK</i>	-13.14		..	.....	.....
		-68.30			+648.68			.....
<i>S</i>	+141.96		<i>K</i>	+252.68		<i>G</i>	-115.22	
		-73.66			+396.00			-115.22
<i>R</i>	+162.92		<i>L</i>	+205.80		<i>F</i>	-128.82	
		+236.58			+190.20			-244.04
<i>Q</i>	+341.58		<i>M</i>	+220.58		<i>D-E</i>	+770.38	
		+578.16			-30.38			$\pm 1,014.42$
<i>H-P</i>	-502.42		<i>N</i>	+228.40		<i>E-Q</i>	-66.16	
		$\pm 1,080.58$			-258.78			$\pm 1,080.58$
			<i>P</i>	+243.64				
					-502.42			

In 2, 5, and 8, + indicates "generation" and - "absorption" of shear flow.

In 3, 6, and 9, the "shear flow" sign convention is used.

from the "force" sign convention in which forces acting in the positive directions of the  $X-X$  and  $Y-Y$  axes are considered positive, or the "stress" sign convention in which the plus sign indicates tension and the minus sign compression.

Since shear flow coming from  $B$  and absorbed at  $C$  would tend to produce clockwise rotation of the forward cell, it is negative according to the shear flow sign convention and it is so recorded in the table. At  $B$  the shear flow absorbed by the stiffener  $B'$  and the skin segment  $B$  amounts to  $55.36 + 66.16 = 121.52$  lb. per in. The total shear flow between  $A$  and  $B$  is therefore  $109.24 + 121.52 = 230.67$  lb. per in. It is also listed as minus since it tends to cause clockwise rotation. The stiff-

ener at  $A'$  and the skin segment at  $A$  generate  $22.78 + 15.00 = 37.78$  lb. per in. of the shear flow between  $A$  and  $B$ . Therefore, the shear flow between  $T$  and  $A$  is  $230.76 - 37.78 = 192.98$  lb. per in., which is also listed as negative.

Continuing around the perimeter in the same manner until the shear flow generated at  $Q'$  and  $Q$  is accounted for, it is found that the shear flow just beyond  $Q$  is  $+578.16$  lb. per in., but whether it should be assumed to flow up the web  $EQ$  or to the right along  $QP$  is undetermined. At this stage it is desirable to make a new start at the slit between  $G$  and  $H$ . Since there is no shear flow between those points on account of the slit, the shear flow between  $H$  and  $I$  is  $105.58$  lb. per in., the amount absorbed at  $H'$  and  $H$ . This shear flow tends to produce counter-clockwise rotation; hence it is listed as positive. One can then proceed from  $H$  to  $P$  in the same manner as from  $C$  to  $Q$ , and find the shear flow in  $PQ$  to be  $-502.42$  lb. per in., acting to the left. In making this computation no allowance need be made for the fact that shear flow is absorbed in the upper and generated in the lower part of the rear web,  $JK$ , only the net change in that member requiring consideration. The flow in  $PQ$  combines with that from the forward cell to produce an upward acting shear flow of  $578.16 + 502.42 = 1,080.58$  lb. per in. This shear flow is listed as  $\pm$  since it tends to produce counter-clockwise rotation of the forward cell.

The shear flow in the front web just above  $Q$  being determined, new starts are made at  $D$  and  $G$ , and in similar manner the flows terminating at those points are combined and the shear flow in the front web just below  $E$  found to be  $\pm(770.38 + 244.04) = \pm 1,014.42$  lb. per in. The net shear flow absorbed in  $EQ$  is  $66.16$  lb. per in. This added to  $\pm 1,014.42$  gives  $\pm 1,080.58$  lb. per in. as the shear flow just above  $Q$ , checking exactly with the previously computed value. If the axial loads of column 6 of Table 16 : 9 and the corresponding values of  $\Delta q$  in column 9 had not been corrected to make the totals for those columns zero, this check would not have been obtained, and the resulting unbalanced shear flow would have been difficult to deal with. The existence of any unbalanced shear flow is impossible, and, while one might question the suitability of the specific correction used, the necessity of making some such correction is unquestionable. If at the conclusion of computations of shear flow there is any unbalanced flow, either  $\Sigma P$  was not balanced or a mistake has been made in the shear-flow computation. In either event, suitable correction should be made before proceeding. The shear flows computed in Table 16 : 10 are preliminary trial values and must be distinguished in some manner from the other shear flows that must be computed. To this end they are designated the  $q_0$  values.

In these computations the shear flow,  $q_o$ , for each segment is the cumulative sum of the values of  $\Delta q$  between that segment and the starting point. This is specified by the symbol  $\Sigma c$  in the operational notes for columns 3, 6, and 9. The  $\Sigma$  indicates a summation, and the letter  $c$  is used to show that it should be a *cumulative* summation of the quantities in the column referred to by the number in bold-face type. Often the figures of one column are the sum of *adjacent* figures from another. That may be specified by the symbol  $\Sigma a$  in the operational notes.

**16 : 10. Computation of Resultant of Trial Shear Flows** — A desirable, though not an essential, step at this stage is to compute the magnitude of the resultant shear force represented by the *preliminary trial* shear flows of Table 16 : 10. This is done in Table 16 : 11. In this

TABLE 16 : 11  
COMPUTATION OF RESULTANT OF  $q_o$  VALUES

1 Segment	2 $q_o$ T 10	3 $\Delta x$ 3-4	4 $\Delta y$ 3-5	5 $q_o \Delta x$ 2 $\times$ 3	6 $q_o \Delta y$ 2 $\times$ 4
ED	+126.42	-5.00	-0.31	-632.1	-39.2
DC	0	-5.00	-0.76	0	0
CB	-109.24	-5.00	-1.52	+546.2	+166.0
...	.....	.....	.....	.....	.....
RQ	+236.58	+5.00	-0.47	+1,182.9	-111.2
QE	.....	.....	.....	0	+12,841.4
QP	-502.42	+8.00	-0.40	-4,019.4	+201.0
...	.....	.....	.....	.....	.....
...	.....	.....	.....	.....	.....
$\Sigma$				+73.6	+21,306.8

Sign Conventions.

2, + if flow is counter-clockwise around cell.

3 and 4, + if  $x$  or  $y$  increases when traversing perimeter of cell counter-clockwise.

5, + if shear force is directed to the right.

6, + if shear force is directed upward.

table the order of the segments is changed from that of Tables 16 : 2 to 16 : 9 to that of Table 16 : 1. This facilitates making summations for each cell independently, since all quantities pertaining to either cell are on adjacent lines. Columns 5 and 6 show the  $X$  and  $Y$  components of the shear forces acting on the respective segments. Except for members  $EQ$  and  $JK$  they are computed by applying Eq. 16 : 5. This is allowable since the shear flow is assumed to change only at the stations and is therefore constant between stations. For the two webs, however, the shear flow must be considered variable since, in computing  $I_{xx}$ ,

terms were included to represent the moment of inertia of each web about an  $X-X$  axis through its centroid. Since each fiber of a web is assumed to make its contribution to the change in shear flow at its actual location, it is desirable to start with the determination of  $q'$ , the *shear-flow gradient* or rate of change of shear flow. From what has gone before it should be clear that the change in shear flow across the width,  $ds$ , of an element  $t$  thick will be equal to  $t ds(\Delta f/\Delta z)$  where  $\Delta f/\Delta z$  is the change in axial stress per inch. In the shell under study since  $V = dM/dz$ , and  $M/V = 50$ ,  $\Delta f/\Delta z = f/50$ . Thus at any point the shear-flow gradient  $q' = f(t/50)$ . The change in shear flow between any two points,  $s_1$  and  $s_2$  may be represented as

$$q_2 - q_1 = \oint_{s_1}^{s_2} q' ds = \oint_{s_1}^{s_2} \frac{ft}{50} ds \quad a$$

From Eq. 16 : 5 the total shear force between the same points is

$$V_{s_1-s_2} = \int_{s_1}^{s_2} q ds \quad b$$

Thus the total shear force between any two points is the second integral of the shear flow gradient between those points. From proposition 12 of Art. 3 : 9 the shear force between any two points can therefore be computed by treating the shear-flow gradient as a distributed load and determining the associated bending moment, which will be equal numerically to the shear force desired. The method of doing this can be illustrated by the appropriate computations for  $EQ$  and Fig. 16 : 6.

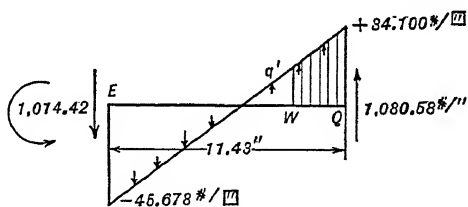


FIG. 16 : 6

Since the shear-flow gradient,  $q'$ , in segment  $EQ$  depends only on the normal stresses in that segment, it varies linearly from  $Q$  to  $E$ . The shear flow,  $q$ , at any point on  $QE$  will be equal to the shear flow at one end, either  $Q$  or  $E$ , plus the area under the  $q'$  diagram between that end and the point in question. The total shear force represented by the shear flow between  $Q$  and any point, such as  $W$ , will be equal to the area under a curve of  $q$  between  $Q$  and  $W$ , or to the moment about  $W$  of the shear flow at  $Q$  plus that of the area of the  $q'$  diagram between  $Q$  and  $W$  about  $Q$ . The total shear force developed on  $EQ$  will be the moment about  $E$  of the shear flow at  $Q$  and the whole  $q'$  diagram. This can be



represented by the expression

$$V_{QE} = q_Q L_{QE} + \frac{q'_Q L_{QE}^2}{3} + \frac{q'_E L_{QE}^2}{6} \quad 16 : 17$$

whence

$$\begin{aligned} V_{QE} &= 1,080.58 \times 11.43 + 34,100 \times \frac{11.43^2}{3} - 45.678 \times \frac{11.43^2}{6} \\ &= +12,351.0 + 1,485.0 - 994.6 = 12,841.4 \text{ lb.} \end{aligned}$$

This can be checked by taking moments of the shear flow at  $E$  and the area of the  $q'$  diagram about  $Q$ . From parallel computations the total shear in  $JK$  is found to be 6,281.6 lb.

The shear flow sign convention, which is most satisfactory for the  $q_0$  values of column 2, would be decidedly unsatisfactory for the shear forces of columns 5 and 6. In those columns, therefore, the "force" convention is used.

On adding the forces listed in columns 5 and 6, the resultant is found to be composed of a component of 73.6 lb. acting to the right and 21,306.8 lb. acting up. These components should have been zero and 20,000. The error in  $\Sigma q_0 \Delta x$  is not serious and may be neglected, but that in  $\Sigma q_0 \Delta y$  is excessive. One source of error is neglect of the shear flows between the centroids of the stiffeners and the adjacent stations on the mid-line of the skin. Except for the line between  $A'$  and  $A$ , all of the lines, such as  $B'B$  and  $C'C$ , joining such pairs of points are either parallel to the  $Y-Y$  axis or nearly so. Each of these lines should be assumed subjected to what might be termed a "branch shear flow" equal to the shear flow generated or absorbed by the stiffener to which it pertains. The vertical components of the forces represented by these branch shear flows are computed in Table 16 : 12, and the total is found to be a downward force of 1,322.1 lb. Subtracting this amount from the total vertical force found in Table 16 : 11 gives 19,984.7 lb. as the total upward force, reducing the error to 15.3 lb., which may be neglected.

**16 : 11. Computation of Correction Shear Flows** — The computations of Tables 16 : 11 and 16 : 12 indicate that the values of shear flow,  $q_0$ , in Table 16 : 10 are consistent not only with the normal force distribution but also with the resultant shear on the cross-section. It should be obvious, however, that an equally consistent, though quite different, set of shear flow values could be obtained if the shear flow were assumed zero at other locations than those chosen. If a constant value be added to the shear flow around either cell, the distribution of the shear forces would be changed, but the magnitude of the resultant would

remain the same. The actual shear-flow pattern developed in *torsionless bending*, which is the immediate objective of the computations, can be obtained by adding the actual shear flow in segment  $CD$  to those figured for segments of the forward cell, and the actual shear flow in segment  $GH$  to those figured for segments of the rearward cell. These "correction shear flows," which are designated  $q_f$  and  $q_r$ , can be evaluated from a study of the deformations of the shell.

TABLE 16 : 12  
COMPUTATION OF BRANCH SHEAR FLOWS

1 Station	2 $q$ 9-9	3 $\Delta y$ 3-3 - 2-6	4 $q\Delta y$ 2 $\times$ 3	5 $\alpha$ Note A	6 $\alpha q \Delta y$ 4 $\times$ 5
$A'A$	+22.78	0	0	-30.56	0
$B'B$	-55.36	+0.51	-28.2	-25.83	+728
$C'C$	-80.90	+0.51	-41.3	-20.87	+862
$D'D$	-93.94	+0.51	-47.9	-15.91	+762
$E'E$	-543.46	+0.64	-347.8	-10.83	+3,767
....	.....	.....	.....	.....	.....
$T'T$	+45.82	-0.59	-27.0	-25.88	+699
$\Sigma$			-1,322.1		-3,599

Note A. Average of 5-3 and 6-3.

In Fig. 16 : 7  $AD$  and  $BC$  represent two longitudinal sections of the shell and  $AB$  a part of a cross-section mid-line,  $ds$  in length. When the shear flow is zero, the angle  $DAB$  is a right angle. If, however, a shear flow of intensity  $q$  is acting along  $AD$  and  $AB$ , there is shear strain and the element  $ABCD$  is deformed to the shape represented by  $AB'C'D$ . From the data of Art. 12 : 9 the angle of shear strain,  $\gamma$ , can be shown to be equal to  $q/(tG)$ , where  $t$  is the thickness of the material and  $G$  is the shearing modulus of elasticity. If the bending of the beam is unaccompanied by torsion, and bending deformation is neglected, sections  $AD$  and  $BC$  remain parallel to the  $Z-Z$  axis, but  $B$  will move to  $B'$  a distance of  $q ds/(tG)$  parallel to the  $Z-Z$  axis. The absolute movement of  $B$  may be somewhat different,  $q ds/(tG)$  being the relative movement of points  $A$  and  $B$  parallel to the  $Z-Z$  axis. The total relative movement, parallel to the longitudinal axis, of any two points,  $M$

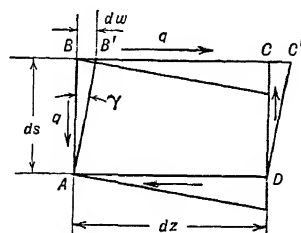


FIG. 16 : 7

and  $N$ , located on the mid-line of the same cross-section may therefore be represented by

$$\Delta z_{MN} \oint_M^N = \frac{q \, ds}{tG} \quad 16 : 18$$

If  $M$  and  $N$  are taken to represent two adjacent points on opposite faces of the imaginary slit in segment  $CD$  or  $GH$ , Eq. 16 : 18 can be used to determine the "relative sliding" of those points implied by any specific system of shear flows. If the points are on the slit in  $CD$  the line integration would be carried out around the perimeter of the forward cell, while for points on the slit in  $GH$  the integration would be carried out around the perimeter of the rear cell. These operations are carried out in Table 16 : 13 to determine the relative slidings implied by the shear-flow system of Table 16 : 10.

Since the entire section is assumed to be made of aluminum alloy, instead of computing values of the relative slidings,  $\Delta z$ , it is more convenient to compute values of  $G \Delta z$ , allowing for the effect of local buckling by the use of an effective thickness for those segments in which buckling is assumed to take place. For most of the segments the shear flow,  $q_o$ , is a constant and the appropriate value of  $ds/t_e$  is that of  $\Delta s/t_e$  computed for column 4 of Table 16 : 1. The relative slidings produced by the deformations of these segments can therefore be computed as the product of these two quantities. For the webs,  $EQ$  and  $JK$ ,  $q$  is not a constant, but  $t$  is a constant, and  $q_o ds$  has been computed for Table 16 : 11. Thus  $G$  times the relative sliding at each slit, due to the deformation of  $QE$ , is computed as indicated in Note A of Table 16 : 13. The relative sliding of the rear slit, due to deformation of  $JK$ , is similarly found to be  $+98,150/G$  in.

By addition of the quantities in column 4 of Table 16 : 13 that pertain to the front and rear circuits, respectively, the total relative sliding along the front slit is found to be  $+167,347/G$  and that along the rear slit  $-127,859/G$  in. Since these slits are imaginary, it is necessary to add constant shear flows,  $q_f$  and  $q_r$ , to the front and rear cells that will reduce these relative slidings to zero. From Eq. 16 : 18 it can be seen that if  $q = 1$ , the relative slidings can be obtained directly from Table 16 : 1. Thus the desired deformation equations are

$$\begin{aligned} 1,422.19 \, q_f - 178.59 \, q_r &= -167,347 \\ -178.59 \, q_f + 3,355.65 \, q_r &= +127,859 \end{aligned}$$

whence

$$q_f = -113.64 \quad \text{and} \quad q_r = +32.05$$

These correction shear flows are added to the values of  $q_o$ , previously computed, and listed in column 5 of Table 16 : 13. The resulting values are designated by the symbol  $q_e$ , the subscript indicating that they are the shear flows produced by a transverse shear force passing through the elastic center of the shell section and causing torsionless bending.

As a check, the values of the resultant shear force represented by the shear flows,  $q_e$ , and the resultant slidings along the imaginary slits are computed in the same manner as those associated with the preliminary trial values,  $q_o$ . These computations are recorded in the last three

TABLE 16 : 13  
COMPUTATIONS OF  $q\Delta s/t_e$

1 Segment	2 $\Delta s/t_e$ 1-4	3 $q_o$ 11-2	4 $q_o\Delta s/t_e$ 2 $\times$ 3	5 $q_e$ Note B	6 $q_e\Delta x$ 5 $\times$ 11-3	7 $q_e\Delta y$ 5 $\times$ 11-4	8 $q_e\Delta s/t_e$ 5 $\times$ 2
...	.....	.....	.....	.....	.....	.....	.....
TS	126.00	-68.30	-8,606	-181.94	-909.7	+120.1	-22,924
SR	125.75	+73.66	+9,263	-39.98	-199.9	+23.2	-5,027
RQ	125.50	+236.58	+29,691	+122.94	+614.7	-57.8	+15,429
QE	178.59	Note A	$\pm 200,647$	Note C	0	+11,176.2	$\pm 174,628$
$\Sigma$ Front	1,422.19		+167,347				+6
QP	200.25	-502.42	-100,610	-470.37	-3,762.9	+188.1	-94,192
PN	250.00	-258.78	-64,695	-226.73	-1,813.8	+27.2	-56,683
...	.....	.....	.....	.....	.....	.....	.....
FE	302.00	-244.04	-73,700	-211.99	+1,695.9	+12.7	-64,021
$\Sigma$ Rear	3,355.65		-127,859				-16
$\Sigma$					+73.7	+21,335.6	

Note A. For QE  $q_o\Delta s = 12,841.4$  from 11-6,  $q_o\Delta s/t_o = 12,841.4/0.064 = 200,647$ . Values for QE are included in the summations for both cells.

Note B.  $q_e = q_o - 113.64$  for front and  $q_o + 32.05$  for rear cell.

Note C. For QE,  $q_e = q_o - 113.64 - 32.05 = q_o - 145.69$ .  $q_e\Delta s = q_e\Delta y = q_o\Delta s - 145.69 \times \Delta s = 12,841.4 - 145.69 \times 11.43 = 12,841.4 - 1,665.2 = 11,176.2$ .  $q_e\Delta s/t_e = 11,176.2/0.064 = 174,628$ .

Sign Conventions.

In 4 and 8, + indicates deformation due to counter-clockwise shear flow around cell. For QE, upper sign applies to front cell.

In 6 and 7, they are the same as in 11-5 and 11-6.

columns of Table 16 : 13. The error in the X component of the resultant force is found to have increased from +73.6 to +73.7 lb. and that in the Y component has changed from -15.1 to +12.7 lb., allowance being made for the branch shear flows which are unchanged. The relative slidings computed from the values of  $q_e$  are only +6/G in. for the front slit and -16/G in. for the rear slit. All these errors are negligible and indicate that the numerical work is sufficiently accurate.

The next step is to determine the location of the resultant shear force represented by the shear flows,  $q_e$ . This is done in Table 16 : 14. At alternate stations on the perimeter the  $X$  and  $Y$  components of the shear forces acting on the adjacent segments of the mid-line are combined and their moments about the centroid of the section are computed. On the next to last line is entered the moment of the branch shear flows, which is computed in Table 16 : 12. The total moment about the centroid is found to be  $-11,102 - 6,996 = -18,098$  in.-lb. Since this is caused by a force of 20,000 lb. in the  $Y$  direction, that force must act along a line 0.905 in. to the left of the centroid, i.e., at  $30.83 - 0.905 = 29.925$  in. to the rear of the leading edge.

**16 : 12. Computation of Net Shear Flows** — The shear flows computed in the preceding articles are those associated with torsionless bending, and it is found that to produce such bending the resultant force must act 29.925 in. to the rear of the leading edge. The original problem, however, was to determine the shear flow resulting when the 20,000-lb. load acts at a distance of 40 in. from the leading edge. Therefore, it is necessary to add to the shear flows of column 5 of Table 16 : 13 those which would be produced by a torsion of 20,000 ( $40.00 - 29.925$ ) = 201,500 in.-lb. The shear flows produced by this torsional couple would be directly proportional to those produced by a torsional couple of 100,000 in.-lb., as computed in Art. 15 : 5. Therefore, it is necessary to add  $q_{tf} = +2.015 \times 79.7 = 160.60$  lb. per in. to the shear flows,  $q_e$ , of the front cell, and  $q_{tr} = +2.015 \times 82.0 = 165.23$  lb. per in. to those of the rear cell. The addition to  $q_e$  of the front web,  $EQ$ , would be  $160.60 - 165.23 = -4.63$  lb. per in.

**16 : 13. Effect of Lack of Symmetry** — In Art. 16 : 6 it is stated that there are three factors of special importance to be taken into account in the analysis of shells although they may be of little consequence in most beam designs. It is desirable to discuss each of these factors in the light of the cycle of computations outlined above.

First of these factors is lack of symmetry. This complication is normally absent with fuselage shells but is characteristic of wing structures. In the computation of the distribution of normal stress over the effective cross-section, lack of symmetry makes it necessary to use Eq. 6 : 18 instead of the simpler Eq. 6 : 2. The equation used is applicable to all unsymmetrical beams and is not limited to shells.

Another effect of lack of symmetry is to make necessary the development of special methods for computing the distribution of shear flow. In the first place it is desirable to locate the point, called the shear center, through which the resultant load on the cross-section must pass if it is to produce torsionless bending. For a doubly symmetrical sec-

tion the shear center and the centroid coincide. For a singly symmetrical section the shear center is on the axis of symmetry but not at the centroid. For an open section like a channel its location can be found by the method of Art. 6 : 5, and that method can be extended to unsymmetrical open sections if Eq. 6 : 18 instead of Eq. 6 : 2 is used in developing a formula for shear flow corresponding to Eq. 16 : 7. With a closed section, particularly a multi-celled one, however, the shear

TABLE 16 : 14  
COMPUTATION OF SHEAR-CENTER LOCATION

1 Segment	2 $q_c \Delta x$ 13-6	3 $q_c \Delta y$ 13-7	4 Station	5 $\bar{x}$ 6-3	6 $\bar{y}$ 6-4	7 $-\bar{y} q_c \Delta x$ 2 $\times$ 6	8 $\bar{x} q_c \Delta y$ 3 $\times$ 5
<i>FE</i>	+1,695.9	+12.7	..	.....	.....	.....	.....
<i>QE</i>	0	+11,176.2					
<i>ED</i>	63.9	-4.0					
<i>DC</i>	+1,632.0	+11,184.9	<i>E</i>	-10.83	+6.61	-10,788	-121,132
<i>CB</i>	+568.2	+86.4					
	+1,114.4	+338.8					
	+1,682.6	+425.2	<i>C</i>	-20.83	+5.54	-9,322	-8,857
...	.....	.....		.....	.....	.....	.....
...	.....	.....		.....	.....	.....	.....
<i>TS</i>	-909.7	+120.1					
<i>SR</i>	-199.9	+23.2					
	-1,109.6	+143.3	<i>S</i>	-20.83	-3.77	-4,183	-2,985
<i>RQ</i>	+614.7	-57.8					
<i>QP</i>	-3,762.9	+188.1					
	-3,148.2	+130.3	<i>Q</i>	-10.83	-4.82	-15,174	-1,411
...	.....	.....		.....	.....	.....	.....
...	.....	.....		.....	.....	.....	.....
Branches from Table 16 : 12							-3,559
$\Sigma$						-11,102	-6,996

center cannot be located directly. The first step of the recommended method is to assume that the shear flow is zero at one point in each cell and to compute the shear-flow distribution compatible with that assumption and the normal force distribution. This stage is based entirely on the principles of statics. The next step is to find the relative movements of two points on opposite sides of imaginary cuts at the points of assumed zero shear flow that would be produced by the shear deformation resulting from the computed shear flows, and also from

constant shear flows of one pound per inch around the perimeter of each cell. The Maxwell-Mohr method of Arts. 13 : 4 to 13 : 7, may then be employed to find the correction shear flows needed to make the relative movements of the points considered equal to zero.

The resultant shear force and its line of action can then be computed from the corrected shear flows. In the example only the  $X$  co-ordinate of the shear center is determined, but, when the total shear on the section acts parallel to the  $Y$ - $Y$  axis, that is the only one required. If the  $Y$  co-ordinate is also desired, a parallel computation based on values of  $V_{xx}$  and  $M_{yy}$  is needed. Sometimes when the direction of the resultant shear is known but is parallel to neither co-ordinate axis, it is satisfactory to make a single computation and either to find the perpendicular distance from the centroid to the resultant that is necessary for torsionless bending or to assume that one component of the resultant passes through the centroid so that the required distance to the other may be computed.

**16 : 14. Buckling Lag** — When subjected to shear or compressive stresses exceeding the critical, the thin sheets used on stressed skin structures buckle and cause a redistribution of normal stresses over the affected region. The difference in resistance to load offered by the buckled sheet and that offered by a fully effective sheet is often described as the effect of "buckling lag."

The effective width methods employed in the analysis of a thin-walled cylinder, Arts. 6 : 8 and 6 : 9, and of stiffened panels, Art. 10 : 6, were developed to handle the effect of buckling on stiffened shell structures where the thin sheet was subjected primarily to compressive stresses acting parallel to the stiffeners. When shear or a combination of shear and compression, is involved, the angle of buckling is altered and the whole problem of effective width is changed. The stress distribution is then dependent on the resistance of the stiffening members to bending in the plane of, and normal to, the sheet, to the efficiency of the riveted connections between sheet and stiffener, and to numerous other factors which vary appreciably with different types of structure.

Lahde and Wagner, in N.A.C.A. Technical Memos. 809 and 814, and Kromm and Marguerre, in N.A.C.A. Technical Memo. 870, have investigated some of the problems connected with flat sheet, while Wagner and Ballerstedt, in N.A.C.A. Technical Memo. 774, Limpert, in Tech. Memo. 846, and Kuhn, in Technical Note 687, have contributed to the analysis of buckling in curved sheets. Each study deals with a rather specialized problem, it being impracticable if not impossible to cover the generalized problem. While each is helpful, none provides a simple general criterion upon which to base the analysis of a wing or fuselage.

In the example presented in Arts. 16 : 5 to 16 : 12, buckling lag in compression was provided for by assuming a width of shell on each side of the rivet lines attaching sheet to stiffeners to be effective and by disregarding the material between such widths. Section properties and normal stress distributions were obtained on the basis that the ineffective material was not present. Actually, even though such material does buckle under compressive stresses, it continues to offer a small resistance to such stresses, but, when "effective" areas are predicated on somewhat arbitrary widths, the futility of trying to allow accurately for compressive resistance after buckling should be apparent.

The redistribution of stress due to shear buckling was provided for by basing section properties and stresses on an "effective sheet" five-eighths as thick as the actual. The ratio five-eighths applies strictly only to flat sheet subjected to shear stresses having intensities several times the critical for the sheet. The covering in the regions of high shear stresses is nearly flat and the maximum shear stress is several times the critical. Curving the sheet tends to reduce its effective modulus,  $G$ , so that the ratio should be somewhat below the five-eighths for a flat sheet. On the other hand, the shear stress at which buckling starts on a curved panel is, according to Kuhn, in N.A.C.A. Technical Note 687,

$$f_{s.cr.} = 0.1 E \frac{t}{R} + 5.0 E \left(\frac{t}{h}\right)^2 \left[1 + 0.8 \left(\frac{h}{d}\right)^2\right] \quad 16 : 19$$

where  $E$  is Young's modulus,  $t$  the thickness of the sheet,  $R$  its radius of curvature,  $h$  the distance around the arc between longitudinal stiffeners, and  $d$  the distance between transverse stiffeners. If  $h$  be greater than  $d$ , the letters and their corresponding quantities should be interchanged in the formula. Kuhn suggests introducing a coefficient of 0.75 when this expression is used for designing a structure to be free from shear buckles.

Equation 16 : 19 is for simply supported sheet, the normal condition for sheet-stiffener structures. When a clamped edge condition is attained on all four edges of a panel, the coefficient 5.0 of the second term may be increased to 7.5. This is based on Wagner's formula, which is the same as Kuhn's for simply supported edge conditions, except that the quantity in brackets in Kuhn's formula is taken as unity by Wagner. Equation 16 : 19 will be found to give critical stresses on curved sheets greater than Eq. 6 : 6 for flat.

For ratios of actual stress to critical exceeding 8 or 10 on flat sheet, taking the effective shear modulus as  $\frac{5}{8} G$  gives good results. For lower stress ratios, the effective  $G$  may be found, to a good degree of approxi-



mation, from the upper curve of Fig. 15 : 5. On curved sheet it is seldom that the actual shear stress exceeds 5 to 10 times the critical, because the buckles become so large as to be objectionable. Even at these low stress ratios, the effective  $G$  may be much less than that for a shear-resistant sheet. Where the effect is to be provided for by reducing  $t$ , it may be necessary to use effective thicknesses as small as one-tenth or one-fifteenth of the actual. The value to be used is, however, a matter of judgment. The five-eighths employed in the illustrative problem is probably high but was decided upon because the areas of covering subject to shear buckles were essentially flat and, for illustrating the tabular analysis of the beam, that coefficient serves as well as any.

**16 : 15. Shear Lag** — When structural members subjected to bending are composed of compact elements, shear strains on any cross-section are small and have negligible effect in redistributing normal stresses. When members involve elements which are wide and thin, shear strains are often great enough to alter the normal stress distribution appreciably, the tendency generally being to reduce such stresses near the center of the wide, thin element. In the shell example, for instance, it was assumed that some of the stiffeners were only partially effective in resisting compression and their actual areas were reduced somewhat when properties of the cross-section were computed.

This reduction was explained as having been made to provide for the effects of "shear lag." Several investigators have studied specific shear-lag problems but, as with "buckling lag," no general solution yet exists. The problems are related, one being concerned with conditions existing when there is no buckling of the sheet, the other involving conditions after buckling.

Kuhn<sup>1</sup> and E. Reissner,<sup>2</sup> among others, have published papers on the effects of shear lag which indicate the variation in normal stress on the wide, thin cover of a box-beam to be a hyperbolic cosine function, for which a parabola is often a good approximation. For preliminary computations on box beams having two shear webs, current practice of some engineers is to determine the properties of the box beam on the assumption that all material in the shear webs and on the tension side of the beam is effective, that a width of sheet about thirty times its thickness acts with each stiffener on the compression side. The stresses in the

<sup>1</sup> "Stress Analysis of Beams with Shear Deformation of the Flanges," P. Kuhn, N.A.C.A. Tech. Reports 608 and 636. Also N.A.C.A. Tech. Notes 704 and 739.

<sup>2</sup> "Stress Distribution in Wide-flanged Box-beams," E. Reissner, *Jour. Aero. Sci.*, Vol. 5, No. 8, June, 1938, pp. 295-299. "Least Work Solutions of Shear-lag Problems," E. Reissner, *Jour. Aero. Sci.*, Vol. 8, No. 7, May, 1941, pp. 284-291.

compression chords adjacent to the shear webs are then computed by the ordinary beam theory and plotted at the points where they occur. They are connected by a straight line. A horizontal line having an ordinate six-tenths of the average of these compressive chord stresses is then constructed, and an approximately parabolic curve is passed through the chord-stress points and drawn tangent to the horizontal line. The effective area of any stiffener on the compression side of the beam between shear webs is then taken as the actual area of the stiffener times the ratio of the ordinate to the parabolic curve at the point where the stiffener acts to the ordinate to the sloping straight line running between the spar-chord stress points. The previously computed stresses in the stiffeners are multiplied by the same ratios, and effective sheet widths are computed by inserting these modified stresses as  $f$  in Eq. 6 : 24.

New cross-section properties are then computed on the basis of the reduced stiffener areas and modified sheet widths on the compressive side of the beam. Stresses are determined with these modified properties by means of the ordinary formula for beams in bending. The stresses on the tension side of the beam, and in the shear webs, obtained by this second approximation are used directly in proportioning sheets and stiffeners. The loads in the sheet and stiffeners on the compressive side are obtained by multiplying the stress computed from this second approximation by the effective area of the section. If a stress is wanted, this load is divided by the actual area of the stiffener in question and its effective sheet.

The above procedure for treating shear lag is similar to the effective width method of Art. 6 : 8 for thin-walled beams, with the added reduction in the effective area of stiffeners on the compression side of the beam. It appears to give satisfactory results on wing beams having two shear webs and on stiffened thin-sheet tension and compression chords, though it disregards shear lag on the tension side of the section. Limited strain-gage data indicate that shear lag exists on the tension side of a beam of this type, but not to the same extent as on the compression side.

With wings of normal proportions, the actual stresses in the chords near the shear webs are seldom greater than 120 per cent of the values determined with properties based on the assumption that the material in the cross-section is fully effective at all points. Because of this, some engineers base wing-design stresses on the assumption of 100 per cent effective sections, and provide for shear lag by having a 15 to 20 per cent positive margin of safety in the shear webs, in thin-sheet chords near the shear webs, and in the riveted connections between chords and webs. Though it is somewhat more arbitrary, this procedure has resulted in satisfactory wing structures on some large airplanes.

**16 : 16. Distribution of Effective Material** — Closely associated with the question of how much of the cross-section should be assumed effective is that of how this material should be assumed distributed when computing centroid locations, moments of inertia, and other required quantities. There are one ideal and two practical methods for handling each part of the cross-section of a thin-walled shell. The ideal method is to assume the effective material concentrated along the mid-lines of the various section elements, full account being taken of any curvature of those mid-lines. The more precise practical method is to assume the material concentrated along the mid-lines, but to assume those mid-lines composed of straight segments located as closely as possible to the actual mid-lines. When a segment of a mid-line is actually straight, this involves no correction; and, when it is curved, by breaking the curve up into a number of straight elements, the error can be reduced to as small a figure as may be desired. Less precise, but more convenient, is to assume all the material of a segment concentrated at or near its centroid.

In the analysis of a single shell any one of these methods may be used for the entire cross-section. With flat plates the first two methods produce the same results, and they are used above for the webs *EQ* and *JK*. The remainder of the effective material is assumed concentrated at the centroids of the stiffeners and the junctions of skin with stiffeners. With most airfoil shells it is believed the system used in the example is the most practical.

Although in the example each segment of skin is adjacent to a stiffener, that is not essential, and the skin material may be divided into segments, some of which are not connected to stiffeners. No special changes in the method of analysis would follow from the division of the skin into a larger number of segments, though the amount of computation labor would be increased. Such further subdivision might be considered advisable near the leading edge of a wing section, to reduce the error involved in assuming the mid-line to be straight between adjacent stations, but normally it would not be worth the extra trouble.

The question of whether the material should be assumed concentrated or distributed along straight lines or curves is not confined to the computation of the centroid location but arises in the computation of the moments of inertia, the normal stresses and total normal forces on the segments, and the shear flows due to transverse load. To obtain consistent results the designer must decide how each segment is to be treated and stick to the chosen method in each of these computations. Thus, if the material in a stiffener or skin segment is assumed concentrated at a point, he should assume the moment of inertia of that area

about its own centroid equal to zero when computing the contribution of that area to the moment of inertia of the shell. Also he should assume all shear flow generated or absorbed by the stiffener or segment to be generated or absorbed at the point where the area is assumed concentrated. In the example these rules are followed for all the effective material except that of the two shear webs. On the other hand, if the material is assumed concentrated along a line, that assumption should be consistently adhered to. Thus if the moment of inertia of a stiffener about its centroid is included in the computation of  $I$  for the shell, the generation and absorption of shear flow by that stiffener should be assumed appropriately distributed along that line. In the example that is done for the webs, where serious error would have resulted from failure to allow for the actual extent of the web in the  $Y$  direction. For the stiffeners and skin elements any attempt to allow for the actual distribution of shear-flow generation and absorption would involve extensive and tedious computations, and the reliability of the final results would not be sufficiently increased to justify the extra labor. Since that situation would result in connection with the shear-flow computations, the moments of inertia of the separate elements (other than the webs) about their own centroidal axes are neglected in order to be consistent.

In the example the centroid of each element of skin is assumed at the "station" where that element is joined to a stiffener. For many of those elements the location of that station is a reasonable approximation to the centroid of the skin segment involved. At Station  $A$ , the nose, and at some of the stations on the compression side of the shell, the centroid of the skin segment is definitely not at the station. Thus the segment of effective skin at  $B$  extends only  $15t = 0.6$  in. to the rear of the rivet line, but halfway to Station  $A$  or 3.32 in. in front of it. Calculations in which the centroidal location of each skin segment is estimated as closely as possible without excessive labor, move the computed position of the centroid of the shell only 0.030 in. to the right and 0.002 in. upward. If this computation were followed by one in which the corrected centroid location is used, and if the moment of inertia of each element about its centroidal axis were included in computing that of the whole shell, the resulting figures for  $I_{xx}$  and  $I_{yy}$  would be increased only about 1 per cent and  $\frac{1}{4}$  per cent, respectively. It may be noticed that the errors in moment of inertia resulting from the procedure followed in the example are on the safe side and are not unreasonable in magnitude.

It might be argued that it would be better to use the more refined methods in the centroid and moment of inertia computations, even though some of the refinements in shear-flow computation that should

accompany them are omitted. The objection is that, unless the designer is consistent in the two portions of the analysis, he is likely to find difficulty in checking the values of shear flow, and the resultant shears computed from the shear flows will not balance the external shear forces. Thus conservatism in the assumptions underlying part of the analysis may result in errors on the unsafe side cropping up in other parts.

At times it may be desirable to assume portions of the skin as well as the web to be distributed along a straight line. There should be no difficulty in applying to such segments the method used in the example for handling the webs. Care must be taken however in applying Eq. 16 : 17 in the computation of the resultant shear on a sloping segment subjected to a parabolically distributed shear flow. The simplest scheme is to compute the total shear force from the formula and resolve it into  $X$  and  $Y$  components. The formula, Eq. 16 : 17, can be easily modified for this purpose.

**16 : 17. Remarks on Practical Procedure** — The computations of the example constitute only one cycle of a complete analysis and remarks are in order regarding some of the more general problems encountered in a complete analysis. As in any complex structure the analysis would be made in a number of cycles. In the earlier cycles many of the figures used by the engineer would be pure assumptions. Others would be the results of rudimentary computations in which only the most important factors would be taken into account. As the work progressed, more and more factors would be considered and a greater proportion of the figures used would be based on previous computation instead of guesses. It is often found convenient to omit corrections for some of the less important factors for several cycles in succession or until it is considered probable that the effect of some factor has changed sufficiently to make a new estimate of its influence necessary. Thus the position of the centroid of the effective section might be assumed unchanged for several cycles or until it is feared that changes in the assumed effective area imply so large a change in the centroid location that the computed moments of inertia may be seriously in error. The decision as to which factors are to be neglected and which variables are to be taken into account and assigned new values for each cycle must be left to the engineer who will learn from experience what is advisable. On the last cycle, however, when the final values of margins of safety are computed, all pertinent factors should be taken into account and the computations brought up to date, though this does not mean that refinements of analysis that do not improve reliability of results sufficiently to justify the extra labor involved must be used.

In the preliminary stages of analysis of most closed shells it will be found desirable to assume the shear center coincident with the centroid,

and a preliminary trial section may be developed by computations similar to those of Art. 6 : 13. In these preliminary computations, also, time will be saved if the  $X$ - $X$  and  $Y$ - $Y$  axes are assumed to be the principal axes. In one of the early cycles it may prove desirable to locate the shear center somewhat more accurately in order to be able to make a better estimate of the torsional shear flows developed by the external force acting at the specified location. This location could then be assumed for a few more cycles before revising that part of the computations.

In the example of Arts. 16 : 6 to 16 : 12 it is assumed that  $V_{xx} = M_{yy} = 0$ , but in practical designs the resultant shear and bending moment usually include both  $X$  and  $Y$  components. Whether the shell should be analyzed for the entire load in a single operation or a separate analysis made for each component of the shear with its associated bending moment is a problem on which opinions vary. The chief objection to a single analysis is that, while it can be used to locate the line of action of a force parallel to the resultant shear and passing through the shear center, it cannot be used to locate the shear center completely. On the other hand, it is often unimportant to know the exact location of the shear center when the information obtainable from a single analysis is available.

Another objection to combining the analyses of the effects of  $X$  and  $Y$  forces is that, unless the ratios  $V_{yy}/M_{xx}$  and  $V_{xx}/M_{yy}$  happen to be equal, the method used in Art. 16 : 9 to compute the changes in shear flow is inapplicable. In most designs these ratios are so nearly equal, and the quantities in the former so overshadow those of the latter, that the error resulting from the use of the former ratio would be inconsiderable. A more accurate method of avoiding this difficulty is included in the "Unit Method," proposed by F. R. Shanley and F. P. Cozzone.<sup>1</sup> In that procedure the shell is first divided into segments by transverse planes and each segment into units (or fibers) by longitudinal planes. The total normal forces on the ends of these units are then computed from Eq. 6 : 18. The difference between the end loads for a given unit divided by the length of that unit is equal to the change in shear flow across its width. The chief difference between this procedure and that of Art. 16 : 9 is that in the latter the units are assumed to be but 1 in. long and the difference in end loads is found by taking advantage of a relation between the total stress and its rate of change that happens to be applicable to the loading under consideration. In practical work it is probably easier to multiply the axial load on each element or unit by a constant ratio of shear to moment than to subtract the loads on one cross-section from those on another and divide by the intervening dis-

<sup>1</sup> *Jour. Aero. Sci.*, April, 1941, p. 246.

tance. The latter procedure, however, is undoubtedly quicker than two applications of the former.

**16 : 18. Shear-flow Determination without Locating the Shear Center** — When a shell is composed of a single cell, the method of analysis illustrated by the example can be greatly simplified. In the first place, there is only one correction shear flow to be added to the preliminary trial shear flows to obtain the flow associated with torsionless bending. Also, no computations are needed for a division of the total torque between cells. As a result it is not necessary to compute either the location of the shear center or the relative sliding of points located on an imaginary longitudinal section. After the normal forces in the elements have been determined the shear flow may be assumed zero at any point and computations made of the implied shear-flow distribution and the location of the resultant shear force. If such computations are made for both an  $X$  force and a  $Y$  force, the intersection of the lines of action of these forces is the *stress center* associated with zero shear flow at the point where that condition is assumed. If the assumed point of zero shear changes, the location of the stress center is correspondingly modified. In general, the stress center will not be at the shear center, and the shear-flow pattern developed would produce relative sliding along a longitudinal section at the point of assumed zero shear. A torque equal to the product of the resultant shear force and the distance from the stress center to the shear center would be required to reduce this sliding to zero. An additional torque, equal to the resultant shear times the distance from its line of action to the shear center, would also be needed to make the action of the shell correspond to that under the specified load. These torques may be added and the actual stress condition found by multiplying the resultant external force by its distance from the computed stress center and by adding to the preliminary trial shear flows,  $q_0$ , a single correction shear flow equal to that torque divided by twice the area enclosed by the mid-line of the section. Changing the point of assumed zero shear used in computing  $q_0$  changes the location of the stress center but makes a corresponding change in the correction shear flow, and the final result will be the same.

The above method of using a "stress center" can be expanded to evaluate the shear flow in a shell composed of two or more cells without locating the shear center. As has been shown in Art. 16 : 11, if the resultant shear passes through the shear center the shear flows are those designated by  $q_e$ , the magnitudes of which are determined from the criterion that  $\oint \frac{q_e ds}{t}$  must be zero for each cell. It is to be noted that the associated rotation of each cell when subjected to the shear flows,  $q_e$ , will also be zero. If the resultant shear does not pass through the

shear center, the total shear flow at any point will be  $q = q_e + q_t$ , where  $q_t$  is the shear flow associated with a torque equal to the product of the resultant shear and its distance from the shear center. Then

since  $\oint \frac{q_e ds}{t_e G} = 0$ ,  $\oint \frac{q ds}{t_e G}$  must be identical with  $\oint \frac{q_t ds}{t_e G}$  for each cell.

Since the latter divided by  $2 A$  has been shown in Art. 16 : 3 to equal the rotation of the cell per unit length, it follows that this rotation can also be determined from the relation

$$L = \frac{1}{2 A G} \oint \frac{q ds}{t_e} \quad 16 : 12a$$

in which  $q$ , the total shear flow, need not be constant around the perimeter of the cell, as was assumed in the development of Eq. 16 : 12.

Equation 16 : 12a is applicable to any one of a group of connected cells, superposition of the shear flows in the intermediate webs, which made necessary extra terms in Eq. 16 : 14, being allowed for by using the actual value of  $q$  at each point and making  $q$  subject to the line integration symbol. In a shell of  $n$  cells,  $n - 1$  independent equations can be formed by equating the expressions for  $\theta/L$  represented by Eq. 16 : 12a, since all cells will have the same rotation per unit length. The additional equation necessary for the complete solution of the problem would be the algebraic expression of the requirement that, for equilibrium, the sum of the moments of the total shear forces on the section elements about any point must equal the moment of the resultant shear about that point.

In writing these equations, the total shear flow at each point would be expressed as a sum of the preliminary trial shear flow,  $q_0$ , at that point, and one or more of the actual shear flows at the locations of the imaginary slits. After insertion of numerical values for  $q_0$ , computed by the method of Art. 16 : 9, the equations can be solved to evaluate the actual shear flows at the slit locations. These can then be added to the  $q_0$  values to obtain the actual shear flow at every point on the section. This line of attack has been developed in detail by F. P. Cozzone, in Lockheed Paper 51, "Unit Method of Beam Analysis (As Applied to Two Cell Structures)."

**16 : 19. Rib and Ring Pressure** — When a thin-walled shell is subjected to bending, the individual fibers which were originally straight and parallel to the longitudinal axis become curved like the element  $AB$  shown in Fig. 16 : 8. The result is that even in pure bending, when the bending moment is constant, the axial load on one end of the element cannot be held in equilibrium by the axial load on the other. As a result there are lateral pressures exerted between the fibers of a beam. With the plate girders and I-beams used in conventional structures, these



pressures are very small and can be easily taken care of by negligible changes in the stress distribution in the web. With thin-walled hollow shells such as airplane wings and fuselages, however, the situation is different, since there may be no web material strategically located for carrying these forces and they tend to collapse the structure. In practice it is therefore necessary to provide transverse ribs or rings which can resist these forces and prevent collapse.

Let  $AB$  of Fig. 16 : 8 represent an originally straight element of length,  $L$ , of a shell subjected to a constant bending moment,  $M$ , and

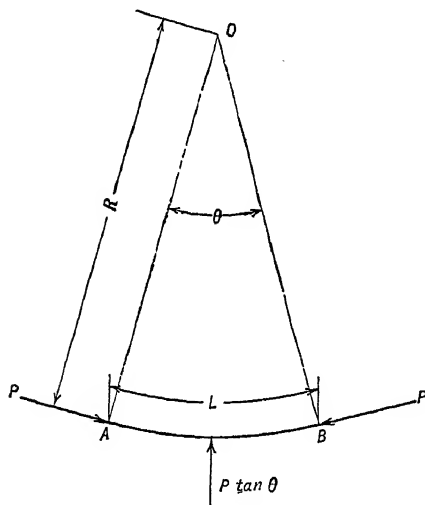


FIG. 16 : 8

let  $\theta$  be the change in slope and  $R$  the radius of curvature of the element resulting from the bending. Also let  $P$  be the axial load, assumed compression, on each end of the element. From the figure it is easily proved that for equilibrium a force  $P \tan \theta$ , normal to the element at its center, is required for equilibrium. If the slope angle,  $\theta$ , is small, and it may be so assumed,  $\tan \theta = \theta$ . But  $\theta = L/R$ . The required force is therefore equal to  $PL/R$ . From elementary-beam theory, however,  $1/R = M/(EI)$ , as stated in Eq. 4 : 5. Therefore, the transverse load required for each element is equal to  $PML/(EI)$ . If the element  $AB$

is the whole compression chord of the beam and  $h$  is the distance between chord centroids,  $P = M/h$ , and the formula for the "collapsing force" becomes

$$F = \frac{M^2 L}{EI h} \quad 16 : 20$$

For thin-walled shells like those used for wings or fuselages, it is not always satisfactory to assume the effect under consideration to result in a single concentrated force on each chord. Each segment of the shell would then be treated separately, being assumed subjected to a force obtained from the relation

$$v = \frac{M f A L}{EI} \quad 16 : 21$$

where  $A$  is the sectional area of the element and  $f$  the unit axial stress to which it is subjected.

In the derivation of Eq. 16 : 20 and 16 : 21 several assumptions were made which are only approximately correct for the conditions met in practice, but the resultant errors in the forces computed from the formulas are small enough to be neglected. First, it is tacitly assumed that the radius of curvature of the element is the same as that of the neutral axis. Secondly, it is assumed that the bending moment is constant. In practice, if  $L$  be taken as the distance between rings or ribs and  $M$  be taken as the bending moment at a ring or rib, the collapsing forces computed from the formulas will be sufficiently accurate. It will seldom be desirable to design ribs or rings for these collapsing forces alone, but such forces should be included in the load systems for such members.

**16 : 20. Normal Stresses Induced by Torsion** — In Chapter VII and in Arts. 16 : 3 to 16 : 5 it is assumed that the entire resistance to torsion is provided by shearing stresses unaccompanied by normal stresses acting on sections perpendicular to the axis of twist. These stresses are usually so distributed that they tend to cause originally plane cross-sections to become warped surfaces. In practical structure such warping may be resisted by the development of normal stresses on the cross-sections which modify the distribution of the shear. This is particularly true in wing structures at the plane of symmetry where, owing to the symmetry, the cross-section must remain plane. These normal stresses, often called the "torsion-bending stresses," and the associated redistribution of the shearing stresses are discussed briefly in this article.

Although the airplane designer is most interested in the torsion-bending stresses developed in closed-section shells, their nature can be more easily explained by study of a simple open section like a thin-walled I-beam or channel. If a member of this type, with unrestrained ends, is subjected to couples parallel to its longitudinal axis, each cross-section will rotate about an axis parallel to the direction of these couples.<sup>1</sup> With equal and opposite end couples this axis of rotation may be any line parallel to the torsional couples. If there is any variation of torsional moment along the length of the member, however, the axis of rotation will pass through the shear centers of the cross-sections.<sup>2</sup> If the torsional moment is constant, the angle of twist per inch length is also constant, and if that angle is small the longitudinal fibers remain

<sup>1</sup> In this article the direction of a couple or moment is that of the vector by which it would be represented in the system described in Art. 9 : 12.

<sup>2</sup> "Twisting Failure of Centrally Loaded Open-section Columns in the Elastic Range," R. Kappus, N.A.C.A. Technical Memo. 851, Washington, 1938, pp. 6-7.

straight. Projections of the cross-sections on planes normal to the axis of twist also retain their original shape.

The nature of the deformation is illustrated in Fig. 16:9, which is an end view of a channel subjected to a counter-clockwise couple at the near end and an equal and opposite clockwise couple at the far end, the angle of twist,  $\theta$ , being much exaggerated. The axis of twist is assumed at  $O$ . As a result of the twist, sections originally plane and normal to the axis of twist no longer remain plane but become "warped," points on such sections moving parallel to the twist axis by amounts that would not, in general, be directly proportional to their distances from some line

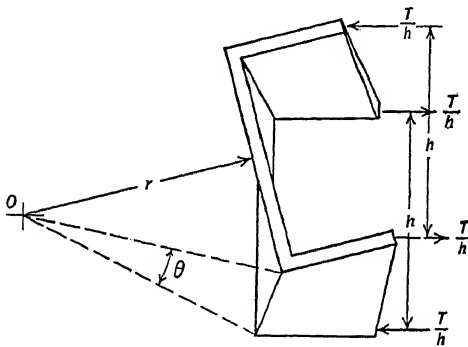


FIG. 16:9

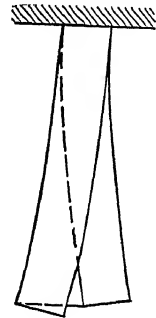


FIG. 16:10

across the section. At the same time shearing stresses are developed on each cross-section, the resultant of which is a couple of magnitude equal to the imposed torque. The distribution pattern of the shearing stresses developed under these conditions may be called the "primary pattern of torsional shear distribution."

If, however, the ends of a member are restrained against movement parallel to the twist axis, the fibers will be elongated or shortened, depending on the direction in which the section elements try to move, and the resulting strains will reveal a change in the pattern of shear distribution and the additional presence of normal stresses on a cross-section. These normal stresses are the torsion-bending stresses to be discussed.

If the member is subjected to equal torques,  $T$ , at its ends and to a torque  $2T$  in the opposite direction on the mid-cross-section, as a consequence of symmetry the mid-cross-section must remain plane and normal to the axis of twist. Then either half of the member may be considered as a unit, subjected to a constant torque,  $T$ , with one end

free to warp and the other completely restrained against warping.

Figure 16 : 10 is a plan view which illustrates how half of such a member would be deformed by a counter-clockwise torque applied to the free end, the upper flange being deflected to the left and the lower to the right. At the free end it is assumed that there are no external forces other than those in the plane normal to the axis of twist. Owing to the twist, these forces may have components parallel to the deflected directions of the fibers that would cause axial loads in them, but, if the angle of twist is assumed small, these will be infinitesimals that can be neglected. At the free end, therefore, the shear may be assumed to follow the primary pattern of shear distribution and the cross-section warped accordingly.

At the fixed end a part of the torsion will be resisted by shear, distributed in the primary pattern, that tends to produce warping of the cross-section. Since, however, this cross-section must remain plane, it must also be subjected to secondary shear and normal forces, the resultant of which is the remainder of the torsion, that prevent warping.

If the radius of sidewise curvature of a flange were constant, the flange would have to be subjected to a constant bending moment parallel to the web. That, however, would require the imposition of normal forces at the free end, and by hypothesis such forces are not present. The alternative is that the curvature, and therefore the bending moment on the flange, in-

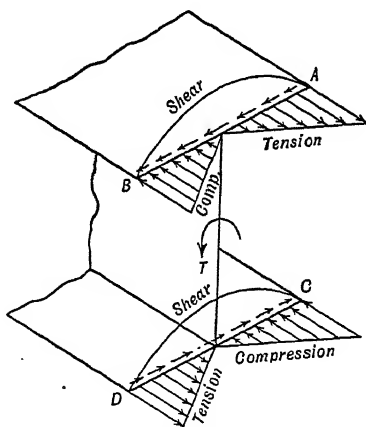


FIG. 16: 11

creases from zero at the free end to a maximum at the fixed end. This situation requires the existence of "secondary shear stress" on each flange. The shear forces in this secondary system must be zero at the free edges of the flanges, and parabolic variation may be assumed between those points. Their resultant is a torsional couple which reduces the torque to be resisted by shear distributed in the primary pattern. The variation in shear implies the presence of normal forces which, in an I-beam, would be anti-symmetrically distributed about the web, as shown in Fig. 16 : 11.

The resultant of the normal forces on the upper flange would be a downward vertical couple, and the resultant of those on the lower

flange would be an upward vertical couple of the same magnitude. The intensity of normal stress at the junctions of the web with the flanges would be zero and there would be no secondary shear or normal stresses acting on the cross-section of the web.

With a channel, however, at the junctions of web and flanges the normal stresses in the web fibers and those in the flange fibers must be of the same intensity. The forces of the secondary system would therefore be distributed as shown in Fig. 16 : 12.

Between *B* and *C* the normal stress varies and must be accompanied by shearing stress of varying intensity. The normal stresses on the web

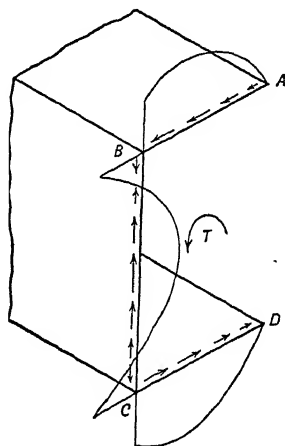


FIG. 16:12a

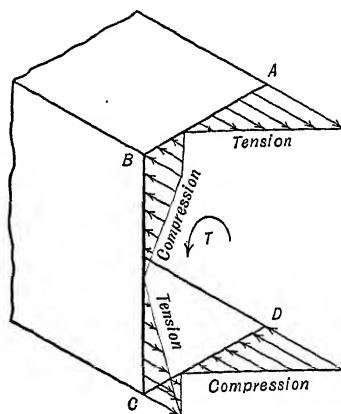


FIG. 16:12b

may be assumed to vary linearly, and their resultant is a couple perpendicular to the web. Since no couple in that direction is included in the assumed external force system, a couple equal and opposite to that in the web must also be included in the internal force system. Such a couple is provided if the intensity of normal stress at *A* and *D* exceeds that at *B* and *C*. Then the resultant of the normal forces on *AB* is a tension in addition to the downward couple, and that of the normal forces on *CD* a compression in addition to the upward couple. This tension and compression constitute a couple perpendicular to the web with the direction and magnitude required.

The secondary shear on the web remains to be considered. These stresses, instead of being distributed as in a rectangular beam subjected to simple bending, are distributed as shown in Fig. 16 : 12a where the shear at *B* and *C* is of opposite sign and double the intensity of that at mid-height. The net area under the curve of Fig. 16 : 12a is zero,

indicating that there is no net shear on the web. It may thus be seen that combination of the normal stresses on the channel cross-section also results in equal and opposite couples, while the secondary shear associated with their variation has as its resultant the torsional couple produced by the secondary shear on the flanges.

Since the objective of the present discussion is primarily to illustrate the nature of the torsion-bending stresses and show why they will be present when the ends of a member subjected to torque are not free to warp, they are considered only qualitatively. For quantitative formulas applicable to I-beams, channels, and similar open sections the reader is referred to Art. 53, Vol. II, of Timoshenko's "Strength of Materials," where the subject is discussed in more detail.

Fortunately for the designer, while the torsion-bending stresses are likely to be comparable to the normal stresses due to bending at the restrained cross-sections, they drop off rapidly and seldom need to be considered in the analysis of other sections. On the other hand, they are produced in closed as well as open sections, and their evaluation for irregular sections is very difficult. L. Lazzarino<sup>1</sup> has developed differential equations for computing their magnitude in a closed shell of arbitrary section, but the solution of those equations is impracticable for routine design work. The problem has also been studied by others, and the recommendations of P. Kuhn, of the N.A.C.A., as outlined in Technical Notes 530 and 691, are followed by many designers, although in the latter report he confesses that what few experimental data there are on the subject do not agree very well with his theory.

The method, as outlined below, is taken almost verbatim from Technical Note 691,<sup>2</sup> which also includes an example of its use.<sup>3</sup>

Consider a rectangular tube symmetrical about both axes, such as that shown in Fig. 16 : 13, and assume the four corner members alone

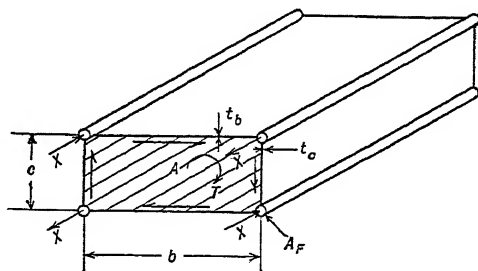


FIG. 16:13

<sup>1</sup> "Twisting of Thin Walled Columns Perfectly Restrained at One End," N.A.C.A. Technical Memo 854, Washington, 1938.

<sup>2</sup> "Some Elementary Principles of Shell Stress Analysis with Notes on the Use of the Shear Center," by P. Kuhn, N.A.C.A. Technical Note 691, Washington, 1939, pp. 24-25.

<sup>3</sup> *Ibid.*, pp. 42-44.

capable of resisting normal forces. The normal force on one of these members that would be produced by complete restraint against warping may be computed from the formula

$$X = \pm 0.56 \frac{T}{A} \left( \frac{b}{t_b} - \frac{c}{t_c} \right) \sqrt{\frac{A_f}{\frac{b}{t_b} + \frac{c}{t_c}}} \quad 16 : 22$$

where the notation is as indicated in the figure. The nature of the force on a given corner member, whether tension or compression, may be determined by the rule that the walls with the smaller ratio of width to thickness tend to act like independent beams, absorbing the torque by bending in opposite directions.

The effect of the end restraint on the shear flow is written most conveniently in the form

$$\Delta q = \pm \frac{T}{2A} \frac{\frac{b}{t_b} - \frac{c}{t_c}}{\frac{b}{t_b} + \frac{c}{t_c}} \quad 16 : 23$$

where  $\Delta q$  is the correction to be applied to the shear flow as determined from Eq. 16 : 8. In Eq. 16 : 23 the minus sign is to be used for the walls with the larger ratio of width to thickness.

In practical design work shells are seldom symmetrical about both axes, as assumed in the derivation of Eq. 16 : 22 and 16 : 23. The simplest method of meeting this situation is to use average values for  $b$ ,  $c$ ,  $t_b$ , and  $t_c$ . This practice is somewhat unconservative, but Eq. 16 : 22 and 16 : 23 are basically conservative because they are derived on the assumption of infinitesimally spaced bulkheads. Furthermore, in practical design complete restraint against warping is seldom if ever encountered, even in continuous wing structures.

The normal stresses determined from Eq. 16 : 22 may be of considerable magnitude, but theoretical studies show that, as one proceeds from a section of complete restraint against warping, the torsion-bending stresses drop off rapidly. In designing wing structures, it is considered desirable to allow for them at the sides of the fuselage, but at the first outboard drag strut or compression rib and at all sections more distant from the plane of symmetry they usually are neglected.

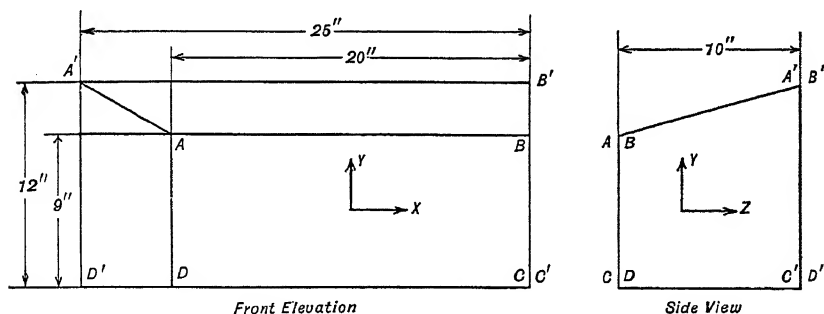
The method of computing these stresses outlined above is not fully satisfactory but is the only one currently available. It is to be hoped that in the near future improved methods will be developed.

**16 : 21. Tapered Shells of Symmetrical Section** — Most shells used for airplane wings and fuselages are not of constant section but are tapered. A part of the total shear on each section is then resisted by a

component of the axial elongation (this term being taken to include both lengthening and shortening) of the material resisting bending, and only a part, instead of the whole, need be resisted by shearing deformation. Completely satisfactory methods for computing the effect of taper have not yet been developed, but it is believed that the procedure proposed below is logical and will give satisfactory practical results.

A constant section shell is analyzed as though it were composed of longitudinal fibers of constant cross-section subjected to axial tension or compression, with shear on both cross-sections and longitudinal planes between fibers but with no lateral compressions or tensions on the latter planes. With taper, either the shell must be treated as if composed of a constant number of tapered fibers or allowance should be made for lateral tensions and compressions. Both lines of attack involve difficulties, but the former appears to be the more likely to lead to a practical and satisfactory design procedure.

Although the shells used in airplane construction are usually curved in section, a study of a flat-sided segment like that shown in Fig. 16 : 14 is more suitable for demonstrating the effects of taper than is an actual



*Segment of Tapered Shell*

FIG. 16:14

fuselage or wing design. This illustrative segment is assumed to be part of a cantilever shell subjected to an upward concentrated load of 12,006 lb., located 10 in. forward of section  $ABCD$  and supported to the rear of section  $A'B'C'D'$ . The figure 12,006 is chosen since it is a common multiple of the section moduli of the two cross-sections shown, and its use facilitates obtaining close checks on the numerical work. The directions of the co-ordinate axes are indicated on the figure.

The distance in the  $Z$  direction between the "rear" cross-section,  $A'B'C'D'$ , and the "forward" cross-section,  $ABCD$ , is 10 in. Therefore, the upper and lower surfaces may be considered divided into tapered "fibers" by planes radiating from a vertical line 40 in. in front



of  $ABCD$ . Similarly, the sides or webs may be considered resolved into fibers by sloping planes radiating from a horizontal line 30 in. in front of  $ABCD$ .

Each fiber may be subjected to a tension or compression acting parallel to its axis, called the "fiber stress," which varies as a function of  $Z$ . In addition to its fiber stress, each fiber may be subjected to shear on its ends and also along the planes separating it from the adjoining fibers. It is assumed, however, that there are no normal stresses acting on the latter planes. It is also assumed that the entire section is fully effective in resisting stress.

Bending moment on a section, such as  $ABCD$ , is resisted by the  $Z$  components of the fiber stresses developed by fiber elongation. In a constant section shell the fiber stresses are all in the  $Z$  direction, and in practical analysis they are assumed to conform to a planar distribution. The equivalent assumption for the analysis of a tapered shell is that the  $Z$  components of the fiber stresses are distributed in planar fashion. The assumption of planar distribution is not precise, even with a constant section shell, and its deviation from the actual distribution is probably greater with a tapered shell. Until, however, a more reasonable or more accurate method of distributing the fiber stresses is developed, it is recommended for practical design. The  $Z$  components of the fiber stresses are therefore obtained from Eq. 6 : 18, which follows directly from the assumption of planar distribution and the principle of equilibrium.

Since the cross-section  $ABCD$  is symmetrical about an axis parallel to the assumed load, Eq. 6 : 18 reduces to Eq. 6 : 2. By the mid-line method of Art. 16 : 1 its moment of inertia is  $40 \times 0.040 \times 4.5^2 + 0.080 \times 729/12 = 37.26 \text{ in.}^4$ , and its section modulus,  $I/y = 37.26/4.5 = 8.28 \text{ in.}^3$ . Thus the  $Z$  component of the fiber stress is  $12,006 \times 10/8.28 = 14,500 \text{ p.s.i.}$  compression along the top and tension along the bottom surface, and varies linearly from  $+14,500$  to  $-14,500 \text{ p.s.i.}$  along the sides. The  $Z$  component per inch of width on the top and bottom surfaces is therefore  $0.040 \times 14,500 = 580 \text{ lb.}$

Owing to its vertical slope, the stress in each fiber of the top surface has a  $Y$  component equal to three-tenths the  $Z$  component, which means that on  $AB$  the fiber stresses include vertical forces amounting to  $580 \times 0.3 = 174 \text{ lb. per in.}$ , or a total of  $20 \times 174 = 3,480 \text{ lb.}$  The slope of the fibers in the "webs" varies from zero at the lower surface to three-tenths at the upper. At any distance,  $y$ , from mid-height, the slope is  $0.15 + y/30$ . Since the  $Z$  component of the fiber stress is  $120,060 y/37.26 = 3,222 y$ , the  $Y$  component is  $3,222 y (0.15 + y/30)$ .

Hence the total of the  $Y$  components of fiber stresses is

$$0.040 \int_{-4.5}^{+4.5} 3,222 y \left( 0.15 + \frac{y}{30} \right) dy = 261 \text{ lb. per web}$$

The resultant of the  $Y$  components of the fiber stresses is therefore a force of  $3,480 + 2 \times 261 = 4,002$  lb. acting midway between the webs.

The  $X$  components of the fiber stresses can be computed in similar fashion. On the top and bottom surfaces they vary uniformly from zero at  $B$  and  $C$  to  $580 \times \frac{5}{10} = 290$  lb. per in. at  $A$  and  $D$ , and act in opposite directions on the two surfaces. The total  $X$  force on each of these surfaces is  $290 \times 20 \times 0.5 = 2,900$  lb., and together they form a couple of  $2,900 \times 9 = 26,100$  in.-lb. There are no  $X$  components on  $BC$ , but on  $AD$  they vary linearly from  $+290$  lb. per in. at  $A$  to  $-290$  lb. per in. at  $D$ . The resultant is a couple of  $290 \times 2.25 \times 6 = 3,915$  in.-lb. The resultant of the couples produced by the  $X$  components of the fiber stresses is therefore

$$26,100 + 3,915 = 30,015 \text{ in.-lb.}$$

$\frac{dv_x}{dx} = C \cdot \downarrow \cdot u$

Since 4,002 lb. of the shear is resisted by  $Y$  components of fiber elongation, only  $12,008 - 4,002 = 8,004$  lb. remains to be resisted by shear deformation. This 8,004 lb., which may be termed the *net shear*  $V_n$ , is distributed over the cross-section

in the manner required to satisfy Eq. 16 : 15 which defines the relation between change in shear flow on a cross-section and the *rate* of change of axial fiber loads. In a constant section shell where  $f = M(y/I)$ , for any fiber  $y/I$  is constant and the rate of change of fiber stress is

$$\frac{\Delta f}{\Delta z} = \frac{\Delta M}{\Delta z} \frac{y}{I} = V \frac{y}{I} = \frac{V}{M} f \quad 16 : 24$$

In a tapered shell  $y/I$  for any fiber varies with  $Z$  and Eq. 16 : 24 is not applicable as it stands. It may be used with shells like that of Fig. 16 : 14 if  $V$  is taken to represent the *net* instead of the *total* shear. This may be demonstrated as follows. In Fig. 16 : 15  $AC$  and  $BD$  represent the axes of a pair of companion fibers, intersecting at  $O$ , which carry a portion,  $dM$ , of the total bending moment on section  $AB$ . For convenience this moment is assumed to be caused by the shear force  $dV$  imposed at  $E$ . If all such pairs of fibers intersect at the distance  $w$  from section  $AB$ , each pair will carry a constant fraction of the total bending

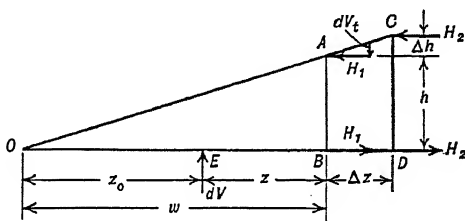


FIG. 16:15

moment, and at section  $CD$  the moment carried by the pair under consideration is  $dV(z + \Delta z)$ . Then the rate of change of the axial fiber load in the direction of the fiber as well as that of its  $Z$  component in the  $Z$  direction may be written

$$\frac{H_2 - H_1}{\Delta z} = \frac{dV(z + \Delta z)}{(h + \Delta h) \Delta z} = \frac{dV z}{h \Delta z} + \frac{h \Delta z + z \Delta h}{h(h + \Delta h) \Delta z} dV$$

By substituting  $\Delta H$  for  $H_2 - H_1$  and  $h(\Delta z/w)$  for  $\Delta h$  and by simplifying, this becomes

$$\frac{\Delta H}{\Delta z} = \frac{w - z}{2(h + \Delta h)} dV = \frac{z_0 dV}{w(h + \Delta h)} \quad b$$

The sum of the vertical components of the fiber loads at  $A$  and  $B$  amounts to  $dV_t = h(H_1/w) = z(dV/w)$ . Then the *net shear* carried by the pair of fibers,  $dV_n = dV - dV_t$ , will be equal to  $z_0 dV/w$ , and

$$dV = w dV_n / z_0 \quad c$$

Substituting Eq.  $c$  in Eq.  $b$  and assuming  $\Delta z$  and  $\Delta h$  to approach zero as a limit gives

$$\frac{\partial H}{\partial z} = \frac{dV_n}{h} \quad 16 : 25$$

Since  $H = dM/h$ ,  $\partial H/\partial z$  can be obtained by multiplying  $H$  by the ratio  $V_n/M$  as stated above.

In the above discussion a single pair of companion fibers is considered, but so long as all such pairs intersect at the same distance,  $w$ , from the cross-section, the results are as applicable to the whole shell and to the resultant shear as to the portion considered. In the shell of Fig. 16 : 14, therefore, the rate of change of shear flow on the cross-section mid-line,  $q'$ , is found by multiplying the  $Z$  component of the fiber stresses per inch width by  $8,004/120,060 = 1/15$ , the ratio of net shear to total bending moment. Thus  $q' = -580/15 = -38.66$  p.s.i. at  $A$  and  $B$ , and  $+38.66$  p.s.i. at  $C$  and  $D$ . From  $A$  to  $D$  and from  $B$  to  $C$ ,  $q'$  varies linearly, while it is constant along  $AB$  and  $CD$ . If the shear flow,  $q$ , is assumed zero midway from  $C$  to  $D$ , computation of the shear forces by the methods of Art. 16 : 10 gives, as the resultant shear forces: zero on the upper and lower surfaces, and a vertical force of 4,002 lb. on each side.

From the above computations the forces on section  $ABCD$  are made up of  $Y$  components amounting to the total shear of 12,006 lb., of which 4,002 lb. is resisted by elongation of the fibers and 8,006 lb. by shear deformation. The resultant of each of these groups of forces lies midway

between the vertical sides of the section. There is also a couple amounting to 30,015 in.-lb., made up of  $X$  components of the fiber forces. The shear center of the section is therefore  $30,015/12,006 = 2.50$  in. to the right of the  $Y$  axis of symmetry. If the 12,006-lb. load were to act opposite the  $Y$  axis of symmetry of section  $ABCD$  it would produce a shear flow of  $12,006 \times 2.5/(2 \times 9 \times 20) = 83.375$  lb. per in., which would increase the shear flow in web  $AD$  and decrease that in  $BC$ .

Two corollaries of the above computations should be noted. The first is that the shear carried at the section by axial elongation of the fibers equals the load which would produce the bending moment on the section if it were applied at the intersection of the upper and lower surfaces. The other is that the shear center is opposite the intersection of the cross-section where the shear is assumed to be applied to the structure and the plane bisecting the dihedral angle between the two sides. Both of these results appear most reasonable and consistent with what is known about tapered beams.

It is not surprising that the taper illustrated in Fig. 16 : 14 causes the shear center to move to the right of the  $Y$  axis of symmetry. The shear center of a thin rectangle is on its axis of symmetry, but, if material is added to its left side to make a channel of the combination, the shear center moves to the right. The effect of taper which involves placing extra material to the left is clearly similar and analogous.

The most apparent defect of the above analysis of a tapered shell is that it is difficult to see just how the  $Y$  components of the fiber stresses in the top surface are generated and transmitted to the fibers by which they are eventually carried. Owing to the variation of section modulus in the  $Z$  direction, the total shear on a cross-section, and hence the shear stress in the web, varies in the  $Z$  direction. Therefore, as one proceeds from section  $ABCD$  to a section to its rear, the shear flow on a horizontal longitudinal section through a web decreases. As a result, normal stresses are developed on these longitudinal sections. They are zero at the bottom and a maximum at the top surfaces. In the shell as shown, the only material available for carrying these  $Y$  forces to the fibers of the top surface midway between the sides is the thin material of the top surface itself. Each transverse strip of this material would appear to be subjected to a uniformly distributed downward load from the fibers and supported at its ends like a simply supported beam. By itself it would hardly be able to withstand the bending produced by this loading unless made much thicker than is normal in airplane construction. What probably happens is that these forces become associated with local stresses and are transmitted from the side walls to the top surface by internal ribs and diaphragms, between which there is buckling

of the skin. Thus, instead of being transmitted to the upper surface continuously, forces are concentrated at the ribs. Little if any study of this problem has yet been made.

On account of symmetry the resultant of the  $X$  components of the fiber stresses in the shell of Fig. 16 : 14 is a couple. Had the shell been unsymmetrical in section, it is probable that this resultant would have been a couple plus a small  $X$  force through the centroid of the section. In practical airplane structures, however, it is unlikely that the resultant of the fiber stresses at a section would have a component normal to the resultant shear on the section of sufficient magnitude to require special attention.

**16 : 22. Practical Analysis of Tapered Shells** — Practical shells are seldom rectangular in section and may differ in other respects from that used in the above example. The procedure to be followed in their analysis would therefore necessarily differ in detail from that of the preceding article, even though based on the same principles. Instead of assuming the material and fiber stresses distributed continuously, it would normally be better to assume them concentrated along a finite number of lines, usually the longitudinal axes of the stiffeners, or along suitable lines parallel to sheet corrugations, depending on the nature of the design. Then instead of dealing primarily with fiber stresses measured in pounds per square inch, the engineer would be more interested in the "fiber force" in pounds acting along each of these "fiber axes." At each cross-section the fiber forces would be found by multiplying the intensity of the  $Z$  component of fiber stress at the intersection of each fiber axis, as obtained from Eq. 6 : 18, by the effective sectional area assigned to the corresponding fiber. The  $X$  and  $Y$  components of the fiber forces could then be computed with the aid of the slopes of the fiber axes, the latter being readily determined from the shell dimensions. The next step would be to subtract the sums of the  $X$  and  $Y$  components of the fiber forces from the corresponding components of the total shear on each cross-section to determine the net shears to be resisted by shear deformation. As in the example of Art. 16 : 5 to 16 : 13, however, it might often prove desirable to assume the material and forces in certain elements, vertical shear webs for example, to be distributed instead of concentrated.

The analysis of the shear forces to determine the shear-flow distribution and the location of the shear or stress center would be very similar to that described above for the constant section shell, and only a few points require special discussion. In determining the change in shear flow between points on a cross-section mid-line, the engineer might either multiply the  $Z$  components of the fiber forces by the ratio of net shear

to bending moment or use the unit method of Shanley and Cozzone. If the latter is employed, he must be careful to recognize that the result of dividing the difference between the end loads on a unit by its length is the *average* change in shear flow across the unit. In a constant section shell the change in shear flow across the ends of a unit are the same as the average, but in a tapered shell this is not true since  $V_n$  varies with  $Z$  although  $V$  may be constant. The nature of this variation can be seen from Fig. 16 : 15 and Eq. c of Art. 16 : 21. Shanley and Cozzone have found, however, that satisfactory results can be obtained if the shear flows obtained by their method are taken as applicable to the cross-section midway between the ends of the units for which they are computed.

Although the  $X$  and  $Y$  components of the fiber forces resist part of the total shear on a section, they are independent of the shear deformation and should be neglected in the computations of the relative slidings of the sides of the imaginary slits for use in the calculation of the correction shear flows. The formula, Eq. 16 : 18, used in the example for computing these movements is not strictly applicable but should serve as a good approximation until a more precise procedure is developed. After the preliminary trial and the correction shear flows have been computed, they should be combined and the magnitude and position of the resultant force determined. The line of application of a force passing through the shear center and parallel to the total shear under investigation can then be found by combining the resultant of these shear flows and the resultant of the  $X$  and  $Y$  components of the fiber forces. The shear center will be at the intersection of the lines of action found in this manner for total shears acting at right angles to each other. The correction shear flow needed to allow for the torque caused by the resultant external force on the section not passing through the shear center can be found by the same procedure as that illustrated for the constant section shell.

It is recognized that the procedure for analyzing tapered shells discussed in this article includes undesirable approximations, and its theoretical basis is not as sound as might be desired. Owing to the paucity of literature on the subject, however, it is considered desirable to present it in the hope that it will encourage further study of the problem.

**16 : 23. Effect of Sudden Change in Section** — Since most stiffened shells are intended to carry bending moments which vary along their lengths, weight is saved by reducing the number or size of the stiffeners in accord with the reduction in moment. While the flanges of stiffening members are often tapered in practice to reduce the abruptness of

the change when a member is discontinued, the parts which are riveted to the skin are usually not tapered, and there is an appreciable change in the geometric properties of the shell when a stiffener is discontinued. The nature of these changes is illustrated in Figs. 16 : 16 and 16 : 17. The former represents a portion of a shell wall having two stiffeners, *A* and *C*, extending its entire length, with a third stiffener, *B*, which is dis-

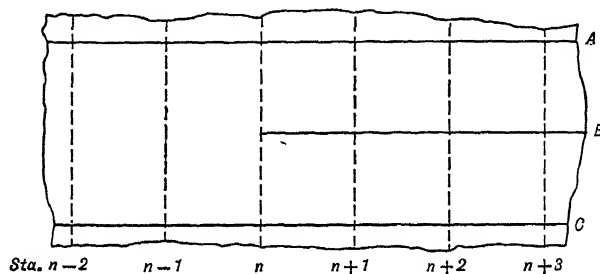


FIG. 16: 16

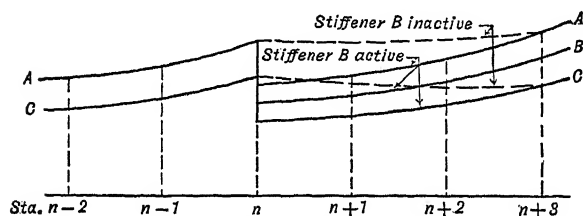


FIG. 16: 17

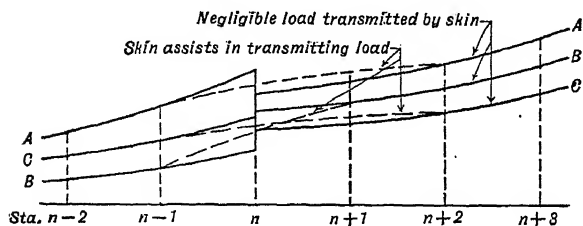


FIG. 16: 18

continued at Station *n*. The broken lines at Stations *n*, *n* + 1, etc., represent transverse stiffening members such as the rings in a fuselage or the capstrips of ribs in a shell wing. The solid curves of Fig. 16 : 17 indicate the variations in axial load in the longitudinal stiffeners as computed by ordinary beam theory. The bending moment is assumed to increase from left to right; and at Station *n* two axial load values are

shown for stiffeners  $A$  and  $C$ , one based on the properties of the section to the right of Station  $n$ , including stiffener  $B$ , the other based on the section without that member. The load curve for stiffener  $B$ , therefore, stops at  $n$ .

According to the curves of Fig. 16 : 17, stiffener  $B$  carries its full share of the load right up to its end at Station  $n$ , where that load is divided between  $A$  and  $C$ . This could happen if the transverse member at  $n$  were infinitely stiff, since it would then act as a beam subjected to a concentrated load at  $B$  and supported at  $A$  and  $C$ . With practical elastic materials, however, some of the load in stiffener  $B$  would be transmitted in this manner, but part would be carried by shear, or by the development of a diagonal tension field, over a finite length of skin. Some of the load would, in all probability, also be transmitted by the bending of the transverse members at Stations  $n + 1$ ,  $n + 2$ , etc. Part may also be carried by an effective "beam," of which the transverse members at Stations  $n$ , and  $n + 1$  are the chords, the skin between those members being the web.

While it is easy to see that the transfer of load into or out of stiffener  $B$  must be accomplished in this general manner, it is difficult to analyze the situation quantitatively even when the sheet and stiffeners all lie in one plane. In the present state of the art, a quantitative analysis on a curved panel is impossible without simplifying assumptions which are often of doubtful accuracy. In practice, curves such as those shown by the broken lines in Fig. 16 : 17 may be drawn for each of the longitudinal stiffeners to "adjust" the loads in the members over a "transition zone" whose length will depend on the judgment of the designer. The design loads for stiffeners  $A$  and  $C$  are thus increased arbitrarily to allow for member  $B$  not carrying the axial load originally computed for it in that region. This adjustment of the stiffener loads should be accompanied by a corresponding change in the shear stresses assumed to act on the skin in the transition zone, and possibly by strengthening the skin in that region so that it may carry the added shear. It may also be necessary to increase the transverse stiffeners to resist the added axial loads produced by the increased shear in the skin.

No general method for handling the problems presented by this type of section change is yet available. In the adjustment shown in Fig. 16 : 17 the entire transition zone lies to the right of Station  $n$ . This is reasonable if stiffener  $B$  be assumed in compression, since little resistance to compression would be offered by the thin skin to the left of  $n$ . If  $B$  were assumed to be in tension, some of the load might well be taken by shear, or by a diagonal tension field, in the panel between Stations  $n$  and  $n - 1$ . If member  $B$  were not discontinued, but were only reduced



in size at Station  $n$ , the transition zone would almost certainly extend on both sides of that station, and the basic axial load curves and their adjustments would be about as shown in Fig. 16 : 18.

**16 : 24. Shear Transfer around Openings**—Some of the most difficult types of section changes are those associated with various openings such as doors, inspection holes, windows, landing wheel wells, and similar discontinuities which are present in all stressed-skin airplanes. The primary objective in the design of the structure around such an opening is to provide whatever reinforcement may be needed to make the reinforced opening as strong and, if practicable, as stiff as the basic structure having neither opening nor reinforcement. The sort of arbitrary adjustment briefly described above may be used for this purpose, but it is difficult to do so with completely satisfactory results. Definite quantitative methods are badly needed but are not yet available. The procedure presented below covers a simple phase of the general problem, and, while it is not presented as a completely satisfactory solution even for that, it does illustrate a line of attack which should prove fruitful when fully developed, and it does show the nature of the problem and the factors involved in its rationalization.

Where covering is removed between transverse or longitudinal stiffeners without cutting them, adequate strength is normally obtained by using "doubling plates" around the opening, that is, by riveting to the main stressed covering around the hole a sheet of the same thickness or of somewhat heavier gage. When stiffeners are cut, a doubling plate usually is used in conjunction with a framed structure riveted around the edges of the hole. The ends of the stiffeners are connected to the frame so that the loads in skin and stiffeners may be transmitted through frame and plate from one side of the opening to the other.

If care be taken to remove stress concentrations near sharp corners in the cut-away area, relatively little difficulty is encountered in proportioning reinforcing members to have the required *strength*. Because of the weight involved it is, however, often impracticable to proportion doubling plates or frames to provide the same *stiffness* as the material removed by the cut-out. On account of using reinforcing members less stiff than a continuous structure would be, the stiffeners which are discontinued are displaced with respect to those which continue around the opening, and they begin to throw off load at some distance from the section where they are cut. They reduce their burden by transmitting load to adjacent members through shear in the sheet, a rather ineffective method where sheets are thin and buckling is not permitted. With very stiff reinforcing frames, normally too heavy to be practicable, stiffener displacements are small and not much of the load in a longitudinal goes

through the skin, no considerable redistribution of normal stress occurs on cross-sections in the vicinity of the cut-out, and no buckling appears in the covering itself. When several longitudinals are cut, or when the reinforcing frame is not excessively stiff, an appreciable redistribution

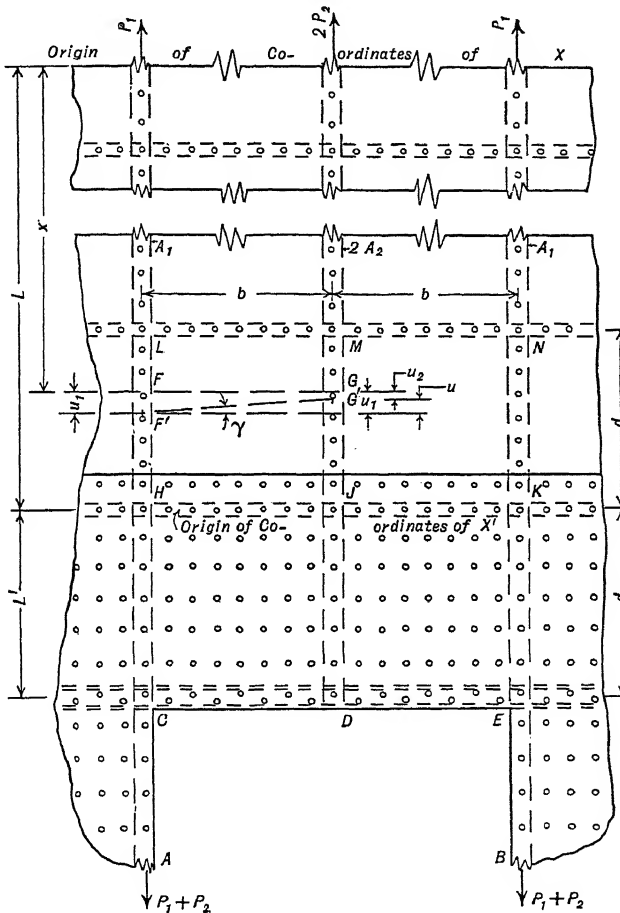


FIG. 16:19

of stress may occur in the vicinity of the cut-out. Under such circumstances it is difficult to prevent the development of shear stresses great enough to cause buckling in some panels of the thin sheet covering.

Where flat sheets and a single discontinuous stiffener are involved, theoretical analyses can be made, with a few simplifying assumptions, to determine the stress in the sheet and the rate of transfer of load

between stiffeners. The procedure which follows presents a rational engineering attack on a simple problem, but students may find that considerable ingenuity is required in extending it to cover particular cases encountered in practice.

Consider the stiffened flat panel shown in Fig. 16 : 19, on which the longitudinal stiffener,  $MJD$ , is assumed to be cut at  $D$ ; the adjacent stiffeners,  $LHA$  and  $NKB$ , to be symmetrically disposed about  $MJD$  and continuous. A part,  $2 S$ , of the tension in  $MJD$  is transmitted to the adjacent stiffeners by the shear in the sheet; a part,  $2 S'$ , by shear in a doubling plate or by bending in the edge-reinforcing member  $CDE$ . For the problem in hand it will be assumed that panel  $HJKEDC$  is reinforced by a doubling plate but that only the skin is used on the structure above stiffener  $HJK$ .

At some distance,  $L$  inches above stiffener  $HJK$ , the relative displacement of the stiffeners and the shear stresses in the sheet will be relatively small. Theoretically, this distance is infinite, but the shear stress in the sheet decays so rapidly that practically the entire load is transmitted from the cut stiffener in a relatively short distance. It is convenient to take the section  $L$  inches from stiffener  $HJK$  as the origin of coordinates, and to represent the load and area of the center stiffener at that section by  $2 P_2$  and  $2 A_2$ . For the side stiffeners at the origin, the corresponding quantities are  $P_1$  and  $A_1$ . Because of the symmetry of the structure half the load in the center stiffener goes to each of the side stiffeners; so the load in sections  $AC$  and  $BE$  of the side stiffeners is  $P_1 + S + S' = P_1 + P_2$ .

Points  $F$ ,  $G$ ,  $x$  inches from the origin will be displaced to  $F'$ ,  $G'$  when the stiffener  $LHA$  elongates  $u_1$  inches under load, while the center stiffener which carries a smaller tensile stress elongates  $u_2$ . The line  $FG$  in the unloaded panel thus becomes  $F'G'$  in the loaded. The shear strain would vary along  $FG$ , but no practical method of taking its variation into account has yet been developed. Therefore, the shear strain at every point along that line is assumed to be represented by the angle  $\gamma = u/b$ .

Since the shear stress,  $f_s$ , equals  $G\gamma$ , one may write  $f_s = Gu/b = G(u_1 - u_2)/b$ . By writing  $f_1$  and  $f_2$  as the unit tensile stresses in the stiffeners at the origin,  $f_1 = P_1/A_1$ ,  $f_2 = P_2/A_2$ . At a section  $x$  inches from the origin

$$f_1 = \frac{P_1}{A_1} + \int_0^x \frac{f_s t dx}{A_1} = \frac{E du_1}{dx} \quad 16 : 26$$

$$f_2 = \frac{P_2}{A_2} - \int_0^x \frac{f_s t dx}{A_2} = \frac{E du_2}{dx} \quad 16 : 27$$

But  $u = u_1 - u_2$ ; so  $du/dx = du_1/dx - du_2/dx$ . Then

$$\frac{du}{dx} = \frac{1}{E} \left[ \frac{P_1}{A_1} + \int_0^x \frac{f_s t}{A_1} dx - \frac{P_2}{A_2} + \int_0^x \frac{f_s t}{A_2} dx \right]$$

On substituting  $f_s = Gu/b$ , this becomes

$$\frac{du}{dx} = \frac{1}{E} \left( \frac{P_1}{A_1} - \frac{P_2}{A_2} \right) + \frac{Gt}{bE} \left( \frac{1}{A_1} + \frac{1}{A_2} \right) \int^x u dx$$

Writing  $k^2$  for  $\frac{Gt}{bE} \left( \frac{1}{A_1} + \frac{1}{A_2} \right)$  and differentiating the above equation with respect to  $x$  gives

for which the solution is

$$u = C_1 \sinh kx + C_2 \cosh kx \quad 16 : 29$$

where  $C_1$  and  $C_2$  are constants to be determined from the boundary conditions.

At  $x = 0$ ,  $u = 0$ , and at  $x = L$ ,  $u = u_L$ , whence  $C_2 = 0$  and  $C_1 = \frac{u_L}{\sinh kL}$ . The displacement  $u$  at any section  $x$  becomes

$$u = \frac{u_L \sinh kx}{\sinh kL} \quad 16 : 30$$

and, since  $f_s = Gu/b$ , the corresponding shear is

$$f_s = \frac{u_L \sinh kx}{b \sinh kL} \quad 16 : 31$$

The total force,  $S$ , transmitted by shear in the sheet from the center stiffener to either side in the distance  $x$  is  $S = \int_0^x f_s t dx$ , whence

$$S = \frac{Gu_L t}{b} \int_0^x \frac{\sinh kx}{\sinh kL} dx = \frac{Gu_L t \cosh kx - 1}{bk \sinh kL} \quad 16 : 32$$

Equation 16 : 32 would give the magnitude of  $S$  for any value of  $x$  if only  $L$  were known. By substituting  $L$  for  $x$ , the equation may be written  $S = \frac{Gu_L t}{bk} \left( \frac{\cosh kL}{\sinh kL} - \frac{1}{\sinh kL} \right)$ , or  $S = \frac{Gu_L t \eta}{bk}$ , where  $\eta = \coth kL - \operatorname{csch} kL$ . Numerical values of  $\eta$  are listed in Table 16 : 15.

Since, in general, the shear flow  $q = f_s t$  and in this problem  $f_s = Gu/b$ , the expression for the total shear transmitted by the sheet in the length,  $L$ , may be simplified to  $S = (q_L/k)\eta$ . If the maximum shear flow in the

skin alone be at stiffener  $HJK$  and have the intensity  $q_m$ , this total shear may be taken as equal to  $q_m/k$ , provided a large enough value be assumed for  $L$  so that  $\eta$  is approximately 1.0. Ninety per cent of this amount would be so transmitted if the origin were  $3/k$  inches from stiffener  $HJK$ , 96.4 per cent if  $L$  were  $4/k$  inches, 98.7 per cent if  $5/k$ , and 99.5 per cent when  $L$  is  $6/k$  inches. For practical design purposes a force  $S = q_m/k$  may be assumed to be transferred from the discontinued stiffener if it extend a distance  $L = 6/k$  inches.

It is seldom that the full load carried by the stiffener at the origin can be transmitted to the adjacent members through the skin in any reasonable distance,  $L$ . With members of normal proportions a major

TABLE 16 : 15  
VALUES of  $\eta = \coth kL - \csc kL$

$kL$	2	3	4	5	6
$\eta$	0.7616	0.9052	0.9638	0.9866	0.9951

part of the load  $2P_2$  will be transmitted in the panel next to the opening, the panel which is usually reinforced by a "doubling plate." The equations just developed will therefore have to be applied once to the part of the stiffener to which only the skin is attached and again to the part in the reinforced panel. If the shear stresses become great enough in either part to cause buckling, further applications will be needed with a reduced value of  $G$ , taken from Fig. 15 : 5, in the tension-field zones. Since it is aerodynamically desirable to have no buckles around openings, designers should proportion doubling plates to carry the loads required of them without buckling.

When tension fields are permitted to develop, the accuracy of this method is doubtful since  $k$  is a function of  $G$  and both the stress  $f_s$  and the transmitted load  $S$  are functions of  $k$ . Even where  $G$  is constant it may be necessary to obtain the solution of a practical problem by trial and error procedure, first with the effective areas  $A_1$  and  $A_2$  assumed constant along the length of the stiffener, then with corrected or averaged values obtained from the stress distribution indicated by the first approximate solution. Furthermore, since this method is based upon relative displacement of the members, cross-sections of a structure which would remain planar under ordinary conditions of bending will be warped by the displacement of the stiffeners near an opening. Some adjustment of stresses in members may therefore be required in the transition zone, and, since no rational method exists for making such adjustments, the somewhat arbitrary procedures suggested in Art. 16 : 23 will prove helpful. For sections beyond the origin, where  $x$  would be

negative, the displacements are negligibly small, cross-sections remain planar, and the ordinary beam theory applies as well as it ever does in a stressed-skin structure.

When more than one stiffener is cut at a given section, the problem of setting up the equations for shear flow in the transition zone becomes complicated since its solution requires a series of simultaneous equations involving the loads in and deflections of each stiffener. It is probably best, under such circumstances, for the engineer to assume a distribution of load in each stiffener and of displacements along the stiffeners. Then, by applying the principles employed in developing the formulas for the simple case, he may make trial and error adjustments until he is satisfied that he has a satisfactory distribution.

If the sheets are curved instead of flat, the shear modulus  $G$  and the critical stress  $f_{s_{cr}}$  must be adjusted for the curvature of the panels. When curved stiffeners are used as reinforcing members around the edges of openings, it must also be remembered that their deflection is the resultant of torsion and bending in the member.

The real unknown in the normal practical problem is the thickness of the doubling plate required to reinforce the panel or panels near the opening. In some cases the stiffness of the frame at the edge of the opening is sufficient to transmit some of the stiffener load by bending. In most practical designs, however, the load carried in this way is small, in many designs it is negligible, but the engineer must determine whether such load is appreciable or negligible if he is to use his material advantageously.

In the article which follows an example is worked to show how some of the difficulties involved in transmitting shear stresses around openings may be handled when the problem is that of a simple flat panel having one discontinuous stiffener. The method presented can doubtless be improved. It can probably be extended to somewhat more complicated problems also; but, before a completely satisfactory solution can be developed for the general case of shear around openings, more data on the physical properties in shear of sheets having single or double curvature must be on hand than have been made available to designers up to the present time.

**16 : 25. Illustrative example** — Consider a flat panel similar to that shown in Fig. 16 : 19, having the dimensions and properties shown in Table 16 : 16.

From Eq. 6 : 6, or 15 : 7, the critical shear stress for a 6- by 9-in. panel is,

$$f_{s_{cr}} = \frac{7.1 \pi^2 E t^2}{10.92 b^2} = 1,147 \text{ p.s.i.}$$

Then the maximum shear flow possible without buckling is  $q_m = 1,147 \times 0.025 = 28.7 \text{ lb. per in.}$  and the load

transmitted from the center to each side stiffener, when the lower end of the panel is about to buckle, is  $S = q_m/k$  or 178 lb. This is but a small part of the load,  $2P_2$ , in the cut stiffener, and there is a load  $2S' = 2(P_2 - S) = 2,344$  lb. to be transmitted through a doubling plate on the end panel or through the end panel acting as a beam.

If, as a first approximation, the assumption is made that the 178 lb. is transmitted above point  $J$ , and that  $2,344/2 = 1,172$  lb. is to be transmitted through the reinforced panels on each side of the stiffener

TABLE 16:16

$d = 9$ in.	$E = 10,300,000$ p.s.i.
$b = 6$ in.	$G = 3,840,000$ p.s.i.
$t = 0.025$ in.	$L$ assumed to be $6/k$
$P_1/A_1 = 15,000$ p.s.i.	$P_2/A_2 = 15,000$ p.s.i.
$A_1 = 0.18$ sq. in., area of side stiffeners with effective sheet	
$A_2 = 0.09$ sq. in., area of one-half center stiffener and effective sheet	
$P_1 = 2,700$ lb.	$P_2 = 1,350$ lb.
$\nu = 0.0259$	$k = 0.161$

$JD$  in its 9-in. length, the average shear flow will be  $1,172/9 = 130.2$  lb. per in. At  $J$  the shear flow is 28.7 lb. per in., so that the maximum at  $D$  would be  $2(130.2) - 28.7 = 231.6$  lb. per in. if the shear were assumed to vary linearly. Then  $231.6 = q_m = f_{s_{cr}} t = K\pi^2 Et^3/10.92 b^2$ . For the same ratio of panel length to width,  $9/6 = 1.5$ ,  $K = 7.1$ , and  $t$  becomes  $(231.6 \times 10.92 \times b^2/K\pi^2 E)^{1/3} = 0.0502$  in. Since an 0.051-in. sheet thickness is a standard size, and since the original 0.025-in. skin will carry some of the load, it is reasonable, for the first trial at least, to assume the doubling plate to be an 0.051-in. aluminum alloy sheet.

The critical shear stress for the 0.051-in. plate is then  $f_{s_{cr}} = 7.1 \pi^2 Et^2/10.92 b^2 = 4,775$  p.s.i. Since it is desirable to keep the intensity of the shear stress in the skin adjacent to stiffener  $HJK$  below  $f_{s_{cr}}$  for the skin, if buckling is to be prevented above the stiffener, and since it is necessary to keep the stress below 4,775 p.s.i. in the panel having the doubling plate if that is not to buckle, we have 9 in. of panel,  $0.025 + 0.051 = 0.076$  in. thick which must carry a mean stress somewhere between 1,147 and 4,775 p.s.i. Were the stress to vary linearly as assumed above, the mean stress would be  $(1,147 + 4,775)/2 = 2,961$  p.s.i., and the load taken out of the stiffener on each side would be  $9 \times 0.076 \times 2,961 = 2,025$  lb.

This is nearly twice the 1,172-lb. load to be transmitted, but the deformation of stiffeners and sheet in panel  $HJKEDC$  under load is probably not compatible with a straight-line variation in the shear stress. It is

therefore necessary that the variation be determined so that the load transmitted from the stiffener  $JD$  may be computed more accurately.

If the doubling plate be carried somewhat beyond stiffener  $HJK$  so that it may be counted upon to act as effective material with the skin and longitudinal stiffeners, both  $A_1$  and  $A_2$  are increased in the panel having the doubling plate. The exact width effective is indeterminate at this stage, but the stresses in the stiffeners at  $H$ ,  $J$ , and  $K$  will not be greatly different from 15,000 p.s.i. whatever this width may be.

Since the stiffeners are subjected to tension, the sheet to which they are attached might well be assumed fully effective between stiffeners, giving an effective area equal to  $6 \times 0.051$ , or 0.306 sq. in., to be added to  $A_1$ . Half as much, or 0.153 sq. in., would be added to  $A_2$ . Were the stiffeners carrying a 15,000-p.s.i. compressive stress, the effective width, as computed from Eq. 6 : 24, would be  $1.7 \times 0.051 \sqrt{10,300,000/15,000} = 2.27$  in., and the effective area to be added to  $A_1$  would be  $2.27 \times 0.051 = 0.116$  sq. in. Neither of these effective areas would be correct where the sheet is carrying shear stresses, since the exact behavior of sheet and stiffeners would then depend on the lateral strains in the panel as well as on the longitudinal. Pending the development of effective width formulas applicable to such conditions, it would seem desirable to use widths near those expected when the stiffeners are in compression, whether they be in tension or compression. Although the reduction involved is larger than would appear necessary in this instance, the stresses in the sheet and the loads transmitted between stiffeners are not affected in the same proportion. In the computations which follow, the effective width is taken as that indicated by Eq. 6 : 24 for a 15,000-p.s.i. compressive load in the stiffeners. This adds 0.116 sq. in. to  $A_1$ , 0.058 sq. in. to  $A_2$ , making them 0.30 and 0.15 sq. in., respectively.

Greater effective widths, say two-thirds or three-quarters of the distance between stiffeners, might be justified for the problem in hand, but these will do for the present approximation. They yield interesting results since they indicate what would happen had the stiffeners been in compression instead of in tension.

Basing  $(k')^2$  on the total thickness of skin and doubling plate,  $(k')^2 = \frac{3,840,000 \times 0.076}{6 \times 10,300,000} \left( \frac{1}{0.30} + \frac{1}{0.15} \right) = 0.04725$ ,  $k' = 0.217$ . In taking the line  $HK$  on the boundary  $HJK$  of panel  $HJKEDC$  as a new origin, the length of the panel is 9 in., so that  $k'L' = 1.953$ , giving  $\sinh k'L' = 3.454$  and  $\cosh k'L' = 3.596$ .

From Eq. 16 : 29,  $u' = C_3 \sinh k'x' + C_4 \cosh k'x'$ , and from the equation preceding Eq. 16 : 28,  $du'/dx' = \frac{1}{E} \left( \frac{P_H}{A_H} - \frac{P_J}{A_J} \right)$  when  $x' = 0$ .



The deflection at the origin for panel *HJKEDC* will be equal to the deflection of the panel above; that is,  $u'_0 = u_L = f_s b/G$ , where  $f_s$  represents the stress in the skin just above stiffener *HJK*. Then  $f_s b/G = C_4 \cosh 0$ ; so  $C_4 = f_s b/G$ . Furthermore, when  $x' = 0$ ,  $du'/dx' = C_3 k' \cosh k'x' + C_4 k' \sinh k'x' = \frac{1}{v} \left( \frac{P_H}{A_H} - \frac{P_J}{A_J} \right)$ . But  $P_H = P_1 + \frac{f_s t}{k}$

and  $P_J = P_2 - \frac{f_s t_s}{k}$ ; so  $\frac{1}{E} \left( \frac{P_1 + \frac{f_s t_s}{k}}{A_H} - \frac{P_2 - \frac{f_s t_s}{k}}{A_J} \right)$  is equal to  $C_3 k' \cosh 0$ . Since, for this problem,  $P_1 = 2 P_2$  and  $A_H = 2 A_J$ , the expression for  $C_3$  simplifies to  $C_3 = \frac{1}{k'E} \left( \frac{3 f_s t_s}{2 A_J k} \right)$  where  $f_s$  is the shear in the skin of thickness  $t_s$  just above the stiffener *HJK*.

The shear stress in panel *HJKEDC* is  $f'_s = Gu/b$ . The force to be transmitted from the center stiffener to each side stiffener in the length of the panel is  $P_2 - \frac{f_s t_s}{k}$ , which also equals  $S' = \int_0^{L'} f'_s t_t dx'$ . Then, using  $f'_s$  for the shear stress, and  $S'$  for the load transmitted through the sheet in panel *HJKEDC*, and writing  $t_t = t_s + t_d$ , the thickness of the skin plus the thickness of the doubling plate,

$$f'_s = \frac{G}{b} (C_3 \sinh k'L' + C_4 \cosh k'L') \quad , \quad 16 : 33$$

$$S' = P_2 - \frac{f_s t_s}{k} = \frac{G t_t}{b} \left[ \frac{C_3}{k'} (\cosh k'L' - 1) + \frac{C_4}{k'} \sinh k'L' \right] \quad 16 : 34$$

For the problem in hand, it is desired to transmit a load  $S' = P_2 - (f_s t_s/k)$  without having  $f'_s$  exceed  $f'_{s_{cr}} = 4,775$  p.s.i. for the 0.051-in. doubling plate near stiffener *CDE*, or  $f_s$  exceed  $f_{s_{cr}} = 1,147$  p.s.i. for the skin near stiffener *HJK*. Since  $C_4 = f_s \times 6/3,840,000 = 0.00000156 f_s$  and  $C_3 = [3 \times 0.025/(0.217 \times 10,300,000 \times 0.30 \times 0.161)] f_s = 0.000000695 f_s$ , if  $P_2$  is to be 1,350 lb.,  $f_s$  as given by Eq. 16 : 34 becomes 763 p.s.i., thus showing that the load in the center stiffener can be transmitted without exceeding the critical stress and without producing buckling in the skin above stiffener *HJK*. When this value of  $f_s$  is introduced in the expressions for  $C_3$  and  $C_4$ , the magnitude of  $f'_s$ , as computed from Eq. 16 : 33, is 3,920 p.s.i. This is less than  $f'_{s_{cr}}$  for the doubling plate and indicates that the load can be transmitted without buckling the doubling plate in panel *HJKEDC*. It is possible that a lighter doubling plate could be used.

The real unknowns in this problem are the doubling plate thickness,

$t_d$ , and the shear stress,  $f_s$ , in the skin just above the panel to which the doubling plate is attached. Since  $k'$  depends upon  $t_t = t_s + t_d$ , and since hyperbolic sine and cosine functions of  $k'x'$  are involved in the equations, a direct solution of  $t_d$  appears impossible. For the problem in hand, however, the approximate determination for the thickness of the doubling plate resulted in a sheet of reasonable thickness and one which proved upon further investigation to be slightly stronger than necessary. It is probably desirable that some positive margin be provided since the computations have been based on constant and rather arbitrary effective areas for sheets and stiffeners in the panel, although it is to be expected that the effective area of sheet acting with stiffener  $JD$  will increase as the stress is reduced, while the effective areas of sheet acting with stiffeners  $HC$  and  $KE$  will be reduced as the stresses in those members increase. Such margin does not have to be large, however, because no account has been taken of the resistance of the transverse stiffeners to bending or of the effect of having the doubling plate extend at least one panel width beyond stiffeners  $HC$  and  $KE$ . Provision for such factors could be made during the second trial computation, using this or a thinner doubling plate, but it seems unnecessary to present the figures here.

In order that the 0.025 skin may withstand a maximum shear stress without buckling equal to  $f'_{scr}$  for the doubling plate, it must be riveted to the latter with a pitch small enough so that waves will not form between the lines of rivets at some lower stress. No general method is available, however, for predicting the pitch required, because the shape of the waves formed depends on the angle between the principal compressive stress and the rivet lines, on the degree of restraint provided by the rivet heads, and on similar factors.

When the longitudinal and transverse stresses in the skin are negligible, as in the problem under consideration, and when the shear stress is uniformly distributed, the compressive stress which tends to produce the waves acts at  $45^\circ$  to the direction of the shear forces and is equal to the shear stress in intensity. It would act in the direction of line  $BB$  in Fig. 16 : 20, and if the horizontal and vertical pitch of the rivets were the same, the principal compressive stress would act along lines perpendicular to lines such as  $AA$  connecting groups of rivets. When waves form in the skin under these conditions, their crests and troughs are parallel to  $AA$  and they buckle *away* from the doubling plate as indicated for Section  $B-B$  in Fig. 16 : 20. Strips of skin parallel to  $BB$  buckle into a series of waves, each of which is analogous to a fixed-ended column of length,  $L_r$ .

In order to be on the conservative side, let us assume the strips to

behave as pin-ended columns of length,  $L_r$ . Since the critical compressive stress for such a column is to equal the critical shear stress for the doubling plate,  $f'_{scr.}$  may be set equal to  $\pi^2 E / [(1 - \mu^2)(L_r/\rho)^2]$ , where  $\rho^2 = t_s^2/12$  for the skin. Substituting for  $\rho^2$  and solving for  $L_r$  yields

$$L_r = 0.95 t_s \sqrt{E/f'_{scr.}} \quad 16 : 35$$

For the problem under consideration, the distance between rows of rivets, measured at  $45^\circ$  to the direction of stiffener  $JD$ , would be  $L_r = 0.95 \times 0.025 \sqrt{10,300,000/4775} = 1.105$  in. To obtain this pitch

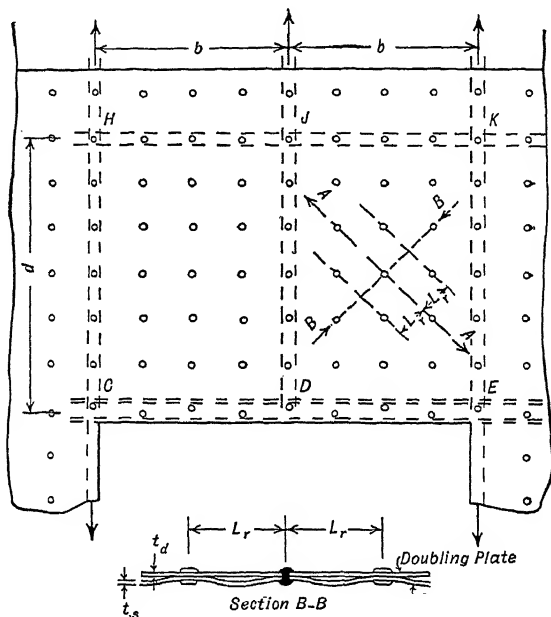


FIG. 16:20

along the  $45^\circ$  lines would require a pitch of  $1.105\sqrt{2}$ , or 1.56 in. along lines parallel to the longitudinal and transverse members. Such an arrangement is indicated in Fig. 16 : 20.

There are no test data to vindicate the assumptions made in this method of obtaining the required pitch, but it appears to be reasonable, somewhat conservative, and for this problem at least it gives quite satisfactory results. A somewhat greater allowable pitch would result were the maximum shear stress, 3,920 p.s.i., obtained from Eq. 16 : 33, substituted for  $f'_{scr.} = 4,775$ . The 1.56-in. pitch obtained above is, however, about sixty times the thickness of the skin and is somewhat

high for the distance between supports on a thin, highly stressed sheet such as this.

When other tensile or compressive stresses are present in the skin, the maximum principal compressive stress and its angle must be determined and Eq. 16 : 35 modified so that  $L_r$  represents the wave length along the line of that stress. A rivet pattern may then be evolved to insure that the distance between rivets shall be less than  $L_r$  along that line. Normal airplane design requires that provision be made for several combinations of loading, and it is not always an easy matter to arrange rivets in a pattern to cover all cases without involving the use of an impractical spacing or number of rivets.

As knowledge of the manner in which loads are transmitted by shear increases, improvements undoubtedly will be made upon the above methods for dealing with discontinuous members and shear around openings. As presented here, they provide a sound procedure for attacking such problems, however, and it is hoped that they may be of use to designers and stress analysts.

## PROBLEMS

16 : 1. Check the values of  $\Delta s/t_e$  shown in Table 16 : 1.

16 : 2. Fill in as much as necessary of the omitted lines of Table 16 : 5 and check the values shown in that table for (a)  $\Sigma Ax$ , (b)  $\Sigma Ay$ , (c)  $\Sigma Ax^2$ , (d)  $\Sigma Ay^2$ , (e)  $\Sigma Axy$ .

16 : 3. Fill in as much as necessary of the omitted lines of Table 16 : 6 and check the values shown in that table for (a)  $\Sigma Ax$ , (b)  $\Sigma Ay$ , (c)  $\Sigma Ax^2$ , (d)  $\Sigma Ay^2$ , (e)  $\Sigma Axy$ .

16 : 4. Fill in as much as necessary of the omitted lines of Table 16 : 9 and check the values shown in that table for (a)  $\Sigma P$ , (b)  $\Sigma Px$ , (c)  $\Sigma Py$ , (d)  $\Sigma Q$ .

16 : 5. Fill in as much as necessary of the omitted lines of Table 16 : 11 and check the values shown in that table for (a)  $\Sigma q_0 \Delta x$ , (b)  $\Sigma q_0 \Delta y$ .

16 : 6. Fill in as much as necessary of the omitted lines of Table 16 : 12 and check the values shown in that table for (a)  $\Sigma q \Delta y$ , (b)  $\Sigma qx \Delta y$ .

16 : 7. Fill in as much as necessary of the omitted lines of Table 16 : 13 which pertain to the front cell and check the values in that table for (a)  $\Sigma q_0 \Delta s/t_e$ , (b)  $\Sigma q_e \Delta s/t_e$ .

16 : 8. Carry out the same operations as in Prob. 16 : 7, but for the rear cell.

16 : 9. Fill in as much as necessary of the omitted lines of Table 16 : 13 and check the values shown in that table for (a)  $\Sigma q_e \Delta x$ , (b)  $\Sigma q_e \Delta y$ .

16 : 10. Check the value shown in the text for  $\oint_{t_e} \frac{q_0}{t_e} ds$  for the rear shear web.

16 : 11. Fill in as much as necessary of the omitted lines of Table 16 : 14 and check the values shown in that table for (a)  $\Sigma -\bar{y} q_e \Delta x$ , (b)  $\Sigma x q_e \Delta y$ .

16 : 12. Compute the shear flows associated with the shear and bending moment of the illustrative example of Arts. 16 : 5 to 16 : 12 in the manner suggested in Art. 16 : 12.

**16 : 13.** Check the magnitude and location of the resultant of the shear flows of Prob. 16 : 12 with the basic data of that problem.

**16 : 14.** Using the data obtainable in Art. 16 : 25, determine the effective areas of skin and doubling plate at  $H$  and  $C$ ,  $J$  and  $D$ ,  $K$  and  $E$ . Base the effective areas of each sheet and stiffener combination on the respective averages and determine  $f'_s$  and  $S'$ . Do you regard the difference in maximum shear stress obtained in this way sufficient to justify making further approximations?

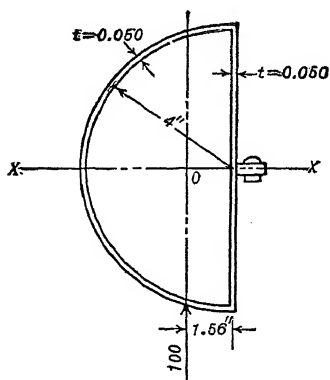
**16 : 15.** Using the loads and structure of Art. 16 : 25, check the practicability of an 0.045-in. doubling plate where no buckling is to be tolerated on skin or doubling plate.

**16 : 16.** An aileron spar is made up of a semicircular shell with a web at the diameter of the semicircle as shown. The centroid of the section is at 0.

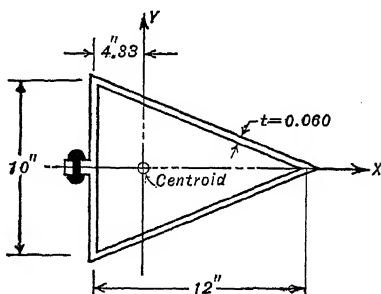
$$I_{xx} = 7.155 \text{ in.}^4$$

$$I_{yy} = 2.542 \text{ in.}^4$$

Assuming a vertical force of 100 lb. acting through the center of gravity, and assuming  $M_{xx} = 10,000 \text{ in.-lb.}$ ,  $M_{yy} = 0$  at this section, set up the expression for, and determine the location of the shear center of the section. (Neglect the riveted flange entirely.) For semicircle,  $(x - 1.56)^2 + y^2 = 4^2$ , taking origin at 0.



PROB. 16:16



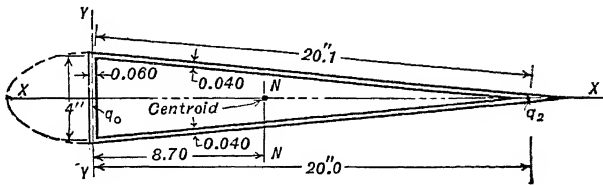
PROB. 16:17

**16 : 17.** An aileron spar is formed from 0.060-in. 24-ST aluminum alloy sheet into a triangular shape as shown. Neglecting the effect of the riveted flange entirely in computing strengths and section properties, find the position of the shear center for the section assuming a vertical force of 100 lb. acting along the  $Y$ -axis, no horizontal force along the  $X$ -axis, a bending moment of 10,000 in.-lb. acting in the plane of the  $Y$ -axis, no moment in the plane of the  $X$ -axis.

$$14.75 \text{ in.}^4 \quad I_{yy} = 15.90 \text{ in.}^4 \quad K = 0.$$

**16 : 18.** At the cross-section of an aileron, shown above, a vertical shear force of 200 lb. acts upward through the shear center. The aileron is made of 24-ST

aluminum alloy sheet and there are sufficient ribs used to maintain the shape of the section. Determine the magnitudes of the shear forces  $q_0$  and  $q_2$ , and the position of the shear center.

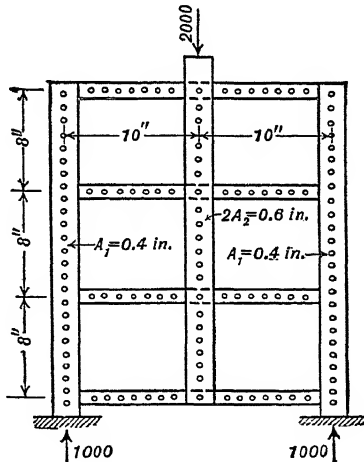


$$\Delta s = 1.005 \Delta x = 10.05 \Delta y \text{ on sloping surfaces}$$

$$I_{xx} = 2.47 \text{ in.}^4 \quad I_{yy} = 74.6 \text{ in.}^4$$

PROB. 16:18

16:19. An aluminum alloy sheet,  $E = 10^7$ ,  $G = 4 \times 10^6$ , is 0.025 in. thick. It is stiffened as shown, the transverse stiffeners being adequate to carry their loads without buckling. Will the sheet transmit the 2,000-lb. load from the center stiffeners to the side stiffeners without buckling the sheet?



PROB. 16:19

16:20. A wing contour forward of the rear web is defined by the following table of ordinates:

Sta. = x	0	8	12	16	24	33
y Upper	0	4.90		6.92	8.25	8.95
y Lower	0		-6.00		-8.25	
Sta. = x	36	42	48	51	60	
y Upper		8.81		7.83	6.00	
y Lower	-9.00		-8.25		-6.00	

Associated with each of the points located by the table of ordinates is a wood stiffener. The centroid of each stiffener may be taken as having the same X co-ordinate as the

point on the skin, but 0.60 in. closer to the  $X$  axis; except that the stiffener at the nose will have its centroid at  $x = 1.00$ ,  $y = 0$ .

Assume: Curved skin  $\frac{1}{8}$  in. thick,

Web at Sta. 60 is  $\frac{1}{8}$  in. thick,

Area of nose stiffener = 2.00 sq. in.

Area at each other stiffener = 1.50 sq. in.

Skin, and web at Sta. 60, incapable of carrying normal stress, any effective area being included in the specified figures for the stiffeners.

Draw sketch of section with stiffeners to  $\frac{1}{8}$  or  $\frac{1}{16}$  scale.

Determine: total area of section effective against normal stress; location of centroid of section;  $I_{xx}$ ,  $I_{yy}$ , and  $I_{xy}$  about axes through the centroid.

**16 : 21.** Assume the shell of Prob. 16 : 20 subjected to an 8,000-lb. force in the  $Y$  direction directed upward and causing a bending moment of 600,000 in.-lb. It is simultaneously subjected to a 2,000-lb. force in the  $X$  direction directed toward the leading edge and causing a bending moment of -100,000 in.-lb.

*a.* Compute the normal stress and axial load on each stiffener.

*b.* Compute the shear flow in each skin panel, assuming  $q = 0$  in the upper skin between Stas. 24 and 33, and indicate the resulting shear flow diagrammatically.

In part *a* carry out the following steps:

1. Compute normal stress,  $f$ , and load on each stiffener,  $P$ , by use of Eq. 6 : 18.

2. Compute  $f$  due to  $M_{xx} = 8,000$  in.-lb. by use of Eq. 6 : 18.

3. Compute  $f$  due to  $M_{yy} = -2,000$  in.-lb. by use of Eq. 6 : 18.

4. Add results of steps 2 and 3 to get increase per inch of normal stress and multiply by stiffener areas to get  $\Delta P$  the increased axial load in each stiffener.

In part *b* use the values of  $\Delta P$  from part *a* to compute  $q$ .

**16 : 22.** Assume that a  $\frac{1}{8}$ -in. thick vertical web is added to the shell of Prob. 16 : 20 at Sta. 24. Compute the shear flow pattern for the loading of Prob. 16 : 21, assuming that  $q = 0$  in the upper skin panels 8-16 and 42-51.

**16 : 23.** *a.* Find the included area of each of the cells forming the shell section of Prob. 16 : 22.

*b.* Assume the section of Prob. 16 : 21 (no web at Sta. 24) subjected to a counter-clockwise couple of 240,000 in.-lb. Determine the shear flow produced by this couple and the combined effect of this couple and the loading of Prob. 16 : 21.

**16 : 24.** Find the shear flow on the shell of Prob. 16 : 22 due to the combination of the torsional couple of Prob. 16 : 23 and the loading of Prob. 16 : 22.

**16 : 25.** *a.* Where will the resultant of the shear flows obtained in Prob. 16 : 21 intersect the axis of symmetry of the skin?

*b.* Where will the resultant of the shear flows obtained in Prob. 16 : 23 intersect the axis of symmetry of the skin?

**16 : 26.** Determine the shear flow in each cell of the shell of Prob. 16 : 22 that would be produced by a counter-clockwise couple of 240,000 in.-lb.

**16 : 27.** *a.* Locate the abscissa of the shear center of the shell of Prob. 16 : 22.

*b.* Locate the ordinate of the shear center of the shell of Prob. 16 : 22.

**16 : 28.** Assume all the shell of Prob. 16 : 20 to the rear of Sta. 24 and all the stiffeners except those at Sta. 1 and 24 removed, thus leaving a shell with three webs and three stiffeners. Assume the resultant force on the section made up of a  $Y$  force of +4,000 lb. and an  $X$  force of +1,000 lb. passing through  $x = +16$ ,  $y = +2$ . Determine the resulting shear flow in each segment of skin.

**16 : 29.** Locate the shear center of the shell of Prob. 16 : 28.

## CHAPTER XVII

### CURVED BEAMS AND RINGS

The determination of the magnitude and distribution of the stresses due to bending of beams which were originally straight is considered in Chapters VI and XV. The expressions presented there may, with little error, be applied to a majority of the curved-beam problems encountered in practice, but their use introduces an error which increases as the ratio of radius of curvature to depth of beam diminishes. Not only is the stress distribution on any cross-section affected by initial curvature but the equation of the elastic curve expressing the relation between applied moments and deflections is also altered. For the design of many of the structural elements in aircraft either or both of these effects must be considered. The purpose of this chapter is to indicate means for doing so.

**17 : 1. Bending Stresses in Curved Bars**—By defining the *centroidal axis* of a curved beam as the line joining the centroids of all cross-sections of the beam, it will be assumed that such a centroidal axis forms a plane curve, either open or closed, and that all external loads lie in the plane

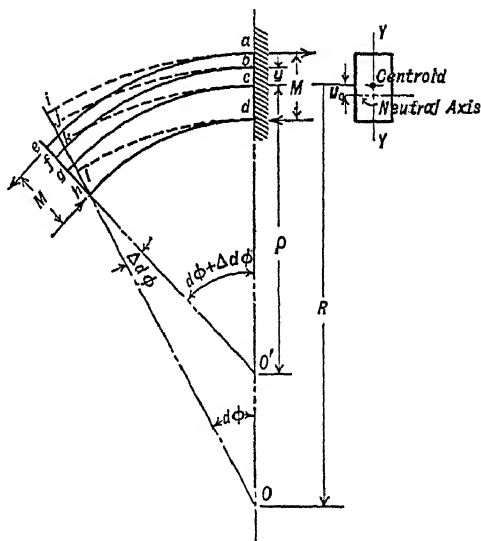


FIG. 17:1

of that curve. It will be assumed that each cross-section has an axis of symmetry, such as  $Y-Y$  of Fig. 17:1, which also lies in the plane of that curve. The line through the centroid and perpendicular to the axis of symmetry of a cross-section may be termed the *central axis* of that cross-section. In a straight beam the central axis and the neutral axis coincide; in a curved beam they do not.

By assuming, further, that the material of the beam is homogeneous, that transverse cross-sections originally plane and normal to the cen-



troidal axis remain so after bending, and that external forces are in equilibrium, it is possible to develop equations for determining the stresses in the beam by using either the neutral axis or the central axis as an axis of reference at any cross-section. There is little to choose between the procedures. Because it is generally convenient to use the central axis for the determination of the moments of inertia of, or for expressing the co-ordinates of a point in, a cross-section, that axis is the more convenient and is used as the reference in the following development. Since the sign convention for straight beams becomes awkward when applied to curved members, it is expedient to adopt a system which will not result in having the sign of the radius of curvature depend on the direction from the beam to its center of curvature. A suitable convention is to take  $y$ , the distance from the central axis to a given fiber, positive when measured outward from the center of curvature, to take a tensile fiber stress, and a bending moment which tends to reduce the radius of curvature of the beam as positive also. Since this convention differs from that for straight beams, care is required in its use.

Let *adli* of Fig. 17 : 1 represent a segment of a beam small enough so that the portion *ck* of the centroidal axis may be treated as a circular arc of radius  $R$  and length  $ds$ , and assume it bent to the shape *adhe* when subjected to the bending couples,  $M$ . The length of the centroidal axis fiber *ck* is  $R d\phi$  before bending; during bending it changes to  $cg = \rho(d\phi + \Delta d\phi)$ . Similarly, the fiber *bj* at the distance  $y$  from the centroidal axis is originally of length  $(R + y)d\phi$ . The bending deforms it to *bf*, of length  $(\rho + y)(d\phi + \Delta d\phi)$ . Letting  $\epsilon_0$  represent the unit strain of fiber *ck*, and  $\epsilon$  the corresponding strain of *bj*,

$$\epsilon_0 = \frac{cg - ck}{ck} = \frac{\rho(d\phi + \Delta d\phi) - R d\phi}{R d\phi} = \frac{\rho - R}{R} + \frac{\rho \Delta d\phi}{R d\phi} = 1 \quad 17 : 1$$

$$\begin{aligned} \epsilon &= \frac{bf - bj}{bj} = \frac{(\rho + y)(d\phi + \Delta d\phi) - (R + y)d\phi}{(R + y)d\phi} \\ &= \frac{(\rho + y)(d\phi + \Delta d\phi)}{(R + y)d\phi} - 1 \end{aligned} \quad 17 : 2$$

From Eq. 17 : 1,  $\frac{d\phi + \Delta d\phi}{d\phi} = \frac{R}{\rho} (1 + \epsilon_0)$ , and from Eq. 17 : 2

$$\sqrt{R + y} \left( \frac{R}{\rho} (1 + \epsilon_0) - 1 \right) = R + y \left( (1 + \epsilon_0) + \epsilon \right) \quad 17 : 3$$

So long as Hooke's law holds, the fiber stress at any point is  $f = E\epsilon$ ,

and, since the resultant normal force on the cross-section is zero,

$$\begin{aligned}\int f dA &= E \int \epsilon dA \\ &= ER(1 + \epsilon_0) \left( \frac{1}{\rho} - \frac{1}{R} \right) \int \frac{y}{R + y} dA + E\epsilon_0 \int dA = 0 \quad 17 : 4\end{aligned}$$

Since the moment of these stresses on plane  $eh = M$ , it follows that

$$M = \int f y dA = ER(1 + \epsilon_0) \left( \frac{1}{\rho} - \frac{1}{R} \right) \int \frac{y^2}{R + y} dA + E\epsilon_0 \int y dA$$

But  $\int y dA = 0$ , since  $y$  is measured from an axis through the centroid of the section; so

$$\frac{M}{E} = R(1 + \epsilon_0) \left( \frac{1}{\rho} - \frac{1}{R} \right) \int \frac{y^2}{R + y} dA \quad 17 : 5$$

From Eq. 17 : 5,  $R(1 + \epsilon_0) \left( \frac{1}{\rho} - \frac{1}{R} \right) = \frac{M}{E \int \frac{y^2}{R + y} dA}$ , and this, when

substituted into Eq. 17 : 4, gives

$$\frac{M \int \frac{y}{R + y} dA}{EA \int \frac{y^2}{R + y} dA} = -\epsilon_0 \quad 17 : 6$$

Then, from Eq. 17 : 3,

$$\epsilon = \frac{y}{R + y} \left[ \frac{M}{E \int \frac{y^2}{R + y} dA} \right] - \frac{M \int \frac{y}{R + y} dA}{EA \int \frac{y^2}{R + y} dA} \quad 17 : 7$$

But

$$\int \frac{y}{R + y} dA = \int \left( 1 - \frac{R}{R + y} \right) dA = A - J$$

where

$$J = R \int \frac{dA}{R + y}$$

and

$$+ y \frac{d^2 f}{dy^2} = 0 - RA + RJ = R(J - A)$$

hence

$$\left. \begin{array}{l} J \\ - \end{array} \right]$$

or

$$M = \frac{RJ}{R - J} \quad 17:8$$

At the neutral axis,  $f = 0$ , and  $y = y_0$ ; so Eq. 17:8 yields  $\frac{J}{A} = \frac{R}{R + y_0}$ , from which the distance  $y_0$  between the central and neutral axes is

$$y_0 = \frac{R(A - J)}{J} \quad 17:9$$

Since  $J$  is greater than the area  $A$ , Eq. 17:9 gives a negative value for  $y_0$ , indicating that the neutral axis of a curved beam will lie on the same side of the central axis as the center of curvature.

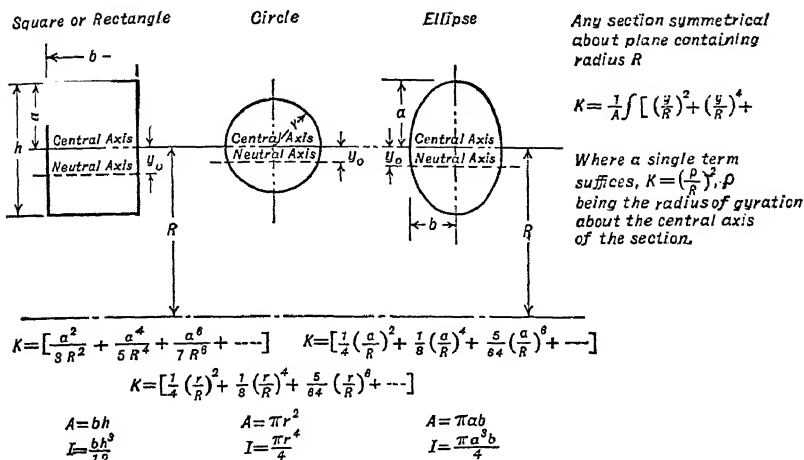
The value of  $J$  depends on the shape of the cross-section under investigation and it is normally but little greater than  $A$ ; so equations involving  $A - J$  entail computation problems and, for satisfactory results, may require the use of several significant figures. Under such circumstances, it is convenient to write  $J$  as  $A(1 + K)$ , where  $K$  represents a series whose terms depend on the shape of the cross-section, and to factor out  $A$  where possible.  $(J - A)/J$  then becomes  $K/(1 + K)$ , for instance, and satisfactory precision may usually be obtained by using two terms in the series for  $K$ . Rewriting Eq. 17:8 and 17:9 in terms of  $K$ , the fiber stress at a point  $y$  units from the *central axis* is

$$f = \frac{M}{RKA} \left( 1 + \frac{y}{R} - \frac{y^2}{R^2} \right) \quad 17:8a$$

and the distance between central and neutral axes becomes

$$y_0 = \frac{-RK}{1 + K} \quad 17:9a$$

Values of  $K$  for typical cross-sections are given in Fig. 17:2.



Values of  $K$  for  $J = A(1 + K)$

FIG. 17: 2

**17 : 2. Graphical Method for Computing  $J$  —** Values of  $J$  for sections having boundaries which cannot be represented by simple mathematical expressions may best be obtained by

a graphical construction, as shown in Fig. 17 : 3. Consider the figure  $abcdef$ , which is symmetrical about the axis  $ad$  and has its center of curvature on that axis at  $O$ . Let  $ec$  be the central axis through the centroid at  $g$ , a distance  $R$  from the center of curvature. Consider a strip  $bf$

of area  $b\Delta y$ . Since  $J = \int \bar{R}^2 + y^2$

$= \sum \frac{Rb}{R + y} \Delta y$ , it is necessary to

construct a new figure such that the width  $b'$  of each strip  $\Delta y$  thick will be equal to  $bR/(R + y)$ . To do this graphically for strip  $bf$ , draw from the center of curvature  $O$  through the axis  $ec$  to  $f$  and  $b$ . By similar triangles,  $gh : fm = R : R + y$ . But

$fm = b/2$  and  $gh = km$ . Hence  $gh = \frac{b}{2} \cdot \frac{R}{R + y}$  or half the desired

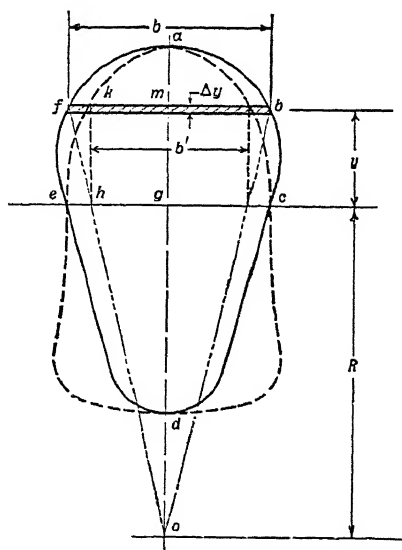
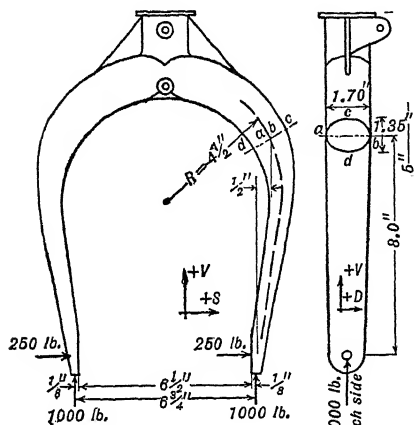


FIG. 17: 3

value of  $b'$ . Then  $\sum b' \Delta y$  is represented by the area bounded by the broken line.

This area may be obtained by using a planimeter or, lacking that, by Simpson's rule.



Front Landing Wheel Fork

FIG. 17:4

**17 : 3. Illustrative Example —**  
A fork for the front wheel of a tricycle landing gear on a small airplane is an aluminum alloy casting having the dimensions shown in Fig. 17 : 4. Assuming it to be subjected to the loads shown, determine the maximum stresses due to bending at section  $abcd$ .

Moment due to vertical component =  $1000 \times 0.5 = +500$  in.-lb.

Moment due to side component =  $-250 \times 8.0 = -2000$  in.-lb.

Moments due to vertical and side components combine to produce

a bending moment of  $-1500$  in.-lb. about axis  $ab$  of section  $abcd$ . For the elliptical section having semi-axes  $0.85$  and  $0.675$  in.,

$$\text{Area} = \pi \times 0.85 \times 0.675 = 1.8025 \text{ sq. in.}$$

$$I_{ab} = \frac{\pi \times 0.85 \times 0.675^3}{4} = 0.2053 \text{ in.}^4$$

$$I_{cd} = \frac{\pi \times 0.675 \times 0.85^3}{4} = 0.3256 \text{ in.}^4$$

$$K = \left[ \frac{1}{4} \left( \frac{0.675}{4.5} \right)^2 \right] = 0.005625$$

The distance from the central to the neutral axis is then, from Eq. 17 : 9a,

$$y_0 = \frac{-4.5(0.005625)}{1.005625} = -0.02517 \text{ in.}$$

and the stress on the inner fiber at the section is, by Eq. 17 : 8a, with  $y = -0.675$  in.,

$$4.5 \times 0.1 \times 1.8025 \left[ - \frac{4.5}{4.5 - 0.675} \right] = 5,617 \text{ p.s.i.}$$

For purposes of comparison, the fiber stress by the formula for straight beams, Eq. 6 : 2, is  $f = (-1500)(-0.675)/0.2053 = 4940$  p.s.i.; so the actual stress is about 14 per cent greater for these conditions than would have been indicated by the ordinary beam formula.

**17 : 4. Deflection of a Curved Beam** — Since the centroidal axis of a curved beam does not lie in the neutral surface, it is subjected to stress and undergoes an extension or shortening when the beam is bent. Assuming the axial forces involved so small as to produce negligible secondary bending moments, the deflection of any point on the centroidal axis due to the primary bending moments on the beam depends upon the changes in curvature and length occurring along that axis. Expressions have been developed <sup>1</sup> for the deflection of members in which the curvature is large in comparison with the cross-section of the beam. They are too cumbersome to be of practical value in ordinary design. The expression for the horizontal component,  $\delta x_1$ , of the deflection of a point on a beam subjected to bending moment,  $M$ , and axial load  $P$ , is, for instance,

while the vertical component,  $\delta y$ , is

$$\frac{M}{-M} x ds - \int_y^{y_1} \left( \frac{P}{AE} + \frac{M}{AER} \right) dy$$

17 : 11

In these expressions,  $x = 0$  and  $y = 0$  at the point on the beam where there is neither deflection nor rotation with respect to the axes of reference, and  $x = x_1$ ,  $y = y_1$  at the point whose deflection is being computed. The bending moment  $M$  is positive when it bends the beam to a sharper curvature. The axial load  $P$  is positive when it produces tension. The quantity  $\frac{M}{AER}$  in the second integral of each of the above expressions appears because of the changes in length of segments along the centroidal axis produced by the non-coincidence of the centroidal and neutral axes.

The majority of the curved beams encountered in airplane design are circular, or approximately circular, rings such as those used for transverse frames in fuselages. The chief exceptions are landing-gear forks and an occasional sharply curved, thick fitting.

<sup>1</sup> "Applied Mechanics," Fuller and Johnson, Vol. II, p. 424, 1919, John Wiley & Sons.

Most transverse rings are thin in comparison with their radii and on any given cross-section,  $y$ , which is measured from the central axis, is small compared to the radius  $R$ . Then  $A-J$  which is equal to  $\int \frac{y}{R+y} dA$  approaches  $\int \frac{y}{R} dA$  which, when the integration is performed over the entire area, is equal to zero. Similarly,  $R(J-A)$ , which is equal to  $\int \frac{y^2}{R+y} dA$ , approaches  $\int \frac{y^2}{R} dA$  or  $\frac{I}{R}$  on a thin section.

Examination of Eq. 17 : 6 shows that  $\epsilon_0$  tends to vanish as  $\int \frac{y}{R+y} dA$  approaches zero, so that Eq. 17 : 5 may be transposed to give

$$\frac{y^2}{R} = \frac{M}{EI} \quad 17 : 12$$

for a section having  $y$  very small as compared with  $R$ , instead of

$$\frac{1}{R} - \frac{1}{\rho} = \frac{-M}{RK(EAR + M)} \quad 17 : 13$$

for a thick curved beam. For thin sections, Eq. 17 : 10 and Eq. 17 : 11 become

$$\delta x_1 = \int_{x=0}^{x=x_1} \frac{M}{EI} dx, \quad M$$

and

The first of the two quantities to be integrated in each expression represents the part of the deflection component due to bending; the second represents the part due to elongation of the centroidal axis. Fuselage rings and similar members are restrained against excessive elongation by the stress-carrying covering of the fuselage. The second of the two integrals is therefore generally ignored, and analyses are made on the basis that the members are circular, that their centroidal axes are "inextensible," and that their cross-sectional dimensions are small in com-

parison with the radius of curvature. They are, however, statically indeterminate and details of their analysis may lead to more or less tedious computation, depending upon the procedures used.

### 17 : 5. Equation of Elastic Curve for Beams Having Circular Central Axes—

Consider a circular ring, the radius to whose centroidal axis is  $R$ , and assume it to be subjected to a system of forces such that it deflects to the shape shown by the dashed curve in Fig. 17 : 5. Using polar co-ordinates measured from an origin at the center of the undeformed ring, point  $P$  moves to  $P_1$ , with co-ordinates that change from  $R, \phi$ , to  $R_1, \phi_1$ ,  $R_1$  being equal to  $R + u$ .

The radius of curvature changes from  $R$  to  $\rho$ , the curvature of the bent ring from  $\frac{1}{R}$  to  $\frac{1}{\rho}$ . But in terms of the co-ordinate system chosen, the curvature is<sup>1</sup>

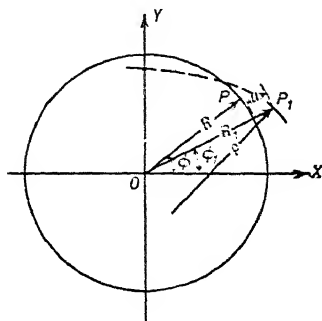


FIG. 17 : 5

$$\frac{1}{\rho} = \frac{R_1^2 + 2 \frac{dR_1^2}{d\phi_1} - R_1 \left( \frac{d^2 R_1}{d\phi_1^2} \right)}{\left[ R_1^2 + \left( \frac{dR_1}{d\phi_1} \right)^2 \right]^{3/2}} \quad 17 : 14$$

Since  $R_1 = R + u$ , and since  $R$  is constant,  $dR_1/d\phi_1 = du/d\phi_1$  and  $d^2 R_1/d\phi_1^2 = d^2 u/d\phi_1^2$ . Furthermore, so long as  $u$  is small compared with  $R_1$ , squares or products of  $u$  and its derivatives may be neglected in comparison with  $R_1$ ; so the curvature becomes

$$\frac{1}{\rho} = \frac{R_1 \left( R_1 - \frac{d^2 R_1}{d\phi_1^2} \right)}{(R_1^2)^{3/2}} = \frac{R + u - \frac{d^2 u}{d\phi_1^2}}{(R + u)^2} \quad 17 : 15$$

By writing this as

$$\frac{1}{\rho} = \frac{1}{R + u} - \frac{\frac{d^2 u}{d\phi_1^2}}{(R + u)^2}$$

<sup>1</sup> "The Engineers' Manual," R. G. Hudson, Section 104, p. 33, 1st or 2nd ed., John Wiley & Sons.



the first term becomes  $\left(\frac{1}{R} - \frac{u}{R^2} + \frac{u^2}{R^3} \dots\right)$ , while the second is  $-\frac{d^2u}{d\phi_1^2} \left(\frac{1}{R^2} - \frac{2u}{R^3} + \frac{3u^2}{R^4} \dots\right)$ . Again neglecting squares and higher powers of  $u/R$ , these terms yield

$$\frac{1}{\rho} = \frac{1}{R} - \frac{u}{R^2} - \frac{1}{R^2} \frac{d^2u}{d\phi_1^2} \quad 17 : 16$$

so the change in curvature becomes

$$\frac{1}{R} - \frac{1}{\rho} = \frac{1}{R^2} \left( u + \frac{d^2u}{d\phi_1^2} \right) \quad 17 : 17$$

while, from Eq. 17 : 12, the relation between curvature and bending moment is  $\frac{1}{R} - \frac{1}{\rho} = -\frac{M}{EI}$ . Then

$$\frac{M}{EI} = -\frac{1}{R^2} \left( u + \frac{d^2u}{d\phi_1^2} \right) \quad 17 : 18$$

for a thin circular ring. The terms on the right side of this equation may obviously be written  $-\frac{u}{R^2} - \frac{d^2u}{R^2 d\phi_1^2} = -\frac{u}{R^2} - \frac{d^2u}{ds_1^2}$ . As  $R$  increases indefinitely, the first of these terms becomes less important, and the radial displacement  $u$ , being measured perpendicular to the element  $ds$ , approaches the displacement  $y$ , measured perpendicular to an element of length  $dx$  on a straight beam until, when  $R$  becomes infinite,  $\frac{u}{R^2} = 0$  and  $\frac{M}{EI} = -\frac{d^2y}{dx^2}$ , as it should for a straight beam.

Equation 17 : 18 is a differential equation involving  $u$  and  $M/I$  as functions of  $\phi$ ,  $E$  normally being constant for a practical structural member. Whether  $M/I$  be constant or vary with  $\phi$ , the solution of Eq. 17 : 18 may be written to give the radial deflection at any point having co-ordinates  $R$  and  $\phi_1$ , as

$$u_{\phi_1} = \left[ \int_0^{\phi_1} \frac{MR^2}{EI} \sin \phi \, d\phi \right] \cos \phi - \left[ \int_0^{\phi_1} \frac{MR^2}{EI} \cos \phi \, d\phi \right] \sin \phi \quad 17 : 19$$

when the section at which  $\phi = 0$  is chosen so that both  $u$  and  $du/d\phi$  equal zero at that section. Inspection of Fig. 17 : 6 shows  $u_{\phi_1} = u_{x_1} \cos \phi_1 + u_{y_1} \sin \phi_1$ , where  $u_{x_1}$  represents the component of the deflection parallel to the  $x$ -axis,  $u_{y_1}$  the component parallel to the  $Y$ -axis.

Hence it may be concluded that

$$u_{x1} = \int_0^{\phi_1} \frac{MR^2}{EI} \sin \phi \, d\phi \quad 17 : 20a$$

$$u_{y1} = - \int_0^{\phi_1} \frac{MR^2}{EI} \cos \phi \, d\phi \quad 17 : 20b$$

These expressions may be converted to the first terms of Eqs. 17 : 10a and 17 : 11a by substituting  $u_{x1} = \delta_{x1}$ ,  $u_{y1} = \delta_{y1}$ ,  $x = R \cos \phi$ ,  $y = R \sin \phi$ , and  $ds = R \, d\phi$ . Either method of development thus leads to the same result when the deflections due to axial forces are negligible.

**17 : 6. Symmetric and Anti-symmetric Loadings** — Equations 17 : 20a and 17 : 20b, expressing relations between bending moments and deflections of curved beams, involve the properties of the beams and simple trigonometric functions. In many practical design problems the actual solution of the equations is rendered difficult or tedious because

the expressions to be substituted for the bending moment are not particularly adapted to easy integration. In airplane structural analysis, however, a great many of the curved beams encountered are circular rings or other members whose centroidal axes describe curves that are symmetrical about some axis or plane, and the tedium of the computations may be considerably reduced if advantage be taken of certain properties of symmetrical sections. The reduction is normally greatest when both load and structure have identical planes of symmetry, but substantial gains are possible with any symmetrical structure since the actual loadings may be replaced by two or more substitute load<sup>1</sup> and reaction systems, each of which is symmetrical or anti-symmetrical about the plane of structural symmetry.

In an anti-symmetrical system each force which acts parallel to the plane of structural symmetry in one direction on one side of that plane has a counterpart which acts in the opposite direction on the other side of the plane; each force acting perpendicular to and toward the plane of structural symmetry on one side has a counterpart acting perpendicular to but away from that plane on the other side; each couple acting on one side of the plane of structural symmetry has a counterpart on the other side acting to produce rotation in the same direction.

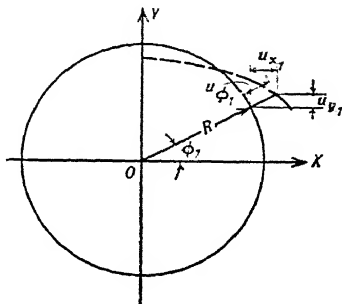


FIG. 17:6

In general, two systems of forces, one symmetric and one anti-symmetric, suffice to give equivalence and ease of analysis so long as the method of superposition is applicable to the structure and load system under consideration. The fundamental scheme for arranging equivalent force systems appears to have been presented in Germany, by W. L. Andree,<sup>1</sup> about twenty years ago. Kaufmann<sup>2</sup> and others have extended its application in later publications.

When the original applied loads are replaced by an equivalent set of symmetric and anti-symmetric forces, certain relations involving not only the forces and moments but also the slopes and deflections may be shown to exist. These relations are presented in statement form below. All twelve follow from the requirements for equilibrium and the principle of consistent deformations, and they will be found useful in establishing equations of condition which are helpful in the analysis of statically indeterminate symmetrical structures in general.

A. For a structure having loads symmetrically disposed about a plane of structural symmetry, it may be shown that

- I. The force components acting on and parallel to the plane of symmetry are zero. (There is no shear on the cross-section of the structure cut by the plane of symmetry.)
- II. The slope of the tangent to the elastic curve at the plane of symmetry is independent of the magnitude of the applied loads on the structure.
- III. The component of the deflection normal to and at the plane of symmetry is zero.
- IV. Components of reactions parallel with the plane of symmetry must be equal in magnitude and act in the same direction.
- V. Components of reactions perpendicular to the plane of symmetry must be equal in magnitude but act in opposite directions.
- VI. Moments serving to fix the slope of the structure at the supports must be equal in magnitude but rotate in opposite directions.

B. For a structure having loads anti-symmetrically disposed about a plane of structural symmetry, it may be shown that

- VII. The components of forces acting perpendicular to the cross-section cut by the plane of anti-symmetry are zero. (This is the only condition compatible with the existence of compression on one side of that plane, tension on the other.)

<sup>1</sup> "Das  $B = U$  Verfahren," W. L. Andree, R. Oldenburg, Munchen and Berlin, 1919.

<sup>2</sup> "Statik der Tragwerk," W. Kaufmann, Springer, Berlin, 1930.

- VIII. The magnitude of the bending moment acting on the plane of anti-symmetry is zero.
- IX. That component of the deflection of the cross-section cut by the plane of anti-symmetry which is parallel to the plane must be zero when measured with respect to a line joining the ends of the structural member through which the plane of anti-symmetry passes.
- X. Components of reactions parallel to the plane of anti-symmetry must be equal in magnitude but must act in opposite directions.
- XI. Components of reactions perpendicular to the plane of anti-symmetry must be equal in magnitude and must act in the same direction.
- XII. Moments serving to fix the slope of the structure at the points of support must be equal in magnitude and must rotate in the same direction.

**17 : 7. Redundant Forces on Section of Circular Ring** — The utility of the symmetric and anti-symmetric load relations may be shown by applying them to the analysis of a circular ring, such as one of the transverse stiffeners which carry seat and floor loads in a circular fuselage structure. These loads normally act vertically, that is, perpendicular to the horizontal axis of symmetry of the ring. In some designs transverse rings also carry horizontal forces and moments due to eccentric forces. A general solution of the problem would therefore require consideration of all three force systems and, in this article, all are investigated.

It is simpler, for the complete analysis of a ring, to deal with radial and tangential forces or components than with vertical and horizontal. The rings investigated therefore carry radial or tangential forces or externally applied couples, the reactions for which are provided by the tangential components of the shear forces developed in the fuselage covering. The shear flow assumed in the covering is that corresponding to the elementary beam theory, with no allowance for "effective" and "ineffective" areas. Were the covering to be stiffened by longitudinal members, as in conventional construction, the actual shear flow would have a saw-toothed variation instead of being a continuous function. The distributions shown in Figs. 17 : 7, 17 : 8, and 17 : 9 may be looked upon as averages, the area of the stiffeners being treated as though distributed around the circumference in the form of an increased thickness of covering. This shear in the covering would actually occur around the periphery of the ring, but it is treated as though acting around the centroidal axis of the ring.<sup>1</sup>

<sup>1</sup> "Stress Analysis of Circular Frames," Fahlbusch and Wegner, N.A.C.A. Technical Memo. 999, Washington, 1941.

Taking the radial force  $F = 2P$  acting at an angle  $\alpha$  to a plane of symmetry as in Fig. 17 : 7a, the actual force system may be considered as a symmetric and anti-symmetric systems of parts  $b$  and  $c$  of Fig. 17 : 7b is considered but two unknowns,  $M_a$  and  $N_a$  are introduced in condition I of the previous

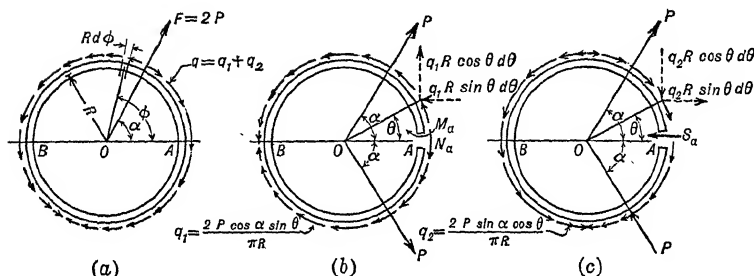


FIG. 17:7

the tangents to the elastic curve at  $A$  and  $B$  undergo no change when the symmetric loads  $P$  are applied, and, from Condition III, the tangential components of the deflection at  $A$  and  $B$  are zero. Since the tangential components  $u_\theta$  are zero at  $\phi = 0$  and  $\phi = \pi$ , Eq. 17 : 20b may be written

$$\int_0^\pi \frac{MR^2}{EI} \cos \phi \, d\phi = \int_0^{\pi R} \frac{MR}{EI} \cos \phi \, ds = 0 \quad 17:21$$

By substituting  $-[u + (d^2u/d\phi^2)]$  for  $MR^2/EI$ , integrating, and having due regard for  $R$  being constant and for  $du/d\phi$  being zero at  $\phi = 0$  and at  $\phi = \pi$ , it is readily shown that

$$\int_0^\pi \frac{MR^2}{EI} \, d\phi = \int_0^{\pi R} \frac{M}{EI} \, ds = 0 \quad 17:22$$

Equations 17 : 21 and 17 : 22 may be employed to determine  $M_a$  and  $N_a$  of the problem in hand when an expression is developed for  $M_\phi$ , the bending moment at any section of the ring whose angular co-ordinate is  $\phi$ , measured from the plane of symmetry  $OA$ . In setting up this expression, it is convenient to use three symbols,  $\alpha$ ,  $\theta$ , and  $\phi$  to designate angular co-ordinates. All are measured from the plane of symmetry  $OA$  and are positive when counter-clockwise.  $\alpha$  is used to designate the co-ordinate of the external load,  $P$ .  $\theta$  is used to designate the angle

from  $OA$  to the shear-flow components, and  $\phi$  to designate the angular co-ordinate of the section under consideration. Then, for  $\phi$  less than  $\alpha$ ,

$$M_\phi = M_\alpha + N_\alpha R(1 - \cos \phi) - \int_\alpha^\phi (q_1 R^2 \cos \theta)(\cos \theta - \cos \phi) d\theta \\ + \int_0^\phi (q_1 R^2 \sin \theta)(\sin \phi - \sin \theta) d\theta$$

and, for  $\phi$  between  $\alpha$  and  $\pi$ ,

$$M_\phi = M_\alpha + N_\alpha R(1 - \cos \phi) - \int_0^\phi (q_1 R^2 \cos \theta)(\cos \theta - \cos \phi) d\theta \\ + \int_0^\phi (q_1 R^2 \sin \theta)(\sin \phi - \sin \theta) d\theta + PR \sin \alpha (\cos \phi - \cos \alpha) \\ - PR \cos \alpha (\sin \phi - \sin \alpha)$$

where  $q_1 = F \cos \alpha \sin \theta / \pi R$  because the tangential component of the shear flow at any point on a cross-section is equal in intensity to the longitudinal shear flow at that point. The longitudinal shear flow is, of course,  $q_L = VQ/I$ . It may be seen from Fig. 17 : 7b that the net shear normal to the plane  $AB$  is zero since the normal components of the forces  $P$  are equal and opposite. There is a shear force of  $V = 2P \cos \alpha = F \cos \alpha$  parallel to  $AB$ , however, and it is this which produces the shear flow.  $Q = \int_0^\alpha R^2 t \cos \theta d\theta = R^2 t \sin \theta$  and  $I = \pi t R^3$ . Then  $q_L = q_1 = F \cos \alpha \sin \theta / \pi R$ .

It is somewhat less confusing to establish the signs for the individual terms involving components of  $q_1$  in the moment equations than to set up criteria for the signs of the shear flows themselves. If one of the components of  $q_1$  produces a moment tending to reduce the radius of curvature of the beam at section  $\phi$ , the term in the equation for  $M_\phi$  involving that component is positive. If the tendency is to increase the radius of curvature, the term has a negative sign.

In the equations which follow,  $q_2$  is obtained by a procedure analogous to that used for  $q_1$ , and its components are treated in the same way when the signs of the terms in the moment equations are established.

If, for the purposes of this investigation,  $R/EI$  be assumed constant, Eq. 17 : 21 becomes  $\int_0^\pi M_\phi \cos \phi d\phi = 0$ , and Eq. 17 : 22,  $\int_0^\pi M_\phi d\phi = 0$ . Substitution of the values for  $M$  and  $q_1$  in these expressions, with integration between the limits indicated and with subsequent simpli-

fication, yields

$$M_a = \frac{FR}{2\pi} \left[ \frac{\cos \alpha}{2} - (\pi - \alpha) \sin \alpha + 1 \right] = FRW_1 \quad 17 : 23$$

$$N_a = \frac{F}{2\pi} \left[ \frac{3 \cos \alpha}{2} + (\pi - \alpha) \sin \alpha \right] = FW_2 \quad 17 : 24$$

The anti-symmetrical loads shown in part *c* of Fig. 17 : 7 are held in equilibrium by the shear flow,  $q_2 = F \sin \alpha \cos \theta / \pi R$ . The bending moment and the normal force at *A*, the section cut by the plane of anti-symmetry, are zero by Conditions VII and VIII; while the radial displacements,  $u_x$ , at this section and at *B* are zero by Condition IX. The shear force,  $S_a$ , is the only unknown, and it may be evaluated by using the criterion that the component of the deflection parallel to  $S_a$  is zero. Since  $u_x = 0$  at  $\phi = 0$  and at  $\phi = \pi$ , and since  $R/EI$  is taken constant, Eq. 17 : 20a may be written

$$M_\phi \sin \phi \, d\phi = \int M_\phi \sin \phi \, d\phi = 0 \quad 17 : 25$$

where  $M_\phi$  for  $\phi$  between 0 and  $\alpha$  is

$$\begin{aligned} M_\phi = S_a R \sin \phi + \int_0^\phi (q_2 R^2 \cos \theta) (\cos \theta - \cos \phi) \, d\theta \\ - \int_0^\phi (q_2 R^2 \sin \theta) (\sin \phi - \sin \theta) \, d\theta \end{aligned}$$

and for  $\phi$  between  $\alpha$  and  $\pi$

$$\begin{aligned} M_\phi = S_a R \sin \phi + \int_0^\phi (q_2 R^2 \cos \theta) (\cos \theta - \cos \phi) \, d\theta \\ - \int_0^\phi (q_2 R^2 \sin \theta) (\sin \phi - \sin \theta) \, d\theta + PR \sin \alpha (\cos \phi - \cos \alpha) \\ - PR \cos \alpha (\sin \phi - \sin \alpha) \end{aligned}$$

Substitution of the above values of  $M_\phi$  and  $q_2$  in Eq. 17 : 25, with the appropriate integration and simplification, yields

$$17 : 26$$

Equations 17 : 23, 17 : 24, and 17 : 26 suffice for the determination of the bending moment, normal force, and shear at section *A* on a circular ring carrying a radial force  $F = 2P$ . If there be more than one force acting, the values of  $M_a$ ,  $N_a$ , and  $S_a$  may be computed for each load and the results added to obtain the total moments and normal and shear

forces at section A. Where precise results are desired, the equations may be used, with the angles  $\alpha$  expressed in radian measure and with the values of sines and cosines taken from Table 14 : 1. For trial designs or less precise results,  $W_1$ ,  $W_2$ , etc., which are  $1/(2\pi)$  times the quantities in brackets in those equations, may be taken from the curves of Fig. 17 : 10 and  $M_a$ ,  $N_a$  or  $S_a$  determined to two significant figures. These are the Wise coefficients,<sup>1</sup> plotted in radians and with signs in conformity with this article.

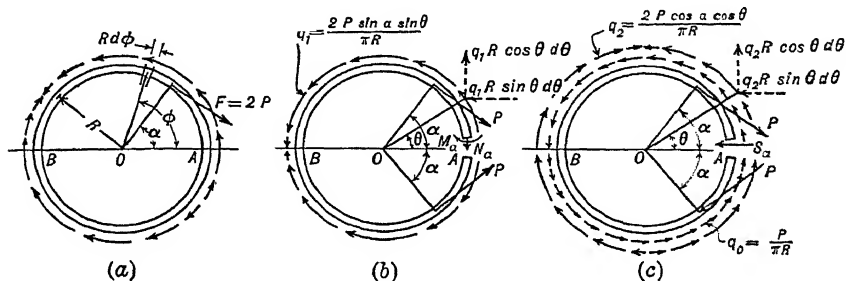


FIG. 17:8

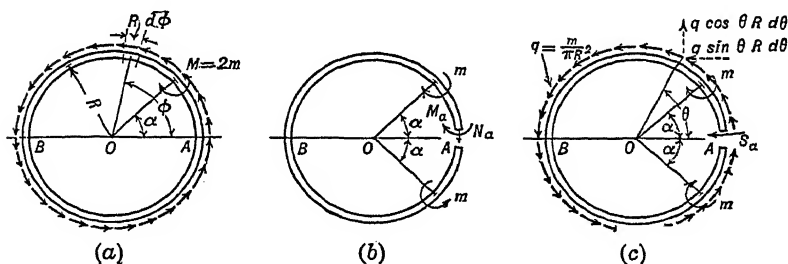


FIG. 17:9

If the force be applied tangentially, as shown in Fig. 17 : 8a, it may be resolved into the symmetric and anti-symmetric loadings of parts b and c of that figure. By methods analogous to those for the radial loads, it may be shown that

$$M_a = \frac{FR}{2\pi} \left[ \frac{3 \sin \alpha}{2} + (\pi - \alpha)(\cos \alpha - 1) \right] = FRW_4 \quad 17 : 27$$

$$N_a = \frac{F}{2\pi} \left[ \frac{\sin \alpha}{2} - (\pi - \alpha) \cos \alpha \right] = FW_5 \quad 17 : 28$$

$$S_a = \frac{F}{2\pi} \left[ (\pi - \alpha) \sin \alpha - 1 - \frac{\cos \alpha}{2} \right] = FW_6 \quad 17 : 29$$

<sup>1</sup> "Analysis of Circular Rings for Monocoque Fuselages," Joseph A. Wise, *Jour. Aero. Sci.*, Vol. 6, No. 11, p. 460, September, 1939.



Figure 17 : 11 gives the Wise coefficients by which  $F$  must be multiplied to give  $M_a$ ,  $N_a$ , and  $S_a$  for a tangential load having angular co-ordinate  $\alpha$ .

The expressions for moment, normal force, and shear at section  $A$  on

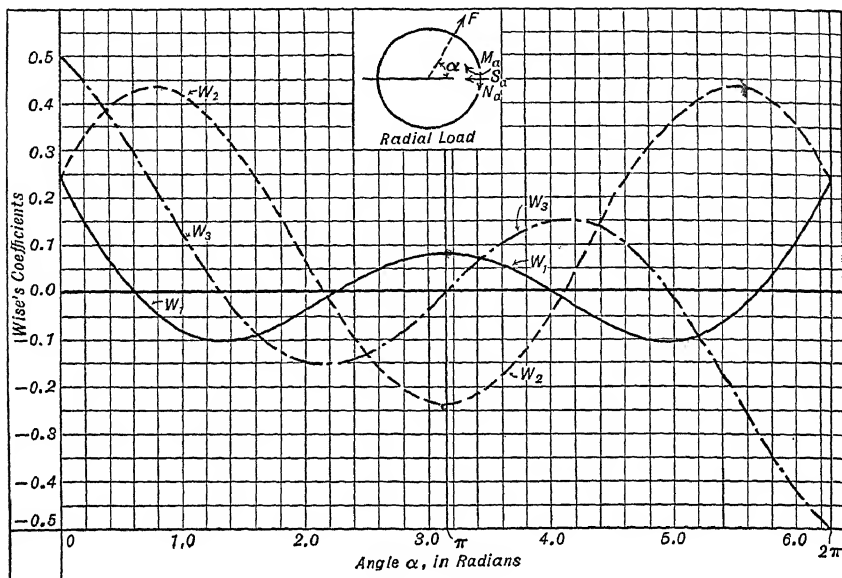


FIG. 17:10

a ring of constant  $EI$ , loaded by a couple,  $M = 2m$ , as shown in Fig. 17 : 9a, are

$$M_a = \frac{M}{2\pi} \left[ 2 \sin \alpha + \alpha - \pi \right] = MW_7 \quad 17:30$$

$$N_a = -\frac{M}{2\pi R} \left[ 2 \sin \alpha \right] = \frac{M}{R} W_8 \quad 17:31$$

$$S_a = -\frac{M}{2\pi R} \left[ 1 + 2 \cos \alpha \right] = \frac{M}{R} W_9 \quad 17:32$$

Figure 17 : 12 represents the Wise coefficients to be used with  $M$  or  $M/R$  in obtaining  $M_a$ ,  $N_a$ , and  $S_a$  to two-figure precision.

The above method has been developed here for circular rings only.<sup>1</sup>

<sup>1</sup> Further data on circular rings may be found in N.A.C.A. Technical Memo. 999, "Stress Analysis of Circular Frames," Fahlbusch and Wegner; in N.A.C.A. Technical Memo. 1004, "Statics of Circular-ring Stiffeners for Monocoque Fuselages," W. Stieda; and in "Stress Analysis of Rings for Monocoque Fuselages," N. J. Hoff, *Jour. Aero. Sci.*, Vol. 9, No. 7, May, 1942.

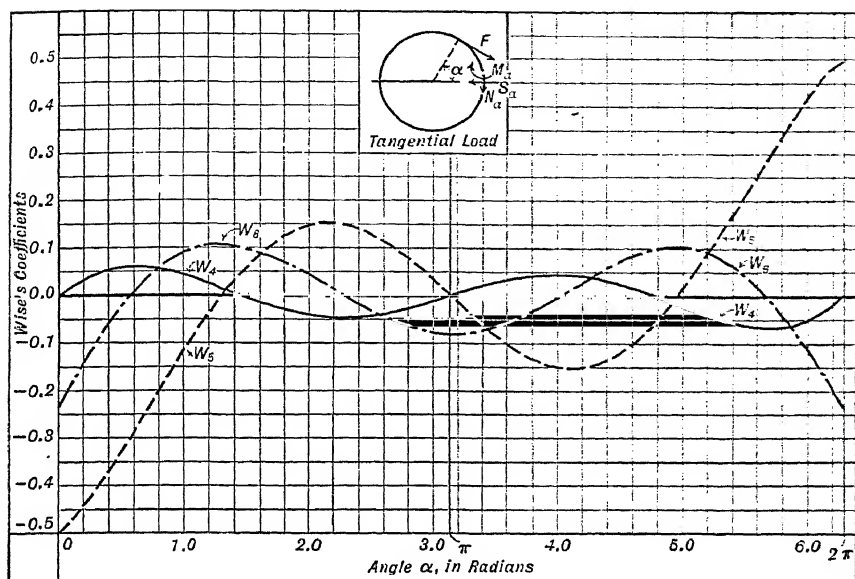


FIG. 17:11

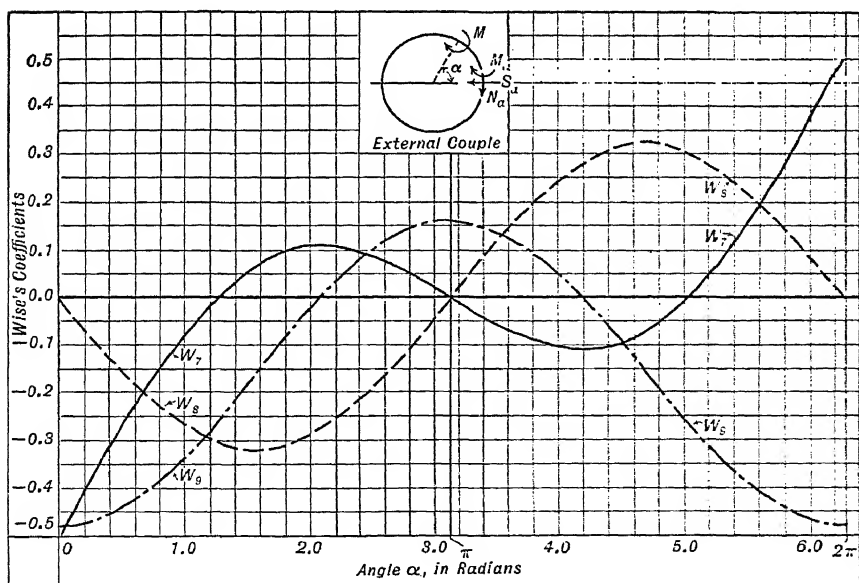


FIG. 17:12

It is also useful in the analysis of square or rectangular frames, but the proportions of such structures vary so greatly that it is not deemed necessary or desirable to present, in this text, functions or curves of coefficients for their analysis. Rings of elliptical shape are rather frequent in airplane fuselages but they, like rectangular frames, vary in proportions so that tables or curves of coefficients become too long for inclusion in this text, especially since they are readily available in N.A.C.A. Technical Note 444, "Working Charts for the Stress Analysis of Elliptic Rings," by Walter F. Burke.

When  $EI$  is not constant, or when the shape of the cross-section does not lend itself to simple integration, Eqs. 17 : 21, 17 : 22, and 17 : 25 may be evaluated by semi-graphical integration. It is convenient, in the analysis of such frames, to note that  $R \cos \phi = x$  and that  $R \sin \phi = y$ , and to substitute finite segments  $\Delta s$  for infinitesimal segments of length  $ds$ . Equation 17 : 21, when so modified, becomes  $\sum \frac{M}{EI} x \Delta s$ ,

and the others can be altered in a similar way. However, since  $M$  may involve  $M_a$ ,  $N_a$ ,  $S_a$ , and  $q$ , the construction of the curve of  $M/EI$  and its integration involves tedious computation. Little work has been done, therefore, on the generalization of methods of analysis for "rings" of non-circular shape. Of the procedures available, Hoff's is as satisfactory as any.

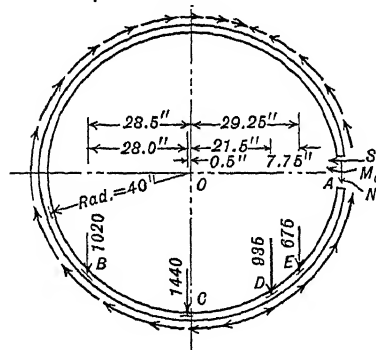


FIG. 17 : 13

**17 : 8. Illustrative Example** — A transverse ring in a large cabin airplane carries floor and seat loads as shown in Fig. 17 : 13. The reactions are provided by the shear flow in the aluminum alloy fuselage covering. By measuring angles in a counter-clock-

wise direction from the horizontal axis  $OA$ , the data in Table 17 : 1 are obtained. Loads at  $B$ ,  $C$ ,  $D$ , and  $E$  are resolved into radial and tangential components in Table 17 : 2. Radial components are considered positive when acting *away* from the center of the ring, tangential components positive when acting to rotate the ring in a *clockwise* direction. The remaining computations may be done in tabular form, Table 17 : 3 providing for the effects of the radial components, Table 17 : 4 for the tangential. The values of  $M_a$ ,  $N_a$ , and  $S_a$ , due to both components, are then obtained by adding the appropriate quantities from these tables.

TABLE 17:1

Angle $\alpha$	$R \cos \alpha$	$\cos \alpha$	Quadrant	$\alpha$ in Radians	$\sin \alpha$
<i>AOB</i>	-28.5	-0.7125	3rd	3.9193	-0.7016
<i>AOC</i>	-0.5	-0.0125	3rd	4.6999	-0.9999
<i>AOD</i>	+21.5	+0.5375	4th	5.2799	-0.8432
<i>AOE</i>	+29.25	+0.7313	4th	5.5326	-0.6820

TABLE 17:2

Station	Load	$\sin \alpha$	Radial Component	$\cos \alpha$	Tangential Component
<i>B</i>	-1020	-0.7016	+715.63	-0.7125	-726.75
<i>C</i>	-1440	-0.9999	+1439.86	-0.0125	-18.00
<i>D</i>	-935	-0.8432	+788.39	+0.5375	+502.56
<i>E</i>	-675	-0.6820	+460.35	+0.7313	+493.63

TABLE 17:3

Station	Radial Component	$R$	$W_1$	$M_a$	$W_2$	$N_a$	$W_3$	$S_a$
<i>B</i>	+715.6	40	+0.0156	+446.5	-0.0833	-59.6	+0.1440	+103.0
<i>C</i>	+1439.9	40	-0.0897	-5166.4	+0.2450	+352.8	+0.0827	+119.1
<i>D</i>	+788.4	40	-0.0850	-2680.6	+0.4153	+327.4	-0.1158	-91.3
<i>E</i>	+460.4	40	-0.0422	-777.2	+0.4341	+199.9	-0.2240	-103.1
Summations				-8177.7		+820.5		+27.7

TABLE 17:4

Station	Tangent Component	$R$	$W_4$	$M_a$	$W_5$	$N_a$	$W_6$	$S_a$
<i>B</i>	-726.8	40	+0.0445	-1293.7	-0.1440	+104.7	-0.0156	+11.3
<i>C</i>	-18.0	40	+0.0118	-8.5	-0.0827	+0.1	+0.0897	+0.2
<i>D</i>	+502.6	40	-0.0439	-882.6	+0.1158	+58.2	+0.0850	+42.7
<i>E</i>	+493.6	40	-0.0606	-1196.5	+0.2240	+110.6	+0.0422	+20.8
Summations				-3381.3		+273.6		+75.0

From the summations in the above tables, the moment, shear, and normal force at section *A* are thus found to be  $M_a = -11560$  in.-lb., hence tending to increase the radius of curvature of the ring at that

section;  $N_a = +1094$  lb., hence producing tension at  $A$ ;  $S_a = +103$  lb., hence acting toward the center of the ring on the part of the section above  $OA$ .

For the complete analysis of the ring, moments, shears, and normal forces should be determined at several sections, say at every half radian around the circumference and at each load point. The computations involved parallel those for section  $A$  with the values of  $\alpha$  changed to conform with the position of the section under consideration. The magnitudes of the radial and tangential components would not change, but the values of the Wise coefficients would since they are functions of  $\alpha$ .

In this, as in all computation methods, care must be taken with signs. Many of them are provided for automatically but some, notably those for the radial and tangential components, must be determined by the direction in which they act, an *outward acting* radial component or a tangential component which acts *clockwise* being positive. External couples are positive when clockwise regardless of the quadrant in which they act.

**17:9. Rings Used to Maintain Form** — The methods of the preceding articles apply to transverse rings or frames carrying floor or seat loads, or other systems of forces which are to be transmitted to the shell of a stressed skin structure. Many of the rings in fuselages carry no such loads but serve to prevent distortion of the fuselage cross-section, that is, they provide elastic support for the longitudinal stringers which might otherwise buckle under the compressive loads to which they are subjected, and they also serve to make the skin buckle into a number of small panels instead of permitting the formation of long buckles of large amplitude. The loads for which such rings must be designed thus depend on the stability and distortion of the skin and members attached to the rings rather than upon any fixed system of applied loads.

The problems involved in the rational determination of such forces are difficult even for the relatively simple case of the circular section of uniform diameter. They appear to be practically insurmountable for elliptical cylinders, or for sections involving the double curvature of skin normal in fuselage design. The analysis of such structures must, at the present time, be based partly on rational, partly on empirical methods. There are several papers<sup>1</sup> which treat the problems

<sup>1</sup> "General Instability of Semi-monocoque Cylinders," E. I. Ryder, *Air Commerce Bull.*, Vol. 9, No. 10, p. 241, April, 1938.

"Instability of Monocoque Structures in Pure Bending," N. J. Hoff, *Jour. Roy. Aero. Soc.*, Vol. XLII, No. 328, p. 281, April, 1938.

"Buckling of Semi-monocoque Structures under Compression," T. K. Wang, *Jour. Appl. Mech.*, Vol. 9, No. 3, p. A-117, September, 1942.

of the cylinder. None offers a complete solution, but each contributes a method of attack and an advance in our knowledge of the behavior of such structures.

One of the latest and most promising methods is that presented by N. J. Hoff.<sup>1</sup> It is primarily a rational procedure and is strictly applicable only to cylinders subjected to pure bending, that is, bending under pure couples but with no torsional or transverse shear. The method includes some empirical coefficients which, it should be noted, are based on rather meager test data and which may be modified as further results become available. It is, however, sound and appears to yield results of the right order of magnitude.

Hoff suggests the following procedure for applying the method. Assume the critical strain,  $\epsilon_{\max}$ , to be the  $P/AE$  value computed from the stress on the most-stressed stringer, and calculate the effective width of skin acting with this stringer from

$$2 w_e = 2 w_c + (\epsilon_{\text{curv}}/\epsilon_{\max}) (d - 2 w_c) \quad 17 : 33$$

where

$$2 w_e = d[\epsilon_{\text{flat}}/(\epsilon_{\max} - \epsilon_{\text{curv}})]^{1/2}$$

$d$  = stringer spacing measured around the arc

$\epsilon_{\text{flat}} = 3.62 (t/d)^2$ , strain of flat sheet under critical compressive stress

$\epsilon_{\text{curv}} = 0.3 t/r$ , strain of curved sheet under critical compressive stress

$t$  = thickness of sheet

$r$  = radius of cylinder

Next determine the moments of inertia of the stringer plus effective width of sheet for bending in the radial direction,  $I_{st r}$ , and for bending in the tangential direction,  $I_{st t}$ . Then calculate  $I_{st}$  from

$$I_{st} = I_{st r} + \frac{5}{8 n^2} I_{st t} \quad 17 : 34$$

assuming  $n = 3$  when no more accurate value is to be had. The value of  $n$  may be expected to lie between 2 and 6 on the basis of the test data now in hand, but further research on cylinders having rings, stringers, and skin of proportions normally found in fuselages is expected to indicate a narrower range for it. It is a function of the wave length of the buckles in the circumferential direction, and 3 is a reasonable value to assume for cylinders having thin skin, and having rings which are stiffer than the stringers for which they provide support.

<sup>1</sup> "General Instability of Monocoque Cylinders," N. J. Hoff, *Jour. Aero. Sci.*, April, 1943.

Next calculate the moment of inertia of the ring for bending in the radial direction,  $I_r$ , assuming the effective width of skin acting with the ring to be equal to the width of the ring. Then, taking  $E_{st}$  as Young's modulus for the stringer,  $E_r$  as Young's modulus for the ring,  $d$  as the stringer spacing,  $L_1$  as the ring spacing, and  $r$  as the radius of the cylinder, the critical stress for the most-stressed stiffener may be found from

$$P_{cr} = n^2 \pi^2 \sqrt{\frac{d}{L_1} \frac{E_{st} I_{st} E_r I_r}{n^2}} \quad 17 : 35$$

When the moment of inertia of the ring is less than that of the stringer, or when the skin is quite thick and the structure buckles as an orthotropic shell rather than by general instability, the assumption that  $n = 3$  may not yield good results. Also, if  $P_{cr}/A_{st}E_{st}$  is not in reasonable accord with the  $P/AE$  used in computing  $\epsilon_{\max}$ , further trials should be made with new assumptions for  $\epsilon_{\max}$  until satisfactory agreement is attained. When making such trials it may, obviously, be desirable to alter the assumed dimensions of ring or stringers in order to bring the computed load on the most-stressed stringer into reasonable accord with the critical load indicated by Eq. 17 : 35.

It should be kept in mind when doing so that if  $P_{cr}$  given by Eq. 17 : 35 exceeds the compressive load in the most-stressed stringer the transverse rings are sufficiently stiff to make the stringers behave as a series of pin-ended columns of length  $L_1$ , provided that the stringers and effective skin are adequate to carry the loads to which they are subjected. The load which the stringers and skin will carry under such circumstances may be predicted by the method given in Art. 10 : 9, using a restraint coefficient  $c = 1$ .

Designers may find it expedient to use this latter load as  $P_{cr}$  and solve Eq. 17 : 35 for  $E_r I_r$  to get an approximation to the stiffness required of the rings. Since such stiffness will vary inversely as  $n^4$ , the result must be checked with due regard for the values of  $\epsilon_{\max}$  and  $n$  used. By taking  $n = 2$ , the indications from currently available data are that the value of  $E_r I_r$  obtained will be on the safe side. The resulting ring sizes will probably be found practicable on small airplanes but may prove too heavy for use in very large fuselages.

There are no data on elliptical cylinders against which to check the applicability of Hoff's method, but it seems probable that reasonable results may be had by taking  $r$  as the length of the semi-major axis when computing  $\epsilon_{\text{curv}}$  in Eq. 17 : 33 and  $P_{cr}$  in Eq. 17 : 35 for the stiffeners at the ends of the long axis of the ellipse. For the stiffeners at the ends of the short axis,  $r$  may be taken as  $b^2/a$ , where  $b$  is the semi-major,

and  $a$  the semi-minor, axis of the ellipse. Similar methods of adapting this procedure to other shapes of structure, and to cylinders subjected to bending, shear, and torsion, will doubtless be developed. It is probable that ring sizes determined by this method for circular cylinders in pure bending will be found reasonable for fuselages carrying shear and bending, since the shear forces acting on fuselages are normally small when compared with the bending moments at the critical sections, and the effect of double curvature of the skin is normally to stiffen the frame to which it is attached. Designers must keep in mind, however, the fact that data are not available to substantiate these assumptions, hence that tests must be made where the members involved are to be closely designed.

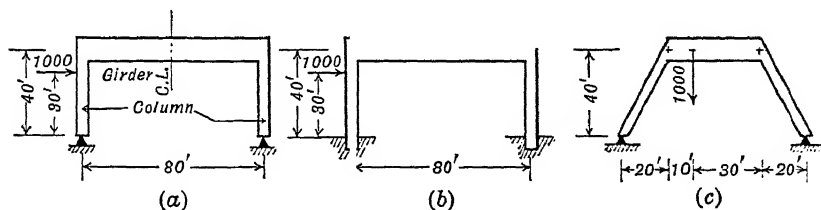
## PROBLEMS

**17 : 1.** Develop the expression from which  $K$  may be found for a round tube having outside diameter  $D$  and wall thickness  $t$ . Assume  $D$  equal  $20t$ ,  $30t$ , and  $40t$ , and plot a curve to show how  $K$  varies with  $D/t$  ratio, when  $R = 5D$ .

**17 : 2.** Assume a  $1 \times 0.049$  mild steel tube bent into the arc of a semicircle having an outside diameter of 13 in. The tube lies in a vertical plane and has its upper end,  $A$ , rigidly fixed in a bracket. On the basis of Art. 17 : 1, how large a concentrated load could be applied at the lower end,  $B$ , without having the stress in the most stressed fiber exceed the elastic limit of the material? The line of action of the load corresponds with  $AB$ , the line between the ends of the tube.

**17 : 3.** What would be the  $X$  and  $Y$  components of the deflection at  $B$  for the tubular beam of Prob. 17 : 2, if the load at  $B$  is 100 lb.? Compare the results obtained by using the method of Art. 17 : 4 with those obtained by Art. 17 : 5, and comment on the effect of the deflections due to the axial forces.

**17 : 4.** Determine the magnitudes of the moments, shears, and normal forces acting on the cross-sections at the center lines of the following structurally symmetrical framed bents. Use the relations of symmetry and anti-symmetry, and assume girder areas are five times column areas and girder moments of inertia are ten times column moments of inertia.



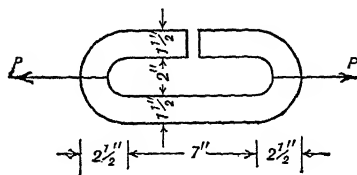
PROB. 17 : 4

**17 : 5.** A thin circular ring of 20-in. radius is subjected to a uniformly distributed load of 5 lb. per in. acting radially outward around the entire ring. Adapt Eqs. 17 : 23, 17 : 24, and 17 : 26 to cover a uniform load and determine the magnitudes of moment, shear, and normal force on any section of the ring.



## CURVED BEAMS AND RINGS

17:6. Using the ring and loading shown in Fig. 17:13, determine moments, shear, and normal forces on sections 1, 2, and  $\pi$  radians from the  $OA$  axis.



PROB. 17:7

17:7. A  $1\frac{1}{2}$ -in. diameter steel rod (chrome molybdenum) was bent and welded to form a link in a chain. Because of a poor weld, the link failed as shown. How large a load,  $P$ , may still be taken on the chain if the maximum tensile stress is not to exceed 30,000 p.s.i. at any point?

$$\text{Area of } 1\frac{1}{2}\text{-in. rod} = 1.767 \text{ in.}^2 \quad I = 0.2485 \text{ in.}^4 \quad \rho = 0.376 \text{ in.}$$

## CHAPTER XVIII

### CRITICAL LOADS

With many types of structure it is sufficient to determine the internal forces developed when they are deformed to shapes in which those forces are in equilibrium with the external loads. With others, particularly when compressive stresses are important, it is also necessary to determine whether the equilibrium is stable or unstable. This has been considered to some extent in connection with columns in Chapter X and with beam-columns in Chapter XIV. Many very practical stability problems require the use of advanced mathematics, and few of the more complex ones have yet been solved. The purpose of this chapter is to discuss the nature of the problem and to serve as an introduction to the more advanced work in the field. For descriptions of that advanced work the reader must turn to other authors.

**18 : 1. Use of Maupertuis' Theorem** — The general criterion for stability is Maupertuis' theorem,<sup>1</sup> often called the *least energy principle*, which may be stated as follows. If a system is in equilibrium and *every* possible change in its configuration implies an increase in its potential energy, it is stable. If *any* possible change in configuration implies a decrease in potential energy, it is unstable. If there is a possible change in configuration that implies no change in potential energy, the system is in a transition stage between stability and instability that may be termed *neutral equilibrium*.

To prove conclusively that a system is in stable equilibrium, it is necessary to show that *all* possible changes in configuration would result in increases of potential energy. To prove it unstable or in neutral equilibrium, however, it is sufficient to prove a *single* possible change in configuration would result in a decrease or in no change in potential energy. A system may be stable with respect to some types of change in configuration, unstable with respect to others, and in neutral equilibrium with respect to still others.

The type of system under discussion consists of a structure composed of one or more members, the external forces or loading to which it is subjected, and the internal forces developed by its deformation. A

<sup>1</sup> E. Mach, "The Science of Mechanics," translated by T. J. McCormack, Open Court Publishing Co., Chicago, 1893, pages 68 ff.

loading associated with a transition from stability to instability is termed the *critical loading* with respect to the type of change of configuration involved. The smallest critical loading for any structure is the *absolute critical loading* for that structure and is the one that determines its true margin of safety with respect to any proportional loading.

An important corollary of Maupertuis' theorem is that a system can pass from one configuration of equilibrium to another without change in potential energy only if it is in neutral equilibrium with respect to that change. The development of the Euler-column formula in Arts. 10 : 4 and 10 : 5 may be considered an application of this corollary, though its basis is there described in a somewhat different manner.

Were the material in those articles used to illustrate the application of this corollary, the system under discussion would include the end loads as well as the column itself. The most important change in the derivation would be that attention would be limited to the work done as the column passes from an initial state of equilibrium with its axis a straight line to an alternative state with the axis curved, the end loads,  $P$ , remaining constant in the process instead of starting with the end loads equal to zero. Then Eq. 10 : 6 would be described as an expression for the potential energy lost by those end loads as the result of their doing positive work, instead of as one measure of the strain energy stored in the column. Similarly, the  $M$  term of Eq. 10 : 8 would be described as an expression for the negative work done by the internal resisting forces instead of as an alternative measure of the strain energy stored. Finally, the basic relation would be expressed in the form

$$U_i - U_e = 0 \quad 18 : 1$$

instead of

$$18 : 2$$

to which Eq. 10 : 9 may be abbreviated. Other verbal changes would also be needed to make the text of Arts. 10 : 4 and 10 : 5 a suitable illustration of the application of Maupertuis' theorem, but essentially they would be as superficial as the difference between Eqs. 18 : 1 and 18 : 2.

Much of the difficulty experienced by students studying the literature of an elastic stability is due to the tendency of various authors to use apparently quite different methods of procedure and to justify them by apparently quite different basic assumptions. Actually, however, both procedures and assumptions are closely related, and the only real differences are in the selections, from related groups of facts, of those to be emphasized and those to be left to implication.

**18 : 2. Representation of Deformation Pattern** — A most important step in computing critical loads is the formulation of equations to define the alternative configurations compatible with neutral equilibrium. These equations usually include parameters, like  $\delta$  and  $w$  in Art. 10 : 5, which make them represent straight lines or planes when the parameters equal zero but curved lines or surfaces when one or more of the parameters is not equal to zero. As stated in Art. 10 : 5, if the absolute critical load is to be obtained, these equations must represent the type of deformation pattern associated with the least storage of strain energy compatible with the development of the internal forces required for equilibrium. For an exact solution the form of the equations must usually be determined by resort to the calculus of variations, but even if that is done, as is shown in Chapter XIX, neglect of important possible types of deformation may lead to erroneous results. On the other hand, if a close approximation to the correct form of equation is used, the computed value of the critical load is very close to the absolute critical. This is illustrated by the parallel computations of Art. 10 : 5. Since the absolute critical is a minimum value, this fact can be taken advantage of by using equations with several parameters, computing the critical load in terms of those parameters and then adjusting the values of those parameters to make the expression for the critical load a minimum. In this way the absolute critical load can be obtained to any desired degree of precision, and usually very few parameters are needed.

In following this line of attack it is often found advantageous to express the deformation patterns by Fourier's sine or cosine series, such as

$$y = C_1 \sin \frac{\pi x}{L} + C_2 \sin \frac{2 \pi x}{L} + C_3 \sin \frac{3 \pi x}{L} \quad 18 : 3a$$

which may be abbreviated to

$$y = \sum_{n=1} \sin \frac{n \pi x}{L} \quad 18 : 3b$$

in which the symbol  $\sum_{n=1}$  indicates a series that includes a separate term for each positive integer. Whether a sine or a cosine series should be used is decided by the boundary conditions which require certain values for the deflection,  $y$ , the slope,  $dy/dx$ , and the bending moment,  $EI d^2y/dx^2$ , at  $x = 0$  and  $x = L$  or at some intermediate point.

By proper choice of the coefficients,  $C_n$ , and by the use of sufficient terms, any continuous curve from  $x = 0$  to  $x = L$  can be approximated to any desired degree of precision. When, as in the stability problems under discussion, one is dealing with elastic curves of beams, the pre-

cision of engineering computations can nearly always be obtained without using more than two or three terms. This proposition is of such importance that an illustration of its truth is desirable. This requires, however, some discussion of the principle of virtual work and of its use in developing specific trigonometric deflection formulas.

**18 : 3. Principle of Virtual Work** — The *principle of virtual work* is also known as the *principle of virtual displacements* or the *principle of virtual velocities*. In his "Glossary of Physics" Weld<sup>1</sup> defines the principle as that which "states that a condition for the equilibrium of a system is that the total virtual work due to all internal and external forces acting upon the system is zero; or, in other words, that the potential energy of the system is a minimum or a maximum or constant." A *virtual displacement* is any infinitesimal displacement which is geometrically possible even though it may not take place. *Virtual work* is the work that would be done by a force as the result of a virtual displacement if such displacement were to be experienced. Thus, in considering virtual displacements and in applying the principle of virtual work, one may deal with imaginary actions, but he is not particularly concerned by the fact that they may never actually occur.

The significance of this principle and the method of using it may be clarified by developing a criterion for the equilibrium of the lever shown in Fig. 18 : 1. If the lever itself be assumed infinitely rigid and if it be assumed balanced on a frictionless pin at  $O$ , its only possible form of motion is rotation about  $O$ . Thus the only possible virtual displacements are those resulting from rotation about  $O$  through the infinitesimal angle  $d\theta$ . In such a virtual displacement, force  $P$  moves through the

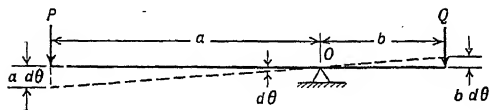


FIG. 18 : 1

distance  $a d\theta$ , and does virtual work equal to  $Pa d\theta$ . At the same time force  $Q$  moves "backward" through the distance  $b d\theta$  and does the negative virtual work  $-Qb d\theta$ .

There is no movement of, and therefore no virtual work done by, the reaction at  $O$ . By applying the principle of virtual work to this situation, a necessary condition for equilibrium is that  $Pa d\theta - Qb d\theta = 0$  or that  $Pa = Qb$ .

In many problems there is more than one possible type of virtual displacement, and in order to obtain complete criteria for equilibrium it is necessary to investigate them all. Consider, for example, the cross-shaped frame, shown diagrammatically in Fig. 18 : 2, which is assumed balanced on a frictionless pivot at  $O$ , the intersection of the two bars.

<sup>1</sup> L. D. Weld, "Glossary of Physics," McGraw-Hill Book Company, 1937, p. 247.

Any possible movement of the frame can be resolved into component rotations about the axes  $AOB$ ,  $COD$ , and a vertical through  $O$ . Assuming a virtual rotation  $d\theta$  about  $COD$  results as above in the relation  $Pa$  must equal  $Qb$ . In that virtual displacement, forces  $R$  and  $S$  do no virtual work since the assumed rotation produces no movement of their points of application. From similar reasoning it can be seen that assumption of a virtual rotation  $d\phi$  about  $AOB$  as an axis produces the additional criterion that  $Rc$  must equal  $Sd$ . A virtual rotation  $d\psi$  about a vertical axis through  $O$ , however, furnishes no additional criterion for equilibrium since it implies no performance of virtual work, all points of application moving in directions normal to the lines of action of the forces. The two equations,  $Pa = Qb$  and  $Rc = Sd$ , constitute necessary and sufficient criteria for equilibrium of the frame, since if they are satisfied the net virtual work done in any imaginable virtual displacement of the system will be zero.

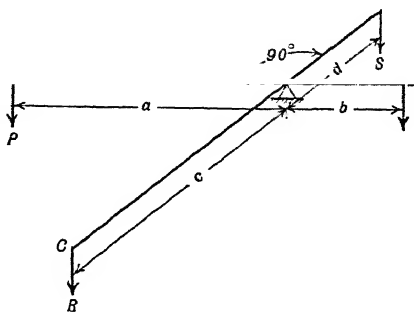


FIG. 18:2

The principle of virtual work can be similarly used to develop criteria for the deformations that must be produced in an elastic body in order to develop the resisting forces required for equilibrium. In such problems the total virtual work to be computed is the sum of the work done by the external forces and the work done by the internal resisting forces, usually negative, as a result of the changes in strain included in the system of virtual displacements.

For practical use the principle needs to be expressed in a formula. For this purpose let  $U$  represent the potential energy of the system under investigation. In general, as the system is subjected to displacements, the potential energy changes. If the displacements are expressed in terms of the mutually independent variables,  $x, y, z, \theta, \phi, \dots$ , the potential energy is some function of those variables and may be represented by

$$U = f(x, y, z, \theta, \phi, \dots) \quad 18:4$$

The principle of virtual work can then be stated as follows: A condition for the equilibrium of a system is that

$$\frac{\partial U}{\partial x} = \frac{\partial U}{\partial y} = \frac{\partial U}{\partial z} = \frac{\partial U}{\partial \theta} = \frac{\partial U}{\partial \phi} = \dots = 0 \quad 18:5$$

This relationship is independent of the method used for determining the form of the function  $f$  in Eq. 18 : 4.

In applying both the virtual work criterion for *equilibrium* and that of Maupertuis for *neutral equilibrium*, a system is assumed to experience a small displacement. In the former operation this displacement must be assumed infinitesimal since, as indicated by Eq. 18 : 5, the criterion is based on the *rate of change* of potential energy at the beginning of the displacement. In the latter it is the *total change* of potential energy that is of interest, and the assumed displacement, though small, must be finite. The two criteria, therefore, are not identical, though they might so appear at first glance.

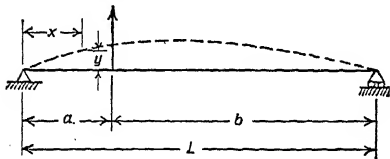


FIG. 18 : 3

**18 : 4. Development of Trigonometric Beam-deflection Formula —**  
The development of trigonometric beam-deflection formulas may be illustrated by that of an expression for the elastic curve of the beam of

Fig. 18 : 3. This beam is assumed simply supported at B and C, subjected to a concentrated load,  $W$ , at A, and of constant  $EI$ . Since the deflection and bending moment at each end is zero, the elastic curve may be represented by Eq. 18 : 3, reducing the problem to that of determining values for the coefficients  $C_n$ .

Each term of Eq. 18 : 3 represents a sinusoidal curve of half-wave length,  $L/n$ , and of maximum amplitude,  $C_n$ . If the proper values of  $C_n$  are used and these curves are superposed the resultant will be, for all practical purposes, the actual deflection curve. Virtual displacements from this deflection curve can be represented by making small changes,  $dC_n$ , in the values of the coefficients. Thus if any particular coefficient,  $C_n$ , be changed to  $C_n + dC_n$ , it is implied that each ordinate is changed by  $dy = dC_n \sin (n\pi x/L)$ . If it can be proved that the virtual work implied by such a change in *any* arbitrarily chosen coefficient is zero, that due to any combination of such changes must also be zero. Then, since any conceivable virtual displacement in the plane of the elastic curve can be represented by such a combination, a general formula for values of  $C_n$  obtained in that manner would give the proper values for those coefficients.

If the amplitude of any one of the sine curves were changed from  $C_n$  to  $C_n + dC_n$ , the movement of the load  $W$  at  $x = a$  would be  $dC_n \sin (n\pi a/L)$  and the virtual work done by that force would be

$$dU_e = W \sin (n\pi a/L) dC_n$$

18 : 6

The virtual work done by the internal resisting forces would be minus the change in the strain energy resulting from the virtual displacement under consideration. By taking from Eq. 10 : 8 the term representing the work due to bending and by making the usual assumption that  $M/EI = d^2y/dx^2$ , the strain energy in the equilibrium position is

$$U_i = \int_0^L \frac{M^2}{2EI} dx = \frac{1}{2} \int_0^L EI \left( \frac{d^2y}{dx^2} \right)^2 dx \quad 18 : 7$$

Then, if  $y$  is represented by Eq. 18 : 3,

$$\frac{d^2y}{dx^2} = -\frac{C_1\pi^2}{L^2} \sin \frac{\pi x}{L} - \frac{C_2 2^2 \pi^2}{L^2} \sin \frac{2\pi x}{L} - \frac{C_3 3^2 \pi^2}{L^2} \sin \frac{3\pi x}{L} - \dots$$

Since  $d^2y/dx^2$  is squared when used in the expression for strain energy, that expression would contain terms of two types,

$$C_n^2 \frac{n^4 \pi^4}{L^4} \sin^2 \frac{n\pi x}{L} \quad \text{and} \quad 2 C_n C_m \frac{n^2 m^2 \pi^4}{L^4} \sin \frac{n\pi x}{L} \sin \frac{m\pi x}{L}$$

where  $m$  and  $n$  are integers and are not equal. Each term must be integrated over the length of the beam, and it can be readily shown that

$$\int_0^L \sin^2 \frac{n\pi x}{L} dx = \frac{L}{2} \quad \text{and} \quad \int_0^L \sin \frac{n\pi x}{L} \sin \frac{m\pi x}{L} dx = 0$$

Hence all terms involving products of the coefficients vanish, while all involving squares remain as  $C_n^2 (n^4 \pi^4 / 2 L^3)$ . The total strain energy of the beam is therefore

$$U_i = \frac{\pi^4}{4 L^3} (C_1^2 + 2^4 C_2^2 + 3^4 C_3^2 + \dots) \quad 18 : 8$$

The virtual work done by the internal forces would be minus the change in  $U_i$  due to  $dC_n$  and may be written

$$\begin{aligned} dU_i &= - \frac{\partial U_i}{\partial C_n} dC_n \\ &= - \frac{\partial}{\partial C_n} \left[ \frac{EI\pi^4}{4 L^3} (C_1^2 + 2^4 C_2^2 + 3^4 C_3^2 + \dots) \right] dC_n \end{aligned}$$

which reduces to

$$dU_i = - \frac{EI\pi^4}{2 L^3} n^4 C_n dC_n \quad 18 : 9$$

Since the net virtual work must be zero to satisfy the principle of virtual work, the right-hand sides of Eqs. 18 : 6 and 18 : 9 may be added and



set equal to zero, whence

$$C_n = \frac{2 WL^3}{\pi^4 EI} \frac{1}{n^4} \sin \frac{n\pi a}{L} \quad 18 : 10$$

By using Eq. 18 : 10 to determine the coefficients and using only the first three terms of the series, Eq. 18 : 3 becomes

$$y = \frac{2 WL^3}{\pi^4 EI} \times \left[ \sin \frac{\pi a}{L} \sin \frac{\pi x}{L} + \frac{1}{2^4} \sin \frac{2\pi a}{L} \sin \frac{2\pi x}{L} + \frac{1}{3^4} \sin \frac{3\pi a}{L} \sin \frac{3\pi x}{L} + \dots \right] \quad 18 : 11$$

when used to represent the elastic curve of the beam shown in Fig. 18 : 3.

If  $a = L/4$  and Eq. 18 : 11 is used to determine the deflection at mid-span where  $x = L/2$ , the result is

$$y = \frac{2 WL^3}{\pi^4 EI} \left[ 0.70711 - \frac{1}{3^4} \times 0.70711 + \dots \right] = \frac{0.01434 WL^3}{EI}$$

From Case 7, Table 4 : 1, this deflection should be

$$y = \frac{WL}{48 EI} \left( L^2 - \frac{L^2}{16} - \frac{L^2}{4} \right) = \frac{0.01432 WL^3}{EI}$$

If more than one side load were acting, the method of super-position would be used and each coefficient would be a sum of terms developed from Eq. 18 : 10, there being a separate term for each load. For a uniformly distributed load,  $W$  would be replaced by  $w da$ , an infinitesimal load producing the infinitesimal deflection  $dy = \frac{2 w L^3}{\pi^4 EI} \sum_{n=1}^{\infty} \frac{1}{n^4}$

$\sin \frac{n\pi a}{L} \sin \frac{n\pi x}{L}$ . If the uniform load extends over the entire span from  $a = 0$  to  $a = L$  the total deflection can be obtained by finding the definite integral of this expression between those limits. Since  $\int_0^L \sin \frac{n\pi a}{L} da = 0$  when  $n$  is an even, and  $2 L/n\pi$  when  $n$  is an odd integer, the result is

$$y = \frac{4 w L^4}{\pi^5 EI} \sum_{n=1,3,5,\dots} \frac{1}{n^5} \sin \frac{n\pi x}{L} \quad 18 : 12$$

For  $x = L/2$ , by using the first two terms of the series, this gives  $y = 0.01302 w(L^4/EI)$ , where the correct value is also  $y = 5 w L^4/(384 EI) = 0.01302 w(L^4/EI)$ . From these figures it can be seen that with the use of only two or three terms the trigonometric formulas produce

results that are less than  $\frac{1}{8}$  per cent in error. Had five terms been used, the results would have been identical to four significant figures. Even if only one term were used, the error would have been only 1.3 per cent for the concentrated and 0.4 per cent for the distributed load.

As indicated by these two checks, Eq. 18 : 3 gives a close approximation to the actual deflection of a simply supported beam. As written, it satisfies the boundary condition requiring  $y = 0$  at  $x = 0$ ,  $x = L$ . Had the deflection at  $x = 0$  been  $A$ , and at  $x = L$  been  $B$ ,  $A + (B - A)x/L$  would have been added to the right side of the equation to provide for their effect. Since  $d^2y/dx^2 = 0$  at  $x = 0$  and  $x = L$ , either expression would accord with the requirement that the moment would be zero at those points. Had the beam been built in at the ends, cosine series would have been used and the  $A + (B - A)x/L$  term added to provide for support deflection if necessary. By choosing functions compatible with the required boundary conditions, it is thus possible to develop readily integrable equations for deflections of beams under various conditions of support and load. This method is of greatest use in practice when it is desired to express the deflection of a beam subjected to a complex load system by a single equation instead of having to divide the span into a number of segments each of which requires a separate formula.

When dealing with plate deflections, instead of using series like that of Eq. 18 : 3, double variable series like

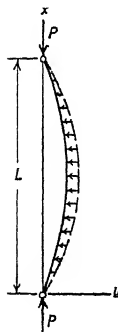
$$z = \sum_{m=1} \sum_{n=1} C_{mn} \sin \frac{m\pi x}{L} \sin \frac{n\pi y}{L} \quad 18 : 13$$

are employed. The mathematical operations required with such series are much more complicated than those with series like Eq. 18 : 3, but they have been used by Timoshenko and others to solve numerous stability problems.

**18 : 5. Critical Load of a Column in an Elastic Medium** — A simple example of the use of Fourier's series in stability investigations is the development of a formula for the critical load of a column in an elastic medium as carried out by Timoshenko.<sup>1</sup> Suppose the pin-ended column of Fig. 18 : 4 is subjected to an axial load,  $P$ , and laterally supported by such closely spaced springs that they may be assumed to form a continuous homogeneous supporting medium. If  $\alpha$  is the spring constant of one spring and  $a$  the spring spacing, the stiffness of support may be represented by the *modulus of foundation*,  $\beta = \alpha a$ . The unit of  $\beta$  is pounds per square inch, and it represents the magnitude of the forces developed per unit length of the column per unit of deflection.

<sup>1</sup> "Theory of Elastic Stability," pp. 108 ff.

If the axis of the column remains straight, it will obviously be in equilibrium regardless of the value of  $P$ . Since the deflection and bending moment at each end must be zero, the elastic curve under the critical load may be represented by the sine series



$$y = \sum_{n=1}^{\infty} C_n \sin \frac{n\pi x}{L} \quad 18:14$$

In passing from the straight to the curved configuration, the column would bend, and the resulting increase of strain energy may be represented by

$$\Delta U_m = \frac{\beta}{2} \sum_{n=1}^{\infty} C_n^2 \quad 18:15$$

FIG. 18:4

as can be seen from comparison with Eq. 18:8.

The lateral reaction of the medium against an element  $dx$  in length is  $\beta y dx$ , and the corresponding strain energy  $\beta y^2 dx/2$ . The total strain energy of the elastic medium is therefore

$$\Delta U_m = \frac{\beta}{2} \int_0^L y^2 dx \quad 18:16$$

Representing  $y$  by Eq. 18:14 and paralleling the procedure used to obtain Eq. 18:8 gives

$$\Delta U_m = \frac{\beta L}{4} \sum_{n=1}^{\infty} C_n^2 \quad 18:17$$

As a result of the bending the distance between the ends of the column changes and the end loads  $P_{cr}$  do the work

$$\Delta U_e = \frac{P_{cr}}{2} \int_0^L \left( \frac{dy}{dx} \right)^2 dx \quad 18:18$$

obtained in the same manner as Eq. 10:6. Substituting Eq. 18:14 in 18:18

$$\Delta U_e = \frac{P_{cr}}{2} \sum_{n=1}^{\infty} \int_0^L \left( \frac{n\pi C_n}{L} \cos \frac{n\pi x}{L} \right)^2 dx \quad 18:19$$

Since the integrations are to be carried from  $x = 0$  to  $x = L$ , when the expression in parentheses is expanded and the terms integrated, those terms which include products of two cosines vanish and those including

squares of cosines become equal to  $\pi^2 n^2 [C_n^2 / (2L)]$ . Therefore

$$\Delta U_e = \frac{P_{cr} \pi^2}{4L} \sum n^2 C_n^2 \quad 18 : 20$$

Since the net change in potential energy of the system must be zero as the column changes shape under the critical load, Eqs. 18 : 15, 18 : 17, and 18 : 20 may be combined, giving

$$\frac{\pi^4 EI}{4L^3} \sum_{n=1}^{\infty} n^4 C_n^2 + \frac{\beta L}{4} \sum_{n=1}^{\infty} C_n^2 - \frac{P_{cr} \pi^2}{4L} \sum_{n=1}^{\infty} n^2 C_n^2 = 0 \quad 18 : 21$$

from which

$$P_{cr} = \frac{\pi^2 EI}{L^2} \frac{\sum_{n=1}^{\infty} n^4 C_n^2 + \frac{\beta L^4}{\pi^4 EI} \sum_{n=1}^{\infty} C_n^2}{\sum_{n=1}^{\infty} n^2 C_n^2} \quad 18 : 22$$

The absolute critical load will be that associated with the values of  $C_n$  which make Eq. 18 : 22 a minimum. It can be shown that an expression of this kind will have its minimum value when all values of  $C_n$  but one are zero.<sup>1</sup>

If the coefficient differing from zero is called  $C_m$ , Eq. 18 : 14 reduces to

$$y = C_m \sin \frac{m\pi x}{L} \quad 18 : 23$$

and Eq. 18 : 22 becomes

$$P_{cr} = \frac{\pi^2 EI}{L^2} \frac{m^4}{m^2} = \frac{\pi^2 EI}{L^2} m^2 \quad 18 : 24$$

The number of half-waves into which the column would bend can now be determined from the condition that Eq. 18 : 24 is a minimum. If there were no elastic medium,  $\beta$  would be zero and  $m$  would have to be equal to 1. Then Eq. 18 : 24 would become identical with the Euler formula, Eq. 10 : 12, as it obviously should, since the conditions would be those of Art. 10 : 5 for a pin-ended column. For very small values of  $\beta$ , Eq. 18 : 24 would still give the smallest value if  $m = 1$ , indicating

<sup>1</sup> If two fractions such as  $a/c$  and  $b/d$  are combined by adding numerators and denominators to form the fraction  $(a + b)/(c + d)$ , the latter will be intermediate in value between the original fractions. This can be extended to a fraction made up of any number of simple fractions in this manner, provided all terms are positive. Since, in Eq. 18 : 22,  $C_n$  is always squared, that expression may be thought of as made up in this manner, and the above statement is proved.

that in a very flexible elastic medium the column would bend in a single half-wave but under a somewhat larger critical load than that for a pin-ended column without elastic support. If  $\beta$  is sufficiently increased, however, a condition is eventually arrived at where Eq. 18 : 24 gives a smaller value for  $m = 2$  than for  $m = 1$ , indicating that there would be a point of inflection at the middle, half of the column bending to the right and the other half to the left. The value of  $\beta$  at which either type of buckling might take place can be found by equating the expression of Eq. 18 : 24 with  $m = 1$  to the same expression with  $m = 2$ . Then

$$1 + \frac{\pi^4 EI}{L^4} = 1 + \frac{4\pi^4 EI}{L^4}$$

from which  $\beta = 4 \pi^4 (EI/L^4)$ . By further increasing  $\beta$ , conditions can be found in which the column would buckle into 3, 4, 5, . . . half-waves.

When Fourier's series are used to represent elastic curves in the determination of critical loads, it is usually sufficient to use one term of the series. When the actual deflections are desired, while one term will sometimes give a sufficiently precise result, it is usually necessary to use two or three terms, but seldom more.

Many problems of stability have been solved by the general method illustrated above. Its applicability is limited, however, to structures which can maintain equilibrium between the external forces without the development of bending deformation. Its use is therefore most widespread in dealing with problems of initially straight columns and flat plates, though it can also be employed with ideal pin-connected trusses. When a structure is bent by loads below the critical, there are no alternative patterns of finite deformations consistent with neutral equilibrium. With such structures, however, the formulas which define the deflections at which the structure would be in equilibrium under load indicate infinite deflections for the loading at the transition from stability to instability. This situation in connection with beam-columns is discussed in Art. 14 : 6.

In the above illustration the material is assumed perfectly elastic. In practical structures the critical loads based on this assumption may produce stresses in excess of the yield point. Then the actual critical load would be reduced by the effect of the resulting plastic flow of the material. The practical effect of this with respect to columns is discussed in Art. 10 : 7 and will not be treated in more detail.

**18 : 6. Types of Instability Failure** — For convenience, instability failures may be classified as "local," "unit," or "group." The distinction between them may be clarified by considering the modes of failure possible on a longitudinal stiffener on the compression side of a

stressed-skin fuselage structure. The stiffener might be constructed, for instance, of material so thin in comparison with its other dimensions that it would buckle locally into a pattern whose half-wave length would be about equal to the width of the stiffener, regardless of how much the bay in which it occurred, or the transverse rings at the end of that bay, might deform under load. Failure resulting from such localized buckling may be classified as due to "local instability."

Were the material thick enough to prevent that type of failure, the stiffener might still become unstable as a column between any two transverse stiffening rings, though the rings themselves might not be appreciably deformed either before or after the longitudinal had deflected excessively under load. Failure resulting from the collapse of a single bay in this manner would be a "unit instability" failure.

Since the longitudinal stiffener is a continuous beam-column, deformation of an intermediate transverse ring might render two adjacent bays of the beam-column unstable although neither would collapse if the ring provided a rigid support. Such a failure would involve the transverse ring and at least two bays of the longitudinal stiffener. It would be of the "group instability" type.

The absolute critical loading of a structure may be associated with any of these three types of instability. While the designer must try to determine this loading, it is not always possible for him to do so. He may usually, though not invariably, use sections so thick that the likelihood of local instability failure is eliminated, but he cannot be certain, with the procedures currently available, that his determination of the loads producing unit or group instability is correct. When he resolves a complex structure into units, he tacitly assumes that the supports for each unit are so rigid that any instability failure will be of the unit or the local type. In any practical structure, however, each unit in a group deforms under the load it transmits to the members supporting it. Since the supporting elements are not composed of materials of infinite stiffness, they also deform and provide an elastic<sup>1</sup> rather than a rigid support. It may be shown that the critical load for an elastically supported unit may be smaller than that for the same unit with rigid supports and hence that the practical unit may be involved in a general instability failure at a load lower than the critical value indicated by a formula developed for ideal end conditions.

In a practical structure it is usually possible to provide supporting elements of such stiffness that changes in critical load resulting from support deflection are of the same order of magnitude as those due to

<sup>1</sup> Although the supporting structure might deform plastically as well as elastically, it would not affect the conclusions of the present argument.

variations in quality of material, in manufacturing tolerances, and in other similar factors. It would be desirable for the engineer to have criteria applicable to complex systems of members which would insure the adequacy of the support given any unit. The problem of group instability failure resolves itself, in fact, to the development of such criteria. While satisfactory solutions have been developed for certain arrangements of members, much remains to be done before criteria are available for the analysis of any type of structure.

### 18 : 7. Stability of a Column Carrying a Variable Transverse Load —

Consider an ideal pin-ended member of length  $L$ , carrying an axial compression  $P$ , and a concentrated transverse force  $W$  which may be varied in magnitude as desired. Assume the column axis to be perfectly free to rotate at each end and to be rigidly restrained against translational

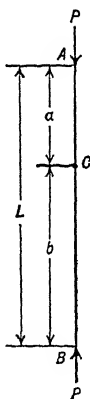


FIG. 18:5a

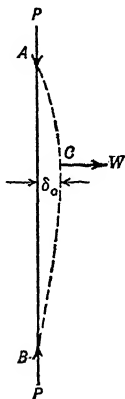


FIG. 18:5b

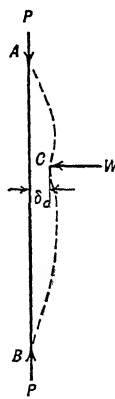


FIG. 18:5c

movement normal to the axis. Let the transverse load first be zero. Then, so long as  $P$  is less than the Euler load,  $\pi^2(EI/L^2)$ , the column axis will remain straight as shown in Fig. 18 : 5a.

Now let  $W$  have any finite magnitude and let it be applied at point  $C$ ,  $a$  units from the top of the column. Even though  $P$  be less than the Euler load, the column will bend and its axis will assume a shape similar to that of Fig. 18 : 5b. Depending on the magnitude of the force  $W$ , the deflection of point  $C$ , as given in Art. 14 : 5, is

$$\delta_c = \frac{W}{P} \left( \frac{j \sin \frac{b}{j} \sin \frac{a}{j}}{\sin \frac{L}{j}} - \frac{ab}{L} \right) \quad 18 : 25$$

For  $L/j$  less than  $\pi$ , Eq. 18 : 25 always gives a positive value for  $\delta_c$ , meaning that the deflection  $\delta_c$  is in the same direction as  $W$ . It is better to say that when  $L/j$  is less than  $\pi$ , if equilibrium is to be maintained by a load at  $C$  when there is deflection of that point, the load must act in the same way as the deflection.

For a given column of constant  $EI$  carrying a specific load  $P$ , there is a definite value of  $j$ ; so Eq. 18 : 25 may be written

$$W = K_c \delta_c \quad 18 : 26a$$

whence

$$K_c = \frac{W}{\delta_c} \quad 18 : 26b$$

in which  $K_c$  is a constant for a given location of point  $C$  and magnitude  $P$ . This constant may be called the "spring constant of point  $C$  of the column for load  $P$ ."

As  $P$  increases,  $K_c$  will decrease until  $P = \pi^2 E(I/L^2)$  and  $L/j = \pi$ , when it becomes equal to zero. This means that when  $P$  is equal to the Euler load no transverse force at  $C$  is needed to maintain equilibrium when the column is bent, a fact already implied in Art. 10 : 5.

If  $P$  exceeds the Euler load, Eqs. 18 : 25 and 18 : 26a remain valid, but  $K_c$  becomes negative. This indicates that the elastic curve has the shape shown in Fig. 18 : 5c and that the transverse load acts in the direction opposite to the deflection if equilibrium is to be maintained.

Thus, to maintain the column in a bent equilibrium position when  $L/j$  is less than  $\pi$ , an "active" load is needed at  $C$  in the direction of the deflection. But if  $L/j$  be greater than  $\pi$ , a "supporting force" in the direction opposing the deflection is required. For  $L/j$  exactly equal to  $\pi$ , the bent column will be in equilibrium only when there is no transverse load at  $C$ .

So long as the spring constant of point  $C$  of the column is positive, the column is stable because  $W$  must be increased to cause an increase in the deflection  $\delta_c$ . If  $W$  be reduced, the column straightens. On the other hand, if the spring constant be negative, the column is unstable since any reduction in the load  $W$  will be accompanied by an increase of both the deflection and the value of  $W$  required for equilibrium. The deflection would therefore increase until the column collapsed.

**18 : 8. Stability of an Elastically Supported Column** — Suppose now that point  $C$  is not free to move laterally but is connected to some "supporting structure." For example, assume that at  $C$  the column be connected by a frictionless pin to the rod  $CD$  of length  $L_r$  and that the rod be rigidly supported at  $D$ , as shown in Fig. 18 : 6. Then any deflection of  $C$  would involve axial deformation of rod  $CD$  which would develop



tensile or compressive stresses in it. If point  $C$  were to move through the distance  $\delta_c$  to  $C'$ , the rod would be shortened and a compressive stress equal to  $E(\delta_c/L_r)$  would be developed in it. This stress multiplied by the sectional area of the rod would then be available as a supporting force to maintain equilibrium.

From Eq. 18 : 26a the supporting force required can be seen to be directly proportional to the deflection. Also the supporting forces developed will be proportional to the deflection  $\delta_c$ . Then if deflection of point  $C$  involves building up a supporting force in the rod at a more rapid rate than the increase in supporting force needed, the deflection will not take place and the column will be in stable equilibrium. Conversely, if the supporting force needed builds up at a more rapid rate than the supporting force developed, once deflection gets started it will continue indefinitely and the column will be unstable.

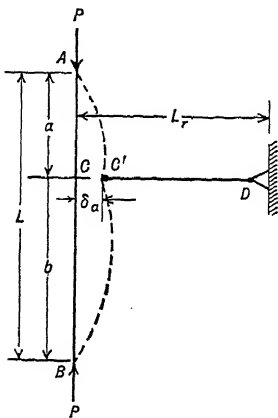


FIG. 18:6

The change in supporting force per unit of deflection is the "spring constant of the supporting structure at  $C$ " and may be designated  $K_s$ . Thus a criterion for stability is that, if the algebraic sum of the spring constants of the column at  $C$  and of the supporting structure at  $C$ ,  $(K_c + K_s)$ , is positive, the column is in stable equilibrium and, if it is negative, the column is unstable. Since the column would be in neutral equilibrium if  $K_c = -K_s$ , the relation between the critical load of the column and the spring constant of the supporting structure is

$$-K_s = \frac{PL \sin \frac{L}{j}}{Lj \sin \frac{a}{j} \sin \frac{b}{j} - ab \sin \frac{a}{j}}$$

the expression for  $K_c$  being obtained by substituting Eq. 18 : 25 into Eq. 18 : 26b and rearranging terms. On multiplying both sides of Eq. a by  $L^3/EI$  to obtain non-dimensional parameters, recognizing that  $P = EI/j^2$ , and simplifying, the relation takes the form

$$EI \left( \frac{L}{j} \right)^4 \sin \frac{L}{j} = \frac{L}{j} \sin \frac{a}{j} \sin \frac{b}{j} - \frac{a}{j} \left( \frac{b}{j} \sin \frac{L}{j} \right)$$

If, for example,  $a = 0.3 L$  and  $L/j = 5.0$ , Eq. *b* gives

$$\begin{aligned} \frac{K_s L^3}{EI} &= \frac{-625 \sin 5.0}{5 \sin 1.50 \sin 3.50 - 1.5 \times 3.5 \sin 5.0} \\ &= \frac{-625 (-0.95895)}{5 \times 0.99749 (-0.35078) - 5.25 (-0.95895)} = 182.5 \end{aligned}$$

In Fig. 18 : 7 a curve of associated values of  $K_s L^3 / (EI)$  and  $L/j_{cr}$  for  $a = 0.3 L$  is shown. For  $K_s = 0$ ,  $L/j_{cr} = \pi$ , as would be expected, since a spring constant of zero is equivalent to no support, and the member would be a pin-ended column of length  $L$ . As  $K_s$  increases,  $L^3/EI$  being constant for any specific column, the critical load, and hence  $L/j_{cr}$ , increases. By comparison of Eq. 18 : 25 and the criterion of Art. 14 : 6 for a pin-ended two-span continuous beam-column it can be proved that the curve of  $L/j_{cr}$  for the elastically supported column as obtained from the former, is asymptotic to the value of  $L/j_{cr}$ , obtained from the latter. This means that as the stiffness of the supporting structure is increased the critical load for the member is increased, but it will never quite attain the value indicated by the methods of Art. 14 : 6, in which it was assumed that the supports were rigid.

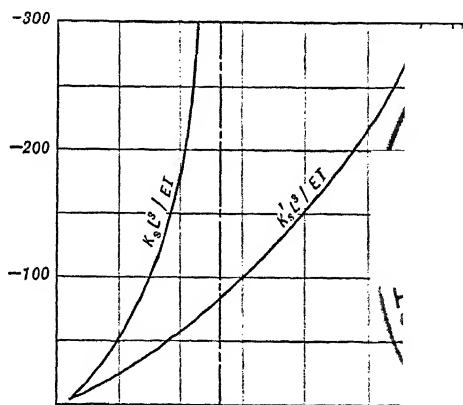


FIG. 18 : 7

If instead of a single elastic support, a column were provided with two symmetrically located supports of equal stiffness, a similar analysis could be made to determine the relationship between the spring constants of those supports and the critical load of the column. If the two supports were at the distance  $0.3 L$  from each end, the relationship would be that indicated by the  $K'_s (L^3/EI)$  curve of Fig. 18 : 7. This curve can also be proved asymptotic to the value of  $L/j_{cr}$ , obtained by the method of Art. 14 : 6 for the corresponding case of the symmetrically loaded beam-column with two rigid supports. It should be noted that, when the second support is provided, the critical load is markedly increased for a given support spring constant and that the asymptotic

load for the member with two supports is also much greater than for the member with one.

**18 : 9. Effect of Non-linear Resistance to Deflection** — In the preceding discussion the resistance to deflection provided by the support at  $C$

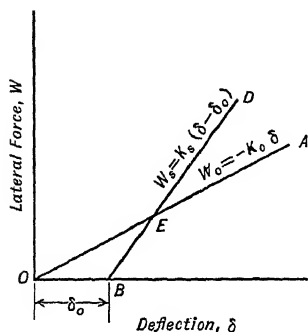


FIG. 18:8

was assumed proportional to the deflection of that point. That is not necessary. For example, there might be play in the joint at  $C$ , which would permit that point to deflect a distance  $\delta_0$  before any resistance would be developed in the supporting structure. If it be assumed that once a resisting force begins to develop it increases linearly with the deflection at  $C$ , the situation can be represented by the straight line  $BD$  of Fig. 18 : 8. The equation of that line is  $W_s = K_s(\delta - \delta_0)$ , where  $W_s$  is the resisting force developed as a result of the deflection  $\delta$  at point  $C$ ,  $K_s$

being the spring constant of the supporting structure, and  $\delta_0$  being the deflection at which it begins to act.

If  $K_c$  is the negative spring constant of the column for point  $C$ , the straight line  $OA$ , the equation of which is  $W_c = -K_c\delta$ , may be added to Fig. 18 : 8. This line indicates the magnitude of the supporting force  $W_c$  required to maintain equilibrium when the deflection of point  $C$  is equal to  $\delta$ . It should then be evident that the intersection of these lines at  $E$  will indicate the magnitude of the resisting force and the deflection at which such a force in the supporting structure will become sufficient to prevent further deflection. It can also be seen from the diagram that, so long as the algebraic sum of  $K_c$  and  $K_s$  is positive, there will be an intersection  $E$ . The combination will be stable and, although the deflection may get a start, it will eventually be stopped by the resistance of the supporting structure. If, however, that algebraic sum is small or if the initial deflection  $\delta_0$  is large, the necessary resisting force may not be developed until excessive unit stresses due to bending have caused plastic flow and failure in a practical column.

If the resisting forces developed are not proportional to the deflection of point  $C$ , but are known functions of that deflection, curve  $BD$  of Fig. 18 : 8 can be suitably modified and the supporting force and deflection associated with equilibrium can be determined if the mathematical procedures involved are not beyond the ability of the engineer.

**18 : 10. Effect of a Transverse Load** — So far it has been assumed that the transverse load acting on the column corresponded to that

which would be developed in a structure supporting the column at  $C$ . The presence of any other transverse load would make no change in the general conclusions as to the criterion for stability, though it would affect the magnitude of the deflection at point  $C$ , at which the system would come into equilibrium.

If the column  $AB$  is subjected to any specific transverse load,  $w = f(x)$ , in addition to the concentrated force,  $W$ , imposed at  $C$ , an expression for the resulting deflection at point  $C$  can be obtained by the method of Art. 14 : 5. If the axial load,  $P$ , is assumed constant, this expression can be simplified to take the form

$$\delta = \frac{W}{K_c} + \delta_w \quad 18 : 27$$

in which  $\delta_w$  is the deflection of point  $C$  consistent with equilibrium when  $W$  is zero,  $K_c$  is the same as in Eq. 18 : 26, and  $\delta$  is the deflection of point  $C$  consistent with equilibrium when the concentrated load at  $C$  is of magnitude  $W$ .

From Eq. 18 : 27 the relation

$$W = K_c(\delta - \delta_w) \quad 18 : 28$$

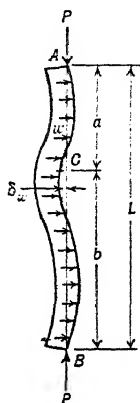


FIG. 18 : 9

follows for the load at  $C$  required to maintain equilibrium when the deflection of that point is equal to  $\delta$  and when the column is subjected to the side load  $w = f(x)$  which, if it were the only side load acting, would produce the deflection  $\delta_w$ .

So long as  $L/j$  is less than  $\pi$  and  $w$  is positive (that is,  $w$  acts in the same direction as the deflection)  $K_c$  and  $\delta_w$ , and hence  $W$  and  $\delta$ , will be positive. In this condition the column will be in stable equilibrium and the deflection  $\delta$  will vary linearly with  $W$ . The chief difference between this situation and that described in Art. 18 : 8 is that when  $w = 0$ , there will be equilibrium with some definite deflection of  $C$  instead of zero deflection of that point.

When  $L/j$  exceeds  $\pi$ ,  $\delta_w$  and  $K_c$  both change sign. This means that for equilibrium when  $W = 0$ , the deflection  $\delta_w$  must be in the opposite direction to the forces  $w = f(x)$ , the elastic curve having a shape similar to that shown in Fig. 18 : 9. If the deflection at  $C$  have any other value, equilibrium will be obtained only by the development of a restraining force  $W$  of opposite sign to the difference  $\delta - \delta_w$ . If there be an elastic support provided at  $C$  with a spring constant  $K_s$ , the equilib-

rium conditions can be represented in the manner of Fig. 18 : 8 by a figure like 18 : 10. From this figure it can be seen that the criterion for stability will again be that the algebraic sum of  $K_c$  and  $K_s$  must be positive.

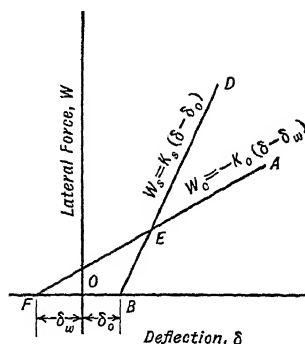


FIG. 18 : 10

**18 : 11. Conclusions Regarding the Spring-constant Criterion** — From this study of a pin-ended column with a single elastic support two important propositions emerge. The spring-constant criterion for stability is not affected by play in the joint between the member and its support or by the presence of a transverse load acting on the member. It is also evident that the criterion is equally unaffected by

initial curvature of the member. Only in ideal cases, however, could the critical load associated with a given value of  $K_s$  be attained. In practical structures there would be excessive deflection of point C under loads approaching the critical, and the resulting bending moments would cause stresses in excess of the yield point of the material, so that plastic failure would occur before the critical load was reached.

It is also found that, as  $L/j$  increases, the value of  $K_s$  required for stability increases and becomes infinite for the value of  $L/j$  associated with unit instability failure, as given by the procedures of Art. 14 : 6 where it is assumed that the supports are absolutely rigid. This has been discussed only in connection with the column of Art. 18 : 7, but it can be seen to be equally true for the others.

The analyses on which the above conclusions are based are for simple academic structures. In almost any practical structure there would be several supports and more than one independent support spring constant. There is no apparent reason to doubt, however, that with beam-columns of several spans resting on supports of different stiffnesses the critical loading is independent of such factors as play in connections to the supports, distribution of transverse load, or initial curvature and that it approaches the values obtained from the procedure of Art. 14 : 6 as the support spring constants approach infinity. Similar relations, though not developed here, appear most likely for other complex structures.

For the structures analyzed above it would be a simple matter to develop criteria of adequacy. Perhaps the simplest would be an arbitrary ratio of critical load computed on the assumption of elastic support

to that based on an assumed rigid support. For single units, where only one support spring constant would be involved, its required value could be obtained from curves like those of Fig. 18 : 7. It has been found, however, that efforts to extend this method to structures having several members or several supports result in such complicated mathematics that it is impractical at present, though it seems to offer some possibilities as a basis on which to develop empirical criteria.

**18 : 12. Stability of Rigid-jointed Trusses** — Professor N. J. Hoff<sup>1</sup> has developed a method for determining the stability of rigid-jointed trusses which is also applicable to continuous beam-columns or to any system of axially loaded members to which the method of moment distribution may be applied.

The first step of Hoff's procedure is to compute the value of  $L/j$  for each member. When this exceeds  $2\pi$  for any compression member having both ends restrained, the loading exceeds the critical and no further investigation is needed. The same is true when any compression member with both ends pinned has a value of  $L/j$  in excess of  $\pi$ , or when a compression member with one end pinned and the other elastically restrained has  $L/j$  in excess of 4.49. High values of  $L/j$  in tension members do not indicate that the critical load is exceeded because high tensile loads do not tend to make a structure unstable.

If all values of  $L/j$  satisfy the above limitations, the stiffness factor for each end of each member is determined from Fig. 14 : 13, Tables 14 : 8 and 14 : 9, or Eqs. 14 : 27 to 14 : 29.<sup>2</sup> The stiffness factors of all members entering each joint are then added algebraically and, when the sum of the stiffness factors for the members entering any joint is negative, the critical load has been exceeded. If the sums of the stiffness factors at all joints be positive, the truss should be analyzed by the moment distribution methods of Art. 14 : 11. This analysis might be made for the secondary joint moments due to the actual transverse loads acting on the structure. Often, however, it is simpler to make the analysis for an arbitrary couple applied at some joint. If this analysis result in a unique set of finite bending moments at the joints, the loading does not exceed the critical. If the computer obtain a set of finite bending moments but suspect that it may not be unique, all he need do is alter the order of balancing the joints. When he still gets essentially the

<sup>1</sup> "Stress Analysis of Aircraft Frameworks," *Jour. Roy. Aero. Soc.*, July, 1941.  
"Stable and Unstable Equilibrium of Plane Frameworks," *Jour. Aero. Sci.*, p. 3, January, 1941.

<sup>2</sup> For six-place tables, see "Tables of Stiffness and Carry-over Factors for Structural Members under Axial Load," E. E. Lundquist and W. D. Kroll, N.A.C.A. Technical Note 652, 1938.

same joint moments, the critical load has not been exceeded and the truss is stable. If he fail to obtain essentially the same joint moments, the critical load has been exceeded.

One great advantage of this method of checking the stability of a rigid-jointed truss is that a single set of computations may be used for the two purposes of checking the stability and determining the bending moments which must be resisted by the truss members. In this feature it is superior to most of the alternative methods that have been suggested. Another advantage is that it is not necessary to subdivide the truss into smaller units in order to make the investigation, but the truss is considered in the manner in which it acts, as a single group.

In addition to proving the validity of this method of determining whether a truss is stable, Hoff devised a method of visualizing the relations between the moment distribution procedure and the basic criteria for stability. With a simple system in which the possible shape changes may be determined by only two independent variables, the relations between the potential energy of the system and those variables can be represented by a surface in three-dimensional space which will be called the *potential energy surface* for the system. Thus if the system were composed of a single span beam with restrained ends and the external forces acting on it, the independent *shape variables* would be the rotations of the two ends. The potential energy surface would be constructed by the methods of analytical geometry, plotting values of the shape variables parallel to mutually perpendicular axes in a horizontal plane. The corresponding values of potential energy would be plotted vertically.

Partial derivatives of the potential energy with respect to each of the shape variables would represent the slopes of tangents to the potential energy surface with horizontal projections parallel to the axis for that variable. Therefore, by the principle of virtual work, any pair of values of the shape variables associated with equilibrium of the structure would be associated with a point on the potential energy surface where the slopes of both such tangents would be zero. Maupertuis' theorem then implies that if that equilibrium is stable, the point in question would be at a low point of the surface, like the bottom point of a bowl. Conversely, if the potential energy surface were shaped like a dome, the point at the top would represent a condition of unstable equilibrium. For neutral equilibrium the point would have to be on a flat horizontal part of the surface.

Each step in a moment distribution analysis reflects an imaginary change in one of the shape variables, and the corresponding change in potential energy could be represented on the potential energy surface

by a curve joining the points associated with the values of those variables before and after the step in question. In the following discussion this curve will be termed the *energy change curve*. Hoff has proved that if the limitations affecting  $L/j$  and stiffness factors mentioned at the beginning of this article are satisfied, each step of a moment distribution analysis of the type described in Art. 14:11 will represent a change in the shape variables that would be associated with a decrease in potential energy of the system. Thus let  $A$  be the point on the potential energy surface representing conditions at the start of the moment distribution analysis when the slopes of both ends of the beam are assumed zero, and  $B$  the point representing conditions after one end has been released and balanced. Then by Hoff's theorem, point  $B$  must be lower than point  $A$ . If  $C$  be the point representing conditions after the second balancing operation, it will be lower than  $B$ . The horizontal projection of segment  $AB$  of the energy change curve will be parallel to the axis for the shape variable assumed to change in the first balancing operation. The projection of segment  $BC$  will similarly be parallel to the axis for the shape variable assumed to change in the second balancing. In a normal moment-distribution analysis of a structure with two independent shape variables, those variables would be assumed to change alternately, and the projection of the energy-change curve would be a series of straight segments parallel to the axes of the shape variables. If the beam were stable, this curve would start at  $A$  and extend down the potential energy surface until it reached the low point representing the equilibrium shape. This would be reflected by convergences of the series of moment increments. If the beam were unstable under the assumed loading, in general the energy change curve would start at  $A$  and continue to descend indefinitely. This would be reflected by the moment increments forming a divergent series.

If instead of only two, there were  $n$  independent shape variables, the potential energy surface would be one in  $n + 1$  dimensional space, and, though difficult to visualize, the same type of relations would apply.

With some special structures and loadings, the moment-distribution analysis may give a finite result although the structure may be in neutral or unstable equilibrium. Thus if the potential energy surface were dome-shaped and one happened to start the analysis, assuming the conditions represented by the top point of the dome, it would appear that no balancing was needed. A more likely situation is that the potential energy surface would be shaped like a mountain pass, with a "saddle point" from which it sloped upward in both directions parallel to one co-ordinate axis and downward in both directions parallel to the



other. An energy-change curve, representing a moment distribution analysis, which started above the saddle point, might happen to bring it down to the saddle point, and a finite result would thus be obtained. With any alternative order of balancing, however, the energy-change-curve would miss that saddle point. On a complex surface with two or more saddle points below the point *A*, the alternative order of balancing might bring the energy change curve to another of these points, and thus a different finite result would be obtained by the moment-distribution process, but usually the changed order of balancing will be represented by a curve which drops indefinitely and by a divergent series of moment increments. It is the possibilities mentioned in this paragraph which make it necessary to require that the results of the moment distribution process be unique as well as finite. In any specific problem, however, the uniqueness of a solution can be easily checked by changing the order of balancing.

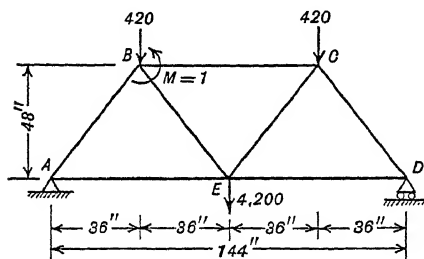


FIG. 18:11

This would mean that the analysis would be reflected on the potential energysurface by a different energy-change curve, but if the structure were stable this new energy change curve would lead to the same low point on the potential energy surface as the first one.

### 18 : 13. Illustrative Example —

Consider a simple truss such as that shown in Fig. 18 : 11, all members being round, mild steel tubes

and all joints being welded. Under the forces applied at *B*, *C*, and *E* the loads in the members are as shown. Table 18 : 1 gives pertinent

TABLE 18 : 1

Members	Size	Load <i>P</i>	Area <i>A</i>	Stress <i>P/A</i>	Eff. $\bar{E}/1,000$	Length <i>L</i>	Mom. of Inertia <i>I</i>	$j^2 = \frac{\bar{E}I}{P}$	<i>L/j</i>
<i>AB</i> and <i>CD</i>	$1\frac{1}{2} \times 0.035$	-3,150	0.1336	-23,577	25,321	60	0.02467	198.31	4.261
<i>BE</i> and <i>EC</i>	$1\frac{1}{2} \times 0.035$	+2,625	0.1336	+19,648	27,775	60	0.02467	261.03	3.714
<i>BC</i>	$1\frac{1}{2} \times 0.049$	-3,465	0.1849	-18,742	27,963	72	0.03339	269.46	4.386
<i>AE</i> and <i>ED</i>	$1\frac{1}{2} \times 0.035$	+1,890	0.1336	+14,147	28,000	72	0.02467	365.48	3.766

data on the sizes of members, their areas, and so forth. It is assumed that sufficient bracing is provided so that the members will not fail by buckling out of the plane of the truss.

The modulus of elasticity for mild steel tubing is taken as 28,000,000 p.s.i. for stress intensities below one-half the yield point of the material

in both tension and compression. For stress intensities greater than this, an effective modulus of elasticity is used as suggested in Art. 10 : 11.

Equation 10 : 23,  $\bar{E} = \frac{P}{A} \left[ 36,000 - \left( \frac{P}{A} \right) \right]$  applies to this steel.

While there is little justification for reducing the modulus in tension to the same extent as in compression, the use of  $\bar{E}$  instead of 28,000,000 p.s.i. for the tubes in tension leads to greater values of  $L/j$  and of  $SL/\bar{E}I$  but to smaller values of the actual stiffness factor,  $S$ . It is therefore conservative to employ some reduction and, for the lack of more exact data as to the variation of  $\bar{E}$  in tension, the assumption that it is the same as in compression is justifiable for investigations of this sort.

Attention is called to the fact that the  $L/j$  of all members lies between  $\pi$  and  $2\pi$ ; so the compression members in the truss would be unstable were they pin-connected. Since they are welded, however, each member is restrained, but not fixed, by those attached to it at each joint, and it is necessary to evaluate the stiffness coefficients for each member before determining whether or not the truss is stable. They are presented in Table 18 : 2, the values of  $SL/\bar{E}I$  having been taken from Table 14 : 8 or 14 : 9, depending upon whether the member was in compression or tension. Values of the carry-over factor,  $C$ , were taken from the same tables.

TABLE 18 : 2

Members	$L/j$	$\frac{SL}{\bar{E}I}$	$\frac{\bar{E}I}{L}$	$S$	$\Sigma SA$	$\Sigma SB$	$\Sigma SE$	$C$
<i>BA</i> and <i>CD</i>	4.261	0.1523	10,411	1,586	1,586	1,586		5.3831
<i>BE</i> and <i>EC</i>	3.714	1.3951	11,420	15,932		15,932	31,864	0.3012
<i>BC</i>	4.386	0.0806	12,968	1,045		1,045		11.642
<i>AE</i> and <i>ED</i>	3.766	1.4048	9,594	13,478	13,478		26,956	0.2981
					15,064	18,563	58,820	

Since the summation of the stiffness factors for the members meeting at each of the joints,  $A$ ,  $B$ , and  $E$ , is positive, a necessary condition for stability is satisfied, but this is not a complete proof that the truss is stable. The latter is obtained by applying a unit couple at joint  $B$  and by distributing it to see whether or not the solution obtained is unique and finite. Carry-over and distribution factors are shown in Fig. 18 : 12*a*, while the balancing and carry-over moments of the first cycle of distribution are entered on Fig. 18 : 12*b*. These computations differ from those of Fig. 13 : 12 in that as each joint is balanced the carry-

over moments are recorded at once and used in the next balancing of each joint where they act. The order of balancing the joints can be followed from the figures in parentheses.

At the end of the cycle shown in Fig. 18 : 12*b*, all joints are balanced, except *B*, at which there is an unbalanced moment of 0.8404 unit. Additional cycles in which the joints are balanced in the same order would obviously produce a series of unbalanced moments at *B*, each 0.8404

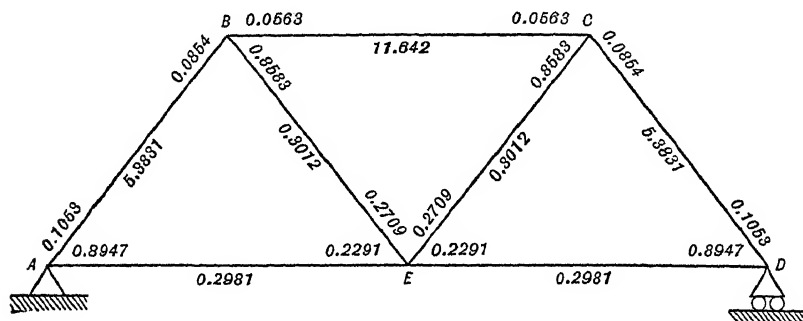


FIG. 18: 12(a)

times that of the preceding cycle. Since this ratio is less than unity, the series would be convergent, its sum equal to  $1/(1 - 0.8404) = 6.25$ , and the truss satisfies Lundquist's criterion for stability.<sup>1</sup> Had the unbalanced moment at *B* resulting from the computations of Fig. 18 : 12*b* exceeded unity, the series would be divergent and the truss shown to be unstable.

A second cycle of moment distribution, carried out with a somewhat different order of balancing the joints, gives  $0.7062 = 0.8404 \times 0.8403$  as the next term of the series of the unbalanced moments at *B*. This shows the moment distribution solution to be unique as well as finite, and that the truss completely satisfies Hoff's criterion.

It is interesting to note that, if values of stiffness coefficients are computed for increasing loads at *B*, *C*, and *E*, their sum at joint *A* passes through zero for loads of 516 pounds at *B* and *C*, 5,160 pounds at *E*. The sum of the coefficients at joint *B* passes through zero for loads of 506 pounds at *B* and *C*, 5060 pounds at *E*. Under loads of these magnitudes, the joints would be equivalent to pin connections at *A* and *D* or at *B* and *C*. Since the  $L/j$  of member *BC* would exceed  $\pi$  when *B* and *C* behaved as pin joints, it would be expected that this structure would collapse. By using Lundquist's or Hoff's criteria, however, it

<sup>1</sup> "Stability of Structural Members under Axial Load," E. E. Lundquist, N.A.C.A. Technical Note 617, 1937.

may be shown that this truss reaches its stability limit when the loads at *B* and *C* are about 440 pounds, that at *E* is 4,400 pounds; so the criterion that the sum of the stiffness factors passes through zero does not yield the critical load for this truss.

When the stability of a truss having a number of members is to be determined, the operations involved in the method of moment distribution become burdensome and lead to error unless the greatest care

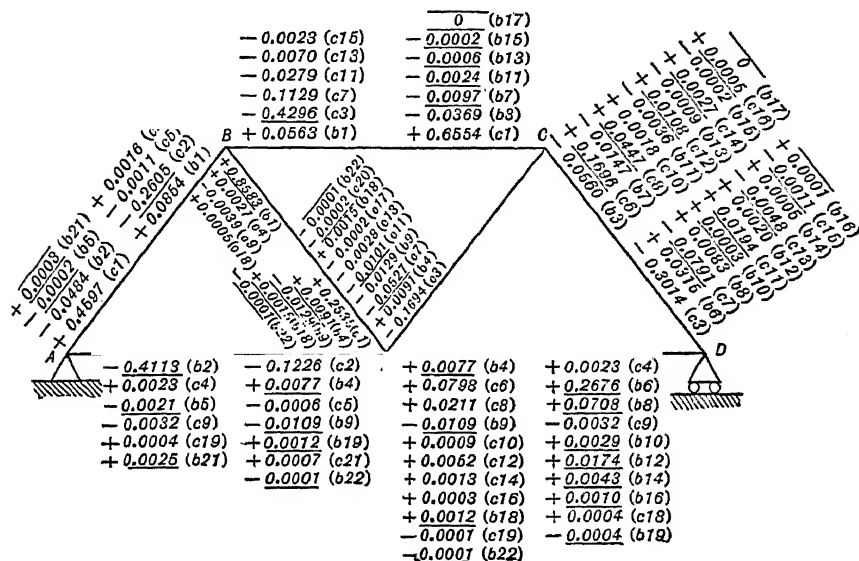


FIG. 18: 12(b)

is exercised with factors and signs. Lundquist<sup>1</sup> has found that satisfactory approximations to the stability of the structure may be obtained by breaking it up into groups of five or six members, applying a unit moment to a joint in each group, and determining whether or not the series involved in the moment-distribution cycles converge or diverge. It is convenient when dealing with such groups to assume pin connections where members of different groups are joined. When the group method is used, a member forming part of one group should under no circumstances be used as part of another. The groups should be so chosen that each member is used but once.

**18 : 14. Empirical Determination of the Critical Load** — When members that become unstable under high loads are subjected to bending deformation by loads less than the critical, the deflections from the

<sup>1</sup> *Op. cit.*

configuration of zero load usually increase at an accelerating rate as the critical load is approached. This is illustrated by the column deflection curves of Fig. 10 : 4. Those curves represent what would be observed if there were no plastic deformation under high stress and are asymptotic to the line representing the load which would be critical under those conditions. That load may be termed the *elastic critical load* to distinguish it from the *plastic critical load*, at which instability would be produced by combined elastic and plastic action of the material.

Southwell has shown<sup>1</sup> how elastic critical loads can be determined from simultaneous readings of load and deflection without the necessity of carrying the test to failure. All that is necessary is to plot points with the measured deflections,  $y$ , as ordinates and the corresponding ratios of  $y/P$  as abscissas. The slope of the straight line most nearly passing through those points is then a measure of the elastic critical load. An important practical objection to this procedure is that the deflections must be measured from the position at zero load, and that position is often difficult to obtain in a test, owing to the difficulty of holding the specimen in place until the load is large enough to take all play out of joints and to seat the specimen firmly in its fittings.

Lundquist has shown<sup>2</sup> that this difficulty can be avoided by substituting for  $P$ , the actual load, and  $y$  the deflection from the zero load position,  $P - P_1$  and  $y - y_1$ , where  $P_1$  is some arbitrary *initial load* and  $y_1$  is the deflection under that initial load. The slope of the curve of  $y - y_1$  plotted against  $(y - y_1)/(P - P_1)$  is then a measure of the difference between  $P_1$  and the elastic critical load.

This procedure is of great value to the engineer since the necessary tests can be made under such low loads that the specimen will not be injured. In fact, it is almost essential that the loading be so limited lest the result be an inferior measure of the plastic critical load under which a failure began to take place. Since the ordinate of each point is  $y - y_1$  and the abscissa is  $(y - y_1)/(P - P_1)$ , the slope of the line joining any point with the origin is equal to the value of  $P - P_1$  for that point. If, then, the member starts to buckle and several deflection readings are obtained for essentially the same load, the points for those readings will be certain to fall on such a line. Since these deflections will probably be considerably greater than those observed before buckling began, the slope of this line is likely to be taken as the measure of critical load. It is a measure of the load causing buckling, but that is a plastic critical which is more reliably determined by the regular

<sup>1</sup> *Proc. Royal Soc., London, Series A*, Vol. 135, p. 601, 1932.

<sup>2</sup> "Generalized Analysis of Experimental Observations in Problems of Elastic Stability," N.A.C.A. Technical Note 658, 1938.

load measuring devices used. For an elastic critical to be determined, it is essential that the plotted points used be associated with loads too small to cause plastic flow.

**18 : 15. Present Status of Theory of Instability Failure** — In general, the structures considered in this chapter are very simple and idealized. Though some of the methods for computing critical loads described here can be extended to apply to more complex structures, this usually involves long and tedious computations or mathematical procedures beyond the ability of the average engineer. Development along these lines has also been restrained by the great discrepancies often found between theoretical and test results. With some types of structure the test specimens have collapsed under about half the computed critical loads. Usually this has been attributed to the inevitable deviations of any practical specimen from an idealized structure amenable to analysis. Thus the mid-line of the cross-section of a fuselage may be assumed to be a perfect circle in the development of a formula for critical load. The true shape of the mid-line will always deviate to some extent from this assumption, and such deviation will result in waves that will probably reduce the ability of the shell to resist compression. The amount of such reduction would be difficult enough to estimate even if the deviations of the actual from the idealized shape were known.

In practice, however, the magnitudes of such deviations not only are unknown but also differ between structures built to the same drawings. Their exact effect on the critical load is therefore impossible to evaluate. The usual method of meeting this situation has been to develop formulas for the critical loads of ideal structures as much as possible like those used in practice and to determine empirically suitable correction factors for use in design. Where these correction factors are between about 0.9 and 1.0, they are considered reasonable measures of the weakening effect of the deviations of the actual from the idealized structure. When, however, they run as low as 0.5 or 0.6, the average engineer cannot avoid suspecting the validity of formulas to which they are applied and is loath both to rely on the latter in design and to spend much time in theoretical studies and computations to which such correction factors must be applied.

Recent studies have shown that for some types of structure a radical change should be made in the method of computing the critical load. In the procedures described in this chapter it is assumed that attention may be limited to the energy changes associated with very small deviations from configurations known to be consistent with equilibrium. Until recently this has been the standard practice of investigators in this field. Now it is being found that for some types of structure used

in airplane design, the computed critical load is much reduced if the assumed deviations are relatively large. This is most evident in connection with curved elements such as spherical shells and thin-walled cylinders. The mathematical obstacles to proper allowance for the possibility of large deviations are considerable, and only a few solutions along this line have yet been obtained. To date the most fruitful work in the development of a "large deflection" theory of instability failure is that of Dr. von Karman and his associates at GALCIT who have published a series of papers<sup>1</sup> in this field. Although these papers do not cover the entire field, they present theoretical values which differ from the test values for the critical loads by amounts that can be considered reasonable reflections of the inevitable deviations of practical from ideal structures. Therefore, although much more work is needed before the general problem of instability failure can be considered mastered, the situation looks much more hopeful than it did a few years ago.

At present, however, the only type of complex structure for which there is available a reasonably satisfactory method of handling the problem of group instability is the rigid-jointed truss, which is amenable to the procedure of Arts. 18 : 12 and 18 : 13. At the other end of the scale is the conventional stressed-skin fuselage, particularly the portions between the wings and tail where there may be no definite loads on which to base the proportions of transverse rings. In such portions of the fuselage the stiffeners are normally designed as continuous beam-columns assumed rigidly supported at each transverse ring. When the rings are designed to transmit the weight and inertia of local fuselage loads, as in Art. 17 : 8, they usually provide sufficient stiffness and support to justify such an assumption. When there are no local loads, the rings may be proportioned by the criteria of Art. 17 : 9, or by similar methods such as those given in Chapter 8 of Sechler and Dunn's "Airplane Structural Analysis and Design." These criteria yield rings of reasonable proportions, but they have not been checked by use on a number of full-sized structures, they do not apply to all shapes of fuselages, nor do they cover all combinations of loads to which sheet, stiffener, and ring systems may be subjected. They must, therefore, be used with caution when applied in practice.

<sup>1</sup> Theodore von Karman and Hsue-shen Tsien, "The Buckling of Spherical Shells by External Pressure," *Jour. Aero. Sci.*, Vol. 7, p. 43, December, 1939.

Theodore von Karman, Louis G. Dunn, and Hsue-shen Tsien, "The Influence of Curvature on the Buckling Characteristics of Structures," *Jour. Aero. Sci.*, Vol. 7, p. 276, May, 1940.

Theodore von Karman and Hsue-shen Tsien, "The Buckling of Thin Cylindrical Shells under Axial Compression," *Jour. Aero. Sci.*, Vol. 8, p. 303, June, 1941.

Hsue-shen Tsien, "Buckling of a Column with Non-linear Lateral Supports," *Jour. Aero. Sci.*, Vol. 9, p. 119, February, 1942.

In judging the appropriateness of a proposed method of determining the critical load for any practical structure, care must be taken to see that the assumptions on which it is based are in agreement with the conditions existing in the actual structure. The fact that a formula is evolved by long and tedious manipulation and simplification of mathematical equations, or by the application of highly advanced branches of mathematics, does not make it apply where the actual conditions deviate in the slightest from the assumptions on which the derivation is based. Normally such deviations will exist, and a formula should not be employed unless its validity, or at least its probable degree of accuracy, has been proved by tests. Students and practicing engineers must therefore keep in mind at all times the assumptions and limitations of the methods they use, realizing how dangerous it is to use empirical or theoretical formulas beyond the range of the data or assumptions from which they sprang.

Although it has been impossible to present in this chapter the desired complete solution of the problem of group instability, that is due primarily to the fact that such a solution does not yet exist. It should, however, be evident to the reader that reliable stability criteria for many types of structure are greatly needed by designers and that their development will furnish an interesting activity to research engineers for some time to come. It is hoped that this introduction to the problem will help the reader to profit by reports on investigations in this field, whether they cover studies made along the lines of the classical "small deflection" theory or the newer "large deflection" theories.

#### PROBLEMS

**18 : 1.** A simply supported beam of length,  $L$ , and uniform section and material is subjected to a uniformly distributed load,  $w$ . Develop the formula for the deflection of the quarter-point,  $x = L/4$ , from the trigonometric formulas of Art. 18 : 4. Determine the percentage errors resulting from (a) the use of only the first term of the series; (b) the use of the first two terms of the series.

**18 : 2.** Do the same for the third-point,  $x = L/3$ .

**18 : 3.** Develop the trigonometric formula for the deflection of a constant section beam fixed at both ends and subjected to a concentrated load at midspan. Apply this formula to determine the deflection at the quarter-point,  $x = L/4$ , and compute the percentage error resulting from (a) the use of only the first term of the series; (b) the use of the first two terms of the series.

**18 : 4.** Do the same for a load uniformly distributed over the entire span.

**18 : 5.** A  $1\frac{1}{4} \times 0.049$  round steel tube ( $E = 29,000,000$ ) 80 in. long is subjected to an axial load of 3,000 lb. If it is pin-supported at its ends, what is the minimum stiffness of an elastic support at midspan consistent with stability?

**18 : 6.** If the spring constant of the elastic support of the column of Prob. 18 : 5 is 120 lb. per in., and if the column deflects 0.10 in. before that support comes into action, what will be the supporting force and what will be the deflection of the column midpoint when equilibrium has been established?



18 : 7. Solve Prob. 18 : 5, assuming the elastic support located 30 in. from one end of the column.

18 : 8. If the column of Prob. 18 : 5 is subjected to a uniformly distributed transverse load of 0.10 lb. per in., and if the spring constant of the elastic support is 120 lb. per in., what will be the reaction at and the deflection of the point of support?

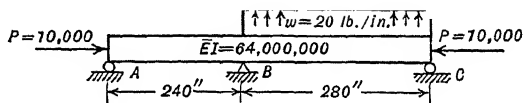
18 : 9. Solve Prob. 18 : 8, assuming the column deflects 0.1 in. before the elastic support comes into action.

18 : 10. Distribute the unit moment applied to the truss of Fig. 18 : 12, using an order of balancing joints which differs from that used in preparing that figure, and compare the results.

18 : 11. Check the stability of the truss of Fig. 18 : 12, assuming the unit couple is imposed at joint  $E$ .

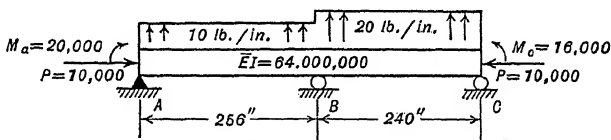
18 : 12. Would the truss of Fig. 18 : 12 be stable if the external loads were increased by 10 per cent?

18 : 13. Is this beam-column elastically stable under the loads shown acting upon it?



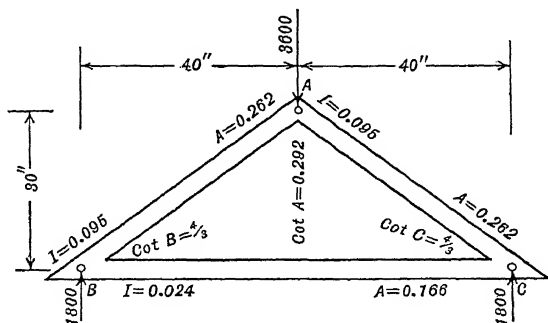
PROB. 18:13

18 : 14. Is this beam-column elastically stable under the loads shown acting upon it?



PROB. 18:14

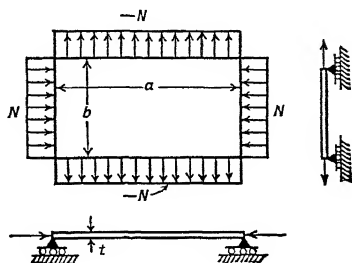
18 : 15. Assuming this truss to be adequately supported at  $B$  and  $C$  and to be braced laterally at  $A$ , show that the members are stable — or unstable — under the loading given.



$$E = 28,000,000 \text{ p.s.i.}$$

PROB. 18:15

18 : 16. A thin rectangular plate, simply supported along all four edges, is acted upon by a uniform thrust in one direction and by a uniform pull of the same amount acting in a direction at right angles to the thrust, as shown. Discuss the problem of the buckling of this plate.



PROB. 18: 16

## CHAPTER XIX

### TORSIONAL COLUMN FAILURE

In Art. 10 : 2 mention was made of the fact that a column sometimes adjusts itself to forcible shortening by twisting as well as bending. This is most likely to occur with open-section columns such as channels and zees that are very inefficient in resisting torsion. It is almost never observed with closed sections like tubes. Although its possibility has been recognized for many years, and its existence observed in many laboratories, it is only recently that much effective study has been devoted to the problem.

The pioneer in the field was H. Wagner in Germany, and his work was further developed by E. E. Lundquist and C. M. Fligg in this country and by R. Kappus in Germany. One of the features of Kappus' development is his use of the calculus of variations, a branch of the calculus which, though it is needed for rigorous proof of some of the most valuable formulas used in engineering, is not as well understood by many engineers as it should be. The first part of this chapter is therefore devoted to an introduction to this method of analysis which closely parallels that of Byerly.<sup>1</sup> This is followed by a rather detailed discussion of its use in obtaining a more rigorous proof of the Euler formula than that given in Chapter X. The bulk of the chapter, however, is devoted to Kappus' application<sup>2</sup> of the method to the problem of torsional column failure.

Subsequent articles show its application to the problem of the failure of a column, such as that shown in Fig. 19 : 1, by twisting. Figure 19 : 1 is a photograph of an aluminum alloy channel having the section shown in Fig. 19 : 9. The column is 70 in. long and is under a load of 2,940 lb. The twist is magnified in the positions of the ends of the five antennae, or rods, attached to the channel web. Until nearly all of the 2,940-lb. load had been developed by axial shortening of the channel, the deviation of the ends of the antennae from a straight line could hardly be detected by the naked eye. When the picture was taken, however, the ultimate load had been reached and additional shortening produced

<sup>1</sup> "Introduction to the Calculus of Variations, W. E. Byerly," Harvard University Press, 1917.

<sup>2</sup> "Twisting Failure of Centrally Loaded Open-section Columns in the Elastic Range," R. Kappus, N.A.C.A. Technical Memorandum 851, Washington, 1938.

further twisting of the column but no increase in axial load. The importance to the designer of this type of failure is indicated by the fact that the critical load for this column, as predicted by the formulas of Chapter X, is 5,540 lb., or 87.5 per cent greater than that at which actual failure took place.

**19 : 1. The Purpose of the Calculus of Variations**—The fundamental problem of the calculus of variations lies in finding the form of the function  $f$  such that if

$y : \dots, \int_{x_0}^{x_1} \phi(x, y, y') \cdot dx$  shall be a

maximum or a minimum. In the latter expression  $\phi(x, y, y')$  represents any desired function of those variables;  $x_0$  and  $x_1$  are any desired values of  $x$ ; and  $y'$  represents the first derivative of  $y$  with respect to  $x$ . For convenience and conciseness, derivatives will be indicated in this chapter by primes, double primes, and so forth, the number of primes representing the order of the derivative.

In ordinary problems of maxima and minima  $y = f(x)$  is a given function and it is desired to find a value  $x_0$  of  $x$  for which  $y$  is greater when a maximum is sought, but less when a minimum is looked for, than for *neighboring* values of  $x$ ; that is, for values of  $x$  differing from  $x_0$  by a sufficiently small amount whether that amount be positive or negative.

To speak in geometrical terms, the calculus of variations is used to find the *form* of a curve for which the definite integral

$I = \int_{x_0}^{x_1} \phi(x, y, y') \cdot dx$  is greater or less

than for any neighboring curve having the same end points.

Let  $y = f(x)$  be the desired curve, and let  $y = F(x)$  be any other continuous curve, as in Fig. 19 : 2, joining the same end points. Then if  $\eta(x) = F(x) - f(x)$ , the equation  $y = f(x) + \eta(x)$  will represent the same curve as  $y = F(x)$ .

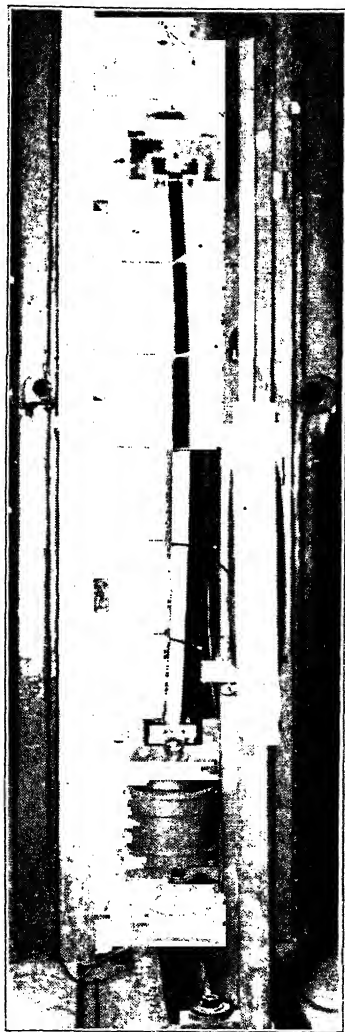


FIG. 19 : 1

Consider now the expression  $y = f(x) + \alpha\eta(x)$  where  $\alpha$  is a parameter independent of  $x$ . This represents a family of curves including  $y = f(x)$  for  $\alpha = 0$  and  $y = F(x)$  for  $\alpha = 1$ .

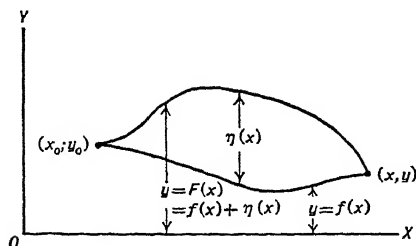


FIG. 19:2

By taking a sufficiently small value for  $\alpha$ ,  $\alpha\eta(x)$  can be made less in absolute value for that and all smaller values of  $\alpha$  and for all values of  $x$  between  $x_0$  and  $x_1$  than any previously chosen quantity  $\xi$ . For such values of  $\alpha$  the curve  $y = f(x) + \alpha\eta(x)$  is said to be a curve in the neighborhood of  $y = f(x)$ .

If  $y = f(x)$  and  $y = F(x)$  are given and, if by definition  $I = \int_{x_0}^{x_1} \phi(x, y, y') dx$ , the value of  $I$  for any one of the family of curves  $y = f(x) + \alpha\eta(x)$  can be represented by

$$I(\alpha) = \int_{x_0}^{x_1} \phi[x, y + \alpha\eta(x), y' + \alpha\eta'(x)] dx$$

and  $I(\alpha)$  will be a function of  $\alpha$  only.

If  $y = f(x)$  is the curve of the family for which  $I$  is to be a minimum, that requirement can be expressed by the statement that  $I(\alpha)$  must be a minimum when  $\alpha = 0$ . A necessary condition for this is that  $(d/d\alpha)I(\alpha) = 0$  when  $\alpha = 0$ . This condition will be expressed by the equation

$$I'(0) = 0^1 \quad 19:1$$

Before showing how this criterion can be applied in a specific problem, it will be advantageous to develop an appropriate system of notation and nomenclature.

**19:2. Calculus of Variations. Notation and Nomenclature**—Assume two points,  $(x_0, y_0)$  and  $(x_1, y_1)$ , joined by two continuous curves,  $y = f(x)$  and  $y = F(x)$ , as in Fig. 19:2. The difference between corresponding ordinates of the two curves may be represented by  $\eta(x) = F(x) - f(x)$ , and  $\eta(x)$  can be thought of as the increment produced in  $y$  if  $f(x)$  is changed into  $F(x)$  without change in  $x$ . It will be called the *variation of  $y$*  and represented by  $\delta y$ . It is a function of  $x$  and, in general, an arbitrary function of  $x$ .

The slope at any point of the curve representing  $y = \eta(x)$  can be seen to be equal to the difference between the slopes of  $y = F(x)$  and  $y = f(x)$ . Therefore just as  $\eta(x)$  is the difference between the ordinates

<sup>1</sup> In this case, since  $I$  is a function of  $\alpha$  only, no confusion should result from using the prime to indicate differentiation with respect to  $\alpha$  instead of  $x$ .

of those curves,  $\eta'(x) = (d/dx)\delta y$  is the difference in the slopes or the change produced in  $y'$  by changing  $f(x)$  into  $F(x)$ . This will be called the *variation of  $y'$*  and will be represented by  $\delta y'$ . It will be, like  $\delta y$ , a function of  $x$ .

Similarly  $\eta''(x) = (d/dx)\delta y'$  will represent the change produced in  $y''$  by the change from  $y = f(x)$  to  $y = F(x)$ . This will be the *variation of  $y''$*  and can be written  $\delta y''$ .

Let  $\phi(y)$  represent any assigned function of  $y$ . If  $y$  is increased by  $\delta y$ , then  $(d/dy)\phi(y) \delta y$  will be an approximation of the increment produced in  $\phi(y)$ , the closeness of the approximation depending on the magnitude of  $\delta y$ . If  $\delta y$  is infinitesimal, this approximation is in error by an infinitesimal of higher order than  $\delta y$ . This approximate increment will be called the *variation of  $\phi(y)$*  and be written  $\delta\phi(y)$ , so that

$$\delta\phi(y) = \frac{d}{dy} [\phi(y)]\delta y \quad 19 : 2$$

If  $y$  and  $y'$  are treated as independent variables,

$$\frac{\partial\phi(y,y')}{\partial y} \delta y + \frac{\partial\phi(y,y')}{\partial y'} \delta y'$$

is in like manner an approximation to the increment produced in  $\phi(y,y')$  by giving  $y$  the increment  $\delta y$  and  $y'$  the increment  $\delta y'$ . It will be called the *variation of  $\phi(y,y')$*  and represented by  $\delta\phi(y,y')$ , so that

$$\delta\phi(y,y') = \frac{\partial\phi(y,y')}{\partial y} \delta y + \frac{\partial\phi(y,y')}{\partial y'} \delta y' \quad 19 : 3$$

The same type of reasoning may be used to obtain the relation

$$\delta\phi(y',y'') = \frac{\partial\phi(y',y'')}{\partial y'} \delta y' + \frac{\partial\phi(y',y'')}{\partial y''} \delta y'' \quad 19 : 4$$

As all these variations are supposed to be caused by changing the form of the function  $f$  in  $y = f(x)$  without changing  $x$ ,

$$\delta\phi(x,y,y') = \frac{\partial\phi(x,y,y')}{\partial y} \delta y + \frac{\partial\phi(x,y,y')}{\partial y'} \delta y' \quad 19 : 5$$

If in Eq. 19 : 2 and 19 : 3 the symbol  $\delta$  is replaced by the symbol  $d$ , the familiar formulas for  $d\phi$  are obtained. Hence variations may be calculated by the use of the familiar formulas and processes of differential calculus. Indeed, if  $y$  is a function,  $f$ , of  $x$ , then  $d\phi$  and  $\delta\phi$  are approximate increments of precisely the same type but differently caused,  $d\phi$  by changing  $x$  without changing the form of the function, and  $\delta\phi$  by changing the form of the function without changing  $x$ .

With the new notation the necessary condition that  $I$ , which is the  $\int_{x_0}^{x_1} \phi(x, y, y') dx$ , shall be a minimum can be written

$$\int_{x_0}^{x_1} \delta \phi(x, y, y') dx = 0 \quad 19 : 6a$$

If the variation of a definite integral be defined as the integral of the variation of the integrand, so that

$$\delta \int_{x_0}^{x_1} \phi dx = \int_{x_0}^{x_1} \delta \phi \cdot dx$$

Eq. 19 : 6a may be abridged to

$$\delta I = 0 \quad 19 : 6b$$

**19 : 3. Application to a Pin-ended Column** — In Art. 10 : 5 it is stated that if an ideal pin-ended column were to bend, the equation of the elastic curve would be  $y = \delta \sin (\pi x/L)$ . No proof was given that the column might not deflect to an equilibrium position defined by some other type of equation. From the principle of virtual work it follows that the curve assumed by the axis of the column must be such that the potential energy of the system composed of the bent column and its end loads must be a minimum. The problem of defining the curve is therefore suitable for illustrating the use of the Calculus of Variations.

As in Chapter X, it is assumed that the column is originally straight and so remains while being subjected to a load  $P$ . After the entire load  $P$  has been imposed, the column deflects to a bent shape, the end load  $P$  remaining constant. During this action of bending, the potential energy of the external load will decrease by the product of that load and the difference between the lengths of the arc of the elastic curve and its chord. At the same time the elements of the column will store up potential energy of strain due to their deformation. It can be seen from the discussion in Chapters X and XVIII that the reduction of potential energy of the external load is equal to the external work

$$U_e = \frac{P}{2} \int_0^L \left( \frac{dy}{dx} \right)^2 dx \quad a$$

while the strain energy stored in the column is equal to the internal work

$$U_i = \frac{EI}{2} \int_0^L \left( \frac{d^2y}{dx^2} \right)^2 dx \quad b$$

Since the potential energy of the system at the moment when the load

$P$  has been applied and bending is about to start is a constant quantity, the potential energy of the system will be a minimum when the change of potential energy due to the bending action is a minimum.

By returning now to the calculus of variations, the problem may be restated as the determination of the form of the function  $y = f(x)$ , which will make  $U = U_i - U_e$  a minimum when  $U_e$  and  $U_i$  are defined as above.<sup>1</sup> Thus the objective is to find the form of  $y = f(x)$  for which  $\delta U = 0$  when

$$U = \int_0^L \left( \frac{EI}{2} y''^2 - \frac{P}{2} y'^2 \right) dx \quad c$$

Since the integrand in this expression for  $U$  is a function  $\phi(y', y'')$ , Eq. 19 : 4 can be applied, the result being the specific criterion

$$\delta U = \frac{EI}{2} \int_0^L 2 y'' \delta y'' dx - \frac{P}{2} \int_0^L 2 y' \delta y' dx = 0 \quad d$$

This may be handled more readily if it is recognized that  $\delta y' = (d/dx) \delta y$ , etc., and Eq.  $d$  is replaced by

$$EI \int_0^L y'' \frac{d}{dx} \delta y' dx - P \int_0^L y' \frac{d}{dx} \delta y dx = 0 \quad e$$

The general formula for integrating by parts is

$$\int_{x_0}^{x_1} u \frac{dv}{dx} dx = [u \cdot v]_{x_0}^{x_1} - \int_{x_0}^{x_1} v \frac{du}{dx} dx \quad 19 : 7$$

where  $u$  and  $v$  are independent functions of  $x$ . Performing this operation on Eq.  $e$  gives

$$EI[y'' \delta y']_0^L - EI \int_0^L y''' \delta y' dx - P[y' \delta y]_0^L + P \int_0^L y'' \delta y dx = 0 \quad f$$

Since the column is assumed pin-ended,  $y = y'' = 0$  at  $x = 0$  and  $x = L$ . The same conditions must hold for any of the neighboring curves that need be considered as representing virtual displacements from the equilibrium position,  $y = f(x)$ ; so  $\delta y = \delta y' = 0$  for the same values of  $x$ . Therefore the terms in brackets vanish and

$$-EI \int_0^L y''' \delta y' dx + P \int_0^L y'' \delta y dx = 0 \quad g$$

By integrating only the first term by parts and noting that the result-

<sup>1</sup>  $U$  is used here instead of  $I$  to represent the definite integral to avoid confusion with the moment of inertia which appears in the integrand.



ing term in brackets will disappear on account of the boundary conditions that  $\delta y = 0$  at  $x = 0$  and  $x = L$ , Eq. *g* is changed to

$$+EI \int_0^L y'''' \delta y \, dx + P \int_0^L y'' \delta y \, dx = 0 \quad h$$

or

$$\int_0^L (EI y'''' + P y'') \delta y \, dx$$

If it is remembered that  $\delta y$  may represent *any* deviation of  $y = F(x)$  from  $y = f(x)$ , it should be clear that in order to satisfy the relation of Eq. *i* it is necessary that

$$EI y'''' + P y'' = 0 \quad 19 : 8$$

This differential equation therefore defines the equation of the elastic curve that will satisfy the condition of equilibrium deduced from the principle of virtual work; that is, that  $\delta U' = 0$ . Its solution will therefore be the desired equation for the elastic curve of the column.

To facilitate the solution of this equation let  $z = y''$ ; so  $z'' = y''''$ . Then Eq. 19 : 8 becomes

$$EI z'' + P z = 0 \quad j$$

which may be written

where  $j^2 = EI/P$  as in Chapter XIV.

Comparison with Eq. *a* of Art. 14 : 1 and with its solution given as Eq. 14 : 2 will show the general solution of Eq. *k* to be

$$z = C_1 \sin (x/j) + C_2 \cos (x/j) \quad l$$

where  $C_1$  and  $C_2$  are constants of integration. Application of the boundary conditions that  $z = y'' = 0$  where  $x = 0$  and  $x = L$  lead to  $C_2 = 0$  and to

$$C_1 \sin (L/j) = 0 \quad m$$

This relation will be satisfied if  $C_1 = 0$  or if  $\sin (L/j) = 0$ . The first alternative would lead to  $y = 0$  as the equation of the elastic curve and shows that the straight line is an equilibrium position for the column regardless of the magnitude of the end load. Of more interest is the second alternative which is satisfied if  $L/j = n\pi$ , where  $n$  is any integer. This shows that there is a bent equilibrium position whenever

$$j = \frac{L}{n\pi} \quad 19 : 9$$

Since  $j^2 = EI/P$ , the loads corresponding to these positions are given by

$$P = \pi^2 n^2 E \frac{I}{L^2} \quad 19 : 10$$

It still remains to find the formulas for the elastic curves of the possible equilibrium positions. Evaluation of the constants of integration have reduced Eq. 1 to  $y'' = z = C_1 \sin(x/j)$ , the second boundary condition having given an expression for the possible equilibrium loads rather than a value for  $C_1$ . Integrating this expression twice produces

$$y = -C_1 j^2 \sin \frac{x}{j} + C_3 x + C_4 \quad n$$

Since  $y = 0$  when  $x = 0$ ,  $C_4 = 0$ . Also, since  $y = 0$  when  $x = L$ , and  $\sin(L/j) = 0$ ,  $C_3 = 0$ . The equation of the elastic curve is then

$$y = -C_1 j^2 \sin \frac{x}{j} \quad o$$

By replacing  $-C_1 j^2$  by  $\Delta^1$  and  $j$  by  $L/(n\pi)$ , this becomes

$$y = \Delta \sin \frac{n\pi x}{L} \quad 19 : 11$$

It should be noted that if  $n = 1$ , Eqs. 19 : 10 and 19 : 11 are identical with the Euler formula for pin-ended columns and for the deflection curve assumed when deriving that formula in Chapter X. In that chapter it was shown that for loads in excess of  $\pi^2 EI/L^2$  such a column would be unstable and that proof need not be repeated. It is sufficient to remark that, while Eq. 19 : 11 with values of  $n$  greater than unity represents possible equilibrium positions, those positions would be unstable and are of little practical interest. Nothing more is needed, therefore, to complete this proof of the validity of the Euler formula for a pin-ended column.

**19 : 4. Warping of Thin Metal Members** — In the development of column theory in the preceding articles, it was tacitly assumed that a long column would adjust itself to forcible decrease in length by bending in the plane containing the minor axes of the cross-sections. It is geometrically possible that the bending might be in the plane containing the major principal axes of the cross-sections. A similar investigation of this possibility would result in parallel expressions for loads consistent with bent equilibrium positions and possible shapes of the elastic curves,

<sup>1</sup>  $\Delta$  is used here instead of  $\delta$  because of the use of the latter symbol to indicate deviations.

the only difference being that  $I$  would be the moment of inertia about the minor axis instead of that about the major axis. Since the former value of  $I$  is greater than the latter, the column would not actually bend in this manner, since it would become unstable with respect to deflection in the plane of the minor axes before the lowest load consistent with bending in the plane of the major axes had been reached.

In the above discussion it is assumed that when the column bends, the movement of each cross-section is one of pure translation, there being no rotation of a section about any axis parallel to the axis of the column. For most compression members used in practice, that assumption is valid. Experience has demonstrated, however, that certain thin-walled open sections have a tendency to twist as well as bend when subjected to axial load. For some of these members the load at which they become elastically unstable with respect to a combination of twisting and bending is considerably lower than that indicated by the Euler formula for bending alone, and it is desirable to investigate the matter more completely. The basic method to be used is the same as that employed above. It will be necessary, however, to include in the expression for the change in potential energy terms to represent the strain energy stored as a result of the deformations produced by the combination of twisting and bending.

In this study it will be assumed that each cross-section of the column retains its shape and rotates about its centroid simultaneously with its movement in translation. If the angle of rotation is  $\theta$ , this entire movement can be described as rotation through the same angle  $\theta$  about some point other than the centroid, the location of that point depending on the components of the translational motion. More refined theory indicates that the axis of rotation formed by the centers of rotation of the individual cross-sections is not a straight line, but the error involved in assuming a straight line parallel to the centroidal axis as the axis of rotation is inconsiderable. This assumption will therefore be adopted.

Strictly speaking, it is not the cross-sections that are assumed to remain unchanged in shape but rather their projections on planes normal to the axis of rotation. As will be apparent later, the different points on a cross-section will have differing movements parallel to the rotation axis, with the result that the cross-sections become "warped," and this warping provides a means of computing the axial load at which deformation of the type under consideration may take place.

On account of the warping, it is desirable to refer to planes normal to the axis of rotation as "transverse" rather than as "cross-sectional" planes. Then, if a column is of constant cross-section, it may be thought of as composed of a large number of longitudinal elements, to be called

"fibers," each of which is normal to the transverse planes before deformation takes place. At the same time each cross-section may be thought of as a combination of differential elements, each the cross-section of a fiber, located in a single transverse plane. If, when the column is deformed, the change in angle of twist,  $\theta$ , per unit of length is a constant, each fiber changes shape from a straight line to a helix with the axis of rotation as its axis. The individual fibers, or more strictly their tangents, are no longer normal to the transverse planes but will be at constant angles to such normals. The magnitudes of these angles will depend on the rate of change in the rotation angle,  $\theta$ , and the distance of the fiber from the rotation axis. If the rate of change of  $\theta$  is not constant, each fiber will be bent into a similar curve which might be called a helix of variable pitch, and angles between its tangents and normals to the transverse planes will vary along its length. The important point is that as the column is deformed the fibers and their tangents become, in general, no longer normal to the transverse planes.

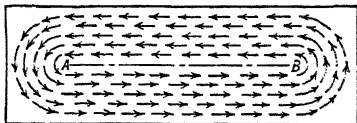


FIG. 19:3

The rotation of a cross-section implies the existence of a torsional couple composed of shearing forces distributed over the section. Proof may be found in textbooks on the theory of elasticity that, when a constant section rectangular bar is subjected to equal and opposite torsional couples imposed on end cross-sections that are free to warp, the distribution of the shearing stresses on each cross-section tends to be as shown in Fig. 19:3. Along the line  $AB$ , midway between the long sides and extending for the greater part of their length, the shear is zero. On one side of that line the shearing forces act in one direction, and on the other side they act in the opposite direction. Pairs of these forces form couples which tend to maintain equilibrium with the external couples. Except near the ends of the long sides, the shear forces are parallel to those sides, and their intensity varies uniformly from zero at the median line to maxima at the free surfaces. When the ratio of the width,  $b$ , to the thickness,  $t$ , is large, it is allowable to assume the shear to be zero along the entire length of the mid-line, the portions near its ends being so small as to be negligible.

Open sections like channels, in which the developed width is large compared with the thickness (16 or more times as great) may be assumed to act in a similar manner under torsion and be subjected to no shear along the median line of a cross-section. This will be true for such "thin-walled open sections" even though the cross-section in-

cludes T-junctions, like those in I-beams, or the curved elements often found in open sections formed from flat sheet. Since the shearing stresses on mutually perpendicular planes must be of equal intensity, there will be no shearing stresses in the "median surface," composed of the median lines of the cross-sections of such members.

Consequently, there will be no shear deformation in that surface. Therefore, if an element of the median line of a cross-section be considered, that element will remain perpendicular to the fiber of which it is a cross-section, regardless of the twisting of the column as a whole. Since the twisting causes the fibers to cease being normal to the transverse planes, the cross-sectional element must cease to be parallel to such planes, and one end will have more movement than the other in a direction parallel to the axis of rotation. In general, the different elements of a median line will come to make different angles with the transverse planes and thus the cross-section will be warped.

Elements of a cross-section that are not on its median line will be subjected to increasing shearing stress as the distance from that line increases, but the effect on shear deformation and warping is small in thin sections and that on one side is largely neutralized by that on the other. Therefore, for the thin-walled sections under consideration, the warping of the entire cross-section may be assumed to be represented by that of its median line.

The type of shear distribution described above and its implications are strictly valid only under very limited ideal conditions. If the ends of the member be not free to warp, if torsional couples be imposed at locations other than the end cross-sections, or if bending moments be imposed on the member, the fibers will be subjected to axial stresses which, in general, will vary along the length of each fiber. Such variation in axial stresses requires the existence of shearing stresses on the cross-sections in order to maintain equilibrium. These shearing stresses will act on the median line as well as on other parts of the cross-section. Unless the column is abnormally short, their magnitudes and those of the related shearing deformations, however, will be relatively so small that they may be neglected. This approximation is comparable to the neglect of shearing deformation in the elementary theory of beams subjected to bending. Therefore, for practical problems it is allowable to assume the median surface to be free from shear distortion and to compute the warping of the cross-sections on that basis.

**19 : 5. Formulas for Unit Warping** — Before deriving formulas for the warping in specific problems, it is desirable to adopt suitable systems of notation and nomenclature and a sign convention. Figure 19 : 4 shows the median line of a thin-walled open section. A

rectangular system of co-ordinates is assumed with its origin at the centroid of one end cross-section,  $C$ . The  $Z_c$  axis is normal to the end cross-section, and the  $X_c$  and  $Y_c$  axes are any mutually perpendicular axes in the plane of the end cross-section and passing through its centroid. In addition to this basic co-ordinate system each point on the median line may be located by a circumferential co-ordinate,  $u$ , with  $u = u_0$  at some selected point. The positive tangential direction,

$t$ , at any point  $(x, y)$  is indicated by that of increase in the circumferential co-ordinate  $u$ . The positive normal direction,  $n$ , is that to the right when looking in the positive  $t$  direction. The distance  $r$  from the  $Z_c$  axis to any point  $(x, y)$  on the median line will be resolved into the components  $r_t$  and  $r_n$ . If a force in the positive  $t$  direction

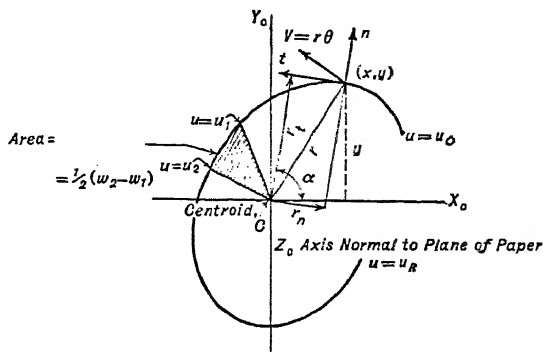


FIG. 19:4

would produce a counter-clockwise moment about  $C$ ,  $r_t$  is positive. Similarly, if a force in the positive  $n$  direction would produce a counter-clockwise moment about  $C$ ,  $r_n$  is positive. The angle  $\alpha$  between the vector  $r_t$  and the  $X_c$  axis is assumed to increase as that vector rotates counter-clockwise.

The first type of warping to be treated in detail is that which results from rotation of the cross-sections about the centroidal,  $Z_c$ , axis when the torsional moment is constant over the length of the member and its ends are free to warp. For these conditions the angle of rotation  $\theta = TL/K_t G$ , where  $T$  is the torsional moment,  $L$  the length of the member,  $G$  the shearing modulus of the material, and  $K_t$  a constant depending on the shape and size of the cross-section. Methods of computing  $K_t$  are discussed in Art. 7:7. From the expression for  $\theta$  it is easily seen that  $\theta' = d\theta/dz$  is a constant. Therefore each segment of the member  $dz$  long should experience the same deformation, and the warping will be independent of  $z$ , although it will be directly proportional to  $\theta'$  and  $T$ . Then the projection on a transverse plane of the displacement of a point  $(x, y)$  of the median line would be given by  $V_c = r_c \theta$ , and its component in the tangential direction by

$$V_{ct} = r_{ct} \theta$$

In these expressions the subscript  $c$  is used to indicate that a quantity is one corresponding to rotation about the  $Z_c$  axis through the centroid  $C$ , and to distinguish it from similar quantities connected with rotations about the parallel axes that will be considered later.

Consider now an element of the median surface,  $dz$  long and  $du$  wide, like that shown in Fig. 19 : 5a. Since  $\theta$  varies linearly with distance in the  $Z$  direction, while  $r_{ct}$  remains constant, the values of  $V_{ct}$  for points along a longitudinal fiber will also vary linearly with  $z$ . If cross-

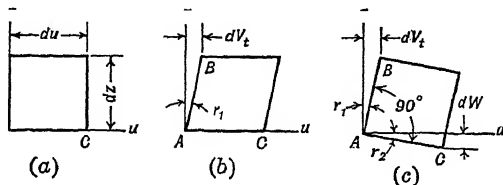


FIG. 19:5

tions remained plane and normal to the rotation axis, as would be the case with a round tube, for instance, shear strain would be produced in the median surface and the resulting shape of the element would be that shown in Fig. 19:5b.

The angle of shear distortion of the element would be  $\gamma_1 = \partial V_{ct}/\partial z$ , partial derivatives being used instead of ordinary derivatives in this expression since  $V_{ct}$  varies in the normal and tangential as well as in the longitudinal direction, but the latter is the only one affecting the angle in question.<sup>1</sup>

Since, however, there will be no shear deformation in the median surface of a thin open section, its elements, instead of being changed to the shape shown in Fig. 19 : 5b will be rotated to the position shown in Fig. 19 : 5c. If  $W$  is the "warping" or movement of a point in the  $z$  direction, its rate of change in the circumferential direction will be  $\partial W/\partial u$ . Then if  $W$  is considered positive when the movement is in the positive  $Z$  direction, in order to satisfy the condition of no shear deformation, a relation to be satisfied is

$$\frac{\partial V_{ct}}{\partial z} + \frac{\partial W_c}{\partial u} = 0 \quad b$$

Since the total warping  $W$  will vary linearly with the torsional moment  $T$  and the angle of twist per unit length  $\theta'$ , it will be convenient to work with a "unit warping"  $w$  corresponding to  $\theta' = -1$ ; so

$$W = -\theta' w \quad c$$

<sup>1</sup> Justification for neglecting  $V_{cn}$ , the normal component of  $V_c$ , in measuring the deformation angle can be obtained by considering an element so located that  $r = r_n$ ,  $r_t = 0$  and  $V_{cn} = V_c$ . Then the movement of the element due to rotations of the cross-sections would be entirely in the normal direction, and the angle between a fiber and the median line would remain a right angle. The movement  $V_{cn}$  therefore has no tendency to produce shear deformation.

By substituting the values of  $V_{ct}$  and  $W_c$  from Eqs. *a* and *c* in Eq. *b*, and observing that  $W$ ,  $w$ ,  $r$ , and  $\theta'$  are independent of  $z$ , one obtains the relation  $dw_c/du = r_{ct}$ . This means that

$$= w_c \int_0^1 r_{ct} du \quad 19 : 12$$

in which  $w_{co}$  is the unit warping at the point chosen for the origin of the circumferential co-ordinate  $u$ .

It is to be noted that dimensionally the unit warping is an area. From Eq. 19 : 12 it may be seen that the difference in unit warping between the points  $u = u_1$  and  $u = u_2$  is equal to twice the area swept through by the vector  $r$  as it moves from  $u_1$  to  $u_2$ . Such an area is shown shaded in Fig. 19 : 4.

In general, the centroidal axis  $Z_c$  need not be the actual axis of rotation for a member with ends free to warp when it is subjected to a constant torque, but the cross-sections may rotate about some parallel axis. It is therefore neces-

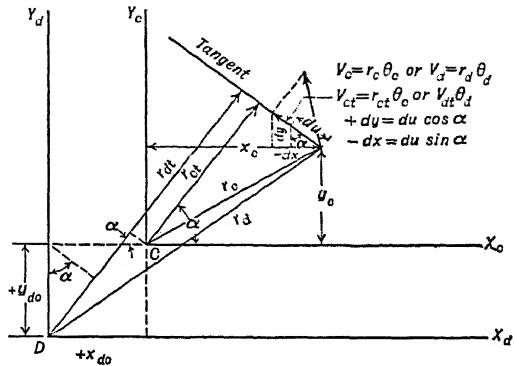


FIG. 19 : 6

sary to develop expressions for the warping resulting from rotation about any axis  $Z_d$  parallel to  $Z_c$  and intersecting the plane of the  $X_c$  and  $Y_c$  axes at some point  $D$ . Let  $x_{cD}$  and  $y_{cD}$  be the co-ordinates of  $D$  measured from  $C$  as the origin and let  $X_d$ ,  $Y_d$ , and  $Z_d$ , passing through  $D$  and parallel to the axes of the former system, be the axes of a new co-ordinate system. The co-ordinates of  $C$  in the new system will then be  $x_{dC}$  and  $y_{dC}$  equal to  $-x_{cD}$  and  $-y_{cD}$ , respectively.

Reasoning parallel to that used to obtain Eqs. *a*, *b*, *c*, and 18 : 12 justifies the formulas

$$\frac{\partial V_{dt}}{\partial z} + \frac{\partial W_d}{\partial u} = 0 \quad d$$

$$V_{dt} = r_{dt} \theta \quad e$$

$$W_d = -\theta' w_d \quad f$$

$$w_d = w_{do} + \int_{\alpha}^u r_{dt} du \quad 19 : 13$$

From Fig. 19 : 6 one can obtain the following relations affecting the



warpings resulting from rotations about the centroidal and the arbitrarily located parallel axis.

$$r_{dt} = r_{ct} + x_{dC} \cos \alpha + y_{dC} \sin \alpha \quad g$$

and

$$du \cos \alpha = dy \quad du \sin \alpha = -dx \quad h$$

Substituting these relations in Eq. 19 : 13 gives

$$w_d - w_{do} = w_c - w_{co} + x_{dC}(y_c - y_{co}) - y_{dC}(x_c - x_{co}) \quad i$$

whence

$$w_d = w_c + x_{dC}y_c - y_{dC}x_c + K \quad 19 : 14a$$

or

$$w_d = w_c - x_{cD}y_c + y_{cD}x_c + K \quad 19 : 14b$$

depending on whether one wishes to use  $D$  or  $C$  as the origin in expressing the relative positions of  $C$  and  $D$ . In both forms of Eq. 19 : 14,  $K$  represents the combination of constants  $w_{do} - w_{co} - x_{dC}y_{co} + y_{dC}x_{co}$ .

**19 : 6. Relations among Stress, Strain, and Warping** — Equation 19 : 14 gives the change in unit warping that results from a change in the rotation axis or, what amounts to the same thing, the addition of translational movement of the cross-section to rotation about its centroid. This change may be seen to be a linear function of the change in position of the axis of rotation plus a constant which will depend on the dimensions of the cross-section.

So far the detailed discussion of warping has been limited to special conditions in which, owing to the constancy of  $\theta'$ , the deformations of all cross-sections are identical and the total warpings  $W$  of points along a given fiber are the same. In the more general practical problem  $\theta'$  is not constant, and the total warping of points along a fiber will vary as a function of  $z$ . This will produce longitudinal strains  $\epsilon_d = \partial W_d / \partial z_d$ . The subscript  $d$  is used here since the strains under consideration are those due to the warping which would result from rotations of the cross-sections about the  $Z_d$  axis.

It is still allowable to assume the absence of shearing strain in the median surface for the reasons already stated in Art. 19 : 4 and, therefore, that Eq. 19 : 13 remains valid. Now, however, as  $W_d$  is a function of  $Z$  as well as of  $u$ , its relation to the unit warping  $w_d$  must be written

$$W_d = -\theta' w_d + f(z) \quad a$$

The strains  $\epsilon_d$  imply the existence of axial stresses  $\sigma_d = E\epsilon_d$  if lateral pressures between the fibers are assumed absent. Applying Eq.  $a$  gives

$$\sigma_d = E\epsilon_d = E \frac{\partial W_d}{\partial z} = -E[\theta'' w_d - f'(z)] \quad b$$

These stresses are those which would be associated with the bending deformations that would cause the axis of rotation to pass through some other point  $D$  instead of through the centroid  $C$ .

It is now time to recall that in the development of the column theory in Art. 19 : 3 it is assumed that the column remains straight until all the critical load  $P$  has been imposed. This causes a shortening  $\epsilon_0 dz = (\sigma_0/E) dz$  of each element, where  $\sigma_0 = P/A$ , the average unit stress. After the critical load has been reached, it is assumed that the column bends, i.e., that each cross-section suffers a movement of pure translation. Here the situation is comparable, except that the cross-section is assumed to be rotated about its centroid as well as translated, the combined movement being envisaged as a rotation about some, as yet unlocated, axis  $Z_d$ . Since the energy transfers connected with this second phase of the action of loading are the only ones of interest, no account need be taken of the axial stresses  $\sigma_0$  built up in the earlier phase, but attention may be limited to the additional stresses  $\sigma_d$  that are developed in the twisting. Since the twisting is assumed to take place under a constant total load  $P$ , the resultant of the forces represented by  $\sigma_d$  will be zero and,

$$\int_A \sigma_d dA = 0 \quad c$$

where  $A$  is the sectional area, the symbol  $\int_A$  calls for integration over the entire cross-section.

Since  $f(z)$  represents a function of  $z$  only, for any one cross-section  $f'(z)$  is a constant. Then if the value of  $\sigma_d$  from Eq.  $b$  is introduced in Eq.  $c$ , the latter may be reduced to

$$f'(z) = \theta'' \cdot \frac{1}{A} \int_A w_d dA \quad d$$

By a suitable choice of  $w_d$  in Eq. 19 : 13 or of  $K$  in Eq. 19 : 14 it is always possible to make

$$\int_A w_d dA = 0 \quad 19 : 15$$

This permits the use of the simple relations

$$W_d = -\theta' w_d \quad 19 : 16$$

whence

$$\epsilon_d = -\theta'' w_d \quad 19 : 17$$

and

$$\sigma_d = -E\theta'' w_d \quad 19 : 18$$

**19 : 7. Energy of a Bent and Twisted Column** — In the preceding article the basic relations between the rotation of the cross-sections about an arbitrarily located  $Z_d$  axis and the resulting strains and stresses were developed. The next step is to obtain expressions for the strain energy stored in the column as the result of combined bending and twisting under a constant axial load. This energy will be the sum of that represented by the work done by the shearing forces and that represented by the work done by the axial loads on the fibers. The relative rotation of two cross-sections  $dz$  apart will be equal to  $\theta' = T/(K_t G)$ . The torsional moment acting on the section will be built up linearly from 0 to  $K_t G \theta'$ . Therefore the work done by the torsional shearing forces will be  $T(\theta'/2) = K_t G(\theta'^2/2)$ . The work done by shearing forces related to the variation in axial stress may be disregarded, as mentioned in Art. 19 : 4, but that due to the axial stresses  $\sigma_d$  is important. The shortening of an individual element will be  $(\sigma_d/E) dz$  due to the linearly imposed force  $\sigma_d dA$ , where  $dA$  is the sectional area of the element. Since  $\sigma_d = E\epsilon_d$ , the energy stored in the element will be  $0.5 E\epsilon_d^2 dA dz$ . Therefore the general expression for the internal work or strain energy stored in the column is

$$U_i = \frac{1}{2} \int_{z=0}^z=L \left( E \int_A \epsilon_d^2 dA + GK_t \theta'^2 \right) dz \quad 19 : 19$$

Since the location of the axis of twist is unknown, it is convenient to combine Eqs. 19 : 17 and 19 : 14 to get  $\epsilon_d$  expressed in terms of warping about the centroidal axis and the co-ordinates of  $D$  with respect to  $C$ . Substituting the value of  $w_d$  from Eq. 19 : 14 in Eq. 19 : 15 and integrating reveals the relation  $K = -\frac{1}{A} \int_A w_c dA$ , the terms including  $x_c$  and  $y_c$  vanishing since those quantities are measured from centroidal axes. Therefore

$$w_d = w_c + x_{dc}y_c - y_{dc}x_c - \frac{1}{A} \int_A w_c dA \quad a$$

The translational movement of the centroid  $C$  due to rotation  $\theta$  about  $D$  as a center may be resolved into the components

$$\xi_c = -y_{dc}\theta \quad \text{and} \quad \eta_c = +x_{dc}\theta \quad 19 : 20$$

in which  $\xi_c$  and  $\eta_c$  are variables with respect to  $Z$ ; so

$$\xi_c'' = -y_{dc}\theta'' \quad \text{and} \quad \eta_c'' = +x_{dc}\theta'' \quad b$$

Then from Eq. 19 : 17

$$\epsilon_d = -\xi_c''x_c - \eta_c''y_c - \theta'' \left( w_c - \frac{1}{A} \int_A w dA \right) \quad c$$

By substituting this value of  $\epsilon$  in Eq. 19 : 19 and using the abbreviations

$$R_{cy} = \int_A x_c w_c dA \quad 19 : 21a$$

$$R_{cx} = \int_A y_c w_c dA \quad 19 : 21b$$

$$C_c = \int_A w_c^2 dA - \frac{1}{A} \left( \int_A w_c dA \right)^2 \quad 19 : 22$$

the expression for internal work reduces to

$$U_i = \frac{1}{2} \int_0^z (EI_y \xi_c''^2 + 2EI_{xy} \xi_c'' \eta_c'' + EI_x \eta_c''^2 + 2ER_{cy} \xi_c'' \theta'' + 2ER_{cx} \eta_c'' \theta'' + EC_c \theta''^2 + GK_t \theta'^2) dz \quad 19 : 23$$

in which  $I_x$  and  $I_y$  are the moments of inertia about the  $X_c$  and  $Y_c$  axes, respectively,  $I_{xy}$  the product of inertia about those axes, and  $K_t$  the torsion constant of the section.  $R_{cx}$ ,  $R_{cy}$ , and  $C_c$  are also functions of the shape and size of the cross-section, but they have no generally recognized names. In the following discussion  $R_{cx}$  and  $R_{cy}$  are termed the "warping moments" of the section about the centroidal  $X$  and  $Y$  axes.  $C_c$  is called the "warping constant."<sup>1</sup>

In computing the external work done by the axial load  $P$  as the column deforms, it is not allowable to consider the column to be a single unit, as is done in the derivation of Eq. 10 : 6, but the member must be treated as a group of fibers, each of sectional area  $dA$  and subjected to the average stress  $\sigma_0 = P/A$ . If the translational movement of each point be represented by the components  $\xi$  and  $\eta$  parallel to the  $X$  and  $Y$  axes, respectively, the difference between a small distance,  $ds$ , measured along a fiber and its projection on the  $Z$  axis,  $dz$ , will be equal to  $\sqrt{\xi'^2 + \eta'^2}$ . Therefore the expression for external work may be written

$$U_e = 0.5 \sigma_0 \int_{z=0}^z \int_A (\xi'^2 + \eta'^2) dA dz \quad 19 : 24$$

Since the translational motion of any point may be resolved into translational movement of a reference point and rotation around that

<sup>1</sup> In checking the validity of the expression for  $C_c$  it is helpful to recognize that since any surface integral like  $\int_A w_c dA$  is a constant, it can be taken from the integration sign and

$$\int_A w_c \left( \int_A w_c dA \right) dA \quad \text{becomes} \quad \left( \int_A w_c dA \right)^2$$

reference point,

$$\xi = \xi_c - y_c \theta \quad \eta = \eta_c + x_c \theta \quad d$$

Consequently, since  $x_c$  and  $y_c$  are measured from centroidal axes,

$$U_e = 0.5 \sigma_0 \int_{z=0}^z=L [A (\xi_c'^2 + \eta_c'^2) + (I_x + I_y) \theta'^2] dz \quad 19:25$$

### 19 : 8. General Differential Equations for a Column; Rotation Axis

**Unknown** — The net change in energy of the system will be  $U_i - U_e$  and can be obtained by combining Eq. 19 : 23 and 19 : 25. From the discussion of the simpler conditions of Art. 19 : 3 it can be seen that not only must  $U_i - U_e = 0$  but also the shape of the deformed column must satisfy the criterion that

$$\delta(U_i - U_e) = 0 \quad 19:26$$

The shape of the deformed column may be defined by the deflection co-ordinates  $\xi_c$  and  $\eta_c$  of its centroidal axis and by the angles of rotation of the cross-sections,  $\theta$ , which are independent functions of  $Z$ . Therefore, if Eq. 19 : 26 is to be completely satisfied, it must be satisfied independently for any arbitrary variations of each of these three variables. If it is assumed there is no rotation of the end cross-sections and no translational movement of their centroids, boundary conditions are that for  $z = 0$  and  $z = L$ ;  $\xi_c$ ,  $\eta_c$ , and  $\theta = 0$ . If the end cross-sections are "fixed," the first derivatives  $\xi_c'$ ,  $\eta_c'$ , and  $\theta'$  are zero at  $z = 0$  and  $z = L$ . Similarly, if a completely pin-ended condition is assumed, the second derivatives  $\xi_c''$ ,  $\eta_c''$ , and  $\theta''$  are zero when  $z = 0$  or  $z = L$ . In each of these cases the variations are subject to the same boundary conditions as the basic quantities.

Assuming a variation of  $\xi_c$  and treating the expression for  $U_i - U_e$  as a function of  $\xi_c'$  and  $\xi_c''$ , application of Eq. 19 : 4 results in

$$\begin{aligned} \delta(U_i - U_e) = \frac{1}{2} \int_0^L (2 EI_y \xi_c'' + 2 EI_{xy} \eta_c'' + 2 ER_y \theta'') \delta \xi_c'' dz \\ - \frac{1}{2} \int_0^L (2 A \sigma_0 \xi_c') \delta \xi_c' dz = 0 \quad a \end{aligned}$$

or

$$\begin{aligned} \int_0^L (EI_y \xi_c'' + EI_{xy} \eta_c'' + ER_y \theta'') \frac{d}{dz} \delta \xi_c' dz \\ - A \sigma_0 \int_0^L \xi_c' \frac{d}{dz} \delta \xi_c dz = 0 \quad b \end{aligned}$$

Integrating by parts

$$\begin{aligned} & [(EI_y \xi_c'' + EI_{xy} \eta_c'' + ER_y \theta'') \delta \xi_c']_0^L \\ & - \int_0^L (EI_y \xi_c''' + EI_{xy} \eta_c''' + ER_y \theta''') \delta \xi_c' dz \\ & - A \sigma_0 [\xi_c' \delta \xi_c]_0^L + A \sigma_0 \int_0^L \xi_c'' \delta \xi_c dz = 0 \end{aligned} \quad c$$

Regardless of whether fixed-end or pin-end conditions are assumed, the expressions within brackets vanish on account of the boundary conditions, whence

$$\begin{aligned} & - \int_0^L (EI_y \xi_c''' + EI_{xy} \eta_c''' + ER_y \theta''') \frac{d}{dz} \delta \xi_c dz \\ & + A \sigma_0 \int_0^L \xi_c'' \delta \xi_c dz = 0 \end{aligned} \quad d$$

Integrating the first expression by parts and noting that the resulting term in brackets vanishes as  $\delta \xi_c$  must be zero at both ends of the member,

$$\int_0^L (EI_y \xi_c'''' + EI_{xy} \eta_c'''' + ER_y \theta'''' + A \sigma_0 \xi_c'') \delta \xi_c dz = 0 \quad e$$

Since Eq. *e* must be satisfied for any arbitrary variation  $\delta \xi_c$ , the expression in parentheses must be zero, and one of the basic differential equations for the shape of the deformed column is

$$EI_y \xi_c'''' + EI_{xy} \eta_c'''' + ER_y \theta'''' + A \sigma_0 \xi_c'' = 0 \quad 19 : 27a$$

From parallel computations based on variations in  $\eta$  and  $\theta$ ,

$$EI_{xy} \xi_c'''' + EI_{xx} \eta_c'''' + ER_x \theta'''' + A \sigma_0 \eta_c'' = 0 \quad 19 : 27b$$

$$ER_y \xi_c'''' + ER_x \eta_c'''' + EC \theta'''' + (\sigma_0 I_p - GK_t) \theta'' = 0 \quad 19 : 27c$$

where  $I_p$  is the polar moment of inertia of the section about its centroid. It should be noted that the three equations of 19 : 27 apply to either pin-end or fixed-end conditions.

The practical solution of Eq. 19 : 27 depends on the appropriate boundary conditions. Most important is the "completely pin-ended condition," in which no bending or torsional moment is applied at either end of the member and the end cross-sections are free to warp. The solution for this condition is

$$\xi_c = a_1 \sin \frac{\pi z}{L} \quad \eta_c = a_2 \sin \frac{\pi z}{L} \quad \theta = a_3 \sin \frac{\pi z}{L} \quad 19 : 28a, b, c$$

This is obviously the particular form where  $n = 1$  of a more general

solution in which  $\sin (n\pi z/L)$  is used instead of  $\sin (\pi z/L)$ . Since the lowest value of average stress,  $\sigma_0$ , compatible with equilibrium in a deformed shape is the only one of practical interest, and it is obtained when  $n = 1$ , the use of that figure is justified. The constants  $a_1$ ,  $a_2$ , and  $a_3$  represent the translational and rotational movements of the cross-section at mid-length. Their absolute values are independent of the loads at which deformation is compatible with equilibrium.

If only one of Eq. 19 : 27 needed to be considered,  $a_1$ ,  $a_2$ , and  $a_3$  might have any values small enough to justify the assumptions that  $\sin \alpha = \alpha = \tan \alpha$ , etc. It is necessary, however, that the values used for these constants be the same in all three equations. Therefore, in general, there are certain mathematical relations that must be satisfied by the constants. Physically this means that, when the column deflects under a critical load, there are definite ratios existing between the deflections parallel to the co-ordinate axes and the rotation about the centroidal axis, which is another way of saying that the cross-sections will rotate about a definite axis. The location of that axis and the critical stress under which that rotation can take place with the column in equilibrium of neutral stability are to be determined from operations on Eq. 19 : 27.

**19 : 9. Action of Column with Doubly Symmetrical Section** — Before studying the more general case of the section of arbitrary shape, it is desirable to investigate those in which the cross-section has axes of symmetry. It will be assumed first that both the  $X$  and  $Y$  axes are axes of symmetry. Then, as is well known,  $I_{xy} = 0$ . From the definition of unit warping,  $w_c$ , it can be seen that for a symmetrical section that quantity will be anti-symmetrical if  $w_{co}$  is so chosen that  $w_c = 0$  where the median line of the section and the axis of symmetry intersect. Therefore, if the  $X_c$  axis is an axis of symmetry, the elements of the median line may be grouped in pairs with the same abscissa,  $x_c$ , and equal and opposite values of  $w_c$ . Then  $R_{cy}$  will be equal to zero. If

some other value were taken for  $w_{co}$ , the effect would be to add  $\int_A w_{co} y$   $dA$  to  $R_{cy}$ , but, since  $w_{co}$  is a constant and  $y_c$  is measured from an axis through the centroid, the new term would also be zero. Thus, regardless of the value chosen for  $w_{co}$ ,  $R_{cy}$  is zero for a section symmetrical about the  $X$  axis and  $R_{cx}$  is zero for a section symmetrical about the  $Y$  axis. Also for sections with "point symmetry" like a conventional  $Z$  with equal flanges,  $R_{cx}$  and  $R_{cy}$  are zero since elements of the median line can be grouped in pairs with the same value of  $w_c$  but with equal and opposite values of  $x_c$  and  $y_c$ . This is true for sections with point symmetry even though the centroidal axes are not principal axes of the section. Practical methods for computing  $R_{cx}$ ,  $R_{cy}$ , and  $C_c$  are described in Art. 19 : 13.

For sections with two axes of symmetry, so many of the constants of Eq. 19 : 27 vanish that they reduce to

$$EI_y \xi_c'''' + A\sigma_0 \xi_c'' = 0 \quad 19 : 29a$$

$$EI_x \eta_c'''' + A\sigma_0 \eta_c'' = 0 \quad 19 : 29b$$

$$EC\theta'''' + (\sigma_0 I_p - GK_t)\theta'' = 0 \quad 19 : 29c$$

Equations 19 : 29, it may be noticed, are independent, and there are no specific relations that must hold between the constants of their solution given by Eq. 19 : 28. This means that the column may deflect normal to the  $Y$  axis, deflect normal to the  $X$  axis, or may rotate about its centroidal axis. Also the load at which it becomes unstable with respect to any of these possible actions is unaffected by those at which it becomes unstable with respect to the other two. Furthermore, there can be no simultaneous combination of these actions unless the critical average stresses for the different actions happen to be equal.

Since  $A\sigma_0 = P$  and  $\xi_c$  represents deflection of the centroid of a section normal to the  $Y_c$  axis, it can be seen that Eq. 19 : 29a and 19 : 8 are fundamentally identical. This means that the latter equation and the Euler formula for critical load developed from it are justified by the more exact theory for doubly symmetrical sections. It also indicates that one may write at once, as an expression for the average stress at which the column becomes unstable with respect to deflection normal to the  $Y$  axis,

$$\sigma_y = \frac{\pi^2 EI_y}{L^2 A} \quad 19 : 30a$$

Similarly, the column becomes unstable with respect to deflection normal to the  $X$ -axis when

$$\sigma_x = \frac{\pi^2 EI_x}{L^2 A} \quad 19 : 30b$$

Substitution of Eq. 19 : 28c in Eq. 19 : 29c gives, as the average stress at which the column becomes unstable with respect to rotation about the centroidal axis,

$$\sigma_r = \frac{\frac{C_c}{L}}{I_p} \quad 19 : 30c$$

In Eq. 19 : 30,  $\sigma_y$ ,  $\sigma_x$ , and  $\sigma_r$  are used in place of  $\sigma_0$ , the subscripts indicating the type of instability with which each is connected.

The action of the doubly symmetrical column may be summarized



by saying that it may fail by bending in the plane of a principal axis of the section in accordance with the Euler formula, or it may twist about the centroidal axis in accordance with Eq. 19 : 30c. Actual failure will take place when the lowest of the three average stresses of Eq. 19 : 30 is reached, and its character will be in accordance with the particular stress attained. The same results apply also to the column with point symmetry. In practical computations for such columns care must be taken to use the principal axes of the cross-section as axes of reference.

#### 19 : 10. Action of Columns with Singly Symmetrical Sections—

The action of sections that are symmetrical about only one axis, like the conventional channel, is somewhat more complex. If symmetry is about the  $X_c$  axis,  $I_{xy}$  and  $R_y$  vanish and Eq. 19 : 27 becomes

$$EI_y \xi_c'''' + A\sigma_0 \xi_c'' = 0 \quad 19 : 31a$$

$$EI_x \eta_c'''' + ER_{cx} \theta'''' + A\sigma_0 \eta_c'' = 0 \quad 19 : 31b$$

$$ER_{cx} \eta_c'''' + EC_c \theta'''' + (\sigma_0 I_p - GK_t) \theta'' = 0 \quad 19 : 31c$$

The first of these is identical with Eq. 19 : 29a and shows that one possible type of failure is by deflection in the plane of symmetry under the average stress  $\sigma_y$  as obtained from Eq. 19 : 30a.

By substituting Eqs. 19 : 28b, c in Eqs. 19 : 31b, c and dividing by  $\sin (\pi z/L)$  the latter become

$$\left( \frac{\pi^2 EI_x}{L^2} - \sigma_0 A \right) a_2 + \left( \frac{\pi^2 ER_{cx}}{L^2} \right) a_3 = 0 \quad a$$

$$\left( \frac{\pi^2 ER_{cx}}{L^2} \right) a_2 + \left( \frac{\pi^2 EC_c}{L^2} + GK_t - \sigma_0 I_p \right) a_3 = 0 \quad b$$

These equations would be satisfied for any value of  $\sigma_0$  if  $a_2$  and  $a_3$  were equal to zero, but that would mean only that the column would be in equilibrium under that stress if there were no rotation or bending. If  $a_2$  and  $a_3$  are not to be zero, the determinant composed of their coefficients must disappear. That is,

$$\begin{vmatrix} \frac{\pi^2 EI_x}{L^2} - \sigma_0 A & \frac{\pi^2 ER_{cx}}{L^2} \\ \frac{\pi^2 ER_{cx}}{L^2} & \frac{\pi^2 EC_c}{L^2} + GK_t - \sigma_0 I_p \end{vmatrix} = 0 \quad c$$

When expanded, this gives a quadratic equation in  $\sigma_0$ , from which can be found two values of average stress at which deflection normal to

the  $X$  axis combined with twist about the centroidal axis is compatible with equilibrium. This determinant and its solution can be simplified by substituting in it the values of  $\sigma_x$  and  $\sigma_r$  from Eqs. 19 : 30b, c, at which a doubly symmetrical section becomes unstable and

$$\rho_x = \frac{\pi^2 E R_{cx}}{L^2 \sqrt{AI_p}} \quad 19 : 32$$

The determinant then may be written

$$\begin{vmatrix} (\sigma_x - \sigma_0)A & \sqrt{AI_p} \rho_x \\ \sqrt{AI_p} \rho_x & I_p(\sigma_r - \sigma_0) \end{vmatrix} = 0 \quad d$$

It can readily be seen that both products in the expansion of this determinant will include the factor  $AI_p$ . Therefore, since the determinant is zero valued, the  $A$  and  $I_p$  terms can be omitted and

$$\begin{vmatrix} \sigma_x - \sigma_0 & \rho_x \\ \rho_x & \sigma_r - \sigma_0 \end{vmatrix} = 0 = \sigma_0^2 - \sigma_0(\sigma_r + \sigma_x) + \sigma_r \sigma_x - \rho_x^2 \quad e$$

Whence

$$\sigma_0 = \frac{\sigma_r + \sigma_x}{2} \pm \sqrt{\left(\frac{\sigma_r - \sigma_x}{2}\right)^2 + \rho_x^2} \quad 19 : 33$$

This formula for the critical stress is similar to that for determining the principal stresses when the normal and shearing stresses on two mutually perpendicular planes are known, and the numerical values of  $\sigma_0$  can be found by a construction analogous to that of Art. 7 : 12, as shown in Fig. 19 : 7. From this figure it can be seen that one of the critical stresses for the member will be less than either  $\sigma_r$  or  $\sigma_x$ , while the other will be greater than either. In both cases the deformation would consist of a combination of bending normal to the axis of symmetry and twisting about the centroidal axis. Alternatively each stress may be considered as that at which the cross-sections would rotate about some point, as yet undetermined, on the axis of symmetry. (For purposes of reference the smaller of these values will be termed  $\sigma_2$  and the larger  $\sigma_3$ .)

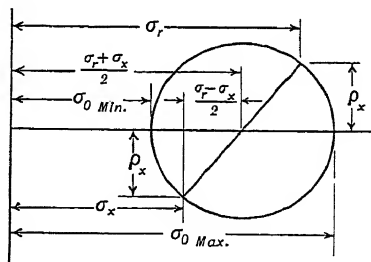


FIG. 19 : 7

Under either critical load  $\sin(\pi z/L)$  will be the same in Eqs. 19 : 28b and c. Therefore  $\eta_c = (a_2/a_3)\theta$ . But from Eq. 19 : 20,  $\eta_c = x_{Dc}\theta$  or

$-x_{cD}\theta$ . Thus the distance from the centroid of the section to the axis of rotation will be obtainable from Eqs. *a* and *b* as

$$X_{cD} = -\frac{a_2}{a_3} = \frac{\frac{\pi^2 E R_x}{L^2}}{\frac{\pi^2 E I_x}{L^2} - A \sigma_0} = \sqrt{\frac{I_p}{A}} \frac{\rho_x}{\sigma_x - \sigma_0} \quad 19 : 34a$$

or

$$X_{cD} = -\frac{a_2}{a_3} = \frac{GK_t + \frac{\pi^2 EC}{L^2} - \sigma_0 I_p}{\frac{\pi^2 E R_x}{L^2}} = \sqrt{\frac{I_p}{A}} \frac{\sigma_r - \sigma_0}{\rho_x} \quad 19 : 34b$$

These formulas for  $x_{cD}$  will give the same result for either value of  $\sigma_0$  obtained from Eq. 19 : 33. The magnitude of that result will depend on which value of  $\sigma_0$  is used. This means that there are two possible locations for the axis of rotation, one associated with each of the possible critical stresses.

**19 : 11. Action of Unsymmetrical Section Column** — When the column section has no axis of symmetry, the three equations of 19 : 27 are coupled, and for the constants  $a_1$ ,  $a_2$ , and  $a_3$ , which represent the magnitudes of the deflections and rotations, to have values other than zero it is necessary to satisfy the criterion that

$$\begin{vmatrix} \frac{\pi^2 E I_y}{L^2} - A \sigma_0 & \frac{\pi^2 E I_{xy}}{L^2} & \frac{\pi^2 E R_{cy}}{L^2} \\ \frac{\pi^2 E I_{xy}}{L^2} & \frac{\pi^2 E I_x}{L^2} - A \sigma_0 & \frac{\pi^2 E R_{cx}}{L^2} \\ \frac{\pi^2 E R_{cy}}{L^2} & \frac{\pi^2 E R_{cx}}{L^2} & \frac{\pi^2 E C_c}{L^2} + GK_t - \sigma_0 I_p \end{vmatrix} = 0 \quad a$$

Using the abbreviations of the preceding article and also

$$\rho_y = \frac{\pi^2 E R_y}{L^2 \sqrt{A I_p}} \quad \rho_{xy} = \frac{\pi^2 E I_{xy}}{L^2 A} \quad 19 : 35a, b$$

this may be written

$$\begin{vmatrix} \sigma_y - \sigma_0 & \rho_{xy} & \rho_y \\ \rho_{xy} & \sigma_x - \sigma_0 & \rho_x \\ \rho_y & \rho_x & \sigma_r - \sigma_0 \end{vmatrix} = 0 \quad b$$

Expanded, this gives the cubic equation

$$\sigma_0^3 - \sigma_0^2(\sigma_r + \sigma_x + \sigma_y) + \sigma_0(\sigma_r\sigma_x + \sigma_r\sigma_y + \sigma_x\sigma_y - \rho_{xy}^2 - \rho_x^2 - \rho_y^2) - (\sigma_r\sigma_x\sigma_y + 2\rho_{xy}\rho_x\rho_y - \rho_{xy}^2\sigma_r - \rho_y^2\sigma_x - \rho_x^2\sigma_y) = 0 \quad 19:36$$

Kappus has shown<sup>1</sup> that all three roots of Eq. 19:36 will be real and positive. This means that each of the three values of  $\sigma_0$  which satisfy it represents an average stress under which deflection combined with rotation is compatible with equilibrium. Connected with each of these possible stresses there is a definite location for the axis of rotation. From combining pairs of Eq. 19:28 and Eq. 19:20

$$\xi_c = \frac{a_1\theta}{a_3} = -y_{cD}\theta = +y_{cD}\theta \quad \text{whence} \quad y_{cD} = \frac{a_1}{a_3} \quad 19:37a$$

and

$$\eta_c = \frac{a_2\theta}{a_3} = +x_{cD}\theta = -x_{cD}\theta \quad \text{whence} \quad x_{cD} = -\frac{a_2}{a_3} \quad 19:37b$$

where  $x_{cD}$  and  $y_{cD}$  are the co-ordinates of the axis of rotation measured from the section centroid as the origin. To obtain numerical values for these co-ordinates the first step is to solve Eq. 19:36 to obtain values of  $\sigma_0$ . The deformation equation can then be reconstructed from Eq. *b* as

$$(\sigma_y - \sigma_0)a_1 + \rho_{xy}a_2 + \rho_ya_3 = 0 \quad d$$

$$\rho_{xy}a_1 + (\sigma_x - \sigma_0)a_2 + \rho_xa_3 = 0 \quad e$$

$$\rho_ya_1 + \rho_xa_2 + (\sigma_r - \sigma_0)a_3 = 0 \quad f$$

in which all values of  $\rho$  and  $\sigma$  would be known. Any two of these equations can be combined so as to eliminate one of the  $a$  quantities and obtain a numerical value for the ratio of the other two. Thus  $a_2$  would be eliminated to obtain  $y_{cD}$  and  $a_1$  to obtain  $x_{cD}$ .

The analytical solution of Eq. 19:36 to determine the values of  $\sigma_0$  is tedious and is best effected in practice by use of the nomogram of Fig. 19:8. This diagram is constructed for the solution of the cubic equation

$$\omega^3 - 3\omega^2 + p\omega - q = 0 \quad 19:38$$

<sup>1</sup> "Twisting Failure of Centrally Loaded Open-section Columns in the Elastic Range," N.A.C.A. Technical Memo. 851, p. 24, Washington, 1938.

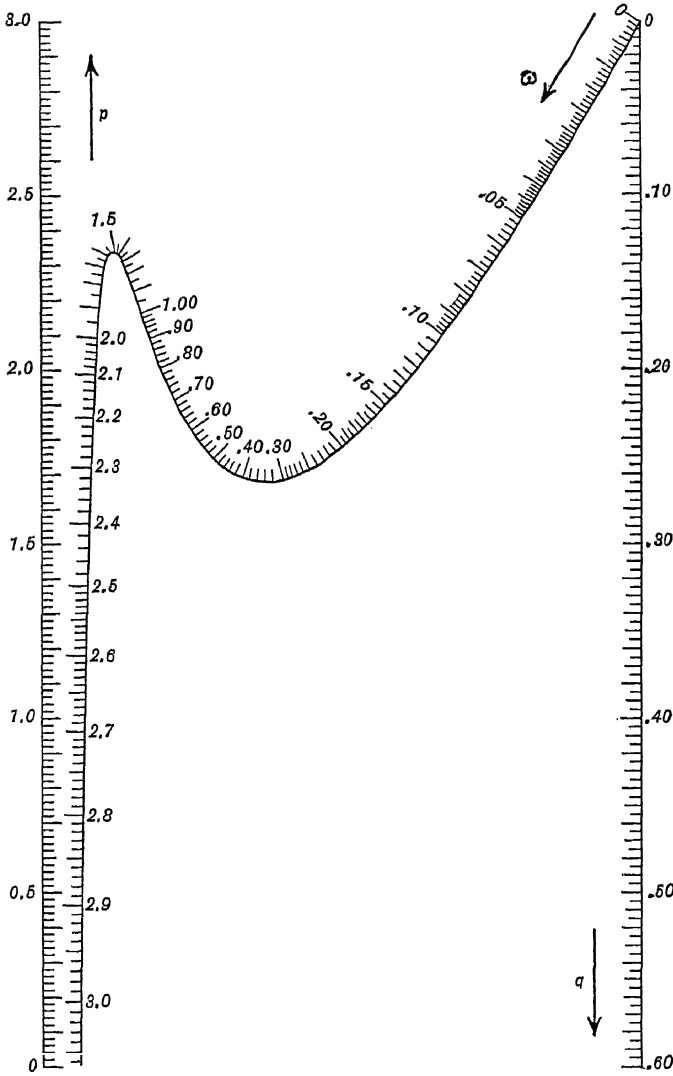


Chart for Determining the Twisting Failure Stress  $\sigma_0 = \omega \sigma_m$  from the Cubic Equation:

$$\omega^3 - 3\omega^2 + p\omega - q = 0$$

FIG. 19:8

In its use let

$$\sigma_m = \frac{\sigma_r + \sigma_x + \sigma_y}{3} \quad 19 : 39a$$

$$p = \frac{\sigma_r \sigma_x + \sigma_r \sigma_y + \sigma_x \sigma_y - \rho_{xy}^2 - \rho_x^2 - \rho_y^2}{\sigma_m^2} \quad 19 : 39b$$

$$q = \frac{\sigma_r \sigma_x \sigma_y + 2 \rho_{xy} \rho_x \rho_y - \rho_{xy}^2 \sigma_r - \rho_y^2 \sigma_x - \rho_x^2 \sigma_y}{\sigma_m^3} \quad 19 : 39c$$

First determine  $\sigma_r$ ,  $\sigma_x$ , and  $\sigma_y$ . Next compute  $\sigma_m$ ,  $p$ , and  $q$ . Then find the value of  $\omega$  from the nomogram. The corresponding stress can then be obtained from

$$\sigma_0 = \omega \sigma_m \quad 19 : 40$$

In practice only the minimum of the three possible values of  $\omega$  would be of interest since it is connected with the stress at which the member would actually become unstable.

**19 : 12. General Equation for a Column with Known Axis of Rotation** — In the preceding articles it has been assumed that the position of the axis of rotation was unknown. In some problems that position is known or can be assumed from the physical conditions of the structure. Under such conditions it is possible to make considerable simplifications in the formulas by using co-ordinates based on the axis of rotation instead of those based on the centroidal axis.

In Art. 19 : 8 the internal energy is given by Eq. 19 : 19 in terms of  $\epsilon_d$ . In that article  $\epsilon_d$  was then expressed in terms of  $\xi_c$ ,  $\eta_c$ ,  $\theta$ , and the unit warpings were related to rotation about the centroidal axis, to obtain a working expression for the internal energy. Alternatively  $\epsilon_d$  may be expressed, as in Eq. 19 : 17, in terms of  $\theta$  and the unit warping corresponding to rotation about the actual axis of rotation. Then

$$U_i = \int_0^L \frac{1}{2} \left( E \int_A w_d^2 \theta''^2 dA + GK_t \theta'^2 \right) dz \quad a$$

or

$$U_i = \frac{1}{2} \int_0^L (EC_d \theta''^2 + GK_t \theta'^2) dz \quad b$$

where

$$C_d = \int_A w_d^2 dA \quad 19 : 41$$

The expression for external work of Eq. 19 : 24 remains valid, but, instead of the formerly used expressions for the value of  $\xi$  and  $\eta$ , it is

better to employ

$$\xi = -y_d\theta \quad \text{and} \quad \eta = x_d\theta \quad c$$

Then

$$U_e = \frac{1}{2}\sigma_0 \int_0^L \int_A (y_d^2\theta'^2 + x_d^2\theta'^2) dA dz \quad d$$

or

$$U_e = \frac{1}{2}\sigma_0 \int_0^L I_{dp}\theta'^2 dz \quad e$$

where  $I_{dp}$  is the polar moment of inertia of the section about the axis of rotation.

Since the axis of rotation is known,  $\theta$  is the only independent quantity of which the variation must be studied. Therefore  $\delta(U_i - U_e)$  may be set equal to zero and operations of the calculus of variations parallel to those of Art. 19 : 8 carried out to obtain the differential equation

$$EC_d\theta'''' + (I_{dp}\sigma_0 - GK_t)\theta'' = 0 \quad 19 : 42$$

This equation is satisfied by  $\theta = a \sin (\pi z/L)$ , insertion of which gives

$$\sigma_0 = \frac{\frac{\pi^2 EC_d}{L^2} + GK_t}{I_{dp}} \quad 19 : 43$$

for the average stress at failure. When the position of the axis of rotation is known, this formula is obviously much easier to apply than Eq. 19 : 36. It is to be noticed, however, that the section constants  $C_d$  and  $I_{dp}$  depend on the location of the axis of rotation.

When the location of that axis is not known, by the use of Eqs. 19 : 51 and 19 : 52 from Art. 19 : 13,  $I_p$  and  $C_d$ , and therefore  $\sigma_0$  also, can be expressed as functions of  $x_{cD}$  and  $y_{cD}$ , the co-ordinates of the center of rotation with respect to the centroid of a section. Then the partial derivatives of  $\sigma_0$  with respect to  $x_{cD}$  and  $y_{cD}$  would be set equal to zero and the resulting equations solved to obtain the values of those variables for which  $\sigma_0$  would be a minimum. This method was used by Lundquist in his development of formulas for torsional failure.<sup>1</sup>

In wing and fuselage construction, stiffeners subject to torsional failure are often attached to the skin in such a manner that the stiffener and a part of the skin must act as a unit. In such construction the stiffener and associated skin, if it twists, must twist about an axis located in the surface of the skin, since rotation about any other axis would be resisted

<sup>1</sup> "On the Strength of Columns that Fail by Twisting," E. E. Lundquist, *Jour. of Aero. Sci.*, Vol. 4, p. 249, April, 1937.

by tensile stresses developed in the skin material. This means that  $x_{cD}$  and  $y_{cD}$  would not be independent variables but would satisfy an equation representing the position of the mid-line of the skin. There would then be only one derivative of  $\sigma_0$  to be set equal to zero. When dealing with a skin and stiffener combination in this manner, the geometrical properties used should be those of the stiffener and effective skin considered as a unit.

**19 : 13. Practical Evaluation of Warping Moments and Constants —** Methods for obtaining most of the section constants appearing in Eq. 19 : 29 and the resulting formulas are well known, and the only special comment to be made is that it is advisable to neglect the effect of the thickness of the section but to use the mid-line method described in Art. 16 : 1. Thus for the channel section of Fig. 19 : 9 the distance from the centroid to the median line of the back is  $4/(2 + 4) = 0.667$  in. The moments of inertia about the principal axes can be computed by the same system. They are

$$I_x = \frac{0.6 \times 4 \times 7}{12 \times 3} = 0.4667 \text{ in.}^4$$

$$I_y = \frac{0.6 \times 4 \times 3}{9 \times 3} = 0.2667 \text{ in.}^4$$

$$I_p = I_x + I_y = 0.7333 \text{ in.}^4$$

$$I_{xy} = 0 \quad \text{since the X-axis is an axis of symmetry}$$

The torsion constant,  $K_t$ , is identical with the constant  $K$  of Art. 7 : 7. For the thin-walled open sections in which torsional failure is likely to be important, it is allowable to compute  $K_t$  as though the cross-section were a rectangle with a width equal to the total length of the median line,  $B$ , and a height equal to the thickness of the material,  $t$ . Then

$$K_t = \frac{Bt^3}{3} \quad 19 : 44$$

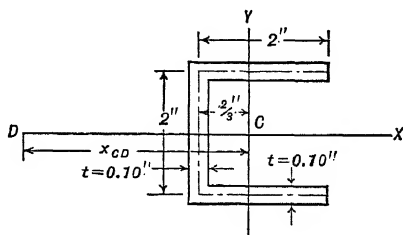


FIG. 19:9

If the thickness is not constant, the section may be divided into segments of constant thickness and  $K_t$  for the entire section taken as the sum of the values of  $K_t$  found for the segments considered individually. For the channel section of Fig. 19 : 9,  $K_t = 6 \times 0.001/3 = 0.002 \text{ in.}^4$

The warping moments,  $R_x$  and  $R_y$ , and the warping constant,  $C$ ,



depend on the distribution of unit warping,  $w$ , along the median line. In Eq. 19 : 12 the unit warping is defined as a constant,  $w_0$ , plus a definite integral. In Fig. 19 : 4 it is shown how half the change in unit warping between two points on the median line could be represented by an area. If a segment of the median line of a section is straight, the difference between the values of  $w$  at its ends can be most conveniently computed by considering that segment of the median line as a vector representing a force and calculating its moment about the point with which the unit warpings are related. If this imaginary force in pounds is numerically equal to the length of the segment in inches, the imaginary moment will be equal to the increment in unit warping in square inches. If the segment is not parallel to one of the reference axes the work is often facilitated by resolving its length into two components and computing the moment in exactly the same manner as that of an oblique force.

While the change in unit warping can be readily computed in this manner, the problem of computing the unit warping,  $w_0$ , at the assumed origin of circumferential co-ordinates remains. The method of handling it depends on whether one is computing unit warpings related to an actual center of rotation,  $w_a$ , or those related to the centroidal axis of the member,  $w_c$ .

For computing values of  $w_a$  there is the criterion of Eq. 19 : 15 that  $\int_A w_a dA = 0$ , which means that the average value of  $w_a$  is zero. Therefore, any point on the median line may be taken as the origin of the circumferential co-ordinate,  $u$ , and any arbitrary value assumed as a trial value for the unit warping at that point. Trial values of the unit warping can then be computed for every point on the median line and the average of these trial values determined. If the section is not of constant thickness, the unit warping at each point would be multiplied by the thickness at that point in computing this average. The actual unit warpings can then be determined by subtracting the average from the originally computed trial values.

This practice cannot be followed in computing unit warpings,  $w_c$ , related to the centroid of the section, since, in general,  $\int_A w_c dA$  is not equal to zero. It can be shown, however, by substituting  $w_c + K$  for  $w_c$  in Eq. 19 : 21 and 19 : 22, that the resulting values of  $R_{cx}$ ,  $R_{cy}$ , and  $C_c$  remain unchanged, since the  $X_c$  and  $Y_c$  axes pass through the centroid and, on integration, all terms including  $K$  vanish. Therefore, any point on the median line may be selected as the origin of  $u$ , and any arbitrary value assumed for  $w_c$  at that point in computing  $R_{cx}$ ,  $R_{cy}$ , and  $C_c$ .

In computing  $R_x$  and  $R_y$  it is usually convenient to visualize the operation as one of computing the moment about the  $X$  or  $Y$  axis of a load distributed along the median line with an intensity at each point equal to the product of the thickness of the section and the unit warping at that point. The validity of this approach should be evident from inspection of the equations defining those constants. By using this method of attack it can be proved that the contribution to  $R_x$  of a constant-thickness straight segment is

$$\Delta R_x = \frac{Lt}{6} [w_a(2y_a + y_b) + w_b(2y_b + y_a)] \quad 19 : 45$$

where  $L$  is the length of the segment,  $t$  the thickness of the section,  $w_a$  and  $w_b$  the unit warpings at, and  $y_a$  and  $y_b$  the ordinates of, the points  $A$  and  $B$  at the ends of the segment. When the segment is parallel to the  $X$ -axis, the increment of  $R_x$  will be equal to the product of the area of the segment, the unit warping at its midpoint, and the common ordinate,  $y$ , of points along the median line. Similar relations hold for the increment in  $R_y$ . These relations lend themselves to convenient tabulation of the computations for complex sections.

In computing the warping constant,  $C$ , it is also convenient to divide the median line into straight segments to permit the application of a type formula for the contribution of a segment to the first term of the definition of this constant in Eq. 19 : 22. Here the problem is to find the area under a curve of  $w^2$  between two points  $L$  inches apart when  $w$  varies linearly. The resulting formula is

$$\Delta C = \frac{Lt}{3} (w_b^2 + w_a w_b + w_a^2) \quad 19 : 46$$

The second term of the expression for  $C$  represents the square of the area under the curve of  $w$  divided by the area of the section.

Actual computations of  $R_{cx}$ ,  $R_{cy}$ , and  $C_c$  will first be illustrated by finding those constants for the unequal leg angle of Fig. 19 : 10, assuming that both legs are of the same thickness,  $t$ . The location of the centroid of the median line is easily checked and it can be seen that, for the leg  $BE$ ,  $r_t = +1.8$  and, for the leg  $EF$ ,  $r_t = +0.8$  in., the sign convention

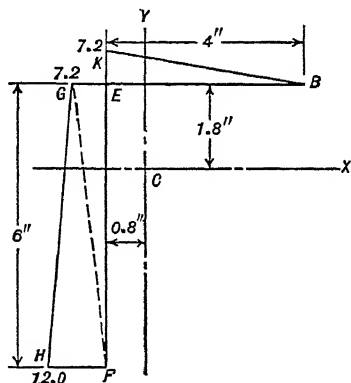


FIG. 19 : 10

being that of Art. 19 : 5 with point  $B$  assumed as the origin of the circumferential co-ordinate. Then if it is assumed that  $w_c = 0$  at  $B$ ,  $w_c = 0 + 4 \times 1.8 = +7.2$  at  $E$  and  $+7.2 + 6 \times 0.8 = +12.0$  at  $F$ . The variation is linear and the values of  $w_c$  are as indicated on Fig. 19 : 9. To determine  $R_{cx}$  and  $R_{cy}$  the section is assumed subjected to a load normal to the paper varying linearly from 0 at  $B$  to  $+7.2 t$  at  $E$  and linearly from  $+7.2 t$  at  $E$  to  $+12.0 t$  at  $F$ . The moment of this load about  $CX$  will be equal to  $R_{cx}$  and its moment about  $CY$  will be equal to  $R_{cy}$ . Then by simple computations

$$\begin{aligned} R_{cx} &= +7.2 \times 2 \times 1.8 t - 7.2 \times 3 \times 0.2 t - 12.0 \times 3 \times 2.2 t \\ &= -57.60 t \end{aligned}$$

$$\begin{aligned} R_{cy} &= +7.2 \times 2 \times (1.333 - 0.800) t - (7.2 + 12.0) \times 3 \times 0.8 t \\ &= -38.40 t \end{aligned}$$

To obtain the value of  $C_c$  from Eq. 19 : 22, Eq. 19 : 46 may be used for the first term. The second term is the square of the total area under the curve of  $w_c$  divided by the area of the section. These relations applied to the angle section give

$$\begin{aligned} C_c &= \frac{4 \times 7.2^2 t}{3} + \frac{6(7.2^2 + 7.2 \times 12.0 + 12.0^2) t}{3} \\ &\quad - \frac{(7.2 \times 2 + 7.2 \times 3 + 12.0 \times 3)^2 t}{10} = +115.20 t \end{aligned}$$

When the cross-section has an axis of symmetry, the computation of the constants is naturally simplified, and it is desirable to develop some special relations that apply when a section is symmetrical about the  $X$ -axis. It has been shown in Art. 19 : 12 that the center of rotation for a section symmetrical about the  $X$ -axis will lie on the  $X$ -axis unless the section is constrained to rotate about some other point. Then if the center of rotation,  $D$ , lies on the  $X$ -axis, it is not necessary to compute trial values of  $w_d$  and correct them, by subtracting the resulting average, but the actual values can be obtained directly by assuming the origin of the circumferential co-ordinate,  $u$ , at the intersection of the median line with the  $X$ -axis and the unit warping at that point to be zero. Furthermore, it can be shown that the actual unit warpings related to rotation about any other point,  $A$ , on the  $X$ -axis can be obtained directly in the same manner.

In the derivation of Eq. 19 : 14 for the relations between  $w_d$  and  $w_c$ , the criterion of Eq. 19 : 15 that  $\int_A w_d dA = 0$  was not utilized. That equation therefore represents the relations between the warpings related

to rotation about any two points in the plane of the cross-section. Thus the relation between  $w_c$  and  $w_a$ , the unit warping related to any point  $A$  on the  $X$ -axis, is

$$w_a = w_c - x_{cA}y_c + K' \quad a$$

Since  $A$  is any point on the  $X$ -axis, Eq.  $a$  must apply when  $A$  and  $D$  coincide. Therefore the criterion that  $\int_A w_a dA = 0$  will be satisfied only by having  $w_c = 0$  at the intercept of the median line with the  $X$ -axis and  $K' = 0$ , or some equivalent. Thus it may be shown that for any section symmetrical about the  $X$ -axis  $w_a = 0$  at the intercept of the median line and the  $X$ -axis and

$$w_a = w_c - x_{cA}y_a \quad 19 : 47$$

since  $y_a = y_c$ .

Symmetry about the  $X$ -axis makes possible additional simplifications in the computations of  $R_x$ ,  $R_y$ , and  $C$ . As explained in Art. 19 : 9,  $R_y$  would be zero. Also, since  $w_c = 0$  at the intercept of the mid-line and the  $X$ -axis,  $w$  would vary anti-symmetrically about that axis and the net area under the curve of  $wt$  would be zero. Therefore the last term in Eq. 19 : 22 defining  $C_c$  would vanish. Further simplification may be obtained if, instead of computing  $R_{cx}$  and  $C_c$  directly, one first computes

$$R_{ax} = \int_A y_a w_a dA \quad 19 : 48a$$

and

$$C_a = \int_A w_a^2 dA \quad 19 : 48b$$

Substituting Eq. 19 : 47 in Eq. 19 : 48 and noting that  $y_c = y_a$  produces

$$R_{cx} = R_{ax} + x_{cA}I_x \quad 19 : 49a$$

$$C_c = C_a + x_{cA}^2 I_x + 2 x_{cA} R_{ax} \quad 19 : 49b$$

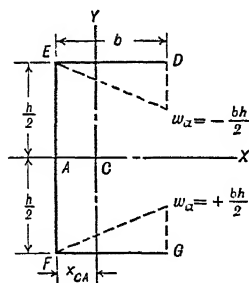


FIG. 19 : 11

In computing the constants  $R_{cx}$  and  $C_c$  for the channel of Fig. 19 : 11 it is convenient to use these relations and compute first  $R_{ax}$  and  $C_a$  with point  $A$  taken at the intersection of the web with the  $X$ -axis. Then Eq. 19 : 49 can be used to find the constants based on unit warping referred to the centroidal axis. For each leg of the channel  $r_t = h/2$ , while for the web  $r_t = 0$ . Therefore the variation in unit warping is as indicated in Fig. 19 : 11 by the broken lines. Hence the warping moment  $R_{ax}$  is  $-2 b^2 h^2 t / 8 = -b^2 h^2 t / 4$ , and the warping constant  $C_a$  is

$2b(b^2h^2t/12) = b^3h^2t/6$ . The abscissa  $x_{cA}$  measured from the centroid  $C$  to point  $A$  is  $-b^2/(h+2b)$ , and the moment of inertia  $I_x = (h^3t/12) + 2(bth^2/4) = h^2t[(h+6b)/12]$ . Substituting these values in Eq. 19 : 49 and combining terms produces as final results

$$R_{cx} = R_{ax} + x_{cA}I_x = -\frac{b^2h^2t}{3} \frac{(h+3b)}{(h+2b)} \quad 19 : 50a$$

$$C_c = C_a + 2x_{cA}R_{ax} + x_{cA}^2I_x = \frac{b^3h^2t}{12} \cdot \frac{2h^2 + 15hb + 26b^2}{(h+2b)^2} \quad 19 : 50b$$

For the special case where  $h = b$  these reduce to,  $R_{cx} = 4h^4t/9$  and  $C_c = 43h^5t/108$ .

When values of  $I_{dp}$  and  $C_d$  are desired for use in Eq. 19 : 43, they may be obtained from the relations

$$I_{dp} = I_p + (x_{cD}^2 + y_{cD}^2) A \quad 19 : 51$$

$$C_d = C_c + x_{cD}^2I_{xx} + y_{cD}^2I_{yy} - 2x_{cD}y_{cD}I_{xy} \\ - 2x_{cD}R_{cx} + 2y_{cD}R_{cy} \quad 19 : 52$$

Eq. 19 : 51 is the standard formula for polar moment of inertia about a point,  $D$ , other than the centroid of a section. Eq. 19 : 52 can be obtained by substituting in Eq. 19 : 41 the expression of Eq. 19 : 14b for  $w_d$ , squaring, integrating, eliminating the terms that vanish on account of  $x_c$  and  $y_c$  being measured from centroidal axes, and simplifying by use of the expressions for  $K$ ,  $C_c$ ,  $R_{cx}$ , and  $R_{cy}$  developed in Art. 19 : 7.

If the axis of rotation,  $D$ , of the angle section of Fig. 19 : 10 is 3.00 in. to the right and 2.00 in. below the centroid,  $C$ ,  $x_{cD} = +3.00$  and  $y_{cD} = -2.00$ . From the preceding computations  $R_{cx} = -57.60t$ ,  $R_{cy} = -38.40t$ , and  $C_c = +115.20t$ . Then

$$A = 10t$$

$$I_{xx} = 4t \times 1.8^2 + 6^3 \frac{t}{12} + 6t \times 1.2^2 = 39.60t$$

$$I_{yy} = 4^3 \frac{t}{12} + 4t \times 1.2^2 + 6t \times 0.8^2 = 14.93t$$

$$I_{xy} = 4t \times 1.8 \times 1.2 + 6t \times 0.8 \times 1.2 = 14.40t$$

$$I_p = 39.60t + 14.93t = 54.53t$$

$$I_{dp} = 54.53t + (3^2 + 2^2) \times 10t = 184.53t$$

$$C_d = 115.20t + 9 \times 39.60t + 4 \times 14.93t + 2 \times 3 \times 2 \times 14.40t \\ + 2 \times 3 \times 57.60t + 2 \times 2 \times 38.40t = 1,203.32t$$

**19 : 14. Experimental Verification for Formulas** — Various experimenters have made tests to verify the formulas of the preceding articles. Among the most extensive of these was the series carried out at Stanford University in 1939. Thirty-three 24-ST aluminum alloy channels of the section shown in Fig. 19 : 9, with lengths ranging from 10 to 90 in., were tested in axial compression and observations made of the critical load and the location of the axis of rotation. Since a complete report on the work has been published as N.A.C.A. Technical Note 733, "Experimental Study of Torsional Column Failure," only a summary is given here.

In order to obtain end conditions approximating those of the underlying theory, special end fittings were constructed in conformity with suggestions made by Mr. E. E. Lundquist, of the N.A.C.A. The most important feature of these fittings was the use of three knife edges at each end of the specimen, one acting at the midpoint of each of the three segments of the median line, to permit the end cross-sections to warp freely. These knife edges were supported by a "saddle" carried by a gimbal ring designed to make the resultant load act along the centroidal axis of the specimen.

Computations of the theoretical values of critical load and location of the axis of rotation are as follows. In Art. 19 : 13 the moments of inertia are found to be  $I_x = 0.4667 \text{ in.}^4$ ,  $I_y = 0.2667 \text{ in.}^4$ ,  $I_p = 0.7333 \text{ in.}^4$ , and  $I_{xy} = 0$ . The sectional area is 0.600 sq. in. Substituting the proper dimensions in Eq. 19 : 50 produces  $R_{cx} = 0.7111 \text{ in.}^5$  and  $C_c = 1.2740 \text{ in.}^6$ . From Eq. 19 : 44,  $K_t = 0.00200 \text{ in.}^4$ . Instead of using this value and an assumed value of the shearing modulus,  $G$ , as was done in Technical Note 733, the experimentally determined value of  $GK_t = 10,000 \text{ lb.-in.}^2$  recorded in that report may be used. The figure used for Young's modulus,  $E$ , will be 10,600,000 p.s.i., obtained by the Bureau of Standards from specimens of the channels tested, instead of the value used in Technical Note 733. In that report the computations were based on  $E = 10,200,000 \text{ p.s.i.}$ , the average result of tests made at Stanford University. As a result of these differences in the values used for  $G$  and  $E$ , the results of the present computations differ somewhat from those of Technical Note 733.

Substituting in Eq. 19 : 30 gives the following expressions for  $\sigma_x$ ,  $\sigma_y$ , and  $\sigma_r$ :

$$\sigma_x = \frac{\pi^2 EI_x}{AL^2} = \frac{\pi^2 \times 10,600,000 \times 0.4667}{0.600 L^2} = \frac{81,380,000}{L^2}$$

$$\frac{\pi^2 EI_y}{AL^2} = \frac{\pi^2 \times 10,600,000 \times 0.2667}{0.600 L^2} = \frac{46,500,000}{L^2}$$

$$\begin{aligned}\sigma_r &= \frac{\frac{\pi^2 EC_c}{L^2} + GK_t}{I_p} = \frac{\pi^2 \times 10,600,000 \times \frac{1.2740}{L^2} + 10,000}{0.7333} \\ &= \frac{181,750,000}{L^2} + 13,640\end{aligned}\quad c$$

From Eq. 19 : 32

$$\rho_x = \frac{\frac{\pi^2 ER_{cx}}{L^2 \sqrt{AI_p}}}{\frac{\pi^2 \times 10,600,000 \times 0.7111}{L^2 \sqrt{0.600 \times 0.7333}}} = \frac{112,150,000}{L^2}\quad d$$

The value of  $\sigma_0$  for any length can be obtained by substituting the value of  $L$  from the above expressions in Eq. 19 : 33. For  $L = 60$  in.:  $\sigma_x = 22,600$  p.s.i.,  $\sigma_y = 12,920$  p.s.i.,  $\sigma_r = 64,130$  p.s.i., and  $\rho_x = 31,150$  p.s.i. Then

$$\begin{aligned}\sigma_0 &= \frac{64,130 + 22,600}{2} - \sqrt{\left(\frac{64,130 - 22,600}{2}\right)^2 + 31,150^2} \\ &= 5,930 \text{ p.s.i.}\end{aligned}$$

The critical load for that length is therefore  $0.600 \times 5,930 = 3,550$  lb. The location of the axis of rotation can be found from Eq. 19 : 34 for a 60-in. length as

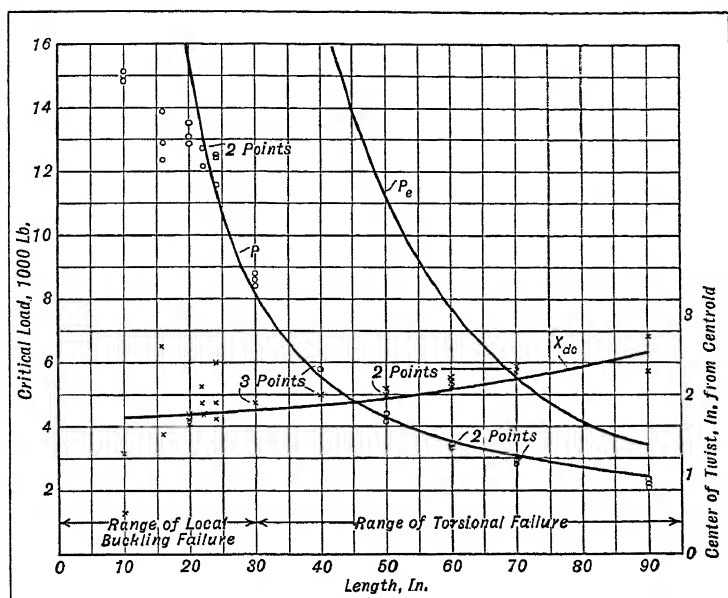
$$x_{cD} = \sqrt{\frac{I_p}{A}} \frac{\rho_x}{\sigma_x - \sigma_0} = \sqrt{\frac{0.7333}{0.600}} \frac{31,150}{22,600 - 5,930} = 2.065 \text{ in.}$$

Since the formula used is based on the assumption that the axis of rotation is at the origin, the plus sign of the result indicates that the centroid of the channel is to the right, i.e., that the channel web is between the axis of rotation and the centroid of the section.

From similar computations for all eleven lengths of channel tested, curves of critical load,  $P$ , and distance from axis of rotation to centroid,  $x$ , versus length of specimen are plotted in Fig. 19 : 12. The experimentally determined values of the same quantities are shown for comparison. It may be noticed that for lengths in excess of 24 in. the agreement is very good, and the tests tend to prove the validity of the formulas. All these longer specimens failed by twisting. The shorter specimens failed by local buckling and, as a result, agreement between the computed and observed quantities was not to be expected.

If the possibility of torsional failure had not been taken into account, it would have been expected that the longer specimens would have

failed by bending in the plane of symmetry when the stress  $\sigma_y$  was reached. The corresponding values of the critical load are represented



Comparison between Test Results and Computed Critical Loads for Aluminum Alloy Channels

FIG. 19:12

by the curve of  $P_e$  shown in Fig. 19 : 12. It may be noticed that, while the observed critical loads and those computed by the formulas of this chapter are in excellent agreement, the values of  $P_e$  are greatly in excess of the observed criticals.

**19 : 15. General Remarks on Torsional Failure** — In developing the formulas of the preceding articles it is assumed, for the most part, that the column is pin-ended and the end cross-sections are free to warp. Obviously these assumptions are not generally applicable. Another ideal case which can be handled conveniently is that in which the column ends are "fixed" and the end cross-sections are completely restrained from warping. Then in the solution of Eq. 19 : 27,  $1 - \cos (2 \pi z/L)$  would replace  $\sin (\pi z/L)$ . The net effect would be the same as if the actual length,  $L$ , were replaced by an effective length,  $L' = L/2$ , in applying the formulas for the member with pin ends, as may be done with the usual column formulas. Similarly for other types of end conditions, the actual column may be replaced by a pin-ended column with an effective length between  $L$  and  $L/2$ .



When the length of the column is small, two factors operate to destroy the validity of the formulas derived above. In the first place, the shearing stresses associated with the variation in longitudinal stress become of appreciable magnitude and it is no longer permissible to neglect them. A precise analysis taking these shearing stresses into account would be very difficult, but Kappus has shown that their effect would be to reduce critical load. If it is the slenderness ratio rather than the absolute length which is small, the critical stresses obtained from the formulas may exceed the yield point of the material. Lundquist and Fligg have investigated this problem and in N.A.C.A. Technical Report 582 have shown how effective moduli of elasticity and shear can be used in the equations. The effective modulus of elasticity,  $\bar{E}$ , is very nearly the same as that described in Art. 10 : 11. For the effective modulus of shear,  $\bar{G}$ , they recommend using the formula

$$\bar{G} = \frac{(\tau + \sqrt{\tau})G}{2} \quad 19 : 51$$

where  $\tau = \bar{E}/E$ .

In computing the geometric constants for a section in the preceding articles it was assumed allowable to compute the properties of the median line and multiply them by the thickness of the section. For the relatively thin sections under consideration this was permissible. If, however, the thickness were considerably increased, the practice would no longer be allowable. Wagner and Pretschner in N.A.C.A. Technical Memorandum 784 have shown how to allow for the effect of section thickness in computing the various constants.

When the section is closed, like an ordinary tube, the torsional stiffness,  $GK_t$ , becomes many times greater than is obtainable with an open section of the same cross-sectional area. In general the formulas developed above are applicable, but the unit warping,  $w$ , becomes much more difficult to determine. Lundquist and Fligg, however, have shown how the warping constant,  $C$ , can be computed for a hollow rectangular tube. Unsymmetrical sections would be even more difficult to handle.

The chief result of the greater torsional stiffness of closed sections is that  $GK_t$  becomes so large that  $\sigma_r$  is much greater than either  $\sigma_x$  or  $\sigma_y$ . If the section be doubly symmetrical, this means that it will fail by bending in the plane of the minor axes of the cross-sections before it becomes liable to fail by twisting. With a singly symmetrical section,  $\sigma_r$  becomes so much greater than  $\rho_x$  and  $\sigma_x$  that the minimum value of  $\sigma_0$  will be approximately equal to  $\sigma_x$ , while the maximum will be but slightly in excess of  $\sigma_r$ . This can be seen from a study of Fig. 19 : 7. Therefore, with closed sections the possibility of torsional or combined torsional

and bending failure may be neglected and investigation by the ordinary column formulas is sufficient.

In practice, open sections are often used as stiffeners in connection with flat or slightly curved thin sheet. The presence of the sheet in the combination has two effects. The first is to offer a constraint which causes the actual axis of rotation to differ in location from the position it would have if the column were free. The second is that a narrow strip of the sheet will act as a part of the column and should be included in computing the geometrical properties of the column section. Precise studies of both of these phenomena offer considerable mathematical difficulties, and little has yet been done along that line. Lundquist and Fligg, however, have some very pertinent remarks to make on the subject, though they apply strictly only when the stiffener section is doubly symmetrical. On the whole, the effect of the skin is to increase somewhat the critical stress of the stiffener.

Tests at Stanford University of panels with various designs of stiffeners having the same sectional areas and same moments of inertia about centroidal axes parallel to the skin showed that the stiffeners with sections likely to fail torsionally tended to do so at lower critical stresses than those not likely to fail in that manner, but the latter were much more likely to fail suddenly.

The whole subject of the torsional failure of columns is one that has received little attention until fairly recently and many important questions in the field remain to be explored. Sufficient work has been done, however, to permit the engineer to estimate when the phenomenon is likely to be important, and to help him avoid difficulties resulting from it.

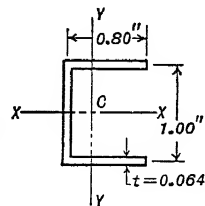
### PROBLEMS

19 : 1. Check the derivation of Eq. 19 : 23 from Eq. 19 : 19.

19 : 2. Check the derivation of Eq. 19 : 27*b*, using the procedure employed to obtain Eq. 19 : 27*a*.

19 : 3. Verify the statement that for either value of  $\sigma_0$ , obtained from Eq. 19 : 33, Eqs. 19 : 34*a* and 19 : 34*b* will give the same value of  $x_{cD}$ .

19 : 4. Compute the values of  $I_{xx}$ ,  $I_{yy}$ ,  $I_p$ ,  $I_{xy}$ ,  $K_t$ ,  $R_x$ ,  $R_y$ , and  $C$  of the channel shown in the figure with respect to the  $X-X$  and  $Y-Y$  axes passing through the centroid of the section,  $C$ .



PROB. 19 : 4

19 : 5. Locate the position of the axis about which the cross-sections of the channel of Prob. 19 : 4 would rotate in a torsional instability failure if free to rotate about any axis.

19 : 6. If the channel of Prob. 19 : 4 is 60 in. long, its ends are free to rotate and warp, and the cross-sections are free to rotate about any axis, would it fail by twist-

ing, bending, or a combination of the two? and what would be the critical load in compression?

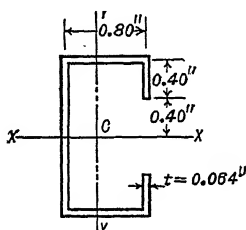
**19 : 7.** What would be the critical load with respect to torsional failure of the column of Prob. 19 : 6 if the cross-sections are constrained to rotate about the centroidal axis?

**19 : 8.** What would be the critical load with respect to torsional failure of the column of Prob. 19 : 6 if the cross-sections are constrained to rotate about an axis intersecting the cross-sections on their axis of symmetry and

- 1.00 in. to the right of the centroid?
- 1.00 in. to the left of the centroid?
- 2.00 in. to the left of the centroid?
- The left-hand surface of the web?

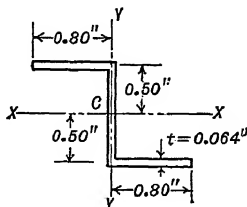
**19 : 9.** What would be the critical load with respect to torsional failure of the column of Prob. 19 : 6 if the cross-sections are constrained to rotate about an axis through the midpoint of the mid-line of the upper horizontal leg of the section?

**19 : 10.** Compute the properties listed in Prob. 19 : 4 for the section shown in the figure.



PROB. 19:10

- 19 : 11.** Work Prob. 19 : 5, assuming the section changed to that of Prob. 19 : 10.
- 19 : 12.** Work Prob. 19 : 6, assuming the section changed to that of Prob. 19 : 10.
- 19 : 13.** Work Prob. 19 : 7, assuming the section changed to that of Prob. 19 : 10.
- 19 : 14.** Work Prob. 19 : 8, assuming the section changed to that of Prob. 19 : 10.
- 19 : 15.** Work Prob. 19 : 9, assuming the section changed to that of Prob. 19 : 10.
- 19 : 16.** Compute the properties listed in Prob. 19 : 4 for the section shown in the figure.



PROB. 19:16

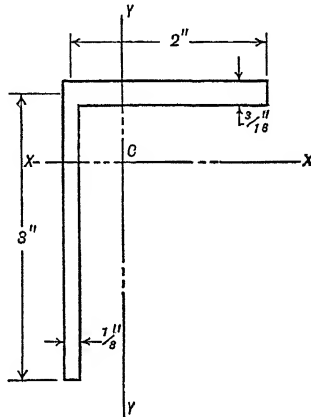
- 19 : 17.** Work Prob. 19 : 5, assuming the section changed to that of Prob. 19 : 16.
- 19 : 18.** Work Prob. 19 : 6, assuming the section changed to that of Prob. 19 : 16.
- 19 : 19.** Work Prob. 19 : 7, assuming the section changed to that of Prob. 19 : 16.

**19 : 20.** What would be the critical load with respect to torsional failure of the column of Prob. 19 : 18 if the cross-sections are constrained to rotate about an axis intersecting the cross-sections on the  $X-X$  axis and

- a. 1.00 in. to the right of the centroid?
- b. 1.50 in. to the left of the centroid?
- c. 2.00 in. to the left of the centroid?

**19 : 21.** Work Prob. 19 : 9, assuming the section changed to that of Prob. 19 : 16.

**19 : 22.** Compute the properties listed in Prob. 19 : 4 for the section shown in the figure. Note the difference in thickness between the two legs.



PROB. 19:22

**19 : 23.** Work Prob. 19 : 5, assuming the section changed to that of Prob. 19 : 22.

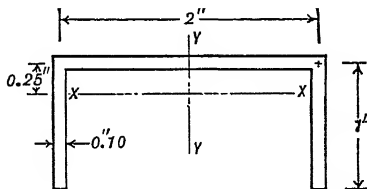
**19 : 24.** Work Prob. 19 : 6, assuming the section changed to that of Prob. 19 : 22.

**19 : 25.** Work Prob. 19 : 7, assuming the section changed to that of Prob. 19 : 22.

**19 : 26.** Work Prob. 19 : 20, assuming the section changed to that of Prob. 19 : 22.

**19 : 27.** Work Prob. 19 : 9, assuming the section changed to that of Prob. 19 : 22.

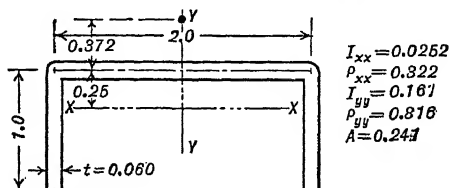
**19 : 28.** What would be the critical load with respect to torsional failure of the column of Prob. 19 : 24 if the cross-sections are constrained to rotate about their shear centers?



PROB. 19:29

**19 : 29.** Assume a channel of dimensions shown to be subjected to a compressive force which is applied through hemispherical blocks at each end so that failure may occur by twisting or buckling. At what loads would you expect failure if the overall length of channel and blocks is 4 in.? if 18 in.? if 60 in.?

**19 : 30.** An aluminum alloy channel,  $E = 10^7$ ,  $G = 4 \times 10^6$ ,  $f_{yp} = 36,000$ , of the dimensions shown is tested between hemispherical blocks so that it may twist



PROB. 19:30

or buckle. Assuming that, if it twists, each cross-section will rotate about a point on the Y-Y axis 0.372 in. behind the center line of the back, at what load would you expect failure to occur if the overall column length is 26 in.?

## CHAPTER XX

### ALLOWABLE STRESS DATA

In order to complete the design of any structure, an engineer must have satisfactory data on the allowable stress properties of the materials in it. In aircraft, materials may be used in solid and compact sections whose strength is essentially the ultimate for the material itself, or in stressed-skin elements and sections formed from thin sheets whose maximum resistance to load depends upon the stiffness and stability of the elements rather than upon the ultimate strengths of the materials in them.

Allowable stress data are distributed throughout this text, but they cover neither all types of structure nor all refinements of method available to the skilled stress analyst. They are adequate for student use and sufficient for many of the problems encountered in practice. For many of the latter, however, solutions differing from those in this text are available and, while it is not possible to cover all such data, an effort has been made to tabulate papers and articles which should be useful to designers and engineers in the aircraft industry. The references are, with one or two exceptions, to papers written in English or for which English translations exist.

While it would be desirable to have such material co-ordinated and presented as a set of allowable stress curves and formulas in a single volume, more space would be required to cover all the aircraft materials than can possibly be spared here. A tabular reference system is used to cover the more important stress problems and this is supplemented by articles on the strength of glass, plastics, and one or two other aircraft materials upon which little has been published. This tabular system permits codifying references and presenting them in a small space. It does not, however, permit classifying them as to merit or as to exact material covered. The individual stress analyst will find it helpful to underline the references he finds of particular value in his work and to add notes of his own. The research engineer, by noting the categories in which few or no references are given, may find fields for future exploration.

**20 : 1. Materials Used in Compact Sections** — Table 20 : 1 presents references to allowable stress data on wood and metallic materials used

in solid or compact sections. The scheme used is to indicate *chapter*, *section*, *article*, *page*, *table*, *figure*, or *equation* in a given reference by an italicized letter, *c*, *s*, *a*, *p*, *t*, *f*, or *e* followed by the appropriate number. Where no bold-faced symbol precedes the letter, the reference is to this text. Where a bold-faced numeral is used, reference is made to texts, journals, or articles tabulated by number in Art. 20 : 3. Publications of the National Advisory Committee for Aeronautics are indicated by a bold-face **R** for a Technical Report, **N** for a Technical Note, and **M** for a Technical Memorandum. Air Corps Information Circulars are indicated by **IC**, British Reports and Memoranda by **RM**.

Detailed references to page, article, or equation are given where justified, but, when a report is short or devoted to but one subject, reference is made to the report only. No effort has been made to present the more important references first in any category, since the importance of any article depends more on the specific problem in hand than on the general applicability of the method described.

**20 : 2. Materials Used in Thin Elements** — Tables 20 : 2 through 20 : 5 give references to the allowable stress data on thin-sheet elements such as flat, curved, and corrugated sheet panels, formed stiffeners, and similar sections in which local buckling failures are important. The system of referencing in these tables is identical with that in Table 20 : 1.

In order to differentiate between sheets whose mid-lines lie in one plane and those whose mid-lines lie on a curve, the former are designated as *flat*, the latter as *curved*. Sheets which are corrugated are so described; those which are curved but not corrugated are called *smooth*. Materials designated *isotropic* have essentially identical properties in any direction, while those termed *an-isotropic* have appreciably higher strength properties in one direction than another. Most of the metals are considered to be isotropic, though their properties parallel with the direction of working, when they are used in the wrought form, may differ by a small percentage from those perpendicular with their direction of working. Woods and many of the plastic materials used in aircraft are definitely an-isotropic, and due regard must be had for their variation in strength when they are used.

**20 : 3. References** — The references on pp. 366-367 constitute a list of texts, handbooks, and articles from which the codified material in Tables 20 : 1 to 20 : 5 was taken. The list does not cover all available documents, but it should prove helpful to student or engineer searching for data applicable to a particular problem. Many of the documents contain further references and bibliographies which will afford further sources of data and information.

TABLE 20:1  
ALLOWABLE STRESS DATA FOR COMPACT SECTIONS

	Aluminum and Magnesium Alloys	Steels	Wood	Plastic Materials
Tension	<i>t</i> 10 : 1, <i>t</i> 20 : 17, 1 <i>c</i> 5, 1 <i>c</i> 6, 15 <i>p</i> 240, 16 <i>p</i> 33, 24, 43 <i>c</i> 2	<i>t</i> 10 : 1, <i>t</i> 10 : 2, <i>t</i> 11 : 11, 1 <i>c</i> 4, 43 <i>c</i> 2	<i>a</i> 6 : 10, <i>t</i> 10 : 3, 1 <i>c</i> 2, 25, 44	<i>t</i> 20 : 8, <i>t</i> 20 : 10, <i>t</i> 20 : 11, <i>t</i> 20 : 12, N 627, N 694, 17 <i>t</i> 3, 26, 40, 42, 43 <i>c</i> 2
Compression	<i>t</i> 10 : 1, <i>t</i> 10 : 4, <i>f</i> 10 : 20, <i>f</i> 10 : 22, <i>t</i> 20 : 17, 1 <i>c</i> 5, 1 <i>c</i> 6, 15 <i>p</i> 240, 16 <i>p</i> 33, 24, 29, 43 <i>c</i> 2	<i>t</i> 10 : 1, <i>t</i> 10 : 4, <i>f</i> 10 : 12, <i>f</i> 10 : 13, <i>f</i> 10 : 14, <i>f</i> 10 : 15, <i>f</i> 10 : 17, <i>f</i> 10 : 18, <i>f</i> 10 : 19, 1 <i>c</i> 4, 29, 43 <i>c</i> 2	<i>t</i> 10 : 3, <i>t</i> 10 : 4, <i>f</i> 10 : 16, 1 <i>c</i> 2, 25, 44	<i>a</i> 20 : 10, <i>t</i> 20 : 13, <i>t</i> 20 : 14, <i>t</i> 20 : 15, N 627, N 694, 17 <i>t</i> 3, 26, 40, 42
Shear	<i>f</i> 7 : 2, <i>f</i> 7 : 3, <i>t</i> 10 : 1, <i>t</i> 20 : 17, 1 <i>c</i> 5, 1 <i>c</i> 6, R 601, 15 <i>p</i> 183, 16 <i>p</i> 33, 24, 28, 29	<i>t</i> 10 : 1, <i>e</i> 11 : 1, <i>f</i> 11 : 5, 1 <i>c</i> 4, R 601, 28, 29, 38	<i>e</i> 6 : 26, <i>t</i> 10 : 3, <i>a</i> 11 : 4, <i>a</i> 11 : 5, <i>t</i> 20 : 16, 1 <i>c</i> 2, 44	N 694
Bending	<i>e</i> 6 : 1, <i>t</i> 10 : 1, 1 <i>c</i> 5, 1 <i>c</i> 6, 27, 29	<i>e</i> 6 : 1, <i>f</i> 6 : 2, <i>f</i> 6 : 4, <i>t</i> 10 : 1, 1 <i>c</i> 4, 27, 29, 38	<i>a</i> 6 : 10, <i>f</i> 6 : 19, <i>t</i> 10 : 3, 1 <i>c</i> 2, 25, 44	N 694, 17 <i>t</i> 3, 26, 40, 42, 43 <i>c</i> 2
Bearing	<i>t</i> 10 : 1, <i>t</i> 11 : 5 to 11 : 9, 1 <i>c</i> 5, 1 <i>c</i> 6, 30	<i>t</i> 10 : 1, <i>t</i> 11 : 2 to 11 : 4, 1 <i>c</i> 4, 43 <i>c</i> 2	<i>f</i> 11 : 11, <i>f</i> 11 : 12, 1 <i>c</i> 2, 44	N 628, N 694, 42
Fatigue	<i>t</i> 10 : 1, <i>t</i> 20 : 17, 1 <i>c</i> 6, 1 <i>c</i> 5 15 <i>p</i> 220, 16 <i>p</i> 33, 18 <i>p</i> 48, 24, 43 <i>c</i> 2	<i>t</i> 10 : 1, 1 <i>c</i> 4, 18 <i>p</i> 223, 43 <i>c</i> 2	45	N 628, N 694, 17 <i>t</i> 3, 17 <i>p</i> 201, 18 <i>p</i> 221



TABLE 20 : 2  
STRESS DATA ON FLAT RECTANGULAR PANELS

	Compression in Plane of Sheet	Shear in Plane of Sheet	Load Normal to Plane of Sheet	Combined Loadings or Stresses
Isotropic sheets	<i>e</i> 10 : 16, <i>e</i> 10 : 17, <i>2 s</i> 2 <i>a</i> 2-3, <i>2 s</i> 3, <i>2 s</i> 4, <i>1 c</i> 1 <i>a</i> 1.610, <i>8 p</i> 37, <i>N</i> 684, <i>M</i> 785, <i>M</i> 814, <i>M</i> 831, <i>M</i> 833, <i>37, 41 c</i> 5, <i>43 c</i> 11	<i>e</i> 6 : 6, <i>e</i> 15 : 7, <i>e</i> 15 : 20, <i>2 s</i> 2 <i>a</i> 4, <i>2 s</i> 11, <i>N</i> 489, <i>M</i> 490, <i>M</i> 592, <i>M</i> 601, <i>M</i> 602, <i>M</i> 604-606, <i>M</i> 705, <i>M</i> 785, <i>M</i> 809, <i>M</i> 831, <i>M</i> 870, <i>41 c</i> 6	<i>3 c</i> 6, <i>5 p</i> 117, <i>6 p</i> 121, <i>11 p</i> 627, <i>13 p</i> 40, <i>p</i> 123, <i>14 p</i> 241, <i>20 p</i> 231, <i>21 p</i> 15, <i>22 p</i> <i>A</i> 173, <i>23 p</i> <i>A</i> 7, <i>p</i> <i>A</i> 114, <i>23 p</i> <i>A</i> 168, <i>41 c</i> 7	<i>1 c</i> 1, <i>a</i> 1.611, <i>3 p</i> 350 and 362, <i>7, 9</i> , <i>M</i> 490, <i>M</i> 785, <i>M</i> 831 <i>p</i> 5, <i>M</i> 870 <i>43 c</i> 11
Corrugated sheets	<i>f</i> 10 : 26, <i>f</i> 10 : 27, <i>2 s</i> 7, <i>41 c</i> 6, <i>IC</i> 699			
Stiffened sheets	<i>a</i> 10 : 10, <i>1 c</i> 1, <i>a</i> 1.711, <i>2 s</i> 6, <i>12</i> , <i>14 p</i> 9, <i>IC</i> 697, <i>IC</i> 705, <i>N</i> 752, <i>N</i> 814, <i>M</i> 785, <i>31, 32, 34, 36, 37, 41 c</i> 6	<i>1 c</i> 1 <i>a</i> 1.721, <i>M</i> 602, <i>M</i> 705, <i>M</i> 756, <i>M</i> 785	<i>N</i> 740	<i>M</i> 490
Combined flat and cor- rugated sheets	<i>2 s</i> 7 <i>p</i> 22, <i>M</i> 933, <i>32, 41 c</i> 6	<i>M</i> 933		<i>33</i>
An-isotropic sheets	<i>a</i> 20 : 10	<i>a</i> 20 : 10, <i>M</i> 601, <i>M</i> 705 <i>p</i> 6		

TABLE 20 : 3  
STRESS DATA ON CURVED RECTANGULAR PANELS

	Compression in Plane of Sheet	Shear in Plane of Sheet	Load Normal to Plane of Sheet	Combined Loadings or Stresses
Isotropic smooth sheets	<i>e</i> 6 : 25, <i>a</i> 10 : 16, 1 <i>c</i> 1 <i>a</i> 1.620, 2 <i>s</i> 8 <i>a</i> 4-5, 3 <i>p</i> 467, 13 <i>p</i> 80 and 93, IC 706, IC 708, M 785, M 831, 37	<i>e</i> 7 : 3, <i>e</i> 7 : 4, 1 <i>c</i> 1 <i>a</i> 1.621, 3 <i>p</i> 480 and 490, 13 <i>p</i> 80, N 343, N 687, M 774, M 831, M 846, M 898	3 <i>p</i> 319 and 445	<i>a</i> 7 : 13, 1 <i>c</i> 1 <i>a</i> 1.622, 3 <i>p</i> 475 and 490, M 831, M 898
Corrugated sheets				
Stiffened sheets	<i>a</i> 10 : 10, 1 <i>c</i> 1 <i>a</i> 1.712, 2 <i>s</i> 9 M 838, M 880	1 <i>c</i> 1 <i>a</i> 1.722, N 687, M 846		
Combined smooth and corrugated sheet	2 <i>s</i> 7, 2 <i>s</i> 10			
An-isotropic smooth sheets				

TABLE 20 : 4  
STRESS DATA ON STIFFENER SECTIONS

	Critical Stresses	Failing Stresses
Compression parallel to axis	$a 10 : 6, a 10 : 9, a 18 : 8, f 10 : 7, f 10 : 9, f 10 : 23, f 10 : 31, f 10 : 32, e 18 : 24, 2 s 5, 2 s 6, 13 p 54, 8 p 41, R 582, 41 c 5, 43 c 13$	$a 10 : 6, a 10 : 9, a 10 : 10, a 10 : 12, f 10 : 31, f 10 : 32, 2 s 5, 1C 708, R 582, N 722, N 726, N 733, N 743, N 752, M 784, M 807, M 838, M 851, 8 p 41, 35, 41 c 5, 43 c 13$
Flexure or bending	$a 6 : 5, a 6 : 6, 6 p 192, M 834$	
Shear loads	$e 15 : 18$	
Torsional loads		$a 7 : 4$
Combined loadings or stresses	$a 19.9, a 19 : 10, R 582, N 686, M 807, M 851$	$N 726$

TABLE 20:5  
DATA ON FUSELAGE AND WING SECTIONS

	Unstiffened Sections	Stiffened Sections
Compression parallel to axis	1 c 1 a 1.630, 1.640, and 1.651, 2 s 8, 3 p 419, 439, and 453, 41 c 8, R 473, M 785	a 10 : 9, 2 s 9, 3 p 470, 41 c 8, N 721
Flexure or bending	1 c 1 a 1.631, 1.641, and 1.652, 3 p 463, N 479, N 523, N 527, N 834, M 785, 39	M 595, M 785, M 838, M 915, 41 c 8
Torsion	1 c 1 a 1.632, 1.642, and 1.653, R 479, N 427, N 527, M 785	19 p 2, RM 1619, RM 1761, M 744, M 785, M 878, M 939, M 997
Combined loadings or stresses	1 c 1 a 1.424, 1.633-1.636, 1.643, 1.654- 1.655, 10 p 795, 11 p 569	M 828, M 933

1. "Strength of Aircraft Elements, ANC-5," Army, Navy, Civil Committee on Aircraft Requirements, Government Printing Office, Washington, 1942.
2. "Progress Report on Methods of Analysis Applicable to Monocoque Aircraft Structures," E. E. Sechler and J. S. Newell, Air Corps Technical Report 4313, Revision I, U. S. Army Air Forces, Matériel Center, Wright Field, Dayton, 1941.
3. "Theory of Elastic Stability," S. Timoshenko, McGraw-Hill Book Co., New York City, 1936.
4. "Theory of Elasticity," S. Timoshenko, McGraw-Hill Book Co., New York City, 1934.
5. "Theory of Plates and Shells," S. Timoshenko, McGraw-Hill Book Co., New York City, 1940.
6. "Strength of Materials, Part II," S. Timoshenko, D. Van Nostrand Co., New York City, 2nd ed., 1941.
7. "Applied Elasticity," J. Prescott, Longmans, Green and Co., London, 1924.
8. "Design Work Sheets," Fourth Series, Product Engineering, New York City, 1937.
9. W. G. L. Yearbook, 1923, paper by H. Wagner, pp. 113-125.
10. *A.S.M.E. Trans.*, Vol. 56, 1934, No. 11, paper by L. H. Donnell, pp. 795 to 806.
11. *A.S.M.E. Trans.*, Vol. 56, 1934, No. 8, paper by Stewart Way, pp. 627 to 636.
12. "Stress Distribution in Stiffened Panels under Compression," E. E. Sechler, *Jour. Aero. Sci.*, Vol. 4, No. 8, 1937, pp. 320 to 323.
13. "Proceedings of the Fifth International Congress for Applied Mechanics," John Wiley and Sons, New York City, 1938.
14. "Stephen Timoshenko," 60th Birthday Volume, The Macmillan Company, New York City, 1938.
15. "The Technology of Magnesium and Its Alloys," translated from German by F. A. Hughes and Co., Ltd., Abbey House, London, 1940.
16. "Magnesium and Its Alloys," J. L. Houghton and W. E. Prytherch, H. M. Stationery Office, London, 1937.
17. "Materials For Airplane Construction," J. B. Johnson, *Jour. Aero. Sci.*, Vol. 6, No. 5, 1939, p. 185.
18. "Prevention of Failure of Metals under Repeated Stress," Battelle Memorial Institute, John Wiley and Sons, New York City, 1941.
19. *Aircraft Eng.*, Vol. XIV, No. 155, January, 1942.
20. "Drang und Zwang," Föppl and Föppl, R. Oldenbourg, Munich, 1924.
21. *Trans. Inst. Naval Arch.*, Vol. XLIV, 1902, paper by I. G. Boobnoff, p. 15.
22. *Jour. Appl. Mech.*, Vol. 4, No. 4, December, 1937.
23. *Jour. Appl. Mech.*, Vol. 6, 1939.
24. "Non-Ferrous Alloys for Airframes and Engines," J. B. Johnson, *Aero Digest*, July, 1942, p. 130.
25. "Strength Characteristics of Plastic Bonded Plywood," George B. Parsons, *Aero Digest*, July, 1942, p. 160.
26. "Properties of Plastics Used by the Aviation Industry," *Aero Digest*, July, 1942, p. 250.
27. "Design Charts for Tubes Subjected to Bending," Walter C. Clayton, *Aviation*, April, 1942, p. 80.
28. "Design Charts for Tubes Subjected to Torsion," Walter C. Clayton, *Aviation*, May, 1942, p. 127.
29. "Design Charts for Tubes Subjected to Axial Loads and Combined Stresses," Walter C. Clayton, *Aviation*, July, 1942, p. 169.
30. "Strength Analysis of Riveted and Bolted Joints," Wayne A. McGowan, *Aviation*, April, 1942, p. 91.

31. "Empirical Formulas for Allowable Compression Loads in Stiffened Sheet Panels," E. Robert Reff, *Jour. Aero. Sci.*, Vol. 6, No. 12, 1939, p. 505.
32. "Measurement of Stiffener Stresses and Effective Widths in Stiffened Panels," H. B. Dickinson and R. J. Fischel, *Jour. Aero. Sci.*, Vol. 6, No. 6, 1939, p. 249.
33. "Corrugated Panels under Combined Compression and Shear Load," P. A. Sanderson and J. R. Fischel, *Jour. Aero. Sci.*, Vol. 7, No. 4, 1940, p. 148.
34. "Effective Widths in Stiffened Panels under Compression," J. R. Fischel, *Jour. Aero. Sci.*, Vol. 7, No. 5, 1940, p. 213.
35. "The Column Strength of Closed, Thin-walled Sections of 18-8 Stainless Steel," Howard W. Barlow, *Jour. Aero. Sci.*, Vol. 8, No. 4, 1941, p. 151.
36. "Permanent Buckling Stress of Thin-sheet Panels under Compression," W. L. Howland and P. E. Sandorff, *Jour. Aero. Sci.*, Vol. 8, No. 7, 1941, p. 261.
37. "The Compressive Strength of Thin Aluminum Alloy Sheet in the Plastic Region," J. R. Fischel, *Jour. Aero. Sci.*, Vol. 8, 1941, p. 373.
38. "Bending and Torsional Design Charts for Round Chrome-molybdenum Tubing," Vincent C. Trimarchi, *Jour. Aero. Sci.*, Vol. 9, No. 6, 1942, p. 213.
39. "Theory for the Buckling of Thin Shells," H. S. Tsien, *Jour. Aero. Sci.*, Vol. 9, No. 10, 1942, p. 373.
40. "Properties of Plastics used by the Aviation Industry," *Aero Digest*, July, 1942, p. 250.
41. "Airplane Structural Analysis and Design," E. E. Sechler and L. G. Dunn, John Wiley and Sons, New York City, 1942.
42. "Plastics for Industrial Use," John Sasso, McGraw-Hill Book Co., New York City, 1942.
43. "Mechanics of Aircraft Structures," J. E. Younger, McGraw-Hill Book Co., New York City, 1942.
44. "ANC Handbook on Design of Wood Aircraft Structures," a publication having restricted distribution.
45. "Fatigue Characteristics of Natural and Resin Impregnated, Compressed, Laminated Woods," F. B. Fuller and T. T. Oberg, *Jour. Aero. Sci.*, Vol. 10, No. 3, 1943, p. 81.

**20 : 4. Glass** — Windshields and windows in airplanes having pressurized cabins for operation in the stratosphere are subjected to loads perpendicular to their midplanes. They may be designed as flat plates supported, but not clamped, around their edges. The modulus of rupture stress for plain or laminated plate glass at 70° F. is 6500, and for heat-strengthened plate glass 29,500 p.s.i. The strength of some of the laminated glasses varies appreciably with temperature as the plastic membrane becomes harder or softer with decrease or increase in temperature. Some of the plastics become so soft at the higher end of the operating temperature scale that the glass behaves more nearly as two separate sheets than as a single unit; some become so brittle at low temperatures that they lose their non-shattering features; and some retain satisfactory characteristics from -40° F. to +120° F. Glass for aircraft purposes is still in a developmental stage, and designers should check carefully the properties obtainable from various glass manufacturers.

It is customary to use large factors of safety in the design of glass

panels, five being employed where actual loads are known accurately, ten being more common where vibration is expected or where loads are not well established. The formulas given in Tables 20 : 6 and 20 : 7 show the relation between the glass thickness  $t$  and the load  $w$  per square inch of clear opening when a factor of safety of 10 is used. For any other factor of safety  $n$ , multiply  $t$  by  $0.316\sqrt{n}$ ,  $w$  by  $10/n$ .

The weight and other properties of glass vary widely with the composition of the particular piece, but for the types of plate used in aircraft the weight may be taken between 0.091 and 0.093 lb. per cu. in. (roughly the same as a sheet of aluminum alloy of the same thickness), the modulus of elasticity between 10,000,000 and 11,000,000 p.s.i., and the tensile strength or modulus of rupture in bending as 6,500 p.s.i. Heat-strengthened plate is about four and one-half times as strong in tension and bending as ordinary plate, that is, 29,500 p.s.i. Poisson's ratio runs about 0.23 or 0.24.

TABLE 20 : 6

## CIRCULAR SHEETS OF GLASS

<i>Plain or Laminated Plate</i>	<i>Heat-strengthened Plate</i>
$t = 0.044 R\sqrt{w}$	$t = 0.6$
	$t = 0.6$

$R$  = radius,  $D$  = diameter of clear opening in inches.  $t$  = thickness in inches.  $w$  = safe load in pounds per square inch of free opening.

For rectangular sheets the thickness may be expressed as  $t = Kb\sqrt{w}$ , where  $b$  is the *short* side of the rectangle and  $K$  varies with the ratio of the short side of the sheet to the long side, as shown in Table 20 : 7,  $K_1$  being for plain or laminated,  $K_2$  for heat-strengthened plate.

TABLE 20 : 7

## RECTANGULAR SHEETS OF GLASS

Short side Long side	1.0	0.9	0.8	0.7	0.6	0.5	0.4	0.3	0.2	0.1
$K_1$	0.0218	0.0230	0.0241	0.0252	0.0264	0.0276	0.0287	0.0298	0.0303	0.0308
$K_2$	0.0098	0.0103	0.0108	0.0113	0.0118	0.0123	0.0128	0.0133	0.0136	0.0138

In mounting windshields and windows, the width of glass bearing against the frame along each edge should be at least equal to the thickness of the glass, and preferably at least twice the thickness. The width required depends partly on the strength of the glass, partly on its deflection; therefore somewhat greater widths are necessary with large areas

than with small. Provision must be made to distribute the load uniformly over the bearing area of the frame; otherwise stress concentrations will cause failure at lower loads than those indicated by the formulas given above. Rubber gaskets are often used to distribute the bearing load against the frame and, at the same time, to insulate the glass against vibrations transmitted through the airplane structure, thus reducing the tendency for such vibrations to crack the glass. The Pittsburgh Plate Glass Company has recently developed a laminated product having semi-tempered plate faces with a thick plastic interlayer which extends beyond the edges of the actual glass. The panel may be bolted or otherwise fastened to the frame through this plastic material, the result being a window that is said to be particularly resistant to breakage under impact loading, static pressure loading, or the torsional and shearing strains developed around the opening in flight.

Glass can be molded to almost any desired contour, and so windows may be streamlined if necessary or desirable. However, care must be taken, when curved glass is used in the pilot's cabin, that images are not distorted and that cross-reflections are not produced in places that will disturb the pilot's vision.

**20 : 5. Plastics** — Plastic materials may be divided into two types, the thermoplastics and the thermosetting plastics. Either may be produced in transparent or opaque sheets, and either may be molded or formed to various shapes. From the standpoint of the aeronautical engineer, the major difference between them is that thermoplastics soften without undergoing chemical change whenever they are heated; whereas the materials of which a thermosetting plastic are composed soften when first heated, undergo a chemical change, polymerize or "set," and remain hard thereafter at all ordinary temperatures. Different plastics respond differently; therefore there is considerable range in properties available between the low limit for temperature,  $-60^{\circ}$  to  $-90^{\circ}$  F. for operation in the stratosphere, and the high,  $+150^{\circ}$  F. for airplanes operating from desert bases, or up to  $+300^{\circ}$  F. for certain instrument or accessory cases.

Few plastic materials have satisfactory strength properties over the  $-60^{\circ}$  to  $+150^{\circ}$  range. They tend to be too brittle at the very low temperature, or too soft at the high. One of the best methods for checking this characteristic is by means of "creep" tests,<sup>1</sup> in which specimens of the plastic are subjected to constant stress for periods ranging from a few minutes to several hours, during which time deflection readings are taken at frequent intervals. By plotting deflection against time,

<sup>1</sup> See "Creep and Cold Flow of Plastics," J. Delmonte and W. Dewar, *Modern Plastics*, October, 1941, p. 73.



it may be determined whether the rate of creep — the rate of increase in deflection per unit of time — tends to approach zero, to remain constant, or to increase with time. Such tests should be made on several specimens at different temperatures and with several loads to cover the range of stresses within the working limits of the given material. The tests may be made on simple tension specimens or by clamping one end of a strip to a bench, letting the other protrude as a cantilever, and applying loads sufficient to produce stresses on the extreme fiber at the "built-in" end of the cantilever of 1,000, 2,000, or more pounds per square inch. A dial gage reading 1/10,000 in. or a micrometer may be used to get deflections at the outer end of the specimen, and readings should be taken at half-minute or one-minute intervals for the first five minutes, at longer intervals for the rest of the test period.

Materials whose deflection curves do not flatten after a short time should not be employed where they will be subjected to appreciable stress for long periods unless large deformations of the structure can be tolerated. Materials which appear satisfactory at room temperatures may be so ductile at temperatures above 100° F. that they will hardly support their own weight. Special attention should therefore be given to creep characteristics at the upper limit of the temperature range in which a given material is to be used. If the material be subject to shock, a creep test at low temperature may give some indication of the behavior of the material, but an impact test will probably be found more satisfactory.

Tensile properties may be obtained by using tensile test specimens of standard dimensions, though it is better to use somewhat wider ends than are employed with metals, in order to reduce stress concentration effects from the jaws of the testing machine. Values are given for some typical materials in Table 20 : 8. Some of these were transparent plastics; some were opaque. Some contained no fibrous materials; others had asbestos, cotton, paper, or other fibrous material mixed with the plastic in order to strengthen it or to reduce its tendency to creep.

By using the same criterion for yield point for these materials as for the aluminum alloys, that is, 0.002-in.-per-in. offset, the tensile yield point is found to be, roughly, 60 per cent of the ultimate tensile strength at room temperature; about 55 per cent at subzero temperatures. Too few data are available to warrant presenting yield-strength values for the materials in Table 20 : 8, but those in hand indicate a decrease in yield-to-ultimate-stress ratio with decrease in temperature, a factor which, if true, must be considered in the design of plastic structures to be used at high altitudes.

TABLE 20 : 8

## TENSILE PROPERTIES OF TYPICAL PLASTIC MATERIALS

Type of Plastic	Transparent	Fiber	Temperature, Degrees F.	Ultimate Tensile Strength, P.s.i.	Modulus of Elasticity P.s.i.
Thermoplastic Methyl methacrylate	Yes	None	-70	14,000	650,000
			+70	7,500	360,000
			+150	525	.....
Thermoplastic Cellulose acetate	Yes	None	-70	11,500	625,000
			+70	5,000	215,000
			+150	725	.....
Thermoplastic Cellulose acetate butyrate	Colored	None	-70	6,600	500,000
			+70	4,000	160,000
			+150	....	.....
Thermosetting Phenol formaldehyde	Opaque	Cloth	-70	9,800	1,300,000
			+70	11,000	1,125,000
			+150	6,500	617,000
Thermosetting Phenol formaldehyde	Opaque	Asbestos	-70	9,000	520,000
			+70	10,000	1,000,000
			+150	6,500	740,000
Thermosetting Phenol formaldehyde	Opaque	Kraft paper	-70	11,500	1,700,000
			+70	13,000	850,000
			+150	8,000	415,000
Thermosetting Phenol formaldehyde	Opaque	Kraft paper	-70	16,200	1,250,000
			+70	19,000	880,000
			+150	6,200	460,000
Thermosetting Phenol formaldehyde	Opaque	Cloth	-70	12,300	950,000
			+70	11,500	900,000
			+150	5,500	280,000
Molded phenolic resin	Opaque	Cotton fiber	-38	30,000	2,600,000
			+78	25,000	2,380,000

The data in Table 20 : 8 suffice to show the wide variation in strength and stiffness available in different plastics and the need for testing different resins or combinations to obtain the particular properties desired. Each of the values in the table is averaged from tests on at least two specimens. They should be looked upon as representative but not sufficiently well founded to be used for final design. Some of the values

are taken from tests on standard materials manufactured under carefully controlled conditions; others from tests on materials of more or less experimental nature produced under laboratory conditions. The importance of temperature on tensile strength and modulus of elasticity is indicated. The thermoplastics, for which two specimens failed at very low stress intensities while the third pulled apart under the weight of specimen and grip plates at the 150° F. temperature, should be noted in particular.

Most of the thermosetting plastics were strongest at room temperature, with reductions of the order of 20 per cent at the low and 40 per cent at the high temperatures. Moduli of elasticity were more erratic but were generally greatest at the low temperature, least at the high. This appears to be true for both the thermoplastics and thermosetting plastics. Were ductility or impact data available on these materials, they would probably be lowest at the low temperature, highest at the high, though one set of data shows practically no change in impact characteristics for the thermoplastic "Plexiglas" between -75° F. and +160° F., by the falling-ball test and the Charpy bar test.

Neither the thermoplastics nor the thermosetting plastics absorb moisture readily, nor do they absorb more than 2 to 5 per cent by weight unless they contain some substance which will of itself absorb liquids. Depending upon the type and concentration of such substances, plastic materials may absorb 4 to 10 per cent of their own weight, sometimes more, but the rate at which such moisture permeates the material is low. The plastics listed in Table 20 : 8 as having no fibrous material absorbed 3 per cent or less of their initial weight when immersed in water at room temperature for three days; those having cloth, paper, or asbestos increased in weight about  $1\frac{1}{2}$  per cent in three days, although one of the paper-base specimens increased about 3 per cent in that time. Few of the plain plastics pick up more than 4 per cent after longer immersions, but moisture does permeate them slowly, and, if they contain hygroscopic substances, the latter will gradually absorb moisture until they become saturated. This fact must be kept in mind when plastics are proposed for use on floats, boat bottoms, or in other places where they will be immersed or subjected to high-humidity conditions over long periods.

**20 : 6. Use of Plastics in Airplane Construction** — Most of the plain plastic materials have specific gravities of approximately unity and are therefore considerably heavier than the woods commonly used in aircraft; yet they have strengths of the same order of magnitude as spruce, mahogany, or birch. They are therefore less desirable than wood for use in highly stressed structural members. These plastics, on the other

hand, have specific gravities less than half those of glass or aluminum alloy, about half of that of magnesium. Therefore they are quite desirable for windows or for lightly stressed parts whose dimensions are established by handling requirements rather than strength. They are particularly useful where high electrical resistance is needed because many of them have excellent insulating properties.

Where clear plastics are used as windows, the maximum stress in the sheet should be kept fairly low, say 1,000 p.s.i. The edges of the sheet should extend into the frame sufficiently so that they will not pull out of the mount if the panel deflects under load or if it contracts at low temperature. Dr. D. S. Frederick<sup>1</sup> shows several methods for mounting Plexiglas windows and gives Table 20 : 9 as typical dimensions for thickness and mounting allowance.

TABLE 20 : 9  
APPROXIMATE DIMENSIONS FOR PLEXIGLAS WINDOWS

<i>Size of Light, In.</i>	<i>Thickness, In.</i>	<i>Mounting Allowance, Each Edge, In.</i>
6 × 6	0.060	$\left\{ \begin{array}{l} 0.625 + 0.002 \text{ times} \\ \text{panel length} \\ 1.00 + 0.002 \text{ times} \\ \text{panel length} \end{array} \right.$
12 × 12	0.080	
18 × 18	0.100	
24 × 24	0.150	

Since Plexiglas is a representative material, the data in Table 20 : 9 may also be used as a guide for proportioning windows of other clear plastics. As in the use of ordinary glass, rectangular sheets may be thinner than squares of equal area, but the exact coefficients to be used are not available as yet. When plastic windshields are used,<sup>2</sup> care must be exercised in curving them or else they will give distorted images and disturbing reflections in the same way that plate glass does.

**20 : 7. Plastics Used as Sealants** — Another type of plastic, about which few published data are available, uses a natural or synthetic rubber base in conjunction with solvents and curing media to yield hard or soft materials for sealing seams in gas tanks, flying boats, and stratosphere airplanes, or for sealing windows, inspection panels, and similar discontinuities in wings and fuselages. The desirable properties of such materials are their ability to resist oil and gasoline or to maintain satisfactory plastic properties over a wide range in temperature.

<sup>1</sup> "Correct Methods of Plexiglas Installation," Dr. D. S. Frederick, *Aviation*, April, 1942.

See also Chapter X, "Plastics for Industrial Use," John Sasso, McGraw-Hill Book Co., New York City, 1942.

<sup>2</sup> "Optical Considerations in the Design of Transparent Plastics Enclosures," Mr. W. F. Bartoe, *Aero Digest*, July, 1942, p. 233.

Plastics of this type play an important role in the design of many airplane structural elements, but they are not counted upon as contributing directly to the strength of such elements; hence their allowable strength properties are relatively unimportant in most applications. No further consideration need, therefore, be given them here.

**20 : 8. Types of Plastic-bonded Plywood** — The older types of plywoods employing blood-albumin or casein glues have been superseded for aircraft use by plastic-bonded plywoods. The plastic provides a bond having better resistance to water and bacteria than the older forms of adhesive, and the wood provides stress-carrying fibers whose strength is of the same order of magnitude as that of the plastic, whose density is less, but whose resistance to creep is considerably greater. A large variety of plastic-bonded plywoods has been developed in the past few years, some using thermoplastics, some thermosetting plastics, some using a mixture of the two types. Other plastic-bonded materials have been developed using cloth, cotton, linen, hemp, sisal, and other fibers to reduce creep and provide strength. While the general remarks in this article pertain to either type of material, the strength-to-weight ratios of the plastic-fiber combinations are generally too low to be suitable for use as aircraft structural materials; hence greater consideration is given the plastic plywoods.

Some of these are made with thermoplastics applied to the single plies by brushing or by immersion in the plastic rendered liquid by heat or solvents. Some are made with thermosetting plastics introduced between the plies in sheet form, or, in some cases, in an aqueous or alcoholic solution. In most of the panels, the separate plies are laid so that the direction of the grain of each is at  $90^\circ$  to the grain of the adjacent plies. In some, the grain direction of adjacent plies varies by  $45^\circ$ , in a few by  $30^\circ$ . Some of the panels employ woven veneers. That is, the wood is cut into strips 2, 4, or more inches wide and then woven in a sort of basket weave to form a single sheet. Panels made from such sheets offer somewhat greater resistance to certain types of load concentration, such as those introduced by bolts and rivets or those that produce a tearing action, than do panels made from ordinary veneer. Their strength-to-weight ratios are not quite so good when the load imposed upon them is limited to one direction, however, since part of a woven material will be nearly perpendicular to the line of action of the load.

Most of the thermoplastic materials are bonded under pressures varying from 50 to 200 p.s.i., with temperatures ranging between  $200^\circ$  and  $300^\circ$  F. The thermosetting resins used in the bag-molding process are set at pressures between 60 and 100 p.s.i.; flat plywood panels are pressed at about 200, and temperatures between  $250^\circ$  and  $300^\circ$  F. are

quite usual. Too great a pressure increases the density of the wood, and, while it may increase the tensile and shear strength-to-weight ratios, it results in lower strength-to-weight ratios on thin panels in compression.

Too high a temperature has a deleterious effect on the wood fibers, making them brittle and less resistant to impact. The moisture content of the wood at the time of bonding is important, though few quantitative data on its effect are yet available. Moisture contents between 7 and 12 per cent appear suitable for dry films, such as the commonly used Tego resin; 5 to 8 per cent for aqueous suspensions.

Except for the poor strength properties which the thermoplastics show at high temperatures and for their extreme brittleness at low, they would be ideal for use in aircraft plywoods since panels made with them can later be heated and molded to shape without destroying the adhesive. If the wood fibers can be bent to a desired shape, the thermoplastic will soften, flow, and adapt itself to the new shape when heat is applied. For many purposes, wood fixtures may be used as male patterns, the plywood may be roughly shaped to them; then fixture and panel may be enclosed in a rubber bag and the whole unit subjected to heat and pressure in an autoclave to mold the panel to exact shape. One practical objection to the use of this method with thermoplastics is that the pressure must be retained until the panel has cooled to 150° or 125° F. so that the plastic will harden enough to keep its shape when the pressure is released. This is difficult when steam is the source of both heat and pressure.

This process was used with cellulose acetate by Mr. Harry Atwood in 1934-35 at the French and Heald Company in Milford, New Hampshire, for compositing the plywood used on the wings, fuselage, landing gear struts, and tail surfaces of the first plastic-bonded plywood airplane built and flown in this country.

Since the thermosetting plastics become sufficiently soft to flow only once, when they polymerize or "set," molded panels using them are generally built on the fixture to be used as the mold, the plastic is inserted between the plies, and the entire operation of bonding and molding is accomplished with a single application of heat and pressure between dies, or by the rubber-bag process. When done, the member bonded with the thermosetting plastic has somewhat better properties, less tendency to creep at the higher temperatures, and less tendency to shatter if struck a sharp blow at low temperatures than does an equivalent panel bonded with a thermoplastic. Airplane structures made with thermosetting plastics should therefore have less tendency to sag or deform under their own weight when standing on the line on a hot

day than has been shown in the past by some of the airplanes employing only thermoplastics.

**20 : 9. Tensile Properties of Plastic-bonded Plywoods** — It is impossible to present, within the limits of this article, complete details or complete allowable stress data on the various plastic-bonded materials available for use in aircraft. There are too many possible combinations of plastics, woods, or other fibers, and new materials are being added almost daily. Complete data are not yet available for any one of the materials because development has heretofore been so rapid that a more promising material or procedure has been developed before tests on an earlier one were completed. The data presented in the tables which follow should therefore be construed as representative strength values obtained from tests on typical materials chosen to include certain plastics and woods or to show the effect of the more important variables.

When tests for the determination of tensile properties are being made, specimens should be long enough and wide enough at the ends so that the load may be transmitted to the specimen without producing severe stress concentrations where the grips of the testing machine bear. For many materials, a minimum width of  $1\frac{1}{2}$  or 2 in. may be desirable in the narrow section of the specimen, with 4 to 6 in. as the width provided under the grips. It is well to attach the grips by four or five bolts at each end of the specimen and to use bolts of  $\frac{3}{8}$ -in. or greater diameter which can be tightened sufficiently so that part of the load will be transmitted by bearing between specimen and bolts, part by friction between specimen and gripping plates. A considerable part of the load should be transmitted by friction when plastic plywood panels are tested, or failures will occur through the bolt holes at the end of the specimen rather than in the test section.

Strain data may be obtained with types of extensometer that clamp onto the specimen, and care should be exercised that they are removed before, or as soon as, the surface plastic starts to rupture. With some plastic plywood materials particularly, it will be found that the plastic on the external faces cracks at a load appreciably less than that causing failure of the specimen. This is especially liable to occur in low-temperature tests, and strain data obtained after part of a specimen has ceased to carry stress are not of sufficient engineering value to warrant endangering the strain gage.

Table 20 : 10 gives typical values for the ultimate tensile strength and tensile modulus of elasticity of ten specimens, six being of 3-ply Honduras mahogany bonded at 310° F. under a pressure of 400 p.s.i. The individual plies were  $\frac{1}{8}$  in. thick, laid so that the grain of the wood in alternate plies differed by 90°, and so that the grain on the faces of the

specimens was parallel to the direction of loading. Specimen 1 was bonded with 100 per cent phenol formaldehyde resin, a thermosetting plastic. Number 2 contained 15 per cent high-viscosity vinyl acetate, a thermoplastic, and 85 per cent phenol formaldehyde; 3 had 30 per cent vinyl acetate; and 4 was bonded with 100 per cent high-viscosity vinyl acetate. Specimen 5 was composited with 100 per cent high-viscosity vinyl butyral, a thermoplastic, while 6 used a special water-soluble phenol formaldehyde resin. Except for Specimen 6, the cementing material was applied to the veneer by immersing the wood in an alcoholic solution of the plastic and removing any excess by wringing between two rollers. The plastic was applied to Specimen 6 in a water solution.

Specimens 7 to 10 were made of New England white birch, sliced 0.025 in. thick and bonded with a thermoplastic, butacite. Panel 7 had 3 plies of birch with a piece of finely woven linen between the core and each face ply. Panel 8 was the same as 7 except that it had no linen. These panels were assembled under 200 p.s.i. pressure at 350° F. for 8 hours. Specimen 9 was the same as 7 except that it was pressed four hours without heat, and specimen 10 was the same as 8 except that it was pressed six hours without heat. The plastic was brushed onto the wood in all cases and the plies were arranged so that the grain of the core was 90° to the direction of the grain of the face plies, the latter being parallel to the direction of loading.

TABLE 20 : 10

EFFECT OF TEMPERATURE ON TENSILE PROPERTIES OF PLYWOOD

Specimen	Ultimate Tensile Stress			Tensile Modulus of Elasticity		
	-60° F.	+70° F.	+150° F.	-60° F.	+70° F.	+150° F.
1	6,420	7,100	6,005	1,240,000	1,240,000	1,240,000
2	7,820	7,605	6,305	1,290,000	1,260,000	1,260,000
3	6,245	5,970	5,685	1,240,000	1,090,000	1,000,000
4	7,025	7,290	*	1,010,000	1,165,000	*
5	5,880	4,850	*	1,060,000	1,320,000	*
6	7,700	7,550	5,925	1,220,000	1,170,000	1,220,000
7	14,520	10,100	7,100	.....	1,101,000	.....
8	13,290	13,980	5,030	.....	1,290,000	.....
9	12,040	8,225	6,110	.....	952,000	.....
10	14,080	12,350	5,660	.....	1,180,000	.....

\* Plastic bond between plies failed while material was being heated.

Table 20 : 11 shows the effect on tensile strength of varying the pressure at which a series of panels was bonded. All employed 100 per cent



phenol formaldehyde resin as the adhesive and each group of specimens contained panels composited at 310° F. under pressures of 200, 400 or 800 p.s.i. Group A was made of 3-ply mahogany, each veneer being  $\frac{1}{28}$  in. thick, with the grain of successive layers varying by 90°. Group B had 9-ply panels of  $\frac{1}{100}$ -in. mahogany with the grain direction of successive plies rotated 45°. Group C was the same as B with the addition of cotton fibers between each ply. Since the change in pressure and addition of cotton fibers affected both weight and strength, the specific gravities of the specimens are included.

There is a definite increase in tensile strength with increase in bonding pressure, but there is also an increase in density sufficient to keep the

TABLE 20 : 11  
EFFECT OF BONDING PRESSURE ON MAHOGANY PLYWOOD

	Group A			Group B			Group C		
Bonding pressure	200	400	800	200	400	800	200	400	800
Ultimate tensile stress	7125	7100	8680	6650	7800	9880	7970	8405	10775
Specific gravity	0.624	0.635	0.756	0.721	0.740	1.055	0.758	0.886	1.105
Factor of merit	0.585	0.574	0.589	0.473	0.541	0.481	0.540	0.486	0.500

strength-to-weight ratio of the material essentially constant as indicated by the factor of merit. The factor given in Table 20 : 11 is, however, not a simple strength-to-weight ratio but a factor showing the weight of a 17-ST aluminum alloy sheet necessary to carry a given load as compared to the weight of a plastic sheet of the same width carrying the same load. It is found from the ratio

$$\frac{(\text{Ultimate tensile stress})_p \times (\text{Specific gravity})_a}{(\text{Ultimate tensile stress})_a \times (\text{Specific gravity})_p} \quad 20$$

where the subscript  $p$  represents the plywood, the subscript  $a$  the aluminum alloy. Since successful aircraft were built of 17-ST aluminum alloy, it seems reasonable to use that as the standard for comparison rather than some of the higher strength alloys which are now available. By taking the ultimate tensile strength of 17-ST at 55,000 p.s.i. and the specific gravity as 2.833, Eq. 20 : 1 may be written

$$F_T = \frac{(\text{Ultimate tensile stress})_p}{(\text{Specific gravity})_p} \times \frac{1}{19,500} \quad 20 : 2$$

closely enough for a comparison of strengths based on material properties alone, without regard to average weight of connection details per pound

weight of actual structure, or to weight of protective coating per square foot, or similar factors which enter a strength-weight criterion applicable to a complete structure. Fortunately, few parts of a stressed-skin structure are designed by tensile-stress criteria, and so low factors of merit in tension do not necessarily indicate that a plastic-bonded plywood structure will be proportionately heavier than one made of aluminum alloy. Such factors of merit are, however, if applied with judgment, useful in comparing materials, and they are included in the tables which follow. They should be considered to give only qualitative and not reliable quantitative information regarding the relative merits of the materials to which they apply.

Table 20 : 12 presents tensile data on typical plastic-bonded plywoods. The values cannot be used for final design because they represent the results of tests made on samples of material submitted by manufacturers during the development of plywoods suitable for aircraft. The properties of the materials used in them were not determined separately, nor was the exact process of manufacture divulged in detail by the manufacturer. The data have been selected from test reports and student theses. They may be regarded as representing strengths that can be obtained, and they may prove useful for preliminary design purposes as well as for comparison with other plywoods and other plastic bonded materials at room temperature. They show the range of variation in strength and stiffness resulting from different combinations of wood and plastic and emphasize the need for testing several possible combinations before adopting any one for use in an airplane or glider.

**20 : 10. Plastic-bonded Plywoods Subjected to Compression —** Since plastic-bonded plywoods are normally employed in stressed-skin shells having stiffeners similar to those used in equivalent metal structures, and since compressive strength properties are usually critical for the design of such members, designers need data from which effective widths may be computed and from which allowable loads on stiffened sheets may be predicted. This calls for data from tests on simply supported flat or curved panels similar to those upon which Eq. 10 : 16a was based. It is difficult to establish a yield-point stress for wood in compression; therefore no upper limit for  $f_{se}$  of Eq. 10 : 16 has been established similar to the yield point used with metals. For purposes of comparison, however, it is convenient to represent  $1.70\sqrt{Ef_{se}}$  by a single coefficient,  $K$ , so that the compressive load carried by a plywood panel having the equivalent of simply supported edges may be represented by

$$P = K_{\mu}t^2$$

TABLE 20 : 12  
TYPICAL TENSILE-STRENGTH PROPERTIES

Plastic	Wood	Ply Thickness, In.	Specific Thickness, In.	Ultimate Tensile Stress, Lb. per Sq. In.	Factor of Merit	Direction of Load to Face Grain	Modulus of Elasticity
Cellulose acetate	African mahogany	$\frac{1}{40}$ , woven	0.038	2,940	0.136	45°	.....
Cellulose acetate	Cuban mahogany	$\frac{1}{40}$ , woven	0.108	5,130	0.245	45°	590,000
Cellulose acetate	Birch	$\frac{1}{40}$ , woven	0.075	4,380	0.215	45°	.....
Cellulose acetate	Hickory	$\frac{1}{40}$ , woven	0.123	4,390	0.209	45°	390,000
Thermosetting	Rotary-cut birch	$\frac{1}{8}$ , core	0.192	11,230	0.705	0° to core	1,500,000
Low-pressure type		0.017 plies				0° to face	
Thermosetting	Sliced birch	$\frac{1}{16}$ , core	0.105	15,700	0.970	0° to core	1,950,000
Low-pressure type		0.010 plies				45° to face	
Thermosetting	Sliced birch	$\frac{1}{40}$ , core	0.063	6,285	0.340	90° to core	482,000
Low-pressure type		0.010 plies				45° to face	
Phenol formaldehyde	Honduras mahogany	$\frac{1}{8}$ , 3-ply	0.104	7,100	0.574	0° to face	1,240,000
Phenol formaldehyde	Honduras mahogany	$\frac{1}{16}$ , 9-ply	0.076	7,800	0.541	0° to face	.....
Phenol formaldehyde	Honduras mahogany plus cotton fibers between plies	$\frac{1}{16}$ , 9-ply	0.093	8,405	0.486	0° to face	986,000
Phenol formaldehyde	Honduras mahogany plus cotton fibers on faces	$\frac{1}{16}$ , 5-ply	0.0705	8,425	0.426	.....	2,030,000

If, for 17-ST aluminum alloy, one takes  $f_{sc} = f_{yp} = 36,000$  p.s.i. and  $E = 10,000,000$  p.s.i., as was done in Chapter X, the value for  $K_a$  would be 1,020,000 in pounds per square inch units. If one takes  $f_{yp} = 32,000$  and  $E = 10,300,000$ ,  $K_a$  becomes 976,000 p.s.i. For simply supported panels of the same length and width carrying the same compressive load, the weight of an aluminum alloy panel would be to the weight of a plywood panel as the factor of merit,

$$F_c = \frac{\sqrt{K_p} \text{ (specific gravity)}_a}{\sqrt{K_a} \text{ (specific gravity)}_p} \quad 20 : 4$$

where the subscript  $a$  refers to the aluminum alloy, the subscript  $p$  to the plywood or plastic. This is approximately

$$F_c = \frac{\sqrt{K_p}}{\text{(Specific gravity)}_p} \times \frac{1}{350} = \frac{\sqrt[4]{E_p f_{sep}}}{\text{(Specific gravity)}_p} \times \frac{1}{350} \quad 20 : 4a$$

for either of the values of  $K_a$  given above. In the tables which follow,  $F_c$  is based on Eq. 20 : 4a.

All the panels used for the edge-compression tests were 10 to 12 in. square. The unloaded edges were supported in slotted tubes or by rods having V-shaped grooves milled into them. The forces acting on the loaded edges were applied through rectangular rods having V-shaped grooves.

Tables 20 : 13 and 20 : 14 are based on edge-compression tests of panels made of the same materials as those used in the tensile tests of Tables 20 : 10 and 20 : 11. The specimen numbers are here modified by C— to indicate compression tests, but they may be identified from the description of the specimen having the same number, or group having the same letter, in the tension-test data.

TABLE 20 : 13  
EFFECT OF TEMPERATURE ON EDGE-COMPRESSION PROPERTIES OF  
PLASTIC-BONDED MAHOGANY PLYWOOD

Specimen	Ultimate Compressive Load			Panel Thickness, Inches			Panel-compression Coefficient, $K_p$		
	-60° F.	+70° F.	+150° F.	-60° F.	+70° F.	+150° F.	-60° F.	+70° F.	+150° F.
C-1	1,545	1,675	1,660	0.098	0.105	0.110	161,000	152,000	137,200
C-2	1,685	1,990	1,550	0.102	0.107	0.101	162,000	174,000	152,000
C-3	1,590	1,720	1,670	0.097	0.106	0.098	169,000	153,000	173,000
C-4	1,955	1,690	*	0.103	0.103	0.100	183,200	159,200	.....
C-5	985	865	*	0.101	0.104	0.104	96,500	80,000	.....
C-6	2,080	2,100	2,020	0.100	0.110	0.107	208,000	173,200	176,200

\* Plastic bond failed while panel was being heated.

The data in Table 20 : 13 indicate temperature effects to be less important for panels in compression than is shown by Table 20 : 10 to be the case for plastic plywood in tension, at least where the bonding material is a thermosetting plastic. The specimens bonded by thermoplastics disintegrated in both cases at less than 150° F., while those bonded by a combination of thermoplastic and thermosetting plastic showed better properties at room temperature than at either high or low.

TABLE 20 : 14

EFFECT OF BONDING PRESSURE ON EDGE-COMPRESSION PROPERTIES

	Group C-A			Group C-B			Group C-C		
Bonding pressure	200	400	800	200	400	800	200	400	800
Compressive load	1690	1675	1685	1395	1250	1170	2025	2035	1825
Panel thickness	0.103	0.104	0.0885	0.080	0.076	0.0565	0.110	0.093	0.075
Coefficient, $\sqrt{K_p}$	399	394	465	467	465	606	410	485	562
Specific gravity	0.624	0.635	0.765	0.721	0.740	1.055	0.758	0.886	1.105
Factor of merit	1.75	1.71	1.68	1.78	1.73	1.58	1.49	1.51	1.40

Each value in these tables is the average of tests on two, three, or four panels, too few to be accepted as definitely establishing properties, but sufficient to indicate the effect of variation in temperature and bonding pressures for these particular combinations of wood and plastic. Designers may find, by suitable research, other combinations having definitely different characteristics under variations of heat and pressure, but the point to be made here is that significant changes in allowable stress properties of a given material may result if the conditions under which it is manufactured are altered or if the temperature ranges under which it is to be used are changed.

Table 20 : 15 presents room-temperature test results for other typical plastic-bonded plywoods and plastic panels. They are representative values, useful in the preliminary design of molded structures, but not to be accepted for final design purposes unless confirmed by tests made on panels produced under conditions exactly duplicating those to be used in manufacturing such structures.

Here again, Table 20 : 15 shows a wide variation in results obtained from different materials. The thermoplastic adhesives, cellulose acetate and butacite, yield lower strength panels and show lower factors of merit than the panels composited with thermosetting resins. The mahogany panels bonded with phenol formaldehyde show particularly good factors of merit, approximately twice those for panels of comparable thickness using cellulose acetate. This material has been used on trim tabs and,

with a structural weight about 10 per cent less, has demonstrated its ability to carry the same static and dynamic loads as its counterpart in aluminum alloy.

**20 : 11. Resistance to Shear and Buckling** — Very few data except those whose distribution is restricted for military reasons are available on the shear strength of plastic plywood panels used for the web members of box spars or in similar structures. Such data as are available were obtained at room temperature and indicate the ultimate shear strengths of the plastic-bonded plywoods to be slightly greater than those of the corresponding casein-glue plywoods. Equation 6 : 26 may be used, therefore, for the design of webs for box spars made of spruce or mahogany plywood until other data or other formulas are made available. A rough approximation to the ultimate shear strengths of other plywoods may be had by multiplying the allowable stress given by Eq. 6 : 26 by the ratio of the allowable shear stress of the other wood parallel to the grain to the corresponding value for spruce.

Data on the critical stress for buckling of these materials in shear or compression are also difficult to obtain. Limited data on the buckling stress in shear for 3-ply birch or mahogany panels indicate that the critical stress may be predicted by an expression similar to Eq. 6 : 6 but with a smaller coefficient than would be obtained by substituting the appropriate values in that equation. By writing Eq. 6 : 6,  $f_{s\ cr} = K_s E (t/b)^2$ , where  $b$  is the shorter side of the panel,  $a$  the longer,  $K_s$  varies as shown in Table 20 : 16.  $K_s$  would be expected to vary with

TABLE 20 : 16

$a$	0.0	0.2	0.4	0.6	0.8	1.0
$K_s$	2.02	2.04	2.09	2.17	2.28	2.42

the number of plies, the angle between the grain of adjacent plies, and the angle between the grain of the face plies and the short side of the panel. The above values of  $K_s$  are for plywood panels whose face grain is parallel to the short side and whose edges are simply supported. It is not possible, as yet, to give the relations between the above values and those for panels loaded at other angles to the grain or for panels loaded in compression instead of shear.

Reference to the Appendix of N.A.C.A. Report 382, "Elastic Instability of Members Having Sections Common in Aircraft Construction," by G. W. Trayer and H. W. March, will suffice to show that the problems involved in establishing equations for predicting critical stresses in an-isotropic materials such as plywood are far more complex than those encountered in treating isotropic sheets.

TABLE 20 : 15  
TYPICAL COMPRESSION PROPERTIES OF PLASTIC-BONDED PLYWOODS

Plastic	Wood	Ply Thickness, In.	Specimen Thickness	Maximum Load	$K_p$	Factor of Merit	Direction of Load
Cellulose acetate	Cuban mahogany	$\frac{1}{40}$ , woven	0.109	1,220	102,680	0.845	.....
Cellulose acetate	Cuban mahogany	$\frac{1}{40}$ , woven	0.098	1,155	120,280	0.820	.....
Cellulose acetate	Birch	$\frac{1}{40}$ , woven	0.068	470	101,600	0.801	.....
Low-pressure thermo-setting	Rotary-cut birch	0.017 core 0.017 plies	0.071	770	153,000	1.21	90° to core 45° to face
Low-pressure thermo-setting	Sliced birch	$\frac{1}{8}$ core 0.010 plies	0.096	1,400	152,000	1.31	0° to core 45° to face
Low-pressure thermo-setting	Rotary-cut elm	0.017 core 0.017 plies	0.083	695	101,400	1.035	0° to core 45° to face
Phenol formaldehyde	Honduras mahogany	$\frac{1}{8}$ , 3-ply	0.104	1,675	155,000	1.71	0° to face plies
Phenol formaldehyde	Honduras mahogany	$\frac{1}{16}$ , 9-ply	0.076	1,250	216,500	1.73	0° to face plies
Phenol formaldehyde	Honduras mahogany plus cotton fiber be- tween plies	$\frac{1}{16}$ , 9-ply	0.093	2,035	235,000	1.51	0° to face plies
Phenol formaldehyde	Honduras mahogany plus cotton fiber on faces	$\frac{1}{16}$ , 5-ply	0.0705	1,650	332,000	1.56	.....
Butacite and heat	Sliced birch plus linen each side of core	$\frac{1}{25}$ , 3-ply	0.065	497	121,900	1.13	0° to face plies
Butacite and heat	Sliced birch	$\frac{1}{25}$ , 3-ply	0.055	401	125,600	1.09	0° to face plies
Butacite, cold	Sliced birch and linen	$\frac{1}{25}$ , 3-ply	0.075	470	85,100	0.95	0° to face plies
Butacite, cold	Sliced birch	$\frac{1}{25}$ , 3-ply	0.064	482	117,900	1.18	0° to face plies

**20 : 12. Moisture Absorption of Plastic-bonded Plywoods** — Because of the greater proportion of hygroscopic material in the plywood panels, three-day immersion tests show that these panels may increase by 20 to 40 per cent of their original weight; seven-day tests show increases of 30 to 60 per cent. The edges of the specimens used in these water-absorption tests apparently were not well sealed by the plastic, and so moisture followed the grain and permeated the wood until it was saturated. It is extremely difficult to get an effective seal on the edges of such panels; so, although these results probably indicate too high a rate of absorption for moisture transmitted through the surface of the panel, they do indicate increases which may be expected after long periods of immersion or when the edges of panels are poorly sealed. No data are available on the tensile, compressive, or shear strengths or on the modulus of elasticity of these materials with various moisture contents. Based on previous data for casein-glue plywoods, strengths and stiffnesses would be expected to decrease as moisture content increased. No quantitative data are available as to the resistance of various plastic coatings to moisture and the actinic rays of the sun. The few qualitative data indicate the phenol formaldehyde resins offer better resistance than the thermoplastics, but well-founded curves giving rates of permeability against time are lacking.

**20 : 13. Connections between Plastic-bonded Plywood Parts** — Connections between parts create one of the greatest problems in the design of plastic aircraft structures. Many of the materials behave very satisfactorily as long as the stresses are well distributed through the covering, but they require an excessive amount of reinforcement or an excessive weight of small bolts distributed over a large area when it becomes necessary to provide a demountable connection between parts, such as joints for wing and fuselage, tail surface and fuselage, or landing gear and wing. This is because the shear and bearing strengths for these materials are low.

Two methods are being developed to circumvent the problem of excessive weight in connection details; one by the use of compressed-wood reinforcements at points where connections are to be made, the other by the use of metal strips attached to the surface of the plywood or inserted between the plies and joined to them by means of a high-strength thermosetting plastic.

The compressed-wood process entails the use of extra plies of wood added to the panel in the region to be reinforced before the panel is subjected to heat and pressure. Where pressures from 100 to 250 p.s.i. would be used to compress the main part of the panel, pressures from 500 to 1,500 lb. might be used over the reinforced sections to increase



the strength and density of the plywood in those regions. Sufficient pressure would normally be used to compress the entire panel to a uniform thickness, with the number of laminations in the reinforced area being gradually reduced or tapered so that there would be no line in the panel where strength and density would be changed suddenly. Messrs. Bernhard, Perry, and Stern<sup>1</sup> show the increases that can be obtained with birch panels by using veneers of various thicknesses when they are bonded at a normal pressure of 200 p.s.i. and at 500, 1,000 and 1,500 lb. They used a phenol formaldehyde resin, available in film form, and bonded all panels at 300° F. for thirty minutes under full pressure. At 1,500 p.s.i. they note a 77 per cent increase in specific gravity, as compared to the panel bonded under 200-lb. pressure, but a 66 per cent increase in block compressive stress and 127 per cent in tensile strength. This method of obtaining high-strength panels, even though it involves an increase in weight, offers excellent possibilities for the design of adequate connections between parts of airplanes. Care is required in working compressed wood after it is once formed, however, because the removal of material tends to relieve internal stresses and produce warping in the vicinity of the disturbed section.

The second method provides local reinforcement by bonding metal or plastic strips to the panels by special adhesives such as the Cycleweld process, developed by the Chrysler Corp. and the Goodyear Tire and Rubber Co. Not only do these adhesives develop sufficient strength between aluminum alloy or steel and wood to produce failure in the wood rather than in the adhesive but they also may be set under temperatures and pressures of the same magnitudes as the thermosetting plastics. They therefore require less elaborate molds and fixtures than does the compressed-wood process, and, because the heat applied to the metal plate can be controlled to insure softening of the adhesive without scorching the wood fibers, it seems probable that metal-plate reinforcements may prove more useful than highly compressed woods, particularly where curved surfaces are involved.

It is difficult, because of the heat-insulating characteristics of wood, to subject a thick block of plywood to heat and pressure with definite assurance that sufficient heat will penetrate the center plies to soften the plastic and give a dependable bond without, at the same time, overheating the wood in the outer laminations. Studies have been made of means to induce heat by high-frequency electric currents passed through the plywood, and considerable progress has been made in that

<sup>1</sup> "Super-pressed Plywood," R. K. Bernhard, T. D. Perry, and E. G. Stern, Wood Industries Division Meeting, Am. Soc. Mech. Eng., Boston, October, 1939.

field, but it cannot yet be said to have reached a state of development sufficient to establish it as a commercial process.

Various "cold-setting" resin adhesives have been developed, and opinion as to their dependability varies. Most of them are urea formaldehydes which tend to be less dependable than the phenols. They do cure at 70° F. with suitable catalysts but generally give better results if heated to 140° F. and if adequate pressure is applied to the joint while they "set." Some manufacturers refuse to use urea-formaldehyde resins, though most find them highly satisfactory. One manufacturer suggests that, where the acidity of the adhesive is too high, deterioration of the wood fibers may be expected after a long period. Such deterioration may be avoided by keeping the pH factor of the adhesive 2.5 or more.

One or two manufacturers of plastic plywood aircraft have found it expedient to air-condition their factories so that the moisture content of parts to be bonded by synthetic resins may be the same. If two parts having different moisture contents are joined, it has been found that the joint tends to warp or to open up when the moisture contents of the parts become equalized. Plastic plywoods are, after all, essentially the same as the older forms of plywood, in whose manufacture control of moisture was of paramount importance. While no data are available to show quantitatively the effect of variations in moisture in plastic-bonded materials, it is undoubtedly one of the most important factors in the production of plywood panels and in the joining of structural elements made of plywood.

The most successful manufacturers appear to use carefully controlled materials and processes throughout their entire fabrication procedure. Even they depend upon a minimum of research to show them how to attain certain characteristics in their product, and few know the entire range of effects attainable by varying any one of the many factors involved in a given procedure. None appears to have even approximate data on the range of effects produced by a simultaneous variation in two or more factors.

As a matter of fact, very little research of a sound and well co-ordinated nature has yet been published on any of the aircraft plastics. As this is written, test and development programs are being undertaken to provide quantitative design data on many plastic-bonded materials, to improve plastics and their properties, and to establish cheaper and more effective methods of fabricating these materials. The authors are of the opinion that the rapid progress being made will render many of the quantitative data given in this chapter obsolescent before publication. They believe, however, that the general observations and

qualitative comparisons will be valid for some years; hence that they will prove helpful to students and aircraft designers.

**20 : 14. Magnesium Alloys** — The wartime expansion of facilities for producing magnesium will doubtless entail a greater use of this metal in aircraft than in the past. Its high-strength alloys weigh 110 to 114 lb. per cu. ft., 0.064 to 0.066 lb. per cu. in., or roughly two-thirds the weight of the aluminum alloys. The ultimate tensile and compressive strengths of some of the wrought alloys exceed two-thirds those of the aluminum alloys, while the modulus of elasticity of 6,500,000 p.s.i. is but slightly less than two-thirds the  $E$  of those alloys. For stiffened flat sheets, whose strength is a function of their thickness squared, the factor of merit in compression is definitely in favor of the magnesium alloys. Where no space limitations exist, magnesium alloy stiffeners may be designed to give a weight saving over steel or the aluminum alloys. Magnesium-casting alloys are also superior to aluminum-casting alloys for many purposes, particularly where members can be given equal stiffness by the use of larger fillets, thicker flanges, or reinforcing ribs. In addition, some of the magnesium-casting alloys may be readily and satisfactorily welded to alloy sheets or bars of different composition, a feature not attainable with the aluminum alloys.

Magnesium alloys are somewhat difficult to protect against corrosion, especially where salt is encountered in a moisture-laden atmosphere. The rate at which corrosion takes place may be greatly reduced by suitable chemical treatments, plus a zinc chromate primer followed by top coats of paint, enamel, or lacquer. Magnesium alloys are particularly susceptible to corrosion when lead and water are present together, hence are not well suited for use as tanks for gasoline containing tetraethyl lead. They have been used for such purposes when a moisture-absorbing salt, such as potassium fluoride, has been added to check corrosion, but this introduces an added maintenance item which may or may not be regarded as burdensome by an airline operator.

Bend radii for the high-strength alloys are greater than for comparable thicknesses of aluminum alloy sheet, from 8 to 10 times the sheet thickness being common on the hard-rolled materials, from 2 to 5 times the thickness being required on annealed sheets. Much sharper bends can be made by working the material in the temperature range between 500° and 700° F., both sheet and tools being heated. There is, however, some reduction in the strength and hardness of the hard-rolled material when heated for forming but none in the properties of the annealed sheet.

The compressive yield points of some of the alloys are low in comparison with the ultimate, and bending operations involving stressing the

material beyond the compression yield point also appear to have an adverse effect on the tensile yield. One series of tests on the J-1 alloy showed a compressive yield at 20,000 p.s.i., a compressive ultimate of 50,000. The tensile yield was in the vicinity of 30,000 p.s.i., but this was found to have been reduced by about 50 per cent after the specimens were loaded slightly beyond the compressive yield. The research upon which these data are based has not been completed, but this effect is considered to have been definitely established, as has a progressive decrease in the modulus of elasticity as the result of a cyclic tensile loading. A modulus of 5,400,000 p.s.i. has been observed on the second cycle under a variable tensile loading, but the range of variation is not stated. It would appear, however, that the alloys of magnesium require further study before their characteristics can be said to be thoroughly understood.

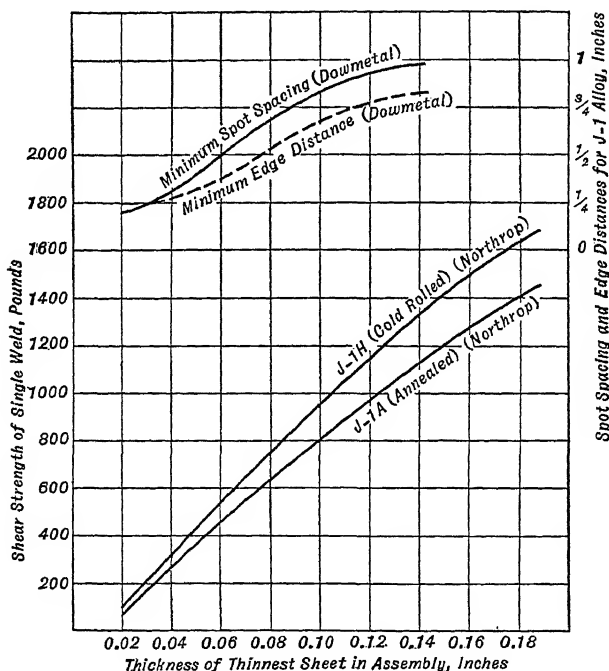
Riveting is usually accomplished with aluminum alloy rivets, 56S being preferred because of its low contact corrosion. Under conditions of mild exposure, A-17S rivets may be used for structural connections and, for low-strength requirements, the easy driving 2S and 3S aluminum rivets may be used. Steel, copper, brass, or bronze rivets should, however, never be used with the magnesium alloys. The design values for 56S rivets and the J-1 alloy in the hard condition are 27,000 p.s.i. for shear, 60,000 for bearing. Table 11 : 9 may therefore be used with somewhat conservative results on such rivets as are limited by shear.

Magnesium alloys may be gas-welded by the oxyacetylene or oxy-hydrogen processes with the aid of proper fluxes. The rod used in gas welding should be of the same composition as the material to be welded, and the joint should be made with the same precautions to avoid warping and distortion as are required when welding aluminum. Arc welding is coming into more extensive use, the Heliarc process, developed by Northrop Aircraft, Inc., and the Dow Chemical Co., showing particular promise. The welding is done by means of an arc in a helium atmosphere and yields sound welds with somewhat larger grain size than the original material but without materially reduced physical properties. It does not cause the alloy to flow into the weld from adjacent material, giving a reduction in thickness near the weld as occurs with steel.

Electric-resistance spot welds, made on conventional a.-c. or d.-c. equipment using copper electrodes, are also used for joining magnesium. Proper machine settings for the various alloys have been established and are available from the manufacturers. In addition to the three variables normally encountered in spot welding, namely, current, pressure, and time, a fourth factor must be provided for in joining the magnesium alloys. It may be called the "holding time," the period through-

out which pressure must be held after the current passage time has elapsed.

Figure 20 : 1 presents data on shear strengths and spot spacings for the commonly used J-1 alloy. The basic data were obtained from Northrop Aircraft, Inc., and the Dow Chemical Co. Large differences in sheet thickness are to be avoided in joints to be spot-welded, a difference of five B & S gage numbers between thickest and thinnest sheets being considered the maximum. Optimum strengths are procured where all sheet thicknesses in the joint are the same.



Shear Strength of Magnesium-Alloy Spot Welds.

FIG. 20:1

Table 20 : 17 presents typical strength data for representative alloys, some of which are suitable for use in extrusions, forgings, or sheet; others for castings. Table 20 : 18 gives the designations for alloys having essentially identical properties but made by different manufacturers.

The strengths of the magnesium alloys vary appreciably with rate of loading, and some tend to creep at stresses between one-half and three-fourths of the yield point of the material, that is, between one-third and one-half the ultimate. While it is possible to assume a short expo-

TABLE 20 : 17

## TYPICAL STRENGTH PROPERTIES OF MAGNESIUM ALLOYS

Alloy Number	Tensile Strength, 1,000 p.s.i.	Tensile Yield Point, 1,000 p.s.i.	Compression Strength, 1,000 p.s.i.	Shear Strength, 1,000 p.s.i.	Endurance Limit, 1,000 p.s.i.	Condition
1	40	30	59	20	13	Extrusions
	38	23	..	..	12	Forgings
	45	35	..	..	..	Sheet
2	42	27	49	18	6	Extrusions
	37	27	..	..	..	Sheet
3	44	30	69	20	15	Extrusions
	41	25	..	21	15	Forgings
4	27	11	45	17	10	Sand cast.
	37	12	46	18	10	Sand cast. h.t.
5	23	14	55	18	10	Sand cast.
	39	14	60	20	10	Sand cast. h.t.

TABLE 20 : 18

## TRADE DESIGNATIONS OF EQUIVALENT ALLOYS

Alloy Number	Dow Chem. Co. (Dowmetal)	American Magnesium Corp.	Permanente Metals Corp. (Permanesium)	German or English Elektron	U. S. Army Air Force Spec.
1	FS	AM52S	P-18	AZ31	11320
2	M	AM3S	P-11	AM503	11317
3	J	AM57S	P-8	AZM	11321
4	H	AM265	P-4	AZG	57-74-1DI
5	C	AM260	P-17	.....	.....

sure to maximum load, five seconds or less, so that no reduction need be made in the ultimate strength values of Table 20 : 17 for designs based on ultimate loads, it appears to be desirable to keep stresses produced by constantly applied loads at low intensities on these alloys when deformation of the structure is undesirable.

The tensile strengths of the magnesium alloys increase with a reduction in temperature and decrease with an increase in temperature. The reduction is not significant, however, until temperatures well above 200° F. are reached, and the increases are too small to be taken into account in design even in aircraft operating at high altitude.

The strength and fatigue properties of magnesium alloy castings closely parallel those of the aluminum alloys, and so designs and patterns suitable for one may frequently be used for the other. The wall thickness of magnesium castings should not be less than  $\frac{5}{32}$  in., except in

small castings, and adequate finish metal should be allowed on surfaces to be machined. A threaded length of two to three times the diameter is necessary to develop the strength of a stud, and stud bosses which carry heavy loads should be connected to the base structure by walls or ribs so that their loading will be distributed over large areas.

Stress concentrations are to be avoided in magnesium castings, and care must be taken to have rounded corners or fillets wherever there is a sharp change in section. Fillets should be proportioned with regard for the thickness of the walls or other parts of the casting they join, a fillet radius equal to the thickness of the thicker section being suitable in most instances. Where this leads to larger radii of fillets than seems expedient, as may occur where thin walls join thick sections, it is desirable to taper the thinner section to about three-fourths the thickness of the thicker one and then to use a fillet in the corners. This taper can be accomplished in a distance of one and one-half or two times the thickness of the thicker section without adding undue weight, and it provides a junction that is stiff and free from stress concentrations.

When holes are made in the walls of castings, they should be beaded or flanged to avoid sharp corners and sudden changes of section. As with the best aluminum alloy casting practice, sharp corners, notches, and tool marks must be avoided because they cause stress concentrations which are particularly objectionable in castings subjected to vibration or repeated reversals of stress. It should be noted that the fatigue strength of castings is not improved by heat treatment, though tensile strength, toughness, and yield strengths may be.

## BIBLIOGRAPHY

Most bibliographies consist of lists of books and periodical articles that may or may not have been used in the preparation of the text to which they are attached and they contain little or no information regarding the scope or value of the items mentioned. Bibliographies of this type are of value to librarians and occasionally to a practicing engineer, but all too often they amount to little but padding. In the following bibliography an attempt is made to give sufficient information about many of the documents listed so that the practicing engineer will find it a useful guide to further studies in the structural design of airplanes. This involves a reduction in the number of titles mentioned, due to space limitations, but the authors believe that this will be more than compensated by the gain in usability.

The first section is devoted to books, some of which are listed for the benefit of the reader who finds his preparation in mathematics and mechanics inadequate for a thorough understanding of this text. The remainder of the books and all the individual reports and articles of the second section are for the engineer who desires a more complete mastery of some of the problems of airplane structural design than he can achieve if his studies are limited to material in this volume. In selecting the references an effort has been made to limit them to articles of importance presenting material that has not been incorporated in this volume or in later books or reports that are listed. A few reports, however, have been listed on account of their historical importance in the development of present accepted practice, although parts of their contents may have been published in more readily available form. In practically all such instances, however, the original report is of value because it also contains much important material not used in the later publication.

In general, the complete title of a book or report is given, but only enough other bibliographical information is presented to permit easy and definite identification. Thus to conserve space, the sources of the individual papers are indicated by abbreviations listed in the Description of Chief Sources. Since few American engineers and students have a good working knowledge of foreign languages, all of the references are to works in English. The fact that many papers and reports are on restricted status limits recent references to articles in technical journals and to translations of foreign papers.

### SECTION I

#### Mathematics

The practicing aeronautical structural engineer must be competent to apply with understanding the methods of algebra, geometry, trigonometry, analytical geometry, and differential and integral calculus. A knowledge of differ-



ential equations is desirable for the engineer doing routine calculations and practically essential for the development of formulas and methods for handling the problems that are constantly being presented by new methods of design and construction. Many textbooks are available covering all these branches of mathematics, and one usually finds that, for purposes of review, the best are those from which he learned these subjects. Sometimes, however, the different approach of another author will help clear up points that were never more than imperfectly grasped, and, for the benefit of the reader who wishes to try a new approach and also for the student who may wish to master some of these branches by home study, some mathematics texts used at Stanford University and the Massachusetts Institute of Technology are listed below.

"College Algebra" by W. L. Hart (Alternate Ed., Heath); "Plane and Solid Geometry" by Wentworth and Smith (Ginn); "Plane Trigonometry" by R. W. Brink (Appleton-Century); "Brief Analytical Geometry" by Mason and Hazard (Ginn); "Elements of Differential and Integral Calculus" by Granville, Smith, and Longley (Rev. Ed., Ginn, 1934); "Differential and Integral Calculus" by H. M. Bacon (McGraw-Hill Book, 1942); "Differential Equations" by H. B. Phillips (3rd Ed., Wiley, 1934); and "Analytical Geometry and Calculus" by H. B. Phillips (Addison-Wesley Press, 1942).

Two books for home study especially recommended by Professor Bacon are "An Introduction to Mathematical Analysis" by F. L. Griffin (Houghton, Mifflin, 1936) and "Analytical Geometry and Calculus" by Woods and Bailey (Ginn). In these works the topics of analytical geometry and calculus are treated without regard to the conventional dividing lines between those subjects. Although this is an unusual approach, it has been found helpful by many students.

The volumes in the above list are written from the point of view of the mathematician to whom practical applications are secondary. "Mathematical Methods in Engineering" by T. von Karman and M. A. Biot (McGraw-Hill Book, 1940) is written from the engineer's viewpoint and shows how differential equations can be used for the solution of many practical problems, many of which are in the field of airplane structural analysis.

Some engineers who find it difficult to grasp the essential nature of the mathematics they are called on to use, when it is developed in the conventional manner, are greatly helped by the unconventional works in the field. Of these works it is desirable to mention "Calculus Made Easy" by S. P. Thompson (2nd Ed., Macmillan, 1927), "Mathematics for the Million" by L. Hogben (Norton, 1937) and "Mathematics and the Imagination" by E. Kasner and J. Newman (Simon and Schuster, 1940). Although these books are especially recommended for the reader who has difficulty with mathematics, all three are well written and would be of considerable interest to anyone engaged in work of a mathematical nature.

### **Mechanics**

The practicing engineer who wishes to improve his mastery of the problems of airplane structural design will find assistance from two types of books.

Of the first are texts on special phases of mechanics which have a bearing on aeronautical practice but are not limited in scope to such applications. Among them are works on mechanics of materials, theory of elasticity, and theory of structures. The second type embraces books written specifically for the airplane designer.

Every engineering student obtains some training in mechanics of materials before graduation, but many of them, on encountering new problems of airplane structural design, find either that this training is inadequate or that, through disuse, they have forgotten what they had once learned. A frequent source of trouble is that they have forgotten some of the assumptions and limitations connected with the formulas with which they became acquainted in college. With more conventional structures this is not likely to be so serious, but in aeronautical work structures which do not conform to the assumptions and limitations on which the common formulas are based are more nearly the rule than the exception. The practicing engineer is therefore wise to begin his study of advanced theory by a careful review of mechanics of materials, using a text which does not stop with listing the basic assumptions and limitations connected with the more common formulas but continues with some discussion of the resulting situation when these assumptions and limitations are not applicable. Probably the best American text for this purpose is "Strength of Materials" by S. Timoshenko (2 Vol., Van Nostrand, 1930). A considerably revised second edition of the second volume appeared in 1940. A somewhat older book in the same field is "Strength of Materials" by G. F. Swain (McGraw-Hill Book, 1927). In general, Swain's work is more detailed on the topics it treats, but it is of narrower scope.

Many of the more advanced topics of mechanics of materials are now considered to form the field of the *theory of elasticity*, which deals with the relations between the internal stresses and strains of elastic bodies resulting from the application of external forces or heat. The best introduction to this branch of mechanics is Timoshenko's "Theory of Elasticity" (McGraw-Hill Book, 1934). Similar in scope, but not as widely or favorably known in this country are "Applied Elasticity" by J. Prescott (Longmans, Green, 1924) and "An Introduction to the Theory of Elasticity" by R. V. Southwell (Oxford, 1936).

The books of the preceding paragraph are limited to discussion of the action of materials when the stresses are below the elastic limit. It is also important at times to know what happens when that limit is exceeded. Relatively little has been written in this field, the most important work being "Plasticity" by A. Nadai (McGraw-Hill Book, 1931).

The above-mentioned works of Timoshenko, Prescott, and Southwell cover the field of elasticity extensively rather than intensively, and there are some works devoted to limited portions of the field that should be mentioned. Most important of these to the aeronautical engineer are "The Theory of Elastic Stability" (McGraw-Hill Book, 1936) and "The Theory of Plates and Shells" (McGraw-Hill Book, 1940), both by Dr. Timoshenko. The former is of particular importance for its development of methods of deter-

mining critical loads for columns and thin plates subjected to compression or shear. The latter, while devoting much of its space to plates of greater thickness than the airplane designer is accustomed to use, also includes much of direct interest to him.

The engineer wishing to learn more of the use and original derivation of the method of least work will be interested in "Elastic Stresses in Structures" by E. S. Andrews (Scott, Greenwood, 1919) because that book is a translation of Castigliano's original work. One desirous of further information on compression members will find in "Columns" by E. H. Salmon (H. Frowde, Hodder & Stoughton, London, 1921) the most complete monograph on the subject in English. Unfortunately it appeared before much had been done on columns of very thin metal and has little information on the special problems resulting from local instability.

In recent years there has been much activity in solving practical problems of elastic behavior, which are difficult if not impossible to handle by analytical methods, with the help of models subjected to polarized light. A good introduction to the methods used and the results obtained in this field is given in "Photoelasticity" by M. M. Frocht (Wiley, 1941). So far only the first volume of this work has appeared but a second is planned.

Up to the present the airplane structural designer has too often attempted to handle problems resulting from vibration by the simple method of forgetting their existence or by rule of thumb procedures to correct the results of his failure to provide for such action. The literature on vibration is very extensive, but the more important results of research in that field have been correlated by J. P. Den Hartog in "Mechanical Vibration" (McGraw-Hill Book, 2nd Ed., 1940). Somewhat more limited in scope, but more detailed in treatment, is "Practical Solution of Torsional Vibration Problems" by W. K. Wilson (2nd Ed., Wiley, 1940).

Closely related to the subject of vibration is that of fatigue, a phenomenon which is an important source of structural failure. To date the engine and propeller designers have been more concerned with fatigue failure than has the designer of the main structure, but the latter is finding it increasingly more important to become familiar with the subject. While many papers have been published in this field, until recently it was very difficult for the designer to obtain the information he needed in concise and practically useful shape. This led the Bureau of Aeronautics of the Navy Department to sponsor the preparation of a handbook on the "Prevention of the Failure of Metals under Repeated Stress" by the Battelle Memorial Institute (Wiley, 1941). Every airplane designer should become familiar with the material in this work which though of general application, draws the majority of its examples from the aeronautical field.

So closely related to the field of theory of elasticity that it is hard to define a boundary between them is the *theory of structures*. In general it may be said that the theory of elasticity deals with the action under load of the infinitesimal elements of which a structure is composed, and the theory of structures is the application of the findings of the theory of elasticity to the design

and analysis of full-sized structures. From this point of view it might be said that the works of Salmon, Andrews, and Den Hartog, and some of those of Timoshenko listed above are actually devoted to theory of structures. While that may be true, it is certain that it is more important that the aeronautical engineer be familiar with the contents of those works than that he be able to classify them with pedantic accuracy.

The books to be listed below as valuable works on the theory of structures have all been written primarily for the designer of bridges, buildings, and similar large constructions. As a result, they include little of direct application to airplane structures that is not outlined in this book. On the other hand, they present alternative methods of developing procedures described here which may be helpful to the reader. They also include discussions of other procedures which the progressive airplane designer may find adaptable to the solution of his problems. Many of the methods described here were adapted from methods presented in this group of works and the authors would be the last to maintain that they had exhausted the possibilities of finding useful procedures from the literature of the structural engineer.

For the simpler phases of structural analysis, and the less advanced methods of handling redundant structures, the authors recommend C. M. Spofford's "Theory of Structures" (3rd Ed., McGraw-Hill Book, 1928) and H. Sutherland and H. L. Bowman's "Structural Theory" (2nd Ed., Wiley, 1942) and "Structural Design" (Wiley, 1938). Probably the American text of widest scope in the field of structural theory is "Modern Framed Structures" by J. B. Johnson, C. W. Bryan, and F. E. Turneaure (10th Ed., Wiley, 1929). This work is in three volumes, of which the second, on statically indeterminate structures, is most likely to provide helpful suggestions to the aeronautical engineer. A somewhat similar work recently published in England is A. J. S. Pippard and J. F. Baker's "The Analysis of Engineering Structures," (Longmans, Green, 1936). This is probably the most accessible source at present for information on a number of new procedures, developed chiefly in England, that are otherwise only to be found in isolated reports.

Two valuable American texts to redundant structures are "Statically Indeterminate Stresses" by J. I. Parcel and G. A. Maney (2nd Ed., Wiley, 1936) and "Theory of Statically Indeterminate Structures" by W. M. Fife and J. B. Wilbur (McGraw-Hill Book, 1937). The former work covers the wider range of problems, while the latter puts more emphasis on the particular principles which underlie all the standard methods of analysis. "Elastic Energy Theory," by J. A. van den Broek (Wiley, 1942), shows how that particular method may be applied to the analysis of various indeterminate structures.

At present the aeronautical engineer has little professional need for the design of arches or reinforced concrete building frames though, as a junior engineer, he may be called upon occasionally to design a hangar or a rigid base for testing structures. Methods originated for the analysis of such structures, however, may prove helpful in the treatment of fuselage bulkhead rings and the rigid-jointed frames used in aircraft. He may therefore find

suggestions of value in C. M. Spofford's "Theory of Continuous Structures and Arches" (McGraw-Hill Book, 1937) and "Continuous Frames of Reinforced Concrete" by H. Cross and N. P. Morgan (Wiley, 1932). The latter book devotes considerable space to the "column analogy" for analyzing frames with not more than three redundants and to short cuts applicable to the moment distribution method when  $L/j = 0$  for all members.

Many types of analysis involve the solution of simultaneous equations which can be most satisfactorily handled by methods of successive approximation. An important development in this field is described in "Relaxation Methods in Engineering Science" by R. V. Southwell (Oxford, 1940). Southwell's method is a general one of which the moment-distribution method may be considered a special case. It was originally developed for the analysis of the highly redundant space frameworks of rigid airships, but Southwell shows additional applications including rigid-jointed frames and vibration problems.

For the occasion of Dr. Timoshenko's sixtieth birthday a number of his friends, who are also leading workers in the field of mechanics, wrote a group of papers that are published in the "S. Timoshenko 60th Anniversary Volume" (Macmillan, 1938). While these papers cover a wide range of special subjects, many of them are on topics of interest to the airplane structural designer.

In general the practicing engineer finds the formulas he wishes to use distributed among a large number of books and papers, and it is often difficult for him to locate desired material. The purpose of handbooks is to bring together the practical findings of the literature and present them in concise form, giving only the results and omitting the proofs in the original papers. An excellent book of this type is the "Handbook of Engineering Fundamentals" by O. W. Eshbach (Wiley, 1936). This covers not only the field of mechanics of materials but also the less advanced phases of most branches of engineering. A somewhat similar work but one restricted to the field of strength of materials is "Formulas for Stress and Strain" by R. J. Roark (McGraw-Hill Book, 1940). This work not only includes most of the published formulas of interest to the structural designer but also well-selected bibliographical references.

### Aeronautics

During the 1920's the chief guide to methods of analysis suitable for airplane structures was the English work "Aeroplane Structures" by A. J. S. Pippard and J. L. Pritchard. As new methods of construction appeared, new methods of analysis developed, and American practice with respect to nomenclature, etc., diverged from the British, this work became less and less suitable for use in this country. When the first edition of "Airplane Structures" was projected, the objective of the authors might well have been described as the production of an American equivalent to Pippard and Pritchard. In a new edition (Longmans, Green, 1935) the latter work was brought up to date, and, while relatively little space is devoted to the special problems of stressed-skin construction, the volume is one which deserves a place in the library of the practicing engineer.

Two other English books on airplane stress analysis require mention. The more important is H. B. Howard's "The Stresses in Aeroplane Structures" (Pitman, 1933), which includes the most complete discussion of the "polar-diagram" method of analyzing beam-columns that has yet appeared. The chief defect of the work is that too little space is devoted to alternative methods. The second is "Practical Aircraft Stress Analysis" by D. R. Adams (Pitman, 1936). In this book, however, the more advanced methods of analysis are unfortunately omitted in spite of the necessity of using them in practice.

The change from fabric-covered to stressed-skin construction resulted in the production of several books, some of which are primarily descriptive, some analytical. M. Langley's "Metal Aircraft Construction" (4th Ed., Pitman, 1941) has many drawings of structural parts which make it one of the best available records of metal airplane structures. Some attention is paid to methods of analysis but, on the whole, the value of the book is primarily descriptive.

F. Loudy's "Metal Airplane Structures" (Henley, 1938) includes a number of pictures of metal construction and some useful tables of standard sizes for metal parts. Much of the book consists of condensations of N. A. C. A. Reports whose value would have been enhanced had the author done more to indicate the relations between the problems covered by these reports and more to show how the material in them could be applied in practical design.

Numerous rules for detail design and some good descriptions of shop practice are given in W. L. Nye's "Metal Construction" (Aviation Press, 1935), but it is short on theoretical material which would help an engineer decide when to use the methods given.

An early work on metal construction was J. E. Younger's "Structural Design of Metal Airplanes" (McGraw-Hill Book, 1935). This has been largely rewritten to bring it up to date, and in its second edition appears as "Mechanics of Aircraft Structures" (McGraw-Hill Book, 1942). The second edition is more largely devoted to structural theory and less to descriptive matter than the first.

Sechler and Dunn's "Airplane Structural Analysis and Design" (Wiley, 1942) is probably the best of the recent books on metal structures. It includes considerable data on weight estimation and preliminary design, and an excellent treatment of the problems entailed in the analysis of stressed skin structural elements.

Of the few books covering the problems peculiar to the design of seaplanes and flying boats, "Seaplane Design" by W. Nelson (McGraw-Hill Book, 1934) is as good as any. The author limits himself to the special problems of the seaplane and devotes a considerable portion of the book to the determination of water loads and to proper methods of detail design.

The most serious gap in aeronautical literature is a text showing the junior engineer how to design in detail the parts of which an airplane is composed. The Society of Automotive Engineers' "Drafting Room Manual" and "Standards Book" are useful in this ~~and as they are~~ in loose leaf

form, they are subject to constant revision and should not get out of date. J. G. Thompson's "Aircraft Drafting Room Manual" (Aviation Press, 1939) is based on the manuals of a number of the airplane manufacturing companies and is very useful in showing draftsmen and engineers some of the standard practices in detail design.

While devoted primarily to the art of welding, and the science of designing welded details, J. B. Johnson's "Airplane Welding and Materials" (Goodheart-Wilcox, 1941) includes an authoritative treatment of the metallic materials used in aircraft and provides a great deal of material that is useful to detail designers and stress analysts.

The books so far mentioned were prepared on the assumption that the reader would know how to go about the general design of his airplane, but the young engineer seldom knows how to get started on a new design with a minimum of lost motion. F. K. Teichman's "Airplane Design Manual" (Pitman, 1939) is intended to help in this regard and, as far as the structural design goes, it does a good job. It contains considerable material on sound proofing, cabin arrangement, and similar matters which are omitted from most textbooks.

Even more valuable is the recent work on "Aircraft Layout and Detail Design" by N. Anderson (McGraw-Hill Book, 1941). This describes how to apply the methods of descriptive geometry to a number of practical design problems encountered in layout work and also includes a considerable amount of good material on the design and analysis of minor parts and connecting fittings.

Like most other branches of engineering, aeronautics has given rise to specialized handbooks with data covering many portions of its field. Most important of these are E. P. Warner and S. P. Johnston's "Aviation Handbook" (McGraw-Hill Book, 1931) and the "Handbook of Aeronautics" sponsored by the Royal Aeronautical Society (Gale and Polden, 1931). The former represents primarily American and the latter British practice. As with most handbooks, neither of these volumes is of particular value as a guide to the use of new procedures, but they are more useful as summaries of procedures more fully described in other volumes and as sources of reference. The "Aircraft Handbook" of Colvin and Colvin (McGraw-Hill Book, 1928) is primarily devoted to engines and includes little material regarding airplane structures.

Although wood construction has long been in eclipse, at least so far as military and transport airplanes are concerned, it has continued to be used in some of the lighter designs for the private pilot. Lack of metals during the war has brought it back into use for military aircraft, with plastic adhesives replacing the older glues. Impregnated wood is also coming into use in some of the "plastic" airplanes being developed in this country. The Forest Products Laboratory at Madison, Wisconsin, has devoted much time in the past to the solution of problems connected with wood construction and has published, mostly through the National Advisory Committee for Aeronautics, a series of excellent reports on the properties of woods. Most of the earlier

work in this field is admirably summarized by G. W. Trayer in "Wood in Aircraft" (National Lumber Manufacturers' Association, Washington, D.C., 1930). This book is not limited to problems of wood construction alone but includes the work done by Trayer and his associates on the more general problems of the torsion of non-circular sections and the lateral buckling of wing spars in airplanes. Though predicated on the use of animal or casein glues, these data are still useful to designers because the properties of the wood itself are critical in most of its applications and a change in adhesives means a change in assembly practice rather than in strength.

Owing to the necessity of keeping the weight of airplanes to a minimum, the designer must use a great variety of materials, and the choice of the proper one for a given part is often a difficult problem. The best available book on the subject is "Aircraft Materials and Processes" by G. F. Titterton (Pitman, 1937). "Airplane Maintenance," by H. G. Lesley (Wiley, 1940), though its title may not indicate it, is also useful as a source of information on materials. The articles on any one material are brief but have been carefully written to present the most important data for the maintenance engineer whose interests, it appears, closely parallel those of the structural designer.

The aeronautical engineer is often asked, "What is a good and sound but not too technical book on airplanes?" The best answer at present is "The Airplane and Its Engine" by C. H. Chatfield, C. F. Taylor, and S. Ober, (4th Ed., McGraw-Hill Book, 1940). It was not intended for this work to go into sufficient detail to satisfy the needs of the airplane designer. It is, however, basically sound and is excellent for the pilot or other interested person who desires an intelligent "layman's knowledge" of airplanes.

## SECTION II

### REPORTS AND PAPERS

#### Description of Chief Sources

Practically all the references to papers in this bibliography are to government-sponsored reports or articles in a group of periodicals devoted to aviation, applied mechanics, or related fields. A brief list of these general sources and of the abbreviations by which they are designated follows.

Most important are the papers published by the National Advisory Committee for Aeronautics. These appear in three distinct series, of which the Technical Reports (abbreviated T.R.) are first published individually and later combined in annual bound volumes. The other series are the Technical Notes (abbreviated T.N.) and Technical Memoranda (abbreviated T.M.), which are published in mimeographed form only. At present the Notes are papers of American origin which are not considered of sufficient importance to rank as Reports or which are in the nature of progress reports on extended projects. The Memoranda are translations of foreign language papers, mostly from German sources. While adhered to at present, this differentiation has not always been in effect. The more recent Technical Reports



and Notes are now confidential, and, since they are not available to the general public, are not listed in this bibliography. Engineers working on defense contracts, however, have access to them and should study those covering topics in which they are interested.

Similar in nature to the N.A.C.A. Reports and Notes are the publications of the U. S. Army. These were originally known as Air Service Information Circulars (abbreviated I.C.) but the name was changed to Air Corps Information Circulars (abbreviated I.C.) without any break in the serial numbering.

Corresponding roughly to the Technical Reports of the N.A.C.A. are the Reports and Memoranda (abbreviated R. & M.) of the British Government's Aeronautical Research Committee (formerly called the Advisory Committee for Aeronautics). These are also published individually and later collected in annual volumes. In general, the Reports and Memoranda tend to be exceedingly concise documents containing a considerable amount of higher mathematics and, as a result, are often difficult to follow. Many of them have therefore been paraphrased by more popular articles in the English technical press.

Next in importance to the governmentally published papers, at least in this country, are papers published by the national societies interested in airplane design and related fields. Most important of these is the Institute of the Aeronautical Sciences which publishes the *Journal of the Aeronautical Sciences* (abbreviated *Jour. Aero. Sci.*). Next in importance is the American Society of Mechanical Engineers. Two of the technical divisions of this society have been responsible for papers of interest to the aeronautical structural engineer, those on Aeronautics and Applied Mechanics, particularly the latter. From about 1927 to 1934 each of these sections published a group of its papers in a separate number of the A.S.M.E. *Transactions*, three or four times a year, with a subtitle indicating the responsible section. In 1935 a new publication system was adopted and the Applied Mechanics section became responsible for publishing the quarterly *Journal of Applied Mechanics* (abbreviated *J. Appl. Mech.*), which constitutes the society *Transactions* for the months in which it appears. Papers from the other technical sections are published in the *Transactions* for the other eight months without any attempt being made to have a single section responsible for all the papers in a given number. The change in publication system and the changes in the subtitles and dating methods under the earlier system make it difficult to refer to these papers. The system adopted here is to refer to *Aero. Trans.* for papers in the numbers prior to 1934 put out by the Aeronautics section, regardless of whether they appeared under the designation of *Aeronautical Transactions* or *Aeronautical Engineering*. Similar reference is made to *Appl. Mech. Trans.* for papers published by the Applied Mechanics section during the same period. For papers of the Aeronautics section published subsequent to the consolidation of the section transactions the reference is to *Trans. A.S.M.E.*

Two other national societies publishing occasional papers of interest to the airplane structural designer are the American Society of Civil Engineers

and the Society of Automotive Engineers. Papers published by the former are denoted by *Trans. A.S.C.E.*, while these of the latter are credited to the *S.A.E. Jour.*

While many advanced theoretical studies are published in this country by the government and the technical societies, the aeronautical press includes relatively few articles of this type. During the past few years, however, the best aeronautical magazines have greatly strengthened their technical sections, and they now publish numerous valuable articles. They are, indeed, the chief source of material on detail design procedures, shop practice, maintenance, and similar subjects of great interest to the airplane designer. Of the various aviation magazines the only ones from which articles have been referred to in this bibliography are *Aviation* and *Aero Digest* and its absorbed predecessors *Aviation Engineering* (abbreviated *Aviation Eng.*) and *Airway Age*.

Of the English societies interested in the field of aviation only the Royal Aeronautical Society publishes a periodical that is well known in this country. This magazine, the *Journal of the Royal Aeronautical Society* (abbreviated *Jour. Roy. Aero. Soc.*) is the source of numerous valuable articles, many of which present in more readable and popular form material that also appears in the Reports and Memoranda.

The British also publish two excellent private periodicals devoted to the field of Aeronautical engineering. These are *Aircraft Engineering* (abbreviated *Aircraft Eng.*) and *The Aircraft Engineer* which appears as a monthly supplement to the weekly magazine *Flight*. References to the latter periodical are made to *Flight*, which reference may refer to articles in the less technical as well as those in the *Aircraft Engineer* section. While the papers of both *Aircraft Engineering* and *Flight* tend to be less concise and to include less advanced mathematics than the Reports and Memoranda, they also tend to exhibit more of these qualities than the American literature.

In order to save space, references to periodical articles include only the dates of the numbers in which they appear, volume and page numbers being omitted since once the desired number is at hand the article can easily be located.

### Arrangement

It would be desirable to arrange the references in a thoroughly logical order according to an easily recognized system. Unfortunately that is hardly practicable, though it is possible to do better than to use a completely alphabetical or chronological list. In this bibliography an attempt is made to group the papers according to their subject matter. Some of the papers pertain to two or more of the classifications, and, since space limitations make repeated references undesirable, the student will usually find it necessary to check up on the papers mentioned under related subjects to find all bearing on that in which he is especially interested. As far as possible, the papers are grouped according to phases of structural theory in the order in which they are taken up in the text. At the end are some papers on subjects that receive little if any attention in the text but are of considerable interest to the airplane structural designer.

### Weights

One of the most important problems connected with the general design of an airplane is that of estimating its probable weight. This is particularly true in connection with the design of a new model. A few suggestions are made in connection with this problem in Art. 1 : 5, but the designer will find them to be very inadequate for his needs.

In the first edition of this book an entire chapter was devoted to weight data and methods of using them. The weights of equipment change as new and improved models are produced and, since up-to-date weight data are now available in the catalogues of the equipment manufacturers, and the publications of the Society of Aeronautical Weight Engineers, it appears unnecessary to include them in a textbook where they rapidly become obsolete. Part of the chapter was devoted to a discussion of methods of estimating the weights of structure and similar parts under the control of the designer. Owing largely to changes in the conventional types of construction, these data had become obsolete by the time the second edition was being prepared, and so all weight data were omitted from that edition. It would have been desirable to have made weight analyses of a group of more modern designs to correct the tables and to include them in this edition, but this was impracticable on account of the confidential nature of many of the data required.

In making a preliminary estimate, the designer can get some help from the "breakdowns" of structural weights in the handbooks and in such articles as "Study of Airplane Weight Complex," by A. A. Gassner (*Aero. Trans.*, April-June, 1932) or the same author's article in *Aviation* for October, 1930. Nearly all the airplanes for which weight breakdowns have been published are, however, of fabric covered structures, and the resulting ratios must be accepted with suspicion when they are applied to stressed skin types. Chapter I of Sechler and Dunn's "Airplane Structural Analysis and Design" (Wiley, 1942) contains useful charts and data for the latter types, and some of the papers of the Society of Aeronautical Weight Engineers are also very helpful.

The situation regarding the effect on weight of modifying an existing design is reasonably good, particularly with respect to the weight of wings. In this connection "Estimation of Wing Weights," by J. E. Lipp (*Jour. Aero. Sci.*, October, 1938) and B. C. Boulton's contribution to the symposium on "The Next Five Years in Aviation" (*Jour. Aero. Sci.*, December, 1936) should be mentioned. W. Semion's paper "Preliminary Design Equations for Aircraft Weight Estimation" (Soc. Aero. Weight Eng. Paper 22) contains formulas for estimating weights of parts and for estimating the effect of modifications in details.

The technique of weight and balance control is briefly mentioned in Art. 1 : 6. More detailed discussions of this subject are to be found in "Weight Control in the Design of Aircraft," by F. Flader (*Aviation*, August 16 and October 19, 1929), "Airplane Weight Control," by J. F. Hardecker and E. E. Lambert (*Airway Age*, September and October, 1929) and "Weight and Balance Control," by J. H. Gunning (*Aviation Eng.*, November, 1932).

These articles describe methods used by Curtiss, the Naval Aircraft Factory, and Douglas, respectively.

### Design Loads

The loads for which an airplane must be designed have two main characteristics, total magnitude and relative distribution. As shown in Chapter II the loads of greatest magnitude may be imposed either in intended maneuvers or by flying in bumpy air. The most important single paper on the loads that may be encountered in intended maneuvers is J. H. Doolittle's *Accelerations in Flight* (T.R. 203, 1925). Later papers have been restricted to reports on less extensive series of tests. The first important paper on the effect of gusts was the *Preliminary Study of Applied Load Factors in Bumpy Air* (T.N. 374, 1931) by R. V. Rhode and E. E. Lundquist. This has been followed by other papers, but the subject matter is in the field of aerodynamics rather than that of airplane structures.

### Continuous Beams

The discussion of the Cross method of moment distribution in Chapters V and XIII does not pretend to cover all the applications and variations of that general method of analyzing continuous beams. The original paper of Professor Cross, "Analysis of Continuous Frames by Distributing Fixed-end Moments" (*Trans. A.S.C.E.*, 1932) is even briefer but is accompanied by about a hundred pages of discussions, some of which are of considerable interest. An alternative method of describing this method of analysis, and one which some students find clearer than that in this volume, is presented by H. A. Williams in "The Application of the Hardy Cross Method of Moment Distribution" (*Trans. A.S.M.E.*, May, 1934). Other papers describing extensions and developments of the Cross method are listed in Art. 13 : 23. The authors of these papers, however, are interested primarily in building frames and, while they present ideas of value to the airplane designer, the papers include little of direct application in the aeronautical field.

### Simple Beams

The tests on which the design figures for the modulus of rupture of aircraft tubing are primarily based are reported on in *Strength of Chrome-molybdenum Tubing under Bending Due to Transverse Loads* (I.C. 686, 1934) by C. G. Brown and F. M. Carpenter. *The Crinkling Strength and the Bending Strength of Round Aircraft Tubing* by W. R. Osgood (T.R. 632, 1938) is a more recent important paper in the same field. Its results, however, are not as well arranged for direct application to practical design.

The classic report on which the design of wood beams is based is *Form Factors for Beams Subjected to Transverse Loading Only* by J. A. Newlin and G. W. Trayer (T.R. 181, 1923). This report is devoted to the design to resist normal stresses on the cross-section. For the design of plywood webs the chief sources of information are *Shear Strength of Plywood Webs of Box Beams* by R. A. Miller (I.C. 587, 1927) and *The Design of Plywood Webs for Airplane Wing Beams* by G. W. Trayer (T.R. 344, 1930). On the whole, Miller's

recommendations have been followed more extensively than those of Trayer, but the designer should also be familiar with the ideas of the latter. With the renewed interest in wood construction, these reports and other work of the Forest Products Laboratory may resume their place as one of the bases of practical design.

### Torsion

**Circular Sections.** The generally accepted theory of failure of *very thin* walled tubes in torsion is that developed by L. H. Donnell in *Stability of Thin-walled Tubes under Torsion* (T.R. 479, 1933). No equally satisfactory theory for the torsional failure of tubes of moderate  $D/t$  ratios has been worked out, and allowable stresses for such members are determined empirically. An important series of tests on such members has been reported by A. H. Stang, W. Ramberg, and G. Back in *Torsion Tests of Tubes*, (T.R. 601, 1937). In the near future the formulas and design charts of this report may supersede the curves of Art. 7 : 3.

Still more recent are the tests reported by R. L. Moore and D. A. Paul in *Torsional Stability of Aluminum Alloy Seamless Tubing*, (T.N. 696, 1939). These tests were on 51-ST tubes with  $D/t$  ranging from 77 to 139 and with  $L/D$  from 1 to 60. The results are compared to theory and found to be in good agreement.

**Non-circular Sections.** Many of the formulas for the torsion of non-circular shafts have been developed by the application of the membrane analogy and experiments with soap films. The mathematical basis of this method, the technique of its use, and the results of its application to several important types of section are discussed in *The Use of Soap Films in Solving Torsion Problems* by G. I. Taylor and A. A. Griffith (R. & M. 333, 1917); *The Determination of the Torsional Stiffness and Strength of Cylindrical Bars of Any Shape* by A. A. Griffith (R. & M. 334, 1917); and *The Application of Soap Films to the Determination of the Torsion and Flexure of Hollow Shafts* by A. A. Griffith (R. & M. 392, 1918). Very much the same field is covered by G. W. Trayer and H. W. March in *The Torsion of Members Having Sections Common in Aircraft Construction*, (T.R. 334, 1930). In the *Journal of the Aeronautical Sciences*, for April, 1937, L. Lombardi compares some test results with Trayer and March's and also Timoshenko's formulas under the title "Torsion of 17-ST Extruded Angles and Channels."

Another important paper in this field is "Structural Beams in Torsion" by I. Lyse and B. G. Johnston (*Trans. A.S.C.E.*, 1936), in which some of the results are in conflict with those of Trayer and March.

### Graphical Methods

Nearly all calculations that can be made analytically can also be made graphically, and numerous papers describing graphical methods have been written. One of the best for describing a graphical system of analysis for that type of member is L. H. Nishkian and D. B. Steinman's work on "Moments in Restrained and Continuous Beams by the Method of Conjugate Points" (*Trans. A.S.C.E.*, 1927).

The graphical method of analyzing plane trusses is much used, but it is difficult to extend the method to three-dimensional frameworks. Methods of accomplishing this, however, are described by F. H. Constant in "Stresses in Space Structures" (*Trans. A.S.C.E.*, 1935) and by E. Moness in "Solving Space Structures Graphically" (*Aviation*, December, 1937 and March, 1938). The Constant paper is somewhat more general in scope but does not give as clear an illustrative example as that of Moness. The latter shows how his method can be applied to the analysis of an engine mount. His paper should be of great interest to an engineer who likes graphical methods, and it illustrates one practical use of descriptive geometry.

### Columns

An excellent general discussion of column theory is found in "Rational Design of Steel Columns" by D. H. Young (*Trans. A.S.C.E.*, 1936). Another valuable paper is that on the "Strength of Steel Columns" by H. B. Westergaard and W. R. Osgood (*Appl. Mech., Trans. A.S.M.E.*, May-August, 1928). This is a study of the design of both straight and slightly curved columns from the viewpoint of the "double-modulus" theory. In "A New Relationship for Use in the Design of Machine Columns" (*Jour. Appl. Mech.*, June, 1938), W. H. Clapp describes as convenient a type of chart for applying the secant type of column formula as has yet been presented. An important feature of Professor Clapp's chart is that the user can choose the degree of accidental eccentricity he wishes to assume.

The problem of the effect of initial bending on the strength of struts is discussed by Westergaard and Osgood in the paper mentioned above, and also by J. E. Younger in the *Strength of Bent Struts* (I.C. 580, 1926). Younger develops not only a formula but also a nomograph for long struts with assumed initial bends. From this nomograph one can determine whether a specified amount of initial bending would reduce the probable strength of the member by more than 10 per cent.

The column formulas of this volume are limited in applicability to members of uniform section, but the designer is often called on to deal with columns of varying section. While many papers have been written on this subject, the only ones to be mentioned here are "A Method for Determining the Ultimate Strength of a Column Swaged at the Ends" by J. M. Gwinn, Jr., and R. A. Miller (*Jour. Aero. Sci.*, May, 1935); "Design of Columns of Varying Cross-section" by A. Dinnik (*Appl. Mech., Trans. A.S.M.E.*, Sept. 30, 1932); and *Compression Struts with Non-progressively Variable Moment of Inertia* by B. Radomski (T.M. 861, 1938).

Many reports have been written describing specific column tests. One of the more important recent ones is that on *Column Strength of Tubes Elastically Restrained against Rotation at the Ends* by W. R. Osgood (T.R. 615, 1938). This covers tests on about 200 tubes, mostly with pin ends. Some, however, were tested with measured restraining moments at the ends. From the results of the tests and the double-modulus theory of column action Osgood develops design formulas and curves, which, though more complex than the formulas of ANC-5, give practically the same results.

The problem of determining the effective degree of restraint in a column test has been attacked by several investigators. One ingenious line of attack is that of B. C. Stephens in "Natural Vibration Frequencies of Structural Members as an Indication of End Fixity and Magnitude of Stress" (*Jour. Aero. Sci.*, December, 1936). In this paper are developed theoretical relations among frequency, restraint coefficient, and axial load that were verified by test. The development is not carried out, however, to the point where the relations can be applied in general practice. Another interesting attack on the same problem is that of W. L. Howland in "A Method of Determining End Fixity" (*Jour. Aero. Sci.*, May, 1939).

Nearly all studies of columns assume that the load is gradually applied and that the problem is one of statics. The question may also arise as to the load that would be critical if applied suddenly and for a very short duration. This is the subject of *Impact Buckling of Thin Bars in the Elastic Range, Hinged at Both Ends* by C. Koning and J. Taub (T.M. 748, 1934), and *Impact Buckling of Thin Bars in the Elastic Range for Any End Condition* by J. Taub (T.M. 749, 1934). These authors find the critical load to be quite dependent on the duration of load application, and if the latter is very short the former will be appreciably greater than the Euler load. The mathematics of these papers is quite formidable.

### Deflections

In "Deflection of Beams of Varying Cross-section" (*Jour. Appl. Mech.*, June, 1937), M. Hetenyi develops a method of representing the change in  $I$  due to a reinforcing plate by a system of hypothetical loads. This method is applicable only when the change is in steps rather than continuous. It can also be adapted, however, to the analysis of columns of varying section. In an appendix, Hetenyi shows how Maclaurin's theorem can be used to simplify the writing of the equation of the elastic curve of a constant section beam. Thus it opens up several interesting lines of study.

A rather complete proof of the impossibility of finding an "effective moment of inertia" for a truss which would permit truss deflections to be computed from the beam formulas is given by A. E. Swickard in *Metal-truss Wing Spars* (T.N. 383, 1931).

Probably the most extensive study of the effect of shear deformation on the deflection of beams is the report by J. A. Newlin and G. W. Trayer on *Deflection of Beams with Special Reference to Shear Deformations* (T. R. 180, 1924). This report includes both a considerable body of test results and the development of formulas for the shear deflection of  $I$  and box beams.

### Statically Indeterminate Structures

The Maxwell-Mohr method of analyzing redundant structures and the method of virtual work for computing deflections and rotations are closely connected in the literature. In the earlier American texts the method of virtual work was used only to compute linear deflections. The extension to computing rotations and the use of rotations so computed in practical

analysis were first described in this country by G. F. Swain, "On a New Principle in the Theory of Structures" (*Trans. A.S.C.E.*, 1919-20). Regardless of one's opinion of Professor Swain's originality, the paper and accompanying discussion are well worth reading.

The method of least work has been the subject of many papers, of which only a few can be mentioned. In his paper *On Castigliano's Theorem of Least Work, and the Principle of St. Venant* (R. & M. 821, 1922-23), R. V. Southwell develops new proofs of these propositions. This paper is an excellent exposition of some of the fundamentals of structural theory. It also includes an interesting discussion showing that Castigliano proved his theorem by a comparison of deflections (Maxwell's method), while the new proof (Southwell's) depends only on superposition and the principle of conservation of energy. The principle of virtual work is not even mentioned as a step in the proof, only those who follow the German tradition initiated by O. Mohr considering that principle to be convenient for the purpose.

In "The Application of the Principle of Least Work to the Primary Stress Calculation of Space Frameworks" (*Aero. Trans. A.S.M.E.*, July-September, 1929), C. P. Burgess develops the basic procedure for applying that method to a rigid airship frame and also discusses several simplifying assumptions. These include the inverse-ratio theory and a clever method of treating the structure as a continuous tube instead of as a jointed framework. The latter might be developed to provide a valuable tool for fuselage shell analysis. In an appendix he shows how to use the Gauss method to solve a group of simultaneous equations. This method does not greatly reduce computation labor but shows up numerical errors before their effect is carried on to later stages of the computations.

The paper *On a Method of Direct Design of Framed Structures Having Redundant Bracing* (R. & M. 793, 1922-23), A. J. S. Pippard presents an interesting variation of the usual method of applying least work. In it the computer assumes unit stresses and develops deformation equations that are solved to determine the required sectional areas. A companion paper by Pippard is on *The Reduction of the Effective Value of Young's Modulus in Flexible Compression Members* (R. & M. 792, 1922-23). In this he shows how one can take account of the difference between the straight-line distance between the ends of a column and the distance measured along the elastic curve as well as the axial shortening,  $PL/AE$ , in a least-work analysis. Another study of the same problem is presented by T. W. K. Clark in "Bow-strain" (*Flight*, Sept. 27, 1934). Clark's paper includes a table of formulas for the difference between the length of the elastic curve and its chord for various loading conditions. Both of these papers should be better known.

An interesting summary of methods used to compute the secondary bending stresses due to joint rigidity is given by C. V. von Abo in "Secondary Stresses in Bridges" (*Trans. A.S.C.E.*, 1926). It does not include the method of moment distribution, however, as that had not yet been published.

While some engineers develop methods of computing the joint-rigidity stresses, others claim that they are not particularly important in design since



yielding of the material takes place at highly stressed points. As a result, it is claimed that the factor of safety and ultimate load is not reduced to anything like the extent that is indicated by the computed secondary moments. This attitude is expressed and backed up by test results in the "Effect of Secondary Stresses upon Ultimate Strength" by J. I. Parcel and E. B. Murer (*Trans. A.S.C.E.*, 1936). Though the authors were interested primarily in bridge structures, their work is of interest to the airplane designer as well.

Another objection to the standard methods of computing secondary stresses is that they depend on the unjustified assumption that the joints between members are absolutely rigid. In "Elastic Properties of Riveted Connections" (*Trans. A.S.C.E.*, 1936), J. C. Rathbun reports on some tests of typical riveted joints to determine their action and also shows how the elasticity of a joint can be allowed for in rigid-frame computations that are being carried out by the Maxwell-Mohr method, moment distribution, or slope deflection. While the test data are hardly applicable to airplane design, the methods of analysis proposed may be found of value.

The method of determining the stresses in a fuselage frame resulting from torsion that is described in Art. 8 : 11 is taken from *The Analysis of Aircraft Structures as Space Frameworks, Method Based on the Forces in the Longitudinal Members* by H. Wagner (T.M. 522, 1929). That report also shows how the same line of attack can be extended to more complex problems. Some of the structures considered are actually statically determinate, but others, like the fuselage frame, are made susceptible to treatment as such only by limitation to the loadings. Though the method appears valuable the report is difficult to follow.

Rigid airship frameworks are so highly indeterminate that they cannot be handled by the standard methods. One result has been the development of methods of analysis in which they are treated as tubes rather than frameworks. The work of Burgess in this line has been mentioned above. In England more extensive work has been done by R. V. Southwell and his associates and is covered by a series of reports under the general title *On the Determination of the Stresses in Braced Frameworks* (R. & M. 737, 1920-21; R. & M. 790, 1921-22; R. & M. 791, 1922-23; R. & M. 819, 1922-23; and R. & M. 1573, 1932-33). The paper by L. Chitty on the *Application of a Method for Determining the Stresses in Braced Frameworks* (R. & M. 1528, 1932-33) is also one of this series. Paralleling the work of Southwell, Professor A. J. S. Pippard carried out *An Experimental Investigation into the Properties of Certain Framed Structures Having Redundant Members* (R. & M. 948, 1924-25, R. & M. 971, 977, and 1002, 1925-26) on a simplified airship model.

Occasionally a new design calls for the development of a new method of analysis. An example is the design of the towers of the Golden Gate Bridge, which is the subject of "Williot Equations for Statically Indeterminate Structures in Combination with Moment Equations in Terms of Angular Displacements" by C. A. Ellis (*Trans. A.S.C.E.*, 1935). Though few airplane designers are likely to be called on to design such large structures, the methods

described might prove valuable in the design of heavy fuselage bulkheads. Perhaps the chief value of the paper, however, is the good description of the various steps taken in making the analysis, showing how one assumption after another is replaced by computed values as the analysis progresses. In this way it gives an excellent description of how to carry out the analysis and design of a complex structure.

### Beam-columns

A convenient method of computing the total bending moments at the half, quarter, and one-eighth span points of a beam-column subjected to a uniformly distributed side load is presented by H. W. Sibert in "A Note on Beams under Combined Side and Axial Loads" (*Jour. Aero. Sci.*, July, 1936). This method is based on a rearrangement of the formulas of Art. 14 : 5.

In "A Deflection Formula for Single-span Beams of Constant Section Subjected to Combined Axial and Transverse Loads" (T.N. 540, 1935), W. F. Burke shows an application of Timoshenko's trigonometric series method described in Art. 18 : 4. The paper also includes a formula for Schwartz's "spring constant" for use in jury-strut problems and tables and charts to obtain the necessary coefficients. The work of Schwartz referred to here is mentioned below in the section Critical Loads.

In Art. 14 : 15 it is shown how polar diagrams can be used to determine the total bending moments on beam-columns. J. D. Akerman and B. C. Stephens have developed the use of "Polar Diagrams for the Solution of Deflections of Axially Loaded Beams" (*Jour. Aero. Sci.*, July, 1938).

The extension of the moment distribution method to beam-columns is the work of B. W. James in "Principal Effects of Axial Load on Moment Distribution Analysis of Rigid Structures" (T.N. 534, 1935). The curves of Figs. 14 : 12 to 14 : 22 are taken from that paper where they are drawn to a larger scale. For practical work, however, the curves are not as convenient as tables, of which the most extensive are the *Tables of Stiffness and Carry-over Factors for Structural Members under Axial Load* (T.N. 652, 1938) by E. E. Lundquist and W. D. Kroll, from which much of the data in Tables 14 : 8 and 14 : 9 are taken. These tables were computed primarily for use with the procedure developed by Lundquist for computing the critical loading for a truss in *Stability of Structural Members under Axial Load* (T.N. 617, 1937).

There is relatively little material on the allowable loads on beam-columns. For wood members there is the very satisfactory report of J. A. Newlin and G. W. Trayer on *Stresses in Wood Members Subjected to Combined Column and Beam Action* (T.R. 188, 1924). For metal there is the report on *Strength of Tubing under Combined Axial and Transverse Load* by L. B. Tuckerman, S. N. Petrenko, and C. D. Johnson (T.N. 307, 1929), which is limited to round steel tubes, and the more recent *Combined Beam-column Stresses of Aluminum-alloy Channel Sections* by R. Gottlieb, T. M. Thompson, and E. C. Witt (T.N. 726, 1939) which is unfortunately limited to a single size of member. There is much room for more experimental work in this field, in connection

with relatively stocky members. To date, however, it has been overshadowed by the attention paid to structures of very thin metal.

### General Reports on Thin Metal

Several reports have been written to summarize the problems connected with the design of thin metal structures and the methods that had been developed to surmount them. Each of these reports has drawn freely from its predecessors and each has been made more and more obsolete by the developments recorded in papers on special phases of the general problem. They retain considerable value, however, in presenting the subject as a whole rather than as a group of separate problems. The three most important of these reports are the *Summary of the Present State of Knowledge Regarding Sheet Metal Construction* by H. L. Cox (R. & M. 1553, 1933); *Methods and Formulas for Calculating the Strength of Plate and Shell Constructions as Used in Airplane Design* by O. S. Heck and H. Ebner (T.M. 785, 1936), which has also been translated under the title "Strength of Plate and Shell Structures in Airplane Construction" (*Jour. Roy. Aero. Soc.*, October, 1936); and the *Progress Report on Methods of Analysis Applicable to Monocoque Structures*, Revision I, by E. E. Sechler and J. S. Newell, Wright Field Serial Report 4313, Revised, 1941. Of the two translations of the Heck and Ebner paper, the British, though perhaps less readily available in this country, is the better.

### Tension-field Beams

The first and most important single paper on the analysis of tension-field beams is still that of H. Wagner on the "Flat Sheet Metal Girder with Very Thin Metal Web" (T.M. 604, 605, and 606, 1929). Since its publication, however, numerous papers have been written on special phases of the subject. One of the most important problems has been that of determining the degree of completeness of the tension field and the effects of the residual diagonal compression. This has been studied by R. Lahde and H. Wagner in *Tests for the Determination of the Stress Condition in Tension Fields* (T.M. 809, 1936) and also by A. Kromm and K. Marguerre in the *Behavior of a Plate Strip under Shear and Compressive Stresses beyond the Buckling Limit* (T.M. 870, 1938). The latter paper contains an extensive mathematical study of the problem and curves for use in design. A pair of interesting British articles on the same subject are "Stiffness in Stressed Skins" (*Aircraft Eng.*, August, 1936) and "Tension Diagonal Fields" (*Aircraft Eng.*, January, 1937) by E. H. Atkin. "Shear Field Aircraft Spars" by J. E. Lipp (*Jour. Aero. Sci.*, November, 1939) is a valuable qualitative discussion of tension-field beams which points out their chief merits and includes a number of remarks on practical design based on the experience of the Douglas Co. "Rational Analysis of Tension-Field Beams" by H. W. Sibert, (*Jour. Aero. Sci.*, November, 1942) presents some formulas for beams of constant or variable cross-section.

## Shells

The method of shell analysis described in Chapter XVI is based largely on a considerable group of papers that has appeared in the last decade. Most of the underlying theory was presented in the earlier papers, the later ones being devoted primarily to simplifying the practical procedure. The earliest of the important papers was *The Torsion and Flexure of Cylinders and Tubes* by W. J. Duncan (R. & M. 1444, 1931). This was highly mathematical and not a very suitable guide for practical design. Almost contemporaneous with Duncan's work was E. H. Atkin's paper on "Torsion in Thin Cylinders" (*Flight*, Sept. 25 and Oct. 30, 1931). While later writers have developed somewhat simpler methods of carrying out the computations or of visualizing their significance, their procedures for handling torsion are essentially those of Atkin. Among these later papers one of the best is "Torsion on a Multi-cell Section with Thin Walls" by J. Lobley (*Flight*, June 18, 1936, with typographical errors listed July 30, 1936). Others are *The Torsional Stiffness of Thin Duralumin Shells Subjected to Large Torques* (T.N. 500, 1934) and *The Initial Torsional Stiffness of Shells with Interior Walls* (T.N. 542, 1935), both by P. Kuhn.

The practical solution of the problem of the distribution of transverse shear on a shell section is based on *Some Features of the Behaviour in Bending of Thin-walled Tubes and Channels* by D. Williams (R. & M. 1669, 1935). This is too highly mathematical for use in practical design but is the basis of the much more practical "Shear Stresses in Hollow Sections" by W. J. Goodey (*Aircraft Eng.*, April, 1936). Since the publication of this paper some of the most important contributions to the subject are those of R. S. Hatcher in "Rational Shear Analysis of Box Girders" (*Jour. Aero. Sci.*, April, 1937) and in a "Letter to the Editor" of the *Journal of the Aeronautical Sciences* in July, 1938. In the letter he developed the concept of the "stress center." The practical application of the method has also been advanced by P. Kuhn in his *Remarks on the Elastic Axis of Shell Wings* (T.N. 562, 1936) and even more in *Some Elementary Principles of Shell Stress Analysis with Notes on the Use of the Shear Center* (T.N. 691, 1939).

A most interesting development of the general procedure is the "Unit Method of Beam Analysis" of F. R. Shanley and F. P. Cozzone (*Jour. Aero. Sci.*, April, 1941) which is partially described in Art. 16 : 17. This paper is of value not only for the method of shell analysis presented in it but also for its discussion and illustration of methods used at the Lockheed Co. for arranging and recording computations. The latter, while basically quite similar to those illustrated in Chapter XVI, differ in detail, and the system shown for indicating when and how to get numerical checks on the computations is much more extensive.

A number of important reports on shells have been translated from the German. Earliest of these is *The Stress Distribution in Shell Bodies and Wings as an Equilibrium Problem* by H. Wagner (T.M. 817, 1937). Practically

contemporaneous is *The Strength of Shell Bodies — Theory and Practice* by H. Ebner (T.M. 838, 1937), which gives an excellent general survey of the problems involved and indicates how they can be handled. It also includes a bibliography which is a good guide to earlier studies of the subject. It is thus one of the best introductions to the special problems of monocoque fuselage design and analysis. This basic paper was followed by the *Calculation of Load Distribution in Stiffened Cylindrical Shells* by H. Ebner and H. Koller (T.M. 866, 1938), in which the methods of calculation are gone into in more detail and some of the more common special problems are considered. The authors also discuss the light thrown on their theory by E. Schapitz and G. Krumling in *Load Tests on a Stiffened Circular Cylindrical Shell* (T.M. 864, 1938). These two reports were prepared in conjunction, one presenting the theoretical and the other the experimental results.

While most of the work on shells has been directed toward the problem of the action of the member in bending, the problem of action under torsion is also of importance. Donnell's work was limited to cylinders without reinforcing members. E. Schapitz in *The Twisting of Thin Walled Stiffened Circular Cylinders* (T.M. 878, 1938) takes up the question of what happens when stiffeners are present and the skin develops incomplete tension fields. The mathematics of this report is rather formidable.

A recent report on the general problem of shell design is *The Strength of Shell and Tubular Spar Wings* by H. Ebner (T.M. 933, 1940).

Few reports have been published on the strength of shells in bending, other than those directed to a determination of the effective width of skin acting with the stiffeners. Two of the best reports of wider scope are the *Experimental and Analytical Investigation of a Monocoque Wing Model Loaded in Bending* by E. Schapitz, H. Feller, and H. Koller (T.M. 915, 1939) and "Corrugated Panels under Combined Compression and Shear Load" by P. A. Sanderson and J. R. Fischel, (*Jour. Aero. Sci.*, February, 1940). In the latter report a formula is developed for the interaction curve for panels subjected to a combination of axial compression and shear, a subject on which there are very few available data.

### Shear Lag

A very interesting though rather unconventional explanation of the phenomenon of shear lag is given by F. R. Shanley in "Box Beams and Shear Lag" (*Aviation*, October, 1937). The most important series of reports on the subject, however, is that of P. Kuhn. This begins with *Stress Analysis of Beams with Shear Deformation of the Flanges* (T.R. 608, 1937). In this introduction to the problem Kuhn handles a few simple cases by presenting and solving the differential equations involved. He also develops a method of solution by successive trials in which the physical actions represented are more apparent than in the equations and which seems to be more susceptible to expansion for use in practical design. Only flat panels and rectangular section boxes, however, are treated. In *Approximate Stress Analysis of Multi-stringer Beams with Shear Deformation of the Flanges* (T.R. 636, 1938), the

methods of Technical Report 608 are expanded for use with cambered boxes, and the method of handling panels with several longitudinal stiffeners is simplified. The report also includes data on tests. These two reports were paralleled by a paper on "Bending Stresses in Box Beams as Influenced by Shear Deformation" (*S.A.E. Jour.*, August, 1938) which is a less mathematical and more descriptive account of the subject. These papers were followed by *Some Notes on the Numerical Solution of Shear-lag and Mathematically Related Problems* (T.N. 704, 1939). Here he gives a simple numerical method of solving differential equations of the type,  $d^2y/dx^2 = K_1y - K_2$ . Since this type of equation is found in other structural problems as well as those connected with shear lag, the method is of considerable interest. Kuhn's most recent unrestricted report in this field is "A Recurrence Formula for Shear Lag Problems" (T.N. 739, 1939).

Paralleling the work of Kuhn is that of E. Reissner. The latter's first paper on the subject is "On the Problem of Stress Distribution in Wide Flanged Box Beams" (*Jour. Aero. Sci.*, June, 1938). This is primarily a theoretical paper limited in scope to corrugated sheet and it is difficult to see how the formulas can be applied in practice. A later paper of wider scope is on "Least Work Solutions of Shear Lag Problems" (*Jour. Aero. Sci.*, May, 1941).

Another paper covering a phenomenon closely related to shear lag is on "A Hidden Safety Factor in the Design of Metal Wings" by H. W. Sibert (*Jour. Aero. Sci.*, December, 1940).

### Torsion-bending Stresses

The method of computing torsion-bending stresses outlined in Art. 16 : 20 was developed by P. Kuhn in "Bending Stresses Due to Torsion in Cantilever Box Wings" (T.N. 530, 1935). In this report only simple types of structures are considered. L. Lazzarino in *Twisting of Thin-walled Columns Perfectly Restrained at One End* (T.M. 854, 1938) developed more general formulas, but they are impractical for use in routine design. In England, J. L. Taylor in "The Theory of Torsion Bending" (*Aircraft Eng.*, October, 1938) took up the subject of the resistance of an open section to torsion when the end section is restrained from warping. This resistance is compared to that of a two-spar wing in which the torsion is taken up by differential bending in the two spars. A rough outline is given of a method for computing stresses and angles of twist, but the mathematical proof appears overcondensed.

### Strength of Intermediate Frames

When a fuselage shell is subjected to load, the chief function of some of the transverse rings is to withstand the forces imposed as a result of the development of diagonal tension fields in the skin. An early paper on this problem is "The Strength of Frames in Monocoque Construction" by C. Gurney (*Flight*, May 27, 1937). In *Loads Imposed on Intermediate Frames of Stiffened Shells* (T.N. 687, 1939), P. Kuhn criticizes Gurney's paper on the grounds that the tension field was assumed "complete," with a wrinkle angle of  $45^\circ$ , instead of

"incomplete," as they would be in practical design. Kuhn then goes into a more thorough discussion of the problem.

Another problem in connection with the design of rings is presented by the existence of openings. Little has been written on the subject, and the problem is still far from a satisfactory solution. Some idea of its difficulty and one promising line of attack are given by H. M. J. Kittlesen in "Openings in Circular Fuselages" (*Aircraft Eng.*, March, 1940).

### Pressurized Cabins

The development of pressurized cabins has brought into existence a number of specialized problems. The most extensive discussion of these problems is that of J. E. Younger in "Structural and Mechanical Problems Involved in Pressure (Supercharged) Cabin Design" (*Jour. Aero. Sci.*, March, 1938). This was written in connection with the design of the first pressurized cabin built by Lockheed. Two other valuable papers in this field, though less extensive in scope are "Tests of Pressurized Cabin Structures" by W. L. Howland and C. F. Beed (*Jour. Aero Sci.*, November, 1940) and "Some Structural Problems Pertaining to Pressurized Fuselages" (*Jour. Aero. Sci.*, June, 1939).

### Curved Beams and Rings

A relatively simple formula for the stresses in sharply curved beams is developed by H. C. Perkins in "Stresses in Curved Bars" (*Appl. Mech., Trans. A.S.M.E.*, September-December, 1931).

Numerous papers have been written regarding the design of rings for airplane fuselages. One of the earliest of these to be mentioned here is that of R. A. Miller and K. D. Wood on "Formulas for the Stress Analysis of Circular Rings in a Monocoque Fuselage" (T.N. 462, 1933). Almost contemporary was W. F. Burke's "Working Charts for the Stress Analysis of Elliptic Rings" (T.N. 444, 1933). These were followed by "General Equations for the Stress Analysis of Rings" by E. E. Lundquist and W. F. Burke (T.R. 509, 1935). One defect of all three of these reports is that the formulas are based on the assumption that  $1/R = M/EI$ , the curvature corrections of Chapter XVII being neglected. The same is true of E. H. Watts' paper on the "Simplified Method of Beam Analogy" (*Aero Digest*, April, 1937), which, however, shows the application of the "column analogy" of Hardy Cross for solving frames with not more than three redundants. The best paper on ring analysis is that on the "Analysis of Circular Rings for Monocoque Fuselages" by J. A. Wise (*Jour. Aero. Sci.*, September, 1939) from which the curves of Figs. 17 : 10 to 17 : 12 were obtained.

### Problems of Elastic Stability

An excellent introduction to the nature of elastic stability problems is presented by L. H. Donnell in "The Problem of Elastic Stability" (*Trans. A.S.M.E.*, October-December, 1933).

The germ of the Spring constant method of attacking problems in this field, as described in Arts. 18 : 7 to 18 : 11, is to be found in the *Analysis of a Strut with a Single Elastic Support in the Span, with Applications to the Design of Airplane Jury-strut Systems* by A. M. Schwartz and R. Bogert (T.N. 529, 1935). Another paper in the same field is that of R. F. Bache and W. B. Klemperer on "The Behavior of Bowed Columns with Intermediate Elastic Supports" (*Jour. Aero. Sci.*, February, 1937).

The problem of the determination of the critical load for a rigid jointed truss has been attacked by several authors. Prior to the solution by N. J. Hoff outlined in Art. 18 : 12 and 18 : 13 the most successful attack was that of E. E. Lundquist in *A Method for Estimating the Critical Buckling Load for Structural Members* (T.N. 717, 1939). The most complete exposition of Hoff's work is to be found in his paper on "Stress Analysis of Aircraft Frameworks" (*Jour. Roy. Aero. Soc.*, July, 1941). Partial accounts are to be found in "Stable and Unstable Equilibrium of Plane Frameworks" (*Jour. Aero. Sci.*, January, 1941) and "The Proportioning of Aircraft Frameworks" (*Jour. Aero. Sci.*, June, 1941).

Southwell's method of determining critical loads experimentally, outlined in Art. 18 : 14, is described and developed in more detail in the papers referred to in that article, all three of which are well worth study.

In most studies of elastic stability the deflections are assumed small in comparison with the thickness of the material used. With the thin metal structures that are commonly used in airplane construction, particularly when the sheet is curved, this results in erroneous conclusions and a technique of attacking the problems by a procedure in which the deflections are assumed relatively large is needed. An early attempt to develop a "large deflection" theory is that of L. H. Donnell in "A New Theory for the Buckling of Thin Cylinders Under Axial Compression and Bending" (*Trans. A.S.M.E.*, November, 1934). More recently Dr. von Karman has taken up the problem and he and H. S. Tsien have produced three papers in this field, "The Buckling of Spherical Shells by External Pressure" (*Jour. Aero. Sci.*, December, 1939), "The Influence of Curvature on the Buckling Characteristics of Structures" (*Jour. Aero. Sci.*, May, 1940), and "The Buckling of Thin Cylindrical Shells under Axial Compression" (*Jour. Aero. Sci.*, June, 1941). L. S. Dunn is also credited with part authorship of the second of these papers. While these three papers do not bring the development of the large deflection theory to the point where it can be used in practical airplane design, they constitute important steps toward that end, and it is to be expected that further work of Dr. von Karman along this line will eventually result in important modifications of present design practice.

An important problem of elastic instability is discussed by E. E. Lundquist "On the Rib Stiffness Required for Box Beams" (*Jour. Aero. Sci.*, May, 1939). This paper is highly mathematical and should be regarded as a basis for developing practical design formulas rather than as presenting such formulas ready for use.



### Torsional Column Failure

Though the subject of torsional failure of columns was discussed by H. Wagner in *Torsion and Buckling of Open Sections* (T.M. 807, 1936) and by H. Wagner and W. Pretschner in a later paper with the same title (T.M. 784, 1936), their formulas are erroneous. This was shown by R. Kappus in *Twisting Failure of Centrally Loaded Open-section Columns in the Elastic Range* (T.M. 851, 1938). Kappus has produced the most complete theoretical treatment of the problem to date. Somewhat antedating Kappus the problem was attacked in this country, and *A Theory for Primary Failure of Straight Centrally Loaded Columns* by E. E. Lundquist and C. M. Fligg (T.R. 582, 1937) and *On the Strength of Columns that Fail by Twisting* by E. E. Lundquist (*Jour. Aero. Sci.*, April, 1937) were published. Though not covering as much ground as the papers by Kappus, these papers are easier to follow. As a sequel to the theoretical work of Lundquist and Fligg, A. S. Niles made a series of tests that are recorded in his *Experimental Study of Torsional Column Failure* (T.N. 733, 1939).

Though fairly old and devoted primarily to wood construction, *Elastic Instability of Members Having Sections Common in Aircraft Construction* by G. W. Trayer and H. W. March (T.R. 382, 1931) is of interest on account of its discussion of the problem of twisting failure of columns that are not of thin metal section. It also records the results of tests on wooden channel and cruciform section struts.

### Columns

Although it appeared before much of the current theory of the action of thin-metal structures under load had been developed, R. A. Miller's report on the *Compression Strength of Duralumin Columns* (I.C. 598, 1927) remains one of the most convenient sources for determining the crippling strength of a column. More recent studies of crippling strength which cover a wider range of sections are to be found in *Local Instability of Symmetrical Rectangular Tube under Axial Compression* (T.N. 686, 1939) and *Local Instability of Centrally Loaded Columns of Channel Section and Z-Section* (T.N. 722, 1939) by E. E. Lundquist, and in *Local Instability of Columns with I-, Z-, Channel and Rectangular Tube Sections* (T.N. 743, 1939) by E. Z. Stowell and E. E. Lundquist.

### Unstiffened Panels

Much of the allowable stress data used in thin metal design has been obtained from tests of small panels. The earlier tests were made on flat or curved sheet without stiffening members besides guides at the otherwise free edges, while the later tests have usually been made on stiffened panels. The first important set of tests in this field were those on the *Strength of Rectangular Flat Panels under Edge Compression* by L. Schuman and G. Back (T.R. 356, 1930) from which von Karman developed the concept of effective width. These tests were followed by others on both flat and curved panels that were reported on by J. S. Newell in the "Strength of Aluminum Alloy Sheets" (*Airway Age*, November and December, 1930). Shortly afterward, the tests

were carried out that were published several years later in *The Column Properties of Corrugated Aluminum Alloy Sheet* by C. F. Greene and C. G. Brown (I.C. 699, 1935). Similar tests on flat sheet were reported on by H. L. Cox in *The Buckling of Thin Plates in Compression* (R. & M. 1554, 1934).

### Stiffened Panels

Since the general adoption of the effective width concept much test work has been directed to the determination of the factors affecting that quantity. One of the earliest reports on this subject is on *Experimental Studies of the Effective Width of Buckled Sheet* by R. H. Lahde and H. Wagner (T.M. 814, 1936). This was followed by the theoretical paper by K. Marguerre on *The Apparent Width of the Plate in Compression* (T.M. 833, 1937). About the same time E. E. Sechler summarized the work on panels that had then been done at GALCIT in "Stress Distribution in Stiffened Panels under Compression" (*Jour. Aero. Sci.*, June, 1937). The *Experimental Study of Deformation and of Effective Width in Axially Loaded Sheet-stringer Panels* of W. Ramberg, A. E. Macpherson, and S. Levy (T.N. 684, 1939) included very elaborate tests on two panels. Among the results was a fairly good confirmation of the Marguerre formulas, but the number of tests was too small to be conclusive.

Several important papers cover work on panels that has been carried out at the Lockheed Co. Among them are "Measurement of Stiffener Stresses and Effective Widths in Stiffened Panels" by H. B. Dickenson and J. R. Fischel (*Jour. Aero. Sci.*, April, 1939); "Effective Widths in Stiffened Panels under Compression" by J. R. Fischel (*Jour. Aero. Sci.*, March, 1940); "Permanent Buckling Stress of Thin-sheet Panels under Compression" by W. L. Howland and P. E. Sandorff (*Jour. Aero. Sci.*, May, 1941), and "The Compressive Strength of Thin Aluminum Alloy Sheet in the Plastic Region" by J. R. Fischel (*Jour. Aero. Sci.*, August, 1941).

While most investigators interpret panel tests in the light of the concept of effective width, in "Empirical Formulas for Allowable Compression Loads in Stiffened Sheet Panels" (*Jour. Aero. Sci.*, October, 1939) E. R. Reff reverts to the alternative method of assuming the strength of the panel to be the sum of the strengths of the sheet alone and the stiffeners alone. In that paper he develops a formula for the load that can be carried by a stiffener when restrained from buckling by a sheet of given thickness.

The last paper on tests of flat panels to be mentioned here is L. G. Dunn's report on *An Investigation of Sheet-stiffener Panels Subjected to Compression Loads with Particular Reference to Torsionally Weak Stiffeners* (T. N. 752, 1940). While some important and previously unknown facts were developed by this investigation, the range of sizes used in the test specimens was very limited and tests made elsewhere indicate that some of the conclusions were broader than were justified by the experiments.

The panels discussed in the preceding group of reports were flat, but it has been recognized from the beginning that the effective width of curved sheet would differ from that of flat. Some early experimental work to determine the effective width of curved sheet was reported by H. Wagner and W.

Ballerstadt in *Tension Fields in Originally Curved, Thin Sheet during Shearing Stresses* (T.M. 774, 1935). A very extensive series of tests in which stainless steel rather than aluminum alloy specimens were used was carried out by the Air Corps, and the results were published in four reports with the general title of *An Investigation of the Compressive Strength Properties of Stainless Steel Sheet-stringer Combinations*. Part I by E. H. Schwartz and C. G. Brown (I.C. 697, 1934) and Part II by E. H. Schwartz (I.C. 705, 1936) cover a very extensive study of flat panels. Part III — *Cylindrical Specimens* by C. G. Brown, J. Matulaitis, and J. E. Younger (I.C. 706, 1936) is devoted to tests made on such large specimens that they had to be tested in the 10,000,000-lb. testing machine at the University of California. Part IV — *Effect of Variations in the Component Parts of Three Particular Types of Stiffeners* by J. Matulaitis and E. H. Schwartz (I.C. 708, 1937) is of considerable value for the light it throws on some questions of detailed stiffener design.

The question of the effective width of curved panels is also covered by *The Buckling of Curved Tension Field Girders* by G. Limpert (T.M. 846, 1938) and by W. A. Wenzek's report on *The Effective Width of Curved Sheet after Buckling* (T.M. 880, 1938). Both reports include test data as well as theoretical discussions.

The Bureau of Standards has done comparatively little testing of panels, but one of their characteristically thorough tests is reported in *Compressive Tests of a Monocoque Box* by W. Ramberg, A. E. Macpherson, and S. Levy (T.N. 721, 1939).

### Miscellaneous Subjects

A report of value which is difficult to classify is that by H. Wagner of *Remarks on Airplane Struts and Girders under Compressive and Bending Stresses. Index Values* (T.M. 500, 1929). In this paper Wagner takes up the question of the degree of intensity of the loading on a structure and shows how it can be expressed quantitatively. This is a field in which little work has been done, and it is unfortunate that Wagner's work has not been followed up.

In the last few years there has been great activity in the use of electrical devices for measuring strains. An important resume of the methods used is to be found in *The Development of Electrical Strain Gages* by A. V. de Forest and H. Leaderman (T.N. 744, 1940). While it is possible to measure strain directly, the investigator is often most interested in determining the stresses that produce the strains. One valuable paper on this subject is "Principal Stresses from Three Strains at 45°" by H. W. Sibert (*Jour. Aero. Sci.*, November, 1939). A more important method, however, seems to be that developed by J. A. Wise in "Circles of Strain" (*Jour. Aero. Sci.*, August, 1940). These circles of strain are similar to Culmann's circles of stress described in Chapter VII.

The photoelastic method of measuring stresses is best described in the book of Frocht mentioned in an earlier section of the bibliography. There are, however, two papers that should be mentioned here. One is *Photoelastic Analysis of Three-dimensional Stress Systems Using Scattered Light* by R. Weller

and J. K. Bussey (T.N. 737, 1939). So far the photoelastic method has been used primarily in investigating plane systems of stress, but the paper in question describes a phase of this type of research which will probably gain in importance. An illustration of how the method can be applied in aeronautical work is supplied by T. J. Dolan and D. G. Richards in "A Photoelastic Study of the Stresses in Wing Ribs" (*Jour. Aero. Sci.*, June, 1940).

The use of thin metal in aircraft results in special problems of testing and requires the use of special procedures, particularly in connection with compressive tests. An important development in the field of determining the compressive strength properties of thin sheet is described by C. S. Aitchison and L. B. Tuckerman in *The "Pack" Method of Compressive Tests of Thin Specimens of Materials Used in Thin-wall Structures* (T.R. 649, 1939). That procedure is not applicable to tubing, for which, however, *The "Plug" Method for Obtaining the Compressive Elastic Properties of Thin-walled Sections* (*Jour. Aero. Sci.*, January, 1941) has been proposed by H. W. Barlow, H. S. Stillwell, and H. S. Lu.

Since much of the testing connected with aeronautic research must be done on models, the experimenter must be familiar with the probable effect of change of scale on the results. A good introduction to this subject is given by J. E. Younger in the "Principle of Similitude as Applied to Research on Thin-sheet Structures" (*Aero. Trans. A.S.M.E.*, October-December, 1933).

Another development of testing technique that is of considerable interest is described by A. V. de Forest and G. Ellis in "Brittle Lacquers as an Aid to Stress Analysis" (*Jour. Aero. Sci.*, March, 1940).

Much has been written about the various materials used in aircraft, and most of it is quickly made obsolescent by new developments. J. B. Johnson's "Materials for Airplane Construction" (*Jour. Aero. Sci.*, March, 1939) was an excellent summary of the material situation as it existed at that time. Narrower in scope but more detailed in their fields are "Recent Developments in Magnesium Alloys" by J. C. Mathes (*Jour. Aero. Sci.*, November, 1940) and "Aircraft Plywoods and Adhesives" by T. D. Perry (*Jour. Aero. Sci.*, March, 1941).

It is impossible to list all the worthwhile papers, the catalogues, handbooks, and house organs treating aeronautical matters. The best source for such material and for papers on applied engineering and aircraft production is the *Aeronautical Engineering Review*, published monthly by the Institute of Aeronautical Sciences. It contains digests of current books and articles, classified as to the fields to which they apply, and while the digests are not as critical of material as is the above bibliography the student and engineer will find them of great assistance in locating material pertaining to any particular subject.



## INDEX

- Abbreviations, papers, 401  
periodicals, 402
- Absolute critical loading, 284, 295
- Active load, 297
- Adams, D. R., 399
- Adhesives, cold setting, 387
- Aero Digest* magazine, 403
- Aircraft Engineer, The*, magazine, 403
- Aircraft Engineering* magazine, 403
- Airway Age* magazine, 403
- Aitchison, C. S., 421
- Akerman, J. D., 411
- Algebra books, 394
- Allowable stress references, aluminum alloys, 361-367  
compact sections, 361, 366  
curved panels, 363, 366  
flat panels, 362, 366  
fuselage sections, 365-367  
magnesium alloys, 361-367  
notation, 360  
plastic materials, 361-367  
shells, 365-367  
steels, 361-367  
stiffener sections, 364, 366  
wing sections, 365-367  
wood, 361-367
- Allowable unit stresses, beam-columns, 84-90, 411  
use of stress ratios, 90
- Aluminum alloys, allowable stress references, 361-367
- American Magnesium Corp., 391
- American Society of Civil Engineers, 402
- American Society of Mechanical Engineers, 402
- Analytical geometry books, 394
- Anderson, N., 400
- Andree, W. L., 268
- Andrews, E. S., 396
- Anisotropic materials, definition, 360
- Anti-symmetric loadings, 267-269
- Apex of polar moment curve, 141
- Approximate computations, beam-columns, 115-116
- Areas, computation of, effective shell sections, 192  
mid-line method, 180  
Simpson's rule for, 35
- Army, Navy, Civil Committee on Aircraft Requirements, 366
- Assumptions, arbitrary, use in solving redundant structures, 2, 30
- Asymmetry, effect on shell analysis, 214
- Atkin, E. H., 412, 413
- Atwood, H., 375
- Aviation* magazine, 403
- Aviation Engineering* magazine, 403
- Axial load, effect of change between supports, 116-117  
general effect, 63-64  
*See also* Beam-columns and Three-moment equation, extended
- Axis, central, 257  
centroidal, 257
- Bache, R. F., 417
- Back, G., 406, 418
- Bacon, H. M., 394
- Bailey, F. H., 394
- Baker, J. F., 397
- Balancing (joint), at junction of more than two members, 39  
under rigid-frame sign convention, 38
- Ballerstedt, W., 216, 420
- Barlow, H. W., 367, 421
- Bartoe, W. F., 373
- Battelle Memorial Institute, 366, 396
- Beam-columns, allowable stress computations, metal, 90  
spruce, 84-90  
applicability of least work method, 25  
approximate computations, 115-116  
bending moments on, *See* Bending moments

- Beam-columns, continuous, computation  
     of reactions, 106  
     extended three-moment equation,  
         *See* Three-moment equation  
     general effect of axial load, 63-64  
     graphical analysis, 151  
     moment-distribution analysis, 120-  
         140  
     critical loads, *See* Critical loads  
     definition, 62  
     deflection of, *See* Deflections  
     elastic limit stress curves, 87, 85  
     graphical analysis, 141-151  
     historical notes on methods, 62, 150-  
         151  
     illustrative computations, 81-88, 130-  
         140  
     non-uniform section, 116-117, 132-140  
     papers on, 411  
     shear on, *See* Shear  
     significant figures needed in computa-  
         tions, 119  
     single span, change in axial load, 116  
         formulas for various loadings, 90-  
             109, 115, 141  
         general effect of axial load, 63-64  
         location of inflection points, 85-89  
         polar diagrams, 141-151  
         relation total to primary moment,  
             115-116  
         shear deflection effects, 118-119  
     slope, 91, 99, 67  
     spring constants, 297  
     stability, *See* Critical loads  
     trial design needed, 119-120  
     use of formulas, 119-120  
     *See also* Beams
- Beam convention for signs, 36-39
- Beams, bending moments on, *See* Bend-  
     ing moments
- complete tension field, 157-159, 412
- continuous, Maxwell-Mohr analysis,  
     8-10  
     papers on, 405, 406  
     solution by influence lines, 34-36
- curved, 257-267, 416  
     bending of, 257-263  
     computation of  $J$  and  $K$ , 261  
     deflections, 263-267  
     papers on, 416
- Beams, curved, sign conventions, 258,  
     263  
     stresses due to bending, 257-263  
     deflections, tension field, 173-178  
     trigonometric series method, 288-291  
     energy of, 288-289  
     incomplete tension field, 156-179, 412  
         analysis assumptions, 160  
         chord stresses, 170  
         deflections, 173-178  
         notation for, 159-160  
         rivets in, 166, 170  
         stiffener design, 166-170  
         web stresses, 160-166, 171-172  
     papers on, 405, 406, 412, 416  
     *See also* Beam-columns
- Bearing, allowable stress references, 362,  
     366
- Beed, C. F., 416
- Beggs, G. E., 36
- Bell Aircraft Corp., 156
- Bend radii, magnesium alloys, 388
- Bending, allowable stress references, 361,  
     364-367  
     curved beams, 257-263  
     rib and ring pressure, 225-227  
     rings, 270-278  
     secondary, beam chords, 171  
         in trusses, 39-41, 409, 410  
     thin-walled shells, 191-242  
         buckling lag, 216-218  
         effect of change in section, 239-242  
         effective material distribution, 220-  
             222, 192-193  
         effective section properties, 192-200  
         normal stress distribution, 200-203,  
             234-235  
         practical analysis, 222-223, 238-239  
         shear flow computation, 203-214,  
             224-225, 235-237  
         tapered, 232-239
- Bending moments, beam-columns, gen-  
     eral formulas, 90, 99, 141  
     graphical analysis, 141-151  
     maximum, 91, 96-98  
     minimum, 99  
     polar curves, 142-150  
     polar formula, 141  
     primary, 63  
     secondary, 63, 133

- Bending moments, beams, computation  
     when end moments are known,  
         38-39, 52  
     definition, 37  
     indication of character, 39, 47  
     qualitative curves, 2-4  
     relation to end moments, 37  
     sign conventions, 36-39  
     work due to, 24-26, 289  
 circular ring, 270-278  
 curved beams, sign conventions, 258,  
     263  
     secondary in trusses, 39-41, 303-310,  
         409, 410  
 Bent equation, 42-46, 50  
 Bernhard, R. K., 386  
 Berry, A., 62  
 Biot, M. A., 394  
 Blocks, filler, 88-89  
 Boeing Airplane Co., 170  
 Bogert, R., 417  
 Boobnoff, I. G., 366  
 Books, aeronautical, 401  
     mathematical, 393  
     structural, 396  
 Boulton, B. C., 404  
 Bowman, H. L., 397  
 Box sections, torsion-bending stresses,  
     231-232  
     *See also* Shells  
 Branch shear flows, 210-211  
 Bredt torsion formula, 185  
 Brown, C. G., 405, 419, 420  
 Bryan, C. W., 397  
 Buckling, beam webs, 157, 160-162,  
     166-168  
     impact, 408  
     plastic-bonded plywood, 383  
     shells, 216-218, 188  
     *See also* Stability, elastic  
 Buckling lag, 216-218  
 Building frame, wind load analysis,  
     41  
 Burgess, C. P., 409  
 Burke, W. F., 276, 411, 416  
 Bussey, J. K., 421  
 Byerly, W. E., 316  
 Cabins, pressurized, 416  
 Calculus books, 394  
 Calculus of variations, 317-323  
     application to derive Euler formula,  
         320  
     application to derive torsional column  
         failure formula, 334  
     nomenclature, 318-320  
     notation, 318-320  
     purpose, 317  
 Carlson, R. M., 89  
 Carpenter, F. M., 405  
 Carry-over factors, beam-columns, curves  
     of, 121  
     location on diagram, 131  
     non-uniform section, 132-135  
     tables of, 122-126  
     sign under rigid-frame convention, 38  
 Castigliano, C. A., 20, 396  
 Castigliano theorems, 20, 21  
 Castings, magnesium alloy, 388  
 Central axis, 257  
 Centroidal axis, 257  
 Channel, torsion-bending stresses, 228,  
     230  
     warping moments and constants, 349  
 Charts, nomographic, pin-ended length  
     of beam-column, 86  
     solution of cubic equation, 342  
 Chatfield, C. H., 401  
 Chitty, L., 410  
 Chord loads, incomplete tension field  
     beams, 170-172  
 Chrysler Corp., 386  
 Circle, hollow, geometric properties, 181  
 Circular rings, *See* Rings  
 Clapp, W. H., 407  
 Clark, T. W. K., 409  
 Clayton, W. C., 366  
 Coefficients, beam-column, fixed-end mo-  
     ment, 122-130  
     stiffness factor, 120-126, 128  
     three-moment equation, 72-78, 107-  
         108  
 Collapsing force, 226  
 Column analogy, 398  
 Column distribution factor, 45  
 Columns, bent, energy of, 320  
     bent and twisted, energy of, 332-335,  
         343-344  
     elastically supported, 291, 297, 300  
     Euler formula derivation, 320-323, 284



- Columns, papers on, 396, 407, 418  
 torsional failure, *See* Torsional column failure  
*See also* Compression
- Combined stresses, allowable stress references, 362-367
- Compact sections, allowable stress references, 361, 366
- Complete tension field beams, 157-159, 412
- Compressed wood, 385
- Compression, allowable stress references, 361-367  
 tests, thin metal, 421  
*See also* Columns
- Compressive strengths, magnesium alloys, 388-391  
 plastic-bonded plywood, 379-384
- Computation checks, moment distribution, no axial load, 38, 46  
 shell analysis, 198-200, 201-203, 207, 210, 213
- Computations, arrangement, 193-198, 31-34
- Condition, equations of, 11
- Connections, impossibility of computing internal work in, 30  
 magnesium alloys, 389  
 plastic-bonded plywood, 385-388
- Consistent deformation, principle of, 4, 30
- Consolidated Aircraft Corp., 156, 164, 168
- Constant, F. H., 407
- Constants for beam-column formulas, axial compression, 92-95, 104  
 axial tension, 100-103, 104-105  
 development for combined loadings, 91, 96
- Continuous beam-columns, *See* Beam-columns; Critical loads; and Three-moment equation
- Continuous beams, *See* Beams
- Correction shear flows, 210-213, 239
- Corrosion, magnesium alloys, 388
- Cosine, computation of, 67, 71  
 definition as series, 64  
 table of, 68-71  
 rule for interpolation, 67
- Cox, H. L., 412, 419
- Cozzone, F. P., 192, 223, 225, 239, 413
- Creep, magnesium alloys, 390
- Creep tests, 369
- Critical loading, definition, 284
- Critical loads, 283-315  
 absolute, 284, 295  
 beam-columns, definition, 109  
 effect of shear deformation, 118-119  
 general criteria, 114-115  
 independent of transverse load, 112  
 relation to ultimate strength, 109-110, 120  
 single-span, 110, 296-303  
 two-span, 111-114, 298-303  
 with concentrated side load, 296, 300
- column in elastic medium, 291-294  
 elastic, 310  
 elastically supported columns, 297-303  
 empirical determination, 309-311  
 fuselage stiffeners, 280  
 plastic, 310  
 rigid-jointed truss, 303-309  
 Southwell method for determination, 309-311  
*See also* Stability and Columns
- Critical stress, shear in beam web, 161, 164  
 shear in curved panel, 217
- Cross, H., 36, 49, 398, 405
- Cross method, 3, 36, 40, 49  
*See also* Moment distribution
- Curvature in polar coordinates, 265
- Curved beams, *See* Beams
- Curved element, effective thickness, 217  
 locus of resultant of constant shear flow on, 185-186
- Curved panels, allowable stress references, 363, 366  
 assumed distribution of material, 220  
 effective shearing modulus, 188, 217  
 effective thickness, 217
- Curves, qualitative bending moment and deflection, 2-4
- Curves of design data, beam-columns, coefficients, 121, 127-130  
 pin-ended length, 86  
 ratio total to primary bending moment, 116  
 spruce, allowable stresses, 87  
 circular rings, Wise coefficients, 274-275

- Curves of design data, tension field
  - beams, correction factors, 158
  - effective shearing modulus, 177
  - torsional column failure, solution of
    - cubic equation, 342
- Cycleweld process, 386
- Deflections, beam-column, axial compression, 91
  - axial tension, 99
  - primary, 63, 133
  - secondary, 63, 134
- beam, curved, 263-267
  - tension field, 173-178
  - trigonometric series method, 288-291
- general formula for superimposed, 4
- Maxwell's law of reciprocal, 10, 34
- papers on, 408, 411
- qualitative curves, 2-4
- redundant structures, 178
- rigid-jointed frames, 48
- rings, 265-267
- support, effect on fixed-end moments,
  - 128, 131, 138
- de Forest, A. V., 420, 421
- Deformation, equations of, arrangement
  - for solution, 32
  - description, 5-6
  - developed from Castigliano's theorem, 20, 22, 27
  - development for shells, 188, 212, 225
  - general method of development, 11-12
  - truss subject to initial stresses, 16-17
- initial, definition, 15
- uncertainty of magnitude, 29
- principle of consistent, 4, 30
- shear, 118-119
- Deformation pattern, representation, 285
- Delmonte, J., 369
- Den Hartog, J. P., 396
- Determinants, solution of simultaneous
  - equations by, 112
  - use for computing critical load, 112-113
- Dewar, W., 369
- Dickinson, H. B., 367, 419
- Differential equations, books, 394
- Differentiation, partial, 21, 23-24
  - relation between derivatives, 23
- Dinnik, A., 407
- Displacements, virtual, 286
- Distribution factor, 39, 45
- Dolan, T. J., 421
- Donnell, L. H., 366, 406, 416, 417
- Doolittle, J. H., 405
- Doubling plates, 242-253
- Doubly symmetrical section, torsional
  - column failure, 336-338
  - warping moments and constant, 336
- Dow Chemical Co., 389, 390, 391
- Dowmetal, 391
- Duncan, W. J., 413
- Dunn, L. G., 312, 367, 399, 404, 417, 419
- Ebner, H., 412, 414
- Effective cross-section, allowance for
  - shear lag, 219
  - computation of geometric properties, 192
  - distribution, 220
- Effective depth, tension field beam, 162, 164
- Effective modulus of elasticity, 140, 307, 354
- Effective shearing modulus, columns
  - subject to torsional failure, 354
  - curved panels, 188, 217
  - flat panels, 177, 217
  - tension field webs, 177
- Effective thickness, computation of, 190, 212, 217
- Effective width, papers on, 419
  - shell skin, 218
- Elastic critical load, 310
- Elastic curve, circular ring, 265-267
  - curved beam, 263-265
- Elastic joints, effect of, 52-53
- Elastic limit stress curves, spruce beam-
  - columns, 87, 85
- Elastic loads, method of, 40, 209
- Elastic medium, column in, 291-294
- Elastic stability, *See Stability and Critical loads*
- Elastically supported column, stability, 291-294, 297-303

- Elasticity, modulus of, *See* Modulus of Elasticity  
 shearing modulus of, *See* Shearing modulus of elasticity  
 theory of, books on, 395
- Electric strain gages, 420
- Elevator spar, analysis as continuous beam-column, 130-132
- Elliptical rings, 276
- Ellis, C. A., 410
- Ellis, G., 421
- Elongation, neglect of deflection due to, 29
- End moments, allowance for known value in slope-deflection equations, 52  
 classed as transverse loads, 91  
 definition, 37  
 relation to bending moment, 37  
 relation to support moment, 37  
 sign conventions, 36-37
- Energy, strain, *See* Internal work
- Equations, bent, 42-46, 50  
 deformation, *See* Deformation, equations of  
 of condition, 11  
 simultaneous, solution, by determinants, 112  
 by successive elimination of variables, 32-33  
 by successive trials, 33-34
- Equilibrium, neutral, 283  
 virtual work criterion, 286-287
- Equilibrium conditions, representation by equations, 1
- Equilibrium equations, detection of mutual dependency, 2  
 use in solving redundant structures, 4, 12, 28
- Equivalent truss, method of computing beam deflections, 173-178
- Eshbach, O. W., 398
- Euler column formula, development, 320-323, 284
- External couple, effect on beam-column, 94-95, 102-103, 104-105
- External work, beam under transverse load, 288-289  
 bent column, 320  
 bent and twisted column, 333, 344  
 column in elastic medium, 292  
 transverse load on beam, 288
- Fahlbusch, H., 274
- Failure, instability, types of, 294
- Fatigue, allowable stress references, 362, 366  
 book on, 396  
 magnesium alloys, 391
- Feller, H., 414
- Field, tension, *See* Tension field beams
- Fife, W. M., 397
- Filler blocks, 88-89
- Fillet, magnesium alloys, 392
- Fischel, J. R., 367, 414, 419
- Fixed-end moments, beam-columns, curves, 127-130  
 formulas, 128, 131  
 tables, 122-126  
 varying section, 137-138  
 sign convention, 38
- Flader, F., 404
- Flat panels, allowable stress references, 362, 366  
 buckling of, 162, 217  
 effective shearing modulus of, 177, 217
- Fligg, C. M., 316, 354, 355, 418
- Flight* magazine, 403
- Flight loads, papers on, 405
- Foppl, A., 366
- Force, collapsing, 266  
 supporting, 297
- Force sign convention, 206
- Form factor chart, spruce beams, 87
- Foundation modulus, 291
- Fourier's series, beam deflection formulas, 288  
 notation, 285
- Frames, building, 41  
 elastic jointed, 52-53  
 rigid jointed, bending-moment diagrams, 39, 47  
 deflection computations, 48  
 moment-distribution analysis, 39-49, 120  
 slope-deflection analysis, 49-52
- Frederick, D. S., 373
- French and Heald Co., 375
- Frocht, M. M., 396
- Fuller, C. E., 263
- Fuller, F. B., 367
- Fuselage rings, 278-281, 312, 415

- Fuselage sections, allowable stress references, 365-367
- GALCIT, 156, 312, 419
- Gassner, A. A., 404
- Geometry books, 394
- Glass, 367-369
- Goldberg, J. E., 52
- Goodey, W. J., 192, 413
- Goodyear Tire and Rubber Co., 386
- Gottlieb, R., 411
- Gottschalk, O., 36
- Gough, B., 151
- Granville, W. A., 394
- Graphical methods, beam-column analysis, 141-151  
papers on, 406, 411
- Green, G. G., 156
- Greene, C. F., 419
- Griffin, F. L., 394
- Griffith, A. A., 406
- Group instability failure, definition, 294, 295
- Gunning, J. H., 404
- Gurney, C., 415
- Gwinn, J. M., Jr., 407
- Handbooks, 398, 400
- Hardecker, J. F., 404
- Hart, W. L., 394
- Hatcher, R. S., 192, 413
- Hazard, C. T., 394
- Heck, O. S., 412
- Heliarc welding, 389
- Hetenyi, M., 408
- Historical notes, beam-column analysis, 62, 150-151  
shell analysis development, 191-192  
torsional column failure, 316  
use of plastic-bonded plywood, 375
- Hoff, N. J., 274, 276, 278, 279, 303, 304, 417
- Hoff's method, fuselage ring analysis, 279-281  
truss stability determination, 303-309
- Hogben, L., 394
- Holes in magnesium alloys, 392
- Houghton, J. L., 366
- Howard, H. B., 150, 151, 399
- Howland, W. L., 367, 408, 416, 419
- Hudson, R. G., 265
- Hughes, F. A. and Co., 366
- I-beam, torsion-bending stresses, 229
- Illustrative computations, analysis of  
circular ring, 276-278  
beam-columns, moment distribution, 130-132  
spruce, allowable stress, 84-88  
use of extended three-moment equation, 81-84  
varying section, 132-140
- beams, trigonometric deflection formulas, 290
- continuous beam, influence lines, 34-36
- curved beams, bending stresses, 262-263
- incomplete tension field beam, 164-176
- Maxwell-Mohr method, multi-redundant structures, 8-10, 13-15, 17-20
- method of least work, 21-24, 26-29
- moment-distribution, no axial load, 41-49
- moment of inertia, mid-line method, 345
- shear transfer near opening, 247-252
- shell in bending, 192-214, 234-237  
branch shear flows, 211  
correction shear flows, 210-214  
geometric properties of shell, 192-200  
net shear flows, 214  
normal stresses, 200-203  
resultant of trial shear flows, 208-210  
shear center location, 214-215  
tapered shell, 234-237  
trial shear flows, 203-208
- shell in torsion, 188-191
- slope-deflection method, 50-51
- stability of rigid jointed truss, 306-309
- supporting structure spring constant, 299
- torsional column failure, critical stress, 351-352  
warping properties, 348, 350
- Inch-kip, 44
- Included structure, statically determinate, 10-11, 30

- Incomplete tension field beams, *See* Tension field beams
- Indeterminate structures, *See* Statically indeterminate structures
- Index values, 420
- Inflection points, location from qualitative curves, 2-4  
location on beam-column, 85-89  
number in span, 37
- Influence lines, use in solving redundant structures, 34-36
- Information Circulars, U. S. Air Forces, 402
- Initial deformation, definition, 15  
uncertainty of magnitudes, 29
- Initial stresses, 15-20
- Instability failure, fuselage rings, 312  
group, 294, 295  
local, 294  
state of theory, 311  
types of, 294  
unit, 294  
*See also* Critical loads and Stability
- Institute of the Aeronautical Sciences, 402
- Integration, by parts, 321  
symbol for line, 181  
symbol for surface, 331, 181
- Internal work, beam under transverse load, 24-26, 288-289  
bent column, 320  
bent and twisted column, 332-333, 343  
column in elastic medium, 292  
element in shear, 186  
general expressions for, 24-26, 22  
in connections, 30
- Interpolation, sines and cosines, 67  
tangents, 71
- Isotropic materials, definition, 360
- Jacobson, J. M., 156
- James, B. W., 120, 411
- Johnson, C. D., 411
- Johnson, J. B., 115, 366, 400, 421
- Johnson, J. B., Bryan, and Turneaure, 397
- Johnson's formula, pin-ended beam-column, 115
- Johnston, B. G., 406
- Johnston, S. P., 400
- Johnston, W. A., 263
- Joints, balancing of, at junction of three or more members, 39  
under rigid-frame sign convention, 38  
elastic, 52-53  
rigid, secondary stresses due to, 39-41, 303-310
- Jones, W. R., 151
- Journal of Applied Mechanics*, 402
- Journal of the Aeronautical Sciences*, 402
- Kappus, R., 227, 316, 341, 354, 418
- Karman, T. von, 312, 394, 417, 418
- Kasner, E., 394
- Kaufmann, W., 268
- Kittlesen, H. M. J., 416
- Klemperer, W. B., 417
- Koller, H., 414
- Koning, C., 408
- Kroll, W. D., 303, 411
- Kromm, A., 216, 412
- Krumling, G., 414
- Kuhn, P., 156, 192, 216, 217, 218, 231, 413, 414, 415
- Lag, buckling, 216-218  
shear, 218-219
- Lahde, R., 177, 216, 412, 419
- Lambert, E. E., 404
- Landing wires, initial stresses in, 17
- Langley, M., 399
- Large deflection theory, 312
- Lazzarino, L., 231, 415
- Leaderman, H., 420
- Least energy principle, 283
- Least work, method of, applicability to beam-columns, 25  
arrangement of computations, 23  
general statement of method, 20-23  
limitations, 29  
numerical examples, 26-29, 21-24  
references, 396, 409  
value of, 29-30  
principle of, 21
- Lesley, H. G., 401
- Lever, solution by virtual work principle, 286
- Levy, S., 419, 420
- Limpert, G., 216, 420

- Line integral, symbol for, 181  
Lipp, J. E., 404, 412  
Load, active, 297  
Load terms, extended three-moment equation, axial compression, 93, 95, 106  
    axial tension, 101, 103, 106  
Loading, critical, 284  
Loadings, symmetric and anti-symmetric 267-269  
Loads, critical, *See* Critical loads  
    in flight, 405  
Lobley, J., 413  
Local instability failure, definition, 294  
Lockheed Aircraft Corp., 192  
Lombardi, L., 406  
Longley, W. R., 394  
Loudy, F., 399  
Lu, H. S., 421  
Lundquist, E. E., 303, 308, 309, 310, 316, 344, 351, 354, 355, 405, 411, 416, 417, 418  
Lyse, I., 406  
  
Mach, E., 283  
Macpherson, A. E., 419, 420  
Magnesium alloys, allowable stress references, 361-367  
    characteristics, 388-392  
Manderla, H., 49  
Maney, G. A., 49, 397  
March, H. W., 383, 406, 418  
Marguerre, K., 216, 412, 419  
Martin, Glenn L., Co., 156, 167  
Mason, T. E., 394  
Materials, papers on, 421  
Mathematics books, 393  
Mathes, J. C., 421  
Matulaitis, J., 420  
Maupertuis' theorem, 283, 304  
Maxwell, J. C., 5, 34  
Maxwell's law of reciprocal deflections, 10, 34  
Maxwell-Mohr method, continuous-beam analysis, 8-10  
    general statement, 11-12  
    illustrative computations, 8-10, 13-15 17-20  
    multipl-redundant structure, 8-10  
        axial loads only, 12-15  
    Iaxwell-Mohr method, neglect of deflection due to elongation, 29  
        singly redundant structure, 5-8  
        value, 29-30  
McGowan, W. A., 366  
    Mechanics books, 394  
Median surface, 326  
Members dropping out of action, 17-20  
Metal construction, books on, 399  
    papers on, 412-420  
Method of elastic loads, 40, 209  
Method of least work, *See* Least work  
Mid-line method of computing section properties, 180, 192, 220, 234, 345  
Miller, R. A., 117, 156, 405, 407, 416, 418  
Models, solution of structures by, 36  
Modulus of elasticity, effective, 140, 307, 354  
    glass, 368  
    magnesium alloys, 388  
    plastic-bonded plywood, 377  
    plastics, 371  
Modulus of foundation, 291  
Modulus of rupture, glass, 367  
Mohr, O., 5, 49  
Moisture, effect on strength, plastic-bonded plywood, 385, 375  
    plastics, 372  
Moisture content of plywood, 385, 375  
Moment diagrams, polar, 141-151  
    rigid frame, 39, 47  
Moment distribution, beam-columns, constant section, 120-132  
    illustrative computations, 130-140  
    varying section, 132-140  
elastic jointed frame, 52  
references, 398, 405  
rigid jointed frame, 39-49, 120  
    check on computations, 46-47  
    convergence of computations, 49  
    illustrative computations, 41-49  
    known joint translation, 39-41  
    stationary joints, 39  
    unknown joint deflection, 41-49  
sign conventions, 36-39  
Moment of inertia, computation for shell section, 198  
effect of change between beam-column supports, 116-117

- Moment of inertia, mid-line method of computation, 180, 220, 345
- Moments, bending, *See* Bending moments
- end, allowance for known, in slope-deflection equations, 52
- classed as transverse loads, 91
- definition, 37
- relation to bending moments, 37
- relation to support moments, 37
- sign conventions, 36-39
- fixed end, beam-columns, uniform section, 122-130, 131
- varying section, 137-138
- support, 37
- support deflection, beam-columns, 128-131, 138-140
- truss joint deflection, 39-40
- warping, definition 333
- doubly symmetrical section, 336
- evaluation, 345
- Moness, E., 407
- Moore, R. L., 406
- Morgan, N. P., 398
- Muller-Breslau, H., 62, 63
- Multipli-redundant structures, general solution, 8-10
- solution for axial loads only, 12-15
- See also* Statically indeterminate structures
- Murer, E. B., 410
- Nadai, A., 395
- National Advisory Committee for Aeronautics, technical publications of, 401
- Nelson, W., 399
- Neutral equilibrium, definition, 283
- Newell, J. S., 366, 412, 418
- Newlin, J. A., 84, 89, 405, 408, 411
- Newman, J., 394
- Niles, A. S., 418
- Nishkian, L. H., 406
- Nomenclature, calculus of variations, 318-320
- tension field beams, 156
- Non-uniform section, beam-columns, graphical analysis, 145-150
- moment-distribution analysis, 132-140
- Non-uniform section, use of average section properties, 116-117
- curved beams, 257-267
- incomplete tension field beams, 171-173, 177
- rings, 270-271, 276
- shells, 232-242
- Normal stresses, curved beams, 257-260
- distribution over shell section, 200
- induced by torsion, 227-232
- relation to shear flow, 183, 204
- tapered shells, 234
- Northrop Aircraft, Inc., 389, 390
- Notation, allowable stress references, 360
- calculus of variations, 318-320
- Fourier's series, 285
- tension field beams, 159-160
- unit warping, 326
- warping moments, 333
- Notes, operation, 193, 196, 198, 208
- reference, 193, 197
- Nye, W. L., 399
- Ober, S., 401
- Oberg, T. T., 367
- Openings, 242
- Operational notes, 193, 196, 198, 208
- Osgood, W. R., 140, 405, 407
- Panels, allowable stress references, 362-366
- curved, assumed distribution of material, 220
- effective  $G$ , 188, 217
- effective thickness, 217
- flat, buckling of, 162, 217
- effective  $G$ , 177, 217
- papers on, 418
- Parcel, J. I., 397, 410
- Parsons, G. B., 366
- Partial differentiation, 21, 23-24
- Parts, integration by, 321
- Pattern, deformation, 285
- Paul, D. A., 406
- Periodicals, aeronautical, 402-403
- Perkins, H. C., 416
- Permanente Metals Corp., 391
- Permanesium, 391
- Perry, J., 115
- Perry, T. D., 386, 421

- Petrenko, S. N., 411  
Phillips, H. B., 394  
Photoelasticity, references, 396, 420  
Pin-ended beam column, Johnson's formula, 115  
    Perry's formula, 115  
Pippard, A. J. S., 397, 398, 409, 410  
Pittsburgh Plate Glass Co., 369  
Plastic-bonded plywood, buckling resistance, 383  
    compressive properties, 379-384  
    connections, 385-387  
    historical note, 375  
    manufacture, 375  
    moisture in, 385, 375  
    research on, 387-388  
    shear resistance, 383  
    tensile properties, 376-380  
    types, 374-376  
Plastic critical load, 310  
Plastic materials, allowable stresses, 361-367, 373  
    cold-setting adhesives, 387  
    properties, 369-372  
    research on, 387  
    sealant, 373  
    types, 369  
Plasticity, 395  
Plywood, plastic-bonded, *See* Plastic-bonded plywood  
Points of inflection, *See* Inflection points  
Poisson's ratio, glass, 368  
Polar co-ordinates, curvature in, 265  
Polar diagrams, beam-columns, 141-151  
Potential energy surface, 304  
Poyer, H. M., 156  
Precision, trigonometric beam deflection formulas, 290  
Prescott, J., 366, 395  
Pressure, bonding, effect on strength of plywood, 377, 382  
Pressurized cabins, 416  
Pretschner, W., 354, 418  
Primary bending moment, definition, 63  
    relation to total moment, 115-116  
Primary shear, 118  
Principles, consistent deformation, 4, 30  
    least energy, 283  
    least work, 21  
    relative rigidities, 30-31  
Principles, similitude, 421  
    superposition, *See* Superposition  
    virtual work, 286-288  
Pritchard, J. L., 398  
Prytherch, W. E., 366  
Qualitative curves of bending moment and deflection, 2-4  
Radian measure, convenience of, 67, 64  
Radomski, B., 407  
Railroad car frame, moment-distribution analysis, 41-49  
    slope-deflection analysis, 50-51  
Ramberg, W., 406, 419, 420  
Rathbun, J. C., 53, 410  
Ratzersdorfer, J., 150  
Reactions, beam-columns, 106  
Reciprocal deflections, 10, 34  
Redundancy, degree of, 1-2  
Redundant structures, *See* Statically indeterminate structures  
Redundants, determination of number, 1-2, 13  
    selection, 12, 13  
Reference notes, 193, 197  
Reff, E. R., 367, 419  
Reissner, E., 218, 415  
Relative rigidities, principle of, 30-31  
Relaxation method, 398  
Reports and Memoranda, Aeronautical Research Committee (British), 402  
Rhode, R. V., 405  
Rib pressure, 225-227  
Richards, D. G., 421  
Rigid-frame sign convention, 36-39  
Rigid-jointed frame, bending-moment diagrams, 39, 47  
    deflection computations, 48  
    moment-distribution analysis, 39-49, 120  
    computation check, 47  
    slope-deflection analysis, 49-52  
Rigid-jointed truss, secondary bending moments, 39-41, 303-310, 409, 410  
Rigidity of structure, definition, 30  
Ring pressure, 225-227



- Rings, circular, bending moments on,  
270-278  
deflection of, 265-267  
illustrative computation, 276-278  
sign conventions, 270, 271, 276, 278  
solution of, 269  
elliptical, 276  
fuselage, instability of, 312  
non-uniform section, 276  
papers on, 416  
used to maintain form, 278
- Rivet correction factor, 163, 165
- Rivet pitch, doubling plates, 251
- Riveted joints, elasticity of, 410
- Riveting, magnesium alloys, 389
- Rivets in tension field beams, web chord  
connection, 166  
web-stiffener connection, 170
- Roark, R. J., 398
- Rotation axis, torsional column failure,  
324, 337, 339, 341, 343
- Rotations, truss members, 40
- Rowe, C. J., 31, 32
- Royal Aeronautical Society, 403
- Ryder, E. I., 278
- Salmon, E. H., 396
- Sanderson, P. A., 367, 414
- Sandorff, P. E., 367, 419
- Sasso, J., 367, 373
- Schapitz, E., 414
- Schuman, L., 418
- Schwalbe, W. L., 52
- Schwartz, A. M., 417, 411
- Schwartz, E. H., 420
- Sealants, plastic, 373
- Seaplanes, 399
- Sechler, E. E., 156, 168, 312, 366, 367,  
399, 404, 412, 419
- Secondary bending moment, beam-col-  
umns, 63, 133  
rigid-jointed truss, 39-41, 303-310,  
409, 410  
tension field beam chords, 171
- Secondary deflection, 63, 134
- Secondary shear, 117-119
- Secondary stress, torsion-bending, 227  
*See also* Joints, rigid
- Section properties, computation for shell,  
192, 220, 234
- Section properties, illustrative computa-  
tions, 345, 348, 350  
mid-line method of computation, 180,  
192, 234, 345
- Semion, W., 404
- Shanley, F. R., 192, 223, 225, 239, 413, 414
- Shear, allowable stress references, 361-  
367  
alternative values, 117  
beam-columns, axial compression, 90,  
118  
axial tension, 99  
polar diagrams, 150  
primary, 118  
secondary, 117-119  
total, 117-118, 90  
on tapered shell section, 235  
work due to, 24, 25, 186
- Shear center, rules for location, 214, 223
- tapered shell, 237, 238
- two-cell shell, 214
- Shear deformation, effect on beam-col-  
umn, 118-119
- slit shell, 211, 239
- Shear distribution factor, beam-columns,  
128, 130, 131, 140  
beams, 45
- Shear flow, direction along thin element,  
182  
in incomplete tension field beam, 161,  
166  
in shell subjected to bending, 203  
branch, 210-211  
computation of trial, 203, 239  
correction, 210-213, 239  
net, 214  
resultant of trial, 208  
sign convention, 205-206  
trial, 239
- in shell subjected to torsion, single  
cell, 184  
subdivided, 187
- near openings, 247
- reaction on circular ring, 269, 271
- relation to normal stress, 183, 204
- relation to total shear, 182
- resultant of constant, 183, 185-186
- resultant of varying, 208
- resultant on curved element of section,  
185-186

- Shear flow gradient, 209, 236
- Shear force, relation to shear flow, 182
- Shear lag, 218-219, 414
- Shear strength, magnesium-alloy spot welds, 390
  - magnesium alloys, 390, 391
  - plastic-bonded plywood, 383
- Shear stress, critical, curved panel, 217
  - near cut-out, 248
  - distribution over section in torsion, 325
  - effect of warping restraint, 227
- Shear transfer, 242-253
- Shearing modulus of elasticity, effective,
  - curved panels, 188, 217
  - flat panels, 177, 217
  - in columns subject to torsional failure, 354
  - tension field webs, 177
- Sheets, flat and curved, allowable stress references, 362-367
- Shells, allowable stress references, 365-367
  - analysis of, 180-256
  - distribution of transverse shear, 191
  - effect of change in section, 239
  - effect of lack of symmetry, 214
  - historical note, 191-192
  - normal stress due to bending, 200
  - illustrative computations, 188-191, 192-215, 234-237
  - papers on, 413
  - practical analysis procedure, 222-223, 238-239
  - rib and ring pressure, 225-227
  - shear center, 214, 223, 237, 238
  - shear deformation, 211, 239
  - shear flow, *See* Shear flow
  - simplified analysis of single cell, 224-225
  - skin buckling, 216-218, 188
  - tapered, 232-239
  - torsion of, single cell, 184-187
    - subdivided, 187-188
  - torsion-bending stresses, 231-232
  - "unit" method of analysis, 223-224, 239, 413
- Sibert, H. W., 411, 412, 415, 420
- Sign conventions, beam, 36-39
  - circular rings, 270, 271, 276, 278
  - curved beams, 258, 263
- Sign conventions, force, 206
  - rigid frame, 36-39
  - shear flow, 205-206
  - stress, 206
- Similitude, principle, of, 421
- Simpson, T., 35
- Simpson's rule, 35
- Simultaneous equations, solution by determinants, 112
  - successive elimination of variables, 32-33
  - successive trials, 33-34
- Sine, computation of, 67, 71
  - definition as series, 64
  - table of, 68-71
  - rule for interpolation, 67
- Singly redundant structure, Maxwell-Mohr solution, 5-8
- Singly symmetrical section, 8
  - torsional column failure, 338-340
  - warping moments and constant, 348-350
- Sliding, relative, in shell analysis, 211
- Slope, beam-columns, 91, 99, 67
- Slope angle, diagonal tension field, 164
- Slope-deflection method, 49-52
- Smith, D. E., 394
- Smith, P. F., 394
- Society of Aeronautical Weight Engineers, 404
- Society of Automotive Engineers, 403
- Southwell, R. V., 310, 395, 398, 409, 410
- Southwell method for critical load determination, 309-311
- Space frameworks, analytical analysis, 409, 410
  - graphical analysis, 407
  - stability of, 417
- Spofford, C. M., 397, 398
- Spring constant, column, 297
- supporting structure, 298
- Spring-constant criteria for stability, 296-303
- Spruce, allowable stresses, beam-columns, 84-90, 411
  - tension, 88
- Stability, elastic, 283-315
  - column in elastic medium, 291-294
  - column with distributed transverse load, 300

- Stability, column with variable transverse load, 296  
 elastically supported column, 297, 300  
 formula for beam web, 161, 167  
 papers on, 416  
 rigid-jointed truss, 303-309  
 single-span beam-column, 109-111  
 spring-constant criterion, 296-303  
 two-span beam-column, 111-115, 299  
*See also* Critical loads
- Stang, A. H., 406
- Static moment  $Q$ , mid-line method of computation, 180
- Statically determinate included structure, 10-11, 30
- Statically indeterminate structures, definition, 1  
 deflections, 178  
 degree of redundancy, 1-2  
 initial stresses, 15-20  
 members dropping out of action, 17-20  
 papers on, 408  
 qualitative bending moment and deflection curves, 2-4  
 solution, by arbitrary assumptions, 2, 30  
   by assumptions based on qualitative curves, 3-4  
   by influence lines, 34-36  
   by Maxwell-Mohr method, 5-20  
     *See also* Maxwell-Mohr method  
   by method of least work, 20-30  
   by models, 36  
   by moment distribution, *See* Moment distribution  
   by relative rigidities, 30-31  
   by slope-deflection method, 49-52  
 symmetrical, solution under symmetrical and anti-symmetrical loadings, 267-269
- Steel, allowable stress references, 361-367
- Steinman, D. B., 406
- Stephens, B. C., 408, 411
- Stern, E. G., 386
- Stieda, W., 274
- Stiffeners, allowable stress references, 364, 366
- Stiffeners, fuselage, critical loads, 280  
 incomplete tension field beam web, 166-170  
   with sheet, torsional column failure, 355
- Stiffness, beam, definition, 139
- Stiffness factors, beam-column, curves, 121  
 formulas, 121  
 symmetrical span, 126  
 tables, 122-126  
 varying section, 132-136  
 sign under rigid-frame convention, 38
- Stillwell, H. S., 421
- Stowell, E. Z., 418
- Strain, circles of, 420  
 relation to warping, 330-331
- Strain energy, *See* Internal work
- Strain gages, 420
- Strength, ultimate, relation to critical load, 109-110, 120
- Strength of materials books, 395
- Stress center, single-cell shell, 224  
 subdivided shell, 224  
 tapered shell, 238
- Stress ratios, 90
- Stress sign convention, 206
- Stresses, allowable, beam-columns, 84-90  
 references, 360-367  
 bending, *See* Bending  
 critical, *See* Critical stress  
 elastic limit, curves for spruce, 87, 85  
 initial, 15-20  
 relation to warping, 330-331  
 web, tension field beams, 157-158, 161-166
- Structure, included statically determinate, 10-11, 30  
 indeterminate, *See* Statically indeterminate structures  
 redundant, *See* Statically indeterminate structures
- Structures, theory of, books, 397
- Superposition, principle of, applicability, 4-5, 29  
 modification applicable to beam-columns, 91, 99, 106, 130  
 statement, 4  
 typical equations resulting from use, 4  
 use with initially stressed truss, 16

- Support deflection effects, beam-columns,
  - moment distribution computations, 128
  - reactions, 106
  - three-moment equation, 106
- Support deflection moments, beam-columns, uniform section, 128-131
  - varying section, 138-140
  - sign under rigid-frame convention, 38
- Support moments, 37
- Supporting force, 297
- Surface, median, 326
  - potential energy, 304
- Surface integration symbol, 331, 181
- Sutherland, H., 397
- Swain, G. F., 40, 395, 409
- Swickard, A. E., 408
- Symmetric loadings, 267-269
- Symmetrical span, relative stiffness factor, 126
- Symmetry, effect of lack in shell analysis, 214
  - effect on section properties, 336, 348
  - effect on torsional column failure, 336, 338-340
- Tables, allowable stress references, 361-365
  - beam-columns, moment-distribution coefficients, 122-126
  - terms for formulas, 92-95, 98, 100-105
  - curved beam sections, formulas for  $K$ , 261
  - extended three-moment equation, coefficients, 72-78, 107-108
  - load terms, 93, 95, 101, 103
  - magnesium-alloy properties, 391
  - plastic materials, compressive properties, 381, 382, 384
  - tensile properties, 371, 377, 378, 380
  - sines, cosines, and tangents, 68-71
  - web stability formula coefficients, 162, 167
- Tangent, definition, 64
  - table of, 68-71
  - interpolation, 71
- Taper, tension field beams, 171-173
  - See also* Non-uniform section
- Tapered shells, practical analysis, 238-239
  - symmetrical section, 232-238
- Taub, J., 408
- Taylor, B., 67
- Taylor, C. F., 401
- Taylor, G. I., 406
- Taylor, J. L., 415
- Taylor's theorem, 67
- Teichman, F. K., 400
- Temperature, effect on strength, of glass, 367
  - of magnesium alloys, 391
  - of plastic-bonded plywood, 375, 377, 381
  - of plastics, 370-372
- Tensile strength, glass, 368
  - magnesium alloys, 388, 391
  - plastic-bonded plywood, 376-380
  - plastics, 371
- Tension, allowable stress references, 361, 366
- Tension field beams, 156-179
  - complete tension fields, 157-159, 412
  - deflections, 173-178
  - incomplete tension fields, chord stresses, 170-172
    - effective depth, 162, 164
    - effective shearing modulus, 177
    - illustrative computations, 164-176
    - non-parallel chords, 171-173
    - shear flow, 161, 166
    - web buckling, 160-162, 166-168
    - web stiffeners, 166-170
    - web stresses, 161-166
  - nomenclature, 156
  - notation, 159-160
- Thermoplastics, definition, 369
  - use in plywood, 374
- Thermosetting plastics, definition, 369
  - use in plywood, 374
- Thickness, effective, 190, 212, 217
- Thin metal construction, reports on, 412-421
- Thompson, J. G., 400
- Thompson, S. P., 394
- Thompson, T. M., 411
- Thompson, W. T., 170

- Three-moment equation, extended, 72-84, 105-108  
     coefficients for axial compression, 72-78  
     coefficients for axial tension, 107-108  
     derivation for uniformly distributed load, 79-81  
     general form for left side, 105-106  
     historical note, 62  
     illustrative example, 81-84  
     load terms, 93, 95, 101, 103, 106  
     notes on use, 119-120  
     terms for support deflection, 106
- Timoshenko, S., 140, 167, 231, 291, 366, 395, 398
- Titterton, G. F., 401
- Torsion, allowable stress references, 361, 364-367  
     Bredt formula, 185  
     normal stress due to, 227  
     papers on, 406, 413  
     shear distribution over rectangular section, 325  
     shear flow in closed sections, 184  
     single-cell shell, 184-187  
     subdivided shell, 187-188  
     tubes, 184-187
- Torsion-bending stresses, 227-232, 415
- Torsion constant, 168
- Torsional column failure, 316-358, 418  
     basic assumptions, 324-326, 353  
     closed sections, 354  
     description, 316-317  
     doubly symmetrical sections, 336  
     effective moduli for, 354  
     end conditions, 353  
     general differential equation, rotation axis known, 344  
     rotation axis unknown, 334  
     general remarks, 353-355  
     historical note, 316  
     illustrative computations, 348, 350, 351-352  
     known rotation axis, 343-345  
     papers on, 418  
     practical evaluation of section constants, 345-350  
     rotation axis, 324, 337, 339, 341, 343  
     singly symmetrical section, 338-340  
     stiffener with sheet, 355
- Torsional column failure, tests, 351  
     unit warping, 326-331, 336, 346  
     unsymmetrical section, 340-343
- Total moments, relation to primary moments, 115-116
- Trayer, G. W., 84, 89, 383, 401, 405, 406, 408, 411, 418
- Trial design, need for, 4, 119-120
- Trigonometric functions, definition as series, 64  
     tables of, 68-71
- Trigonometric series method, beam deflections, 288-291
- Trimarchi, V. C., 367
- Truss, equivalent, 173-178  
     members dropping out of action, 17-20  
     rigid-jointed, computation of stresses in, 39-41  
     rotations of members, 40  
     stability of, 303-309  
     secondary bending moments due to joint rigidity, 39-41, 409, 410  
     Vierendeel, 41-51, 128, 157  
     wing, initial stresses, 17
- Truss joint deflection, effect on moment distribution computations, 39
- Tsien, H. S., 312, 367, 417
- Tubes, torsion of, 184-187
- Tuckerman, L. B., 411, 421
- Turneaure, F. E., 397
- Twist, angle of, closed tube, 186
- Twisting, energy of, 332, 343
- Ultimate strength, relation to critical load, 109-110, 120
- Unit instability failure, definition, 295
- Unit load system for deflection computation, 178
- Unit method, shell analysis, 223-224, 239, 413
- Unit warping, doubly symmetrical section, 336  
     evaluation, 346  
     formulas, 326-331  
     relations to stress and strain, 330
- Unsymmetrical section, torsional column failure, 340-343

- van den Broek, J. A., 397
- Variations, calculus of, *See* Calculus of variations
- Varying section, *See* Non-uniform section
- Velocities, virtual, 286
- Vibration, books on, 396
- Vierendeel, A., 41
- Vierendeel truss, 41-51, 128, 157
- Virtual displacements, 286
- Virtual work, definition, 286
  - statement of principle, algebraic, 287
  - verbal, 286
  - use for computing beam deflections, 288
  - use in equilibrium problems, 286
- von Abo, C., 409
- Wagner, H., 156, 157, 177, 216, 217, 316, 354, 366, 410, 412, 413, 418, 419, 420
- Wang, T. K., 278
- Warner, E. P., 400
- Warping, column sections, 323, 326
  - relation to stress and strain, 330-331
  - unit, 326-331, 336, 346
- Warping constant, definition, 333, 343
  - doubly symmetrical section, 336
  - evaluation, 345
  - singly symmetrical section, 348-350
- Warping moment, definition, 333
  - doubly symmetrical section, 336
  - evaluation, 345
  - singly symmetrical section, 348-350
- Watts, E. H., 416
- Way, S., 366
- Web stiffeners, incomplete tension field
  - beams, 166-170
  - oblique, 159, 173
- Web stresses, complete tension field
  - beams, 157-158
- incomplete tension field beams, 160-166, 171-172
- Wegner, W., 274
- Weights, glass, 368
  - magnesium alloys, 388
  - papers on, 404
- Weld, L. D., 286
- Welding, magnesium
  - references, 400
- Weller, R., 420
- Wentworth, G., 394
- Wenzek, W. A., 420
- Westergaard, H. B., 407
- Width, effective, papers on, 419
  - shell skin, 218
- Wilbur, J. B., 52, 397
- Williams, D., 132, 151, 192, 413
- Williams, H. A., 405
- Williot diagram, 40
- Williot equations, 410
- Wilson, W. K., 396
- Wind loads, 41
- Windows, glass, 367
  - plastic, 373
- Windshields, glass, 367
  - plastics, 373
- Wing sections, allowable stress references, 365-367
- Wing spar, analysis by extended three-moment equation, 81-90
  - computation of bending moments, 81-84
  - computation of effective slenderness ratios, 85, 88-89
  - spruce, computation of section properties, 81-82
  - computation of allowable normal stress, 84-89
  - effect of filler blocks, 88-89
- Wing trusses, initial stresses, 17
- Wise, J. A., 273, 416, 420
- Wise coefficients, definition, 273
  - diagrams of, 274-275
  - use, 276-278
- Witt, E. C., 411
- Wood, K. D., 416
- Wood, allowable stress references, 361-367
  - allowable stresses, 84-90
  - compressed, 385
  - See also* Plastic-bonded plywood
- Woods, F. S., 394
- Work, external, *See* External work
  - internal, *See* Internal work
- Yield stress, magnesium alloys, 389, 391
  - plastics, 370
    - D. H., 407
    - E., 113, 367, 399, 407, 416,